4. SITE 534: BLAKE-BAHAMA BASIN[1]

Shipboard Scientific Party[2]

HOLE 534

Date occupied: 21-22 October 1980

Position: 28°20.6'N, 75°22.9'W

Water depth (corrected sea level; m, echo-sounding): 4973

Bottom felt (m, drill pipe from rig floor): 4984

Penetration (m, jet test): 87.5

Number of cores: 1

Total length of cored section (m): 2.1

Total core recovered (m): 2.1

Core recovery (%): 100

Oldest sediment cored:
Depth sub-bottom (m): 2.1
Nature: Biogenic calcisiltite
Age: Quaternary

Basement: Not reached

HOLE 534A

Date occupied: 29 October-29 November 1980 and
6 December-19 December 1980

Position: 28°20.6'N, 75°22.9'W

Water depth (sea level; corrected m, echo-sounding): 4971

Bottom felt (m, drill pipe from rig floor): 4976

Penetration (m): 1666.5

Number of cores: 130

Total length of cored section (m): 1130.2

Total core recovered (m): 629.8

Core recovery (%): 56

Oldest sediment cored:
Depth sub-bottom (m): 1635
Nature: Reddish brown shale
Age: middle Callovian
Measured velocity (km/s): 2.5

Basement:
Depth sub-bottom (m): 1635.0-1666.5
Nature: Basalt
Velocity (km/s): 5.2

Principal results: Continuous coring between 536 and 1666.5 m below the seafloor yielded a detailed ocean-basement and overlying sedimentary record spanning over 140 m.y. of Atlantic Ocean history. Callovian through Albian, Cenomanian, Maestrichtian, late Eocene, and early Miocene sediments were recovered. The younger, unsampled section can be extrapolated from the findings at Site 391. The sedimentary sequence reflects largely continuous, quiescent 0.1 cm/10^3 yr. or less hemipelagic sedimentation mostly between the calcium carbonate compensation depth (CCD) for foraminifers and nannofossils. On this is supperimposed periodic and much more rapid sedimentation by turbidite, debris flows, or deep currents of slope and shelf carbonates and carbonaceous claystone. Three-quarters of this sediment (decompacted thickness) was deposited in the first 50 m.y. after the site appeared on the mid-ocean ridge. Most of the overlying younger sediment was deposited in the Neogene. The results are as follows:

1) Massive debris flows up to 30 m thick in the lower part of the Miocene Great Abaco Member can be correlated over the 22-km distance between Sites 391 and 534, attesting to their widespread nature. Multiple sources in shallow water and deep bathyal areas supplied the transported material, which disrupted the indigenous basinal hemipelagic clay sediments and incorporated the clasts in this lower Miocene deposit.

2) The upper Eocene cherts and porcellanites of the Bermuda Rise Formation (27 m thick) discovered at Site 534 indicate that Oligocene erosion in the Blake-Bahama Basin did not totally remove the Paleogene sediments. The remnants of these slowly deposited sediments indicate that a long period of slow deposition in the Paleogene resulted in only a thin deposit of sediments. This information contradicts previous conclusions, based on vitrinite reflectance of the Cretaceous black shale of Site 391, that 800 m of post-Cenomanian to pre-Miocene sediments were eroded. The presence of chert indicates that seismic Horizon A^c is merged with the Horizon A^u as a single wavelet in the Blake-Bahama Basin.

3) Continuous coring of the shales of the Maestrichtian Plantagenet Formation and the Cenomanian-Barremian Hatteras Formation (186 m thick) reveals the slow accumulation (<1 cm/1000 yr.) of clay mineral and organic matter in depths beneath the CCD. Green clays alternating with black shale in the carbonaceous parts of the Hatteras Formation suggest low-oxygen to anoxic conditions, which were brought about when the poorly ventilated ocean basin was overwhelmed with organic matter. Peaks in organic matter concentrations are found in the lower Aptian, (?)middle Aptian-lower Albian, middle Albian, and Cenomanian. The variegated claystones of the Maestrichtian Plantagenet Formation are interpreted as having resulted from the basin-wide oxygenation in the presence of sluggish bottom-water currents. Similar variegated claystone, this time with winnowed silt beds, in the middle of the Hatteras Formation is attributed to another previous oxygenation under the influence of improved bottom circulation. A weak

---

[1] Sheridan, R. E., Gradstein, F. M., et al., *Init. Repts. DSDP*, 76: Washington (U.S. Govt. Printing Office).

[2] Robert Sheridan (Co-Chief Scientist), Department of Geology, University of Delaware, Newark, Delaware; Felix Gradstein (Co-Chief Scientist), Bedford Institute of Oceanography, Geological Survey of Canada, Dartmouth, Nova Scotia, Canada; Leo A. Barnard, Department of Oceanography, Texas A&M University, College Station, Texas; Deborah M. Bliefnick, Earth Sciences Department, University of California, Santa Cruz, California; Daniel Habib, Department of Earth and Environmental Sciences, Queens College, Flushing, New York; Peter D. Jenden, Institute of Geophysics and Planetary Physics, University of California, Los Angeles, California; Hideo Kagami, Ocean Research Institute, University of Tokyo, Nakano, Tokyo, Japan; Everly M. Keenan, Department of Geology, University of Delaware, Newark, Delaware; John Kostecki, Lamont-Doherty Geological Observatory, Columbia University, Palisades, New York; Keith Kvenvolden, U.S. Geological Survey, Menlo Park, California; Michel Moullade, Centre de Recherches Micropaleontologiques, Université de Nice, Nice, France; James Ogg, Geological Research Division, Scripps Institution of Oceanography, La Jolla, California; Peter H. Roth, Department of Geology and Geophysics, University of Utah, Salt Lake City, Utah; Thomas Shipley, Deep Sea Drilling Project, Scripps Institution of Oceanography, La Jolla, California (present address: University of Texas, Institute of Geophysics, Austin, Texas).

LEG 76 EXTENSION: Jay L. Bowdler, Union Oil Company of California, Houston, Texas; Pierre H. Cotillon, Département de Géologie, Université Claude Bernard, Villeurbanne, France; Robert B. Halley, Branch of Oil and Gas Resources, U.S. Geological Survey, Denver, Colorado; Hajimu Kinoshita, Department of Geophysics, Chiba University, Chiba, Japan; James W. Patton, Marathon Oil Company, Littleton, Colorado; Isabella Premoli-Silva, Istituto di Paleontologia, Universita di Milano, Milano, Italy; Kenneth A. Pisciotto, Deep Sea Drilling Project, Scripps Institution of Oceanography, La Jolla, California (present address: Sohio Petroleum Company, San Francisco, California); Margaret M. Testarmata, Galveston Marine Geophysics Laboratory, University of Texas at Austin, Galveston, Texas; Richard V. Tyson, Department of Earth Sciences, The Open University, Bucks, United Kingdom; David K. Watkins, Department of Geology, Florida State University, Tallahassee, Florida.

reflector is associated with this older variegated claystone and is called β', which might be an unconformity caused by the oxygenating currents.

4) Continuous coring of the Berriasian to Barremian Blake-Bahama Formation (392 m thick) indicates sedimentation of alternating turbiditic (detrital to organoclastic) and pelagic biogenic deposits well above the CCD. The organic shale and terrigenous quartz-rich sands and silts derived from the land occur in greater quantities in the Blake-Bahama Formation at Site 534 than at Site 391, indicating a lateral facies transition from clastic- to limestone-dominated sedimentation. Seismic Horizon β is correlated with the Barremian turbiditic limestone near the top of the Blake-Bahama Formation, and another prominent reflector called C′ is correlated with the Berriasian limestones at the bottom of the Formation.

5) Continuous coring of the Cat Gap Formation (153 m thick) indicates deposition of red calcareous claystones and transported limestones in an environment near the CCD and ACD (aragonite compensation depth). Relatively detailed biostratigraphy using nannofossils, foraminifers, and calpionellids shows the Cretaceous/Jurassic boundary to be at the top of the Cat Gap Formation. The top of the red shaly limestones of the Cat Gap correlates with seismic Horizon C. Another possible unconformity in the Kimmeridgian separates the red shales of the Cat Gap from the lower, limestone-rich subunit of the same formation. This unconformity is seismic reflector D′.

6) Continuous coring of the oldest sediments (140 m thick), deposited in the Callovian and Oxfordian, reveals a stratigraphic transition from an organic, phosphatic dark red and green and black Callovian shale to a siliceous radiolarian-rich, green black silty claystone mixed with displaced Oxfordian turbiditic slope limestones. The oldest sedimentary unit reflects above-average organic input; bottom water may have been depleted in oxygen concentration at the sediment/water interface. Evidence for at least some deep circulation comes from current ripple laminations, phosphatic lag gravels, and winnowed lenticular beds; seismic evidence at Site 534 indicates the existence of current-deposited bed forms below Horizon D. Horizon D itself is correlated with the lower Oxfordian turbiditic limestones.

7) Fractured oceanic basalt (31.5 m thick) with several 1 to 5-cm-thin silicified red limestone beds was recovered from below a strong clear basement reflector that agrees with the sharp contact observed in the base of Core 127. Well-cemented basalt breccia zones and well-developed mineral veins attest to the long period of diagenesis that this oldest basement rock has undergone. These factors prove that a normal oceanic crust exists under the outer (Jurassic) magnetic quiet zone.

8) Dating the sediments just above oceanic basement at Marine Magnetic Anomaly M-28 as middle Callovian yields a spreading rate of approximately 3.8 cm/yr. for the Blake-Bahama Basin between the Blake Spur Anomaly and M-22. This constant spreading rate agrees reasonably with the paleomagnetic dating of Anomalies M-22 and M-25 by Ogg (1980). Thus an age of latest Oxfordian for M-25 (143 m.y. old) is established—2 to 6 m.y. younger than previous estimates. Projecting this relatively high spreading rate yields an age of early Callovian (±155 m.y.) for the Blake Spur Magnetic Anomaly, which is 20 m.y. younger than previously thought. Therefore, the major spreading-center jump associated with the Blake Spur Anomaly and the opening of the modern North Atlantic are judged to have occurred much more recently than previously projected.

BACKGROUND AND OBJECTIVES

Blake-Bahama Basin

The continental edge of eastern North America is the passive margin with the oldest geological history available in the modern oceans. Rifting and seafloor spreading between the North American and African continents began in the late Triassic to Early Jurassic. A possible spreading-center jump and reorganization in spreading at the time of the Blake Spur Magnetic Anomaly (?Bathonian) left some of the oldest crust on the western margin of the North Atlantic (Vogt et al., 1971; Klitgord and Behrendt, 1979; Sheridan, 1978) (Fig. 1). The spreading-center jump isolated a portion of the most ancient Atlantic Ocean crust between the East Coast and Blake Spur anomalies off the United States. Only in the westernmost Pacific may similarly old ocean basement and sediment be present, but not within easy reach of the drill. Penetration and sampling of such old ocean crust and the immediately overlying pelagic sedimentary cover, consisting of Middle Jurassic and younger strata, has long been a key objective in oceanographic research. This objective was accomplished at Site 534 (Fig. 2).

Jurassic Paleogeography and Paleoenvironment

The Middle Jurassic central North Atlantic Ocean was still much constricted and certainly did not measure more than a few hundred kilometers across (e.g., Sclater et al., 1977; 1980). Initially it was an elongate, narrow, embaymentlike extension of western Tethys, the major seaway through southern Europe and South Asia. Tethys linked through the Norwegian Sea-Arctic Ocean and through South Asia with the Jurassic Pacific (Fig. 3).

Just when in the Jurassic a westward equatorial connection became established between Tethys through the incipient North Atlantic "embayment" extending across Central America and into the Pacific is not well known. There are marine epicontinental Middle and Upper Jurassic deposits in Cuba and particularly in Mexico (Barr, 1974; Maldonado-Kourdell, 1956), and Upper Jurassic marine oceanic sediments in the Gulf of Mexico. Some authors (Hallam, 1975; Westermann, 1977; in press, and personal communication, 1981) use generalized paleogeography or intricate biota dispersal to defend such a Middle Jurassic connection. Others (see Ager, 1975; Thiede, 1979) do not show a Jurassic western equatorial ocean passage until well into the Late Jurassic.

Although the Jurassic was a time of relatively warm, equable climate with weak thermal gradients in the ocean (the results of a warm climate, large epicontinental seas, low relief, marine polar regions, and close packing of continents along the N–S line), a sluggish ocean circulation may have existed. The establishment of a global surface circulation pathway in the equatorial belt may have created different ocean environments and enhanced opportunities for ocean micro- and macrobiota dispersal. In this context it is tempting to speculate that the advent of true planktonic foraminifers in the earliest part of the Middle Jurassic is related to such an oceanographic event. Arguments against this relation are that these calcareous microfossils (and many others) are a minor biomass in Jurassic oceans and, unlike modern ones, are relatively "shelf" bound. The poorly known dispersal of this group in the Jurassic to Early Cretaceous may be independent of ocean pathways.

It is unlikely that vigorous and widespread deep-water flow existed in the North Atlantic before the opening of the South Atlantic in the mid-Cretaceous. Nevertheless, indications of Jurassic contour-following currents can be interpretated from the appearance of basal Middle

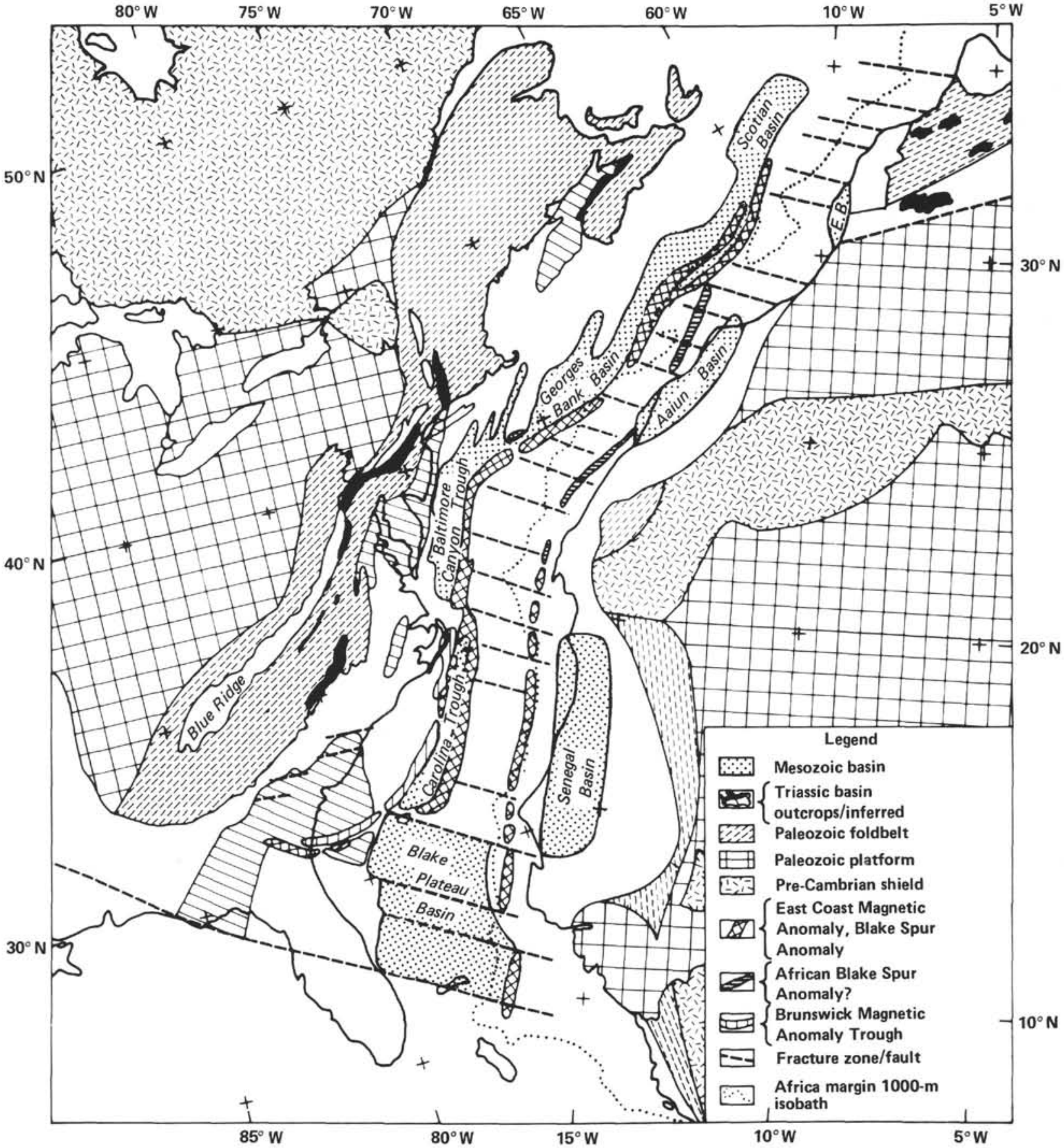

Figure 1. Reconstruction of the North Atlantic at the time of the Blake Spur Anomaly (after Klitgord and Schouten, 1977). (Locations of the major Mesozoic sediment-filled basins are indicated for the African and North American margins (from Klitgord and Behrendt, 1979).

Jurassic sediments on high-quality seismic reflector profiles near Site 534 (Sheridan et al., this volume). More evidence comes from a study of the sediments drilled at Site 534. In this respect, direct paleobathymetric information can be derived from the backtracking and stripping technique shown in Figure 4. The paleobathymetric track is the one at nearby Site 391 corrected for thermal cooling, sediment compaction and loading, and isostatic rebound. The superimposed levels of the CCD follow from the known and estimated stratigraphic position of the carbonate-shale units. At least two major cycles existed (Fig. 4), with a possible third upward excursion of the CCD in the Late Jurassic.

Jurassic Marine Biostratigraphy

Jurassic marine biostratigraphy is founded on the diversified and rapidly evolving ammonite macrofossil record, which is generally tied to stratotypes (Fig. 5). Standard zonations are in existence for the shallow marine Tethyan and boreal realms (Mouterde et al., 1971;

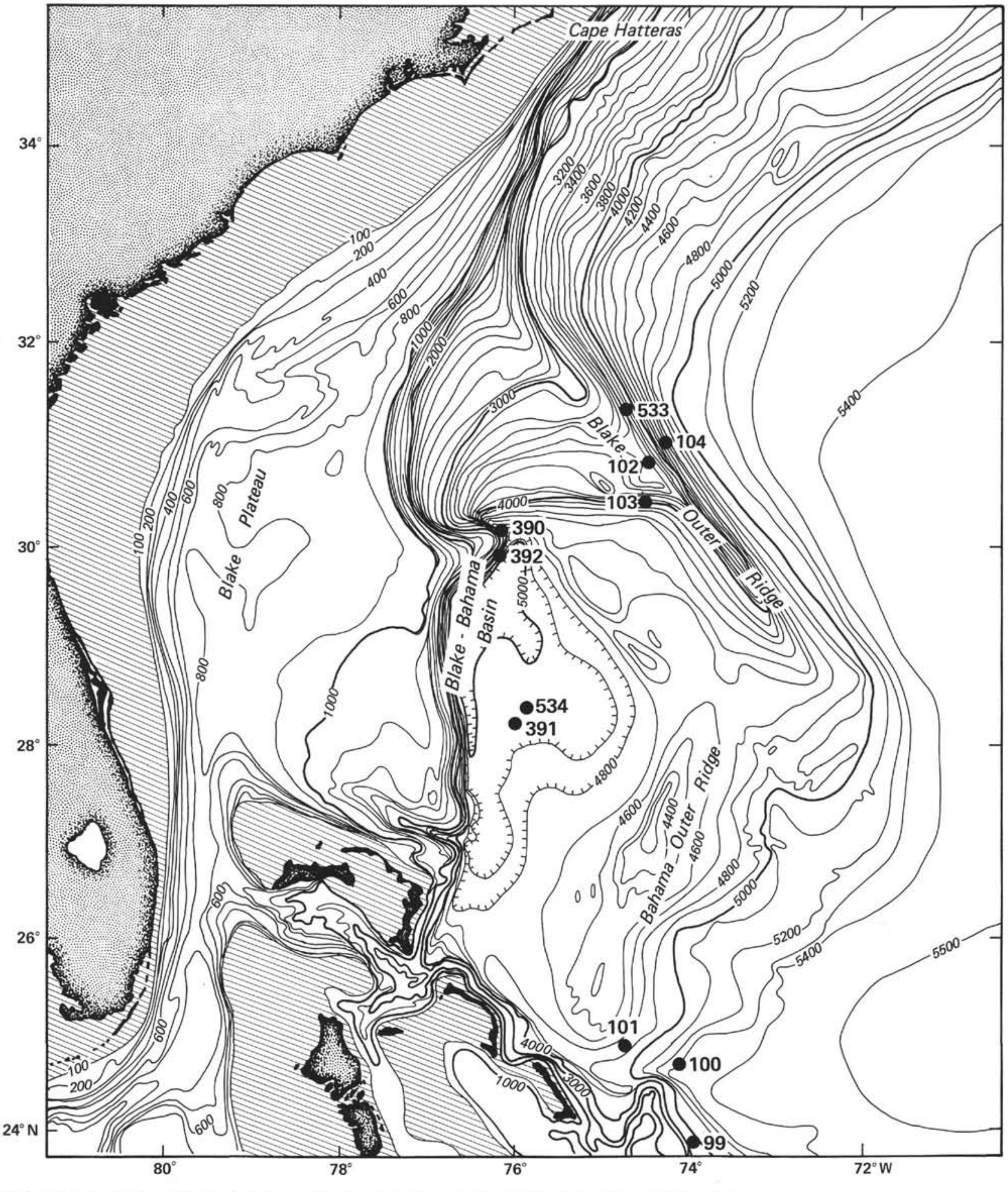

Figure 2. Locations of Sites 533 and 534 relative to previous DSDP sites and general physiography.

Hallam, 1975). Locally, marine bivalves (e.g., Buchia), pelagic crinoids, and algae have proven to be zonally useful.

Jurassic microfossil biostratigraphy, as applicable to the North American Basin, is far from standardized, an exception being the calpionellid zonation for Jurassic/Cretaceous boundary beds (Alleman et al., 1971; Remane, 1978). Jurassic stratigraphies based on nannofossils (Barnard and Hay, 1974; Hamilton, 1979), planktonic and benthic foraminifers (Gradstein, 1976; 1978b), ostracodes (Oertli, 1963; Ascoli, 1976), and dinoflagellates (e.g., Bujak and Williams, 1977) are essentially local zonations. These zonations apply to a particular epicontinental basin, marginal to the incipient Atlantic.

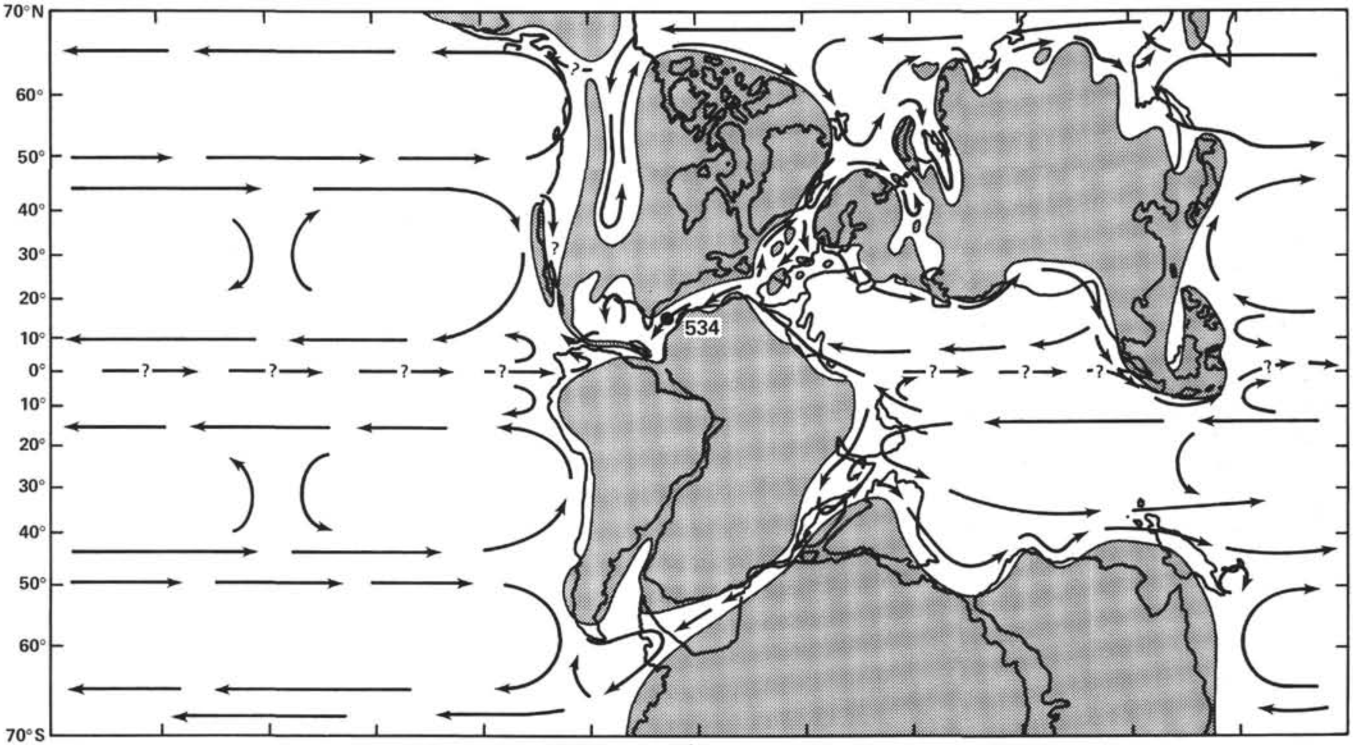

Figure 3. Late Jurassic paleogeography and surface circulation, after Ager (1975). (According to G. Westerman [personal communication, 1981 and in press] the same scenario existed in the Middle Jurassic.)

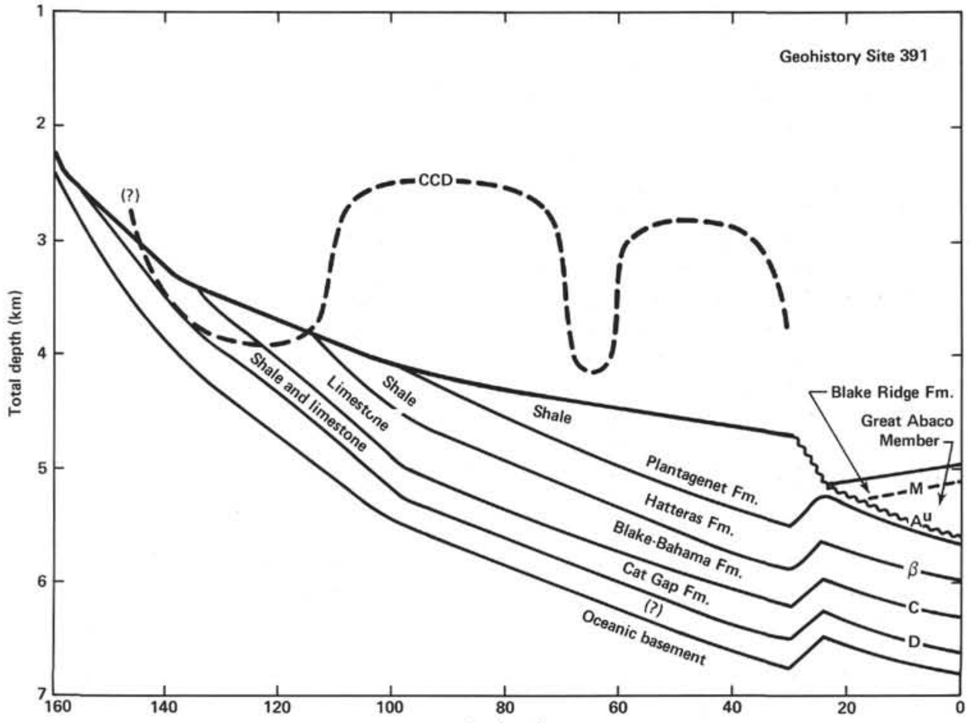

Figure 4. Geohistory plot of Site 391 constructed prior to drilling at Site 534. (Superimposed CCD curve is after Jansa et al. [1979]. Figure is corrected for thermal cooling, sediment loading, isostatic rebound, and sediment compaction, assuming 800 m of erosion in the Oligocene [Dow, 1978].)

Stratigraphic resolution is generally at the stage level (there are 11 Jurassic stages covering a 55-m.y. period). Biostratigraphic interrelation and chronostratigraphic precision are ill understood. This situation is even more characteristic of the Jurassic zonations in oceanic sediments; it is probably a true statement that no such zonation(s) exist, although a middle part of the Late Jurassic radiolarian zonation for southern Europe (Tethys) (Baumgartner et al., 1980) may well be applicable to the Atlantic region.

Aptychi, planktonic crinoids, smaller benthic foraminifers, nannofossils, small ostracodes, and palynomorphs were used to date the Late Jurassic deposits of three Leg 11 sites in the North American Basin (see studies by Renz, Hess, Luterbacher, Wilcoxon, Oertli, and Habib in Hollister, Ewing, et al., 1972). Biomass and taxonomic diversity is relatively low.

For some of these groups of fossils, there is good affinity with southern European–Tethys facies. Stratigraphic resolution is less than in the epicontinental record, and several age discrepancies remain to be solved.

At Site 534, the continuous coring of Middle and Upper Jurassic rocks considerably extends the deep-sea record. The site provides an excellent opportunity for basic biostratigraphic studies applicable to further explorations of the deep sea and the continental slopes.

Stratigraphic Relationships

Oceanographic events and geomagnetic and biostratigraphic scales and zonation are not well established for the Jurassic Atlantic Ocean. Better integration and calibration of geologic information (s.l.) has been achieved for the Early Cretaceous. Figure 5 (back pocket) brings together biostratigraphic, tectonic, and oceanographic information deemed relevant to drilling at Site 534. This multiple stratigraphic account summarizes the "state of the art" and provides a prognosis for the evaluation of the Site 534 Mesozoic data. The lithostratigraphic information for the oceanic Cat Gap, Blake-Bahama, and Hatteras formations comes from Benson, Sheridan, et al. (1978) and Jansa et al. (1979). The time-scale concept is from van Hinte (1976a, b). The magnetostratigraphy scales are discussed separately in this report (see the Time Scale and Magnetostratigraphy section). The paleontological zonations and events summaries come from recent literature and from compilations by participants in Leg 76 studies. The nannofossil biostratigraphy for the Cretaceous comes from Roth (1978). Documentation of ranges of Jurassic nannofossils is still inadequate for a zonation; first and last occurrence levels will be used for age assignments and are largely based on studies by Rood et al. (1971), Rood and Barnard (1972), Barnard and Hay (1974), Thierstein (1976), Wind (1978), and Medd (1979).

In Figure 5 we present the calpionellid zonation for Tethyan, open marine, carbonate sediments (Remane, 1978). This zonation, which has been applied to Atlantic Deep Sea Drilling sites (e.g., Legs 11, 50), may be expected to help considerably in providing a chronostratigraphy for Tithonian–Valanginian strata. The sediment magnetic reversal scale after Ogg (1980) is calibrated with the calpionellid zones as listed. Also, the disappearance of the foraminifers *Epistomina uhligi* and *E. stellicostata* on the Grand Banks is in one of the subzones of calpionellid Zone B (Jansa et al., 1980).

Middle and Late Jurassic biostratigraphic ranges and "datums" of foraminifers are based on information from Lutze (1960), Simon and Bartenstein (1962), Espitalié and Sigal (1963), Pazdro (1969), Wernli and Septfontaine (1971), Ohm (1967), Ruget (1973), Bielecka and Geroch (1974), Gradstein (1976 and unpublished data), and Jansa et al. (1980). The Early Cretaceous foraminiferal biostratigraphy, which, because of the planktonic foraminiferal record, has been more firmly established than the Jurassic one, is based on studies by Bartenstein et al. (1957, 1966, 1973), Moullade (1966, 1974, 1980), compilations by Sigal (1977) and van Hinte (1976b), and regional studies in the western North Atlantic by Luterbacher (1972) and Gradstein (1978a).

The taxa listed in the Jurassic part of the foraminiferal column have been selected from among many other forms for conspicuous morphology and known presence in circum-Atlantic marginal basins, notably Portugal, Morocco, and The Grand Banks. Exclusively shallow neritic taxa, including several excellent index forms among the larger foraminifers, have been omitted from the figure. The Early Jurassic taxa that may be encountered in a deep basin are *Marginulina prima* s.l., *Lingulina tenera* s.l., *Brizalina liassica, Frondicularia terquemi, Nodosaria regularis*, and *Lenticulina d'orbignyi*. The appearance of Jurassic globigerinids, *Garantella* spp. (except *G. rudia*), *Lenticulina tricarinella, L. quenstedti*, and *Epistomina mosquensis*, and the disappearance of *Reinholdella crebra* and *Epistomina regularis* is of use in Middle Jurassic stratigraphy. The presence of *Gaudryina heersumensis*, the disappearance of *Lenticulina quenstedti, Epistomina uhligi*, and *E. stellicostata* can be used to broadly subdivide Upper Jurassic strata.

A special case is the presence and disappearance of the Jurassic globigerinids. Jurassic globigerinids, represented by a dozen form species, first appear in the Bajocian. This group of tiny planktonic forms extends stratigraphically upward into Oxfordian or Kimmeridgian beds. Occurrences are on the Grand Banks, in Portugal, the French circum-Mediterranean area, central Europe, and southern U.S.S.R.

In the Atlantic realm there is no record of globigerinids in upper Tithonian through Valanginian strata. The reappearance of these globigerinids is in the form of *Caucasella hotervica*, a Hauterivian through basal Aptian marker. The latter, like the Jurassic globigerinids, has largely been recorded in neritic deposits with rare deeper marine incursions.

The taxa listed in the Cretaceous part of the column devoted to foraminifers also represent a selection of mostly planktonic species, the biostratigraphic value of which is well known and calibrated in the Tethyan realm and its margins (Mesogea); these species have been recorded on the previous western North Atlantic DSDP Legs (e.g., 4, 11, 44).

As we have already stated, valuable and detailed foraminiferal zonations are presently available for the Cretaceous and, particularly, the Lower Cretaceous, but instead of repeating them in Figure 5, a choice has been made to include only the most important biostratigraphic events (FADs, LADs, extension of some conspicuous species).

In the Neocomian (Berriasian to Hauterivian), planktonic foraminifers were practically not yet represented, with the exception of *Caucasella*; and only small benthic foraminifers are used for zonations and biostratigraphic correlations. There was in fact an important acceleration of the speciation rate among benthic foraminifers in the middle part of the Valanginian (Moullade, 1980), the result of which was to enrich progressively the poor lower Neocomian assemblages inherited from the Jurassic. This phenomenon is well evidenced in the Mesogean realm but probably for ecological reasons is not clearly depicted in the western North Atlantic.

In this domain several biostratigraphic events, well calibrated with the chronostratigraphic scale, are nevertheless of use, like FAD of certain species of nodosarids (*Lenticula nodosa*, which appears close to the Berriasian/Valanginian boundary), *L. busnardoi*, lituolids (*Dorothia praehauteriviana*), and the first osangulariids (*Gavelinella sigmoicosta*).

In the uppermost Hauterivian a noticeable event is represented by the first appearance of small hedbergellids, as *Hedbergella sigali* and *H. infracretaca* group, which corresponds to the beginning of an uninterrupted period of development of Cretaceous planktonic foraminifers. In the Mesogean and Atlantic realms, this period is delineated by the successive appearances of short-ranged species, as *Blowiella blowi, Schackoina cabri, Globigerinelloides ferreolensis, G. algerianus, Hedbergella trocoidea* (Aptian), *Ticinella primula, T. praeticinencis, T. breggiensis, Planomalina buxtorfi, Rotalipora appenninica* (Albian, incl. Vraconian), and *Rotalipora brotzeni* (Cenomanian). For example, in the Tethyan realm the interval that comprises the Aptian and Albian stages can be subdivided into 14 zones, based on the FAD of index planktonic forms.

In the DSDP samples, where planktonic foraminifers happen to be rather often dissolved, use of benthic forms can be helpful. In the upper Lower Cretaceous *Gavelinella barremiana* (appearing in the upper lower Barremian) and *Pleurostomella* spp. (appearing in the uppermost Aptian), among others, can be used biostratigraphically.

The Lower Cretaceous dinoflagellate biostratigraphy is the one developed by D. Habib for the western North Atlantic (Habib, 1978); the "state of the art" in Jurassic sediments is explained in detail by Habib and Drugg (this volume).

Recently a radiolarian zonation of the middle part of the Upper Jurassic has been published for southern Europe (Tethys) (Baumgartner et al., 1980) that may well be applicable to the Atlantic Ocean region. The zonation makes use of the concurrent range zone concept of "unitary associations," as formulated statistically by J. Guex and E. Davaud (1982). Figure 5 presents the seccession of radiolarian zones (Al–E12) and their approximate chronostratigraphic assignments.

Mid-Cretaceous and Neocomian Cycles

The discovery of widespread "black" shale facies in the Atlantic has been one of the major discoveries of the Deep Sea Drilling Project (Arthur, 1979). The mid-Cretaceous was a time of equable climates and most probably a climatic optimum, after which the Earth cooled quite drastically. Sedimentation patterns in the Cretaceous show a dramatic shallowing of the calcium carbonate compensation depth by over 1 km during the mid-Cretaceous (Fig. 4). Organic carbon was preserved in concentrations greater than before or after that time period. Cyclic sedimentation was very widespread during the mid-Cretaceous, both along continental margins and in oceanic settings far removed from any sources of detrital input. Strong east–west gradients in nannoplankton distributions and in the source of the organic matter have been demonstrated (Roth and Bowdler, 1979; Tissot et al., 1979). The cyclical nature of nannoplankton assemblages and light stable isotopes in cores from the Tethys strongly indicate cyclic changes in paleoceanographic and paleoclimatological parameters. The periodicity of such cycles seems to be on the order of 10^4 to 10^5 yr. Biostratigraphic resolution is on the order of 5×10^6 yr. (i.e., one to two orders of magnitude less than the period of the observed cycles). Thus a continuous and high-resolution section is essential for a study of the mid-Cretaceous cycles. Such continuous sections have been recovered in the eastern Atlantic. But at none of the sites in the western Atlantic had a sufficiently continuous section been recovered that would be adequate for a study of "black" shale cycles. The following questions need to be answered before we can fully understand the "mid-Cretaceous event":

1) Why did the CCD become so much shallower in the mid-Cretaceous, leading to a transition from pelagic carbonates to marls and shales around the Barremian (Fig. 4)?

2) What caused the cyclic sedimentation—cyclic changes in detrital input, carbonate dissolution, or surface water productivity?

3) Are the cycles in the eastern and western Atlantic synchronous and thus caused by ocean-wide rather than local effects?

4) Where was the boundary between oxic and anoxic conditions with respect to the sediment/water interface?

A combination of sedimentological, micropaleontological (foraminifers, nannofossils, palynomorphs), and geochemical analyses (organic geochemistry, light stable isotopes) should result in a better understanding of mid-Cretaceous cycles and the underlying causes of the oceanography and climate of the mid-Cretaceous, the last climatic optimum before the decline of global surface temperatures. Therefore one of the objectives at site 534 was to recover a complete section of mid-Cretaceous and Neocomian sediments that would provide adequate material for sedimentological, geochemical, and micropaleontological studies in order to answer these fundamental paleoceanographic and paleoclimatological questions.

Seismostratigraphy

During the last five years over 20,000 km of new multichannel seismic reflection profiles have been collected by various institutions along the eastern North American margin. Most of these data continue from the oceanic section of the lower continental rise to the continental shelf to give a good picture of the North American margin structure and stratigraphy. The survey of the *Robert Conrad* near Site 534 is an example of such continental margin data (Fig. 6). The new seismic data have led to the mapping over a wide area of three major pre-β seismic horizons. Of these only C has been dated (at Site 391) and probably is of the Late Jurassic (Fig. 7) (Bryan et al., 1980). It was hoped that the deepest reflector seen in the Blake-Bahama Basin, called Horizon D (Bryan et al., 1980; Fig. 7), would be penetrated at Site 534. Horizon D was expected to correlate with Horizon J_2 to the north (Klitgord and Grow, 1980); thus an important stratigraphic tie could be established. Another seismic horizon that needs better dating is A^u, between the Cretaceous (Cenomanian) claystone and lower Miocene debris flow. Horizon A^u reflects the tremendous erosion that took place between the late Eocene and early Miocene (Tucholke and Mountain, 1979) and may be the expression of multiple oceanographic events of regional and ocean-wide significance.

For better correlation of these very significant reflectors, Site 534 was logged as thoroughly as possible. Velocity and density logs were used to calculate synthetic seismograms for precise correlations of the seismic reflectors at the site.

Time Scale and Magnetostratigraphy

The accuracy of time scales is critical to the development of models dealing with the correlation, succession, and rate of change of oceanographic and geologic events. The Jurassic time scale is an order of magnitude less detailed than that for the Cretaceous and particularly for the Cenozoic. For reference the commonly used Jurassic scale compiled by van Hinte (1976b) is reproduced in Figure 5. This scale largely makes use of the equal duration of stages and equal duration of ammonite zones with few, broadly spaced, and somewhat tentative radiometric control points. Even with its uncertainties (which might be on the order of 10%), the van Hinte (1976b) time scale was chosen for studies of Leg 76 data. One of the best ways of improving any time

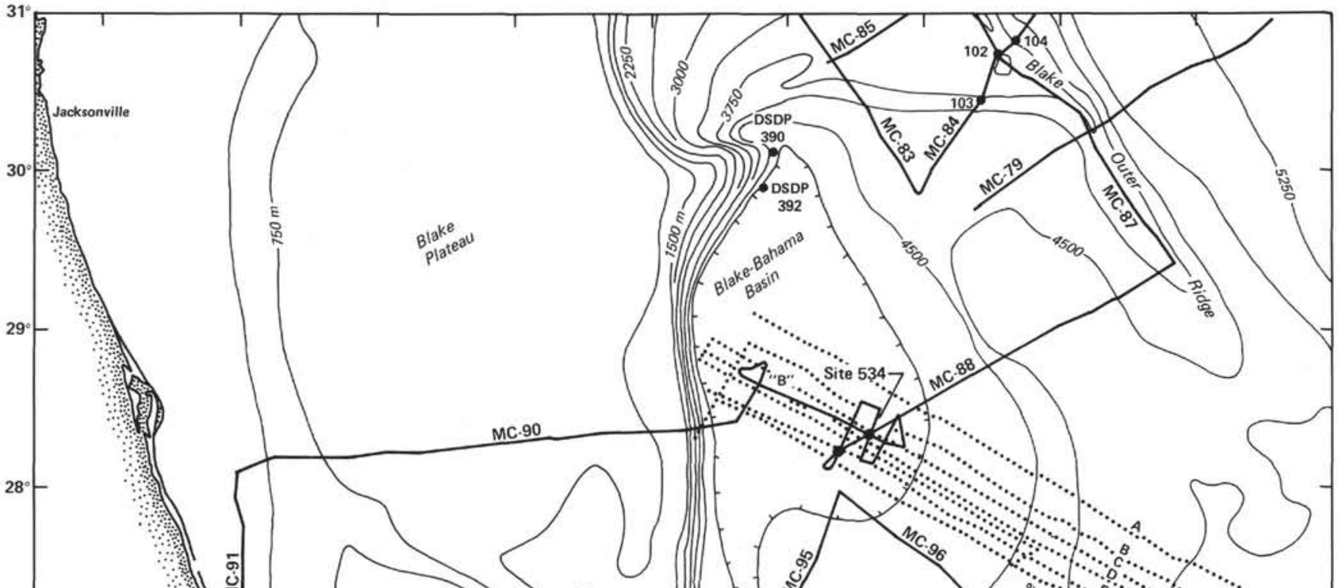

Figure 6. Location of seismic reflection profiles at Site 534 (solid track lines) and magnetic profiles (dotted lines) (after Bryan et al., 1980).

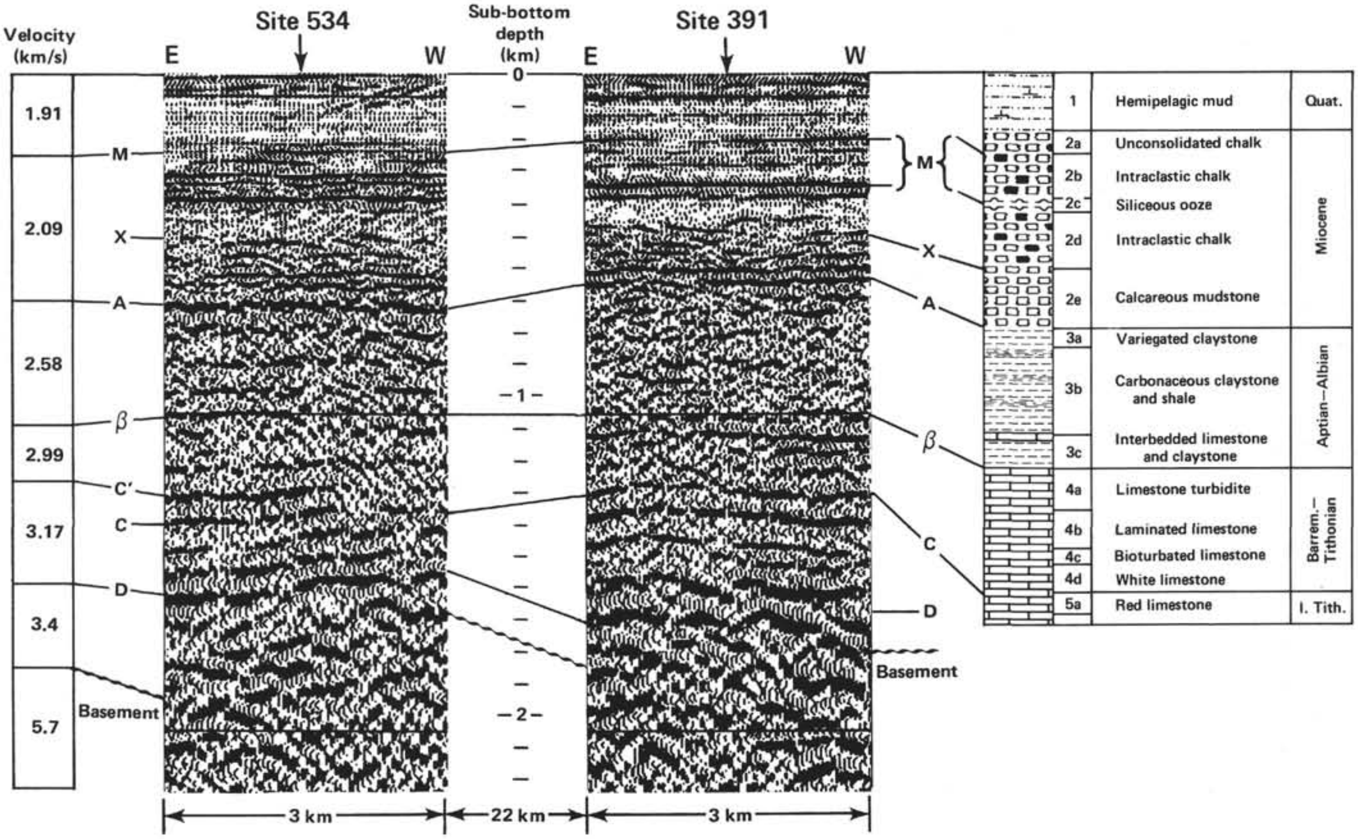

Figure 7. Previous correlation of seismic horizons at Site 534 with those at Site 391. (Depth sections were computed using the sonobuoy velocities given at the left and compared with the lithostratigraphic column at Site 391 [this was modified after Benson et al., 1978]. The corrected seafloor depth is 4970 m at Site 534 and 4965 m at Site 391 [after Bryan et al., 1980]. Note that the drilling at Site 534 and reexamination of the profiles have changed this correlation of Horizon C [after Bryan et al., 1980].)

scale is to provide close ties between such variables as biostratigraphy, magnetostratigraphy, and geochronology. In the case of the Jurassic, there is little information on this relation below reversal M-25 at the base of the Keathley Sequence. Site 534 offered an excellent opportunity to study the sedimentary and magnetic polarity record between Anomaly M-26 and the Blake Spur Anomaly in the Jurassic magnetic quiet zone and its ties to the stratigraphic record (Figs. 8 and 9).

The selection of a magnetic time scale to be used as a working hypothesis on Leg 76 was a difficult matter in that the most recently published scales for the Keathley Sequence (Cande et al., 1978; Vogt and Einwich, 1979) were in need of revision. The basic data source for the relative lengths of the polarity zones older than M-25 was from the Cande et al. (1978) scale of marine magnetic anomalies that are well mapped in the Pacific where the spreading rates are high (4.7 cm/yr.). However, Cande et al. (1978) use the London time scale, so these magnetic reversals had to be recalculated according to the van Hinte (1976b) scale, which was accomplished by assuming a constant ratio between the London and van Hinte scale for the anomalies older than M-25. Once converted, these older reversals were added to the table of Vogt and Einwich (1979) for a complete Keathley Sequence fitted to the van Hinte (1976b) time scale (Table 1).

More recently than the Vogt and Einwich (1979) revision, there have been two paleomagnetic studies of the Cretaceous and Jurassic parts of the section in southern Europe (Lowrie et al., 1980; Ogg, 1980). These newest biostratigraphic calibrations require recalculation of the marine magnetic anomaly time scales of Vogt and Einwich (1979) and Cande et al. (1978).

We recalculated the marine magnetic anomaly time scale by accepting the ages of M-O (basal Aptian) and M-17 (basal Berriasian) of Lowrie et al. (1980) and Ogg (1980), respectively. These control dates implied that the length of the sequences in between must be compressed by a constant factor of 0.82. This ratio was applied to the intervals published on the Vogt and Einwich (1979) magnetic polarity time scale between M-O and M-17.

We also revised the magnetic polarity time scale below M-17 by accepting the biostratigraphic correlations of Ogg (1981) and Ogg et al. (1981) for M-17 (basal Berriasian) through M-25 (latest Oxfordian). The M-26 of Bryan et al. (1980) that we refer to here corresponds to M-26 through M-29 of Cande et al. (1978). These were converted to absolute ages by using the van Hinte (1976b) time scale. The resulting duration of the anomaly sequence can be closely approximated by compressing the Vogt and Einwich (1979) scale, as modified by the addition of M-26 derived from the data of Cande et al. (1978), by a factor of 0.70. This compression ratio of

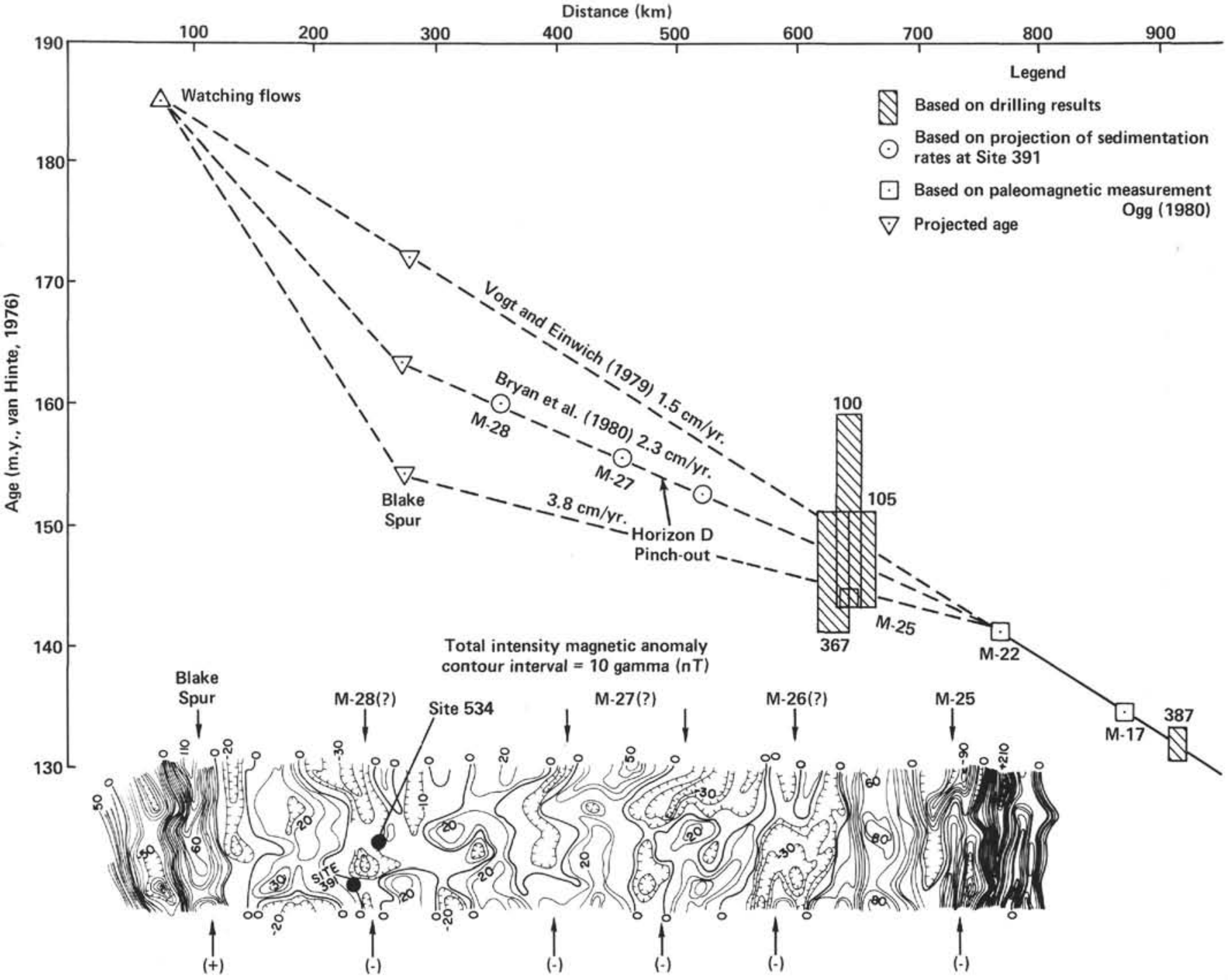

Figure 8. Magnetic anomalies of the outer magnetic quiet zone and calculation of spreading rates (after Bryan et al., 1980; Vogt and Einwich, 1979; and Ogg, 1980).

0.70 yielded the ages for anomalies shown in Table 1 and illustrated on Figure 5.

For anomalies older than M-26, namely M-27, M-28, and the Blake Spur anomalies (Bryan et al., 1980), two different ages can be assigned. In one technique, constant spreading rates for these mapped marine anomalies are assumed; by measuring the distance from M-26 to the anomaly, one may calculate its age. This technique has been used to derive the ages of M-27, M-28, and the Blake Spur anomalies in Table 1. However, an alternate set of ages for M-27, M-28, and the Blake Spur anomalies can be estimated by applying a constant sedimentation rate to the undrilled sediment above seismic basement at Hole 391C, located over Anomaly M-28. Bryan et al. (1980) have done so to predict an age of 160 m.y. for the basement at M-28, and an age of 156 m.y. for Horizon D, which pinches out against the younger M-27 reversal. With M-27 and M-28 thus dated, the age of the Blake Spur Anomaly can be extrapolated. Accordingly, these alternate ages for M-27, M-28, and the Blake Spur anomalies are also included in Table 1 and illustrated on Figure 5.

Tectonic Implications

The age determined for Horizon D will provide a better estimation of the age of the Blake Spur Anomaly and the Blake Spur spreading-center jump. This is because the spreading-center jump seems to have created a basement escarpment and ridge structure, which is coincident with the Blake Spur Anomaly for a large part of the western North Atlantic Ocean (Fig. 10) (Sheridan et al., this volume; Sheridan et al., 1979; Klitgord and Grow, 1980). All along the Blake Spur Ridge Horizons D and J_2 lap against it from the northwest, and only in a few places, such as at Site 534, does the sediment below Horizons D and J_2 fill pockets in the shallow relief of the oceanic crust just seaward of the Blake Spur Magnetic Anomaly. After examining all the available seismic data on the U.S. Atlantic margin, there is no target, other than Site 534, where Horizon D is accessible, cer-

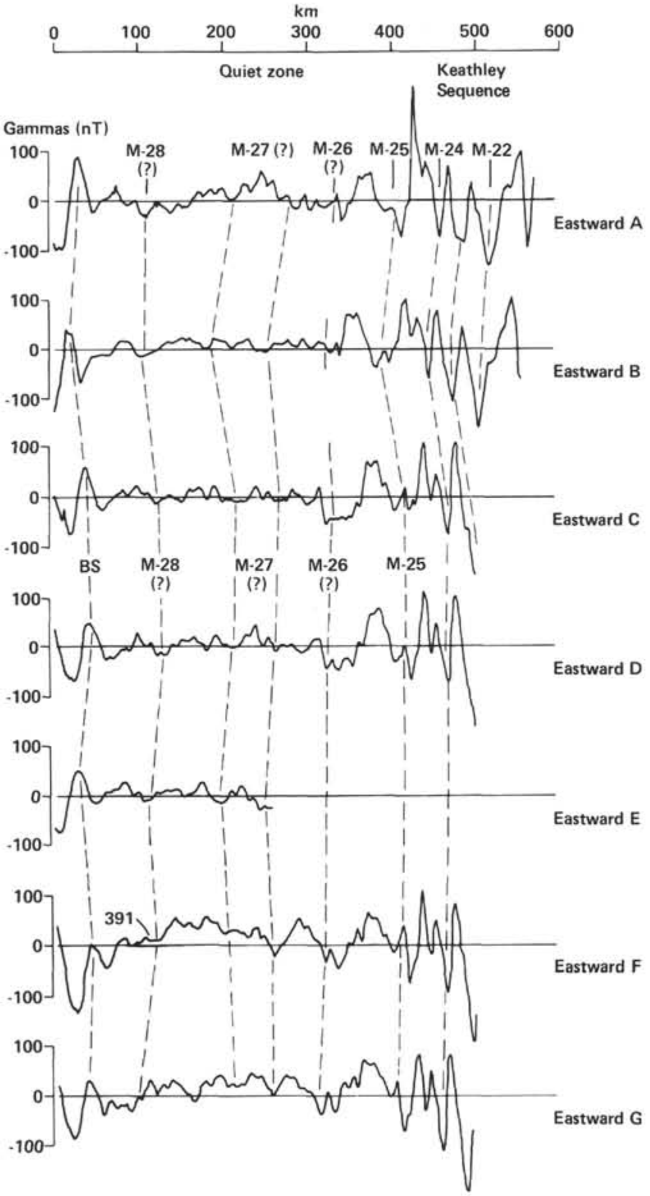

Figure 9. Stacked total-intensity magnetic anomaly profiles A through G across the Blake-Bahama Basin (locations shown in Fig. 6). (The IGRF [International Geomagnetic Reference Field] and a residual linear trend have been removed. Mesozoic Magnetic Anomaly M-25, tentatively identified Mesozoic Anomalies M-26–M-28, and the Blake Spur Anomaly [BS] are labeled [from Bryan et al., 1980].)

tainly not on the Blake Spur Anomaly itself or landward of the associated basement ridge.

With Horizon D more precisely dated, the plate reconstructions at this Anomaly (Fig. 1) can be timed more carefully. Also, events such as breakup unconformities associated with the Blake Spur rift will be possible to identify on the surrounding coastal plains and shelves of the North Atlantic.

The age of the Blake Spur Anomaly can be guessed by extrapolating spreading rates determined in the Keathley (M-0–M-25) Sequence (Vogt and Einwich, 1979), by

Table 1. Revised magnetic time scale.

End of reversed interval (Ma)	Beginning of reversed interval (Ma)	Magnetic anomaly	
	112.04		
112.20	114.86	M-0	
115.38	117.67	M-1	
117.99	118.67	M-3	
120.09	120.90	M-5	
121.34	121.46	M-6	
121.54	121.67	M-7	
122.00	122.27	M-8	
122.46	122.70	M-9	
123.08	123.38	M-10	
123.65	124.03		
124.07	124.33		
124.35	124.60	M-10 N	
124.81	125.47		
125.84	125.88	M-11	
125.18	126.76		
126.85	127.10	M-12	
127.70	127.77		
127.93	128.20		
128.29	128.59	M-13	
128.94	129.16	M-14	
129.82	130.35	M-15	
130.76	132.22	M-16	
132.82	133.18	M-17	
134.54	134.99	M-18	
135.31	135.40		
135.47	136.25	M-19	
136.60	136.75		
136.89	137.40	M-20	
138.05	138.90	M-21	
139.26	140.46		
140.50	140.85		
141.27	141.34	M-22	
141.98	142.09		
142.23	142.51		
142.72	142.75	M-23	
143.77	143.80	M-24	
143.95	144.04		
144.25	144.52		
144.65	144.87	M-25	
145.07	145.19		
145.24	145.32		
145.38	145.49		
145.57	145.65		
145.71	145.77		
145.83	145.89		
145.93	145.08	M-26[a]	M-26[b]
146.20	146.36	M-27[a]	
146.48	146.70	M-28[a]	
146.86	147.58	M-29[a]	
147.99	148.94	M-27[b]	
149.54	150.98	M-27[b]	
151.44	152.99	M-28[b]	
153.47	154.90		
155.58	155.98	Blake Spur	
Alternate ages for oldest reversals[b]			
	154.47	M-27	
155-32	157.38	M-27	
158.04	160.25	M-28	
160.93	162.97		
163.65	164.50	Blake Spur	

Note: N = normal.

[a] Cande et al. (1978).

[b] Bryan et al. (1980).

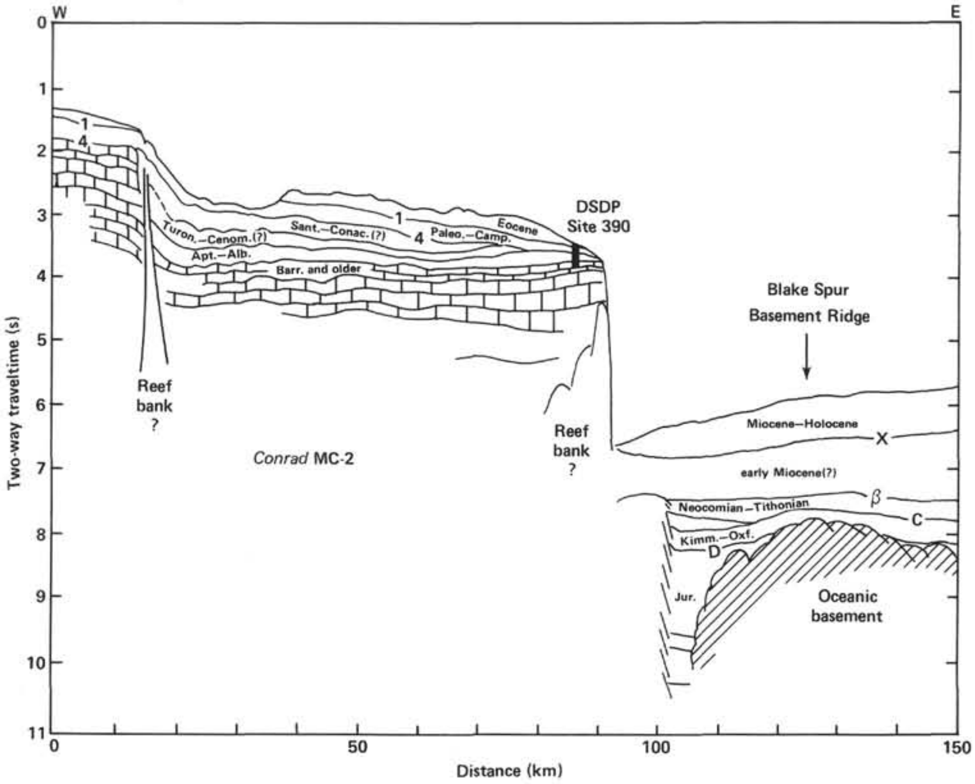

Figure 10. Interpretation of seismic reflection profile across the Blake Escarpment and Blake Spur basement ridge (from Sheridan et al., 1979).

extrapolating sedimentation rates at Site 391 and dating Anomalies M-28 and M-27 (Bryan et al., 1980), or by dating the actual M-anomaly reversals in the stratigraphic record and extrapolating to the Blake Spur (Ogg, 1980) (Fig. 8). These extrapolations based on recent publications illustrate the range of our ignorance—from approximately 153 to 173 Ma (Callovian to Aalenian). The Jurassic biostratigraphic zonations are precise enough to be used to determine the most probable ages of the Blake Spur Anomaly and also M-28. As noted earlier, this resolution will have great implications for the stratigraphy and plate tectonic reconstructions of North America.

Another more far-reaching implication of dating the M-28 and Blake Spur anomalies is the determination of the correct spreading rate for the Jurassic magnetic quiet zone. Based on recently published ages of the M-sequence magnetic anomalies (Fig. 8), calculated spreading rates for the magnetic quiet zone vary from 1.5 cm/yr. to 3.8 cm/yr. These great differences can be resolved by drilling into the basement on M-28 at Site 534.

Several lines of evidence suggest that the Late Jurassic spreading rates should have been as high as the rates during the mid-Cretaceous. There apparently was a eustatic rise in sea level during the Late Jurassic, which can be attributed to worldwide increases in spreading rate at about that time (Vail et al., 1977). Also, there is a smoother oceanic basement under the Jurassic quiet zone, as opposed to that under the Keathley Sequence. Smoother basement is generally associated with rapid spreading, such as in the Pacific Ocean today.

If the Jurassic magnetic quiet zone was formed during times of high spreading rates, just as the Cretaceous quiet zone was formed in times of global high spreading rates, a very significant link is suggested between the plate driving processes acting in the upper mantle and the magnetic field processes acting at the core/mantle boundary. Such a link has been proposed by Vogt (1975). If this link exists, it indicates that surface tectonics and movements might have been controlled by the processes in the very core of the Earth. An objective of the drilling at Site 534 was to discover stratigraphic evidence to elucidate such hypotheses.

Site 534: Location and Prognosis

The unusual physiographic and structural position of the Blake-Bahama Basin (Fig. 2) provides a window to drill through the Cenozoic, Cretaceous, and Jurassic ocean sediments. Although to the north of the Basin there is a massive continental rise with several kilometers of sediments, seismic observations indicate that the Basin only contains 1700 to 2500 m (?) of strata (Dillon et al., 1976; Sheridan, Pastouret, et al., 1978; Bryan et al., 1980). Water depth is at 5 km, making it congruent with a deep abyssal plain. The Basin apparently had been sediment starved and eroded in the early Tertiary (?Oligocene) (Benson et al., 1978; Sheridan, Enos, et al., 1978; Jansa et al., 1979).

Because of its favorable geological situation, Blake-Bahama Basin drilling was the first priority during Leg 44 of the Deep Sea Drilling Project in 1975 (Benson et al., 1978). But malfunctioning of the reentry cones to change drill bits only allowed a single-bit attempt in

Hole 391C, which terminated at 1412 m in lower Tithonian red shaly limestone, some 300 to 400 m short of basement. Drilling at Site 534 (Fig. 7), 22 km from Hole 391C (thus avoiding confusion with one of the three 1975 reentry cones), was therefore our Leg 76 objective. Local water depth at this site is 4950 m and sediment thickness 1800 m, as based on linear extrapolation of sedimentation rate (1.9 cm/10^3 yr.) and the seismic velocities determined from two sonobuoys at the site (Bryan et al., 1980). Site 534 lies in the Middle Jurassic magnetic quiet zone, just seaward of the Blake Spur Anomaly (Fig. 8). The basal sedimentary record should show the M-26 and M-27 reversals, and basement age should be that about of M-28. As a result, the crust is estimated to be on the order of 156 to 165 m.y. old, which roughly agrees with the age of the basal sediments as a function of the calculated sub-bottom depth at Site 391.

Site 534 penetrated, in descending stratigraphic order; ±650 m of upper Cenozoic hemipelagic clays and Miocene debris flows (Great Abaco Member of the Blake Ridge Formation) (Jansa et al., 1979), 300 m of the lower part of the Middle Cretaceous dark colored and variegated shales (Hatteras and Plantagenet formations), 330 m of Lower Cretaceous light colored limestones (Blake-Bahama Formation), Upper Jurassic brown and green shaly limestones (Cat Gap Formation), and Middle Jurassic unknown (?) hemipelagic sediment before reaching basaltic ocean crust approximately 153 m.y. of age.

Summary of Objectives

1. Extend lithostratigraphy below the Upper Jurassic and correlate to the Tethys facies of the same age. Provide multidisciplinary geological information on one of the thickest ocean sections of Cretaceous dark shales in order to further delineate its origin.
2. Establish a multiple Jurassic deep-marine biostratigraphy and attempt to resolve discrepancies in dating of Leg 11 deposits. Correlate to the Tethyan province.
3. Date seismic Horizon D and determine its genetic origin.
4. Make Jurassic, Cretaceous, and Cenozoic paleobathymetric estimates based on corrected backtracking, and relate the subsidence with the history of sedimentation and biofacies as a function of the carbonate dissolution regime.
5. Relate the Site 534 geological–paleontological record to the paleogeography of the early ocean basin and establish arguments for dating the early connection between the Tethys and Pacific.
6. Trace the evolution of the pelagic biota in the early Atlantic Ocean.
7. Relate the magnetostratigraphic record at the base of and below the Keathley Sequence to the biostratigraphy, sedimentation rates, and rates of seafloor spreading in order to furnish a more precise Jurassic time scale.
8. Date the Jurassic spreading-center jump in the western North Atlantic Ocean.
9. Compare the Jurassic and Cretaceous spreading rates and relate these to the temporal distribution of the magnetic quiet zones.

OPERATIONS

Immediately after leaving Site 533 at 0000 hr., 20 October 1980, en route to multiple reentry Site 534 in the Blake-Bahama Basin, the *Glomar Challenger* suffered the total loss of the number three engine. This loss reduced our effective speed and meant that during subsequent drilling operations one of the stern thrusters would be without power. As a consequence, drilling during bad weather might have had to be suspended to improve station-keeping capacity. Although all on board realized the potentially troublesome situation, the captain and operations manager felt that at least the cone could be set without problems; thus the *Challenger* proceeded to Site 534. Weather conditions were almost perfect—thus occupation of the site would allow a thorough appraisal of current and bottom conditions.

Shortly before arriving at Site 534, speed was reduced to sychronize ETA (estimated time of arrival) with a satellite pass. This accomplished, we released the 13.5-kHz beacon on 20 October at 2012 hr. at position 28° 20.6′W, 75°22.9′N. Two more satellite fixes were made within a one-half mile radius from the first one. Unfortunately, attempts to position on Benthos beacon 15 were thwarted by the inexplicable loss of signal within 1000 ft. of the site and a stronger signal when we steamed away from the beacon. At 2242 hr., a 16.0-kHz Benthos beacon number 11 was dropped at the site, and stable positioning was achieved by 2400 hr. Pipe was run in the hole and at 1012 hr., 21 October, Hole 534 was spudded. The drill pipe pinger was deployed but developed loss of signal at depth. One mudline core was taken at 4984.5 m, which recovered 2.1-m sections, thus confirming the seafloor depth as 4984 m. Subsequently a 87.5-m jet-in test was done to determine the length of the conductor casings below the cone. Upon review of the technical condition of the ship, on 21 October the Deep Sea Drilling Project decided to divert us to port for an engine overhaul. Word was received to abort Site 534 and proceed to Port Everglades, Fort Lauderdale, Florida for emergency repairs to the number three engine. Between 1345 and 2230 hr. on 21 October, pipe was pulled and at 2244 hr. we departed for port.

After completion of the engine overhaul on 28 October 1980, we sailed again for Site 534 (Fig. 11), where we arrived the next evening, 29 October 1980, aided by two satellite fixes prior to arrival. We acquired the signals of the 13.5- and 16.0-kHz beacons on the site at 2135 hr., and at 2200 hr. The *Challenger* was again in stable automatic positioning mode at 28°20.6′N, 75° 22.9′W. Seas were calm and the weather balmy, with an outlook for more of the same. The ship's crew immediately proceeded with keelhauling of the previously prepared reentry cone, which was hung under the moon pool. The next 83 m of 16-in. casing string was suspended under the core and latched onto it. The bottom-hole assembly with the casing running tool was entered

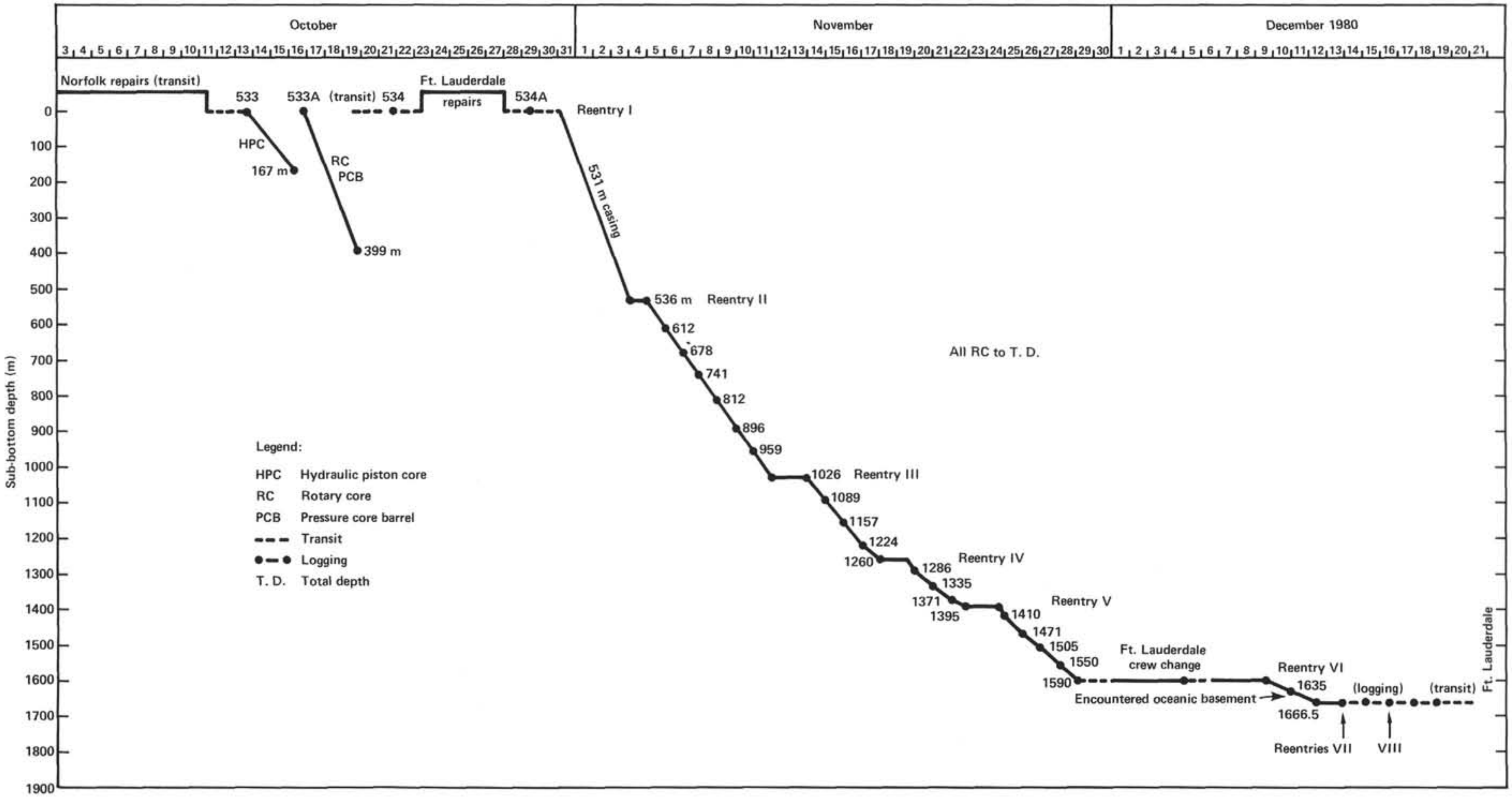

Figure 11. Graphic summary of operations during Leg 76, western North Atlantic, 11 October to 22 December 1980.

and latched to the cone–casing combination. The elaborate construction was run to the seafloor, and just before spudding in, the Bowen sub unit and heave compensator were installed. The casing pipe was spudded in at 2154 hr. on 30 October at 4976 m, which is 8 m shallower than in the first hole of Site 534. Based on this difference and the nature of the hyperbolic echos on the depth record, small-scale topographic relief is thought to exist at the site.

Washing in proceeded rapidly, and the cone was landed at 2330 hr. On 31 October at 0035 hr., the wireline-operated shifting tool disengaged the cone and casing string from the drill pipe, upon which further washing was continued to 531 m below the seafloor.

This depth was achieved at 1400 hr. and the drill string pulled on deck where it arrived on 1 November at 0130 hr. Subsequently, 529 m of 11 3/4-in. casing was assembled, hung in the moon pool, and latched to the bottom-hole assembly (Fig. 12). Shortly after 1700 hr. on 1 November, the pipe was again on its way down and reentered in the cone. The first reentry operation took about 18 hr., including a wire-line trip which involved a delay of six hours to change the first sonar scanning tool that had been improperly assembled and had ceased to rotate. At 1400 hr. the second tool was run in and performed well, allowing a perfect three reflector stab to be made at 2302 hr. The end of the drill string with approximately 40 tons of casing attached was very sluggish in its movements toward the reentry cone. Movement was resisted until the *Challenger* was offset over 30 m. Even with these offsets, the pipe swung very slowly and was apparently out of phase with ship movements. It was thought the inertia of the extra casing weight was acting as an anchor. Now bottom currents at Site 534 are also postulated to explain the pipe drag.

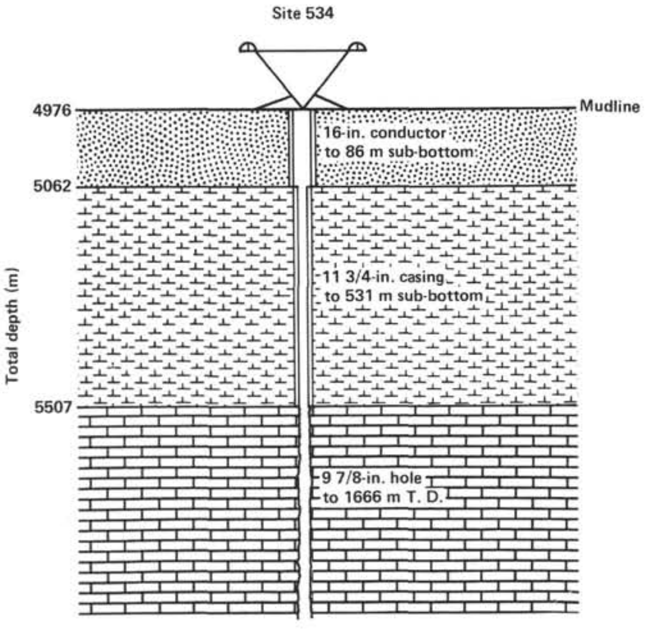

Figure 12. Casing hierarchy used at Site 534.

When at 0000 hr. on 3 November 1980 the second sonar tool had been retrieved, the 11 3/4-in. casing was rapidly lowered to the prewashed depth of 531 m and cemented in the hole. Another round trip was made to assemble the 9 7/8-in. bit and coring assembly; reentry in the cone was achieved on 4 November at 1427 hr. Again the movement of the pipe just above the cone was sluggish even without the casing weight. This caused the reentry operation to take a long time, ~12 hr. However, in spite of this slow procedure, all three reflectors of the cone were observed, and a perfect reentry was achieved. The pipe seemed to move with more ease to the southeast, and with more resistance to the northwest, as if a weak bottom current crosses the site from northwest to southeast. Working with and against this apparent near-bottom current improved our chances to move the pipe and to stabilize it over the cone when ready to stab. These maneuvers finally led to a successful reentry.

After drilling out the cement plug and swabbing the hole, regular continuous coring started at 0100 hr., 5 November 1980, at a depth of 5363 m. The first core failed to recover any sediment, but subsequent cores showed progressively better recovery. During drilling of Core 8, apparently the bit got plugged with a particular hard piece of intraclast limestone, which led to only 0.25 cm recovery and high circulation pump pressure. A chisel bit was sent down to clean the bit opening, and this rectified the problem. After the bit was set down for further coring, T.D. (total depth) was found to be 7 m shallower than when Core 8 was first drilled; one possible reason may be a slight straightening of bends in the drill string above the seafloor. Such occurrences can happen when the ship changes heading.

A problem developed during the cutting of Core 15. Rotation for one half hour failed to take any weight off the bit and either the bit hit something very hard or the core barrel could have jammed. The core was pulled at 1530 hr. and found empty and clean. It was interpreted that the pipe might have been chafing on the lip of the reentry cone, that some weight had been taken up at that point, and the bit was not reaching the bottom of the hole. Also, chafing was noted at the upper end of the pipe at the horn beneath the moon pool. It was possible that a mid-water current was bending the pipe to cause contact at the upper and lower extremes. A careful appraisal of the positioning system and its heading-related error was made, which failed to show an excursion of *Challenger* during drilling of Core 15. The positioning system was verified as functioning properly. Thus to avoid chafing below the moon pool, the ship was moved a few hundred feet to bring the pipe vertical at its upper end. Then Core 15 was redrilled at the correct interval and 1.5 m of sediment was recovered. The core was out of round in its lower section and showed unusual wear, but at least the bit was open and was indeed reaching the bottom of the hole. Nevertheless, the possibility remained that some chafing was still occurring at the reentry cone.

To check this out, the Totco Eastman survey tool was lowered on a wire line to measure the pipe angle just above the cone. Angles of 5 and 10° were recorded. A similar (7°) reading of the tool was made the next day. This indicated that although the pipe might indeed have been bent by mid-water currents, the angle of entry in the cone was near vertical and the pipe was not chafing. After additional offsets of 100 ft. south and 100 ft. east to bring the ship closer to the last reentry position and thus relieve stress, Core 16 was cut. Stiffer coring joints were added at the upper end of the pipe to absorb possible strains when drilling through potential hard layers. Consequently, only 9.0-m coring intervals were possible.

Core 16 recovered 3.2 m of intraclast chalk, most of it in the form of badly downward-tapered "cookies" with closely spaced external scratch "rings." This was the result of the use of a hard-rock type of core-catcher that was subsequently replaced by an intermediate-rock type. Cores 17, 18, 19, and 20 showed satisfactory recovery, although drill time was slowed down on several 5- to 10-cm layers of chert. Core 21 again failed to recover more than a few chips. This time the core barrel may not have seated properly during cutting of the core, resulting in a pileup of cored sediments above the bit. As a result pump pressure should have been higher than normal, an adjustment that was consequently made. The bit was cleaned with a stabbing tool in front of the core barrel. This procedure was repeated for Core 23.

In the meantime, the ship was slightly offset again to relieve rubbing of the drill string in the moon pool horn. When setting down for cutting Core 21, T.D. was again found to be shallower than before, this time about 3 m.

From November 7 through 11 coring continued at a regular pace of 2.5 to 3.5 hr. between cores. The weather continued to be pleasantly warm with light to moderate winds and negligible to light swell. Hurricane Jeanne stayed well west of the ship and never posed a serious threat. Sediment recovery, which had varied widely and fared poorly in Cores 19 through 33 (only 33 out of 126 m were recovered), improved. Cores 19 through 33 were very clayey between harder stringers (black and green clays of the Bermuda Rise, Plantagenet, and upper Hatteras formations); most of this material was lost while coring. From Cores 39 through 56, 204.5 m of sediment were cored and 123.5 m recovered. Vertical deviation of the hole as measured at 775 m and 1000 m sub-bottom depth amounted to 0.3 and 0.4°. On November 10, coring was suspended for 4 hr. to slip 10 m of wire on the main winch and thus run a fresh stretch of it through the pulleys of the traveler block. This is a normal maintenance and safety procedure. At 0030 hr. on 12 November there was a slight pickup of current from NNW, which caused a 200 ft. excursion from the site. All engines were brought on line to reoccupy the correct offsets and headings to maintain position in the hole.

After Core 50, the occurrence of hard limestones at the top of the Blake-Bahama Formation caused the drilling rate to decrease markedly—to less than 5 m/hr. Although this decrease was similar to the marked decrease at Horizon β as encountered at Site 391, there was some suspicion on the part of the operations manager that the Smith F93CK (long-tooth) bit was not cutting as well as it should be in these kinds of rocks. Perhaps it had been damaged in drilling the unexpected cherts in the overlying Bermuda Rise Formation. Some slight decrease in the diameter of the recovered cores, such as Core 55, also suggested possible wobble of the rollers and deterioration of the bit bearings. Based on these considerations, and the fact that the heavy wall 9.0-m drilling pipe had to be tripped anyway, it was decided to pull the entire string for a bit change. This procedure was begun at 0300 hr., 12 November 1980, after spending 136 min. cutting Core 56. The bit arrived on deck at 1700 hr. after 38 hr. of coring; three of the roller bearings were damaged; one or two of the rollers probably would have sheared off soon.

Reentry maneuvers commenced on 13 November at 1145 hr. and took nearly 8 hr. to achieve. Again the bit moved very slowly over the bottom but at a livelier speed than the previous two successful reentries. This time the bit was brought very quickly, within close proximity of the cone (within 10 m), and the best maneuvers were swings in the east-west direction. On at least two occasions the bit was inside the radius of the cone but off slightly to one side, not directly over the hole. The stab was not made because we hoped to let the pipe swing farther over the center of the cone. To our frustration, the pipe then swung away and out of the cone. The third time that this happened, when the pipe was just inside the radius of the cone but not centered, the cone was stabbed at 1930 hr., 13 November 1980.

Reentry was successful. However, by 0100 hr., 14 November 1980, the drill string stopped against a possible bridge or shoulder at approximately 808 m sub-bottom in the range of the Hatteras Formation. Washing permitted the pipe to be lowered to 808 m, when the Bowen sub was installed to allow rotation. The obstruction at this level was reamed out and the hole was apparently cleared; this obstacle was a shale flow-in and/or possible debris accumulation on and above a washed-out ledge near the Hatteras/Blake-Bahama transitional chalks. Apparently the hole was clear below the chalks, where it was more in gauge.

The bit stopped at a total depth of 5992.5 m rather than the previously established 6011.5 m—this was 19 m shallower than before reentry. The most likely explanation is that a combination of changes in ship positioning relative to the cone and the bending of the pipe in the deep current changed the distance from the ship to the bottom of the hole.

Because it would have been difficult to correct in a systematic way all the total depths of cores already recovered, without speculating how the current might have affected the pipe as well, it was decided not to change the record. This was the best decision, given that sub-bottom depth and total depth are calculated based on the accumulation of drilled and cored intervals. Presumably these cored and drilled intervals were each in error, one more than the other, if the ship movements and the currents were moving the pipe in the water in some unknown way.

As a result of this depth discrepancy, the depth error, which can be assigned to the recorded depth of a cored interval (Table 2), is ±2%. This order of uncertainty in

Table 2. Coring summary, Hole 534A.

Core no.	Total depth (m)	Sub-bottom depth (m)	Cored (m)	Recovered (m)	Lithology	Age
H1	4976–5507	0–531	Wash core	9.2	Nannofossil ooze; intraclast chalk	middle Miocene
1	5512.3–5521.8	536.3–545.8	9.5	0.0	dark green mudstone	early middle Miocene
2	5521.8–5531.4	545.8–555.4	9.6	1.7	dark green mudstone	early middle Miocene
3	5531.4–5541.0	555.4–565.0	9.6	4.1	dark green mudstone	early middle Miocene
4	5541.0–5550.5	565.0–574.5	9.5	7.3	Chalk, intraclast chalk	late early Miocene
5	5550.5–5560.0	574.5–584.0	9.5	8.6	Chalk, intraclast chalk	late early Miocene
6	5560.0–5569.5	584.0–593.5	9.5	7.2	Chalk, intraclast chalk	late early Miocene
7	5569.5–5579.0	593.5–603.0	9.5	7.4	Chalk, intraclast chalk	middle early Miocene
8	5579.0–5581.5	603.0–605.5	2.5	0.3	Chalk, intraclast chalk, dark green mudstone	middle early Miocene
9	5581.5–5588.5	605.5–612.5	7.0	0.0		middle early Miocene
10	5588.5–5598.0	612.5–622.0	9.5	6.6		early early Miocene
11	5598.0–5607.5	622.0–631.5	9.5	2.4		early early Miocene
12	5607.5–5617.0	631.5–641.0	9.5	7.6		early early Miocene
13	5617.0–5626.5	641.0–650.5	9.5	5.8		early early Miocene
14	5626.5–5636.0	650.5–660.0	9.5	7.6		early early Miocene
15	5636.0–5645.5	660.0–669.5	9.5	1.5	Intraclast chalk	early early Miocene
16	5645.5–5654.5	669.5–678.5	9.0	3.2	Intraclast chalk	early early Miocene
17	5654.5–5663.5	678.5–687.5	9.0	9.5	Intraclast chalk	early early Miocene
18	5663.5–5672.5	687.5–696.5	9.0	2.7	Intraclast chalk	early early Miocene
19	5672.5–5681.5	696.5–705.5	9.0	4.2	Zeolitic siliceous variegated mudstone; graded sandstone; porcellanite	late Eocene
20	5681.5–5690.5	705.5–714.5	9.0	4.1		late Eocene
21	5690.5–5699.5	714.5–723.5	9.0	0.0		?
22	5699.5–5708.5	723.5–732.5	9.0	0.1		?
23	5708.5–5717.5	732.5–741.5	9.0	0.3		Maestrichtian
24	5717.5–5726.5	741.5–750.5	9.0	6.3	Variegated claystone	early Maestrichtian
25	5726.5–5735.5	750.5–759.5	9.0	1.6	Variegated claystone	early Maestrichtian
26	5735.5–5740.5	759.5–764.5	5.0	1.6	Variegated claystone	early Maestrichtian
27	5740.5–5750.0	764.5–774.0	9.5	4.4	Black to green carbonaceous claystone	Vraconian
28	5750.0–5759.5	774.0–783.5	9.5	3.6		Vraconian
29	5759.5–5769.0	783.5–793.0	9.5	5.3		Vraconian
30	5769.0–5778.5	793.0–802.5	9.5	0.6		late Albian
31	5778.5–5788.0	802.5–812.0	9.5	1.3		late Albian
32	5788.0–5797.5	812.0–821.5	9.5	1.6		late Albian
33	5797.5–5807.0	821.5–831.0	9.5	1.8		late Albian
34	5807.0–5816.5	831.0–840.5	9.5	3.5		middle Albian
35	5816.5–5826.0	840.5–850.0	9.5	6.5		middle Albian
36	5826.0–5835.5	850.0–859.5	9.5	4.7		early middle Albian
37	5835.5–5845.0	859.5–869.0	9.5	5.8		early middle Albian
38	5845.0–5854.0	869.0–878.0	9.0	7.0		early middle Albian
39	5854.0–5863.0	878.0–887.0	9.0	6.8		early Albian
40	5863.0–5872.0	887.0–896.0	9.0	0.2	Variegated claystone	early Albian
41	5872.0–5881.0	896.0–905.0	9.0	8.7	Variegated claystone	Aptian
42	5881.0–5890.0	905.0–914.0	9.0	3.7	Variegated claystone	Aptian
43	5890.0–5899.0	914.0–923.0	9.0	3.2	Carbonaceous claystone	Aptian
44	5899.0–5908.0	923.0–932.0	9.0	6.7	Carbonaceous claystone	Aptian
45	5908.0–5917.0	932.0–941.0	9.0	7.0	Carbonaceous claystone	Aptian
46	5917.0–5926.0	941.0–950.0	9.0	1.3	Carbonaceous claystone	Barremian–Aptian
47	5926.0–5935.0	950.0–959.0	9.0	6.0	Calcareous and nannofossil claystone; limestone; minor carbonaceous claystone	Barremian
48	5935.0–5939.5	859.0–963.5	4.5	8.7		Barremian
49	5939.5–5948.5	963.5–972.5	9.0	9.5		Barremian
50	5948.5–5957.5	972.5–981.5	9.0	6.7		Barremian
51	5957.5–5966.5	981.5–990.5	9.0	1.5		Barremian
52	5966.5–5975.5	990.5–999.5	9.0	7.3		Barremian
53	5975.5–5984.5	999.5–1008.5	9.0	6.2		Hauterivian–Barremian
54	5984.5–5993.5	1008.5–1917.5	9.0	3.6		Hauterivian–Barremian
55	5993.5–6002.5	1017.5–1026.5	9.0	4.6		Hauterivian–Barremian
56	6002.5–6011.5	1026.5–1035.5	9.0	4.3		Hauterivian–Barremian
57	6011.5–6020.5	1035.5–1044.5	9.0	6.1		Hauterivian–Barremian
58	6020.5–6029.5	1044.5–1053.5	9.0	6.6	Laminated nannofossil chalk and limestone, siltstone, minor carbonaceous claystone	Hauterivian
59	6029.5–6038.5	1053.5–1062.5	9.0	4.7		Hauterivian
60	6038.5–6047.5	1062.5–1071.5	9.0	6.1		Hauterivian
61	6047.5–6056.5	1071.5–1080.5	9.0	6.6		Hauterivian
62	6056.5–6065.5	1080.5–1089.5	9.0	0.6		Hauterivian
63	6065.5–6074.5	1089.5–1098.5	9.0	3.7		Hauterivian
64	6074.5–6083.5	1098.5–1107.5	9.0	6.7		Valanginian–Hauterivian
65	6083.5–6092.5	1107.5–1116.5	9.0	8.3		Valanginian–Hauterivian
66	6092.5–6101.5	1116.5–1125.5	9.0	7.1		Valanginian–Hauterivian
67	6101.5–6106.0	1125.5–1130.0	4.5	4.7		late Valanginian
68	6106.0–6115.0	1130.0–1139.0	9.0	8.4		late Valanginian
69	6115.0–6124.0	1139.0–1148.0	9.0	9.3		late Valanginian
70	6124.0–6133.0	1148.0–1157.0	9.0	8.1		late Valanginian
71	6133.0–6142.0	1157.0–1166.0	9.0	7.9		early Valanginian
72	6142.0–6151.0	1166.0–1175.0	9.0	8.4		early Valanginian
73	6151.0–6160.0	1175.0–1184.0	9.0	7.1	Bioturbated nannofossil-radiolarian limestone and chalk, minor siltstone	early Valanginian
74	6160.0–6169.0	1184.0–1193.0	9.0	8.6		early Valanginian
75	6169.0–6178.0	1193.0–1202.0	9.0	9.0		early Valanginian
76	6178.0–6187.0	1202.0–1211.0	9.0	8.9		early Valanginian
77	6187.0–6191.5	1211.0–1215.5	4.5	5.4		early Valanginian
78	6191.5–6200.5	1218.5–1224.5	9.0	7.7		early Valanginian
79	6200.5–6209.5	1224.5–1233.5	9.0	8.6		early Valanginian
80	6209.5–6218.5	1233.5–1242.5	9.0	6.9		early Valanginian
81	6218.5–6227.5	1242.5–1251.5	9.0	6.0		early Valanginian
82	6227.5–6236.5	1251.5–1260.5	9.0	2.2		late Berriasian
83	6236.5–6244.0	1260.5–1268.0	7.5	7.5		late Berriasian

Table 2. (Continued)

Core no.	Total depth (m)	Sub-bottom depth (m)	Cored (m)	Recovered (m)	Lithology	Age
84	6244.0–6253.0	1268.0–1277.0	9.0	9.6	Bioturbated nannofossil-radiolarian limestone and chalk; stylolites	late Berriasian
85	6253.0–6262.0	1277.0–1286.0	9.0	7.6		late Berriasian
86	6262.0–6271.0	1286.0–1295.0	9.0	6.5		late Berriasian
87	6271.0–6280.0	1295.0–1304.0	9.0	8.0		early Berriasian
88	6280.0–6289.0	1304.0–1313.0	9.0	8.0		early Berriasian
89	6289.0–6298.0	1313.0–1322.0	9.0	7.6		early Berriasian
90	6298.0–6307.0	1322.0–1331.0	9.0	7.5		latest Tithonian–earliest Berriasian
91	6307.0–6316.0	1331.0–1340.0	9.0	8.0		latest Tithonian–early Berriasian
92	6316.8–6325.0	1340.0–1349.0	9.0	8.2	Grayish red calcareous claystone	Tithonian
93	6325.0–6329.5	1349.0–1353.5	4.5	4.5		Tithonian
94	6329.5–6338.5	1353.5–1362.5	9.0	5.4		Tithonian
95	6338.5–6347.5	1362.5–1371.5	9.0	6.7		Tithonian
96	6347.5–6356.5	1371.5–1380.5	9.0	6.6		Kimmeridgian–Tithonian
97	6356.5–6365.5	1380.5–1389.5	9.0	0.5		Kimmeridgian–Tithonian
98	6365.5–6371.5	1389.5–1395.5	6.0	0.0		Kimmeridgian–Tithonian
B1	6357.0–6371.5	1381.0–1395.5	(?)	0.1		Kimmeridgian–Tithonian
99	6731.5–6377.0	1395.5–1401.0	5.5	5.2		Kimmeridgian–Tithonian
100	6377.0–6386.0	1401.0–1410.0	9.0	5.6		Kimmeridgian–Tithonian
101	6386.0–6395.0	1410.0–1419.0	9.0	7.9		Kimmeridgian–Tithonian
102	6395.0–6404.0	1419.0–1428.0	9.0	7.5		Kimmeridgian–Tithonian
103	6404.0–6413.0	1428.0–1437.0	9.0	1.6	Gray, micritic to bioclastic limestone, greenish gray to brown calcareous claystone	Kimmeridgian
104	6413.0–6422.0	1437.0–1446.0	9.0	6.4		Kimmeridgian
105	6422.0–6431.0	1446.0–1455.0	9.0	2.8		Oxfordian–Kimmeridgian
106	6431.0–6440.0	1455.0–1464.0	9.0	2.4		Oxfordian–Kimmeridgian
107	6440.0–6444.5	1464.0–1468.5	4.5	2.7		Oxfordian–Kimmeridgian
108	6444.5–6453.5	1468.5–1477.5	9.0	1.1		Oxfordian–Kimmeridgian
109	6453.5–6462.5	1477.5–1486.5	9.0	0.2		Oxfordian–Kimmeridgian
110	6462.5–6471.5	1486.5–1495.5	9.0	0.3		Oxfordian–Kimmeridgian
111	6471.5–6480.5	1495.5–1504.5	9.0	0.3	Variegated, reddish brown to grayish green claystone	Oxfordian
112	6480.5–6489.5	1504.5–1513.5	9.0	1.1		Oxfordian
113	6489.5–6498.5	1513.5–1522.5	9.0	0.8		Oxfordian
114	6498.5–6507.5	1522.5–1531.5	9.0	1.8		Oxfordian
115	6507.5–6516.5	1531.5–1540.5	9.0	1.1	Gray micritic limestone; dark gray, green, brown radiolarian claystone	Oxfordian
116	6516.5–6525.5	1540.5–1549.5	9.0	0.9		Oxfordian
117	6525.5–6534.5	1549.5–1558.5	9.0	0.6		Oxfordian
118	6534.5–6543.5	1558.5–1567.5	9.0	1.1		Oxfordian
119	6543.5–6548.0	1567.5–1572.0	4.5	0.2		Callovian–Oxfordian
120	6548.0–6557.0	1572.0–1581.0	9.0	1.0		Callovian–Oxfordian
121	6557.0–6566.0	1581.0–1590.0	9.0	0.6		Callovian–Oxfordian
H4	5507.0–6566.0	531.0–1590.0	Wash core	0.1		Callovian–Oxfordian
122	6566.0–6570.0	1590.0–1594.0	4.0	2.6		Callovian–Oxfordian
123	6570.0–6579.5	1594.0–1603.5	9.5	5.9		Callovian–Oxfordian
124	6579.5–6588.5	1603.5–1612.5	9.0	1.5		middle–late Callovian
125	6588.5–6597.5	1612.5–1621.5	9.0	8.5	Black and red to green shale	middle–late Callovian
126	6597.5–6606.5	1621.5–1630.5	9.0	6.2		middle–late Callovian
127	6606.5–6615.5	1630.5–1639.5	9.0	4.9		middle–late Callovian
128	6615.5–6624.5	1639.5–1648.5	9.0	5.6	Basalt in core catcher only	
129	6624.5–6633.5	1648.5–1657.5	9.0	5.6		
130	6633.5–6642.5	1657.5–1666.5	9.0	7.0		
			1130.2	629.8		

Note: For an explanation of Core B1 see Operations section. Cores preceded by H indicate wash cores. (Cores H2 and H3 were not described or preserved.)

depth of the core samples will affect the calculations based on intervals, such as sedimentation rates and seismic interval velocities.

Normal operations resumed with the cutting of Core 57 at 1035.5 m sub-bottom at 0500 hr. on 14 November 1980. Recovery was largely shale cuttings and 60 cm of hard Blake-Bahama limestone.

From 1035.5 m to 1260.5 m below the seafloor (Cores 57–82), coring was only interrupted by the loss of the heave compensator. It developed a broken piston in the pressure housing on deck and was taken off the drilling assembly for the rest of the cruise. The passing of a low on November 16 to 17, with winds of up to 35 knots, did not affect operations. The ship was easily held on station. On November 17, at 1500 hr., the decision was made to pull pipe for reason of the poor performance of the drill bit after it had cored for only 29.5 hr. Cores 79 to 82 had showed progressively less recovery, and core diameter fell below the size of 5.4 cm, which was used as the criterion to change bits. Many cored limestone fragments showed signs of excessive abrasion. The F93CK (long tooth) bit arrived on deck at 0315 hr. on 18 November 1980; one roller was wobbling on its bearing, and another bearing seal was gone.

After replacement of the damaged bit with a Smith F94CK (short-tooth) one, the drill string was run in the hole from 0400 through 1400 hr., 18 November 1980. At 1600 hr. the reentry tool arrived at the bottom of the pipe and tool rotation was accomplished. However, the return signal looked as if the transducer was below the mudline. Confused by this, we raised the tool and pipe as much as 4 m in hopes of getting it out of the mud, but the return pattern never changed. We assumed that the transducer was dirtied with pipe dope; the tool was then withdrawn up into the pipe for flushing with pressure up to 30 strokes. Upon lowering the transducer, the normal return pattern was suddenly presented on the screen; we concluded that the tool had been up in the pipe all the while. At 1710 hr. both tool and drill pipe were lowered 4 m to be at 4966.5 m and the cone was well detected at a 150-ft. range. Bad luck caught up with us at 1754 hr., when the tool ceased rotating and transmitting (this failure was later concluded to have been caused by a leaky rotor motor sealing sleeve). The malfunctioning tool was recovered and a new reentry tool landed at the bottom of the pipe at 2200 hr. In the fastest reentry operation thus far on Leg 76, the tool found the cone in a little less than 1 hr. and the stab was made at 2312 hr.

On its way down the hole, the pipe was stopped at 840 m sub-bottom, approximately 30 m deeper than during the previous reentry. The Bowen sub was installed in the drill string to remove the blockage, which may have been a bridge on a shoulder of a thin hard limestone bed in the Hatteras shales. Only a little effort was needed to break through to where the hole was clean through the Blake-Bahama Formation.

Normal operations were resumed with the recovery of Core 83 at 1515 hr., 19 November 1980. Recovery was good, but drilling was slow. The limestone was less hard and more marly than anticipated, and as a result the 94 short-tooth bit probably was sliding more than cutting.

When the tugboat *Orca* arrived at 1230 hr., 22 November 1980, the crew and scientists took a few minutes to welcome the new members to the shipboard party, the major social event of the cruise. Unfortunately, an oil filter on one of the propulsion motors chose just this moment to malfunction. To repair the filter the propulsion motor had to be taken off the line for 4 or 5 hr. In the meantime, full propulsion capacity was needed to maintain the *Challenger* in position for the rendezvous and personnel transfer. The transfer was no easy task as it required jumping from an inflatable boat to the boarding ladder in a heavy swell.

Consequently, the ship's officers and operations manager decided to borrow power from the Bowen sub motor and, therefore, the drilling had to cease. However, the draw works motors could still function. To utilize the time (4–5 hr.) it was decided to pull the pipe to replace the Smith F94CK (short-tooth) bit, which was not achieving good penetration rates. Core 98 was halted after 6.0 m of cutting and the pipe was pulled out of the hole at 1245 hr. It was found to be empty, suggesting a possibly plugged bit, which might also explain the poor recovery rate for Core 97.

Upon arrival of the bit on deck at 0530 hr., 23 November 1980, it was found to be plugged very tightly by a very hard, gray clay, which was so dry it crumbled. This was in contact with a small fragment of red shale above it. Following the procedures of the Deep Sea Drilling Project, this is labled Core B1 in Table 2.

Preparations were begun for our fourth return to the hole. Between 0530 and 0745 hr., *Challenger* was maneuvered back over the hole because it had drifted as far as 5 mm during the pulling of the string. For safety and comfort on the rig floor *Challenger* was headed into the heavy 3-m swell, rather than positioned to stay on station. Magna fluxing the joints during this run found some fatigue cracks in three inner core barrels, which were set aside for repair. The magna fluxing procedure adds about 4 hr. to the normal trip time.

At 1058 hr., Captain Clarke ordered another 13-kHz sonar beacon launched to replace the original 13-kHz beacon, which no longer could be "heard" by the positioning computer. This was done to provide backup for the 16-kHz beacon, which was the present reference for Site 534, and give a longer-lived signal for eventual return to the site.

All was ready for the next reentry of the cone on 23 November at 2030 hr. The 94-type bit had been replaced by the better cutting type (F93CK, long tooth). Within half an hour, the cone was found and successfully stabbed at 2114 hr. The reentry again was complicated by the occurrences of bridges at 850 and at 950 m sub-bottom. The bridge at 950 m was particularly troublesome, because at this depth the limestones of the Blake-Bahama Formation form a ledge, above which the Hatteras Formation shales are eroded into a cave. Apparently the ledge was becoming larger, so that the bit set down some distance off the hole in the limestone. This time it took approximately 1 hr. from 0430 to 0530, to raise and lower the pipe until the bit was slipped into the hole. After this second "reentry" at the ledge, the drill string lowered easily to the bottom of the hole.

The hole was cleaned with mud, and the core level was pulled, as was Core H3, to examine the cuttings for information on the bridging problem. However, the wash core only had a few cuttings mixed with muddy water. Apparently, the high pressure on the bit kept it clean. At 1145 hr., the inner core barrel landed for Core 99, but pressure became abnormally high, which suggested a plugged bit (with the pressure vents, rather than the center bit opening, filled with mud). Several techniques were employed to unplug the bit, including stabbing of the bit with the unplug tool and hard landing of the core barrel with full pump stroke. None gave a definitive clue to the state of the bit, and it was decided to core 5.5 m and hope for the best. Coring took only 40 min. and at 1645 hours, 5.2 m of the Cat Gap Formation was retrieved. Coring routine was reestablished.

In the early morning of November 25, we passed beyond the sub-bottom-depth penetrated at Site 391 (1412 m), with the red shales, Cores 99 to 103, coming up every 3 hr. Unfortunately, the gray, micritic limestones and shales below Core 103 down to Core 111 retarded the pace considerably. In addition, "the deep current" reappeared and caused considerable pipe stress and uncertainty on the weight indication during drilling of Core 107, which was pulled after cutting only 4.5 m in 210 min. From Core 112, at 1504 m sub-bottom, down to Core 117 hard shales again speeded up the coring, but recovery was much below normal. Maybe the bit had been damaged when drilling through the hard limestones.

On Saturday, 29 November 1980, it became clear that the bit was likely past reflector D strata and that we had reached the hitherto unexplored basal sedimentary unit. The next highlight of drilling would be basement, to be attempted during the continuation of Leg 76 in December, after the port call and crew change in Ft. Lauderdale. Time constraints created by the need to change Global Marine and Scripps crews made the 1 December 1980 ETA at Ft. Lauderdale a must; therefore the coring operations were terminated when Core 121 had been cut. Drill torque had much increased and a seized drill roller cone was feared. In any case, the core diameter indicated bit wear, which was to be expected, given the bit model and number of drilling hours. Core 121 arrived on deck at 0015 hr. on 29 November. The hole was flushed with heavy mud and the drill string pulled. All gear arrived safely on deck at 1415 hr. The bit was inspected for damage, but nothing unusual was found. All the cones were wobbling as if the seals were gone and bearings worn; the cones were obviously damaged and might have dropped off with further use. The decision to pull pipe was indeed a correct one. Having amassed 52 hr. of bit life, this model 93 had served us well—it penetrated 195 m over a 4-day period.

The drilling crew spent a short time magna fluxing the Bowen sub joints on the rig floor. At 1800 hr. on 29 November 1980, *Glomar Challenger* headed for Ft. Lauderdale (to return in a week's time for completion of deep, multiple reentry drilling at Site 534 in the Blake-Bahama Basin). Arrival at Ft. Lauderdale at 1000 hr. on 1 December 1980 began a 4-day port call to change crews and reprovision the ship.

On December 5, 0700 hr., *Glomar Challenger* headed again for Site 534. Crew change and fitting out for the extension of Leg 76 and for Leg 77 were completed, including repairs to the heave compensator. The Leg 77 scientific team had largely come aboard, except for the co-chief scientists, a paleontologist, and the organic geochemist. Of the Leg 76 scientists, the two co-chief scientists and two of the sedimentologists had stayed aboard in order to complete the coring and logging at Site 534 to basement. We hoped to complete the Leg 76 extension by 16 December 1980, as approved by the Deep Sea Drilling Project.

Under stable weather conditions with 15 to 25 knot winds and a light to moderate NNE swell, we reoccupied Site 534. The ship was again in automatic positioning over the beacon at 2000 hr. on 6 December. After bleeding air from the heave compensator, at 2230 hr. the pipe was run down with a Smith F94CK (short-tooth) bit and three bumper subs and drill collars. The offsets relative to the beacon to bring the ship over the cone had been estalished during the previous reentry. A slight delay to slip and cut the drilling cable put the running in of the reentry tool at 0955 hr. At 1240 hr. on 7 December the reentry tool was at the bottom of the pipe and rotating. Returns seemed normal, including a mudline reflector, but there was no sign of the cone.

A box-type search pattern was begun, first with 100-ft. and then with 300-ft. offsets. After we had not seen the cone for some time, we suspected that the tool was not seated and out of the pipe. At 1800 hr. the tool was pulled up and set down and a definite loss of weight was indicated, but 6 m deeper than previously, which suggested that the tool was not out of the pipe. However, when seated the tool failed to rotate properly. At 1820 hr. the tool was winched back on deck; the problem was traced to improper assembly of the tool, which prevented proper seating in the bit. A new, properly assembled tool was sent down, but this one also stopped rotating at the bottom of the pipe. On chance that an obstruction might have been present in the bottom-hole assembly, the operations manager decided to employ the bit deplugger before lowering a third reentry sonar tool. In the meantime, the heave compensator had started leaking and was not fit for operation until seals on the hydraulic piston were replaced.

At 2330 hr. 7 December 1980, the deplugger was run and seated with high pressure. This should have cleared the obstructions from the bit. At 0130 hr. on 8 December 1980, the overshot was sent down after the deplugger. In the meantime, the operations manager discovered that the opening of the Smith F94CK bit installed at the end of the drill string was not the correct diameter for normal cores, that is, 2 7/16 in.; rather it was a smaller-diameter bit for the pressure core barrel, 2 1/8 in. This 5/16-in. reduction in diameter was apparently what was preventing the reentry tool from getting out of the bit. There were scratches on the reentry tool sonde, which attested to the presence of the narrower bit opening. We decided to leave this type of bit on and live with smaller cores rather than trip the pipe to replace it. We were assured by the drilling operations manager and tool pusher that recovery would not be affected.

At 0315 hr., the third reentry tool was sent down with a sonde that was apparently of a smaller diameter than the bit opening. Upon reaching the bottom at 0530 hr., the tool again got stuck in the bit opening and refused to rotate. Twice the tool was lowered and twice it was stuck, with approximately 2000 lb. of overpull needed to dislodge it from the too-small bit. At 0535 hr. 8 December 1980, we decided to pull pipe in order to change to a proper bit size. This whole problem, which could easily have been avoided by more conspicuous labeling of the proper bits and by checking the bit opening diameter before bit installation, cost the program two days of operations at Site 534.

At 0730 hr. on 8 December, the reentry tool arrived on deck, and we found that the entire 45° transducer had been ripped off. Apparently this was still lodged in the bit opening. However, at 1545 hr. the bit arrived on deck without any fragments of the broken transducer. Upon changing to a normal-diameter bit, the BHA (bottom-hole assembly) was reassembled and running in the hole was begun. At midnight, the transducer reentry tool was again on its way down the pipe, but mysteriously stopped rotating at 1000 m. When retrieved, no sign of malfunction could be detected; in the early morning hours of 9 December, the fifth reentry tool trip in three days time was started.

Running in the hole which we had left 10 days ago was accomplished in 10 hr. under near-perfect weather conditions—almost no swell and a light, pleasant breeze. As a result, the drill string was virtually stationary. The stable drilling string condition probably facilitated the drill string's slipping past the feared bridges at 800 and 950 m sub-bottom. Only two minor obstructions were encountered at 802 and 860 m sub-bottom, which were cleared easily with the help of some pipe rotation and flushing when the Bowen sub had been installed. The bottom of the hole was felt at 2200 hr., about 8 m deeper than anticipated, based on the "old" bookkeeping record. The last seven single pipe lengths before touching bottom went down through fill because of cavings and required more pump pressure. Next the hole was thoroughly flushed with mud for 1.5 hr., after which the inner core barrel was retrieved. This one was empty except for only 20 cm of *in situ* sediments, which proved the hole to be thoroughly clean. At 0230 hr. of 10 December, we were coring again in Oxfordian claystones and limestones. The first core, Core 122, arrived on deck at 0600 hr. with 3 m of dark shale and limestone. Cores 123 to 126, with black to red green shale and limestone, came on deck at intervals of 5 to 8 hr.; cutting was slow due to the nature of the shaly limestone and claystone, which tended to obstruct the core catcher and resist bit penetration. During the cutting of Core 127, we feared we had finally come across Jurassic chert levels, which caused the drilling to slow down. Great was our surprise when the core contained shale and the core catcher 7 cm of fine-grained basalt. The next three cores were all basalt, which confirmed that ocean basement had been reached at 1635 m instead of at 1700 m, as estimated. Nannofossil biostratigraphy showed the basal sediments to be Callovian. We were sampling the oldest stage of Atlantic Ocean history—approximately 153 m.y. old.

At 1000 hr. on 12 December, the coring operation at Site 534 was terminated; total depth reached was 1666.5 m. The Totco reading showed the bottom 9 m of the hole to be 2.5° off vertical. Now the hole was flushed with heavy mud for 1.5 hr., after which the pipe was pulled back on deck and a logging type bit added. The reason for pulling pipe prior to logging of the hole was that we could not use the hydraulic bit release. First, a drill bit at the bottom would obstruct potential seismic experiments in the hole at a future date. Second, if we dropped the bit outside the hole, the open-ended drill string would not likely slip past the bridges in the 800 to 1000 m interval sub-bottom. The addition of the wide throat, nonroller type of bit to the drill string would also aid in reentering the hole and logging the section below the bridges.

At 2200 hr. on 12 December 1980, the drilling bit arrived on deck and was changed for the logging bit. By 0800 hr. on 13 December 1980, pipe was run in the hole to just above the cone, followed by the EDO reentry tool at 1000 hr. By 1030 hr. the reentry cone was within 25-ft. range, but then it eluded the pipe until 1645 hr., when the stab was successfully made.

After reentering the hole, pipe was run-in to the bridge at 850 to 1000 m, where the Bowen sub was installed to work the pipe through. After that bridge, no other major obstructions were felt until 3 m above bottom where rubble had accumulated. At 0450 hr., the rubble was pumped out with heavy mud for a long enough time to fully circulate the mud and cuttings out of the hole. By 0700 hr., the pipe was broken and pulled up to the position just below the upper contact of the Blake-Bahama Formation where logging of the lower half of the hole was to be done. However, at 1000 hr. the pressure on the water in the pipe after reconnection of the circulation pump was found to indicate high back pressure, as if the bit were plugged. (We now believe that actually the hole was plugged, leading to over-pressure after pumping.) Because there was some overpull, 500,000 to 650,000 lb., on withdrawal of the pipe it was thought some cuttings and talus had caught around the external parts of the pipe and gotten between the hole wall and the drill collars. In hopes of rubbing this debris off the pipe, it was then pulled up into the casing. This did not deplug the bit. From 1130 to 1500 hr., sinker bars were attached to the wireline overshot and lowered to "punch" the debris from the bit. Upon failing to accomplish deplugging, the bit was then raised out of the reentry cone to try using regular inner core barrels to core the debris out of the pipe. After several trips the operations manager deemed it fruitless to continue trying to deplug near bottom, so the pipe was pulled.

By 0600 on 15 December 1980, the bottom-hole assembly was pulled on deck with as much as 70 m of debris in the pipe, including chunks of spalled boulders at least 30 cm along their long axis.

Again an attempt was made at logging. By 1330 on 15 December 1980, the pipe was above the cone, and 2 hr. later the EDO reentry tool was at the bottom of the pipe. However, the EDO tool did not appear to be out of the pipe, and it was reseated several times. Finally, at 1655 hr. the tool failed to rotate and had to be pulled.

By 1930 hr. this first EDO tool was returned to the deck where the rotation motor shaft was found to be broken. No explanation was given for this. A new tool was sent down and by 2130 hr. on 15 December 1980, it was again seated several times, but it still seemed like it was not out of the pipe. Only a shadow of a mudline echo was seen on the scope, as if the transducer was shielded.

Again this tool was brought up on deck and an extension to the transducer shaft was installed to be sure it stuck out of the pipe when seated. However, at 0230 hr. on 16 December 1980 when the extended tool was seated and rotating, it had the same symptoms as the last tool—no mudline echo, as if the tool were not out of the pipe. However, the returns did change when the EDO tool was pulled up into the pipe where a pipe echo was observed. This seemed to indicate the tool was malfunctioning and was indeed properly seated. The receiver circuit was suspect so the tool was again pulled at 0300 hr.

The recovered EDO tool was thoroughly checked out and seemed to be functioning all right. Possibly some loose solder joints in the connector and cable head had been the problem. These were resoldered and a new tool was sent down. At 0900 hr. on the 16 December 1980, the new EDO was out of the pipe, rotating, functioning well, and giving a nice "picture" of the cone at 60-ft. range. By 1217 hr., the cone was successfully stabbed and reentry made.

At 1900 hr. we had washed in with the aid of the Bowen sub to a depth of 5920 m, just below the bad bridge at the constriction in the hole at the upper Blake-Bahama Formation contact. The sheaves were set for logging. The logging tool, composed of natural gamma ray, borehole-compensated density, and temperature sensors, was run in to a depth of 6390 m, where a bridge stopped further progress. This bridge apparently occurs at reflector D′, where hard limestones again constrict the hole beneath a crumbly shale section. By 0344 hr., 17 December 1980, logging with the density tool was accomplished from the Cat Gap Formation to the upper part of the Blake-Bahama Formation, over a depth of 6400 to 5950 m.

Early in the morning of 17 December 1980, it was necessary to pull pipe up into the casing for equipment safety. The weather front passing over at that time caused 40-knot winds and 3-m swells, which required full propulsion powers to withstand. Because the No. 3 engine was in disrepair again, power was drawn from the drawworks by assigning its motor to one of the propulsion systems. With the weather front around, there was always the possibility the *Challenger* would not be able to maintain station, and the pipe would have to be pulled rapidly through the casing to save the equipment.

In the meantime, two logs were run, the borehole-compensated density log and the borehole-compensated sonic log, over the 280-m interval below the casing. Again the tools stopped at a shale bridge at a 5760-m depth. The density logging was completed by 1415 hr. 17 December 1980. The sonic log with natural gamma ray detector was sent down, but the gamma ray sensor failed to operate on the way down. The tool was pulled and replaced with a new one, which apparently functioned well. Three sonic runs were needed to get reproducibility, and the sonic log from the upper part of the section just below casing was completed at 2208 hr. 17 December 1980.

After the sonic log survey of the interval just below the casing, the weather calmed and the logging of the deeper part of the hole was pursued. At 0420 hr. 18 December 1980, pipe was run in to 5920 m depth with the help of the Bowen sub to work through the bridges. The target depth was reached at 0500 hr. and the sonic logging tool was run in. Unfortunately, the tool could get in only a few meters below the pipe opening, as if the hole were bridged again. The tool was pulled at 0700 hr. Upon arriving on deck at 1030 hr., the tool was found damaged, with the caliper bent and the gamma ray source spilled out. Apparently the caliper was still opened when the tool entered the pipe, and it was bent upon contact. This stress of the jammed caliper plus the stress of trying to hammer through the bridge with the tool had caused the logging wire to bend near its head. The wire took two hours to be repaired, and this slowed up the logging operation. From 1200 to 1600 hr. the pipe was washed to the T.D. of the hole to pump out the cuttings with 40 barrels of mud. In this way, we hoped to clear the way for logging the very bottom of the hole. By 2300 hr. 18 December 1980, the pipe was pulled back up to 6340 m and the log sent down to the bottom, but the logging tool could only penetrate 20 m. Thus the tool was pulled again and the pipe washed to a deeper ledge at 6430 m. The density log was sent down to record the log data for the interval from the deepest point accessible to 30 m below the pipe. Unfortunately, the logging tool again settled on a bridge, this time at 6510 m. From this depth to 6460 m, 50 m of density log was obtained. By 0359 hr. 19 December 1980, the density log over the deepest accessible interval had been completed with three rather well-reproducible runs. Time constraints then required that the tool be pulled, followed by the drill string, which terminated the operations at Site 534. By 0625 hr. the logging tool was on deck, followed by the core pipe at 1645 hr., and *Glomar Challenger* departed Site 534 at 1700 hours 19 December 1980 to head for the port call at Ft. Lauderdale. Thus ended the Leg 76 operations.

LITHOLOGY

Blake Ridge Formation (Unit 1)

Only one core was obtained from the Quaternary Blake Ridge Formation (Jansa et al., 1979) at Hole 534—a mudline test—drilled at 4973 m water depth and penetrating 2.1 m below the seafloor, with 100% recovery. The lithology is 40 cm of light olive gray and 135 cm of light greenish gray to bluish gray (5B6/1), slightly burrowed, foraminifer–nannofossil silty ooze. The ooze is underlain by 35 cm of greenish gray nannofossil marl. Smear-slide analysis of Sample 534-1-1, 100 cm indicates about 19% detrital content, 5% nannofossils, and 14% siliceous microfossils. Closer examination of the nannofossils shows many of them to be reworked from pre-Pleistocene strata, indicating that some of the sediment was transported by bottom currents.

This finding appears plausible when compared with work by Heezen et al. (1966), who hypothesized the existence of fairly active bottom currents in the vicinity of Site 534. The sharp color change that occurs at 25 cm in Section 2 indicates a change in deposition patterns possibly caused by increased turbidity current and bottom current activity during the last glacial event, more than 12,000 yr. ago. The increased concentration of pyrite below this boundary suggests a reducing environment possibly caused by a greater rate of deposition.

The Holocene/Pleistocene boundary was placed at 40 cm sub-bottom, based on a color change. Foraminiferal assemblages indicate this boundary to be accurate within the limits of sampling error. A Holocene sedimentation rate of 3.5 to 4.0 cm/1000 yr., derived from the above assumptions, suggests moderate detrital input, possibly through bottom-current transport.

Great Abaco Member (Unit 2)

At Site 534, two holes, 534 and 534A, were drilled in the Blake-Bahama Basin in water depths of 4973 and 4971 m respectively. Hole 534A was washed from 0 to 531 m, followed by continuous coring. Sediments from the Great Abaco Member occur in Cores 534A-1 through 18 to a sub-bottom depth of 696.5 m. Total recovery was 83.5 m, composed mostly of intraclastic chalk, siliceous and calcareous claystone and mudstone, and minor limestone, all early Miocene (see Fig. 13, back pocket).

Similar and coeval lithologies occur at Site 391, 22 km to the southwest of Site 534. A more extensive Miocene section was spot-cored at Site 391, where five subunits (designated 2a–e) were delineated in what was termed the Great Abaco Member (Benson et al., 1978; Jansa et al., 1979). Drilling depth and lithologic types recovered at Site 534 indicate we cored only the equivalent of Site 391 subunit 2e. Thus our cored interval represents the lowest lithostratigraphic unit of the Great Abaco Member. Within this unit, continuous coring allowed us to distinguish subdivisions, which are based mainly on the mode of deposition (i.e., turbidite versus debris flow versus hemipelagic sedimentation) and less on lithologic variations.

A total thickness of 160.2 m of lower Miocene material was cored at Site 534, of which 83.5 m were recovered (52%). Unit 2 is characterized by interbedded chalks, intraclastic chalks, and calcareous and siliceous mudstones, and can be divided into four subunits (labeled a–d) on the basis of lithology and mode of deposition (Figs. 13, 14).

Subunit 2a

Subunit 2a consists mainly of intraclastic chalk interbedded with siliceous and calcareous mudstones and extends from 545.8 to 566.6 m sub-bottom. The mudstone beds, on the order of a meter and a half in thickness, are grayish olive (10Y 4/2) and contain abundant siliceous microfossils (mainly diatoms and radiolarians) and calcareous nannofossils. The intraclastic chalks are marly, grayish yellow green (5GY 7/2), and contain numerous 1.5- to 3-cm, evenly distributed, elongate, horizontally oriented clasts. The clasts consist of pale colored (5Y 8/4) chalk and dark brownish gray and dark greenish gray (5Y 3/2, 5Y 4/4, and 10Y 4/2) muddy siliceous ooze. The distinct outlines and lack of distortion of many clasts indicates they were sufficiently lithified at the time of deposition to resist deformation.

Sedimentary structures and bedding contacts indicate that the intraclastic chalks were deposited by repeated debris flows and fluidized grain flows grading upward into turbidity currents. Some laminated sequences with sharp tops and bottoms (Fig. 15) may have been deposited, and/or reworked by bottom currents. Between influxes of chalk, mudstone was deposited, which in some cases was also reworked by bottom currents.

Subunit 2b

Subunit 2b (566.6–595.0 m sub-bottom) is composed predominantly of yellowish gray and green (5Y 8/1 and 5Y 6/1) chalk as well as intraclastic chalk, which varies from yellowish gray (5Y 8/1) to pale olive (10Y 6/2) to light olive gray (5Y 6/1). The chalk is generally homogeneous, although frequently bedded. The intraclastic chalk is very similar to that in Subunit 2a. Mudstones are a minor component, with one 4-m interval of siliceous mudstone (11% siliceous microfossils) near the top of the subunit and thinner intervals of calcareous mudstone farther down in the subunit.

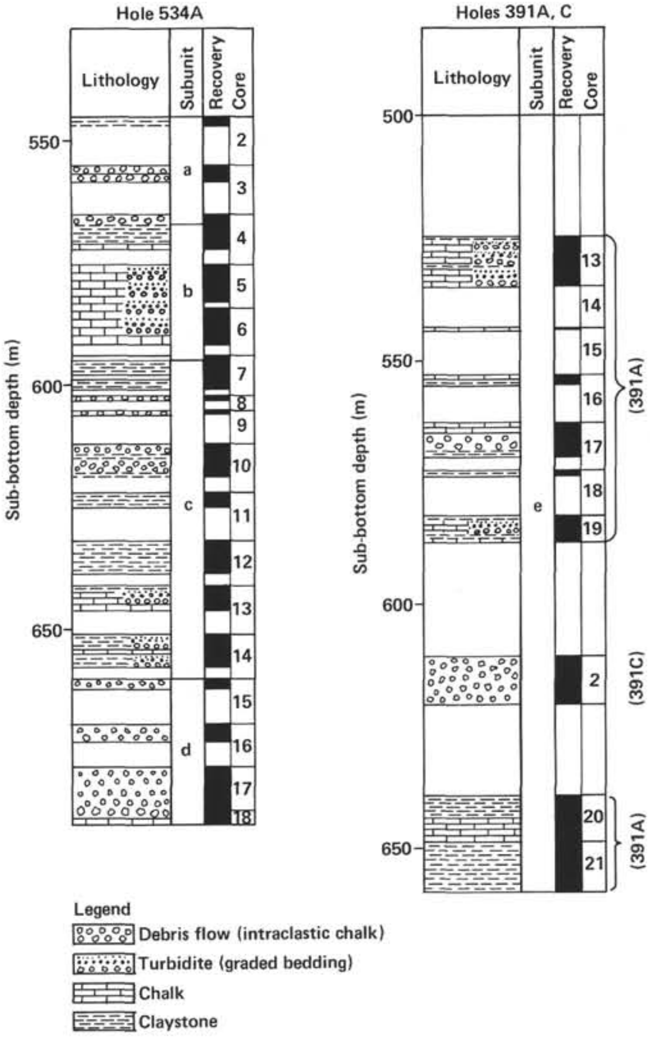

Figure 14. Generalized stratigraphic logs showing correlation of relative thickness, lithologies, and core recovery of the Miocene Great Abaco Member at Sites 391 and 534.

The chalk beds, especially, show the erosional bases and graded bedding of partial (sometimes complete) Bouma sequences indicative of turbidite deposition (Fig. 16). These chalk beds contrast to the relatively rare occurrence of turbidite beds in Subunit 2a. Scoured contacts and laminated sequences present in the mudstones indicate they have been reworked by bottom currents. The first chalk turbidite encountered at the top of this subunit has a coarse basal sand composed of *Amphistegina* foraminifers, indicating transport of some of the chalk material from a shallow water carbonate platform, probably the Bahama Banks. These turbidity currents have scoured down to Eocene rocks and have incorporated pieces of them as clasts. The nannofossils identified in the clasts contrast sharply with the Miocene forms found in the chalk matrix.

Subunit 2c

Subunit 2c (Cores 534A-7–14, 595.0–660.0 m sub-bottom) is the most variable of the subdivisions noted in the Great Abaco Member and exhibits a wide range of

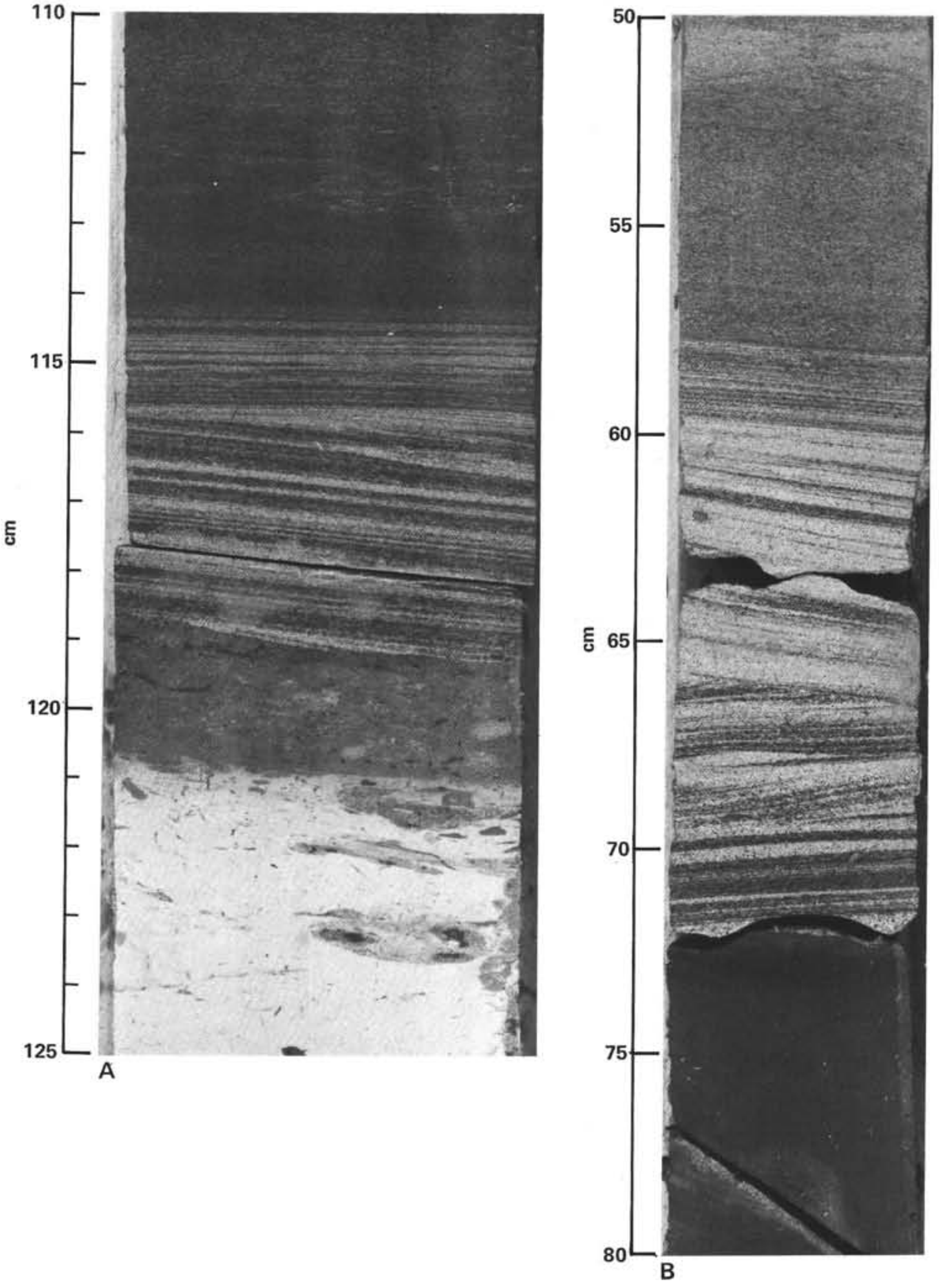

Figure 15. Laminated chalk (light)/siliceous mudstone (dark) sequences with sharp tops and bottoms indicating deposition and/or reworking by bottom currents. (Scale is in cm.) (A. Sample 534A-7-1, 110–125 cm. B. Sample 534A-12-2, 50–80 cm.)

lithologic types. It is dominated by interbedded light colored chalks and olive gray mudstones. Intraclastic chalk comprises most of Core 534A-10 but otherwise is a minor constituent. Other minor lithologies found in this subunit include light gray (N7) limestone cobbles containing abundant sand-sized clasts of bluish green gray (5BG 5/1) mudstone; variegated medium bluish gray (5B 5/1) to dark olive gray (5Y 3/1) muddy porcellanite; and bioturbated, olive gray (5Y 4/1) diatomaceous mudstone.

The calcareous mudstones and some of the siliceous calcareous mudstones exhibit sedimentary structures indicative of turbidite deposition. The turbidite units are stacked one on top of the other and in some cases (Cores 534A-7 and 14), the basal layers are composed of fine to medium sand-sized grains. The siliceous mudstones show little or no evidence of current reworking. In Cores 534A-10 and 13, a different depositional mechanism is evident—debris flows. The slumps and convolute bedding are especially obvious in Core 13, and lithologic

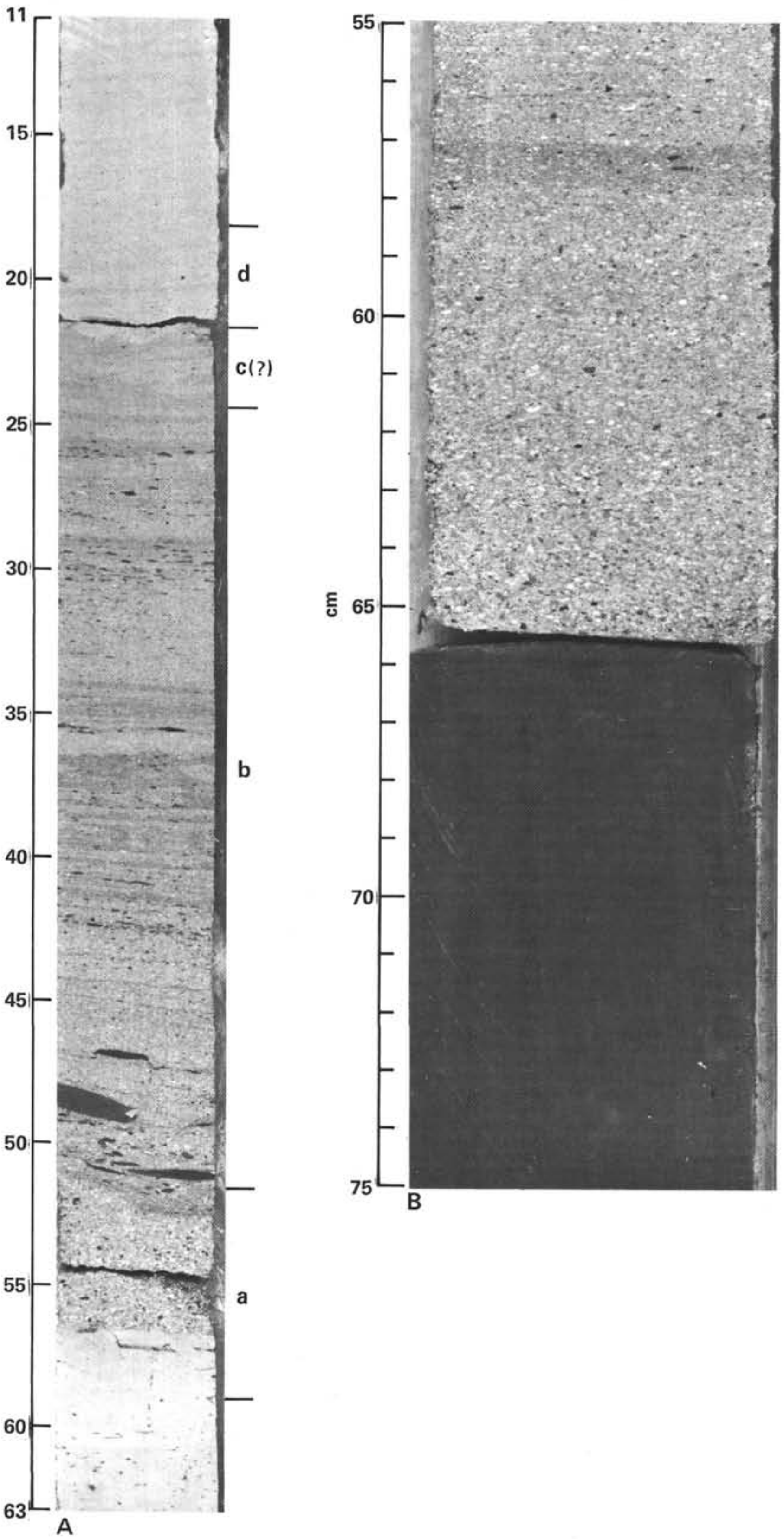

Figure 16. A. Sample 534A-4-2, 11-63 cm—nearly complete Bouma sequence with intervals a through d present, indicating deposition by a turbidity current. (Dark clasts are composed of siliceous mudstone. Light spots are benthic foraminifers and other carbonate grains.) B. Sample 534A-7-1, 55-75 cm—close-up of erosional base and graded bedding of coarse foraminifer turbidite deposited on top of siliceous mudstone. (Scale for A. and B. in cm.)

variation is more pronounced (includes intraclastic chalk, shallow-water foraminifer chalk, siltstone, and mudstone).

Subunit 2d

Subunit 2d is a relatively uniform sequence of greenish gray (5GY 6/1) chalk and intraclastic chalk comprising Cores 534A-15 to 18 (660.0–696.5 m sub-bottom). The density of clasts and overall grain size increase downward. Clast size increases from 0.5 cm in Core 16 to 2 to 3 cm near the base of Core 17, and the texture varies from a mudstone to a calcareous sandstone or even a calcareous conglomerate. Clasts are of three main types: dark greenish gray (5G 4/1) and medium bluish-green gray (5BG 5/1) siliceous mudstone; yellowish gray (5Y 7/2) limestone; and light pinkish gray (5YR 8/1), angular foraminifer-rich carbonate grains of shallow-water origin. The base of Core 17 also contains a 35-cm limestone clast and a 2-cm pyrite nodule. The structures, textures, and composition of these four cores indicate that deposition was by a combination of debris flow and turbidite, approximately 30 m thick.

The boundary between Subunits 2c and 2d at 660 m coincides with the only significant change in physical properties observed in the Great Abaco Member. Below this boundary, porosity is lower and density is higher, possibly reflecting either the massive debris flow and turbidite origin of Subunit 2d or diagenetic alteration (cementation) of the subunit.

Discussion

The same lithologic succession cored in Hole 534A was also recovered at Site 391 on DSDP Leg 44 (Benson et al., 1978). The Miocene section recovered at Site 391 was divided into five subunits, and the interval cored in Hole 534A can be correlated with Subunit 2e from Site 391 (Fig. 14). Site 391 is 22 km southwest of Site 534, is closer to the possible source of the turbidites and debris flows, and is somewhat shallower (about 60 m) than equivalent levels at Site 534. Poorer recovery at Site 391 makes detailed correlations difficult, but broad sequences of lithologic types plus nannofossil zones can be correlated between the two sites.

Our evidence corroborates the ideas put forth by Benson et al., (1978) concerning the intrabasinal origin of the mudstone clasts contained in the chalks. Their similarity in age and lithology to the interbedded siliceous mudstones present elsewhere in the section indicates this lithology was the "background" pattern of sedimentation into which the calcareous material was introduced. Shallow-water and slope carbonates, transported by gravity-flow processes into the Blake-Bahama Basin, eroded and incorporated pieces of siliceous mudstone that became the clasts in the intraclastic chalks. Continuous "background" sedimentation and periodic pulses of carbonate flows produced the observed interbedded lithologies.

Bermuda Rise Formation (Unit 3)

Approximately 27 m of the Bermuda Rise Formation, dated as late Eocene, were cored at Hole 534A, of which 8.4 m were recovered, representing about 31%. The upper boundary of the Bermuda Rise Formation at this site is taken where the varicolored siliceous claystones are overlain by nannofossil–chalks and redeposited facies typical of the Miocene Great Abaco Member (Core 18). The unconformity at the top of Unit 3 was not recovered in a single core. The low recovery of the Bermuda Rise Formation prevents any subunits from being recognized. The lower boundary of the Bermuda Rise Formation at Site 534 is taken to be at the top of Core 22. This boundary shows up as a prominent density contrast in the well logs, but is otherwise arbitrary, as recovery is poor and the lithologies are transitional. The uppermost facies of the Plantagenet Formation, seen in the lower part of Cores 23 and 24, although also varicolored claystone, appears to be less siliceous and zeolitic in comparison with the Bermuda Rise Formation.

Lithologic Description

(1) Claystones and Fine-Grained Siltstones

Volumetrically, the Bermuda Rise Formation sediments recovered consist almost entirely of greenish claystones (>90%) (e.g., Fig. 17B). Colors recorded include pale yellowish green (10GY 7/2), grayish olive green (5GY 3/2), yellowish green (6GY 3/2), yellowish gray (6GY 7/2), dusky yellowish green (5GY 5/2), olive (10Y 5/2), and exceptionally very pale orange (10YR 8/2) to medium gray (N6).

The fine-grained siltstones that are volumetrically minor are mostly finely parallel laminated with occasional intervals up to 7 cm thick that show normal grading, small-scale ripple cross lamination and convolute lamination (e.g., Samples 534A-20-1, 90–97 cm; 534A-20-2, 40–48 cm and 70–78 cm). Approximately 23 to 30% of the cored claystones are moderately to strongly bioturbated (e.g., Sample 534A-20-1, 30–37 cm, 60–70 cm, and 110–120 cm). Core 20, Section 3 is entirely mottled, most likely due to burrowing.

In smear slides, the claystones, textually, contain up to 20% sand and 40% silt, the rest being clay. Compositionally, clay predominates (15–64%), with a marked occurrence of zeolite (up to 74%). Quartz reaches 15% in Core 19. Calcareous nannofossils range up to 10% in the claystones. Several smear slides contain well-preserved radiolarians. Minor constituents, also present in the smear slides, include feldspar, mica, glauconite, unspecified carbonate, pyrite, goethite, zircon, and sphene.

Two samples of claystone from Core 20 were subjected to whole-rock X-ray diffraction on the ship. Section 1, at 135 cm, consists (in decreasing order of approximate abundance) of quartz, clinoptilolite, smectite, and mixed-layered clays, with minor calcite in addition. Section 2, at 114 cm, was found to contain clinoptilolite, smectite, and mixed-layered clays (minor constituents are quartz, feldspar, and calcite). On this basis the zeolite in the smear slides is identified as well-crystallized clinoptilolite. The initial suggestion that volcanogenic material was present (e.g., devitrified volcanic glass, plagioclase, etc.) was not confirmed by more careful examination of the smear slides at high magnifications.

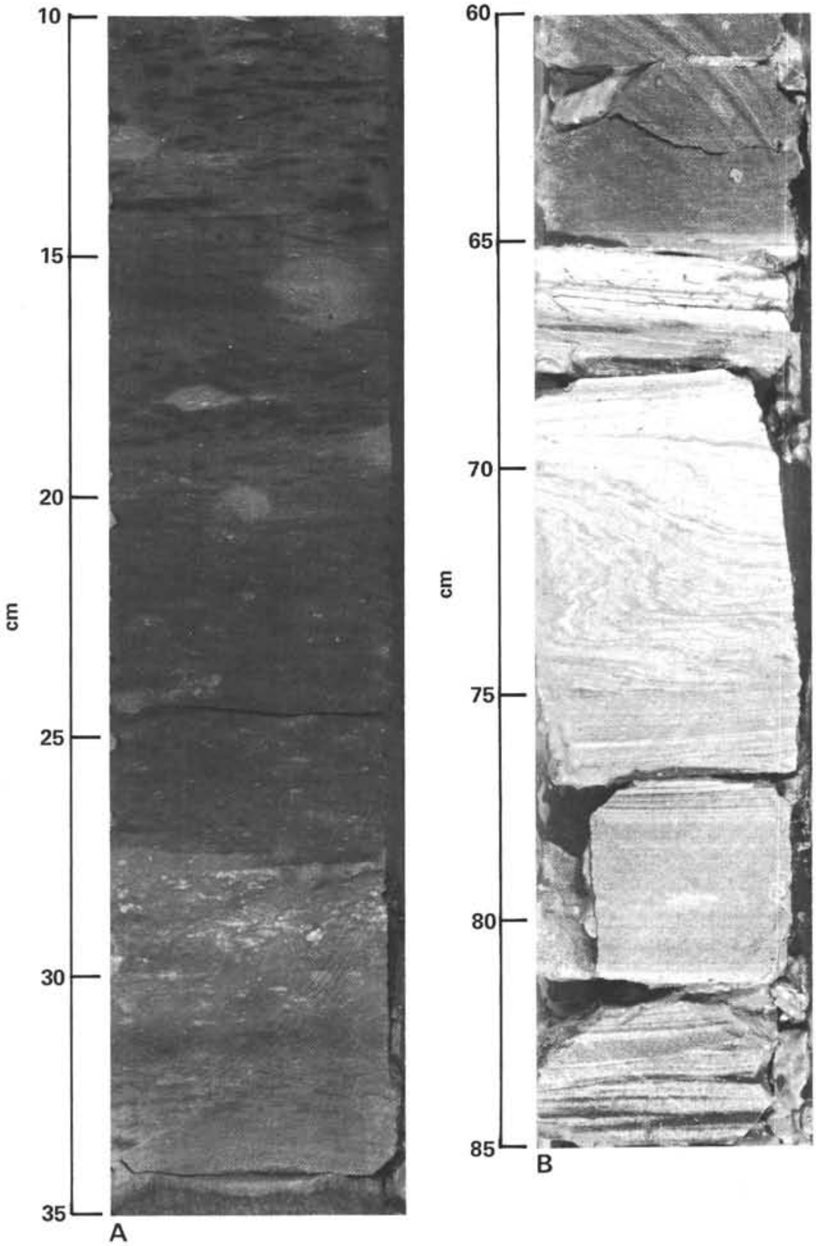

Figure 17. Close-up photographs of cores of the Bermuda Rise Formation. A. Sample 534A-20-3, 10–35 cm. (Typical varicolored claystone. Note the dark gray mottling due to bioturbation and the diffuse medium gray, circular areas that are reduction spots.) B. Sample 534A-19-2, 60–85 cm; calcareous siltstone (75–85 cm) within typical varicolored claystone. (Note the Bouma sequence [grading, parallel at convolute lamination], diagnostic of turbidity current deposition.)

Most of the material tentatively identified as devitrified volcanic glass is probably fine-grained clinoptilolite, as confirmed by the X-ray diffraction.

(2) Silty Micritic Chalk

Although almost all the claystones are moderately calcareous (they fizz gently in 5% HCl), a smear slide of one gray green sediment from Core 19, Section 2 (79 cm) was found to contain 60% unspecified carbonate (calcite) that has undergone extensive recrystallization. A thin section from Core 19, Section 2 at 46 cm was found to be a quartz-silt-rich pelmicrite (wackestone) containing glauconite. Both intervals are characterized by grading and parallel and convolute lamination.

Interpretation

The sedimentary structures in the typical greenish claystones (parallel lamination, burrows, etc.) point to slow condensed deposition, possibly affected by some reworking through bottom currents. The microfossils show that accumulation took place above the carbonate compensation depth, at least for calcareous nannoplankton. Several thin intervals of calcareous siltstones and silty micritic chalk, described earlier, show structures identified as b-c-d-e, c-d-e, and d-e intervals of Bouma sequences of turbidites. The redeposited quartz silt material is of terrigenous, continental origin. Many of the samples contain poorly to well preserved radiolarians, indicative of high productivity of siliceous plankton in the late Eocene, as recorded at Hole 534A. During diagenesis, these radiolarians were partly or completely converted to chalcedonic quartz, associated with the formation of substantial volumes of well-crystallized clinoptilolite; whether or not any volcanic material is involved is not yet known. The origin of the green color may reflect the presence of glauconite and reduced ion (Fe^{2+}). By contrast, the pale orange (10YR 8/2) claystones, which contain goethite, may reflect more oxidizing bottom conditions. Additional mineralogical and chemical data are clearly needed to understand more fully the deposition and diagenesis of those unusual sediments.

Regional Comparisons

The Bermuda Rise Formation was not cored at Site 391 (Benson et al., 1978), which was interpreted to be the result of erosion rather than nondeposition. Elsewhere (Fig. 18), the formation has been cored on the Bermuda Rise (Sites 387, 386, 6, 7, and 9), eastwards toward the Mid-Atlantic Ridge (Site 10), between the Sohm and Hatteras abyssal plains (Site 8), at Vogel Seamount (Site 385), and on the continental rise (Site 106) (discussed by Jansa et al., 1979). At all these sites, the Bermuda Rise Formation is siliceous. The age is latest middle Eocene to latest Eocene. Marked regional compositional variation exists. At the type locality (Site 387), the cherts and associated sediments are greenish gray (5V42) to olive gray (5G 5/1), in contrast to the varicolored greenish claystones cored from Hole 534A. In this regard, these claystones are more comparable

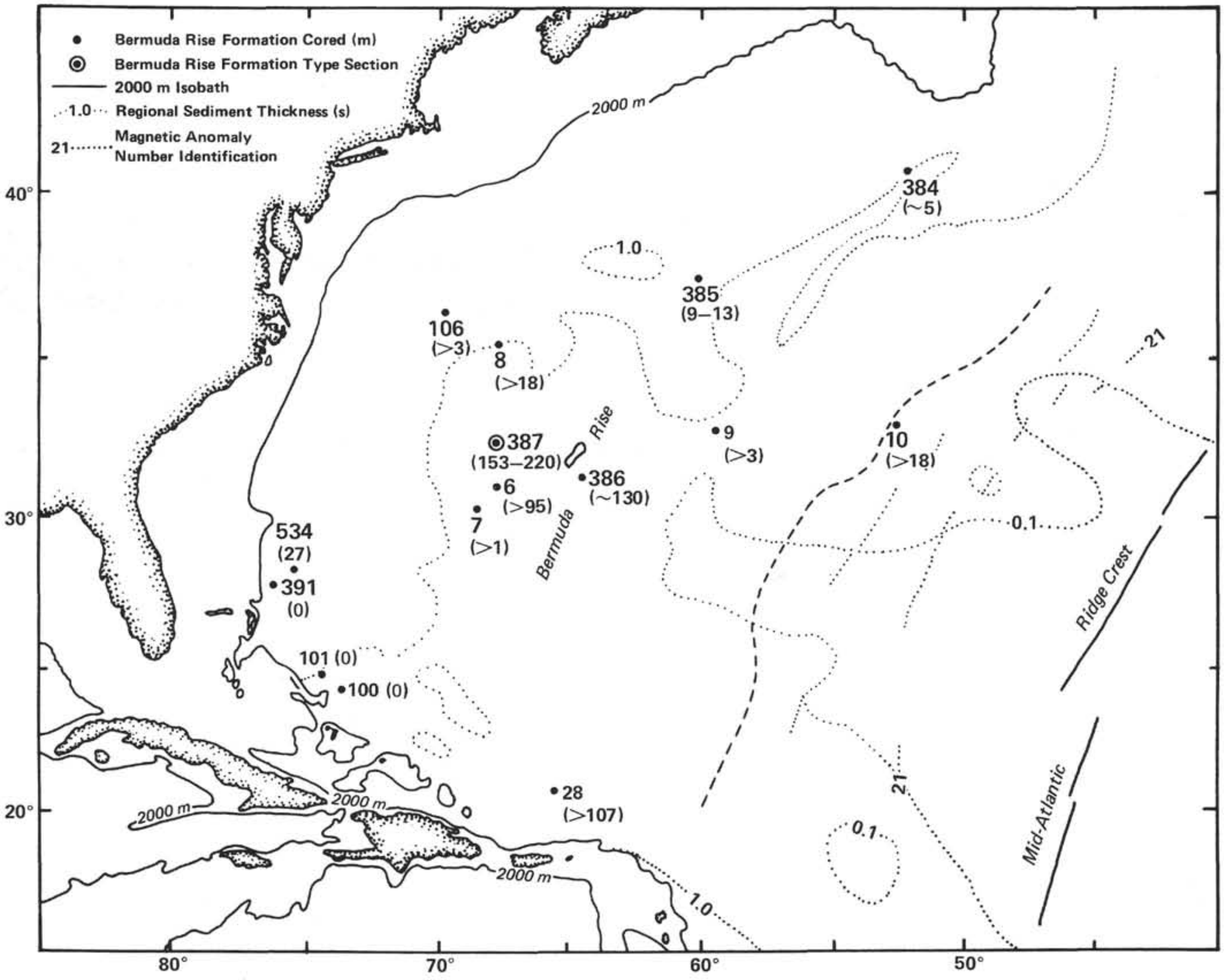

Figure 18. Location of holes that have penetrated the Bermuda Rise Formation. (Formation thickness [m] is shown in parentheses. Note that 27 m of the Formation were drilled at Site 534, in contrast to Site 391, where the Bermuda Rise Formation is not present.)

with the upper Eocene varicolored clays cored at Site 28 on the Antilles Outer Ridge, which lies between the north wall of the Puerto Rico Trench and the Nares Basin to the north (Bader et al., 1970).

Plantagenet Formation (Subunit 4a)

Variegated, locally zeolitic, noncalcareous claystones overlying the black claystone of the Hatteras Formation are identified as Plantagenet Formation (Jansa et al., 1979). The upper boundary of the Plantagenet Formation is represented by a facies change from variegated claystone typical of the Plantagenet Formation to mostly greenish zeolitic and cherty sediments of the Bermuda Rise Formation. This boundary is tentative because of poor recovery, but future micropaleontological study may clarify the problem; therefore in this report we define the boundary to be between Cores 21 and 22, in view of the density contrast seen in the well logs.

The transition from the Plantagenet to the top of the Hatteras Formation is taken to occur at the increase in organic carbon and at the color change to black and green. This transition is also confirmed by a paleontological hiatus.

The Plantagenet Formation consists mainly of variegated claystones of reddish brown (10R 5/4), dark yellowish orange (10YR 6/6), greenish gray (5GY 4/1), and medium bluish gray (5B 5/1) colors and extends from 723.5 m in Core 22 to 764.5 m sub-bottom in Core 26 (41.0 m thick). The main detrital minerals are quartz, feldspar, and mica. The clay minerals on the whole rock basis consist of abundant illite and subordinate amounts of quartz, smectite, and kaolinite. Authigenic minerals are not observed by the bulk sediment X-ray analysis. Mica flakes observed in a washed paleontological sample (534A-24-4, 42 cm) are identified as illite by X-ray and microscopic observation. Sedimentary structures are rare, except for a few parallel laminations in places. The variegated intervals record oxidation of bottom sediments that presumably took place during periods of slower sedimentation and may have been aided by periodically intensified, deep-oceanic circulation. This conclusion is supported by the observation of a few millimeter-thick silty layers composed mainly of quartz and feldspar. Calcium carbonates in the silty layers may be dissolved. Also, the clay minerals are composed of a weathering-resistant suite, such as illite, kaolinite, and mixed-layered clays.

A very small volume of porcellanite recovered in the core catcher of Core 23 is dark yellowish (10YR 4/4) with a vitreous conchoidal fracture, showing patches of incomplete silicification.

In thin section, the porcellanite from Core 23 is a partly silicified, marly, planktonic foraminiferal chalk. Planktonic foraminifers and radiolarians are densely packed with a micritic clay-rich matrix that has been mostly converted to fine-grained chalcedonic quartz, with segregations of opaque particles. The radiolarian shells have almost been converted to chalcedonic quartz. Some isotropic silica (?Opal C) persists within foraminifer shells.

Hatteras Formation (Subunits 4b–d)

The upper boundary of the black claystone of the Hatteras Formation is represented by a hiatus that shows a strong facies change from black claystone of the Hatteras Formation to variegated claystone of the Plantagenet Formation. The Hatteras Formation can be subdivided into three subunits based on the whole-rock clay mineralogy and a variegated interval (Subunit 4c) in the middle. The upper subunit (4b) is characterized by comparative abundance of smaller clay mineral sizes (smectite) and marine organic matter, both of which favor depositions toward the open sea. On the other hand, the lower subunit (4d) is represented by abundance of primary clay types (illite, mixed layered) and terrestrial organic matter. The lower boundary of the Hatteras Formation is rather arbitrary; it is placed where the calcium carbonate content in the background pelagic sediment (identified by the presence of burrowed layers) exceeds over 20%, according to the definition of the CCD (van Andel, 1975).

A total of 185.5 m of the Hatteras Formation was penetrated from 764.5 to 950.0 m sub-bottom.

Subunit 4b

Subunit 4b, at the top of the Hatteras Formation, is composed predominantly of carbonaceous claystone of black (N1), grayish black (N2), dark gray (N3), and greenish black (5GY 2/1) color and interbedded silty claystone, dark greenish gray (5GY 4/1) and greenish gray (5GY 6/1) in color. The upper parts of the subunit, from Cores 27 to 30 (764.5–802.5 m sub-bottom), are dominantly silty claystones except Core 29, where the carbonaceous abundance peak is recognized. This peak may support previous work, which suggested a relatively high content of marine organic matter (Tissot et al., 1979). In the silty claystone-rich interval, the carbonaceous claystones range from 2 to 30 cm in thickness, whereas interbedded silty claystones are 5 to 50 cm in thickness (Fig. 19). The sedimentary structures in the upper part are obscure. The millimeter-thick lenticular and wavy laminations in the background (burrowed) silty claystones are observed. One of these silty stringers is composed of illite, kaolinite, and dolomite, with quartz and feldspar, indicating a detrital origin (Core 27, Section 1, 14 cm). Attapulgite is also found in a silty stringer (Core 36, Section 1, 60 cm). On the smear slide, silty stringers in the background sediment are composed of quartz, feldspar with the presence of microcline, and blue amphibole of metamorphic origin (Fig. 20). The lower part of the subunit, from Cores 31 to 39 (802.5–887.0 m sub-bottom), is composed mainly of carbonaceous claystones of 2 to 60 cm in thickness. They are black (N1), grayish black (N2), dark gray (N3), and greenish black (5GY 2/1). Macroscopic pyrite concretions occur in places. Interbedded silty claystones are dark greenish gray (5GY 4/1) and greenish black (5GY 2/1), and range from 1 to 50 cm in thickness (Fig. 21). Abundance of smectite and kaolinite in the clay fractions characterizes the subunit and may suggest pedo-

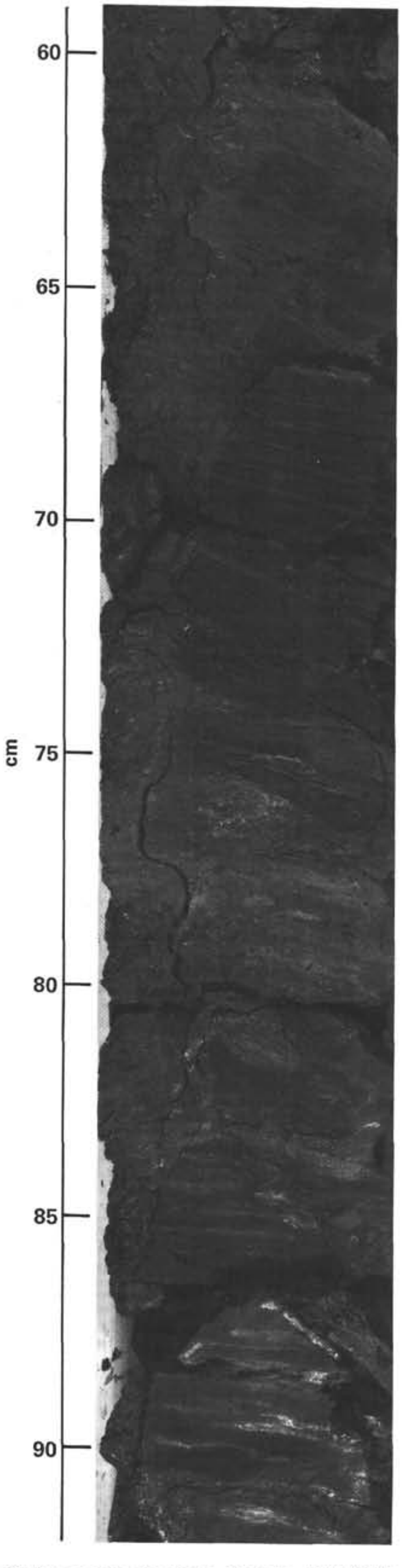

Figure 19. Carbonaceous claystone, Sample 534A-29-2, 59–92 cm. (Black [N1] carbonaceous claystone, 59–74 cm; dark grayish green [5GY 4/1] silty claystone with lenticular and mottled laminae, 74–80 cm; grayish black [N2] silty claystone with numerous flaser-type laminae, 80–92 cm.)

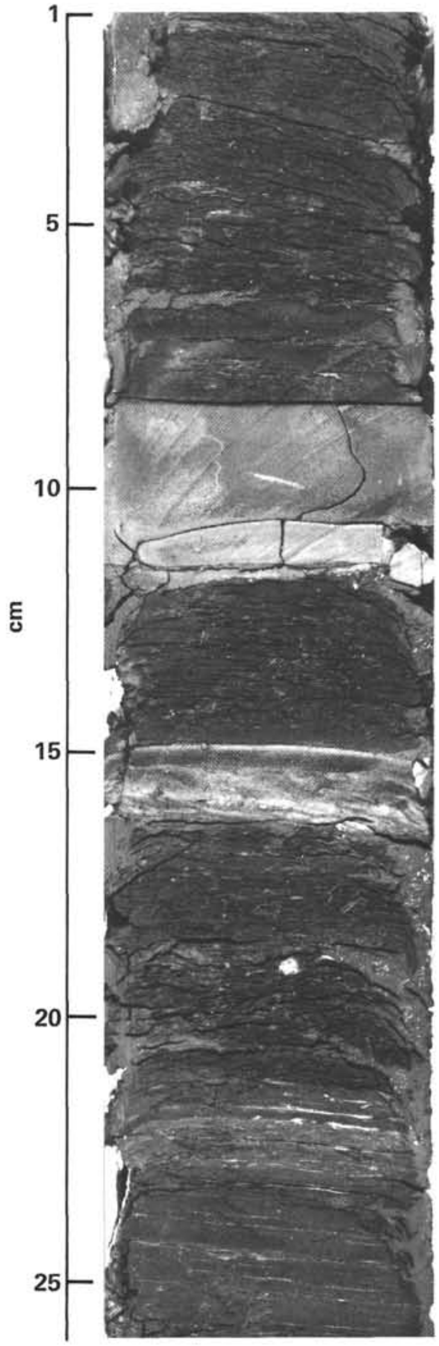

Figure 20. Carbonaceous claystone, Sample 534A-34-2, 1–26 cm. (Grayish black [N2] clay-rich carbonaceous claystone, 1–8 cm, 12–15 cm and 17–21 cm. Dark greenish gray [5NG 4/1] calcareous siltstone with vague parallel lamination and pyrite concretion, 8–12 cm. Concentration of many silty layers composed mainly of quartz, with a small amount of recrystallized calcite, 15–17 cm. Greenish black [5G 2/1] claystone with numerous intercalations of flaser-type silt layers, 21–26 cm.)

genic genesis of these clays on the land, controlled by a hot and humid climate (Chamley, 1979). Calciturbidites up to 30 cm in thickness occur frequently.

Subunit 4c

Subunit 4c is composed of variegated claystones of yellowish red (10R 4/2), dark yellowish brown (10YR

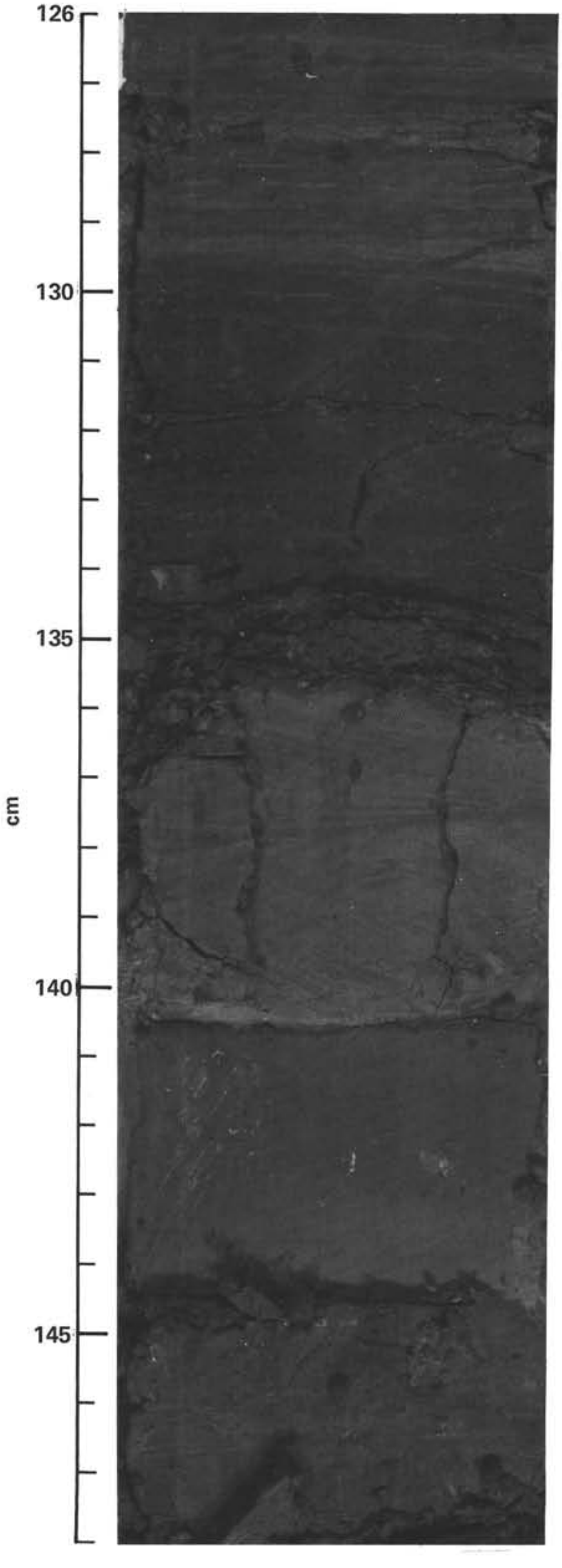

Figure 21. Carbonaceous claystone, Sample 534A-38-2, 125–148 cm. (Black [N1] homogeneous carbonaceous claystone with a few laminae only in the upper part, 130–136 cm. Olive gray [5Y 4/1] calciturbidite with climbing ripples, 136–140 cm. Dark greenish gray [5G 4/1] calcareous silty claystone, becoming siltier toward the bottom, 140–144 cm. Greenish black [5G 2.1] silty claystone with numerous flaser-type silty stringers, 125–130 and 145–148 cm.)

4/2), moderate brown (5YR 3/4), grayish olive (10Y 4/2), and greenish gray (6GY 6/1) colors. The interval spans from Cores 40 to 42 (887.0–914.0 m sub-bottom). The thickness of the bed is 27.0 m. Illite and mixed-layered clays are only recognized in the whole-rock sample analysis. Color change and resistant clay compositions indicate slow or winnowing deposition for this interval. One of the characteristics of the subunit is frequent occurrences of silty layers (millimeters thick) of turbidite origin (Fig. 22). In one sample, attapulgite is recognized (Sample 534A-41-5, 90 cm). In the background sediments, small burrows are frequently observed and sporadic occurrences of wavy or flaser-type laminations are noted. In the lower part of the subunit a few carbonaceous claystones of 2 to 7 cm thickness are intercalated. They are dusky brown (5Y5 2/2) to dark greenish gray (5GY 6/1) in color.

Subunit 4d

The lower part of the Hatteras Formation, Subunit 4d, consists of two carbonaceous cores in the upper and two calcareous claystone cores in the lower parts. It

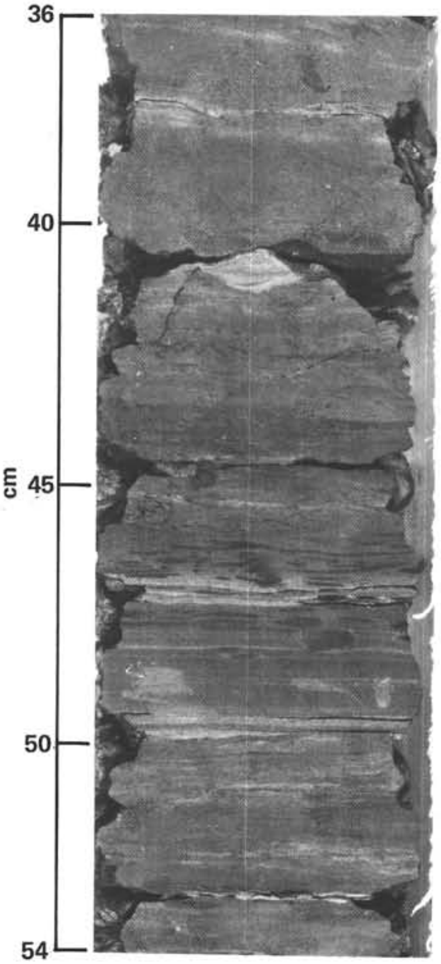

Figure 22. Variegated claystone, Sample 534A-41-6, 36–54 cm. (Moderate brown [5Y 3/4] claystone, 36–43 cm. Graded quartzose siltstone, 41 and 49.5 cm. Olive gray [5Y 3/1 to 4/1] claystone with numerous elongated lenticular beds of burrows, 44–54 cm.)

spans Cores 43 to 46 (914.0–950.0 m sub-bottom). The carbonaceous claystones are greenish black (5G 2/1) and olive black (5Y 2/1) to dark gray (N3) and are 2 to 25 cm in thickness. Silty stringers are abundantly intercalated, and pyrite concretions are occasionally observed in the black portion. The background silty claystones are dark greenish gray (5GY 4/1) and olive gray (5Y 4/1), and range from 3 to 70 cm. Burrows and wavy laminae are present, but burrows tend to be concentrated in olive gray (5Y 4/1) calcareous claystone. (Clay minerals are characterized by illite and mixed-layered clay on the whole-rock analysis. The lower part of the subunit is characterized by the presence of laminated calcareous claystones that range from 10 to 15 cm in thickness. The percentage of the calcareous claystones reaches 28% of the core at the bottom of the subunit. Calciturbidites up to 15 cm thick are present. Thus the subunit is transitional into the carbonate facies of Unit 5 below. During the deposition of Subunit 4d, calcium-carbonate accumulation decreased drastically. The termination of the carbonate accumulation might have been caused by the rapid lowering of the CCD starting at the end of the Barremian (Tucholke and Vogt, 1978). Yet little terrigenous material was supplied to Hole 534A except terrestrial organic carbon. As a result, terrestrial organic carbon content reached the highest level in this interval (Habib, this volume).

Blake-Bahama Formation (Unit 5)

In Hole 534A, 392 m of the Blake-Bahama Formation were cored (Cores 47–92), of which 298.4 m were recovered (76%). The upper boundary of the Formation is at the top of Core 47 where the *in situ* background sedimentation becomes calcareous, marked by the presence of well-cemented chalks. Below the boundary, the abundance of carbonaceous claystone progressively diminishes. The exceptionally high recovery of the Blake-Bahama Formation makes it possible to investigate in considerable detail depositional trends in the Early Cretaceous. Four distinct subunits, based on relative abundance of lithologies, are recognized and correlated with the type section of the Formation at Site 391 (Jansa et al., 1979). Distinctive intervals within the individual subunits are discussed later. The lower boundary of the Blake-Bahama Formation is located at the top of Core 92, where typical gray limestones pass into pink and red limestones and claystones characteristic of the Cat Gap Formation.

General Lithologic Description

In contrast to the overlying Hatteras Formation, almost all the lithologies of the Blake-Bahama Formation are calcareous. In approximate order of abundance, the lithologies are nannofossil-radiolarian micritic limestone, nannofossil chalks and marls, claystones, quartzose and calcareous siltstones, quartzose sandstones, and minor chert. Subunit 5a of the Hauterivian to the early Barremian ranges from Core 47 to 64. Starting with a transitional facies from the Hatteras Formation, which gives way downward to a sequence characterized by intercalations of quartzose and calcareous siltstones and sandstones, Subunit 5a shows structures indicative of turbidity current deposition (which is discussed later). Below this sequence, Subunit 5b (Cores 65–75) is marked by very finely laminated calcareous nannoplankton marls and chalks interstratified with bioturbated chalks containing minor intercalations of siltstones and claystones. Subunit 5c (Cores 75–84) is more heterogeneous, and is composed of interstratified, parallel laminated nannofossil chalks, bioturbated limestones, and minor claystones and siltstones. Lastly, Subunit 5d (Cores 84–92) is marked by more uniform, well-cemented limestones with only minor claystone partings and laminae. The Cat Gap Formation begins where the limestones and claystones change from gray to mostly pink and red.

Subunit 5a (Cores 47–64; 950–1107 m sub-bottom depth)

It is in Core 47 the *in situ* sediments, carbonaceous claystones, become markedly calcareous. Cores 47 to 49 constitute a transitional facies dominated by calcareous claystones, nannofossil claystones, and minor dolomitic limestones. Thin intercalations of dolomitic limestone and carbonaceous claystones (olive black 5Y 2/1) are reminiscent of the lower part of the Hatteras Formation. Sedimentary structures in this interval include parallel lamination and burrowing in subordinate intervals; scattered pyrite nodules are present. Smear slides confirm that, in contrast to the Hatteras Formation, well-preserved calcareous nannofossils are abundant. Several thin limestone intercalations (e.g., Core 48, Section 1, 98 cm), which are carbonaceous, are seen in thin section to be radiolarian micrites (wackestones) with scattered grains of quartz and calcite, compositionally very similar to redeposited material in Subunit 4d of the overlying Hatteras Formation.

Beginning at Core 49, it is clear that the majority of calcareous claystones, some of which are carbonaceous, are typically massive, graded, and unburrowed, often pyrite-rich. The thickness of individual beds of calcareous claystones rarely exceeds 15 cm; 5 to 10 cm is typical. Thin sections show that the calcareous claystones that occur throughout Subunit 5a are typically wackestones, with 15% micritic pellets, 3% quartzose silt, 75% clay matrix, 5% organics, and 2% pyrite.

From Core 51 downward there is progressively greater abundance of quartzose and calcareous siltstones and sandstones, showing grading, parallel and convolute lamination, and other features diagnostic of Bouma sequences of turbidites. For example, in a thin section of Core 51, Section 1, 139–141 cm, marly nannofossil chalk is seen to be a radiolarian micrite, with bioclasts of shallow-water carbonate material. The bioclasts include ooids, pisoliths, calcareous and algal fragments, together with micritic pellets and rare quartz grains. Of note is a thin section of Core 52, Section 1, 71–73 cm which contains a single grain of feldspathic basalt. The turbidites reach greatest thickness and relative volume in Core 58. In this core the turbiditic intercalations reach 1 m in thickness, with Bouma a–e units and combinations thereof. Section 2 of this core contains an intraclastic-bearing, debris-flow interval containing intraclasts of claystone (Fig. 23). Petrographically, the turbidites and the debris-flow component in this section contain variable admixtures of shallow-water carbonate and terrigenous quartzose material. For example, the terrigenous components of the sandstones (e.g., Core 58, Section 13, 127 cm) contain (in approximate order of abundance) quartz, muscovite, plagioclase, biotite, orthoclase, microcline, perthite, hornblende, epidote, and other heavy minerals, including zircon. In general, compared to the sandstones, the siltstones contain much greater volumes of muscovite and biotite. After the zenith of turbidite and debris-flow deposition in Core 58, the turbidites gradually wane in thickness, volume, and grain size. Downward, the thinner redeposited intervals tend to contain more calcareous than terrigenous material. For example, Core 59, Section 1, 100 cm, consists of micritic pellets, echinoderm plates and spines, shells, and rare benthic foraminifers without redeposited platform carbonate material.

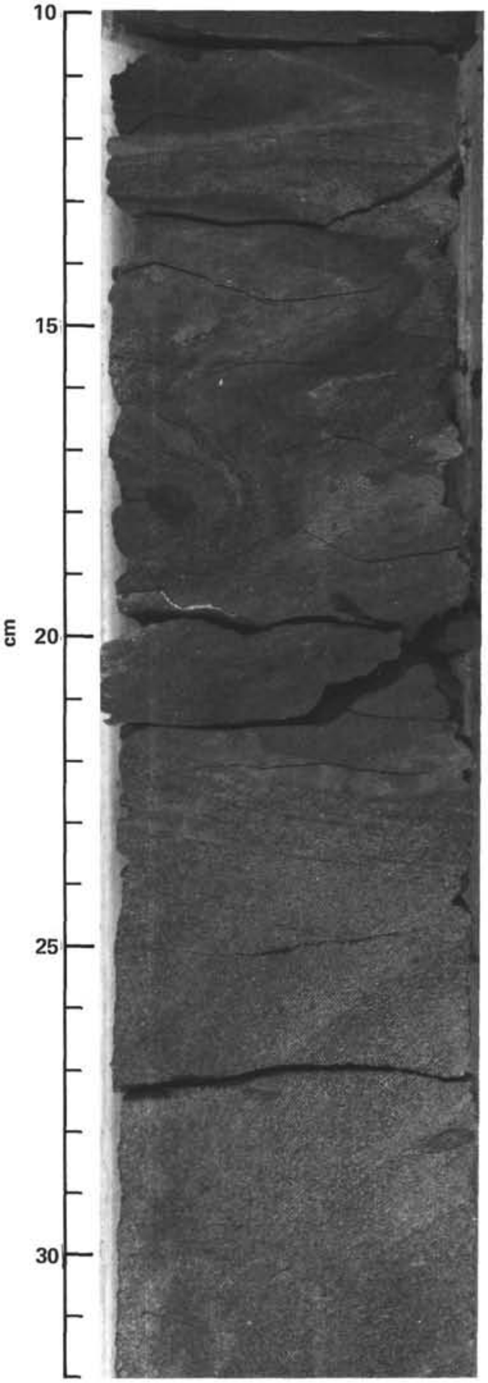

Figure 23. Subunit 5a—convolutely laminated dolomite, sandy limestones, and claystones. (The convolute lamination, which is attributed to slumping, occurs in the thickest turbidite intervals toward the base of Subunit 5a. Note the lower part [22–32 cm] is the base of a 1-m-thick turbidite intercalation. Finely laminated claystones are seen near the top [10–16 cm]. Sample 534A-58-2, 10–32 cm.)

Thin, intercalated, turbiditic calcareous claystones persist throughout Subunit 5a, becoming particularly abundant toward the base. Typically these claystones are greenish gray (5G 6/1). When viewed at high magnification, almost all the claystones are graded, the bottom 1 to 3 mm being silty. These claystones are invariably massive or contain very small-scale *Chondrites* burrows. Smear slides show that these claystones typically contain well-preserved calcareous nannofossils, in contrast to the interbedded nannofossil marls and limestones. Notably, all the dark gray to black carbonaceous intervals in Subunit 5a are associated with the graded calcareous claystones. In smear slides, organic matter ranges up to 21% but is normally very much less (< 10%). The organic material is in the form of anhedral lumps, intepreted as residual reworked organic matter.

Interpretation

The calcareous claystones and marly nannofossil chalks at the top of the Blake-Bahama Formation mark the last sediment to be deposited well above the carbonate compensation depth before the shallowing of the CCD during deposition of the Hatteras Formation. Carbonaceous claystone intercalations characteristic of the Hatteras Formation decrease downward in number and thickness; this may represent a lesser supply of organic matter to the basin during the Early Cretaceous or dilution of the same organic input by carbonate. The calcareous claystones are redeposited pelagic sediments dominated by clay and calcareous nannofossils. Notably, all the organic material in this subunit is associated with these turbiditic claystones. The source area may be the continental rise. In marked contrast, the thicker, coarser, and less persistent silt- and sand-sized turbidites represent a mixture of terrigenous and shallow calcareous material transported into the basin by turbidity currents. The terrigenous material was ultimately derived from plutonic igneous and metamorphic source areas. The assemblage of calcareous bioclasts is typical of a carbonate platform. The single intercalation of debris-flow material may present a violent event (e.g., earthquake, slump, or storm) in the source area. In general the gradual increase, then decrease, of the turbidites could reflect some combination of changes in sea level, rapid subsidence of the site, or tectonic movements in the source area.

Subunit 5b (Cores 65–75; 1107.5–1202.2 m sub-bottom depth)

After Core 64, the turbiditic siltstones are reduced to minor graded partings that are volumetrically insignificant. Subunit 5b, Valanginian–Hauterivian, is characterized instead by rhythmical intercalations of finely parallel-laminated marly chalks, bioturbated chalks, and minor graded claystones up to 5 cm thick, similar to those in Subunit 5a. Typically, the marly chalks and nannofossil chalks range from medium light gray (N4) to light gray (N3) and light olive gray (5Y 6/1). These characteristic chalks are invariably very finely laminated, generally totally unburrowed (Fig. 24). The laminated unburrowed units, often 10 to 30 cm thick, alternate with moderately to very highly burrowed nannofossil chalks and limestones in which there is either no lamination or else a vague lamination is preserved. By Core 67, the last turbiditic quartzose siltstones from Subunit 5a have disappeared. Thin, graded claystones persist, however; some are carbonaceous, as in Subunit 5a (e.g., greenish black 5G 2/1). Typically the burrowed intervals tend to be composed of purer carbonate than their finely laminated counterparts (e.g., up to 70%) as seen in a smear slide from Core 67, Section 1, at 50 cm. Particularly after Core 68, the burrowed material tends to be better cemented and transitional to limestones, whereas the laminated intervals are invariably marly nannofossil chalks. From Core 69 downward, the burrowed limestones are typically medium light gray (N4) to dark greenish gray (5GY 4/1) or dark gray (N3) to light bluish gray (5B 8/1). A notable feature is the presence of numerous calcispheres up to 2 mm in diameter. In thin section, these calcispheres are seen to be calcified radiolarians that may be moderately to highly abundant. Radiolarians are also abundant in the finely parallel-laminated chalk intervals, but in this case the radiolarian shells are usually elliptical due to compression during diagenesis. Occasional radiolarians that are partly to completely pyritized are always perfectly spherical; Freeman and Enos (1979) made a similar observation at Site 391. In Subunit 5b, chert is extremely rare but is found as occasional nodules, for example, in Core 69, Section 1, 5–10 cm. The fine lamination that characterizes these radiolarian-nannoplankton chalks becomes almost invisible when viewed in thin section. Many of the fine laminae are associated with relatively greater concentrations of quartz, and particularly mica. By contrast, the paler bands contain proportionately more carbonate. Poorly preserved radiolarians tend to be elliptical in the thicker dark laminae that contain more terrigenous material, whereas they are more spherical in the paler, more carbonate-rich laminae.

Interpretation

Subunit 5b is characterized by intercalations of very finely laminated marly radiolarian nannofossil chalks, bioturbated chalks, and limestones with minor claystone and siltstone partings. The lamination is unusual in its regularity and persistence over long intervals. The general aspect is reminiscent of lacustrine-type lamination.

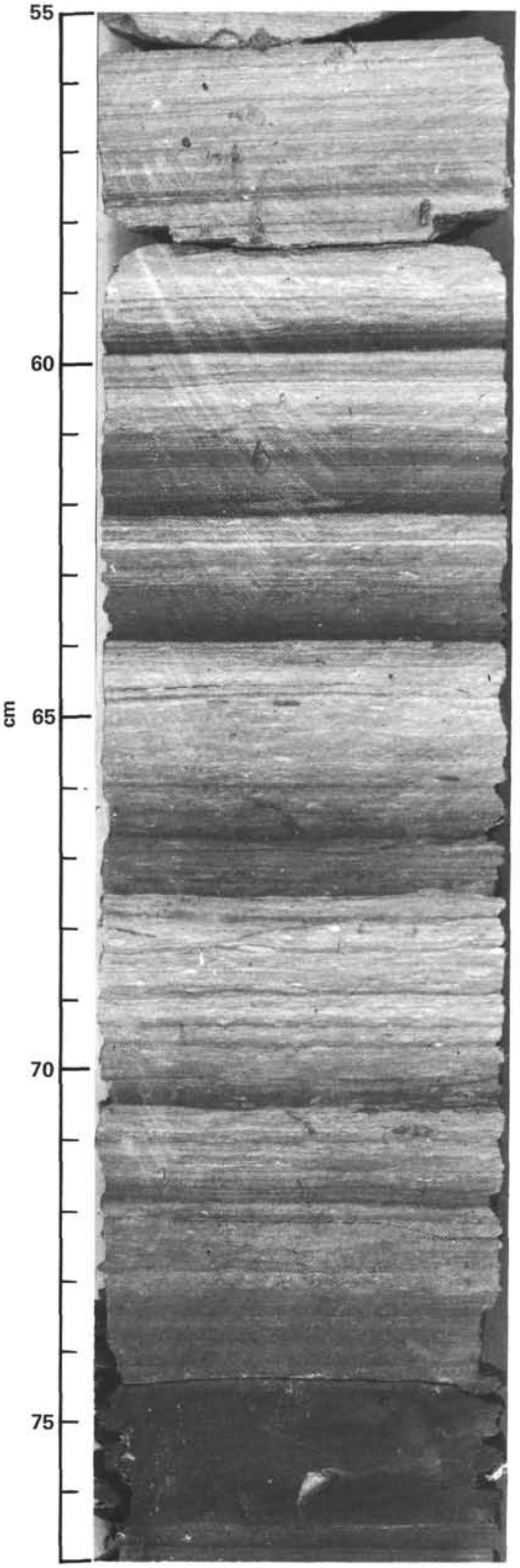

Figure 24. Subunit 5b—characteristic alterations of pale gray to dark gray, finely laminated nannoplankton chalk. (The dark laminae are relatively enriched in organic matter, mostly of terrigeneous origin. Note the massive dark gray claystone at 57–66 cm. This is a graded turbidite component mostly of clay and well preserved calcareous nannoplankton. Sample 534A-66-5, 55–77 cm.)

An understanding of the origin of the lamination must await more detailed studies, but factors that could generally play a role include (1) subtle changes in input of terrigenous material, perhaps related to major storms, earthquakes, and so on; (2) cyclical changes in productivity in calcareous and/or siliceous plankton; (3) current reworking; (4) diagenetic remobilization of calcite; and (5) differential compaction during diagenesis. From sedimentation rate calculations, the laminae occur at 20- to 50-yr. intervals. Notably, the finely laminated units are virtually totally unburrowed. Many of these intervals are gray due to an abundance of organic matter. The obvious interpretation is that bottom conditions were reducing and thus hostile to bottom life. By contrast, the very highly burrowed intercalated limestones presumably document periods of relatively oxidizing bottom conditions, possibly related to deposition below the oxygen minimum zone. In this context it is worth pointing out that the generally higher content of carbonates in these burrowed intervals may reflect the utilization and removal of organic matter by the burrowing organisms during periods of more oxidizing conditions. The thin graded claystones closely resemble those in Subunit 5a; they are again interpreted to be the result of redeposition of mostly pelagic calcareous nannofossil and radiolarian-rich material, with only minor terrigenous material concentrated in the several millimeter-thick graded base of individual beds. As noted earlier, a few turbiditic siltstones persist from Subunit 5a; the carbonate in these is mostly shelly micrite rather than carbonate platform material, as in Subunit 5a.

Subunit 5c (Cores 76–83; 1202.0–1268.0 sub-bottom depth)

Subunit 5c, late Berriasian–Valanginian, is characterized by essentially the same lithologies as Subunit 5b, but the assemblage is more heterogeneous from core to core. One distinct difference is that the burrowed intervals are limestones, in contrast to the chalks that predominate over limestones in Subunit 5b (Fig. 25). In general, the subunit consists of thinly parallel-laminated marly chalks, bioturbated limestones, thin graded calcareous siltstones, and intervals marked by a return of graded calcareous siltstones, as in Subunit 5a.

The finely parallel laminated intervals are almost identical to those in Subunit 5b. Colors range from light olive gray (5Y 6/1) to olive gray (5Y 4/1), medium dark gray (N4), and dark gray (N3). Some of the darker parallel laminated intervals contain distinctly carbonaceous claystone partings up to 0.3 cm thick. Again, conspicuous calcite grains are found, in thin sections, to be calcite-replaced radiolarians that have been flattened. The burrowed limestones may or may not show traces of parallel lamination. Stylolites appear and become generally more abundant downward, occurring only in relatively clay-poor limestones. Larger burrows are often filled with micritic pellets, possibly of fecal origin. Calcareous claystones, similar to those in the overlying units, are again present in Subunit 5c. Colors are dark greenish gray (5G 4/1) to olive gray (10Y 4/2), typically graded and free of burrows. The proportion of parallel-laminated bioturbated limestones and claystones differs markedly from core to core, in contrast to Subunit 5b, where the relative abundances of these lithologies are much more uniform. Core 73, for example, contains few thin burrowed intervals; there are more calcareous claystones relative to Cores 72 and 74. By contrast, burrowed limestones are relatively much more abundant in Core 75. Core 76 is marked by the return of turbiditic claystones, whereas Core 77 has more burrowed inter-

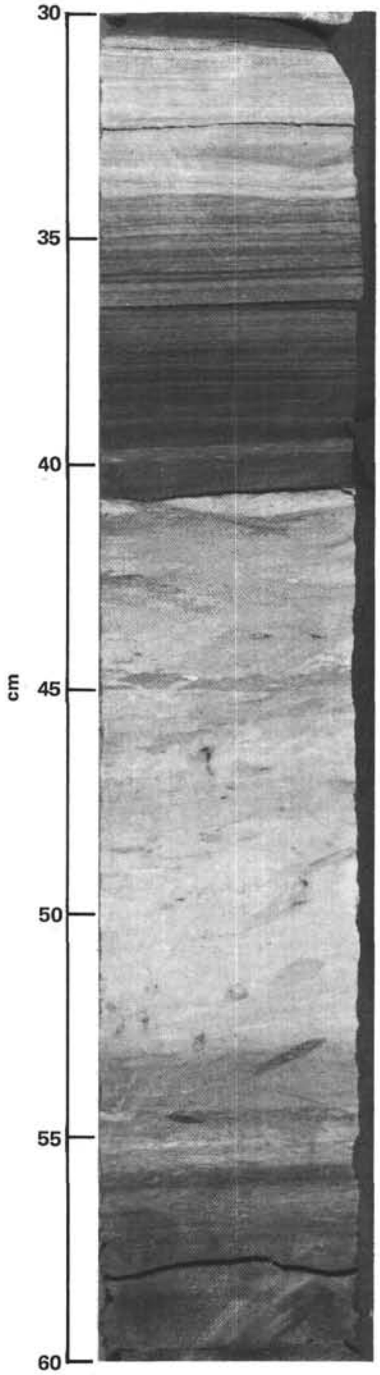

Figure 25. Subunit 5c—typical alternation of pale to dark gray finely laminated nannoplankton chalks and highly bioturbated nannoplankton radiolarian-rich limestones. (Sample 534A-74-1, 30–60 cm.)

vals, recalling the situation in Core 74. Cores 78 and 79 are distinctly dominated by parallel-laminated claystones with only volumetrically minor burrowed limestones.

Thin sections show that the bioturbated limestones are nannoplankton radiolarian micrites, in which, as in Subunit 5b, the radiolarians are entirely replaced by calcite or pyrite. Rare quartz grains are present and minor volumes of phosphate. In the finely laminated chalk intervals radiolarians are again moderately to highly abundant. Some of the individual pale laminations comprise fused, en echelon, flattened radiolarian shells replaced by calcite. In other cases the laminations are characterized by subtle variations of carbonate and fine-grained terrigenous material, as in Subunit 5b.

Interpretation

Subunit 5c comprises similar lithologies to those of Subunit 5b, but it is markedly more heterogeneous in detail. Also, the bioturbated intervals tend to be composed of limestone rather than the chalk in Subunit 5 intervals, where diagenesis is less advanced. Variations in the relative volumes of the various lithologies in individual cores may reflect some combination of changes in sea level, climate, and sedimentation rate, with oxygenated versus reduced seafloor conditions. The different variables operating in Subunit 5c can only be disentangled by postcruise laboratory studies, particularly of mineralogy and chemical analysis. One notable point is that the spherical shape of the calcite-replaced radiolarian shells in the bioturbated limestones indicates that they were cemented prior to the occurrence of significant compaction; in marked contrast, the radiolarian shells in the parallel-laminated chalks are strongly flattened, indicating that significant compaction had taken place prior to lithification. The difference in time of lithification correlates with the relative abundance of clay; fine-grained clays that are abundant in the finely laminated chalks are known to inhibit diagenetic carbonate cementation. Another notable point is that despite the abundance of radiolarians, chert is extremely rare. This factor suggests that dissolution of the siliceous microfossils and loss of silica to seawater occurred close to the sediment/water interface.

Subunit 5d (Cores 84–92; 1268.0–1342.0 m sub-bottom depth)

Around Core 84 there is a marked change in lithology to more uniform radiolarian nannofossil marls, chalks, and limestones with minor claystone partings. The uniformly parallel-laminated chalks that characterize Subunits 5b and 5c disappear. Quartzose and calcareous redeposited facies are also absent. Typically, in Berriasian Subunit 5d, two lithologies are interbedded with gradational contacts: marly nannofossil chalk, which is transitional to limestone (color 5GY 6/1 to 5G 5/1), and nannofossil claystone (dark greenish gray 5GY 4/1 to 5Y 4/1) (Fig. 26). In the lower part of the subunit, light gray (N7) and light bluish gray (5B 7/1) nannofossil limestones are abundant. The marly nannofossil chalks and limestones are typically moderately to strongly burrowed. The burrow-fill material is both darker and

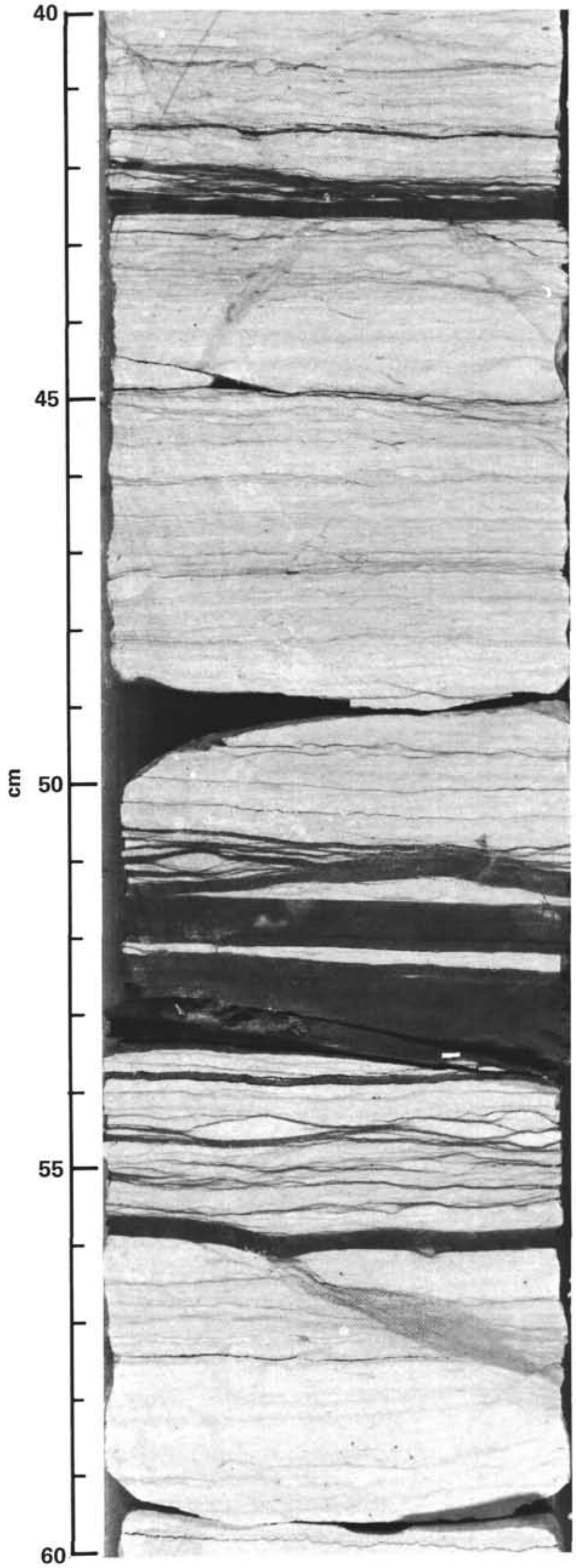

Figure 26. Subunit 5d—typical radiolarian nannoplankton limestones intercalated with seams of calcareous claystone. (Note the anastomosing stylolites composed of material that is identical in the thicker claystone seams. Sample 534A-81-3, 40–60 cm.)

lighter in some cases than the host sediment. Burrows are normally seen to have severely disrupted the original parallel lamination. By contrast, the nannofossil marls are less intensely burrowed and less well cemented, with laminae of clay-rich material spaced about 0.5 to 0.3 mm apart. Compositionally similar clay layers reach 1.5 to 3 cm in thickness. Numerous stylolites, particularly in the pure limestones, give the effect of a wavy, highly irregular or anastomosing texture in places. Occasional intervals up to 5 cm thick (e.g., Core 85, Section 2, 75 cm) possess a micronodular texture due to diagenetic precipitation of calcite. Synsedimentary microfaults have been noted. Aptychi are abundant, but molds of ammonite shells are found occasionally. Several intervals contain occasional nodules of vitreous replacement chert up to 5 cm in diameter (e.g., Core 86, Section 1, 54 cm). A single occurrence of small-scale slumping was observed in Core 91, Section 2, 140–150 cm. Another feature in these cores are intervals up to 7 cm thick containing numerous, subrounded to elliptical segregated clasts of micritic limestones, which are typically lighter in color than the host sediments ("microbreccias"). These appear to be primary in origin. Finally, in Section 2 of Core 92, the typical gray limestones give way to pink and red carbonate characteristic of the Cat Gap Formation.

Interpretation

Subunit 5d is lithologically much more uniform compared to those above it. Both the marly chalks and limestones are seen in thin section to be radiolarian nannofossil micrites. The marly chalks contain a greater abundance of fine-grained terrigenous material and are, again, less cemented than their more burrowed limestone equivalents. Some silica was apparently retained in the sediments long enough to favor the diagenetic formation of chert nodules composed of vitreous chalcedonic quartz. The claystones, as throughout the whole formation, remain terrigenous in origin; thicker (up to 6 cm) partings show extremely fine-scale grading and parallel lamination signifying turbidite deposition. A single intercalation of red and pink calcilutites in Core 83, Section 5 represents a return to conditions characteristic of the underlying Cat Gap Formation. The red color may be due to a period of more highly oxidizing bottom conditions, a greater input of oxidized iron, reduced input of organics, or some combination of these variables.

Regional Comparisons

Site 391 is the type section of the Blake-Bahama Formation (Jansa et al., 1979). In Volume 44 of the *Initial Reports* (Benson et al., 1978), four subunits were recognized that closely correspond to those at Site 534, which are shown in Figure 27. In the definition of the type section, Jansa et al. (1979) chose to combine Subunits 4b and 4c at Site 391 to a single middle subunit, composed of parallel laminated and burrowed marls, chalks, and limestones, with subordinate calcareous claystones. By contrast, in the Cat Gap area (Sites 4, 5, 99, and 100; Fig. 28) the Blake-Bahama Formation is less lithified as a result of a thinner overburden. Oceanward, on the Bermuda Rise (Site 387), the Blake-Bahama Formation contains significant volumes of quartzitic chert, dolomite, and siderite, in contrast to Site 534. At Site 105 the sequence consists of alternations of hard, white to pale gray, micritic limestone, and soft laminated greenish gray clayey limestone. Data are summarized by Jansa et al. (1979). By contrast, at Site 534, the closest site yet drilled relative to continental margin sources, the Blake-Bahama Formation contains a relatively high abundance of terrigenous and detrital carbonate material, as well as carbonaceous material, particularly near the contact with the Hatteras Formation.

Finally, it is worth noting that sequences of Early Cretaceous pelagic limestones are also present both in the eastern Atlantic and the western Mediterranean. General comparisons have been drawn by Bernoulli (1972) and Bourbon (1978).

Conclusion

Excellent recovery of the Berriasian to Barremian Blake-Bahama Formation allows the Early Cretaceous history of the Blake-Bahama Basin to be elucidated in considerable detail. The various facies record a delicate interplay between detrital and pelagic sedimentation strongly modified by diagenetic processes. Postcruise laboratory studies are needed to gain a better understanding of the various factors affecting the genesis of this interesting Formation.

Units 6 and 7—Cat Gap Formation and Unnamed Unit

In Hole 534A, 292.5 m of Middle and Upper Jurassic sediments were drilled (sub-bottom depth interval of 1342.0–1635.5 m), of which 112.5 m were recovered (38%). These were subdivided as follows (Fig. 29):

Unit 6
Subunit 6a—grayish red calcareous claystone
Subunit 6b—limestone turbidites interbedded with dark greenish gray claystone

Unit 7
Subunit 7a—variegated dark reddish brown to grayish green claystones
Subunit 7b—gray limestone turbidites interbedded with dark variegated claystones
Subunit 7c—dark gray, marly limestones interbedded with dark greenish gray radiolarian-rich claystones
Subunit 7d—greenish black to black claystone with radiolarian silt lenses
Subunit 7e—dusky red calcareous claystone

Subunits 6a and 6b are similar in several aspects to the Cat Gap Formation of Jansa et al. (1979); Subunit 7a is perhaps a lower transition facies of the Cat Gap

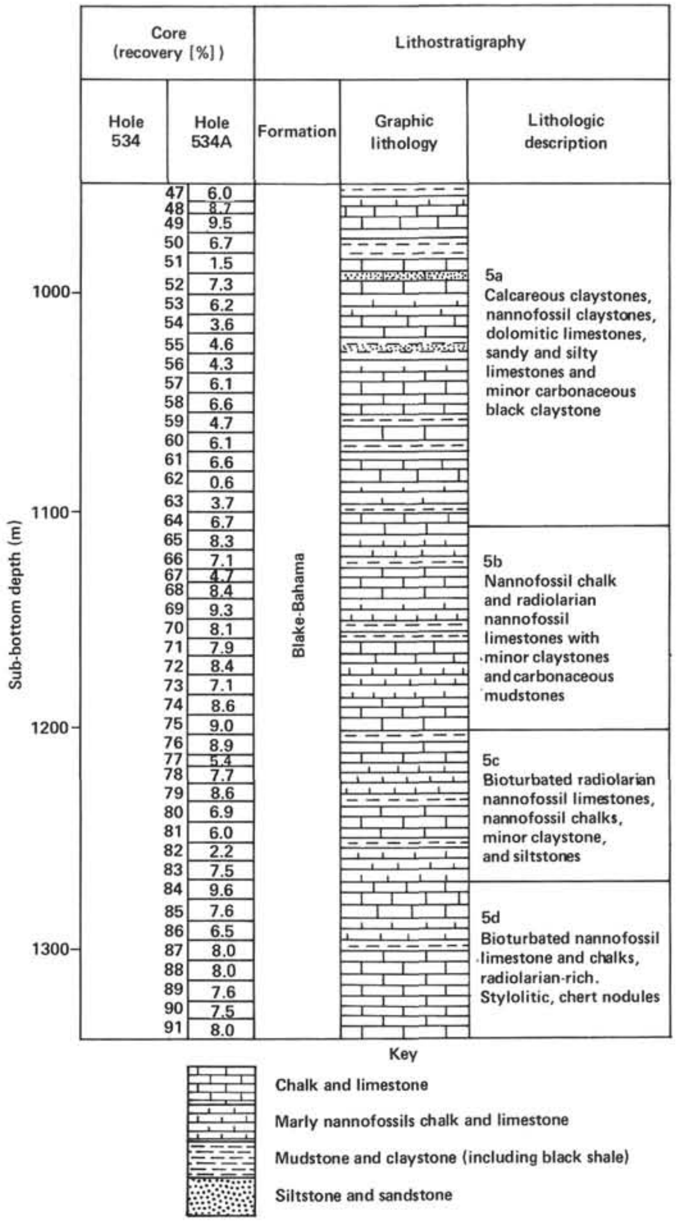

Figure 27. Generalized stratigraphic logs showing the relative thickness, age, and lithologies of the Blake-Bahama Formation at Site 534.

(Ogg et al., this volume); and Subunits 7b through 7e[3] have not been encountered before in DSDP holes in the western Atlantic. These units will be discussed separately.

Subunit 6a—Grayish Red Calcareous Claystone

Subunit 6a (Core 92, Section 2, 40 cm to Core 103, Section 1, 107 cm, 1342.0–1429.0 m sub-bottom) ranges from Tithonian to Kimmeridgian. Coring of this interval spanned 87 m, of which 57 m were recovered (68%).

Contacts

The contact of Subunit 6a to the Blake-Bahama Formation is placed at the highest occurrence of red calcareous claystone interbeds between white limestones (Core 92, Section 2, 40 cm). There is a gradual increase in the ratio of limestone to calcareous claystone from Cores 94 to 91 with no apparent break in sedimentation, and a gradual decrease in abundance of red calcareous

---

[3] Note that Subunits 7b and 7c originally belonged in a Subunit 7b as defined during the cruise; likewise Subunits 7d and 7e originally were defined as a Subunit 7c, as indicated:

Definition of lithological Subunits 7a through 7e.

Lithological subunit	Shipboard assignment by sample (core-section, cm level)	Site 534 report assignment by sample (core-section, cm level)
7a	111-1, 7 through 117-1, 26	111-1, 7 through 117-1, 26
7b	117-1, 26 through 125-4, 14	117-1, 26 through 120 (top)
7c	125-4, 14 through 127,CC (10)	120 (top) through 125-4, 14
7d		125-4, 14 through 126-3, 75
7e		126-3, 75 through 127,CC (10)

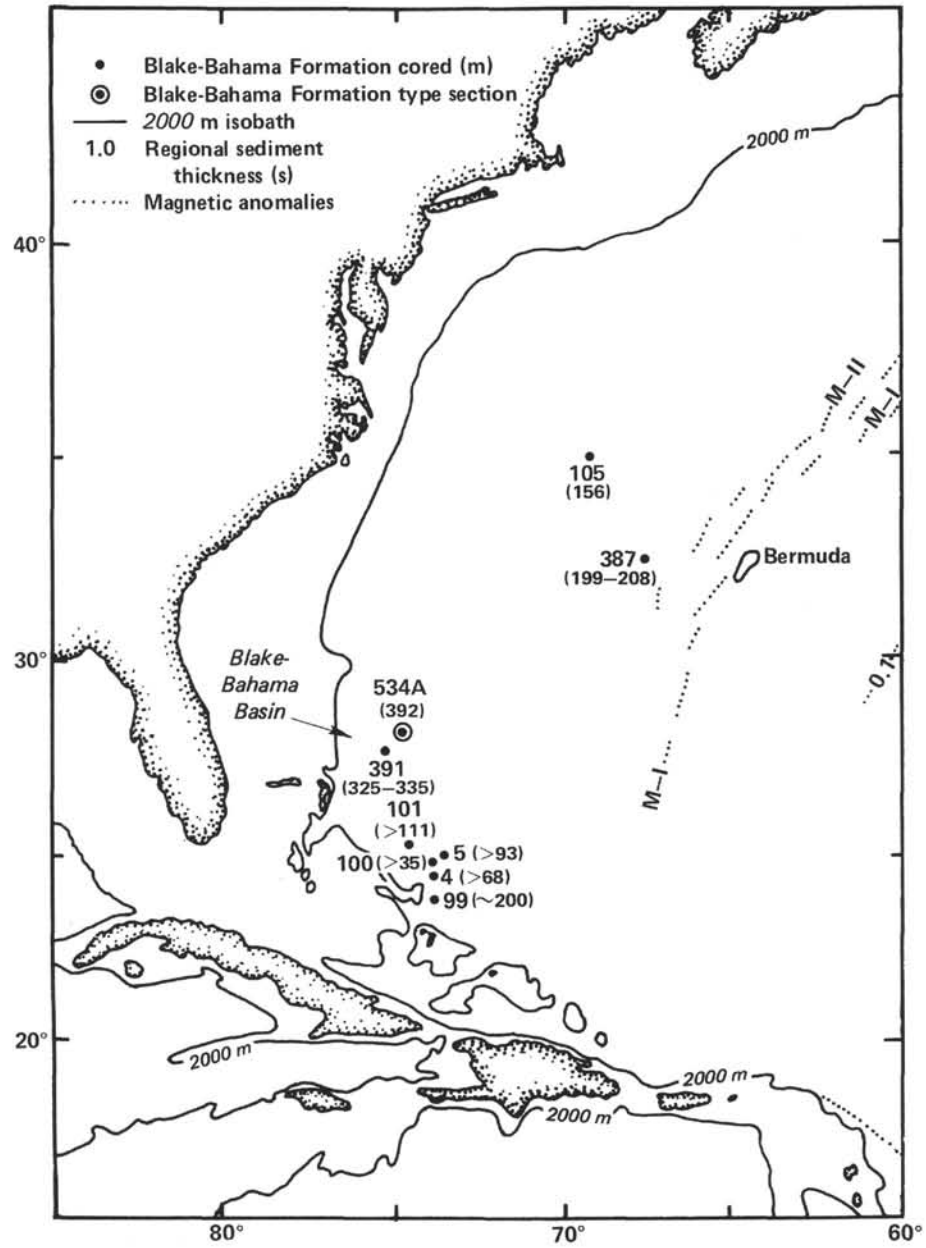

Figure 28. Boreholes where Blake-Bahama Formation sediments have been cored. (Formation thickness in meters is shown in parentheses. Horizon β correlates approximately with the top of the Blake-Bahama limestone; the eastern boundary indicates mapped pinch-out on basement [after Mountain and Tucholke, 1977], near Magnetic Anomaly M-11. This anomaly has been interpreted by van Hinte [1976a] to be Valanginian. Note that the section at Hole 534A, 392 m, is the thickest sequence of the Blake-Bahama rocks cored to date. [Figure after Jansa et al., 1979].)

claystone interbeds and intensity of red color from Cores 94 to 92. Arbitrarily defining the upper boundary of Subunit 6a by the highest occurrence of any red color follows the subdivisions in the Upper Jurassic used at other DSDP sites (Sites 99, 100, 105, 367, and Hole 391C) and the Cat Gap Formation definition of Jansa et al. (1979).

The basal contact between Subunits 6a and 6b is placed at Core 103, Section 1, 107 cm, at the top of the highest thick bed of light gray bioclastic-pelletal limestone. This lower boundary is also transitional, because these limestone turbidite beds occur as high as Core 100, but are usually much thinner and of finer-grained texture. Below Core 103, grayish red claystones are a very minor lithology.

Lithologic Description

The major lithology of Subunit 6a is grayish red calcareous claystone, the color ranging from dusky red (10R 3/4) to grayish red (5R 4/2) to dark reddish brown (10R 3/4) to grayish brown (5YR 2/2), with a general trend toward darker colors near the base of the unit. Greenish gray mottles occur locally, especially around shell fragments and burrows, and as bands parallel to bedding.

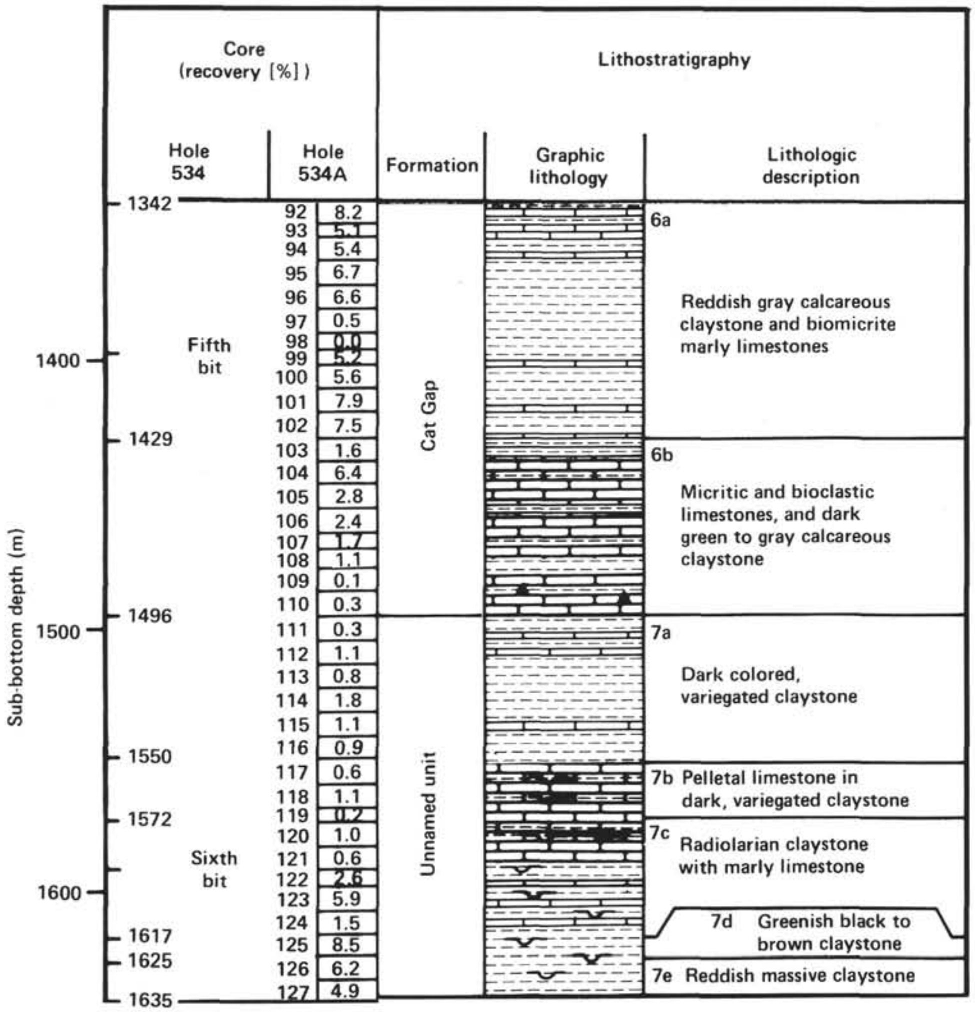

Figure 29. Lithology summary of Cat Gap (Unit 6) and unnamed unit (Unit 7).

This is probably a local reduction of the iron oxide. The composition ranges from a calcareous claystone to marly nannofossil chalk. Interbeds of pale red (5R 6/2) to greenish gray (5GY 6/1) marly limestones occur with increasing abundance toward the top of the subunit. In the top 20 m (Cores 92, 93) these limestone beds are dominant. In both limestones and claystones, laminations are frequently disrupted by bioturbation (especially *Chondrites*).

The main fossils found in Subunit 6a are nannofossils, abundant calcified radiolarians, calpionellids (to Core 94), calcispheres, rare pieces of the pelagic crinoid *Saccocoma* (in Core 94), and rare ammonites, aptychi, and shell fragments. An ammonite and numerous shell fragments that retain a pearly luster were found in Core 100.

Within the interval between Cores 99 and 101 occur several black carbonaceous claystone layers and one large pyrite nodule. Siliceous limestone nodules and thin microbreccia layers are found sporadically in the upper 30 m. There is a nodular texture in a few thin marly layers.

Depositional Environment

The red calcareous claystone and associated marly chalk were deposited on a quiet bottom above the carbonate compensation depth (CCD); there was an oxidizing environment within the sediment as well as moderate bioturbation. This description is based on the lack of slump or current features, abundant nannofossils and other bioclasts, frequent burrows in a vaguely laminated sediment, and the red color. Redeposited beds are minor but increase in abundance and thickness from Core 100 downward. The red claystones were deposited above the aragonite compensation depth (ACD) during part of the interval. This event is indicated by the rare ammonites and pearly luster on shells in Core 100 and the XRD (X-ray diffraction) identification of aragonite in the claystones of several cores (see the clay mineralogy section that follows).

Regional Correlation

The upper facies (''*Saccocoma*'' microfacies) of the Cat Gap Formation at Sites 99, 100, 105, and Hole 391C

(Jansa et al., 1979) is a red calcareous claystone that has overlapping age assignments and a general sedimentary character similar to Subunit 6a of Hole 534A. However, the microfacies of the red calcareous claystones of 534A do not have a *Saccocoma*-rich interval that is a characteristic of the upper portion of the Cat Gap. Because *Saccocoma* is found predominantly in the lower Tithonian, perhaps this interval was not recovered from Hole 534A. The facies of Subunit 6a is also much richer in radiolarians, especially in the upper portion. The facies of Subunit 6a is similar to the Upper Jurassic sediments of Site 367 in the eastern Atlantic (Jansa et al., 1978). The red color is also common to Upper Jurassic pelagic limestones and marls of the Tethys (Rosso ad Aptychi, Ammonitico Rosso Superiore), which suggests that an oxidizing environment within pelagic sediments was typical of both the Tethys and the Atlantic during the Late Jurassic.

Subunit 6b—Interbedded Light Gray Limestones and Dark Greenish Gray Claystones

Subunit 6b (Core 103, Section 1, 107 cm to Core 111, Section 1, 7 cm, 1429.0–1495.6 m sub-bottom) spans the early Kimmeridgian to the Oxfordian. The interval cored was 66.6 m, of which 17.6 m were recovered (27%).

Contacts

The top of Subunit 6b is placed within Core 103 because the lower portion of this core and the underlying next few cores are dominated by light gray limestones of turbidite origin with interbedded greenish gray calcareous claystones. Between Cores 103 and 104, fine pelagic bivalves, which are abundant in Subunit 6b, seem to disappear, which suggests a possible hiatus in sedimentation that was not recovered (the drilling of Core 103 indicates penetration of a hard zone in the unrecovered[?] lower 5 m).

The base of Subunit 6b is placed at Core 111, Section 1, 7 cm, below which dark variegated claystones dominate the recovered sediments. The contact is probably gradational; and extremely poor recovery in Cores 109 through 113 complicates definition of the boundary.

Lithologic Description

Three main types of sediments are interbedded throughout Subunit 6b: (1) Calcareous claystone with dark gray colors ranging from medium dark gray (N4) to greenish black (5GY 2/1). The claystone is laminated to moderately bioturbated with *Chondrites* burrows; the fossil assemblage is mainly nannofossils, tiny pelagic bivalves, and calcified radiolarians. The pelagic bivalve shells generally have prismatic sparry calcite overgrowths. (2) Micritic limestone that is light gray (N7) to dark greenish gray (5GY 4/1). The common (5% or less) bioclasts are generally micritized. Partial recrystallization to microspar is common. The beds are massive with minor bioturbation or with vague laminations. (3) Limestone of packed skeletal–pelletal microsparite to sparite; ranging from light gray (N7), light bluish gray (5B 7/1), yellowish gray (5Y 8/1), light olive gray (5Y 6/1), to greenish gray (5GY 5/1). The microfacies consists mostly of pellets and micritized grains in addition to ooids (Core 106), benthic shallow water foraminifers, and echinoderm and shell fragments. The beds generally have features of turbidite deposits (including graded bedding, current cross-bedding, convolute to parallel laminations, claystone interclasts [Core 106], flute casts, and scoured bases), with burrows in upper portions. Figure 30 shows some of these turbidite features in medium-grained limestone beds. In Section 2 of Core 107, there is an interesting feature—complex normal- and reversed-graded intervals within a single bed.

A minor lithology (found in Cores 105, 108, and 110) is grayish red to blackish red calcareous claystone, perhaps a forerunner of the overlying facies of Subunit 6a. These occur only within calcareous claystone intervals that lack abundant limestone beds. Other minor lithologies are thin microbreccias(?) (Cores 104, 108) and a yellowish brown chert (fragment in Core 109).

Two interesting diagenetic textures seen here are (1) the boudinage and pinching of thin micrite limestone beds when they are interlayered between clay beds and (2) fibrous spar overgrowths on tiny bivalve shells in the claystones that may coalesce to form discontinuous en echelon spar layers within the sediment (sometimes called "beef" texture in the Lias of Southern England). This latter texture is well developed in Core 104.

Depositional Environment

The claystones of Subunit 6b are interbedded with two types of limestones. One is an obvious turbidite of transported shallow-water carbonate; the other is a fine micritic limestone that is probably a redeposited fine-mud carbonate, also of shallow origin. Seismic reflection data indicate that Subunits 6a and 6b thicken towards the Bahamas and increase in interval velocity, suggesting that more carbonate turbidites occur in that direction. Those carbonate banks were probably the source of the coarse skeletal-pelletal turbidites. The micritic limestones may be turbidites, possibly derived from the continental slope.

The dark greenish gray claystones represent the pelagic background sedimentation. When there is an interval with few limestone turbidites, the claystones become dark reddish gray in color, suggesting that the turbidites either buried organic matter in the claystones before it was oxidized by bottom water or that the turbidites transported organics, which then created a reducing environment during diagenesis. Another possibility is that the bottom waters were slightly anoxic during most of this period. No evidence of bottom currents were observed in the claystones. Burrowing organisms were relatively rare.

Regional Correlation

The presence of fine bivalve shells in the claystone and some of the limestones is also a characteristic of the "filament" microfacies of the lower part of the Cat Gap Formation at Site 105 (Jansa et al., 1979). However, limestone turbidites dominate Subunit 6b; they were not important in the Site 105 facies (unless the distal ends of such turbidites are the thin limestone layers that later

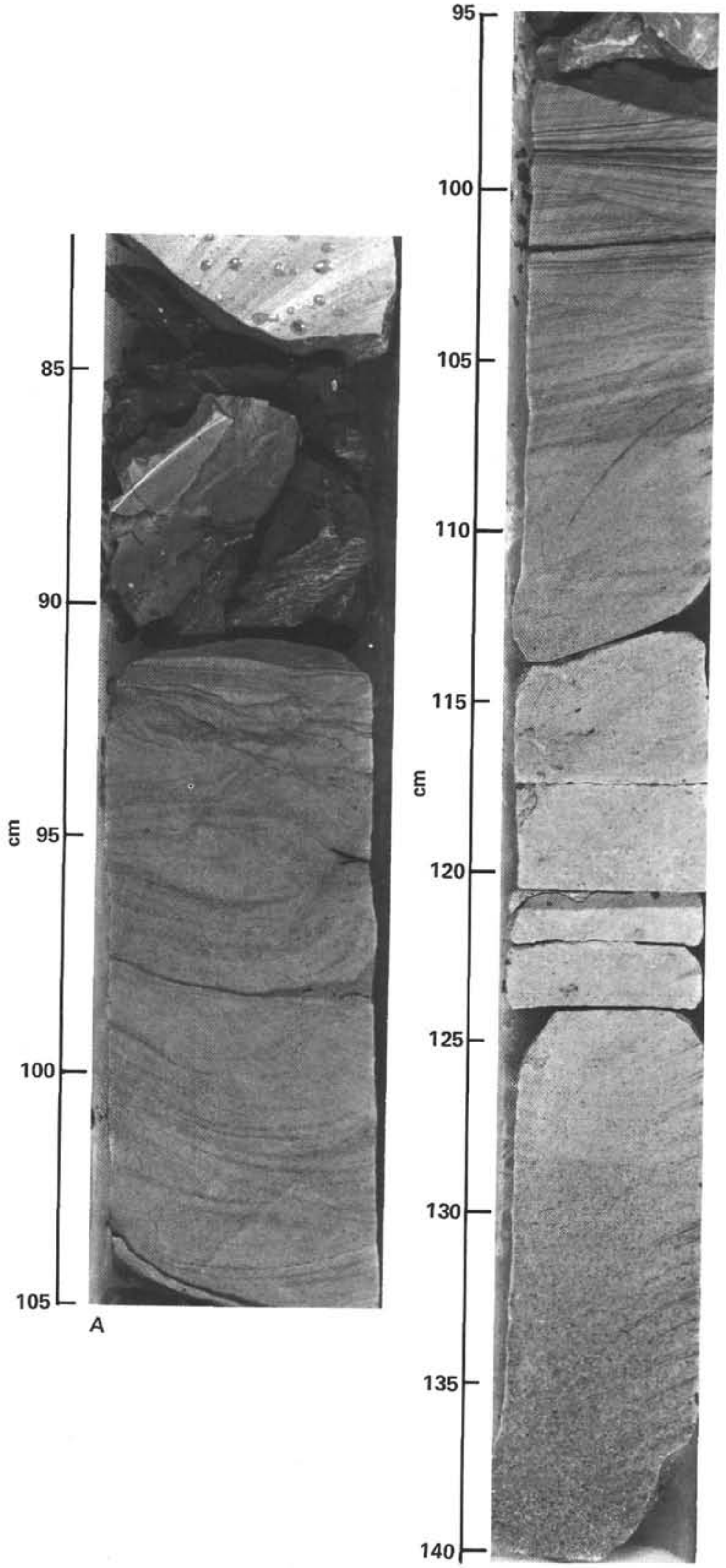

Figure 30. A. Interbedded light gray turbidite limestone and dark greenish gray claystone in Sample 534A-105-1, 82–105 cm of Subunit 6b, Cat Gap Formation. B. Graded tan gray turbiditic limestone interbeds in Sample 534A-106-1, 95–140 cm of Subunit 6b. Cat Gap Formation.

became the limestone clasts in the claystone of Site 105, as suggested by Bernoulli [1972]). Therefore, Subunit 6b is regarded as a lateral equivalent of the "filament" microfacies of the Cat Gap Formation, but the subunit cannot be regarded as identical to that facies at the "type" section.

Subunit 7a—Dark Variegated Claystones

Subunit 7a (Core 111, Section 1, 7 cm to Core 117, Section 1, 26 cm; 1495.6 to 1549.8 m sub-bottom) is an Oxfordian interval that spans 54.2 m, 6.2 m of which were recovered (11%).

Contacts

The upper contact is placed at the top of the highest interval of dark variegated claystones that were recovered (Core 111, Section 1, 7 cm). The basal contact is placed at the top of the first thick limestone turbidite at Core 117, Section 1, 26 cm. Due to the very poor recovery throughout this interval and at the "contacts," these assignments are based partly on the drilling time per core. The interval from Core 111 to 117 had rapid drilling times compared to overlying Subunit 6b or underlying Subunit 7b, indicating the predominance of claystone over limestone in 7a. The boundaries are probably transitional, and the contacts are assigned on the basis of incomplete data.

Lithologic Description

Subunit 7a has dark variegated claystones occasionally interbedded with redeposited micritic limestones. The claystones have three basic color types: (1) "reddish"—pale red (5R 6/2), grayish red (5R 4/2), dusky red (5R 3/4), medium brown (5YR 3/4), grayish brown (5G 6/1), or blackish red (5R 2/2); (2) "greenish"—olive gray (5Y 4/1) to greenish gray (5GY 6/1); and (3) "black—dark bluish gray (5B 4/1), dark greenish gray (5GY 4/1), greenish gray (5G 6/1), olive black (5Y 2/1), or dark gray (N3). These three types occur in 1- to 5-cm color bands with either sharp or gradational contacts. Some general characteristics suggest cyclic turbidite deposition. For example, the "black" (color type 3) layer always has a sharp upper contact to overlying "reddish" (color type 1) or "greenish" (color type 2) layers, but often a transitional contact to the underlying layers, with *Chondrites* burrows carrying dark greenish gray clay down into the reddish gray or olive gray. At the base of the "reddish" or "greenish" layers there is often a very thin (0.5 cm) layer of greenish gray, finely laminated calcareous siltstone, which may grade upward into the claystone. The "greenish" (color type 2) layer frequently occurs as mottles in the reddish gray. These indications suggest that the dark greenish gray ("black") claystone is the background sediment, and that there was abundant turbidite input of reddish gray ("reddish") clays (commonly with calcareous silt), which were often reduced to give an olive gray ("greenish") color. The allochthonous (possibly redeposited) "reddish" olive gray claystones (subsequently referred to as "allochthonous" claystones) appear to comprise about 75% or more of the recovered claystone sediments of Subunit 7a. The abundance of nannofossils in the host and (possibly redeposited) allochthonous claystones show no consistent variations. Up to 5% quartz silt grains are present in some layers.

Interbeds of micritic and pelmicritic limestones occur occasionally within the variegated claystones. These limestones are very light gray (N8) to greenish gray (5GY 6/1), are massive to laminated with occasional convolute laminations, and also have a very low abundance of bioclasts (except a bed in Core 116, which has 20-25% echinoderm fragments and calcified radiolarians).

Depositional Environment

The dark variegated claystone of Subunit 7a had turbidite input from two sources that fed into a slowly accumulating background sediment of dark greenish gray clay. The dark greenish gray clay (10–15% of the recovered sediment) is often burrowed and shows no evidence of current reworking. The dominant type of turbidite is reddish brown claystone with minor calcareous silt. Reduction after deposition caused abundant olive gray mottling, especially where the reddish claystone is in contact with the dark greenish gray claystone (background sediment). This mottling suggests that the bottom sediment was organic-rich or in an anoxic environment, whereas the turbidite clays were low in organic content or came from an oxidizing environment. The source area of the turbidite clays was pelagic, because they are low in carbonate and terrestrial clastics (indeed, these clays are very similar in composition to the background claystone). The second type of turbidite is bioclast-poor micritic limestones, which are similar to those in Subunit 6b. Their source area must have been more carbonate-rich than the claystone turbidites, but not in shallow water depths. The shallow-water limestone turbidites of Subunit 6b are not present.

Regional Correlation

This facies has not been recovered at any previous site. It may be included later as a transitional lower facies of the Cat Gap Formation, but is distinctly different from any sediments at Sites 100 or 105, which are the basis of the definition of that Formation. For further discussions see Ogg et al. (this volume) and Gradstein and Sheridan (Leg 76 synthesis, this volume).

Subunit 7b—Olive Gray Limestones in Dark Variegated Claystone

Subunit 7b (Core 117, Section 1, 26 cm to the top of Core 120; 1549.8–1572.0 m sub-bottom) is also Oxfordian. It encompassed 22.2 m, 2.95 of which were recovered (8%).

Contacts

The upper contact of Subunit 7b is placed at Core 117, Section 1, 26 cm, below which gray limestones compose a significant portion of the sedimentary sequence. This transition is indicated by a rapid increase in the drilling time per core compared to the drilling of the claystones of Subunit 7a. Extremely poor recovery (10%) prevents determination of a precise unit boundary, and it is probable that the increase in limestone turbidites downward is a gradation phenomenon.

The lower contact is placed between Cores 119 and 120. Core 120 still has gray limestone beds, but they are interbedded with a greenish radiolarian-rich claystone with thin radiolarian-sand layers, a distinctive facies that characterizes the underlying Subunits 7c and 7d.

Lithologic Description

Subunit 7b is composed of gray limestones interbedded with dark variegated claystones. The limestones are light olive gray (5Y 6/1) to greenish gray (5G 6/1, 5GY 6/1 to 5G 4/1) to olive gray (5Y 4/1). The limestone beds commonly exhibit graded bedding, laminations, convolute laminations, and interaclasts of claystone. *Chondrites* burrows are common in the upper portions of the beds. Two unusual microbreccia(?) levels occur within the limestones of Core 118 (Fig. 31 and 32). The textures range from loosely packed bioclastic pelletal microspar-sparite to pelletal micrite to biomicrite to homogeneous micrite. The coarser, more bioclast and pellet-rich textures are found near the bases of the thicker limestone beds. Bioclasts include echinoderm fragments, pyritized and calcified radiolarians, and rare benthic foraminifers.

The interbedded, dark variegated claystones resemble those of Subunit 7a: blackish red (5R 2/2) to olive gray (5Y 4/1) claystones are between thin greenish black (5G 2/1) claystones and have faint laminations and minor amounts of bioturbation.

Depositional Environment

The abundant pelletal limestones, which are the dominant rock type of Subunit 7b, are calcareous turbidites that were deposited within a changing claystone sequence.

The dark variegated claystones are very similar to those of Subunit 7a and are interpreted similarly: blackish red claystone turbidites interbedded with thin layers of a host sediment of greenish black claystone. The only distinction, then, between Subunits 7b and 7a is the sharp change in the abundance of the calcareous turbidites. This could reflect either a reduction in turbidite activity, or increased dilution by the claystone turbidite component, or both.

The source region for the pelletal limestone turbidites was possibly the continental slope or the Blake Spur Anomaly Ridge. The high coccolith content of the pellets and lack of any shallow-water material implies that the initial sediment was a pelagic carbonate.

Given the interpretaton that most of the claystones are also redeposited (from a deeper and possibly closer source), the apparent amount of normal pelagic sediment (greenish black clay) is a very minor fraction of Subunit 7b.

Regional Correlation

These facies have not been recovered at other sites, but are known by geophysical mapping and laws of superposition to be older than any previous recovered sediments in the Atlantic. On the basis of seismic reflection profiles, the limestone turbidites appear to be a widespread, basement topography-smoothing episode. However, until this facies and those of underlying Subunits 7c, 7d, and 7e have been identified at another site, it is premature to assign any formation name or status to them.

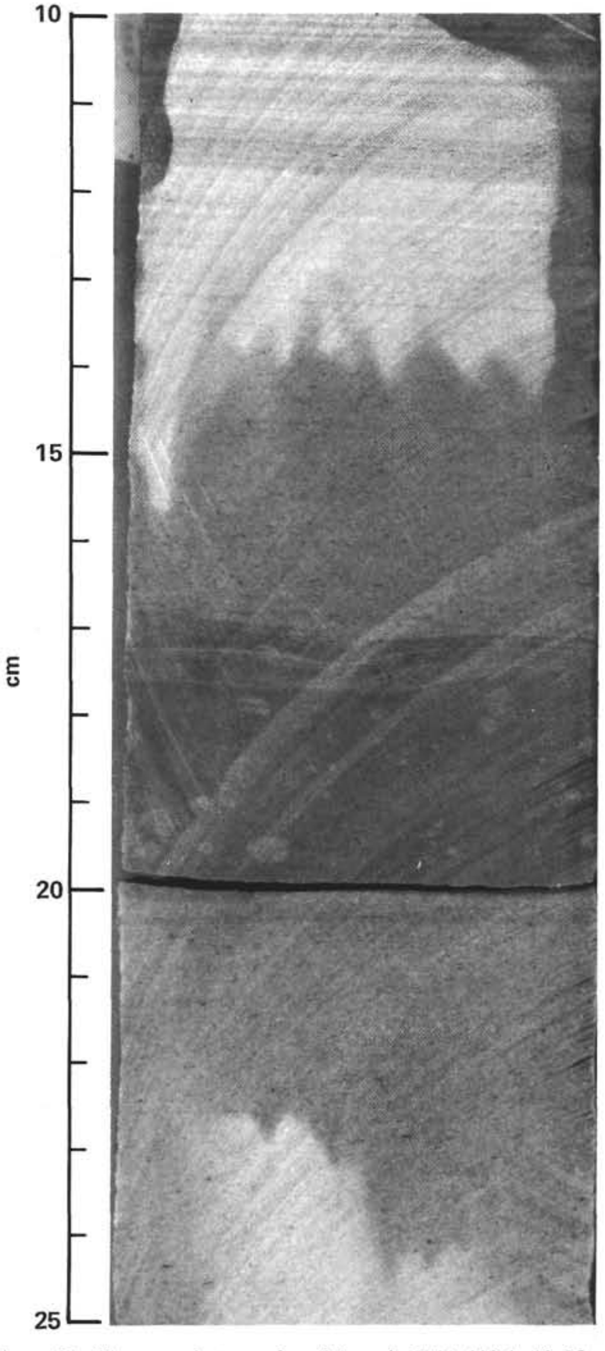

Figure 31. Close-up photography of Sample 534A-118-1, 10–25 cm, showing a microbreccia found in the limestone of Subunit 7b between 17 and 20 cm.

Subunit 7c—Olive Gray Limestones in Dark Greenish Gray Radiolarian-rich Claystones

Subunit 7c (top of Core 120 to Core 125, Section 4, 14 cm; 1572.0–1617.1 m sub-bottom) is Oxfordian to

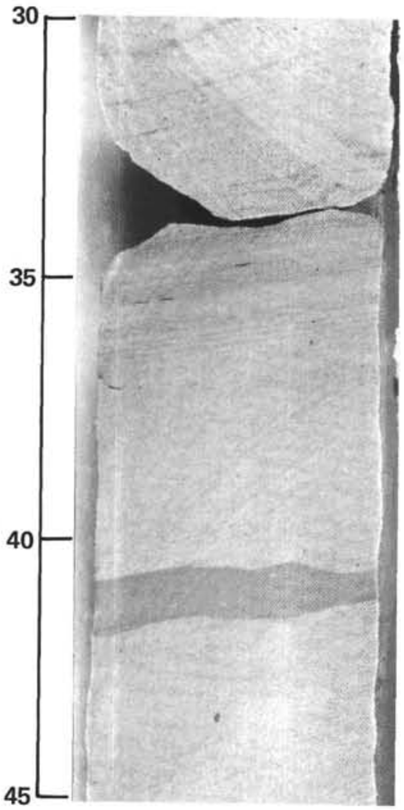

Figure 32. Microbreccia in Sample 534A-118-1, 30–45 cm similar to that found in Figure 31. (The layer, between 40 and 41 cm, is thinner than that found between 17 and 20 cm in the same core.)

Callovian and spanned 45.1 m, of which 14.9 m were recovered (33%).

Contacts

There was a sudden change from variegated claystone to dark greenish gray radiolarian claystone between Cores 119 and 120, although poor recovery prevents identification of the nature of this change. The upper boundary of Subunit 7c is therefore arbitrarily placed at the top of Core 120.

The lower contact at Core 125, Section 4, 14 cm is identified at the base of the lowest olive gray limestone occurrence. The abundance of limestones rapidly increases in the upper part of Core 125 and dominates Core 124.

Lithologic Description

Subunit 7c is composed of olive gray limestones interbedded with dark greenish gray claystone containing silty layers of concentrated radiolarians. The limestones in the upper part of Subunit 7c are similar to those of Subunit 7b, but those in the lower part are generally darker and more marly. Colors range from greenish gray (5G 6/1, 5GY 5/1 to 5G 4/1) to olive gray (5Y 4/1), with a downward trend toward darker limestones. The limestone beds commonly exhibit graded bedding, laminations, and convolute laminations, and have bioturbation and *Chondrites* burrows in the upper portions. The textures range from bioclastic pelletal microspar–sparite, to pelmicrite, to homogeneous micrite. There is a downward trend toward finer-grained and more marly limestones. Bioclasts include small bivalve shell fragments ("filaments"), pyritized and silicified radiolarians, echinoderm fragments, and rare benthic foraminifers.

The claystones of Subunit 7c range from siliceous radiolarian-rich claystone (Cores 120 and 121), to claystone (Core 122), to nannofossil claystone (Cores 123–125) as the abundance of radiolarians and quartz silt decreases and nannofossil abundance increases. Throughout the claystone sequence occur thin (0.5–1.0 cm) layers or lenses of radiolarian silt containing 30 to 50% radiolarians in a clay matrix similar to the host sediment (Figs. 33, 34). These radiolarian concentrations have sharp contacts, are often laminated, and decrease in abundance toward the base of the unit. The color of the claystones changes from dusky purplish blue green (5BG3/2 + 5P3/2) and dark greenish gray (5GY4/1) in Cores 120 to 122 to olive black (2Y2/1) and greenish black (5G2/2) in Cores 123 to 125. From Cores 122 through 126 there is an increasing frequency of carbonaceous claystone layers and laminae (Fig. 35—Subunit 7d), together with glauconite grains and lenses and sand-sized phosphate concretions in the host claystone. The sparse radiolarians in the claystones of Cores 122 to 125 are replaced by pyrite, whereas the abundant radiolarians in the claystones of Cores 120 to 122 and the interbedded radiolarian silt layers throughout the unit are silicified, often with chalcedonic quartz interiors. Fragments of pelagic bivalves, some fish phosphatic debris, and scattered plant debris occur in the claystones of Cores 124 to 125.

Depositional Environment

The upward trend of increasing abundance, thickness, and coarse carbonate content of the limestone beds through Subunit 7c along with their sedimentary structured strongly suggest a calcareous turbidite progression from relatively feeble distal types to relatively larger events. The source of the pelagic carbonate was probably the continental slope or Blake Spur Ridge to the west. Of course, there is the possibility that some of the nongraded, marly limestone beds are *in situ* deposits caused by changes in pelagic carbonate productivity or fluctuations in the CCD.

One distinctive characteristic of the claystone sediments is the sporadic occurrence of thin radiolarian silt layers. These radiolarian-rich bands and lenses suggest (1) occasional bottom-current activity winnowing the radiolarian fraction from an original radiolarian-bearing claystone, (2) transportation of radiolarians from another source area, or (3) episodes of high productivity of radiolarians. The abundance of radiolarians in this sediment relative to the overlying Late Jurassic sediments may indicate either a higher radiolarian productivity, less dilution by other components, better preservation of the radiolarians in the sediment, or a combination of factors. Similar radiolarian silt layers occur

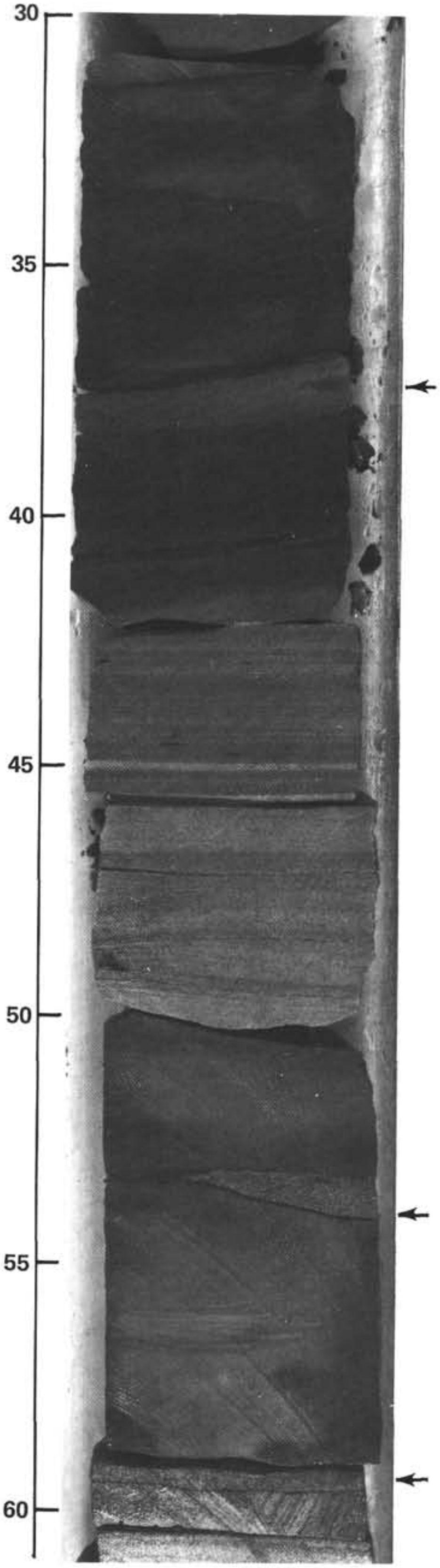

Figure 33. Olive gray limestone interbedded with dark greenish gray claystone containing silty layers of concentrated radiolarians at a, b, and c from Section 534A-120-1 of Subunit 7c (the unnamed lithostratigraphic interval underneath the Cat Gap Formation).

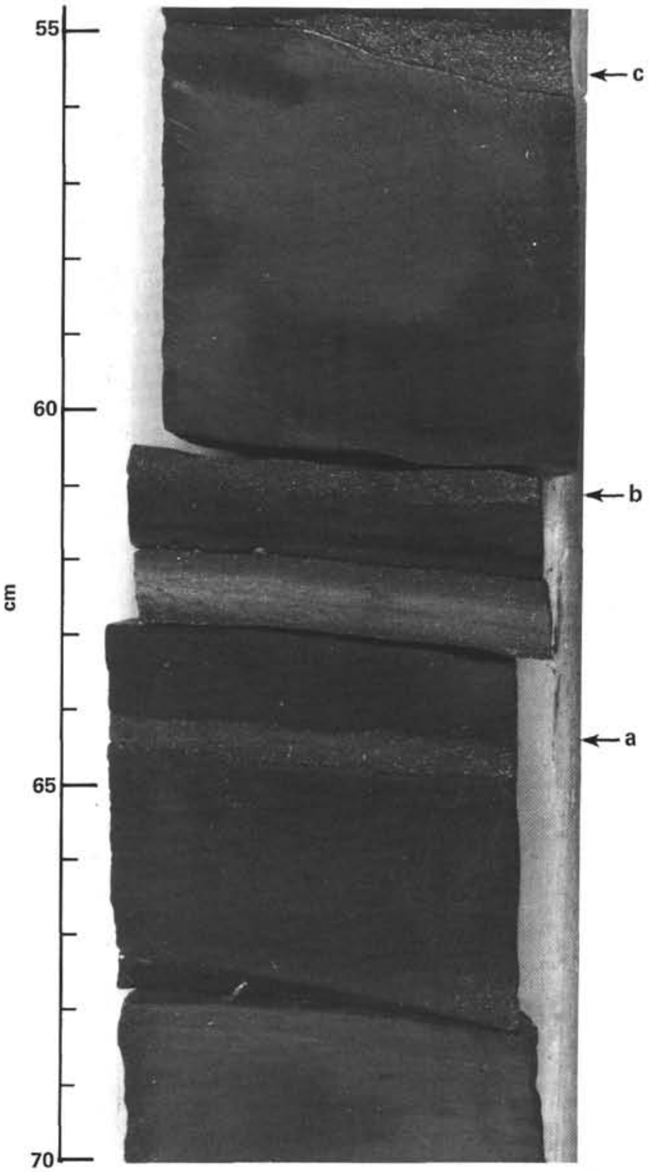

Figure 34. Close-up of the lower part of the section shown in Figure 33 depicting the lenticular shape of the radiolarian silt layers—at a, b, c—from Section 534A-120-1 of Subunit 7c (the unnamed lithostratigraphic interval underneath the Cat Gap Formation.)

within the Late Cretaceous greenish claystones that were recovered at Site 387 (see the discussion in McCave, 1979).

The very low calcareous nannofossil content (1–5%) and poor preservation within the claystones in Cores 120 to 123 suggest a depositional environment close to the local CCD during this interval. The upward decline in nannofossil content from 25 to 35% (smear slide estimates) in Core 126 to 3 to 5% in Core 123 also suggests a change in the CCD. The carbonate content begins to increase again in Core 119. An alternative explanation for the low carbonate content and poor preservation is diagenesis caused by the increased dissolution of carbonate as the organic carbon content of the claystone rose.

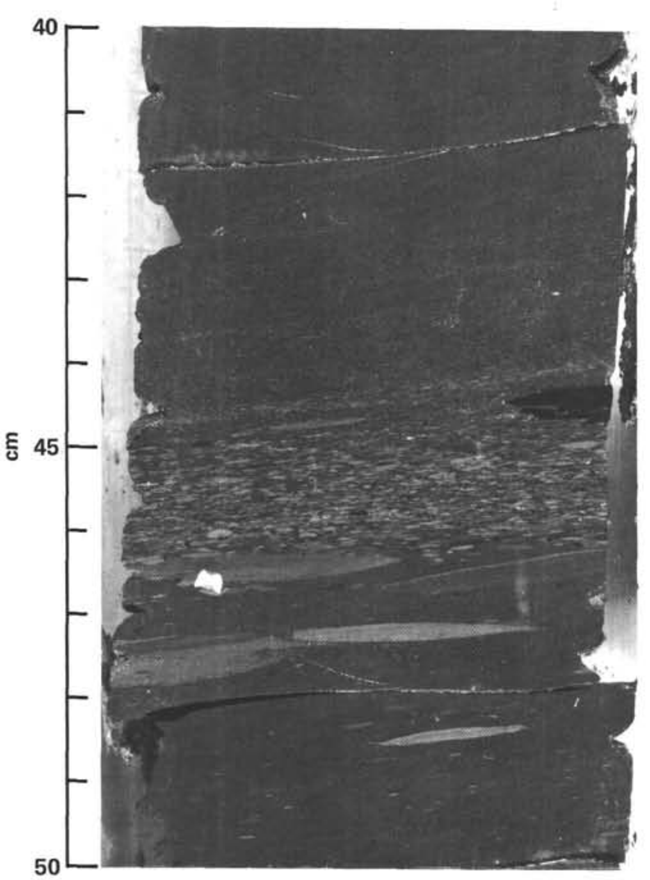

Figure 35. Layers of nannofossil-rich claystone clasts in greenish black, organic-rich claystone—Section 534A-126-3, Subunit 7d (unnamed lithostratigraphic interval underneath the Cat Gap Formation).

There are many carbonaceous black claystone layers within the dark greenish gray claystone. Some of the organic material is terrestrially derived, and these layers may be organic-rich turbidites from the shelf, although no turbidite sedimentary structures were observed. The glauconite grains, quartz silt, and small phosphate concretions observed in thin sections of the greenish claystones were possibly transported by currents to the site. Subunits 7c and 7d have the only significant (though minor) abundance of quartz silt in the Jurassic sediment sequence. The superb preservaton by pyrite of many radiolarians in both the claystones and limestones suggests an anoxic environment within the sediments very near or at the sediment/water interface.

The apparent inclination of bedding in Subunit 7c is 5 to 15° (the measured deviation of the bottom of the drill string was about 2.5°). However, the only indication of synsedimentary slumping is a slight contortion of some limestone layers in Core 125. The overlying Subunit 7b has nearly horizontal apparent inclinations, which suggests the possibility that tectonic tilting occurred between the deposition of the sediments of Subunits 7c and 7b. The slight contortion in Core 125 could be an artifact of drilling.

Regional Correlation

This facies has not been recovered at other sites. It is known, by geophysical mapping and regional correlation, to be older than any previous recovered sediments in the Atlantic.

Subunit 7d—Greenish Black Nannofossil Claystone

Subunit 7d (Core 125, Section 4, 14 cm to Core 126, Section 3, 75 cm; 1617.1-1625.3 m sub-bottom) is Callovian; coring of this interval spanned 8.2 m, of which 7.5 m were recovered (91%).

Contacts

The upper contact was placed at the base of the lowest marly limestone of Core 125 at Section 4, 14 cm. The basal contact is at the top of the dusky brown claystone, or Core 126, Section 3, 75 cm.

Lithologic Description

The dominant lithology of Subunit 7d is greenish black (5G 2/1) to olive black (5Y 2/1) nannofossil claystone to carbonaceous nannofossil claystone. It is predominantly laminated, but many beds are massive or have a graded texture. The greenish claystone levels generally have small elongate dark mottles, interpreted as burrows. Thin sections show that the laminae are discontinuous concentrations of fine organic material and pyrite-Fe oxide particles and/or nannofossil micrite. Thin radiolarian sand layers, similar to those of Subunit 7c, occur sporadically. The abundance of both carbonaceous claystone and radiolarian silt layers increases upward in Subunit 7d. Pyritized radiolarians, fine pelagic bivalve shells, phosphatic fragments and concretions, plus about 5% quartz and mica silt are minor components of the nannofossil claystone, in addition to 2 to 5% organic matter. Laminae replaced by pyrite and nodules of pyrite are common.

The beds have 10 to 15° inclinations; synsedimentary slumping, folds, and shear planes are present (Fig. 36). Beds with flattened elongate claystone intraclasts are abundant throughout Subunit 7d and range from 4-cm-thick layers with clasts less than 2 mm in length to spectacular 45-cm-thick beds with clasts exceeding 3 cm in length. The clasts are usually shades of greenish gray, but include clasts identical to the host claystone, fish debris and phosphate concretions, and plant debris. Some of the greenish gray clasts (Fig. 37) contain up to 40% nannofossils, significantly more than either of the host claystones do. These intraclast levels are often graded or associated with synsedimentary slump features. Some horizons with changing inclinations of lamination are perhaps portions of ripples, cross-bedding, and current scour, though no unambiguous examples were observed.

Depositional Environment

The greenish black claystone of Cores 125 and 126, with its glauconite and phosphate grains and high content of organic material and pyrite, suggests variable, including reducing, bottom conditions in the sediment.

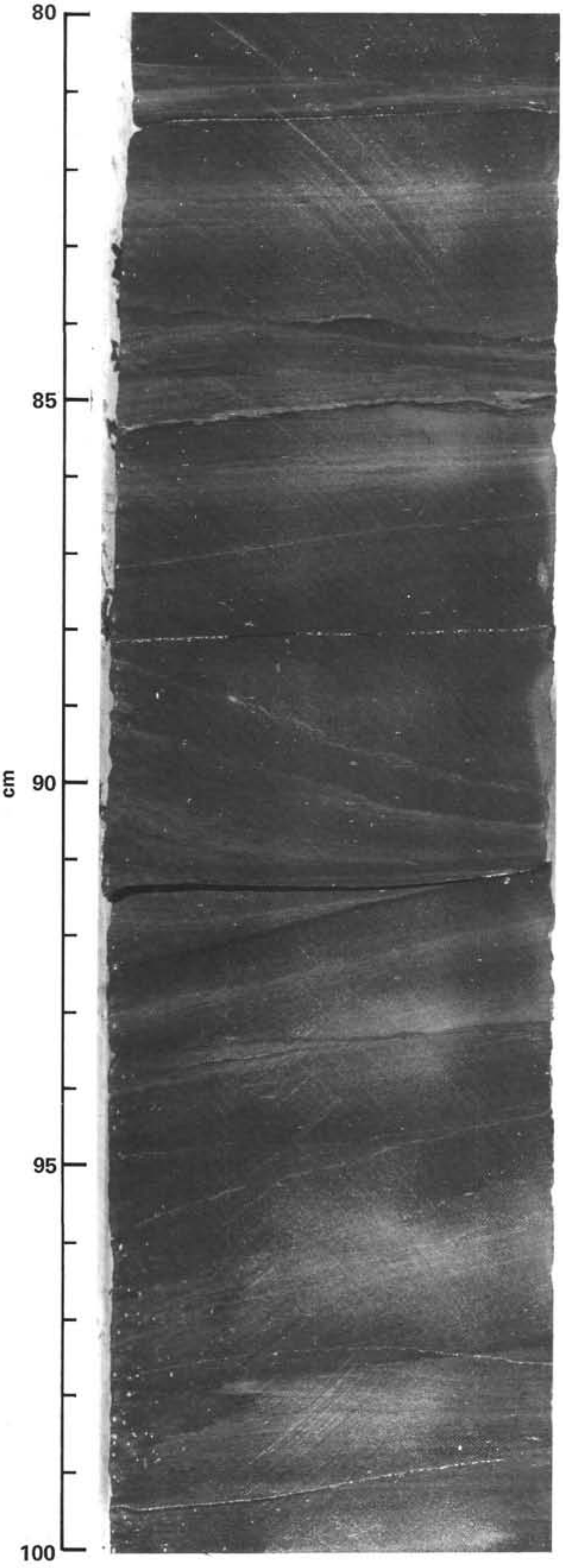

Figure 36. Close-up of Sample 534A-125-4, 80–100 cm showing the occurrence of low-angle cross-bedding, which occurs in Subunit 7d. (Apparent erosional surfaces occur at 84 and 85.5 cm.)

The 10 to 15° inclination of the beds, synsedimentary slumping, and shear planes indicate deposition on a slope, which would have resulted from sediment build-up, tectonic tilting, or both. These sequences may have also been formed by contour currents. In addition, current winnowing could have produced some of the intraclastic intervals. The claystone intraclasts are probably locally derived. Sloping and hummocky bedding is apparent on the seismic reflection profiles. The levels with graded or poorly sorted elongate claystone intraclasts may represent redeposition associated with slumping events farther upslope, perhaps from gravity loading of over-steepened slopes in soft sediment.

Regional Correlation

The sediments of Subunit 7d are older than any sediments ever drilled in the oceans. Therefore it is difficult to judge whether the black claystones reflect a widespread low oxygen event, lack of bottom circulation, or a local basin receiving organic-rich turbidites. In the Tethys and on bordering margins there are either many organic-rich sediments or indications of a reducing environment within the upper Callovian through lower Oxfordian sediments, for example, the "Terres Noires" of southeastern France and the green radiolarian cherts of northern Italy.

Subunit 7e—Dusky Brown Nannofossil Claystone

Subunit 7e (Core 126, Section 3, 75 cm to Core 127,CC [10 cm]; 1625.3–1635.3 m sub-bottom) is a Callovian interval that spans 10.0 m, of which 7.5 m were recovered (75%).

Contacts

The upper contact of Subunit 7e is placed at the highest occurrence of dusky brown claystone in Core 126, Section 3, 75 cm. The basal contact is at the top of the basalt, or Core 127,CC (10 cm).

Lithologic Description

The dominant lithology of Subunit 7e is dusky brown (5YR 2/2) to grayish brown (5YR 3/2) nannofossil claystone. It is massive to irregularly laminated, with greenish gray intervals of claystone intraclasts and a couple of thin radiolarian silt layers (Fig. 38). These greenish gray intervals are similar to the features in Subunit 7d. Some of the greenish gray clasts contain up to 40% nannofossils (smear-slide estimates), significantly more than the 15 to 30% nannofossil content of the dusky brown claystone. Fine pelagic bivalves ("filaments") were observed in thin sections of the claystones and of the similar, dusky brown, calcareous claystone within the basalt flows.

Sedimentary Environment

The dusky brown, nannofossil claystones of Subunit 7e have no carbonaceous black claystone intervals or pyrite occurrences, unlike overlying Subunit 7d. This indicates a more oxidizing environment within the sediment, perhaps owing to an initial lower organic content or more oxidizing bottom waters. The higher nannofossil content of these claystones relative to the overlying

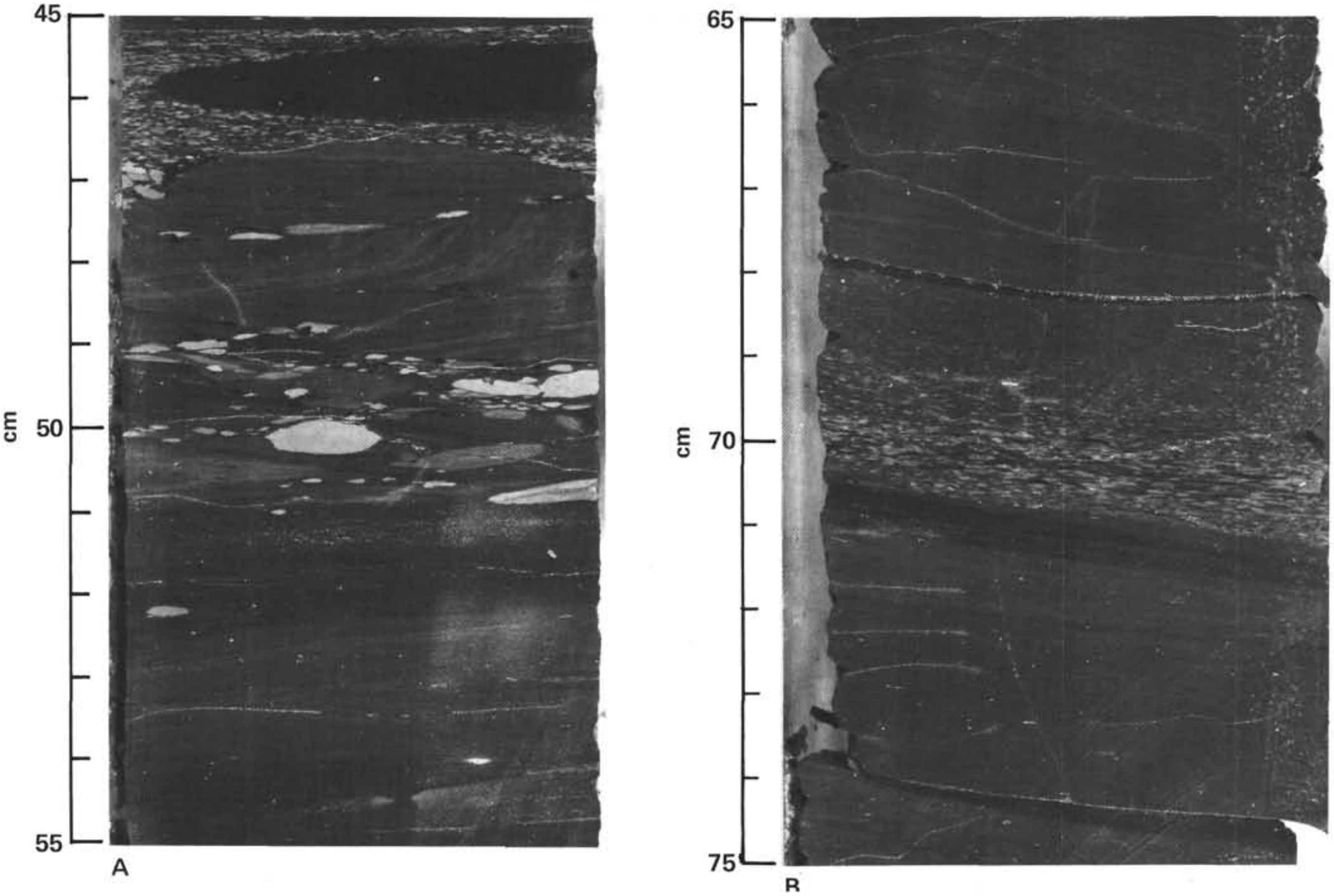

Figure 37. A. Evidence of possible lag gravel pavement and cross-bedding in Subunit 7d. (A close-up of Sample 534A-125-5, 45–55 cm shows small intraclasts grading upward into small-scale cross-bedding [48 cm], which suggests that this sequence may have been a coarse lag deposit that was rolled along on an erosional surface.) B. Evidence of synsedimentary slumping in Subunit 7d. (A close-up of Sample 534A-125-6, 65–75 cm shows a typical sequence of graded intraclasts.)

greenish black claystones may reflect either a higher carbonate productivity, greater preservation of nannofossils within an oxidizing sediment environment, or a lower CCD. Only minor bioturbation features were observed, primarily within the greenish gray horizons. No evidence of current activity was observed, but the homogeneous character of the dusky brown claystone may conceal any sedimentary structures.

The direct contact of the sediments to the basalt is unfortunately missing. The rare interbeds of sediment between basalt flows resemble the claystones of Subunit 7e but are commonly more siliceous. There are no obvious hydrothermal deposits or metalliferous sediments within Subunit 7e. One sediment interbed within the basalts is a brighter red color, possibly owing to thermal effects from the overlying flow.

Regional Correlation

This claystone is the oldest pelagic sediment recovered at any site in the Atlantic. It is impossible to determine at this time if it is a basinal or only very local facies.

Clay Mineralogy

Shipboard X-ray diffraction analysis was carried out on dried suspensions of bulk sediments using a special preparation procedure. For a description of the suspension, see the Site 506 report, Volume 70 (Honnorez, Von Herzen, et al., in press). The preparation procedure is: (1) Dry the sample in an oven at a temperature of less than 60°C. (2) Grind the sample to a fine powder; add a small amount of KCl as an internal standard. (3) Place the powdered sample on two glass slides; drop ionized water on one, and ethylene glycol on the other. (4) Flatten the sample to orient the clay minerals. (5) Dry the slides in an oven for one hour at less than 60°C. (6) Leave for one day at room temperature. (7) Electric current on *Glomar Challenger* fluctuates frequently; duplicate runs are therefore required for critical key lines. and (8) Relative abundance is obtained from intensities of peaks for the well-crystallized minerals (quartz, calcite, etc.). An intensity factor is applied only for calcite (Cook et al., 1975). The abundance of clay minerals is estimated from the peak height as well as the peak area.

Results

The results presented here are only tentative, because of the fluctuating power supply and lack of special treatment of clays before X-ray analysis.

The Cat Gap Formation and underlying units are divided into three groups according to combinations of clay minerals (see Table 3). Group I is characterized by

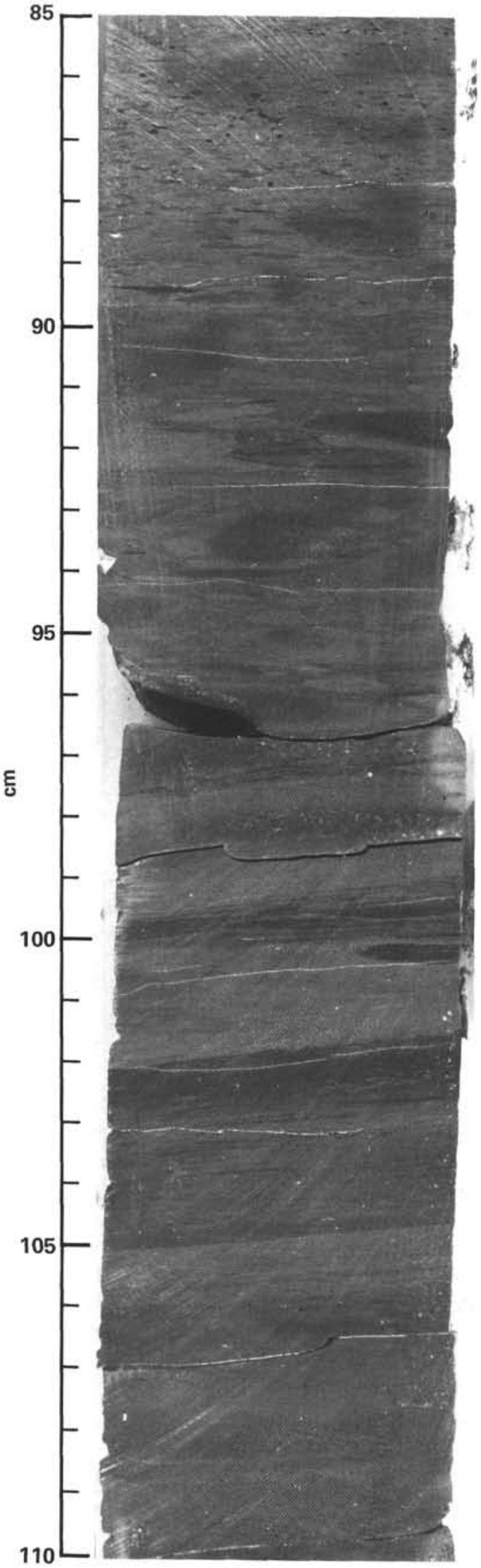

Figure 38. Examples of the irregularly laminated sediments with claystone intraclasts typical of Subunit 7e, Sample 534A-126-3, 85–110 cm

an abundance of smectite and traces of kaolinite, indicating a terrigenous input. Hematite is present and is responsible for the sediment color. Because hematite commonly occurs despite changes in color and sediment type, it is also considered to be a land-derived mineral. This mineral was reported from the Oxfordian section at Site 105 (Zemmels et al., 1972). Aragonite is also abundant in Group I. Abundant aragonite needles, observed in smear slides under the microscope, are thought to be derived from shells formed at shallower water depths. They are also reported from Unit 5 of Hole 391C (Flood, 1978).

Group II is characterized by the presence of illite and chlorite. Smectite content decreases dramatically compared to that in Group I. Quartz and calcite are the dominant constituents. Aragonite is again present. Smectite from the lower stratigraphic horizons of this interval tends to be richer in Mg content (stevensite). This is different from smectites in Group I, which have a Na-rich affinity (montmorillonite). The combinations of clay minerals in Group II may indicate slow input of terrigenous material together with diagenetic alteration of the clays.

Group III is characterized by an abundance of smectite of the Mg-rich affinity. Quartz and calcite are again the dominant constituents, with kaolinite indicating a terrigenous input. Another Mg-rich mineral characteristic of this interval is palygorskite, which is associated with the black shale and quartzose chert layers. In this material the radiolarians are completely transformed to quartz with or without calcite and carbonate-apatite.

Discussion

The change in mineralogy of the smectites is interesting and may indicate diagenetic alteration. The sub-bottom sediments might also have become gradually more Mg-rich stratigraphically downward.

Magnesite was found for the first time at this site. However, the key line at 2θ of 33° is confused by other minerals, such as hematite, aragonite, and carbonate-apatite, so that the identification is only tentative at present.

Millot (1970) showed that lacustrine deposits with sepiolite, palygorskites, and magnesite from many places have the following characteristics in common—presence of carbonates, common occurrence of chert, and hypersalinity. Although we cannot exclude the possibility that the magnesite is land-derived, the development of dense hypersaline stratification of the ocean could favor the precipitation of magnesite and palygorskite as authigenic minerals, and may also have led to stagnant sea-bottom conditions.

During the Triassic, clay minerals on land were dominantly illitic, associated with smectite and its transformed affinity, 14Å mixed-layered clays (Millot, 1970). Abundance of illite, mixed-layered clays, and smectite associated with chlorite is reported from the Kimmeridgian-Oxfordian interval at Site 105 (Chamley, 1979). In view of these previously published results, it can be stated that the clay mineral assemblage in Group II may have a detrital origin.

Table 3. Relative abundance of clay minerals, Hole 534A.

Sample (core-section, cm from top of section)	Lithology	Illite	Chlorite	Kaolinite	Smectite	Quartz	Plagio-clase	Calcite	Hematite	Aragonite	Magnesite	Paly-gorskite	Carbonate-Apatite
Group I													
92-4, 73	Red claystone	+	–	–	+ +	+ + +		+ +					
93-3, 121	Red claystone	–				+ +		+ + +					
94-4, 71	Blue claystone	+	–	–	+ + +	+ +	+	+	–				
95-2, 40	Red claystone	+	–	–	+ +	+ +	+	+ +	–	+			
99-2, 135	Black claystone	+	–	–	+ +	+ +	–	+			–		
99-3, 100	Red claystone	–			+ +	+ +	–	+	–				
Group II													
103-1, 145	Gray limestone					+		+ + +					
104-4, 139	Red claystone	+	–		+	+ +	–	+		–			
106-2, 20	Gray claystone	+	–		+	+ + +	–	–					
107-2, 101	Red claystone	+	–		–	+	–	+ +			–		
108-1, 33	Red claystone	+	–		–	+ + +	+	+ +	–				
111-1, 10	Gray claystone	–	+		–	+	–	+ +	–				
Group III													
112-1, 48	Red claystone			–	–	+ +	–	+ +				–	
113-1, 34	Burrowed chalk	–		–	–	+	–	+ + +					
114-2, 2	Gray claystone	+		–	+ + +	+ + +	+	+			–	–	
114-2, 3	Red claystone	+		–	+ +	+ + +	–	–			–		
115-1, 38	Red claystone	–	–	–	+ + +	+ + +	–	–	–				
116-1, 53	Black claystone	–		–	+ +	+ + +	–	+					
120-1, 50	Radiolarian layer					+ + +		+ + +					–
120-1, 70	Black claystone	–	–	+		+ + +			–			–	
120-1, 90	Radiolarian layer	–	–	–		+ + +							

Note: + + + = abundant; + + = common; + = rare; – = present; and blank spaces indicate absent.

Preliminary Sedimentological Interpretation of the Callovian "Black" Shales within Cores 122 through 127

"Black" shales were first encountered in Core 122, Section 2 and continued stratigraphically downward to Core 124, Section 1 as thin layers of predominantly 2 cm or less in thickness. In Core 125, in the vicinity of the transition between Subunits 7c and 7d (see Table 4), they represent 3.9 m out of the total 8.5 m recovered and are most abundant in Core 125, Sections 3 to 6. In Cores 122 to 124 the "black" shale occurs in a sequence dominated by turbiditic marly limestones, whereas in Core 125, the background sediment is mainly composed of dark-colored or green claystones with only minor redeposited sediments. The percentage lithological composition of the individual core sections is shown in Table 4, as calculated from detailed observations and the visual description sheets; the percentage of claystone is given as the remainder after the calculation of the abundance of the other lithologies. The data in this table clearly demonstrate the lithological transition occurring at the boundary between Subunits 7c and 7d; there is a significant downward decrease in the abundance and bed thickness of the turbiditic marly limestones and a corresponding increase in the percentage of "black" shales. Slump structures and graded claystone units characterize Subunits 7d and e. It should be appreciated that these contrasts are accentuated by the poor recovery (16.7%) in Core 124.

The "black" shales are actually greenish black (5G2/1) to olive black (5Y2/1) and are finely laminated, whereas the ordinary claystones have a planar but somewhat mottled fabric, which probably resulted from some degree of bioturbation. Both the black shale and the green claystones are relatively organic rich. Recorded organic carbon values are $\leq 2.5\%$ (black shale) and $\leq 1.4\%$ (claystone). The laminated nature of the black shales may indicate that the bottom waters were poorly oxygenated at the time of deposition (i.e., ≤ 0.5 ml/l O_2). This view could be supported by the presence of phosphatic oolitic concretions in the sequence. At the present time such concretions are only known to form in areas of < 1.0 ml/l of dissolved oxygen, where the pH lies between 7.1 and 7.5 and the Eh between 0 to -200 mV, and where the sedimentation rate is at least periodically very slow. Although at present these conditions occur only at the margins of oxygen minimum zones on the continental slope, the paleobathymetric position of Site 534 in the Callovian (at least 2.8 km deep, based on backtracking) indicates that the oxygen minimum model for black-shale genesis is inappropriate for this sequence. No evidence of bottom-water currents was observed within the individual black-shale beds, although there is good evidence for such activity in the claystone slumps, and graded, redeposited sediments are sometimes intercalated. In the intermittent absence of good bottom circulation, a pool of oxygen-depleted water could periodically have formed on the floor of the basin. Alternatively, the black, organic-rich muds would have been rapidly transported into the basin by turbidity currents and then buried to produce subsurface reducing conditions.

The development of black shales during the Callovian is a relatively rare phenomenon. Some organic-rich intervals are found in Northwest Europe, but these are probably controlled by "local" facies and paleogeography; and there is no indication of a global "oceanic anoxic event," as observed in the Toarcian or in parts of the Cretaceous. The pattern of the distribution of the black shales within the cored interval at Hole 534A imlies that the factors resulting in their formation (e.g., bottom-water oxygenation, organic-matter input, sedi-

Table 4. Percentage lithologic composition of Cores 122 through 127.

	Core	Section	Thickness (cm)	Radiolarian silts (%)	Marly limestone (%)	No. limestone beds	Average thickness (cm)	Black shale (%)	Claystone (%)	Graded intraclastic claystone units (%)	No. graded beds	Average thickness (cm)	Claystone slumps (%)	No. slumped beds	Average thickness (cm)
Subunit 7c	122	1	150	5.2	56.7	8	10.3	0	38.1	0			0		
		2	105	1.8	76.2	8	9.9	2.9	19.1	0			0		
	123	1	145	0.6	80.7	10	11.3	5.5	13.1	0			0		
		2	150	1.7	64.7	9	10.3	4.7	28.9	0			0		
		3	150	1.9	53.3	10	3	1.3	43.5	0			0		
		4	125	0	72	9	10.2	4.8	23.2	0			0		
	124	1	95	0	78.9	8	9.5	2.1	19	0			0		
Transition	125	1	150	1.5	12	5	3.4	11.3	67.9	7.3	3	3.7	0		
		2	150	1.6	40	14	3.9	24.7	36.7	0			0		
		3	150	3.3	32.7	7	4.9	64	0	0			0		
		4	150	4.5	2.7	1	4	72.7	3.4	6.7	3	3.3	10	1	15
Subunit 7d		5	120	1.6	0			52.5	32.5	6.7	2	4	6.7	2	4
		6	97	1.0	0			68	22.8	8.2	2	4	0		
	126	1	150	0.7	0			0	72.6	16.7	5	5	10	1	15
		2	150	0.9	0			0	87.8	3.3	3	1.7	8	1	15
Subunit 7e		3	150	0	0			0	78.7	14	4	5.3	7.3	3	3.7
		4	150	0	0			0	70	7.3	2	5.5	22.7	4	8.5
	127	1	150	1.0	0			0	68.4	26.7	1	4.0	5.3	1	8
		2	150	0	0			0	100	0			0		
		3	150	0	0			0	100	0			0		
		4	20	0	0			0	100	0			0		

Note: Blank spaces indicate item not applicable.

mentation rate) were delicately balanced. Shipboard evidence suggests that the sub-bottom of the early to middle Callovian Atlantic was periodically oxygen-depleted.

Fine-grained, woody carbonaceous debris was observed macroscopically, in smear slides, and in thin sections taken from Cores 122 through 127. Eight sediment samples were submitted for examination by the Rock-Eval pyrolysis method (Table 5). The resulting oxygen indices indicate predominantly Type III kerogens (i.e., woody, terrestrially dominated), but the two black-shale samples exhibited significantly higher hydrogen indices than those from more oxygenated facies, suggesting a more mixed composition. These data are insufficient to enable us to make any speculations on the nature of the black-shale depositional mechanism, but there are three main alternatives:

1) Inputs of allochthonous organic matter increased periodically, creating an oxygen demand greater than could be filled by bottom-water oxygen renewal.

2) Poor circulation led to oxygen depletion and hence greater preservation of the backround organic matter input.

3) Organic-rich sediments were rapidly deposited and buried without reworking, leading to subsurface reducing conditions (in this case bottom water need not have been reducing).

These models are not mutually exclusive and need further investigation.

Table 5. Organic carbon data, Hole 534A.

Sample no.	Sample (core-section, cm from top of section)	Lithology	Org. C (%)	Subunit	
1	122-1, 14	Marly limestone (turbiditic)	0.38	7c	
2	123-2, 79	Marly limestone (turbiditic)	0.47	7c	
3	123-2, 99	Dark claystone	1.30	7c	
4	124-1, 56	Marly limestone (turbiditic)	0.34	7c	Transition zone
5	125-3, 100	Black shale	1.80	7c	
8	125-4, 70	Black shale	2.40	7d	
7	126-2, 30	Calcareous claystone	1.10	7d	
6	126-4, 20	Calcareous claystone	0.16	7e	

Igneous Rocks (Unit 8)

Figure 39 summarizes the igneous rock sequence encountered at Hole 534A. We distinguished 29 cooling units on the basis of texture, occurrences of glassy margins and sediment intercalations, and alteration zones. Dark greenish gray, phyric basalt is the principal igneous rock type in this sequence. Vesicles are common, averaging about 2 to 5% of the rock volume; most of these are filled with dark green, yellow to brown clays (smectites, celadonite[?]) and/or sparry calcite, which gives the rocks a porphyritic appearance. These basalts are moderately fractured, with calcite as the common fracture filling. Calcite is also the common mineral filling vesicles in zones around these fractures. In addition, green claystone and reddish brown siliceous limestone fill some fractures. Glassy margins, used to distinguish cooling-unit boundaries, are generally darker-colored and more fine-grained than the basalt away from the margin. Almost all of these glassy zones are devitrified and altered to green and brown clays. Several cooling units are not bounded by glassy margins (e.g., cooling Units 6 and 14), but are composed of basalts that are texturally similar to those with glassy boundaries.

Basalt breccias and alteration zones occur in several cores (e.g., Core 129, Section 1, Piece 13 and Core 129, Section 2, Piece 1; Fig. 40). Basaltic fragments in the breccias are angular, moderately to intensely altered, and are set in a matrix of quartz, calcite, and green clay. Yellowish brown palagonite(?) occurs in the breccias, probably as an alteration product of basaltic glass. Alteration zones appear to be mixtures of sparry, coarsely crystalline calcite, quartz, and fine green clay (smectite). In Piece 1 in Core 129, Section 1, a layer of calcite rims vesicular basalt. The calcite, in turn, is coated by green clay, then quartz; the quartz has a botryoidal surface. Pieces 3A and 3B in Core 129, Section 2, are composed

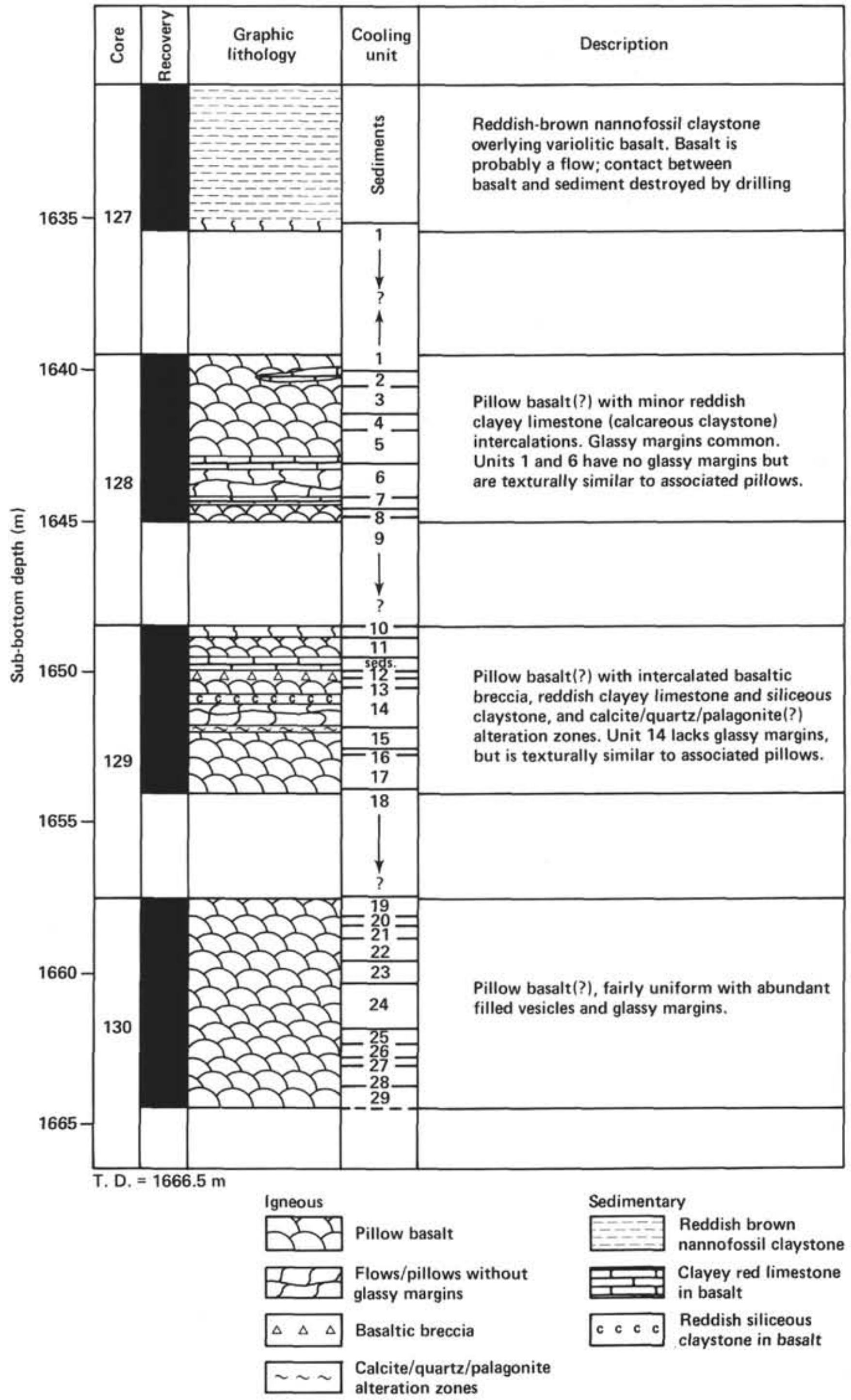

Figure 39. Summary of igneous rocks recovered from Hole 534A—Unit 8.

of irregularly laminated green smectite, calcite, and quartz below coarsely crystalline calcite and quartz. These observations are confirmed by thin-section analyses.

Sedimentary rocks intercalated with these basaltic rocks include reddish brown clayey limestone and siliceous claystone. The limestones are micritic with abundant clay. The siliceous rocks are aphanitic, irregularly shaped, and altered to greenish colors near the contacts with basalt. We observed abundant filament microfossils in a thin section of the limestone in Sample 534A-128-3, 107–109 cm. Both the claystone and limestone yielded rare, recrystallized, and indeterminate nannofossils.

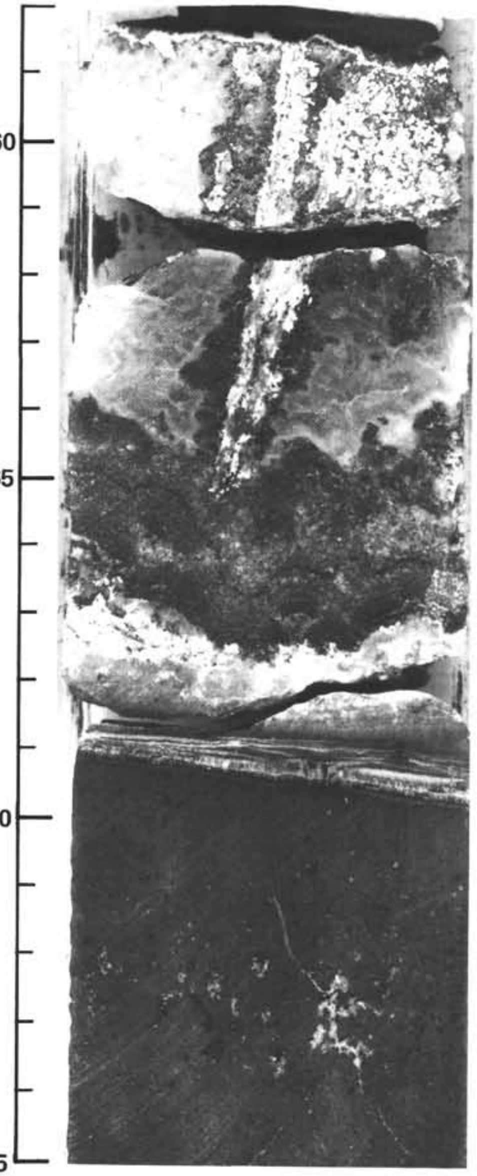

Figure 40. Moderately fractured basalt with calcite as the common fracture filling (Sample 534A-129-2, 58–75 cm).

Petrography

Samples examined from Hole 534A are aphyric to microporphyritic basalts containing phenocrystic calcic plagioclase and augitic clinopyroxene in an altered mesostasis of devitrified basaltic glass, opaque minerals, calcite, and clay. Plagioclase occurs as small (0.1–0.5 mm), skeletal (very thin elongate-tapered, swallow-tailed, and hollow) crystals with common albite twins, and, less often, as larger (0.5–1 mm), box-shaped, and equant grains in clusters. The latter sometimes show Carlsbad twinning. The average plagioclase composition is An_{60-75}. Many of the larger crystals have thin, more sodic rims.

Augitic clinopyroxene ($Z \wedge C \simeq 42°$) appears to be the only pyroxene in these basalts, and it occurs only in the coarser-grained portions of flows, away from glassy margins. These crystals are small (~0.2 mm) and occur either as single, euhedral grains with corroded edges (clay alteration, not reaction with the melt) or, more commonly, as irregular masses near the center of clusters of slender plagioclase laths (subophitic to intersertal texture) and plumose crystals associated with these glomerocrystic feldspar masses.

Olivine is not present, however, several samples from the middle of flow units contain sparse, euhedral olivine pseudomorphs, now completely altered green clay.

The mesostasis of these basalts is a variolitic mixture of devitrified glass and opaque minerals, with variable amounts of alteration products, principally green clay and calcite. Groundmass plagioclase and pyroxene phases increase in amount in the coarser-grained portions. Opaque minerals (principally titanomagnetite) are small (< 100 μm), skeletal to subhedral crystals (reflected light). These occur most commonly in the glass between plagioclase laths and concentrated along the edges of plagioclase clusters and crystals. Vesicles in these rocks are filled with green, yellowish brown clays (smectites, celadonite[?]), and/or calcite.

Textures of these basaltic rocks ranges from glassy to hyalopilitic. Most samples examined are variolitic and hyalopilitic with interstitial altered glass. Over a distance of 2 to 5 cm across a glassy margin, textures progress from glassy, to variolitic, to granular intersertal. Glomerocrystic plagioclase and augite have intersertal to hyalophitic textures. We did not examine textural progressions over distances of more than several centimeters in any single cooling unit. Once away from glassy margins, however, textures appear to be fairly uniform within any unit. Textural differences among cooling units include variations in the abundance of phenocrysts and the degree of alteration. Cooling Units 1 and 14 are composed of vitrophyric basalts that have been almost entirely altered to clays. No augite occurs (or remains) in the samples examined from these two units. Both units are bounded by sediments rather than delineated by glassy margins or alteration zones, as are all the other cooling units. Almost all the other cooling units that were examined petrographically contain some augite in samples taken away from glassy margins.

Interpretation

Based on preliminary textural and compositional data, the basaltic rocks recovered at Hole 534A probably are oceanic tholeiites similar to those recovered at DSDP Sites 100 and 105 (Bryan, 1972). The mineral paragenesis suggested is: plagioclase → plagioclase + pyroxene → opaques (titanomagnetite?). Olivine may have been a minor primary phase. Later alteration products include green and yellow phyllosilicates (nontronite[?], celadonite[?], palagonite[?], calcite, and quartz. Composition and textural similarities among the flow units at this hole suggest that all may have come from a common source. We interpret the abundant glassy margins marking the boundaries between these flow units as rinds of pillow lavas that were abruptly chilled when extruded on the seafloor. Intercalated sediments, basaltic breccias, and rock fragments composed of sparry calcite and quartz (sometimes with horizontal layering) were deposited and/or precipitated in the voids between adjacent pillows.

BIOSTRATIGRAPHY

Blake Ridge Formation

Foraminifers

At Site 534 2.1 m of this Formation were penetrated. Three samples (534-1-1, 0–2 cm; 534-1-1, 90–110 cm; 534-1,CC) have yielded common to abundant, moderately to well-preserved foraminifers. Planktonic forms prevail and represent 92 to 97% of the assemblages. Rare benthics include miliolids and anomalinids.

Samples 534-1-1, 0–2 cm and 534-1-1, 90–110 cm contain *Globorotalia truncatulinoides* (few to common), *G. tumida tumida* (common), *G. tumida flexuosa* (few), *G. hirsuta, G. inflata* (few), *G. crassaformis, Globigerinoides* spp., *Pulleniatina obliquiloculata,* and *P. finalis.* These assemblages, predominantly composed of keeled and warm-water forms, have been tentatively identified as Holocene. In Sample 534-1,CC, the same species have been found, however, the proportion of keeled forms is strongly reduced and the population of globorotalids is dominated by *Globorotalia inflata.* This cooler-water assemblage, in which *Pulleniatina finalis* is still present, has been assigned to the late Pleistocene.

Great Abaco Member

About 160 m of intraclastic chalks and siliceous mudstones were cored between 536 and 696 m below the seafloor. The unit is assigned to the Great Abaco Member of the Blake Ridge Formation. Foraminifers are generally rare and poorly preserved; planktonic forms prevail. Calcareous nannofossils are common and moderately well preserved. The wash-core at the top of the section (H1) is dated as middle Miocene; the remainder of the section recovered is early Miocene. Larger foraminifers, exclusively found in the redeposited beds, are dated as late Eocene. Reworked Paleogene and Late Cretaceous nannofossils occur throughout the cored interval of the Great Abaco Member (Table 6).

Foraminifers

The cores of Hole 534A, which lithologically correspond to approximately 150 meters of the Great Abaco Member of the Blake Ridge Formation, have yielded early and middle Miocene foraminifer assemblages. As a result of deposition close to the CCD, most of the core-catcher samples were barren. The use of additional samples that were selected in turbiditic levels was thought to yield better recovery. Few of these turned out to be fossiliferous and only yielded few, poorly preserved planktonic foraminifers. Wash-core H1 (Sample H1,CC) contains an assemblage with *Globorotalia fohsi peripheroronda, Globoquadrina dehiscens, G. altispira, Orbulina suturalis,* and also few displaced larger benthic foraminifers such as *Amphistegina* sp. The assemblage is assigned to the middle Miocene *Globorotalia fohsi* Zone.

Sample 534A-3-2, 83–85 cm yielded *Globigerinoides sicanus* and *Globoquadrina dehiscens. Orbulina* is absent, and therefore Core 3 is placed in the *Globigerinatella insueta* Zone. The age is late early Miocene.

In Cores 7, 10, and 14, more impoverished assemblages have been found, which comprise *Globigerinita (Catapsydrax) dissimilis, Globorotalia siakensis* (7,CC), and *G. kugleri* (10,CC, 14,CC). As a result, the interval from Cores 10 to 14 has been assigned to the *G. kugleri* Zone. The age is early early Miocene.

In some assemblages, a few small calcareous benthic foraminifers such as *Bolivina* and *Cibicides* occur.

Several cores (for instance, Cores 7 and 17) have coarser levels with calcarenitic facies containing numerous and moderately preserved larger benthic foramin-

Table 6. Preliminary biostratigraphy of the Great Abaco Member, Cores 1 through 18, Hole 534A.

		Biostratigraphy	
Age	Cores	Foraminifers	Coccoliths
middle Miocene	H-1	*G. fohsi*	
	1		
early to middle Miocene	2		*S. heteromorphus*
late early Miocene	3	*G. insueta*	*H. ampliaperta*
late early Miocene	4		*H. ampliaperta*
late early Miocene	5		*S. belemnos*
late early Miocene	6		*S. belemnos*
middle early Miocene	7	*C. dissimilis* (?)	*T. carinatus*
middle early Miocene	8		*T. carinatus*
middle early Miocene	9		*T. carinatus*
early early Miocene	10	*G. kugleri*	*T. carinatus*
early early Miocene	11	*G. kugleri*	*T. carinatus*
early early Miocene	12	*G. kugleri*	*T. carinatus*
early early Miocene	13	*G. kugleri*	*T. carinatus*
early early Miocene	14	*G. kugleri*	*T. carinatus*
early early Miocene	15		*T. carinatus*
early early Miocene	16		*T. carinatus*
early early Miocene	17		*T. carinatus*
early early Miocene	18		*T. carinatus*

ifers, such as *Lepidocyclina* (common), *Nummulites* (few), *Assilina, Operculina, Amphistegina* (rare), *Discocyclina,* and *Heterostegina* (very rare), and some planktonics. Tentatively, this shallow marine (photic zone) assemblage has been identified as late Eocene.

A similar assemblage was found in the Miocene debris flow deposits at Site 391. The origin of this redeposited fauna is thought to be in the Bahama channels, where shallow marine Paleogene deposits crop out.

Nannofossils

Lower Miocene nannofossils are common and generally moderately well preserved. In the siliceous mudstones, the coccoliths are usually etched. Secondary overgrowths are observed in the majority of the samples from the intraclastic chalks. Core 1 of Hole 534A did not recover any sediment. Core 2 contains an assemblage assigned to the *Sphenolithus heteromorphus* Zone, with *Discoaster exilis* and *Sphenolithus heteromorphus.* This zone straddles the early and middle Miocene boundary. Cores 3 and 4 recovered coccolith assemblages that belong to the *Helicosphaera ampliaperta* Zone, with rare occurrences of the marker species and a predominance of *Discoaster deflandrei* over slim-rayed discoasters. Cores 5 and 6 are assigned to the *Sphenolithus belemnos* Zone, based on the presence of the nominate taxon. Cores 7 through 18 contain *Triquetrorhabdulus carinatus* and only rare *Reticulofenestra abisecta* and thus belong to the upper part of the *Triquetrorhabdulus carinatus* Zone, which is dated as earliest Miocene. Reworked Paleogene and Late Cretaceous coccoliths occur throughout this lower Miocene interval, especially in the intraclastic chalks and other redeposited carbonates.

Sedimentation Rates

We have assigned an age of about 14.5 m.y. to Core 2 and about 21 m.y. to the bottom of the Great Abaco Member cored at this site. This age assignment yields a sediment accumulation rate of 23 m/m.y. for the recovered part of this stratigraphic unit.

Bermuda Rise, Plantagenet, and Hatteras Formations

The Bermuda Rise Formation contains upper Eocene nannoplankton in Cores 19 and 20. The Plantagenet Formation is probably lower Maestrichtian, on the basis of planktonic foraminifers in Cores 24 through 26. Core 25 contains some Tertiary nannofossils that are possibly downhole contaminants. The upper part of the Hatteras Formation is upper Albian (Vraconian); Core 27 has rare Vraconian-Cenomanian foraminifers, and Cores 27 to 30 are identified by palynology as Vraconian (uppermost Albian). Cores 31 through 33 in the middle part of the Hatteras Formation are upper Albian, based on dinoflagellates, and Cores 34, 35, and 38 are middle Albian, according to evidence provided by dinoflagellates and nannofossils. This identification agrees well with palynology that places the underlying Core 39, Section 6 in the lower Albian and Cores 41 and 42 in the upper Aptian. There were no diagnostic foraminifers or nannofossils found in Cores 39 through 43. The foraminifers and nannoplankton in Core 44 are lower middle Aptian. On the basis of calcareous nannofossils and foraminifers, Cores 45 and 46 belong to the upper Barremian; dinoflagellates indicate that these cores are lowest Aptian (Table 7).

Foraminifers

Bermuda Rise Formation

The three cores (19–21) that have been assigned to the Bermuda Rise Formation yielded very rare foraminifers. Sample 534A-19,CC contains a single specimen of *Cibicides,* and Sample 534A-20,CC has very rare and tiny specimens of poorly preserved Globigerinids, which might possibly be attributed to *Acarinina senni* and to the *G. eocaena* group. This tentative identification would agree with that of the Eocene for Cores 19 through 20, based on coccoliths.

Plantagenet Formation

Sample 534A-23-1, 21–23 cm yielded rare upper Campanian-lower Maestrichtian *Globotruncana arca, G.* gr. *stuartiformis,* and *Heterohelix* sp., and one specimen of *Racemiguembelina* sp., which is an upper Maestrichtian genus. In addition, Sample 534A-23,CC from a turbidite shows in thin section Santonian to lower Maestrichtian *Globotruncana lapparenti lapparenti* and *G. linneiana bulloides.* Core 23 has therefore been assigned to the Maestrichtian.

Cores 24 to 26 have provided rare and moderately preserved, mostly agglutinated benthic and calcareous planktonic foraminifers. On the basis of the different nature and preservation of the tests, it seems that the reddish agglutinated forms do represent the nondissolved remaining part of the *in situ* very deep microfauna, whereas the white chalky, and frequently broken planktonic shells could have been transported to this site by some kind of turbiditic process. As a result, we cannot be entirely certain that the planktonic forms give us the time of deposition at Site 534.

Samples 534A-24-2, 8–10 cm, and 534A-24-3, 74–76 cm have provided very rare and undiagnostic small trochamminids. Samples 534A-24-4, 41–43 cm, 534A-24, CC, 534A-25,CC and 534A-26,CC yielded a rather scanty microfauna, including *Globotruncana arca, G.* cf. *ventricosa, G. stuartiformis, G.* gr. *stuarti, Rugoglobigerina* spp., *Heterohelix* sp., and *Pseudotextularia* sp., accompanied by agglutinated general such as *Bathysiphon, Glomospira, Ammodiscus, Haplophragmoides,* and so on. The planktonic part of the assemblage indicates that deposition took place in the early Maestrichtian.

If a reworking of this Maestrichtian assemblage had taken place in the Paleocene through the middle Eocene, we could also have expected to find the planktonics of this time interval, but only Campanian-Maestrichtian forms were found. Foraminiferal oozes of both ages occur on the nearby Blake Plateau and Escarpment. Also, Maestrichtian microfaunas and/or floras have already been found in the lower part of the Plantagenet Formation at several North Atlantic sites (Holes 386, 387, 391C,

Table 7. Preliminary biostratigraphy of the Bermuda Rise, Plantagenet, and Hatteras formations, Cores 19 to 46, Hole 534A.

Litho-stratigraphy	Cores	Foraminifers	Coccoliths	Dinoflagellates	Age
Bermuda Rise Formation	19		*D. barbadiensis* to *D. saipanensis*		late Eocene
	20				late Eocene
	21				?
Plantagenet Formation	22				?
	23	*G. mayaroensis to G. stuarti*			Maestrichtian
	24	*G. stuarti*			early Maestrichtian
	25	*G. stuarti*			early Maestrichtian
	26	*G. stuarti*			early Maestrichtian
Hatteras Formation	27	*P.* and *H. delrioensis*		*S. echinoideum* (p.p.)	Vraconian
	28			*S. echinoideum* (p.p.)	Vraconian
	29			*S. echinoideum* (p.p.)	Vraconian
	30			*S. echinoideum* (p.p.)	Vraconian
	31			*S. echinoideum* (p.p.)	Albian
	32			*S. vestitum*	late Albian
	33			*S. vestitum*	late Albian
	34		*P. cretacea*	*S. vestitum*	middle Albian
	35		*P. cretacea*	*S. vestitum*	middle Albian
	36		*P. cretacea*	*S. perlucida*	middle Albian
	37		*P. cretacea*	*S. perlucida*	middle Albian
	38		*P. cretacea*	*S. perlucida*	early Albian
	39			*S. perlucida*	early Albian
	40				?
	41			*S. perlucida* (and *D. deflandrei* LAD)	late Aptian
	42			*S. perlucida*	late Aptian
	43			*S. perlucida*	Aptian
	44	*G. blowi; H.* sp. aff. *planispira*	*C. litterarius*	*S. perlucida*	early Aptian
	45	*H.* sp. aff. *planispira*	*W. oblonga*	*S. perlucida*	early Aptian to late Barremian
	46	?	*W. oblonga*	*S. perlucida*	early Aptian or late Barremian

391C, Jansa et al., 1979). We have therefore tentatively dated the Plantagenet Formation as defined at Hole 534A as early Maestrichtian.

Hatteras Formation (Cores 27–46)

Rare and not particularly age-diagnostic agglutinated benthic foraminifers have been found in Cores 27, 28, 31, 33 to 37, 40, and 41. Cores 34 to 37 contain *Trochammina vocontiana, Ammodiscus cretaceus, A. gaultinus, Dorothia filiformis, Haplophragmoides bulloides,* and so on, that is, an Early Cretaceous assemblage, which, in the Tethyan realm, is frequently found in the upper Aptian–Albian interval. Nevertheless, this relatively unprecise dating is consistent with the age that has been given to this interval by the coccoliths and dinoflagellates. In addition to some unidentified trochamminids, Sample 534A-27,CC (near the top of the Hatteras Formation) has also provided a single specimen of *Praeglobotruncana delrioensis* and very rare *Hedbergella delrioensis.* Core 27 has therefore been assigned to the Vraconian–Cenomanian.

The interval comprising Cores 44 and 45 has yielded, in addition to the usual trochamminids, few and generally poorly preserved calcareous specimens. Sample 534A-44-1, 131–133 cm contains *Hedbergella sigali, Clavihedbergella bizonae, Gavelinella* sp. Sample 534A-44-4, 30–32 cm shows a few *Gavelinella* sp. aff. *brielensis,* thus permitting us to assign Core 44 to the middle and lower Aptian. Sample 534A-45-4, 8–10 cm yields rare *Gavelinella* cf. *barremiana, Dorothia ouachensis, Hedbergella* sp. aff. *planispira* (sensu Moullade, 1966, non *H. similis* Longoria). In Sample 534A-45,CC few *H.* sp. aff. *planispira,* rare *H. sigali, H. infracretacea,* and *Clavihedbergella eocretacea* have been found. Core 45 is therefore assigned to the lower Aptian–upper Barremian, with a higher probability that Sample 534A-45,CC belongs to the Barremian rather than to the Aptian. Core 46 was devoid of foraminifers.

On the basis of the frequent absence of foraminifers and the presence of only impoverished agglutinated microfaunas in some levels, the shaly Bermuda Rise, Plantagenet, and Hatteras formations seem to have been deposited very close or just below the CCD, at slightly greater depths than at adjacent Hole 391C.

Nannofossils

Bermuda Rise Formation

Poorly preserved coccolith assemblages, which include *Discoaster barbadiensis, D. saipanensis, Reticulofenestra umbilica,* and *R. scrippsae* were found in Cores 19 and 20. Dissolution resulted in the destruction of some of the stratigraphically important forms. Thus zonal assignment of these two cores to an interval from the *Discoaster saipanensis* Subzone of the *Reticulofenestra umbilica* Zone to the *Discoaster barbadiensis* Zone is considered tentative. However, an upper Eocene assignment for these cores seems certain. Core 21 lacks calcareous nannofossils.

Plantagenet Formation

Cores 23 and 24 are devoid of calcareous nannofossils. The core catcher of Core 25 contains a very sparse nannofossil assemblage composed mostly of Tertiary forms, such as *Cyclicargolithus floridanus, C. pelagicus, C. eopelagicus,* and *Discoaster deflandrei.* Although these forms have long stratigraphic ranges, the assemblage is definitely indicative of a Tertiary age, possibly late Eocene. Only two Upper Cretaceous specimens were recoverd from Core 25, namely *Arkhangelskiella cymbiformis* and *Micula staurophora.* This mixed assemblage is either the result of reworking of Cretaceous forms into Eocene sediments or of downhole cavings mixed into a very poor Cretaceous assemblage during drilling. Core 26 does not contain any coccoliths.

Hatteras Formation

The upper part of the Hatteras Formation (Cores 27–33) lacks coccoliths. Carbonate-rich layers in Cores 34, 35, and 38 contain assemblages including *Parhabdolithus angustus* and rare *Deflandrius cretaceus;* they are assigned to the middle Albian Zone NC8. Samples from Cores 36, 37, and 39 through 42 are devoid of calcareous nannoplankton. Increasing carbonate content in Cores 43 through 46 resulted in the preservation of rich calcareous nannofossil assemblages. Cores 43 and the upper part of 45 still contain *Chiastozygus litterarius* and rare *Vagalapilla matalosa* and are thus assigned to the lower Aptian Zone NC6. Cores 45 (lower part) and 46 contain *Nannoconus colomi* but lack *C. litterarius* and *V. matalosa* and therefore belong to the upper Barremian Zone NC5a.

Palynology

The Hatteras Formation extends from the stratigraphic level of Core 27 down to that of Core 49. For the purpose of this report, the base of the sediment transitional to the underlying Blake-Bahama Formation is placed in Core 49. The dinoflagellates at the top of the Blake-Bahama Formation in Core 391C-14 (Benson et al., 1978; Habib, 1978; Jansa et al., 1979) are used to make this assignment in Core 49. The top of the Hatteras Formation lies within the *Spinidinium echinoideum* Zone, which ranges from Cores 27 to 30 (Sample 534A-30-1, 15–17 cm). This zone ranges from lower Cenomanian to Vraconian (uppermost Albian). However, the highest sample investigated, 534A-27-1, 66–68 cm, contains *Spinidinium vestitum* Brideaux and *Hystrichosphaeridium arundum* Eisenack and Cookson, which indicates that it is older than the Albian/Cenomanian boundary. On the basis of this evidence, the top of the Hatteras Formation in Hole 534A is Vraconian, which correlates with Core 6 in Hole 391C and with Core 11 in Hole 105 (Habib, 1977). Core 32 through Sample 534A-36-1, 88–90 cm are upper Albian to middle Albian in the *Spinidinium vestitum* Zone. *Palaeohystrichophora infusorioides* Deflandre has its lowest occurrence in this Zone. The samples containing the *Spinidinium vestitum* and *Spinidinium echinoideum* Zones yielded appreciable organic residues; the vast majority of these residues, however, is small terrigenous carbonized debris, which represents the altered and comminuted tracheal tissue of land plants (micrinitic facies). Palynomorphs are less well represented and consist of as many as 20 to 25 species of dinoflagellates in high relative percentages.

Sample 534A-36-2, 88–90 cm contains the micrinitic facies but is devoid of palynomorphs. Sample 534A-36-3, 88–90 cm through Core 39 are middle Albian to lower Albian in the upper part of the *Subtilisphaera perlucida* Zone. Dinoflagellates are still the dominant palynomorphs, except that samples from Cores 37 and 38 contain abundant residues rich in pollen grains of *Classopollis* and bisaccates, and larger fern spores. These cores represent the first downhole occurrence where *Classopollis* is abundant, although this genus ranges to the top of the investigated section. The residue is still largely carbonized, but there is now a large amount of both well-preserved and carbonized larger tracheids (tracheal facies).

Cores 41 and 42 consist of reddish to yellowish variegated claystones, in contrast to the primarily black clays higher in the section. Samples 534A-41-1, 42–44 cm, 534A-41-2, 42–44 cm, and 534A-41-3, 42–44 cm consist of reddish hematitic clay containing very little, entirely carbonized, organic residue of the micrinitic facies. These samples are barren of palynomorphs. Sample 534A-41-6, 42–44 cm contains very little carbonized residue and also few poorly preserved dinoflagellate cysts and no sporomorphs. *Cleistosphaeridium polypes* (Cookson and Eisenack), *H. arundum, Subtilisphaera perlucida,* (Alberti) and *Druggidium deflandrei* Habib occur. The highest occurrence of *D. deflandrei* places this sample in the lower part of the *Subtilisphaera perlucida* Zone, and indicates an age not younger than late Aptian. Samples 534A-42-1, 15–17 cm and 534A-42-2, 15–17 cm are composed of very small amounts of carbonized, debris and are barren of palynomorphs. The stratigraphic interval from 534A-42-3, 15–17 cm through 534A-49-3, 30–32 cm is Aptian in the lower *Subtilisphaera perlucida* Zone. This interval lies mostly within the transitional lithology at the base of the Hatteras Formation. Cores 44 and 45 contain an especially rich residue containing the tracheal facies. Sporomorph species and specimens are numerous and include a number of large fern spore species, including those in *Cicatricosisporites, Appendicisporites,* and *Costatoperforosporites. Classopollis* remains the dominant sporomorph. Amorphous (xenomorphic) debris is common and well-preserved, and there is an abundance of chitinous linings of benthic(?) trochoidal foraminifers.

Blake-Bahama Formation

The Blake-Bahama Formation consists of turbiditic sediments in the upper part, ranging downward to laminated limestones and marls, to uniform radiolarian-nannofossil limestones lacking clay laminae in the lowest part. It contains common and moderately well preserved nannofossils and dinoflagellate cysts. Foraminifers appear to be rare and poorly preserved. Age-diagnostic forms have only been found in a few samples. Age assignments based on calcareous nannoplankton, foraminifers, and dinoflagellates are generally in good agreement, except that foraminifers and nannofossils date Core 45 as latest Barremian and dinoflagellates date Core 49 still within the earliest Aptian. The ages based on these fossils are summarized in Table 8. Few to abundant radiolarians (replaced by calcite or pyrite) were observed in most of the washed residues. Fragments of ammonite aptychi were also observed from Cores 64 to 89. Calpionellids were observed and stratigraphically evaluated in Cores 87 to 91. Only Sample 534A-90-4, 19–20 cm yielded a good fauna, indicating a level in the middle part of Zone B, very close to the Tithonian/Berriasian boundary. The oldest Berriasian dinoflagellate flora was found in Core 90, Section 2. On the basis of nannofossil data, the Cretaceous/Jurassic boundary is placed at the base of Core 91.

Foraminifers

Twenty-one core-catcher and seven additional samples were investigated from the 390 m of alternating white limestones and gray shales representing the Blake-Bahama Formation in Hole 534A (Cores 47–91). Only few samples yielded rare and moderately well preserved age-diagnostic foraminifer assemblages. Sample 534A-47-4, 72–74 cm contained few and poorly preserved spe-

Table 8. Preliminary biostratigraphy of the Blake-Bahama Formation, Hole 534A.

Cores	Foraminifers	Nannofossils	Dinoflagellates	Calpionellids	Age
47	*C. eocretacea*	*W. oblonga*	*S. perlucida*		late Barremian or early Aptian
48	*C. eocretacea*		*S. perlucida*		late Barremian or early Aptian
49	*H. sigali–C. eocretacea*		*O. operculata/P. neocomica*		late Barremian or early Aptian
50			*O. operculata/P. neocomica*		Barremian
51			*O. operculata/P. neocomica*		Barremian
52	*H. sigali*		*O. operculata/P. neocomica*		Barremian
53	*H. sigali*		*O. operculata/P. neocomica*		Barremian
54	*D. ouachensis–G. eichenbergi*		*O. operculata/P. neocomica*		Barremian
55			*O. operculata/P. neocomica*		Barremian
56			*O. operculata/P. neocomica*		Barremian
57			*O. operculata/P. neocomica*		Barremian
58			*O. operculata/P. neocomica*		Barremian
59		*C. cuvillieri*	*O. operculata/P. neocomica*		Hauterivian
60			*O. operculata/P. neocomica*		Hauterivian
61			*D. rhabdoreticolatum*		Hauterivian
62			*D. rhabdoreticolatum*		Hauterivian
62			*D. rhabdoreticolatum*		Hauterivian
63			*D. rhabdoreticolatum*		
64	*H. vocontianus*		*D. deflandrei*		Hauterivian
65			*D. deflandrei*		Hauterivian
66			*D. deflandrei*		Hauterivian
67			*D. deflandrei*		Hauterivian
68			*D. deflandrei*		Hauterivian
69		?	*D. deflandrei*		Hauterivian
70		? *T. verenae–O. rectus*	*D. deflandrei*		Valanginian
71	*D. hauteriviana*		*D. deflandrei*		Valanginian
72			*D. deflandrei*		Valanginian
73			*D. deflandrei*		Valanginian
74			*D. deflandrei*		Valanginian
75			*D. deflandrei*		Valanginian
76			*D. apicopaucicum*		Valanginian
77			*D. apicopaucicum*		Valanginian
78			*D. apicopaucicum*		Valanginian
79		*R. neocomiana*	*D. apicopaucicum*		Valanginian
80			*D. apicopaucicum*		early Valanginian
81			*D. apicopaucicum*		early Valanginian
82			*B. johnewingii*		late Berriasian
83			*B. johnewingii*		late Berriasian
84			*B. johnewingii*		late Berriasian
85			*B. johnewingii*		late Berriasian
86			*B. johnewingii*		late Berriasian
87		*N. colomi*	*T. salpinx*		early Berriasian
88			*T. salpinx*		early Berriasian
89			*T. salpinx*		early Berriasian
90				*Calpionella* B, middle	latest Tithonian or earliest Berriasian
91				*Calpionella* B, middle	latest Tithonian or earliest Berriasian

cimens of *Clavihedbergella eocretacea,* thus confirming the age at the top of the Blake-Bahama Formation to be Barremian. Samples 534A-49-3, 32–34 cm and 534A-49,CC yielded a relatively more diversified Barremian assemblage, composed of few agglutinated forms (*Ammodiscus cretaceus,* Trochamminids), some nodosarids (including *Pseudonodosaria humilis*), *Gavelinella* sp., *Hedbergella sigali,* and (Sample 534A-49,CC only) *Clavihedbergella eocretacea.* Samples 534A-52,CC and 53, CC provided rare and tiny specimens of *Hedbergella sigali,* accompanied in 53,CC by *Dorothia ouachensis* and *Gaudryinella eichenbergi.* Therefore, the Hauterivian/Barremian boundary can be set between Cores 52 and 53 (Moullade, 1966, 1974, in press; Magniez-Jannin, personal communication, 1980). Sample 534A-54,CC contains few *Dorothia ouachensis,* rare *Ammodiscus gaultinus, Pseudonodosaria humilis, Lenticulina* spp. (gr. *muensteri-gibba-crassa*), and *Gavelinella* sp., and corresponds to the upper part of the *D. ouachensis* Zone. In the Tethyan realm the genus *Gavelinella* is known to appear first in the late Hauterivian; consequently, Sample 534A-54,CC has been assigned to the upper Hauterivian. This assignment is consistent with that for Core 53—the uppermost Hauterivian, indicated by both foraminifers and coccoliths. The interval comprising Cores 55 to 63 is barren of foraminifers based on the study of both core-catcher and few additional samples. In Sample 534A-64,CC, rare *Haplophragmoides vocontianus, Ammodiscus gaultinus, Pseudonodosaria humilis,* and *Trochammina* sp. have been found. In the Tethyan realm *H. vocontianus* ranges from the uppermost Valanginian to the lower upper Hauterivian (Moullade, 1980, in press). Also taking into account the coccolith data, the Valanginian/Hauterivian boundary has thus been tentatively set between Cores 63 and 64. No foraminifers were found in the sequence of Cores 65 to 70. Sample 534A-71,CC yielded the most diversified Lower Cretaceous assemblage of Hole 534A. This assemblage comprises common *Dorothia hauteriviana* and rare transitional specimens between this species and its phylogenetic ancestor, *D. praehauteriviana,* thus indicating an age of early late Valanginian. The age is in agreement with the simultaneous occurrence of rare specimens of *Lenticulina nodosa* (Moullade, 1980, in press). The assemblage from Core 71 can be correlated with the "*D. praehauteriviana* assemblage" that was found at approximately the same sub-bottom depth in Hole 391C (Cores 24 and 26; Gradstein, 1978a); it also occurs at Site 105 (Cores 19–21) and in Hole 101A (Core 10) (Luterbacher, 1972).

On the basis of a study of core-catcher samples, the interval from Cores 72 to 82 is devoid of foraminifers. Cores 83, 86, and 89 contain poor and non age-diagnostic assemblages comprising few agglutinated benthics such as "*Spirillina*"-like *Ammodiscus, Bathysiphon, Reophax, Ammobaculites,* very rare trochamminids, and few calcareous nodosariid benthics such as *Lenticulina* (*muensteri, gibba, crassa,* etc.) and *Pseudonodosaria humilis.* On the basis of additional samples, we believe that further investigations will be needed before these unusual and still poorly known Berriasian assemblages can be fully described.

The scanty and sporadic foraminifer occurrence in the Neocomian Blake-Bahama Formation from the western North Atlantic deep ocean stands in contrast to the contemporaneous and rich Tethyan microfaunas (Moullade, 1966). This contrast is probably due to the greater depth of deposition of the Blake-Bahama Formation, closer to the CCD level. Early diagenetic dissolution may have also impoverished the autochthonous microfossil assemblage.

Palynology

Samples 534A-49-4, 30–32 cm through 534A-61-2, 73–75 cm contain the lower lower Aptian to upper Hauterivian *Phoberocysta neocomica/Odontochitina operculata* Zones. *Phoberocysta neocomica* (Gocht) has its highest occurrence in the highest sample of this Zone. This species has been used by palynologists to define the Aptian/Barremian boundary, although Millioud (1969) reported it in the lower Aptian of the Angles stratotype section. It is also known to range through the lower half of the Bedoulian in its stratotype (Habib and Drugg, this volume). Cores 49 through 61 show a transition in the recovered residues from little micrinitic debris or admixed micrinitic-xenomorphic debris (49–51) to a rich residue containing well-preserved xenomorphic debris, numerous pollen grains (*Classopollis*), and foraminiferal linings (52–55), to a rich residue containing a well-developed tracheal facies (56–61) similar to that found in Cores 44 and 45. The distribution of organic facies corresponds fairly closely to that of the lithology. From Core 51 downward, the lithology becomes increasingly more turbiditic, with turbidites attaining greatest thickness in Core 58. It remains turbiditic through Core 61, but to a lesser extent.

Samples 534A-62-1, 41–42 cm and 534A-63-2, 38–40 cm contain very little residue of admixed xenomorphic/micrinitic debris in the Hauterivian *Druggidium rhabdoreticulatum* Zone. *Druggidium apicopaucicum* Habib has its highest stratigraphically persistent occurrence in Sample 534A-63-2, 38–40 cm, which supports the Hauterivian assignment. This species occurs also in Core 49, but it is believed to be reworked there because of the large stratigraphic gap between these two levels of occurrence. Samples 534A-65-5, 40–42 cm through 534A-75-1, 43–44 cm contain the Hauterivian to upper Valanginian *Druggidium deflandrei* Zone. The highest occurrence of *Scriniodinium dictyotum* Cookson and Eisenack in Sample 534A-72-2, 34–36 cm indicates that this sample is not younger than Valanginian. Samples in Cores 67 to 69 contain abundant carbonized debris, including many large carbonized tracheids, and numerous poorly preserved pollen grains (mostly *Classopollis*) and xenomorphic debris, as well as numerous chitinous linings of foraminifers (oxidized tracheal facies?). In Cores 72 to 74, the organic facies consists of abundant and well-preserved xenomorphic debris, pollen grains, and foraminiferal linings. The facies of Cores 67 to 74 lie within laminated chalks and graded claystones alternating with burrowed chalks.

Samples 534A-76-3, 10–12 cm through 534A-81-1, 61–62 cm are assigned to the lower upper Valanginian to lowest Valanginian *Druggidium apicopaucicum* Zone in thinly laminated marly chalks and bioturbated limestones. A well-preserved and well-developed tracheal facies is present, which ranges up into Core 75.

Samples 534A-82-1, 53-55 cm through 534A-86-1, 148-150 cm contain the upper Berriasian *Biorbifera johnewingii* Zone. *Amphorula metaelliptica* Dodekova is restricted to this Zone in the North Atlantic. Beginning with Core 84, there is a marked change of lithology downward to uniform pelagic oozes and marls lacking laminated clay layers. Reddish calcilutites similar to those of the underlying Cat Gap Formation occur in Core 84. The organic facies reflects this change in the *Biorbifera johnewingii* Zone. Core 82 contains relatively little organic residue but a well-preserved xenomorphic facies containing numerous *Classopollis* and foraminiferal linings. However, in Cores 83 through 86, there is very little residue of poorly preserved xenomorphic debris containing only few dinoflagellates. In Cores 85 and 86, *B. johnewingii, P. neocomica, Prolixosphaeridium granulosum* (Sarjeant), *Tanyosphaeridium salpinx* Norvick, *Cometodinium whitei* (Deflandre and Courteville), and *A. metaelliptica* are the only stratigraphically persistent species. This facies change affects the downward range of at least several dinoflagellate species.

Samples 534A-87-6, 7-8 cm through 534A-90-2, 0-1 cm are characterized by the same organic facies, lithofacies, lack of pollen grains, and paucity of dinoflagellates. This situation extends to the bottom of the Blake-Bahama Formation in Core 92. The highest sample contains *P. neocomica below the lowest occurrence of B. johnewingii,* indicative of an earliest late Berriasian or early Berriasian deposition. Few other species are present, but *P. granulosum, T. salpinx,* and *C. whitei* are persistent. The Cretaceous/Jurassic boundary is placed between Core 91, Section 2 and Core 91, Section 3, based on the lowest occurrence of *P. granulosum* and *T. salpinx* in Sample 534A-91-2, 57-58 cm. These species first appear in the early Berriasian in European stratotype material. *Polygonifera evittii* Habib has its highest occurrence in Sample 534A-90-2, 0-1 cm.

Nannofossils

A section of 390 m of limestones and alternating marls in Cores 47 through 91 contains common and generally well preserved nannofossil assemblages. On the basis of calcareous nannofossil evidence, neither the upper nor the lower boundary of the Blake-Bahama Formation coincides with a biostratigraphic boundary. Age assignments based on nannofossils and tentative correlations with European stages are shown in Table 8. Cores 47 through 59 contain assemblages typical of the upper part of Zone NC5 (Barremian), with *Watznaueria oblonga* and *Nannoconus colomii.* Cores 52 through 58 yielded similar nannofossil assemblages that also included *Calcicalathina oblongata*; thus these cores are assigned to the lower part of Zone NC5 (lower Barremian–upper Hauterivian), that is, Subzone *N. bucheri.*

Cores 59 (lower part) through 67 (upper part) belong to Zone NC4 (upper Hauterivian–upper Valanginian), as indicated by the presence of *C. cuvillieri, Spectonia colligata,* and *Nannoconus colomii.* Cores 67 (lower part) through 79, Section 4 are assigned to Zone NC3 (upper–lower Valanginian), on the basis of the presence of *Tubodiscus verenae.* Cores 79 (lowermost part) through 86 contain assemblages that are assigned to Zone NC2 (upper Valanginian–upper Berriasian), because of the presence of *Retecapsa neocomiana, R. angustiforata,* and *Nannoconus colomii.*

Cores 85 through 91 yielded assemblages that include large specimens of *Nannoconus colomii,* thus these assemblages belong to Zone NC1 (Berriasian). Small specimens of *Nannoconus* cf. *colomii* and *Nannoconus dolomiticus* occur in the Upper Jurassic. Therefore the first occurrence of the genus *Nannoconus* cannot be used to define the Cretaceous/Jurassic boundary.

Calpionellids

In the Blake-Bahama Formation sequence, shipboard (by M. Moullade) and shore-based (by J. Remane) observations have shown common and moderately well preserved calpionellids in Cores 89, 90, and 91 (thin sections of Samples 534A-89-3, 64-66 cm, 534A-90-1, 70-72 cm, 534A-90-4, 138-140 cm, and 534A-91-3, 82-84 cm). Abundant *Calpionella alpina,* the predominant species, is accompanied by very rare *Crassicollaria parvula* and *Tintinnopsella carpathica.* Using the Remane zonation (1978), we assigned these cores an age very close to the Tithonian/Berriasian boundary (B Zone, middle part), which agrees well with the dinoflagellate and coccolith age assignments.

Macrofossils

Dr. T. A. Jeletzky (Ottawa, Canada) submitted the following opinion on a pelecypod fragment in Sample 534A-83-1, 24-25 cm: "A flattened fragment of a finely and bluntly ribbed pelecypod, which cannot be identified even to the suborder."

Cat Gap Formation and Unnamed Unit

The interval from Core 92, Section 2 to Core 111, Section 1 is characterized by limestones and claystones. Calcareous nannofossils and dinoflagellate cysts are distributed throughout the interval (Table 9). The nannofossils are rare to abundant and moderately to poorly preserved. Many of the marker species present in the boreal realm are absent, which results in a reduced biostratigraphic resolution. Dinoflagellates are not as abundant as they are in the higher formations and are not as well preserved. Pollen grains and a few spores are most abundant in the lowermost lithostratigraphic unit, but elsewhere are generally absent. Cores 92 and 93 yielded identifiable calpionellids; their presence in Cores 94 to 96 is doubtful. The boundary between calpionellid Zones A and B is in Core 92. On this basis, the age of the lower part of Core 92 is late Tithonian. Several intervals also contain age-diagnostic foraminifers. Calcisphaerids occur in Cores 99 and 114. Pyritized radiolarians are present in the cores. Ammonite aptychi occur in Tithonian Core 95, in the remains of pelagic mollusks ("filaments") in Cores 127 and 128, and in sediments intercalated in basalt (Table 10).

Table 9. Preliminary biostratigraphy of the Cat Gap Formation, Hole 534A.

Cores	Foraminifers	Nannofossils		Dinoflagellates	Calpionellids	Age
92		*C. mexicana* Zone	*P. beckmannii* Subzone		*Calpionella* B/Zone A	latest Tithonian
93				LAD: *S. jurassica*	Zone A	late Tithonian
94						
95						Tithonian
96			*H. cuvillieri* Subzone			Kimmeridgian or Tithonian
97						
98						
99	*E.* aff. *uhligi* and *L. quenstedti*					
100		*V. stradneri* Zone				
101						
102						
103						
104				FAD: *C. whitei*		Oxfordian or Kimmeridgian
105						
106				FAD: *S. jurassica*		
107						
108						
109						
110	*"G." helvetojurassica*			LAD: *G. jurassica*		
111						

Note: FAD = first appearance datum; LAD = last appearance datum; braces in Age column indicate uncertainty in age assignment.

Table 10. Preliminary biostratigraphy of unnamed unit.

Cores	Foraminifers	Nannofossils		Dinoflagellates	Age
111		*V. stradneri* Zone			early Oxfordian
112	*L. quenstedti, F.* aff. *parallela*			FAD: *G. nuciformis*	
113					
114	*L. quenstedti*	*S. bigotii* Zone	*C. margereli* Subzone		
115					
116	*L. quenstedti*				
117				LAD: *C. pachydermum*	
118					late Callovian or Oxfordian
119					
120				LAD: *L. jurassica*	
121				LAD: *H. pectinigera* and	late Callovian or early Oxfordian
122				FAD: *P. evittii*	
123			*S. hexum* Subzone		middle Callovian or Callovian
124				LAD: *C. norrisii*	
125					
126					
127				FAD: *C. norrisii*	

Note: See Table 9 for explanation of symbol and abbreviations.

Foraminifers

Cores 92 to 110, between 1340 and 1498 m sub-bottom depth, recovered 69 m of the 160-m thick Cat Gap Formation. Samples processed for foraminifers yielded a moderately well-preserved and generally low-diversity assemblage. The red brown, gray black, and green shales appear to have a low carbonate content and may have lost much of an indigenous fauna. The intercalated gray micritic to coarse bioclastic limestones could not be processed, but thin sections show a lack of calcareous shelly microfauna, except for the bioclastic one to be discussed.

Core-catcher Samples 534A-92,CC and 534A-94,CC were virtually barren. Core 99, Section 3 to 99,CC contain *Lenticulina quenstedti, L. major, Epistomina uhligi, E. uhligi-parastelligera, Neobulimina* sp. (probably a new species), *Frondicularia nikitini, Ophthalmidium carinatum, Guttulina pygmaea, Turrispirillina amoena, Bigenerina jurassica*, and a number of other agglutinating taxa. Similar assemblages were reported by Luterbacher (1972) at Site 100 in ?Oxfordian to ?Kimmeridgian beds and by Gradstein (1978a) at nearby Site 391, Cores 50 to 52, assigned to the early Tithonian to Oxfordian. On the Grand Banks of Newfoundland, *E. uhligi* extends into upper Tithonian strata, and *L. quenstedti* ranges into Kimmeridgian (*sensu gallico*) beds (Gradstein, 1978b). These findings agree with those in Core B1 and in Core 99, Section 1, in Hole 534A, where *E. uhligi* without *L. quenstedti* was noted. The lower part of Core 99 is therefore assigned to the Kimmeridgian. A similar assemblage, including *L. quenstedti*, was found in Sample 534A-103-1, 86–87 cm.

Samples 534A-103,CC, 534A-104,CC, 534A-107,CC, and 534A-109,CC provided impoverished and diagnostically dissimilar benthic assemblages, including agglutinated forms (*Bigenerina, Ammodiscus, Glomospira, Reophax, Rhizammina, Bathysiphon*, etc.) and nodosariids (smooth *Lenticulina, Pseudonodosaria, Lingulina*, etc).

Core 110 recovery was very poor (only 30 cm in the core catcher), however, relatively diversified assemblages were recovered from the upper 20 cm. Planktonic foraminifers are present in the 44 to 65 μm size fraction of this sample (at 10–11 cm); these foraminifers are associated with slightly larger calcareous benthic and agglutinating taxa. The benthics are almost all smooth forms of *Lenticulina, Lingulina, Vaginulina, Dentalina, Lagena, Nodosaria, ?Epistomina*, and *Trocholina nodulosa, Conorbina* sp., *?Conorboides paraspis, Spirillina, Glomospira, ?Pelosina, Sorosphaera, Ammodiscus*, and *Bathysiphon*. The planktonics are of the type of *"Globigerina" helvetojurassica* Hauesler or *"G." ox-*

fordiana Grigelis. These forms, like almost all of the Jurassic planktonic form species, are stratigraphically and taxonomically poorly documented. The morphotypes are known to occur in Oxfordian strata of western Europe. Reddish colored limestones (Sample 434A-110,CC is a reddish calcareous claystone) with "globigerinids" frequently occur in the western Mediterranean and are generally Oxfordian (Colom and Rangheard, 1965). Such an age is tentatively assigned to Sample 534A-110,CC.

The foraminiferal fauna from the Cat Gap Formation at Hole 534A is predominantly composed of deep water benthics, that is, simple agglutinated benthics and nodosariids, but in Cores 99, 106, 107, and 110, transported shallow-water to upper-bathyal organisms are also present: epistominids, *Trocholina, Discorbis*, and *Baccinella irregularis* (calcareous algae in Sample 534A-106-1, 133–135 cm). In Cores 106 and 107, this presumably largely neritic microfauna is represented in a few thin levels of coarser oolitic limestone. It is worth mentioning that ostracodes occur in some amounts in the same layers as the transported shallow-water organisms.

Below Core 110 down to Core 116, benthic foraminiferal assemblages can be very common and diversified (i.e., Samples 534A-112,CC, and 534A-113-1, 24–26 cm), rare and poorly diversified (Sample 534A-114-1, 105–107 cm), or absent (Sample 534A-112-1, 62–64 cm; 534A-114-1, 10–11 cm).

The benthic foraminifers generally display a very small size (< 150 μm and frequently < 100 μm). Such size can be related to unfavorable habitat (for instance, a water depth too great for species that in general may have their optimal environment in the upper bathyal zone); or their even dimension is simply the effect of a size sorting due to redepositional processes. The second hypothesis, which would also explain the absence of these benthic foraminifers in the more fine-grained layers, would agree with the type of sediments we are dealing with.

The largest benthic assemblages consist of a number of nodosariids such as *Astacolus* aff. *major, Frondicularia* aff. *subparallela, Ramulina* sp., *Lenticulina quenstedti*, and agglutinated forms such as *Haplophragmium* cf. *aequale, Ammobaculites suprajurassicus, Rhizammina*, and so on. The specimens of *Frondicularia* aff. *subparallela* are reminiscent of *Frondicularia nikitini* but lack the striations. This assemblage is not strictly age-diagnostic but contains several species that are generally more abundant in Callovian–Oxfordian strata. *L. quenstedti* accompanied by a few other forms (such as *L. gibba, Ramulina* sp., *Dentalina* sp., polymorphinids, and "primitive" agglutinated forms) in Samples 534A-113-1, 59–61 cm, 534A-114,CC, and 534A-116, CC represents an impoverished assemblage characterizing the intermediate layers within a single graded sequence.

Similar depositional patterns control the abundance of benthic foraminifers in the lower Subunits 7b and 7c (Core 117–Sample 534A-127,CC). Relatively larger-sized specimens occur, associated with abundant radiolarians in the radiolarian claystones, much coarser than the coarsest layers from the overlying subunit. The benthic faunas from this lowest interval are similar to those of the upper units, however, representatives of *Dentalina, Trochammina*, and *Haplophragmoides* are more frequent in contrast to *Lenticulina, Rhizammina*, and so on, which dominated in the units above.

Several specimens of *Tolypammina*, a sessile foraminifer, are recorded from Sample 534A-127,CC. In absence of evidence for transportation, the hard substratum on which they grow may be provided for by shells of pelagic pelecypods, which occur abundantly in the same layer.

In Sample 534A-125,CC, small agglutinated foraminifers served as nuclei to phosphatic concretions.

Calpionellids

Cores 92 and 93 contain common moderately preserved calpionellids. In Cores 94 to 96, calpionellids are very rare and badly preserved; their identification or even their presence is not always certain. In samples from Core 92 (534A-92-1, 80–82 cm; 534A-92-2, 70–72 cm; 534A-92-4, 91–93 cm), *Calpionella alpina* is largely predominant, which indicates Zone B, close to the Tithonian/Berriasian boundary. In Sample 534A-92-5, 50–52 cm, the genus *Crassicollaria* becomes more abundant; consequently this association belongs to Zone A, which is definitely upper Tithonian. *Crassicollaria* spp. were also observed in Sample 534A-93-4, 44–45 cm.

Calcareous Nannofossils

Abundant to rare and moderately to poorly preserved nannofossils were recovered from this section of shales and limestones.

None of the existing nannofossil zonations can be used in this hole. Many of the marker species used in the boreal Jurassic are absent or exceedingly rare. Thus a new zonation is proposed in a later chapter of this book (Roth); it is based on forms recognizable in the light and electron microscopes.

The interval from Cores 92 to 96, Section 3 contains abundant *Conusphaera mexicana*, small specimens of *Nannoconus* (*N.* cf. *colomii* and *N. dolomiticus*) and *Polycostella beckmannii* but lacks *Stephanolithion bigotii*. This interval is assigned to the *Polycostella beckmannii* Subzone of the *Conusphaera mexicana* Zone.

The stratigraphically highest occurrence of fragmented *Stephanolithion bigotii* occurs in Core 97, Section 1. This occurrence defines the top of the *Hexapodorhabdus cuvillieri* Subzone of the *Conusphaera mexicana* Zone, which has its base in Core 101, Section 5. The assemblage includes *Conusphaera mexicana* and *Stephanolithion bigotii* but lacks *Polycostella beckmannii* and *Nannoconus* spp. The relationship of the nannofossil zones and the classical Jurassic stages is somewhat problematic. The extinction of the *Stephanolithion bigotii* is used to place the Kimmeridgian/Tithonian boundary. This means that *Conusphaera mexicana* ranges into the uppermost Kimmeridgian.

Cores 102 through 113, Section 1, at 47 cm contain *Vagalapilla stradneri* and *Stephanolithion bigotii* and are assigned to the *Vagalapilla stradneri* Zone. *Parhabdolithus embergeri* makes its first occurrence in the uppermost part of this interval; due to the gradual size increase and transition of this form from its ancestor, *P. embergeri* is not used here as a zonal marker. The Kimmeridgian/Oxfordian boundary falls within the *Vagalapilla stradneri* Zone and is tentatively placed at the base of Core 104, because of a change of specimen abundances. The base of this zone appears to coincide with the boundary of the middle and lower Oxfordian.

Core 113, Section 1, at 60 cm through Core 123, Section 2 belong to the *Stephanolithion bigotii* Zone–*Cyclagellosphaera margereli* Subzone. These cores contain common *Stephanolithion bigotii* but lack *Vagalapilla stradneri* and *Stephanolithion hexum*. A rare occurrence of *Axopodorhabdus rahla* in Core 118 is used as an indication of the Oxfordian/Callovian boundary in the vicinity of this core. The base of the *Stephanolithion bigotii* Zone–*Cyclagellosphaera margereli* Subzone (i.e., just above the last occurrence of *S. hexum*) coincides with the junction between the upper and middle Callovian. The joint occurrence of *Stephanolithion bigotii* and *S. hexum* in the intervals from the lower part of Core 123 to Core 126 is characteristic of the *Stephanolithion bigotii* Zone–*S. hexum* Subzone, which is middle Callovian. Shipboard paleontologists reported *S. bigotii* in Core 127, but this was not confirmed during shore-lab studies.

Palynology

The upper boundary of the Cat Gap Formation occurs in Core 92, Section 2 and is characterized by a lithologic change to bioturbated grayish red calcareous claystones. The uppermost Tithonian is located in the Blake-Bahama Formation in Samples 534A-91-3, 40–41 cm through 534A-92-2, 9–10 cm. It consists of the same poorly preserved organic facies characteristic of the lower Berriasian. Few fossils were recovered, including those in *Cometodinium whitei* and *Polygonifera evittii. C. whitei* ranges down to Sample 534A-104-2, 59–61 cm, which indicates an age no older than Tithonian for this sample. This species has its lowest occurrence in the Tithonian of France. On the basis of this evidence, the grayish red claystones in Hole 534A to the base of Core 103 are entirely Tithonian.

Sample 534A-93-2, 99–101 cm contains a rich organic residue of well-preserved and diversified dinoflagellates and extremely few pollen grains (bisaccates, *Classopollis, Exesipollenites*) in a matrix of abundant and well-preserved fine-grained xenomorphic–micrinitic debris. Species occurring in this sample that do not range into the Cretaceous include *Senoniasphaera jurassica* (Gitmez and Sarjeant), *Gonyaulacysta ambiguua* (Deflandre), *G. nuciformis* (Delflandre), *Chytroeisphaeridia chytroeides* (Sarjeant), and *Sentusidinium verrucosum* (Sarjeant). This sample also contains the uppermost occurrence of *Sirmiodinium grossii* Alberti sensu Warren, 1973. The North Atlantic specimens possess a pentagonal outline and a pericyst with an antapical perforation. They closely resemble *S. jurassica*, from which they can be distinguished by their perforate cysts. *S. grossii* is known to range from the Upper Jurassic through the Neocomian, but appears to be restricted to the Kimmeridgian–Tithonian in the North Atlantic. Warren (1973, fig. 7) showed that the pentagonal forms are concentrated in the Upper Jurassic of California. Samples 534A-94-4, 68–70 cm through 534A-103-1, 95–96 cm contain a large number of Upper Jurassic species. Pollen grains are virtually absent in residues consisting of poorly preserved xenomorphic–micrinitic debris. A number of black clay samples from Cores 99, 100, and 101 yielded only poorly preserved dinoflagellates in an abundant residue composed almost completely of small carbonized (micrinitic) particles and large carbonized tracheids. The color of these samples is attributed to the black color of the carbonized residue, which is considered to have formed in an oxidizing environment. The red clay residues of Samples 534A-99-3, 79–80 cm, 534A-100-2, 127–128 cm, and 534A-101-3, 67–68 cm consist of carbonized tissue quite similar to that in the red clay residues of Core 41.

Cores 104 to 111 consist of dark greenish claystones interbedded with light gray limestones. Samples 534A-104-2, 59–61 cm through 534A-106-1, 3–4 cm are composed of fossiliferous dinoflagellates and a few pollen grains in a rich xenomorphic–micrinitic residue. The lowest sample contains the lowest occurrence of the pentagonal forms of *S. grossii*, indicating an age not older than Kimmeridgian. Samples 534A-107-2, 98–100 cm and 534A-108-1, 23–25 cm are devoid of palynomorphs in a small residue made up entirely of small carbonized debris (micrinitic facies). Samples 534A-109,CC through 534A-111-1, 27–29 cm yielded rich residues of poorly preserved xenomorphic debris. Dinoflagellate fossils are relatively few but consist of a number of species. Sample 534A-110,CC contains the highest occurrence of *Gonyaulacysta jurassica* (Deflandre), which suggests deposition in the Kimmeridgian. The highest occurrence of this species is in Core 8 at Site 100.

Cores 111 to 127 consist of variations of dark variegated claystones, greenish gray claystones and limestones, and, near the base of the sedimentary section, greenish black laminated radiolarian claystones. Sample 534A-112-1, 69–71 cm has the lowest occurrence of *G. nuciformis*, which indicates an age close to the Kimmeridgian/Oxfordian boundary. Samples 534A-113-1, 0–2 cm through 534A-116-1, 76–68 cm possess poorly preserved dinoflagellates with an Oxfordian aspect, including species with fenestrate cingular septa in the genus *Wanaea* and in *Systematophora complicata* Neal and Sarjeant, *G. jurassica*, and *G. ambiguua*. Beginning with Core 117 and downward toward the bottom of the section, there is an increasing diversification of spheroidal dinoflagellates with epicystal archeopyles referable to *Ctenidodinium* Deflandre sensu Lentin and Williams (1973). Samples from Cores 117 and 118 contain the thicker-walled species *Ctenididinium pachydermum* (Deflandre) and the lowest occurrence of Oxfordian *Scriniodinium dictyotum*. Sample 534A-119-1, 120–121 cm yielded few fossils, including *S. complicata*, in a residue of fine carbonized debris. Sample 534A-120-1, 43–45 cm contains the highest occurrence of *Lithodinia jurassica* Eisenack, of the early Oxfordian. This sample also contains the first downhole occurrence of *Stepha-*

nelytron scarburghense Sarjeant and spinate species in the plexus *Ctenidodinium combazii* Dupin/*C. ornatum* (Eisenack). Samples 534A-121-1, 8–10 cm through 534A-123-1, 92–94 cm contain *L. jurassica, C. combazii/C. ornatum*, aff. *Acanthaulax cladophora* (Deflandre), *Stephanelytron redcliffense* Sarjeant, *S. scarburghense*, and *Hystrichogonyaulax pectinigera* (Gocht), which indicate deposition in the early Oxfordian. The lowest occurrence of *P. evittii* in the uppermost sample of this interval indicates an age not older than earliest Oxfordian.

Sample 534A-124-1, 54–56 cm through the stratigraphically lowest sample studied, 534A-127-2, 33–35 cm, contain dinoflagellates assigned to *Ctenidodinium norrisii* (Pocock) and *Wanaea indotata* Drugg, which indicate the Callovian. Species of *Stephanelytron* extend down through Core 127, indicating that this stratigraphic level is not older than middle Callovian.

Throughout the section ranging from the lower upper Berriasian through the lower Oxfordian, palynological study of the investigated samples indicates that much of the recognizable organic matter is of marine origin, with only short intervals of concentrated carbonized tracheal tissue. In the stratigraphic interval represented by Cores 121 through 127, however, the sediments contain rich organic residues of abundant and well-preserved xenomorphic debris (of fecal pellet origin) and foraminiferal linings, and also numerous *Classopollis*, diversified large fern spores including at least four species of *Cicatricosisporites, Ephedripites* (including *Steevesipollenites*), both well-preserved and carbonized large tracheids, and cuticular tissue—all of which indicate an episode of a large influx of terrigenous organic matter in the middle Callovian to early Oxfordian. The occurrence of *Cicatricosisporites* in sediments as old as Callovian is unusual, but is entirely consistent with large contributions of organic materials derived from the continents.

Radiolarians

Radiolarians are common to abundant throughout the lower part of the Blake-Bahama Formation, the Cat Gap Formation, and the unnamed Lithologic Unit 7. The tests are predominantly replaced by calcite or in certain levels by pyrite (Cores 75–83 and Cores 120–126). Radiolarians preserved as silica are very rare.

The abundant pyritized radiolarians of Cores 120 to 126 represent very well-preserved assemblages assignable to the lowermost Zone A (Unitary Association 1—or U.A. 1) of Baumgartner et al. (1980). In the Tethyan realm these associations are dated as ranging from middle/late Callovian to early Oxfordian.

The base of *Eucyrtidium ptyctum* s. str. in Sample 534A-122-1, 43–45 cm and the final appearance of an undescribed early form of *Mirifusus* sp. in Sample 534A-123-1, 29–31 cm make it possible to separate a new Unitary Association "O" from U.A. 1 of Baumgartner et al. (1980). Both U.A. "O" and U.A. 1 have been recognized in the lower part of the basal, ribbon-bedded, green radiolarites of the Lombardy Basin of northern Italy and allow a precise biostratigraphic correlation to be drawn between Tethyan and Atlantic radiolarian-rich formations (see Baumgartner, this volume).

Macrofossils

Dr. G. E. G. Westermann (Hamilton, Canada) studied a number of minute ammonite shells in Core 100 and provided the following written opinion: "2 to 12 mm diameter, juvenile Ammonoidea, crushed and with most of the shells dissolved, except for a thin iridescent (nacreous, aragonitic) film. Probably originally without ornament; the present fine crinkles of the peri-umbilical area are due to plastic deformation after partial decalcification. No septal sutures were preserved and no stratigraphic conclusion is feasible."

Dr. J. A. Jeletzky (Ottawa, Canada) provided the following written opinion on shell fragments in Sample 534A-101-1, 33–34 cm: "Fragment of an ?ostreid pelecypod, strongly resembling *Pycnodonite* Fischer de Waltheim (1835) but not definitively identifiable. *Pycnodonte* suggests an Early Cretaceous age."

Sediments between Basalt Flows

In Core 128, calcareous claystone occurs in Section 1, 75–82 cm, and in Section 3, 107–109 cm. The latter sample contains common to abundant fragments of molluscan shells that are very similar to the so-called "filaments." Rare, small, silicified benthic foraminifers also occur: they can be attributed to the genera *Glomospira, Dentalina, Pseudonodosaria*, and possibly *Turrispirillina*. Radiolarians are rare, and fish debris appear to be absent. Calcareous nannoplankton could not be isolated because of the heavy recrystallization. The microfacies with abundant pelagic molluscan shells recalls the facies from *Posidonia* Beds, a formation widespread in the Tethys realm from the Bajocian to the Callovian.

SEDIMENTATION RATES

Bermuda Rise, Plantagenet, and Hatteras Formations

Biostratigraphic resolution in these formations is not adequate to calculate firm sediment accumulation rates, especially for the upper part of this interval. We assume the presence of a hiatus between the base of the lower Miocene and upper Eocene. Sediment accumulation rates of about 2.5 m/m.y. for the Bermuda Rise and Plantagenet intervals are only a crude approximation. Numerous hiatuses could be present in this poorly dated interval. A hiatus embracing most of the Upper Cretaceous (Campanian through Turonian) is postulated between the Plantagenet and Hatteras Formations. Biostratigraphic control is relatively detailed in the Hatteras Formation. The overall net rate is about 10 m/m.y., with a condensed sequence or possibly hiatuses in the early Aptian through the early Albian (Figs. 13 and 41).

Blake-Bahama Formation

Good stratigraphic control provided by a continuous nannoplankton zonation and some foraminiferal and calpionellid age determinations indicate relatively constant

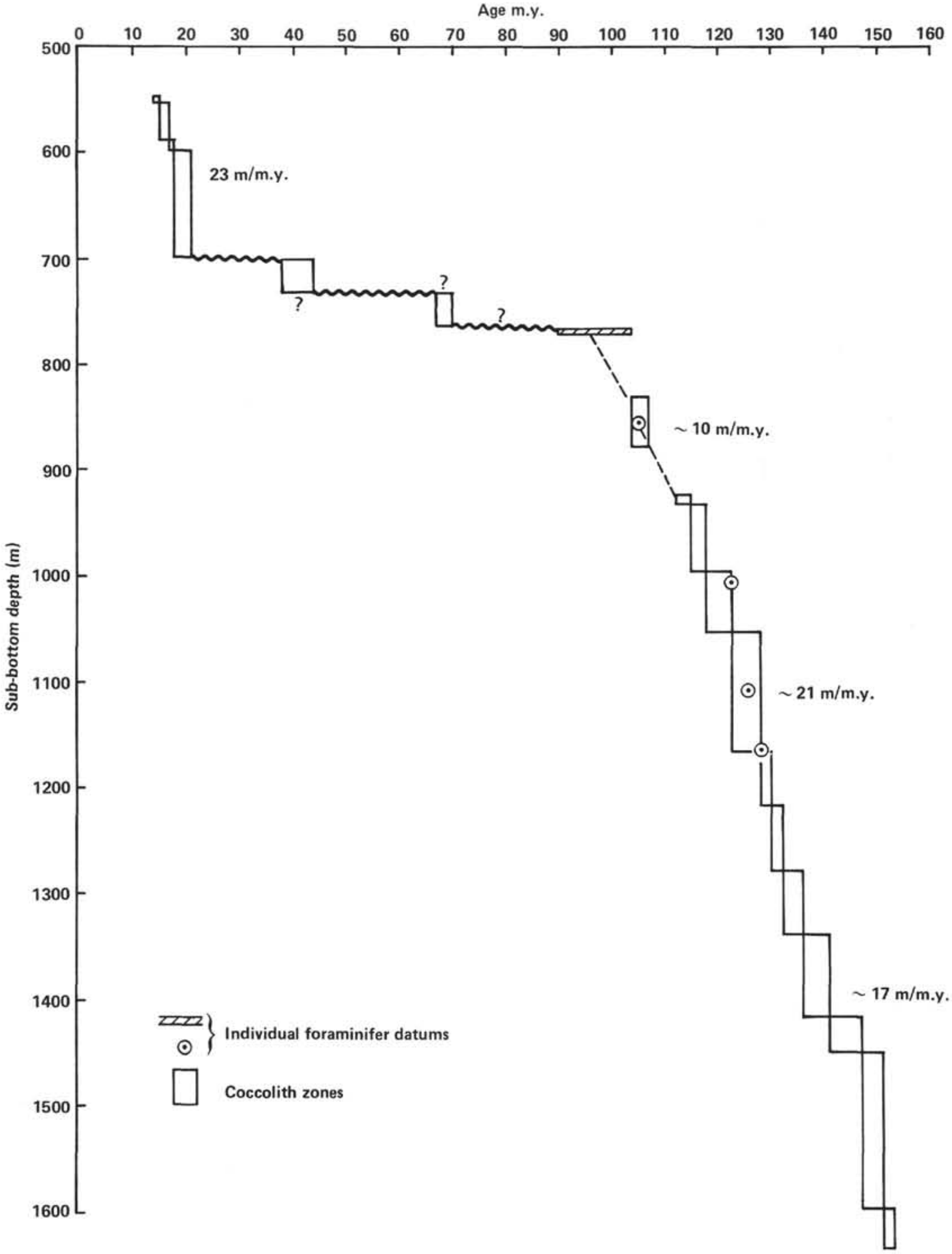

Figure 41. Sedimentation rates for Hole 534A. (Dashed line indicates apparent continuous sedimentation.)

sedimentation rates of 21 m/m.y. for the Blake-Bahama Formation.

Cat Gap Formation and Lithologic Unit 7

Although biostratigraphic resolution is not very good for the Jurassic part of this hole, we were able to calculate an average sediment accumulation rate of about 17 m/m.y.

ORGANIC GEOCHEMISTRY

Shipboard Rock Eval Analyses

Previous studies of the carbonaceous black shales of the Hatteras Formation collected at Site 391 demonstrated that the kerogen in the samples analyzed was thermally immature and contained significant amounts of terrestrially derived organic matter (Cardoso et al., 1978; Deroo et al., 1978; Dow, 1978). Investigation of lipids extracted from three Site 391 samples also indicated the terrestrial nature of the organic matter (Cardoso et al., 1978). Forty-six samples collected from the Cretaceous black shales and overlying and underlying units of Hole 534A were examined to determine the origin and maturity of their kerogen. The results of these determinations were similar to the results obtained for the material collected 22 km away at Site 391.

The kerogen in the samples was analyzed using the Girdel Rock Eval and CHN Analyzer. The Rock Eval utilizes a standard pyrolysis method employed in source-rock characterization and evaluation. The instrument consists of a pyrolysis unit linked to dual detectors—flame ionization (FID) for hydrocarbons and thermal conductivity (TC) for CO_2. Samples were ground to a coarse consistency, placed in sintered steel crucibles, and heated from 250°C to 550°C at 25°/min. in an inert (He) atmosphere. The gas stream released during the program was split; half was directed towards the FID and half towards the TC. The CO_2 evolved during the heating was collected from 250° to 390°C and stored in a trap until the programming was finished. It was then reheated and directed toward the TC. Samples were held at the initial temperature (250°C) for 5 min. while the indigenous hydrocarbons present in the rocks were volatized and swept by the helium to the FID. The total hydrocarbon yield during that time period corresponded to the amount of free hydrocarbons (oil and gas) contained in the sample. This is called the S_1 peak and is expressed in mg hydrocarbons (HC)/gram of rock.

The programming of the unit from 250° to 550°C results in the cracking of the kerogen contained in the sample. The corresponding peak is called S_2 and is also measured in mg HC/gram rock. As the kerogen in a sample increases in maturity, the S_1 peak will increase and the kerogen (S_2 peak) will decrease. The temperature at which the S_2 peak is evolved is monitored during the analysis and is related to the maturity of the kerogen. Immature material will crack between 400 and 435°C, whereas kerogen from a mature zone will crack between 435° and 460°C. The quantity of CO_2 evolved between 250° and 390°C is the S_3 peak. A cut-off of 390° was chosen for the collection of CO_2, because siderite decomposes at 400°C and calcite and dolimite decay between 500° and 600°C.

Plots of the hydrogen index (mg hydrocarbon found in S_2 peak/gram organic carbon) and the oxygen index (mg CO_2 found in S_3 peak/gram organic carbon) have been used to display the results of the Rock-Eval analyses for Hole 534A (Fig. 42). Generally, the hydrogen index is low, which indicates that the samples are too immature or too depleted in hydrogen to be considered petroleum sources. Their immature character is also indicated by the relatively low temperatures (400–425°C) at which the kerogen cracked (Fig. 43). This plot of the oxygen index versus depth shows that there is a sharp reduction in oxygen content below 765 m. This oxygen reduction below 765 m corresponds to the lithologic transition from calcareous chalks and varicolored claystones above 765 m to the underlying carbonaceous claystones (black shales) of the Hatteras Formation. Within the Hatteras Formation (764–950 m), the oxygen indexes remain fairly constant, with ratios ranging from 50 to 100 mg CO_2/gC_{org}, which implies a steady input from terrestrial organic sources. The hydrogen indexes do not follow lithologic boundaries as closely as do the oxygen indexes (Fig. 43). A probable input from marine organic sources is indicated by the higher values downhole. The percent of organic carbon also increases at this lithologic transition from a low of 0.03% in the overlying varicolored claystones, to 0.65% at the top of the carbonaceous claystones, to a maximum of 4.62% near the top of the Blake-Bahama Formation. (Figs. 43 and 13). Organic carbon decreases and the oxygen index increases near the Hatteras/Blake-Bahama formations boundary. Most of the values for organic carbon within

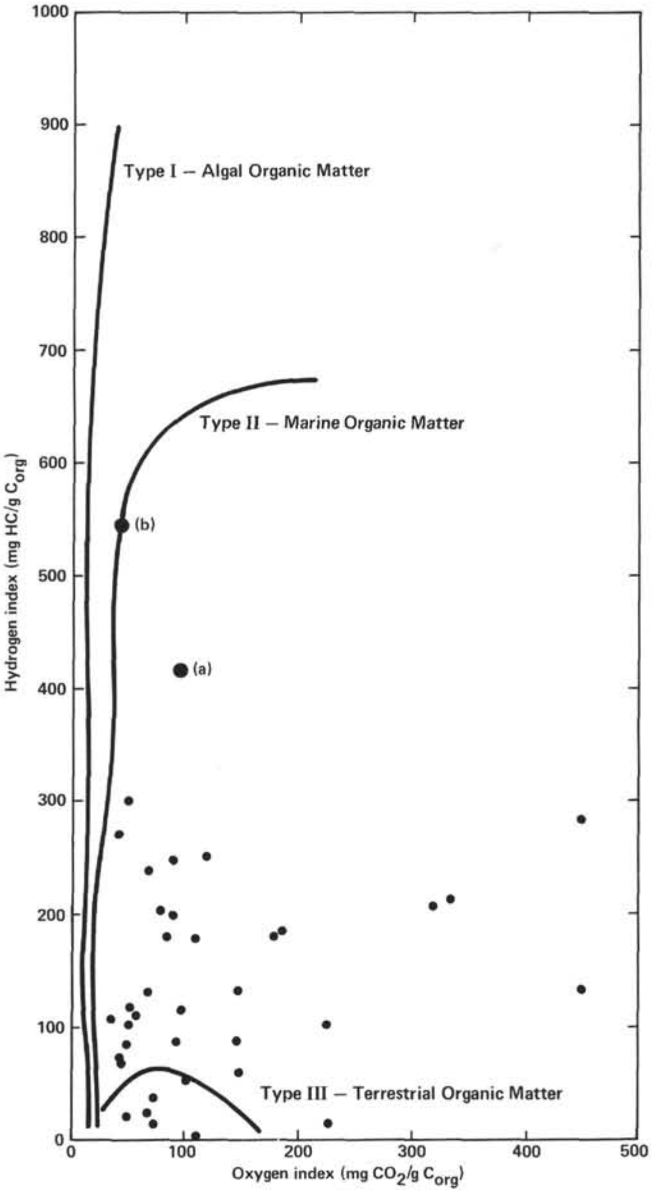

Figure 42. Hydrogen index versus oxygen index, Site 534. (See text for explanation of points a and b.)

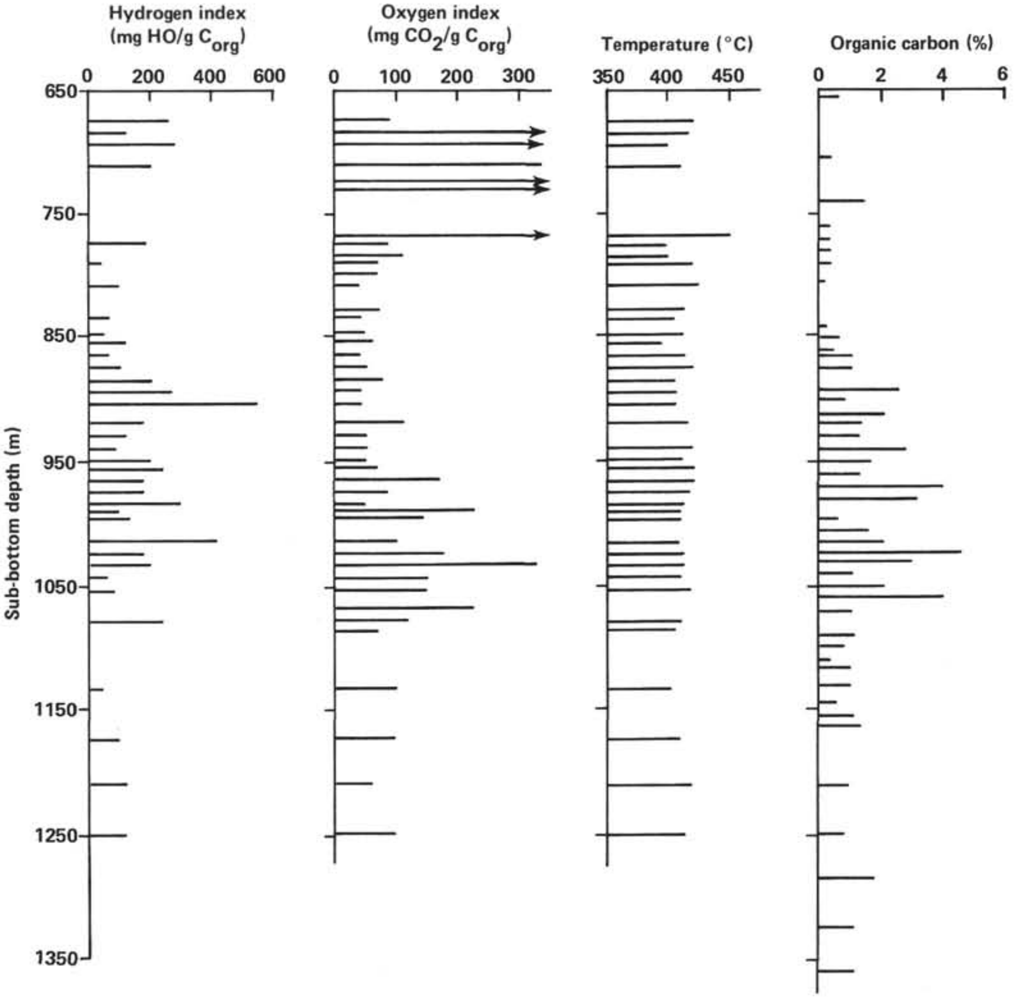

Figure 43. Hydrogen, oxygen, temperature, and organic carbon indexes for Hole 534A.

the black shales exceed the lower limit of organic carbon (0.4%) thought to be needed for petroleum generation.

Different types of kerogen can be displayed on a Van Krevelen diagram (Fig. 44) where atomic H/C is plotted versus atomic O/C. Type I kerogen is rich in hydrogen and contains predominantly lipids such as fatty acids, alcohols, and waxes. It closely resembles the constituents of petroleum and is considered as good source-rock material. Type II kerogen is derived from marine algal material. Type III, rich in oxygen, is composed of derivatives of cellulose such as carbohydrates and lignin and is not a likely petroleum precursor. It is probable that gas or coal would be produced from the maturation of Type III materials. As the kerogen of any one type is subjected to time and temperature, it initially becomes depleted with respect to oxygen, and later the H/C ratio decreases also. Figure 44 shows three types of kerogen and their evolution from immaturity to maturity. It can be seen from Figure 42 that the predominant type of kerogen present in the samples from Hole 534A is terrestrial in origin (Type III) and therefore a potential gas source. However, two samples containing Type II kerogen (a and b, Fig. 42) may be regarded as potential petroleum sources.

Four samples in Cores 124, 125, and 126 of Lithologic Subunits 7c and 7d were analyzed on the Rock Eval, and eight for organic carbon. The results are summarized in Table 11.

Two samples proved low in organic carbon (Sample Nos. 4 and 8 were only 0.34 and 0.16%, respectively). Three others were found to be above average, ranging from 1.1 to 2.4%. The worldwide average for shales is about 1.0% for organic carbon.

The hydrogen index is low for all of the samples, but very low for two of them—Samples 4 and 8. This information, coupled with the relatively high values of the oxygen index, suggests that the organic matter in Samples 4 and 8 is essentially vitrinitic in nature, or a kerogen Type III, using Tissot's terminology, and so has a terrestrial source. The other samples, 6 and 7, although showing a higher hydrogen index, also must be judged to contain primarily terrestrial plant debris, probably a mixture of Types II and III (typified by exinite for Type II and vitrinite for Type III, using Tissot's terminology).

All of the samples appear to be immature, none having reached a maturation stage of significant hydrocarbon generation.

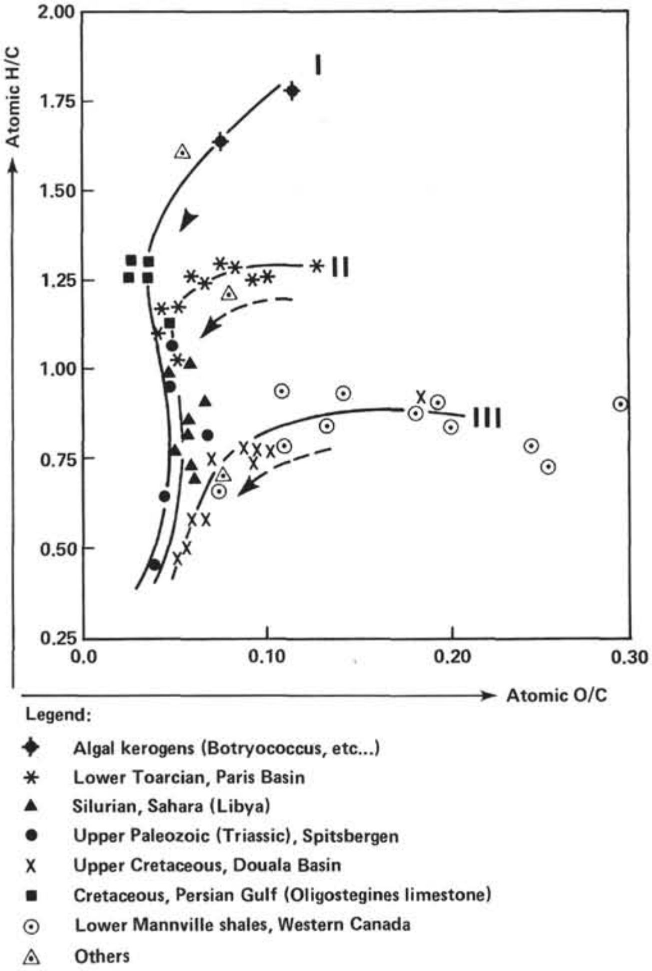

Figure 44. Classification of the various types of kerogen in an atomic H/C–O/C diagram (after Espitalié et al., 1977).

INORGANIC GEOCHEMISTRY

Observed values for interstitial water pH, alkalinity, salinity, chlorinity, magnesium, and calcium are recorded in Table 12 and are plotted versus sub-bottom depth in Figures 45 and 46. The analytical procedures used are explained in the Explanatory Notes to this volume. Twenty-two interstitial water samples were squeezed from 15-cm-long full-core sections taken from 550 to 1100 m sub-bottom. Gradual induration of the sediments precluded pH and alkalinity measurements below 1000 m, and analyses for salinity, chlorinity, calcium, and magnesium were terminated at 1100 m when squeezes from deeper samples failed to recover any water.

A brief comparison of the interstitial water data from Site 534 with that from Site 391 (Leg 44) 22 km away shows that depth profiles of all the components measured (with the exception of pH) almost overlap below 500 m. This observation suggests rather uniform sedimentology throughout the central Blake-Bahama Basin. The more detailed observations of the present site indicate, however, that chloride and salinity in the Cretaceous Plantagenet and Hatteras formations vary more widely than previously thought. The variations, 1.5% in chloride and 3% in salinity, are approximately an order of magnitude larger than analytical error. Because the black shales, especially, are fissile and hygroscopic, variation due to contamination by surface seawater during the coring operation cannot be ruled out. Soft, highly deformed core samples from 815 and 872 m yielded unusually large quantities of water after squeezing less than one hour at 15,000 psi, which suggests possible contamination. Data points for these samples are enclosed in parentheses in Figures 45, 46, and 47.) Generally, however, surface seawater contamination should produce sharp negative deflections in the calcium profile corresponding to sharp positive deflections in the magnesium profile; such behavior is not observed. The chloride and salinity variations therefore appear to be real. Although no attempt is made to explain these observations at the present time, it is worth noting that a possible correlation may exist between chlorinity and salinity variations and clay porosity. Figure 47 shows clay porosity and chlorinity plotted against depth in the Plantagenet and Hatteras formations. Within the precision of the data, between 700 and 900 m, low chlorinities appear to correspond to minima in clay porosity, and, conversely, high chlorinities appear to correspond to maxima in clay porosity. Superimposed on these small-scale variations are a gradual decrease in porosity and a gradual increase in chlorinity with depth.

Except for minor variations in the Plantagenet and Hatteras Formations, magnesium remains almost constant at about 35 mmol/l throughout the interval cored. Apparently, diagenesis in the clay units and the carbonate units penetrated has not resulted in net uptake of magnesium. Calcium, on the other hand, shows a large increase with depth and behaves as if it were completely independent of magnesium. The relatively smooth profile suggests a net diffusion of calcium upward in the statigraphic column. Reaction with bicarbonate ion to produce calcium carbonate and carbon dioxide between

Table 11. Organic geochemistry summary, Hole 534A.

Sample no.	Sub-bottom depth (m)	Sample (interval in cm)	Org. carbon (%)	Hydrogen index (mg HC/g C_{org})	Oxygen index (mg CO_2/g C_{org})	S_2 (°C)	Lithology
1	1590.0	122-1, 13–15	0.38	—	—	—	Marly limestone
2	1595.5	123-2, 78–80	0.47	—	—	—	Marly claystone
3	1595.5	123-2, 98–100	1.30	—	—	—	Dark claystone
4	1603.5	124-1, 55–58	0.34	32	166	435	Marly limestone
5	1607.0	125-3, 98–101	1.80	—	—	—	Olive green black claystone
6	1608.5	125-4, 69–71	2.40	52	46	426	Olive green black claystone
7	1623.0	126-2, 28–31	1.10	54	88	418	Calcareous claystone
8	1626.0	126-4, 19–21	0.16	23	260	415	Calcareous claystone

Note: — indicates no measurement made.

Table 12. Summary of shipboard geochemical data, Hole 534A.

Sample no.	Sample (interval in cm)	Sub-bottom depth (m)	pH	Alkalinity (meq/l)	Salinity (‰)	Calcium (mmol/l)	Magnesium (mmol/l)	Chlorinity (‰)
IAPSO	—	—	7.67	2.37	35.50	10.55	53.99	19.38
SSW	—	—	8.17	2.37	36.77	10.59	55.47	20.00
38	3-2, 135-145	558.28-558.35	7.15	8.81	34.27	15.28	34.63	20.07
39	7-2, 140-150	596.40-596.50	7.02	8.11	34.87	17.56	34.26	20.11
40	10-3, 105-120	616.55-616.70	7.01	8.91	34.49	18.96	32.63	20.31
41	14-2, 135-150	653.35-653.50	7.08	7.35	34.38	20.66	33.11	20.04
42	17-5, 135-150	685.85-686.00	—	—	—	—	—	—
43	20-2, 135-150	708.35-708.50	7.27	3.94	34.43	25.46	34.45	20.20
44	24-2, 135-150	744.35-744.50	7.47	3.25	33.55	28.32	34.04	19.42
45	27-1, 135-150	765.85-766.00	8.23	2.10	32.62	26.79	31.38	18.83
46	29-2, 135-150	786.35-786.50	8.24	2.60	35.31	29.08	35.20	20.19
47	32-1, 132-150	814.82-815.00	7.61	2.29	36.30	31.23	38.60	20.53
48	34-1, 105-120	833.55-833.70	8.10	2.30	33.80	31.55	33.22	19.62
49	36-2, 135-150	852.85-853.00	8.05	2.19	35.83	33.49	34.44	20.91
50	38-4, 135-150	871.85-872.00	8.09	1.77	36.71	34.08	38.08	20.57
51	41-4, 135-150	898.85-899.00	8.42	1.25	34.21	34.90	35.03	19.67
52	43-1, 135-150	916.85-917.00	7.70	0.94	37.02	36.57	36.56	21.29
53	45-2, 135-150	934.85-935.00	7.47	0.77	37.02	36.74	36.21	21.49
54	47-3, 134-150	954.34-954.50	—	—	—	—	—	—
55	49-2, 140-150	966.40-966.50	—	—	37.51	39.52	37.06	21.69
56	52-1, 0-15	990.50-990.65	7.43	0.33	37.46	43.59	36.54	21.56
57	56-1, 140-150	1027.90-1028.00	—	—	37.51	47.57	36.96	21.61
58	58-2, 135-150	1047.35-1047.50	—	—	38.45	56.33	36.50	21.87
59	61-2, 127-142	1074.27-1074.42	—	—	39.22	63.10	35.28	22.37
60	63-2, 105-120	1092.05-1092.20	—	—	39.33	63.81	35.96	22.37
61	64-4, 135-150	1104.35-1104.50	—	—	38.72	64.42	35.13	21.86
62	68-3, 135-150	1134.35-1134.50	—	—	—	—	—	—
63	71-3, 135-150	1161.35-1161.50	—	—	—	—	—	—

Note: — = insufficient water for analysis.

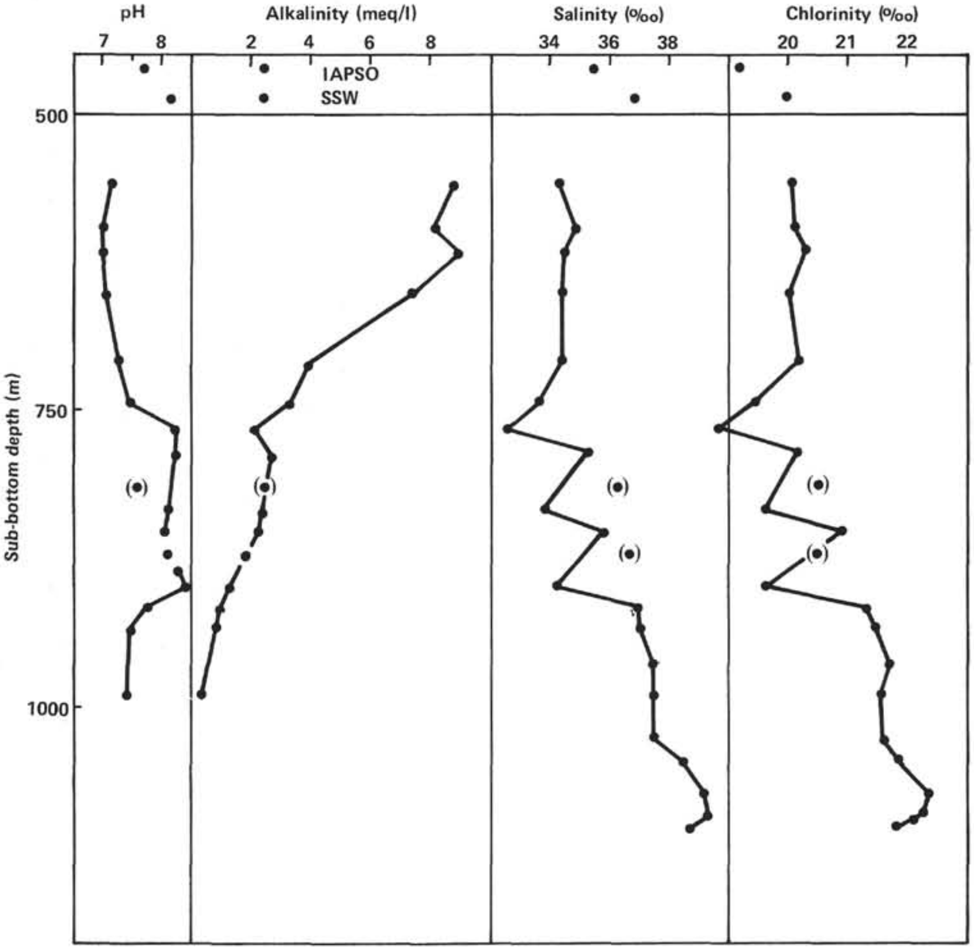

Figure 45. Alkalinity, salinity, and cholorinity, Site 534. (See text for an explanation of data points enclosed in parentheses; also for Figs. 46 and 47).

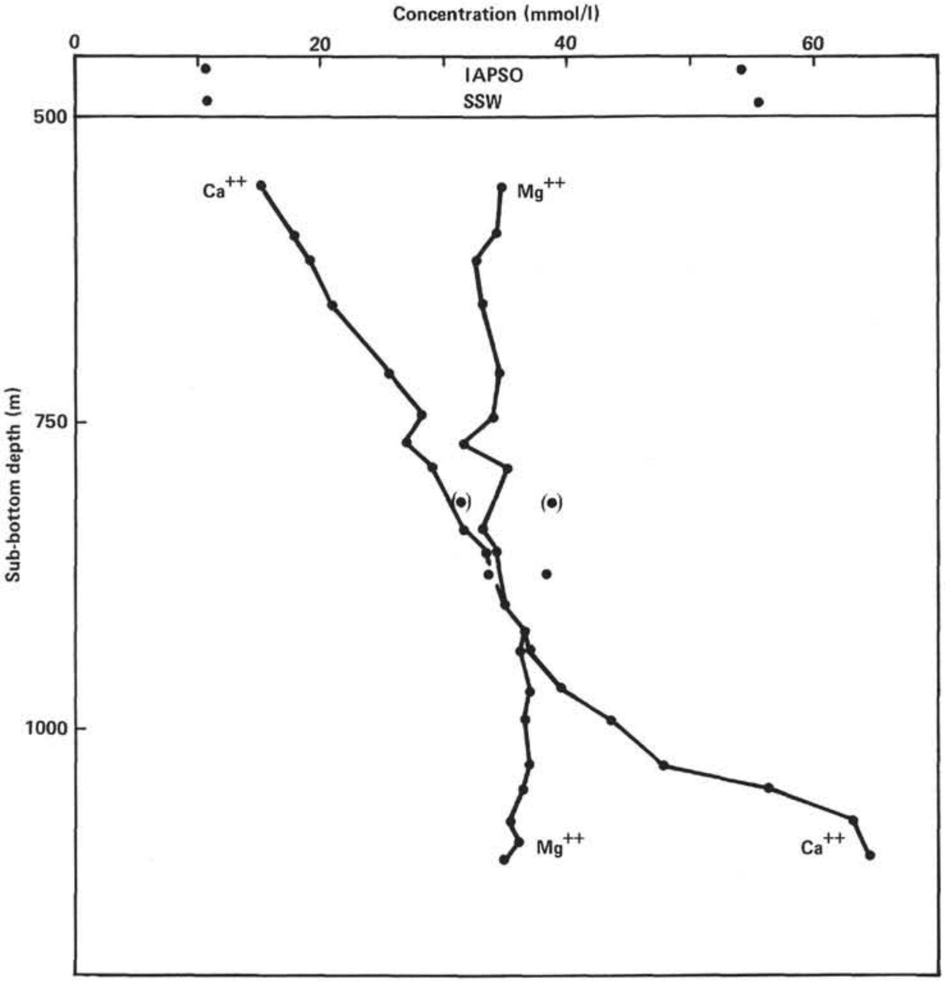

Figure 46. Ca^{++} and Mg^{++} concentrations, Site 534.

600 and 750 m sub-bottom depth would explain the sharp drop in alkalinity and relatively low pH observed for this region.

Between 750 and 900 m sub-bottom, pH values of 8 to 8.5 are observed. These high values reflect the presence of clay-rich sediments of the Bermuda Rise, Plantagenet, and Hatteras formations and contrast sharply with the pHs of 7 to 7.5 for the carbonate sediments above and below. It is not certain whether the observed pH difference reflects *in situ* conditions or a squeezing effect.

PHYSICAL PROPERTIES

The physical property data from Site 534 are summarized in Figure 48 and Tables 13 and 14. Additional data are included in the site summary diagram (Fig. 13) and in Shipley (this volume).

Great Abaco Member

The chalks, mudstones, and limestones of the Great Abaco Member were little disturbed by drilling and provide reliable physical-property data. The cored portion of the Great Abaco Member contains about 65% chalk, 25% mudstone, and 10% limestone. The average sound velocity, bulk density, and porosity of each of these lithologies is given in Shipley (this volume).

Chalk thermal conductivities were measured in duplicate at two depths, 599.3 and 653.9 m. The values, 1.74 and 1.66 mcal/cm-°C-s, appear reasonable. No thermal conductivity values were reported at Site 391.

Porosity rebound for chalks at this depth of burial is about 5% and for mudstone about 8% (Hamilton, 1976). The porosity rebound effect results in measured laboratory velocities being about 0.1 km/s lower than *in situ* values for the chalk porosity rebound and about 0.02 km/s for mudstone porosity rebound (Boyce, 1976).

Bermuda Rise Formation

Only three mudstone samples were available for physical property measurements from the Bermuda Rise Formation, because of the very low recovery and drilling disturbance.

Plantagenet Formation

Four samples of mudstone and one of chert were examined from the thin Plantagenet Formation. There is no obvious significant variation in velocities, densities, or porosities between the Plantagenet Formation clay-

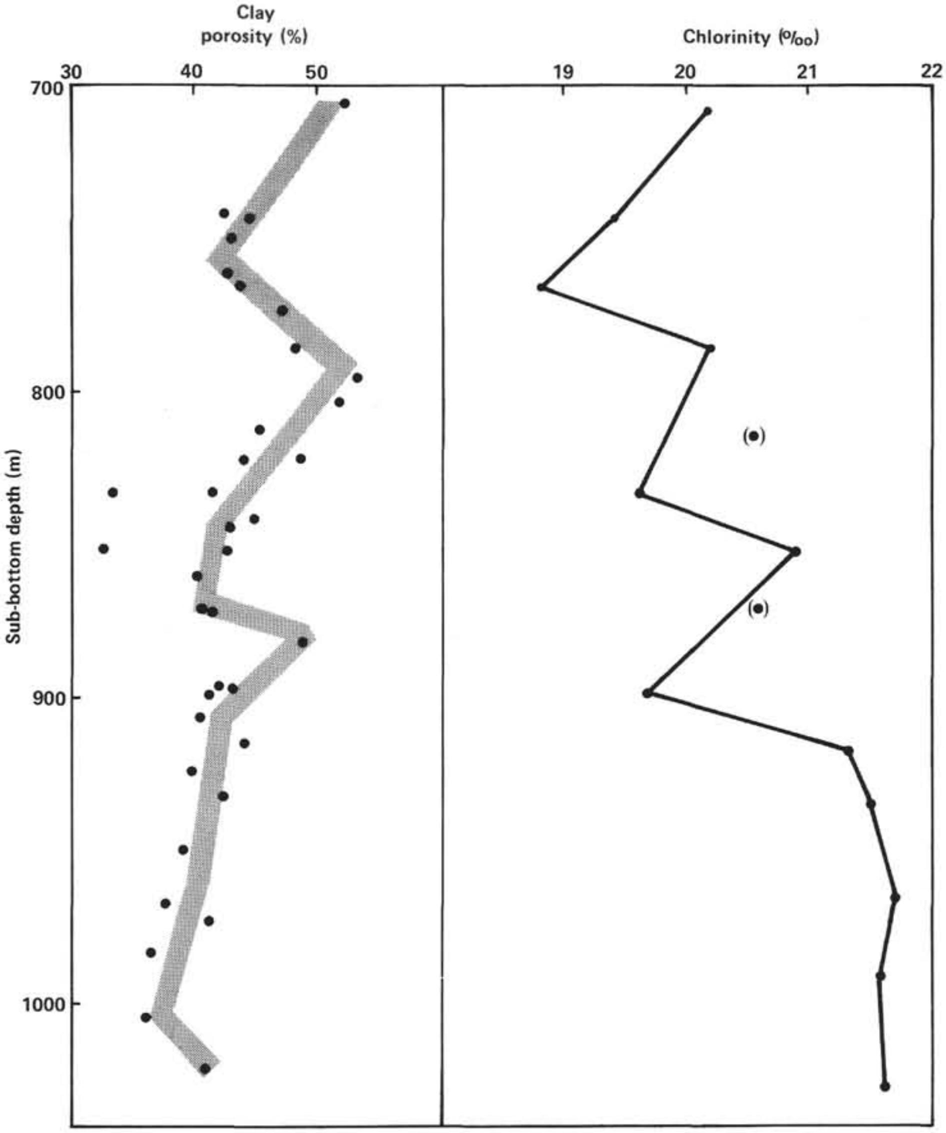

Figure 47. Clay porosity and chlorinity, Site 534.

stones and those of the overlying Bermuda Rise or the underlying Hatteras Formations.

Hatteras Formation

The claystones of the Hatteras Formation were only slightly disturbed in the coring process and generally yielded good physical property data. The claystones are water absorbing, and care was exercised to trim contaminated material before velocity and gravimetric measurements were undertaken. The fissile nature of the black shales made velocity measurements parallel to bedding difficult. Gravimetric determinations are probably only accurate to 1 or 2% because of water absorption. No analytical problems were encountered with the chalks or limestones.

At this depth of burial, porosity rebound for the claystones is estimated at 8% or 9% (Hamilton, 1976). The effect on the *in situ* vertical velocity for the claystones is about 0.25 km/s. There was insufficient coring at Site 391 to make an adequate comparison of physical properties to Site 534.

Blake-Bahama Formation

The heterogeneous lithologic components and gradational changes of the claystones, chalks, and limestones produce a wide range of physical properties within the Blake-Bahama Formation. The rocks are well-indurated, and thus there is little core disturbance that could affect the laboratory measurements. The abundance estimates of the lithologic components within this formation are only accurate to about 10% because of the gradational changes between lithologies.

Thermal conductivity was measured in a claystone, chalk, and limestone; results were 2.1, 2.8, and 2.7 mcal/cm-°C-s, respectively. The range of values may reflect, in part, the variations in porosity.

The affect of porosity rebound cannot be determined from data of Hamilton (1976) for depths greater than

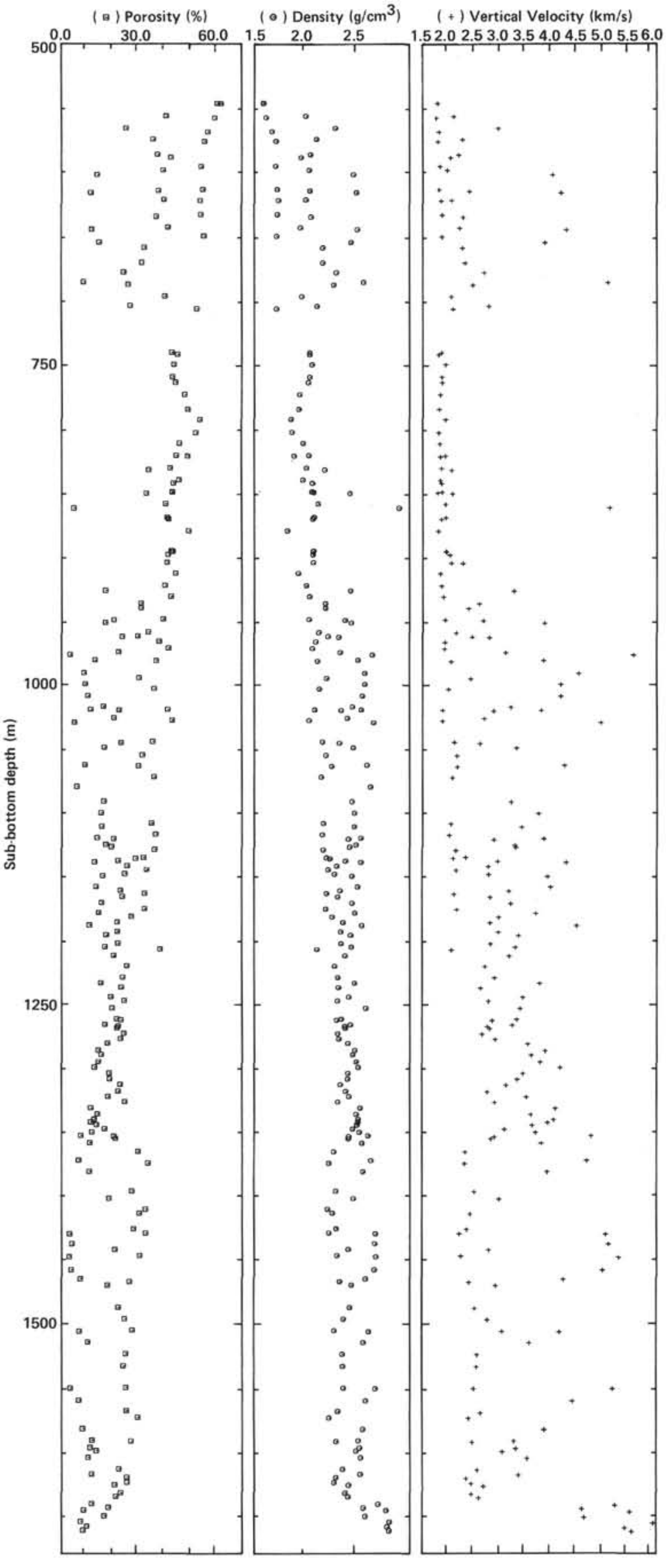

Figure 48. Laboratory physical properties data, Hole 534A.

Table 13. Physical property data, Site 534.

Sample (core-section, cm from top of section)	Depth in hole (m)	Velocity (km/s)		Thermal conductivity (mcal/cm-°C-s)	GRAPE wet-bulk density[a] (g/cm^3)	Gravimetric (wet)			Lithology
		Parallel to bedding	Normal to bedding			Bulk density (g/cm^3)	Water content (%)	Porosity (%)	
Hole 534									
1-1, 121					1.50				
Hole 534A									
2-1, 95	546.8	1.84	1.68		1.57	1.59	37.9	60.3	Mudstone
3-1, 148	556.9	2.12	1.99		2.03	2.00	20.3	40.4	Chalk
3-2, 119	558.1	1.92	1.65		1.65	1.61	36.8	59.3	Mudstone
4-1, 148	566.5	3.02	2.86		2.25	2.28	10.9	24.9	Chalk
4-3, 112	569.1	1.91	1.71		1.62	1.67	33.9	56.6	Mudstone
5-1, 63	575.1	1.98	2.16		2.13	2.10	16.9	35.4	Chalk
5-2, 68	576.7	1.93	1.69		1.74	1.71	32.4	55.3	Mudstone
6-3, 20	587.2	2.17	2.09		2.02	2.04	18.2	37.1	Chalk
6-4, 95	589.5	1.96	1.93		2.00	1.95	21.7	42.3	Friable chalk
7-2, 129	596.3	1.95	1.72		1.69	1.70	31.7	54.0	Mudstone
7-4, 130	599.3	1.92	1.87		2.01	2.03	19.4	39.3	Chalk
7-4, 131	599.3			1.74					Chalk
7-4, 131	599.3			1.73					Chalk
8-1, 7	603.1	4.08	3.91		2.41	2.46	5.6	13.8	Limestone
10-2, 52	614.5	1.92	1.71		1.75	1.72	31.8	54.6	Mudstone
10-3, 3	615.5	2.26	2.30		2.06	2.04	18.4	37.5	Chalk
10-4, 19	617.2	4.50	4.08		2.45	2.49	4.6	11.4	Limestone
11-1, 64	622.6	2.21	1.95		1.99	2.00	19.9	39.7	Chalk
11-1, 121	623.2	2.03	1.75		1.76	1.73	31.0	53.7	Mudstone
12-2, 146	634.5	2.01	1.78		1.72	1.72	31.3	54.0	Mudstone
12-3, 137	635.9			1.64					Chalk
12-3, 137	635.9			1.67					Chalk
12-4, 27	636.3	2.32	2.18		2.05	2.05	17.4	36.7	Chalk
13-3, 59	644.6	2.14	2.12		1.93	1.95	21.2	41.3	Chalk
13-4, 81	646.3	4.25	4.18		2.46	2.50	4.7	11.8	Limestone
14-1, 81	651.3	2.00	1.77		1.54?	1.71	32.2	55.2	Mudstone
14-4, 127	656.3	4.24	3.76		2.42	2.44	6.0	14.6	Limestone
15-1, 18	660.2	2.32	2.16		2.17	2.16	14.8	32.0	Chalk
16-2, 79	671.8	2.33	2.22		2.17	2.16	14.4	31.1	Chalk
17-1, 80	679.3	2.76	2.59		2.27	2.29	10.5	24.0	Chalk
17-6, 118	687.2	4.93	4.98		2.59	2.56	3.3	8.5	Limestone
18-1, 141	688.9	2.53	2.36		2.22	2.27	11.4	25.8	Chalk
19-1, 141	697.9	2.00	1.95		1.95	1.96	20.4	39.9	Claystone
20-1, 5	705.6	3.06	2.68		2.09	2.10	12.6	26.6	Claystone
20-2, 50	707.5	2.26	1.98		1.74	1.71	30.5	52.3	Red claystone
23-1, 3	732.5		4.87		2.48			12.0	Chert
24-1, 14	741.6	1.87	1.76		2.08	2.03	21.0	42.6	Green claystone
24-2, 13	743.1		1.70			2.03	22.1	44.8	Red claystone
25-1, 35	750.8	1.74	1.83		2.10	2.05	21.1	43.4	Red claystone
26,CC (6)	760.5		1.76			2.03	21.1	42.8	Green claystone
27-1, 39	764.9	1.97	1.77		1.78	2.02	21.7	43.9	Black claystone
28-1, 28	743.1	1.84	1.73		2.01	1.94	24.5	47.4	Black claystone
29-2, 64	785.6		1.71		1.92	1.93	25.2	48.6	Black claystone
30-1, 55	793.6	1.80	1.84			1.85	28.9	53.5	Black claystone
31,CC (18)	803.8		1.70			1.86	27.8	51.9	Black claystone
32-1, 29	812.3	1.83	1.72		2.01	1.97	23.1	45.6	Green claystone
33-1, 33	821.5	1.99	1.83		2.05	2.03	21.9	44.3	Green claystone
33-1, 74	822.2		1.74			1.88	25.9	48.7	Black claystone
34-1, 50	831.5	1.96	1.76		2.02	2.00	20.9	42.0	Black claystone
34-2,	832.8	2.03	1.96			2.18	15.4	33.6	Green claystone
35-1, 35	840.8		1.73			1.97	23.1	45.3	Black claystone
35-2, 132	843.3		1.76			2.06	21.0	43.2	Green claystone
36-1, 7	850.1		1.77		2.08	2.06	20.8	42.8	Green claystone
36-1, 46	850.5		1.68		2.04	2.07	20.7	42.9	Black claystone
36-1, 121	851.2	2.02	1.97		2.46	2.43	13.5	32.8	Green siltstone
37-1, 5	859.5		1.84			2.12	19.1	40.3	Green claystone
37-3, 57	863.1	5.19	5.02		2.87	2.90	1.6	4.7	Limestone
38-1, 101	870.0	2.12	1.85		2.08	2.08	19.7	40.7	Black claystone
38-2, 86	871.4		1.76			2.07	20.0	41.4	Green claystone
39-2, 115	880.6		1.70			1.82	27.0	49.2	Black claystone
41-1, 63	896.6		1.85		2.02	2.07	20.5	42.4	Brown claystone
41-1, 85	896.8	2.24	1.86			2.07	20.8	43.0	Brown claystone
41-3, 49	899.5	1.97	1.92		2.09	2.07	19.9	41.2	Green claystone
42-1, 70	905.7	2.18	1.95		2.09	2.07	19.7	40.8	Green claystone
43-1, 8	914.1		1.74			1.92	22.9	44.1	Black claystone
44-1, 64	923.6	1.88	1.76			2.00	20.0	40.0	Black claystone
44-4, 9	927.6		3.17		2.52	2.43	7.0	17.0	Chalk
45-1, 19	932.2		1.80			2.03	20.8	42.4	Black claystone
45-4, 106	937.6	2.88	2.49		2.20	2.19	14.1	30.8	Chalk
46-1, 35	941.4	2.75	2.29		2.24	2.19	14.1	30.8	Chalk
47-1, 17	950.2	2.01	1.83			2.03	19.4	39.4	Gray claystone
47-1, 75	950.8	2.82	2.58			2.38	8.6	20.4	Chalk
47-2, 127	952.8	3.86	3.76			2.44	7.0	17.0	Limestone
48-1, 124	960.2		2.05		2.21	2.12	15.8	33.6	Chalk
48-3, 138	963.4	2.73	2.37		2.20	2.21	13.4	29.6	Chalk
49-1, 42	963.9	3.18	2.70		2.32	2.32	10.2	23.6	Chalk
49-3, 113	967.6		1.83			2.10	18.1	37.9	Black claystone
50-1, 42	972.9		1.82			2.06	20.1	41.5	Black claystone

Table 13. (Continued).

		Velocity (km/s)				Gravimetric (wet)			
Sample (core-section, cm from top of section)	Depth in hole (m)	Parallel to bedding	Normal to bedding	Thermal conductivity (mcal/cm-°C-s)	GRAPE wet-bulk density[a] (g/cm^3)	Bulk density (g/cm^3)	Water content (%)	Porosity (%)	Lithology
Hole 534A									
50-3, 47	976.0	3.54	3.02		2.33	2.33	9.5	22.2	Chalk
50-4, 103	978.0		5.49		2.73	2.65	1.3	3.3	Limestone
51-1, 67	982.2	3.83	3.74		1.80?	2.51	5.2	13.1	Limestone
51-1, 127	982.8		1.95			2.11	17.4	36.7	Black claystone
52-2, 21	992.2	4.52	4.43		2.58	2.57	3.4	8.7	Limestone
52-4, 104	996.0	2.74	2.33		2.11	2.20	13.7	30.0	Chalk
53-1, 116	1000.7	4.22	4.08		2.62	2.57	3.6	9.2	Limestone
53-4, 24	1004.2		1.90			2.13	16.9	35.9	Green claystone
54-1, 135	1009.8		4.08			2.55	4.0	10.3	Limestone
55-1, 66	1018.2		3.11		2.47	2.45	6.6	16.3	Limestone
55-2, 145	1020.4		1.78			2.08	19.7	41.1	Claystone
55-3, 2	1020.5	4.06	3.70			2.54	4.5	11.3	Limestone
55-3, 53	1021.0	3.19	2.78			2.34	9.5	22.3	Chalk
56-1, 54	1027.0		2.59			2.40	8.5	20.3	Chalk
56-2, 84	1028.8		1.78			2.03	21.0	42.7	Claystone
56,CC (10)	1030.6		4.85			2.66	1.9	4.9	Limestone
58-1, 93	1045.4	2.28	2.01		2.05	2.16	16.3	35.2	Claystone
58-2, 38	1046.4	2.67	2.51		2.18	2.32	9.9	23.0	Calcarenite
58-4, 95	1050.0		3.22			2.46	6.7	16.5	Limestone
59-2, 87	1055.9		2.06			2.19	14.2	31.5	Chalk
59-3, 100	1057.5			2.16					Black claystone
59-3, 100	1057.5			2.12					Black claystone
60-1, 110	1063.6		4.15		2.70	2.59	3.5	9.0	Limestone
60-2, 46	1064.5	2.30	2.07		2.24	2.25	13.2	29.7	Laminated chalk
61-1, 134	1072.8	2.32	1.97			2.15	16.7	35.7	Black claystone
63-2, 95	1092.0		3.11			2.44	6.7	16.3	Laminated limestone
64-2, 90	1100.9		3.64			2.47	6.2	15.2	Laminated limestone
65-1, 139	1108.9		1.94			2.17	16.0	34.7	Black claystone
65-3, 92	1111.4	4.10	3.31			2.47	6.3	15.5	Laminated limestone
66-1, 114	1117.6	2.21	1.91			2.16	16.9	36.3	Black claystone
66-3, 98	1120.5	4.04	3.74		2.49	2.53	5.4	13.7	Limestone
66-4, 28	1121.3		2.78		2.47	2.41	8.3	20.0	Laminated limestone
67-1, 25	1125.8		3.18		2.43	2.48	6.9	17.1	Limestone
67-2, 53	1127.5		3.20		2.43	2.42	8.0	19.3	Laminated limestone
67-3, 113	1129.6	2.40	2.04		2.17	2.17	16.6	36.0	Black claystone
68-1, 131	1131.3		1.99			2.20	14.5	31.8	Laminated chalk
68-2, 56	1132.1		2.23			2.23	12.8	28.7	Laminated chalk
68-3, 87	1133.9		2.86			2.38	9.2	22.0	Laminated chalk
69-1, 35	1139.4		4.18			2.54	5.1	12.9	Limestone
69-3, 32	1142.3	3.40	2.67			2.30	11.1	25.5	Laminated chalk
69-5, 23	1145.2	2.38	2.04			2.21	14.9	33.0	Black claystone
70-1, 60	1145.8	3.29	2.68		2.24	2.28	10.8	24.5	Laminated chalk
70-2, 75	1150.2		3.82		2.52	2.45	6.5	16.0	Limestone
71-2, 10	1158.6		3.87			2.50	5.4	13.4	Limestone
71-4, 11	1161.6		3.07			2.33	9.8	22.8	Laminated chalk
71-5, 87	1163.9	2.27	2.00			2.20	14.6	32.2	Black claystone
72-1, 43	1166.4	3.35	2.70		2.39	2.31	10.2	23.6	Laminated chalk
72-4, 82	1171.3	4.05	3.05		2.48	2.45	6.3	15.5	Limestone
73-1, 87	1173.9	2.44	2.06			2.19	14.6	32.1	Black claystone
73-1, 112	1176.1			2.76					Chalk
73-1, 112	1176.1			2.76					Chalk
73-3, 96	1179.0	4.17	3.59		2.47	2.48	5.8	14.4	Limestone
73,CC (19)	1182.0	3.39	2.87		2.42	2.25	12.0	27.1	Laminated chalk
74-2, 80	1186.3	3.26	2.70		2.46	2.36	9.2	21.6	Laminated chalk
74-4, 20	1188.7	4.51	4.38		2.59	2.54	4.3	10.9	Limestone
75-1, 58	1193.6	3.61	2.87		2.37	2.34	9.3	21.7	Laminated chalk
75-3, 30	1196.3	3.36	3.26		2.40	2.43	7.2	17.4	Limestone
76-1, 77	1202.8	3.31	2.72		2.35	2.34	9.4	21.9	Laminated chalk
76-3, 50	1205.5	3.47	3.20		2.49	2.44	6.9	16.8	Limestone
76-4, 85	1207.4	2.31	1.96		2.28	2.11	18.1	38.2	Black claystone
77-1, 127	1212.3	3.56	3.08			2.38	8.5	20.2	Laminated chalk
78-4, 30	1220.3	3.04	2.60			2.28	11.1	25.3	Laminated chalk
79-4, 22	1229.2	3.20	2.80			2.31	10.3	23.8	Laminated chalk
80-1, 10	1233.6		3.67			2.47	6.2	15.3	Limestone
80-3, 56	1237.0	3.00	2.52		2.89	2.32	10.0	23.2	Laminated chalk
81-2, 46	1244.5	3.56	3.34		2.37	2.41	7.9	19.2	Limestone
81-4, 37	1247.4		2.67			2.31	10.5	24.3	Laminated chalk
82-2, 25	1253.2	3.54	3.29		2.38	2.58	7.6	19.6	White limestone
83-1, 117	1261.7	3.52	3.22		2.33	2.34	9.1	21.4	White limestone
83-2, 52	1262.5	3.24	2.75		2.28	2.30	10.0	23.1	Laminated chalk
83-3, 145	1265.0			2.64					Limestone
83-3, 145	1265.0			2.76					Limestone
83-4, 114	1266.1	3.39	3.14		2.42	2.43	6.9	16.9	Green limestone
83-5, 85	1267.4	2.73	2.65		2.36	2.38	9.2	22.0	Red claystone
84-1, 91	1268.3	3.01	2.70		2.39	2.38	9.0	21.5	Green limestone
84-4, 59	1273.1	2.94	2.54		2.30	2.31	10.5	24.2	Laminated chalk
85-1, 26	1277.3	3.27	2.80		2.31	2.32	9.9	22.9	Laminated chalk
85-3, 75	1280.8	3.68	3.43		2.38	2.41	7.4	17.9	Gray limestone
86-1, 24	1286.2	4.01	3.77		2.43	2.47	5.8	14.3	Gray limestone
86-3, 65	1289.6	3.29	3.50		2.49	2.45	6.3	15.4	Gray limestone
87-1, 31	1295.3	3.94	3.68		2.43	2.49	5.7	14.2	Gray limestone
87-4, 19	1299.7	4.27	4.07			2.51	5.1	12.8	Gray limestone

Table 13. (Continued).

Sample (core-section, cm from top of section)	Depth in hole (m)	Velocity (km/s)		Thermal conductivity (mcal/cm-°C-s)	GRAPE wet-bulk density[a] (g/cm³)	Gravimetric (wet)			Lithology
		Parallel to bedding	Normal to bedding			Bulk density (g/cm³)	Water content (%)	Porosity (%)	
Hole 534A									
88-1, 19	1304.2	3.59	3.34		2.40	2.41	7.7	18.5	Gray limestone
88-4, 21	1308.7	3.55	3.23		2.38	2.40	7.8	18.7	Gray limestone
89-1, 12	1313.1	3.20	3.02		2.34	2.33	9.7	22.7	White limestone
89-4, 84	1318.3	3.12	2.65			2.38	9.2	21.9	Green limestone
90-1, 40	1322.4	3.56	3.41		2.46	2.42	7.5	18.0	White limestone
90-4, 8	1326.6	2.76	2.80		2.31	2.31	10.6	24.5	White limestone
91-1, 29	1331.3	3.95	3.97		2.53	2.53	4:5	11.4	White limestone
91-4, 65	1336.2		3.50		2.48	2.49	5.6	13.9	White limestone
92-1, 13	1340.1	4.19	3.94		2.46	2.51	5.0	12.7	White limestone
92-2, 89	1342.4	4.06	3.82		2.52	2.50	4.5	11.4	White limestone
92-4, 2	1344.5	3.81	3.52		2.48	2.49	5.4	13.5	Red limestone
92-6, 17	1347.7	3.37	2.99		2.42	2.45	6.8	16.7	Red claystone
93-1, 117	1350.2	3.85	3.59		2.53	2.52	4.7	11.8	White limestone
93-3, 85	1352.8	4.56	4.66		2.64	2.60	2.8	7.4	White limestone
93-4, 6	1353.6	3.22	2.79		2.43	2.41	8.4	20.2	Red claystone
94-2, 13	1355.1	3.29	2.73		2.36	2.41	8.6	20.8	Red claystone
94-4, 65	1358.6		3.70		2.63	2.54	4.3	10.9	White limestone
95-2, 135	1365.4		2.22			2.27	13.1	29.6	Red claystone
95-3, 128	1364.3			2.41					Limestone
96-1, 66	1372.1	4.76	4.58		2.67	2.63	2.5	6.6	White limestone
96-2, 138	1374.4	2.61	2.21			2.22		34.4	Red claystone
97-1, 41	1380.9	3.96	3.81			2.55	4.2	10.8	Red limestone
99-1, 62	1396.1	2.74	2.40		2.26	2.29	11.9	27.3	Red claystone
100-1, 90	1401.9	3.29	2.88			2.46	7.5	18.4	Limestone
101-3, 47	1413.5	2.68	2.25			2.26	13.3	30.1	Red claystone
102-5, 47	1425.5	2.49	2.25		2.10	2.29	12.2	27.9	Red claystone
103-1, 82	1428.8	2.44	2.11		2.24	2.22	14.6	32.5	Red claystone
103-1, 138	1429.4	5.45	4.94		2.74	2.68	1.2	3.1	Gray limestone
104-1, 8	1437.1	5.25	5.00		2.70	2.67	1.5	4.0	Gray limestone
104-4, 1	1441.5	3.26	2.68		2.45	2.41	8.6	20.6	Red claystone
105-1, 20	1446.2	2.61	2.14		2.24	2.30	13.1	30.2	Black claystone
105-1, 107	1447.1	5.32	5.19		2.69	2.68	1.1	2.9	White limestone
105-1, 144	1447.4			2.82					Limestone
106-2, 68	1457.2	5.12	4.88		2.68	2.66	1.4	3.6	White limestone
107-1, 30	1464.3	4.20	4.13		2.63	2.58	2.8	7.3	Gray limestone
107-2, 92	1466.4		2.30			2.33	11.3	26.4	Green claystone
108-1, 60	1469.1	3.10	2.82		2.47	2.44	7.3	17.9	Red claystone
110,CC (12)	1486.6	2.88	2.41			2.43	9.1	22.0	Red claystone
111-1, 15	1495.6	2.73	2.66			2.37	10.3	24.5	Black claystone
112-1, 15	1504.6	3.34	2.94		2.63	2.28	12.0	27.4	Green claystone
112-1, 75	1505.2	4.16	4.05		2.64	2.61	2.7	6.9	Green limestone
113-1, 36	1513.9	3.71	3.47		2.74	2.56	4.0	10.3	Green claystone
114-1, 54	1523.0	2.94	2.45			2.36	10.6	24.9	Gray claystone
115-1, 94	1532.4	2.95	2.44			2.36	10.2	24.0	Brown claystone
117-1, 11	1549.6	2.88	2.39		2.33	2.37	10.6	25.0	Brown claystone
117-1, 44	1549.9	5.14	5.04			2.68	1.3	3.5	White limestone
118-1, 86	1559.4	4.40	4.31		2.79	2.59	2.6	6.8	Green limestone
119-1, 109	1568.6	2.95	2.53			2.31	10.9	25.3	Black claystone
120-1, 65	1572.6	2.54	2.30		2.24	2.23	13.3	29.6	Black claystone
121-1, 38	1581.4	4.03	3.76		2.60	2.56	3.2	8.3	White limestone
122-1, 32	1590.3	3.63	3.18			2.51	4.8	12.0	Limestone
122-1, 87	1590.9	2.87	2.37			2.30	11.8	27.0	Claystone
123-2, 63	1596.1	3.72	3.21			2.53	4.4	11.2	Claystone
123-4, 4	1598.5	3.41	2.95			2.49	5.5	13.6	Claystone
124-1, 25	1603.8	3.76	3.42			2.54	4.1	10.5	Claystone
125-1, 11	1612.6	3.03	2.47			2.36	9.5	22.3	Claystone
125-3, 120	1616.7	3.58	3.27			2.54	4.6	11.8	Claystone
125-5, 68	1619.2	2.73	2.25			2.30	11.0	25.4	Claystone
126-2, 23	1623.2	2.62	2.35			2.28	11.2	25.4	Claystone
126-3, 82	1625.3	3.15	2.59			2.42	8.6	20.7	Claystone
127-1, 107	1631.6	2.88	2.36			2.39	9.6	23.0	Claystone
127-3, 108	1634.6	3.01	2.50			2.42	8.8	21.3	Claystone
128-1, 69	1640.2	5.20	5.14			2.71	4.4	11.9	Basalt
128-3, 56	1641.3	4.52	4.50			2.56	7.2	18.4	Basalt
128-4, 102	1645.0	5.16	5.41			2.79	3.2	8.8	Basalt
129-1, 123	1649.7	4.61	4.54			2.59	6.5	16.8	Basalt
129-4, 96	1654.0	6.19	5.87			2.82	2.7	7.6	Basalt
130-1, 31	1657.8	5.35	5.33			2.80	3.6	10.0	Basalt
130-3, 26	1662.3	5.52	5.46			2.82	3.0	8.5	Basalt

[a] 2-minute count.

1000 m. Further correction of laboratory data to *in situ* conditions is discussed by Shipley (this volume). Detailed correlation with Site 391 is not possible because the two data sets differ in their classification of chalks and limestones.

Cat Gap Formation

Red to green to black claystones and limestones produce a bimodal distribution of physical properties in the Cat Gap Formation. The claystones were again fresh-water absorbing and tended to break into small fragments. Velocity was quickly measured after sampling and the rocks were further trimmed for gravimetric determinations. Poor recovery (<20%) reduces the reliability of the abundance estimates in these intervals.

Thermal conductivities measured in one limestone at 1364 m give a value of 2.41 mcal/cm-°C-s.

Appropriate data were not available for this depth of burial to estimate the porosity rebound effect. See Shipley (this volume) for other methods used to estimate *in situ* physical properties.

Unnamed Unit (1495.6 m–1635.3 m)

The section beneath the Cat Gap Formation consists largely of claystones and some limestones. The very poor recovery and fractured nature of the claystones make estimates of abundance difficult. The physical properties were measured on fragments that appeared undisturbed except for fracturing. The rather high velocities, 2.7 km/s, reflect the calcareous nature of many of the claystones.

Basement

Samples of basaltic basement yielded high velocities (5.2 km/s), which represents a large contrast to the overlying claystone interval.

Table 14 is a summary of the physical properties on a formation basis. In some cases the formation and obvious physical property boundaries coincide, but more often they do not. This is not surprising, because the definition of formations is based on different criteria, including first occurrences of color, diagnostic sediment process or mineral composition, and so on, which may not be reflected in the physical properites.

Table 14. Leg 76 physical properties summary, by formation.

Formation[b]	Wet-bulk density (g/cm^3)	Porosity (%)	Vertical velocity (km/s)	Number of samples
Great Abaco Member				
Mudstone (25)	1.7 ± 0.1	56 ± 2	1.7 ± 0.1	9
Chalk (65)	2.1 ± 0.1	35 ± 6	2.2 ± 0.3	14
Limestone (10)	2.5 ± 0.1	12 ± 2	4.2 ± 0.5	5
Weighted mean	2.0	38	2.3	
Bermuda Rise				
Mudstone (100)	1.9 ± 0.2	40 ± 13	2.2 ± 0.4	3
Plantagenet				
Mudstone (75[c])	1.8 ± 0.5	43 ± 1	2.0 ± 0.1	4
Chert (25[c])	4.9		2.5[a]	1
Weighted mean	2.6		2.1	
Hatteras				
Claystone (95)	2.0 ± 0.1	44 ± 5	1.8 ± 0.1	26
Chalk (5)	2.3 ± 0.1	26 ± 8	2.6 ± 0.5	3
Limestone	2.9	5	5.0	1
Weighted mean	2.0	43	1.8	
Blake-Bahama				
Claystone (15)	2.2 ± 0.1	35 ± 6	2.0 ± 0.3	18
Chalk (45)	2.3 ± 0.1	25 ± 4	2.6 ± 0.3	30
Limestone (40)	2.5 ± 0.1	15 ± 4	3.7 ± 0.6	45
Weighted mean	2.4	22	3.0	
Cat Gap				
Claystone (55)	2.4 ± 0.1	25 ± 6	2.5 ± 0.3	14
Limestone (45)	2.6 ± 0.1	8 ± 4	4.4 ± 0.6	12
Weighted mean	2.5	17	3.4	
Unnamed				
Claystone (70)	2.4 ± 0.1	21 ± 6	2.7 ± 0.4	19
Limestone (30)	2.6 ± 0.1	7 ± 4	4.1 ± 0.7	5
Weighted mean	2.5	17	3.1	
Basement				
Basalt	2.7 ± 0.1	12 ± 4	5.2 ± 0.5	7

[a] Density from 2-minute GRAPE; other density and porosity values by gravimetric methods.

[b] Estimates of lithologic abundance in percent shown in ( ).

[c] Approximate estimate.

Although the formation physical properties, as defined, do not necessarily have a relationship to the acoustics, the "mean" impedance plot in Figure 13 shows some general interval-dependent trends. For example, the interval A to β corresponding approximately to the Hatteras Formation black claystone contains few impedance contrasts and few internal reflections, whereas the alternating limestones, chalks, and claystones of the Blake-Bahama Formation and deeper units produce numerous impedance contrasts that correlate in a general way with the reflections in the intervals β to C and C to D.

It is interesting to note that within the limits of the recovered cores at Site 534 the defined top and bottom of the Blake-Bahama Formation do not correspond to obvious breaks in the physical properties. The upper contact is a transitional zone related to the decreasing carbonate component upsection. The top of the Cat Gap Formation is defined as the first occurrence of red-colored limestones. No significant break in the physical property trend should be expected from a change in oxidation state, nor is such a break detected at this boundary in the recovered core. There is some evidence from the marked drilling rate decrease in Core 92 that a hard zone, not recovered, may exist at the Formation boundary.

The relationship between the physical properties and the major seismic reflections is not straightforward. The major reflections are more likely caused by a complex interference from impedance contrasts on the scale of beds and from the integration of these effects over a larger area than sampled in Hole 534A. Lack of recovery, such as the chert in the Bermuda Rise Formation, prevents accurate detection of obviously sigificant events needed to understand fully the acoustics of the section. The details of seismic to well-hole correlation using the laboratory and logging physical property data are discussed in Shipley (this volume).

PALEOMAGNETISM

The emphasis of the Hole 534A paleomagnetic sampling was to identify and date the Early Cretaceous–Late Jurassic magnetic polarity sequence (the "M-sequence"). Oriented minicores were drilled from every core from Cores 47 through 130. Density of sampling varied from one per section to every 50 cm. Hard limestone layers were sampled preferentially to claystones; however, in portions of the Upper Jurassic where claystones are dominant, samples of these claystones were obtained with plastic cubes. A total of 524 sediment and 51 basalt samples were taken.

Approximately 150 of the Lower Cretaceous and Upper Jurassic sediment minicores were run on the Digico spinner on board the *Glomar Challenger*. Of these, only 29 had initial NRM (natural remanent magnetism) intensities greater than 1×10^{-6} emu/cm^3. (The Digico had a fluctuating sensitivity for weak samples below 1×10^{-5} emu/cm^3, and measured intensities could vary by an order of magnitude between measurements of the same sample; therefore true intensities were estimated by comparing to a 1.5×10^{-6} standard run sequentially.) The sandy carbonates of the Hauterivian and red marly limestones of the Upper Jurassic yielded the strongest NRM intensities.

No demagnetization of samples was undertaken on board the ship due to the very weak intensities of the samples, unreliable results from the spinner at low intensities, lack of magnetic shielding, and lack of thermal demagnetization apparatus. The detailed analysis of the samples was done using cryogenic magnetometers (in a mu-metal room at Caltech, and in a steel room at the University of Wyoming).

Analysis of a large suite of samples from Cores 87 through 96 (Berriasian-Tithonian) yielded a pattern of normal and reversed polarity zones (Fig. 49). This apparent polarity sequence was obtained when these white to pink limestones and red marls were thermally demagnetized above 300°C. The carrier of these magnetic directions in the pink and red-colored sediments is hematite, because the intensities are constant under alternating field demagnetization and the directions remain stable through 600°C. The pattern of polarity zones is similar to M-16 through M-20 of the marine magnetic anomaly sequence, and the biostratigraphic ages correlate to the same magnetostratigraphic pattern in limestones of northern Italy (Ogg, 1981).

The clay-rich sediments from Cores 97 and below failed to yield a reliable polarity sequence during the preliminary runs.

Basalt Magnetics

From the basalt cores (Cores 127-130) of Hole 534A, 51 samples were taken from 26 cooling units, interpreted as pillows. The NRMs were run aboard ship; they are tabulated in Table 15. Histograms of the inclinations and intensities are shown in Figure 50.

All the samples had normal directions with a mean of 29.7° and a standard deviation of 9.9°. The predicted mean magnetic field inclination of 28° for Hole 534A in the Late Jurassic (estimated paleolatitude = 15°) is in close agreement with this value. The few samples with higher inclinations are from two flows (Cooling Units 4 and 22), which perhaps represent secular variation of 15° from the mean pole position or overprint of the present-day field or both.

As a crude test of the stability of the NRM directions against viscous acquisition, a subset of the samples was exposed to the present magnetic field for 24 hr., then remeasured. All remeasured directions were identical to the initial measurements within the accuracy (±2.5°) of the *Glomar Challenger's* spinner magnetometer. Also, multiple samples from the same block have identical NRM directions, although the intensities decrease away from the chill margin.

Some of the NRM directions may be an artifact of the sampling procedure. A drilling-induced remanence was observed by Ade-Hall and Johnson (1976) in Leg 34 and Leg 45 basalt cores. Bleil and Smith (1980) on Leg 51 show an example of a spurious magnetization direct-

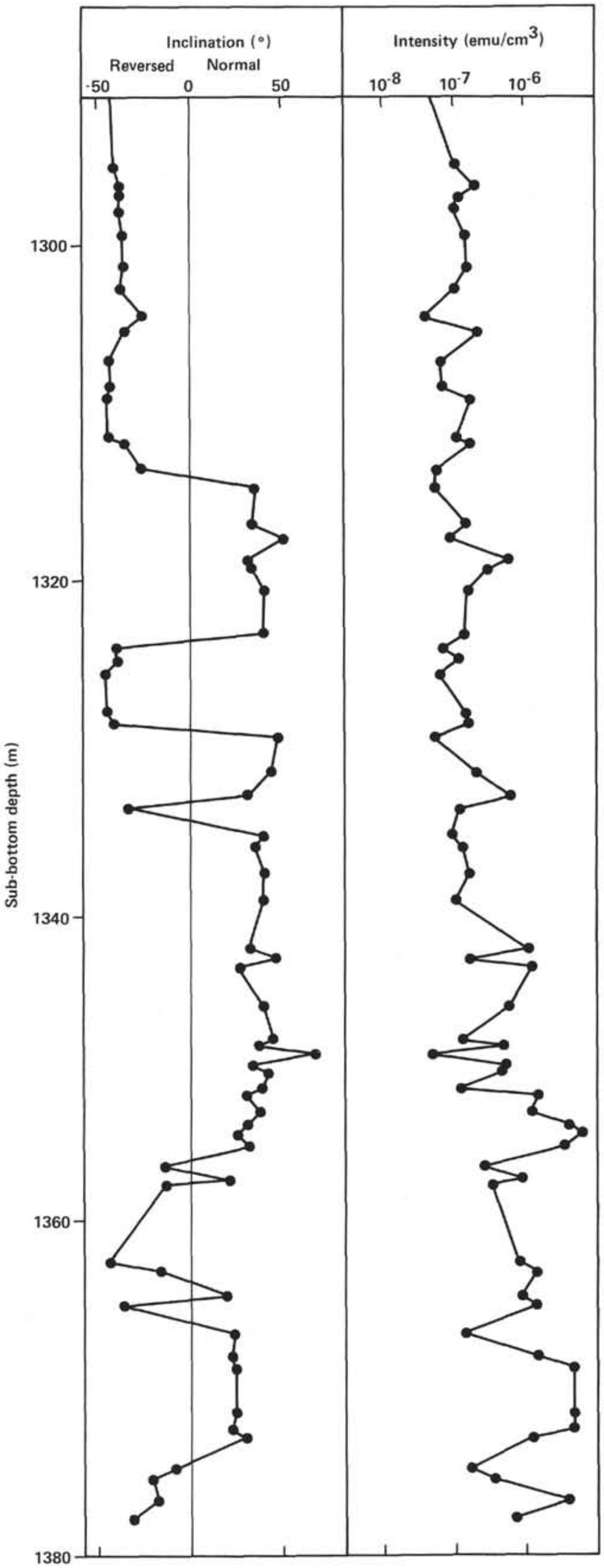

Figure 49. Inclinations of magnetization in samples of Cores 87 through 96. (Alternating frequency demagnetization at 350°C.)

Table 15. Basalt NRMs of Hole 534A.

Cooling unit	Sample (core-section, cm from top of section)	Intensity (× 10^{-3} emu/cm^3)	Declination (°)	Inclination (°)
0	127,CC (16)	4.48	294	33.5
	128-1, 13	7.08	18	21.7
1	128-1, 38	5.99	21	18.7
	128-1, 41	5.66	24	19.5
	128-1, 46	3.39	26	19.9
2	128-1, 97	5.01	193	28.0
3	128-2, 11	3.82	90	31.2
	128-2, 82	5.85	203	47.7
4	128-2, 86	3.26	202	47.3
	128-2, 138	5.99	210	48.9
	128-3, 84	4.01	250	21.9
5	128-3, 87	3.75	262	39.0
	128-4, 8	9.06	315	25.8
6	128-4, 11	6.84	317	27.2
	128-4, 15	3.90	316	28.2
	128-4, 107	5.72	209	33.3
	128-4, 112	5.44	207	31.9
8	128-4, 45	5.01	216	23.2
9	128-4, 100	7.04	294	21.2
10	129-1, 22	3.26	338	20.7
11	129-1, 102	3.02	213	34.1
12	129-2, 37	3.95	13	21.8
	129-2, 40	3.65	17	20.5
13	129-2, 50	4.16	86	23.6
	129-2, 72	8.25	254	22.6
14	129-2, 75	7.73	251	22.8
	129-2, 115	3.09	315	28.4
15	129-3, 90	4.55	197	20.2
	129-4, 18	10.58	223	35.6
	129-4, 23	7.20	220	33.9
17	129-4, 81	3.68	204	32.5
	129-4, 83	3.81	207	32.9
	129-4, 86	3.05	209	42.8
18	129-5, 15	4.84	151	32.5
19	130-1, 3	6.66	265	19.3
	130-1, 5	4.07	265	19.5
21	130-1, 106	5.53	125	33.8
	130-2, 20	3.68	210	42.8
22	130-2, 53	3.08	215	54.1
	130-2, 56	2.40	230	59.8
23	130-2, 129	3.58	298	19.8
24	130-3, 18	4.46	20	36.0
	130-3, 52	5.40	5	30.1
	130-3, 55	3.84	6	37.4
	130-3, 127	6.74	22	27.6
	130-4, 38	6.86	141	21.3
25	130-4, 78	3.90	123	36.6
26	130-5, 40	2.61	22	25.5
28	130-5, 119	6.90	115	19.0
29	130-6, 49	3.77	24	20.1
	130-6, 54	3.52	24	17.8

ed along the axis of the minicores, apparently acquired during the shipboard sampling process. It is disturbing that for the Leg 76 basalt minicores, 55% of the NRM declinations of individual blocks lie either between 5 to 25° or 195 to 225°, a nonrandom pattern. Whether this is simply a change distribution of a discrete sample set or an artifact of the sample drilling is unknown. The agreement of minicore declinations to the declinations measured on uncut full-round cores with the long core spinner suggests the former.

The magnetic studies of Middle Cretaceous pillow basalts recovered on Leg 51 (Bleil and Smith, 1980) showed that these fine-grained basalts display very minor directional changes upon alternating field demagnetization, thus the NRMs were similar to the directions after demagnetization. If this same behavior holds for the Middle Jurassic pillow basalts recovered at this site, then the NRM results imply a normal Jurassic polarity for the upper 30 m of basalt flows. Because Site 534 was drilled on the east edge of Reversed Magnetic Anomaly M-28, then these upper flows may have been extruded during the normal polarity following M-28. The source of the magnetic anomaly may be in basement rocks deeper than the drilling penetration.

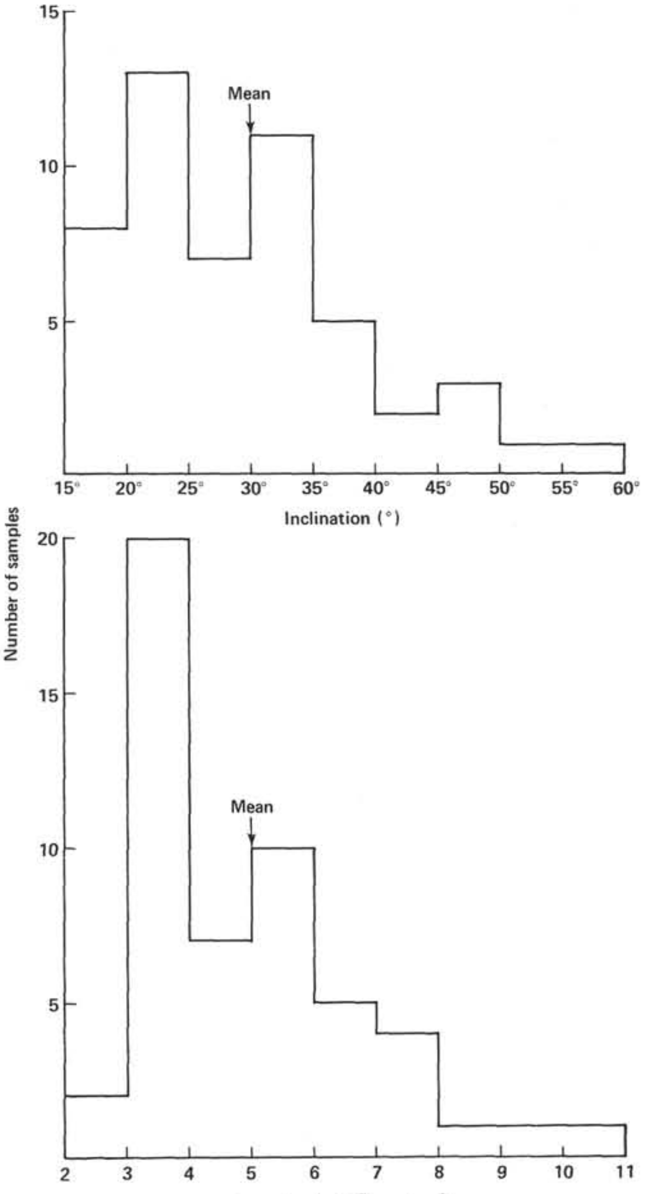

Figure 50. Basalt NRMs, Hole 534A. (Of 51 samples, mean inclination was 29.7°, $\sigma = 9.9$; mean intensity was 4.96×10^{-3} emu/cm^3, $\sigma = 1.8$.)

DOWNHOLE MEASUREMENTS

Gearhart-Owen Well Logs

Objectives

The objectives of the logging program at Site 534 were to obtain data for integration with other geological and geophysical information already available. First, we wished to gather representative *in situ* geophysical data, such as gamma ray scattering (a measure of bulk electron density), sonic traveltime (a measure of bulk rock velocity), temperature (already discussed above), and natural gamma ray emission (a measure of rock lithology). From these measurements the acoustic velocity, acoustic impedance, density, and porosity can be calculated. Comparisons of these *in situ* determinations can be made with the laboratory measured values and the calculated *in situ* corrections based on empirical porosity rebound data. The log data provide *in situ* measurements to verify the assumptions used in the rebound calculations and to extend the empirical measurements to older and more deeply buried rocks that are for the first time available for logging. These independent logging results, especially of the sonic velocity and impedance measurements, can then be correlated, via synthetic seismograph modeling, with the remotely determined seismic reflection and refraction data.

Second, the density and porosity logs combined with the natural gamma logs and sonic logs allow the identification of the mineral grain density and, therefore, provide an identification of lithology in parts of the drilled section where recovery was poor. Limestone versus quartz sandstone can be distinguished by logs, for example.

Finally, the natural gamma radiation is a measure of the small particles of minerals containing uranium, potassium, and thorium, all radioactive sources. Because these minerals occur more commonly in shales, this lithology should have a high count of emissions, versus limestones and clean quartz sandstones, which have a low count.

Methods

The following suite of Gearhart-Owen logging tools were run in Hole 534A:

1) Sonic Log (Bore Hole Compensated System, 9.21 cm diameter, 30 cm receiver spacing), Caliper, and Natural Gamma Ray Log (GR).

2) Density Log (Bore Hole Compensated Compton Scattering Gamma Ray Detection Log [CDL], 6.98 cm diameter), Caliper, Natural Gamma Ray Log (GR), and Temperature Log (Thermocouple).

Because of the hole conditions observed during the first logging attempts (i.e., the extensive bridging and the extensive washouts, with diameters in excess of 40 in. in some shales), it was decided not to run the additional neutron and induction logs. The time was better spent running multiple logging trips in different parts of the hole between bridges using the two primary porosity logging tools, sonic and density. These two tools tell more about the physical properties of the rocks, whereas the neutron and induction logs tell more about the pore fluids. Because the pore fluids in the case of Hole 534A are all salt water, there was less need for the neutron and induction logs.

Results of Gearhart-Owens Well Logs

Because the hole is divided by a series of bridges, mainly at places where hard limestones form constrictions with soft crumbly shales above, the logs had to be done in increments between the bridges. For this reason, it is convenient to discuss the recovered logs in segments in the order they were recorded. Moreover, the weather conditions, which were severe on several of the log runs, apparently created varying degrees of oscillations in the logging wire and sonde, so each log has a more or less "noisy" character. This characteristic is especially true for the washed out part of the section, where hole diameters of 40 in. or more permitted swinging and possibly some heave of the sonde. Thus detailed comparison of one logging run to another shows discrepancies.

Temperature Measurements

Two forms of temperature measurements were recorded at Site 534: (1) the Gearhart-Owen (GO) thermal log, and (2) the attached thermometer technique. The GO thermal log was run on the first density logging survey into Hole 534A after the hole was left undisturbed for two days. Temperatures increased regularly below the mudline inside the drill pipe, and an abrupt rise in temperature of 10° was recorded as the probe entered the bare hole. Although the increase in temperature with depth was gradual as expected, there were several spots down the hole where the temperature change decreased or the temperature was constant for several meters. No weight loss was indicated on the winch, as if the tool might have been stuck on a ledge, so a real change in gradient may have been detected. However, disturbance by the pumped drilling water might have followed the logging tool down the hole (Fig. 51).

Upon stopping at the bridge in the Cat Gap Formation at 1414 m sub-bottom depth, the temperature was

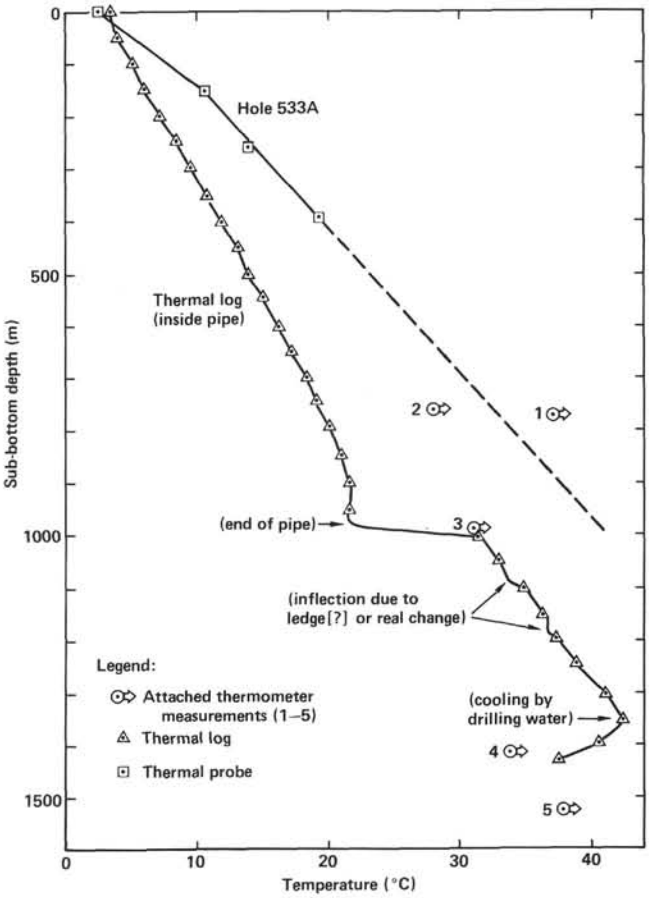

Figure 51. Temperature measurements in Hole 534A. (For comparison, the temperature measurements for Hole 533A are plotted.)

measured as approximately 38°C. This gradually cooled to 37°C as drilling water reached the bottom of the hole after 10 min. of equilibration. We assumed the higher temperature to be more accurate, which yielded a temperature gradient of approximately 2.5°C/100 m, assuming a linear gradient. This value is quite reasonable and normal for this age crust. We note that this gradient for Site 534 is somewhat less than the 3.6°C/100 m gradient measured at Site 533, which probably indicates the lack of equilibrium in Hole 534A. The thermal probe technique used at Site 533, where the thermistor is allowed to equilibrate in the soft mud, probably is a better measurement of the *in situ* temperature than the thermal log measurement in the drilling water at Site 534.

The thermometers attached to the various logging runs record the maximum temperature reached, presumably at the bottom of the logging run. These measurements are listed in Table 16, with the calculated thermal gradient.

The thermal gradients determined by attached thermometer measurements 1 and 2 are higher than those determined by the thermal log and more in agreement with the thermistor probe technique used at Site 533. Alternatively, these higher gradients for the upper part of the hole might indicate a nonlinear gradient, as found at Site 533, where a gradient of 4.9°C/100 m in the upper part gives way to a 3.5°C/100 m gradient in the lower part. Perhaps in Hole 534A there is a higher 3.3–4.5°C/100 m gradient in the upper part of the hole, and a lower gradient in the lower part to give a 2.5°C/100 m overall gradient from 1414 m to the seafloor. This hypothesis is supported by the deeper thermometer measurements 3, 4, and 5, which recorded 2.9, 2.3, and 2.3°C/100 m thermal gradients, respectively, assuming a constant linear situation between the seafloor and the measurement depth (Fig. 51).

First Density Log Run, 6385–5935 m

First, it must be pointed out that the depths used to calibrate the log runs are originally the depths read off the Schlumberger logging-winch meter wheel. These Schlumberger depths were deeper by some 34 m relative to drill pipe depths when calibrated against the location of the end of the pipe noted on the temperature log and the end of the casing noted on the density log. The lithologic boundaries and seismic-stratigraphic and physical-unit boundaries referred to in other parts of the site chapter are based on cored interval summations in drill pipe depth. The Schlumberger log depths have been converted as closely as possible to this same measurement system. These Schlumberger winch depths converted to total depths are shown in Figures 52 to 55. Thus the comparison of drilled lithologic boundaries in drill pipe depth to the log "kick" based on Schlumberger winch depths converted to total depths has to be made with these inaccuracies in mind.

Table 16. Attached thermometer measurements.

Measurement number	Date and time	Sub-bottom depth (m)	Temperature (°C)	Thermal gradient (°C/100 m)
1	17 Dec. 1980, 1300	778	37	4.5
2	17 Dec. 1980, 2145	769	28	3.3
3	18 Dec. 1980, 0700	997	31	2.9
4	18 Dec. 1980, 2300	1411	34	2.3
5	19 Dec. 1980, 0330	1534	38	2.3

The density log between 6385 and 5935 m records the transition from the red shaly Subunit 6a of the Cat Gap Formation to the hard, thick-bedded Berriasian limestone of the base of the Blake-Bahama Formation. The top of the Cat Gap Formation is correlated with seismic Horizon C, and the top of the basal Blake-Bahama Formation limestone is correlated with reflector C′ (Fig. 52). Above reflector C′ are the interbedded shales and limestones of the laminated Blake-Bahama Formation.

The gamma ray (GR) log shows a slight indication of the increased clay content of the red shale of the Cat Gap Formation below Horizon C, reading between 20 and 25 API units. A sharp drop in the GR reading to 5 to 10 API units above Horizon C indicates the presence of the hard Berriasian limestone. However, there is less of an effect in the GR log across reflector C′, and the log gives little indication of this boundary.

The caliper log indicates a highly washed-out section in the red shales below Horizon C and a constricted borehole at the Berriasian limestone. Above reflector C′, the interbedded shales and limestones of the Blake-Bahama laminates are also washed out, but less than the red shale of the Cat Gap Formation.

Where the caliper measurement of the borehole is low, the density log (Fig. 52) shows a less noisy and more reliable reading. The massive hard limestone between reflectors C and C′ stands out clearly. Above and below this limestone, the density log is a crude saw-toothed pattern, which may reflect real interbeds of thin limestones and shale, or oscillations and swing of the tool against the side of the enlarged borehole. From the coring of the Blake-Bahama laminates, we know there are real intercalations of limestone and shale present, but this would be difficult to prove from the log alone.

Quantitatively, the log determination of the density in the hard Berriasian limestone as 2.6 to 2.7 g/cm^3 is close to the 2.5 g/cm^3 mean density determined in the laboratory for the rocks from the interval. Where the borehole is constricted, the log density data seem to be accurate. Above reflector C′ the oscillatory log density data do follow a trend around 2.3 g/cm^3, which is the laboratory-measured value of density for this interval, so the log is reasonably representative here as well. Below Horizon C, however, the log values for density trend along values below 2.0 g/cm^3, distinctly lower than the 2.3 g/cm^3 laboratory determined values (Fig. 52). Here the hole size is so large that the log data are deemed to be unreliable. Probably the tool is swinging in the drilling water most of the time, and the sensor pad only hits the side of the hole sporadically. This irregularity was shown with the duplicate run of the log over this interval, when none of the individual peaks of the density log could be repeated.

Second Density Log Run, 5740–5500 m

The density log between 5740 and 5500 m records the transition from the variegated shales of the Plantagenet

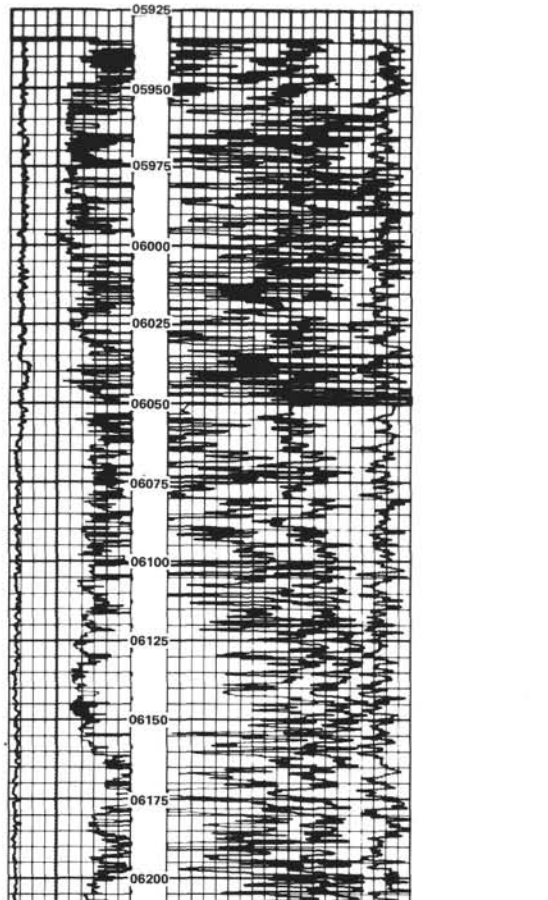

Figure 52. First density log run, Hole 534A. (Also located are the shipboard identification of depths to reflector C′ and Horizon C. Comparisons of laboratory measures of *in situ* densities and log densities for the indicated interval are shown. ϱ (LAB) = mean density determined in the laboratory; ϱ (LOG) = mean density determined by logging. Scales refer to the following: GR = gamma ray in API units; caliper is in inches; $\Delta\varrho$ is a dimensionless ratio used as a correction factor in determining density (ϱ) in g/cm^3; ϕ is porosity (in %) calculated from the CDL [compensated density log]. These explanations also apply to Figs. 53–55.)

Formation through the 27-m-thick Bermuda Rise siliceous claystones, to the massive turbiditic limestones and debris flows of the basal part of the Great Abaco Member. This transition involves the merged wavelets of the reflection Horizons A^c and A^u, as discussed in the section on seismic stratigraphy.

The caliper measurement indicates the hole is extensively washed out in the Plantagenet variegated shales below 5706 m. Hole diameter improves upward to reasonable diameter at the base of the Great Abaco Member at 5670 m and continues to hold up until above the massive turbiditic limestones between 5670 and 5630 m. Above these limestones, the hole is again enlarged where the softer chalks of the Great Abaco Member occur.

The gamma ray log indicates a steady and low value across the massive limestone beds from 5670 to 5625 m. Above and below this interval the GR log is variable, which may represent noise from oscillations in the oversized hole. The GR should be higher below 5670 m, and it does rise somewhat at that depth, which is the transition from the Great Abaco Member chalks and limestones to the Bermuda Rise Formation claystones. However, below 5706 m, the GR should rise again in the Plantagenet claystones, but instead it drops. This drop might be due to the extensive washout of the hole and enlarged diameter (off the scale).

The density log is a very saw-toothed pattern reflecting both real, thin-bed intercalation and probably a swinging tool in an enlarged hole. The duplicate run of this log did not show reproducibility of each peak and trough. When the caliper is good in the basal limestones of the Great Abaco Member, the density log is smoother and may be more reliable. Here the measured density by the log is 2.2 to 2.4 g/cm^3, which is in the range of the 2.2 g/cm^3 average laboratory value for the same cored interval (Fig. 53).

The reflection wavelet $A^u = A^c$, discussed in the next section on seismic stratigraphy, corresponds to some positive density log peaks in the Bermuda Rise Formation interval. These positive peaks are below negatives at 5673 and 5680 m, which are the softer claystone of the Bermuda Rise just beneath the hard linestone of the base of the Great Abaco Member. The combination of these positive and negative densities (therefore impedance contrasts) convolved with the negative density contrast at 5706 m between the Bermuda Rise cherts and the Plantagenet claystone below produces the wavelet called $A^u = A^c$. The density log appears to show these thin bedded negative and positive acoustic impedance contrasts at this critical transition zone.

Sonic Log Run, 5735–5500 m

The first sonic log run made in Hole 534A crossed the Plantagenet and Bermuda Rise Formations and the basal part of the Great Abaco Member (Fig. 54). This run was, therefore, a good measurement of the *in situ* sonic velocity across the rocks producing the A^c and A^u merged wavelet. The estimated depth of Horizon $A^u = A^c$ based on the coring data fits pretty well with the sonic log that shows the higher velocity spikes of possible chert and porcellanite layers in the Bermuda Rise Formation at that point. Below, the soft shales of the Plantagenet

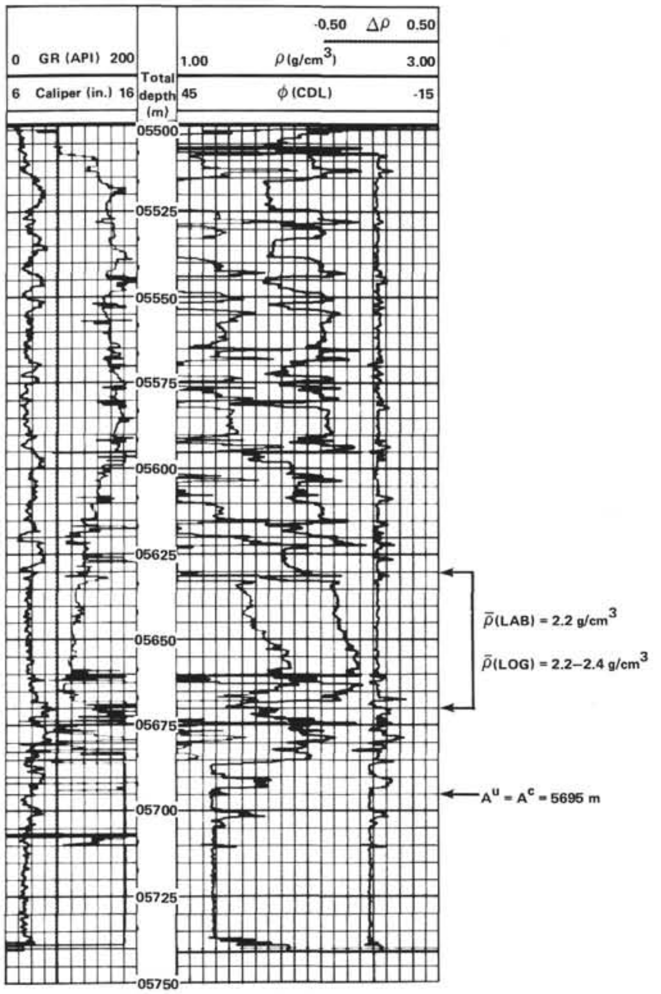

Figure 53. Second density log run, Hole 534A. (Position of Horizon $A^u = A^c$ as determined aboard ship is shown. Comparison of the laboratory *in situ* corrected densities for the indicated interval is shown.)

Formation are so washed out that the hole diameter prevents a reliable sonic transit time reading.

Quantitatively, the sonic log can be converted to *in situ* compressional wave velocity (Fig. 54). The values determined by the log in the part of the hole above the base of the Great Abaco Member are reasonably close to laboratory values. The velocity inversions at the Great Abaco/Bermuda Rise and the Bermuda Rise/Plantagenet contacts are indicated on the log, but the velocity measured for the Plantagenet is not reliable.

Third Density Log Run, 6490–6420 m

Only a short run was possible at the bottom of the hole because of bridging. The third density log crossed the interbedded limestones and claystones of the base of the Cat Gap Formation and the top of Lithologic Unit 7 (Fig. 55). The density and gamma ray and caliper logs all indicate interbedding of hard limestones and soft shales that were recovered in the poor coring of this interval.

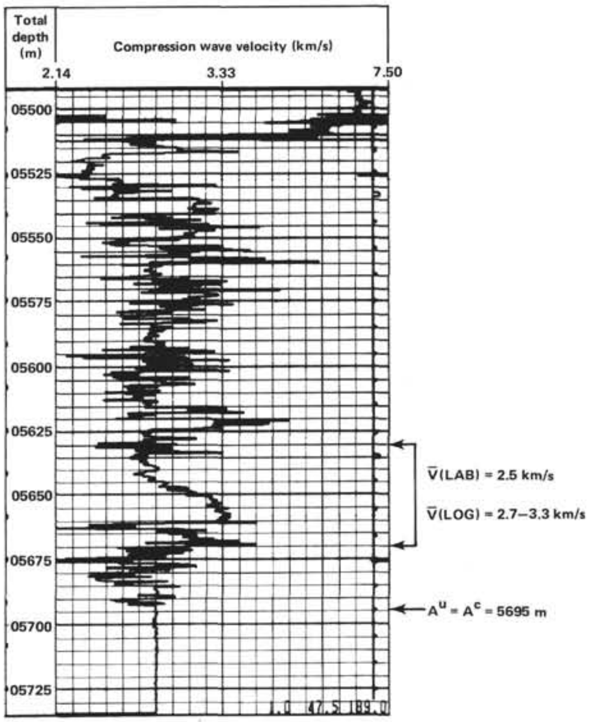

Figure 54. First sonic log run, Hole 534A. (Depth of Horizon $A^u = A^c$ as determined aboard ship is shown. Also indicated is the laboratory *in situ* corrected velocity compared to log velocity over the interval shown.)

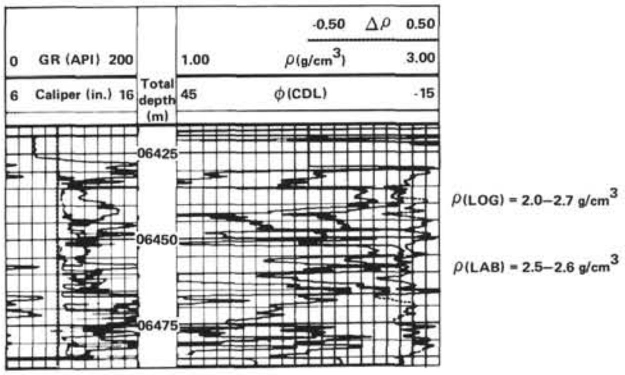

Figure 55. Third density log run, Hole 534A. (Comparison of laboratory *in situ* density and log density is indicated.)

Quantitatively, the log densities include a lower range of values, 2.0 to 2.7 g/cm³, compared to that measured in the lab, 2.5 to 2.6 g/cm³, indicating that more soft shale was washed out preferentially in the coring, and probably more of the hard limestones and indurated claystones were recovered. Therefore the laboratory averages for the physical properties of this interval are biased on the high side.

This logged interval is between seismic reflectors D and D′, and therefore it is no surprise that no significant or major density and acoustic impedance contrast is indicated by the log.

SEISMIC STRATIGRAPHY

High quality 24-channel multichannel seismic reflection profiles were made by Bryan et al. (1980) across Site 534 during Cruise 2102 of the *Conrad* (Fig. 56).

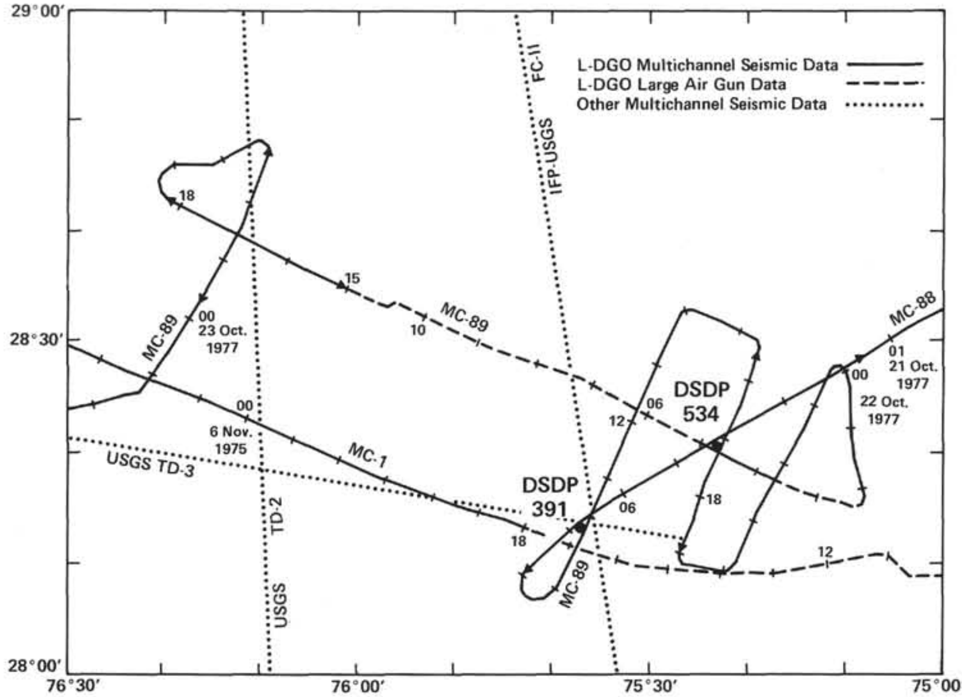

Figure 56. Track chart of the multichannel seismic survey carried out at Site 391 and the area of Site 534 (lines MC-88 and -89) as well as other multichannel lines around which the survey was designed (after Bryan et al., 1980).

Cross lines are MC-88 and MC-89, which were shot on an approximately 8-km spacing. These lines were oriented northeast-southwest (paralleling the magnetic anomalies) and northwest-southeast (perpendicular to the magnetic anomalies). The magnetic anomalies in the area of Site 534 reveal trends of linear, small-amplitude anomalies (+20 nT to −20 nT) superimposed by smaller-amplitude (−10 nT to −15 nT) anomalies of a more circular character (Fig. 57). The seismic mapping indicates that the circular anomalies, such as that between Sites 391 and 534, are caused by small-scale (200–300 m deep) pockets or troughs in oceanic basement. Detailed mapping in the Site 534 area suggests that the trough in basement at this position has a slight northwest-southeast trend (Fig. 58) and that it might correspond to a fracture zone trough that has terminated the lobes in the northeast trending magnetic anomalies without producing lateral offsets (Fig. 57). In this trough the deepest and oldest Jurassic oceanic sediments are ponded below the well-identified seismic Horizon D (Fig. 59). Because the previously unsampled sediments below Horizon D were the first-priority target for drilling at Site 534, the site was located on the northeast rim of this basement trough, where the reflector is so clearly developed yet the basement is in reach of *Glomar Challenger*'s drill string limit of 6800 m (Fig. 7).

Detailed calculations of two orthogonal sonobuoys at the site were used to calculate the depths to the various reflectors (Table 17) (Bryan et al., 1980). All the regionally mappable reflection horizons, M, X, A^u, β, C, D, and oceanic basement, appeared to be within reach of the drill.

Based on previous correlations of the reflectors with Site 391 (Fig. 7), the horizons were correlated with Site 391 lithologic units as follows (Benson et al., 1978; Sheridan, Pastouret, et al, 1978; Bryan et al., 1980; Jansa et al., 1979):

M = middle Miocene intraclastic chalk (top of Subunit 2b of Great Abaco Member)
X = lower Miocene intraclast chalk mudstone (top Subunit 2e of Great Abaco Member)
A^u = unconformity between Miocene intraclastic chalk (Great Abaco Member) and Cretaceous variegated claystone (Plantagenet Formation)
β = Barremian white limestones (top of Blake Bahama Formation)
C = lower Tithonian red shaly limestone (top of Cat Gap Formation)

Horizon D and basement were not penetrated at Site 391, and these were the prime objectives of Site 534.

Continuous coring in Hole 534A below 536 m has provided new and surprising results regarding the correlation of the seismic stratigraphy. Beginning in the Great Abaco Member below Horizon X, the cores contained a reasonably high amount of chalk with velocities above 2.0 km/s, and some layers of limestone with velocities above 4.0 km/s. A time-average calculation for the velocity of the lower part of the Great Abaco Member, between X and A^u, gave 2.4 km/s. This calculation is in substantial agreement with the 2.09 km/s velocity measured by the sonobuoys at Site 534 (and with the 2.25 km/s velocity calculated for the same interval at Site 391 [Benson et al.,1978]). The new and surprising

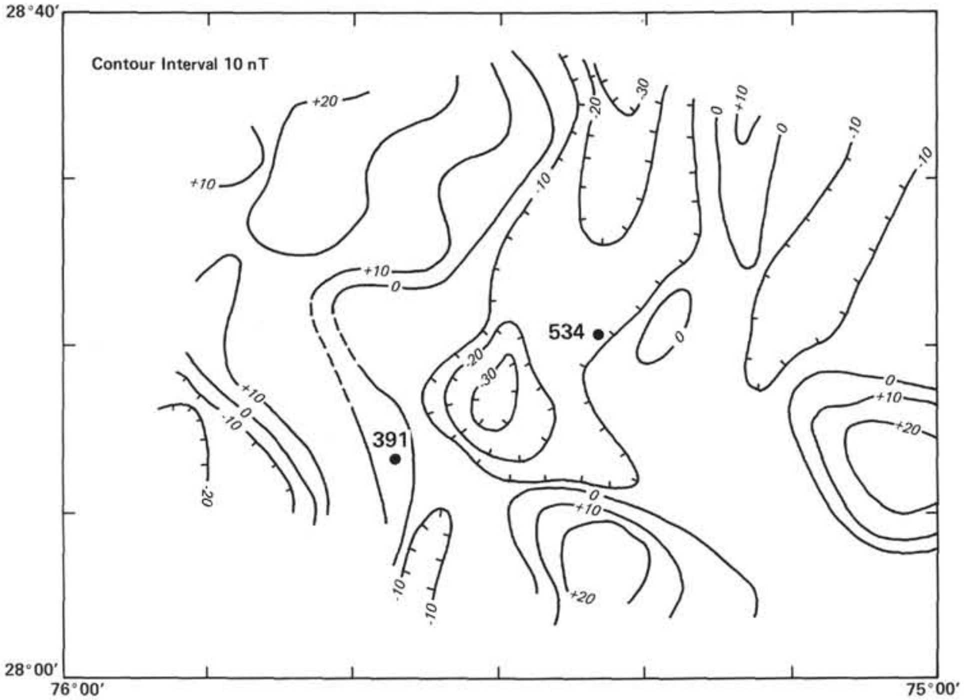

Figure 57. Total-intensity magnetic anomaly map derived from the *Eastward* magnetic survey (from Bryan et al., 1980). (The data were contoured in order to facilitate locating Site 534. The lineations represented here trend NE-SW; the negative anomaly between Sites 391 and 534 is caused by a basement trough.)

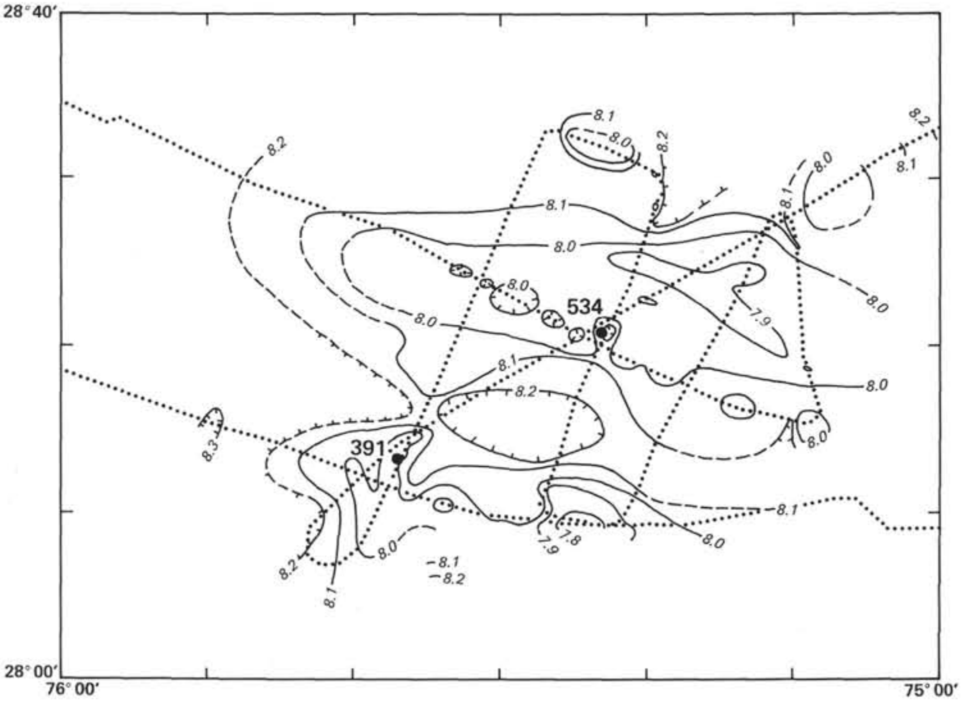

Figure 58. Contour map of depth to basement in the vicinity of Sites 391 and 534. (Track lines [MC-88, MC-89, and MC-1] are dotted [after Bryan et al., 1980]. Units are two-way traveltime [in seconds] below sea level.)

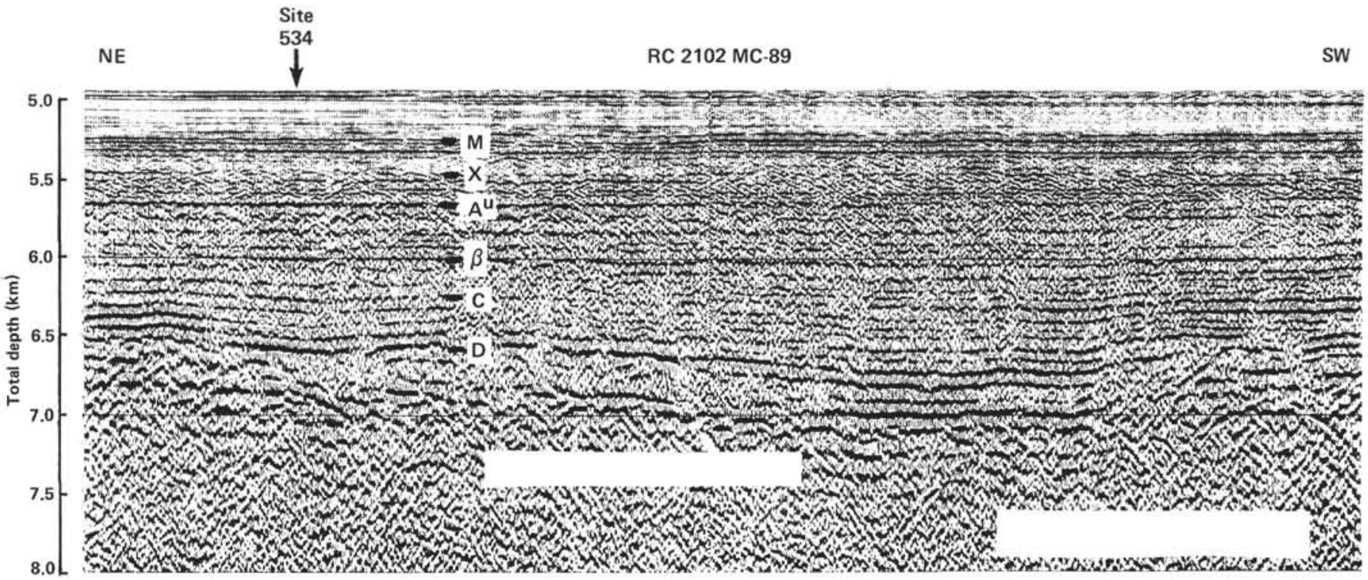

Figure 59. Depth section of multichannel seismic reflection profile made aboard the *Robert Conrad* near Site 534 (after Sheridan et al., this volume).

Table 17. Seismic units predicted at Site 534 (after Bryan et al., 1980).

Seismic horizon (two-way traveltime in s)	Two-way traveltime within interval (s)	Calculated thickness (m)	Calculated sub-bottom depth (m)	Measured sonobuoy velocity (km/s)
Seafloor (6.57)			0	
to	0.21	200		1.91
M (6.78)			200	
M (6.78)			200	
to	0.32	334		2.09
X (7.10)			534	
X (7.10)			534	
to	0.19	199		2.09
A^u (7.29)			733	
A^u (7.29)			733	
to	0.23	297		2.58
β (7.52)			1030	
β (7.52)			1030	
to	0.20	299		2.99
C (7.72)			1329	
C (7.72)			1329	
to	0.17	269		3.17
D (7.89)			1598	
D (7.89)			1598	
to	0.13	221		3.4
Basement (8.02)			1819	
Basement (8.02)			1819	5.7

seismic correlation at Site 534 is the discovery of the 27-m-thick Eocene siliceous claystones and chert of the Bermuda Rise Formation below the Great Abaco Member and above what is the $A^u = A^c$ unconformity (Fig. 60). This Formation was absent at Site 391 only 22 km away, where the Miocene Great Abaco Member overlies directly the variegated claystones of the Cretaceous Plantagenet Formation and where no cherts and siliceous claystones of the Paleocene–Eocene Bermuda Rise Formation were found.

The local presence of this thin unit of Bermuda Rise Formation just below the A^u unconformity complicates the correlation of the A^u seismic horizon at Site 534. One reason is that the impedance contrast between the cherty Bermuda Rise Formation and the underlying watery claystones of the Plantagenet Formation should also produce a reflection horizon, known as A^c (Tucholke and Mountain, 1979). This Bermuda Rise unit is so thin that the A^u and A^c reflections would nearly merge at Site 534 and would be within about one wavelet of each other. The time difference between A^u and A^c can be calculated from the equation:

$$\Delta t = \frac{2\Delta H}{V} \tag{1}$$

where H is the unit thickness of 27 m and V is the interval velocity of approximately 2.5 km/s. For these values $\Delta t = 0.02$ s, which is close to a wavelet for 25- to 50-Hz-frequency seismic waves.

On this basis Seismic Horizon A^u is thought to merge with Horizon A^c at Site 534, and the convolution interference of these two reflections is interpreted to result in single positive wavelet found at 7.29 s sub-bottom two-way traveltime (Fig. 60). Such a correlation would put the Horizon $A^u = A^c$ interface at 719 m in the drill hole, which is close to the 733-m calculated sub-bottom depth based on the sonobuoy measurements (Tables 17 and 18). This correlation also gives a reasonably good velocity, 2.04 km/s for the interval between $A^u = A^c$ and the seafloor, which compares well with the sonobuoy and shipboard velocity data for the same interval.

It is interesting to note that this high-amplitude, single, positive wavelet of Horizon $A^u = A^c$ does not extend to the southwest where the A^u reflector has a lesser amplitude at Site 391, as seen in Figure 7. Another interpretation related to the seismic stratigraphy of Site 391 Subunit 2e of the Great Abaco Member deals with the hummocky nature of the internal reflections in that unit (Fig. 7). This characteristic seems to be caused by real initial dips of the debris flow units and lobes. It was noted that in certain cores, the bedding in the debris-flow and fluid-grain-flow units had dips of about 5° throughout the thickness of several distinct flows. Some prograding and outbuilding of the individual flows might be producing the dips of the reflectors in the X to A^u interval.

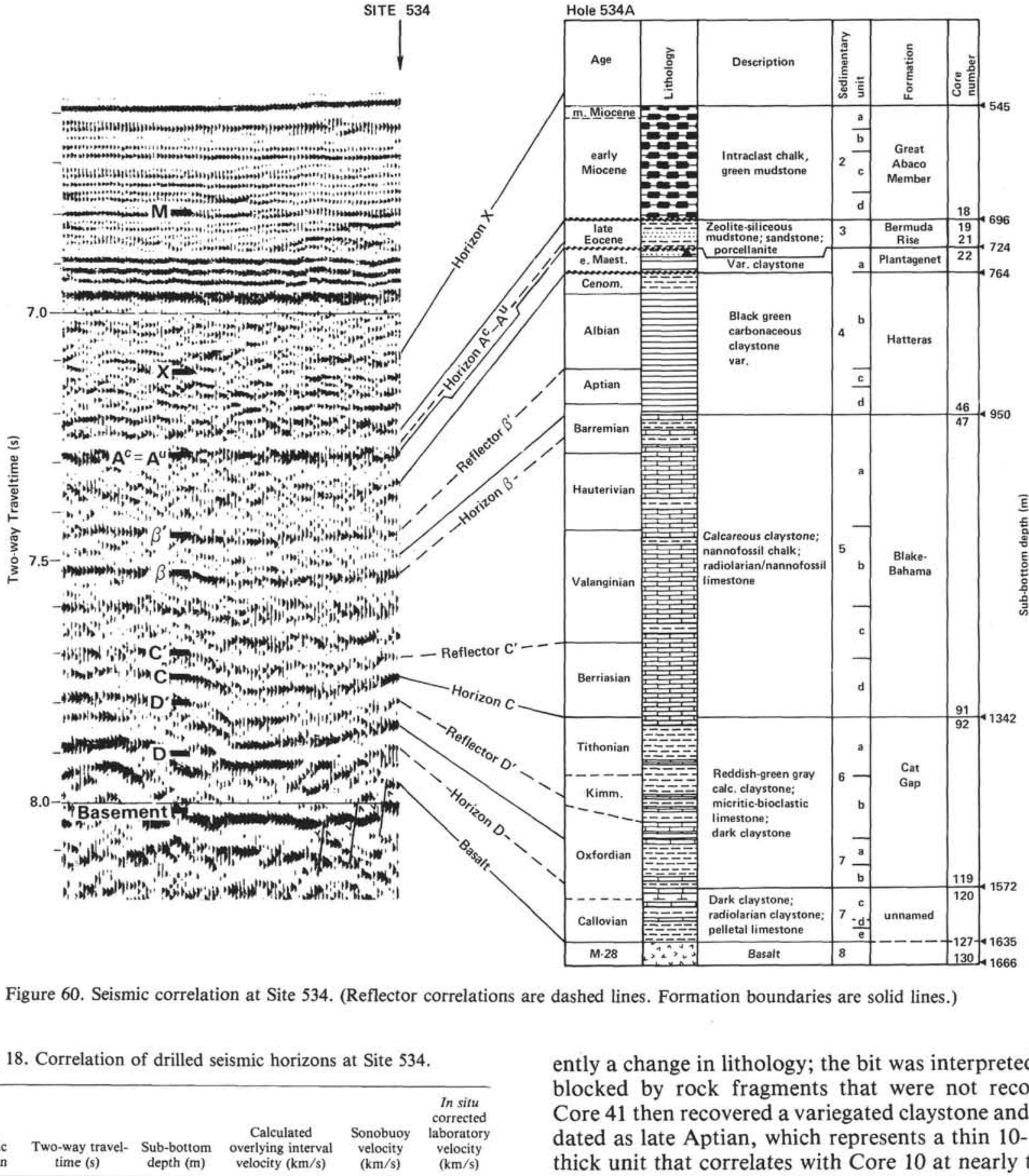

Figure 60. Seismic correlation at Site 534. (Reflector correlations are dashed lines. Formation boundaries are solid lines.)

Table 18. Correlation of drilled seismic horizons at Site 534.

Sesimic horizon	Two-way travel-time (s)	Sub-bottom depth (m)	Calculated overlying interval velocity (km/s)	Sonobuoy velocity (km/s)	*In situ* corrected laboratory velocity (km/s)
Seafloor	6.57	0	—	—	—
X	7.10	525	2.02	2.00	—
$A^u = A^c$	7.29	719	2.04	2.09	2.3
β′	7.46	887	1.98	2.58	2.1
β	7.52	975	2.93	2.58	2.0
C′	7.72	1250	2.85	2.99	2.9
C	7.77	1340	3.90	2.99	3.3
D′	7.83	1432	3.06	3.17	3.0
D	7.89	1552	4.00	3.17	3.4
Basement	7.97	1635	2.18	3.40[a]	3.1

[a] Refraction velocity.

Further drilling in Hole 534A through the Hatteras Formation encountered two important lithologic and physical breaks, which are correlated with seismic reflection horizons. In Core 40 at 887 m there was apparently a change in lithology; the bit was interpreted to be blocked by rock fragments that were not recovered. Core 41 then recovered a variegated claystone and shale, dated as late Aptian, which represents a thin 10- 15-m-thick unit that correlates with Core 10 at nearly the exact same level of Hole 391C (Core 10 is dated as late Aptian to early Albian). Now it appears that this unit marks a significant and abrupt change in physical environment over a wide area. Lithologic changes, such as the disappearance of thin quartz-rich layers below this boundary, suggest that a significant sedimentological event occurred between the late Aptian and early Albian.

Examination of the seismic reflection profile at Site 534 indicates the presence of a weak reflector at 7.46 s two-way traveltime. If this reflection event is correlated with this late Aptian to early Albian event at 887 m, this correlation would give a velocity of 1.98 km/s for the above interval ($A^u = A^c$ to β′) in agreement with the physical properties measurements (Fig. 60 and Table 18). Although the physical properties immediately above and below this late Aptian to early Albian horizon do not change markedly, the reflection horizon might be produced by harder rocks not recovered in Core 40. Alternatively, it has been suggested that a mid-Aptian erosional hiatus should exist in the deep western North Atlantic (Vail et al., 1980; Shipley and Watkins, 1978), and perhaps a similar hiatus is causing the reflector at 7.46 s identified here. Terminations of bedding reflections along this low-angle unconformity might produce the weak seismic reflector even in the presence of only subtle physical properties changes. This reflector may also correlate with the so-called Horizon β' mapped farther to the north in the western North Atlantic basin (B. E. Tucholke, personal communication, 1980); therefore, we have used this nomenclature for the reflector.

Deeper drilling at Site 534 eventually crossed the transitional (≈ 50 m) contact between the Hatteras and Blake-Bahama Formations. Below reflector β', more and more carbonate is found in the cores until nannofossil chalk becomes the background sediment, with the carbonaceous components being interbeds. The sedimentologists on board the *Glomar Challenger* placed the upper boundary of the Blake-Bahama Formations at 950 m, on the basis of the first occurrence of nannofossil chalks. Increasing amounts of transported carbonates forming hard limestone beds occurred at Cores 50 and 51. These first significant appearances of hard limestones are correlated with seismic Horizon β taken to be at 975 m (Fig. 60 and Table 18).

This correlation of Horizon β will result in a velocity in the interval from Horizon β to β' of 2.93 km/s, which is higher than the velocity of 2.58 km/s measured for the same interval by sonobuoys (Tables 17 and 18). This discrepancy is opposite to that above β', where the drilling correlation gives a lower sonobuoy velocity of 1.98 km/s. These opposing discrepancies are partially explained by the fact that the sonobuoy measurements apparently combined the 2.93 and 1.98 km/s intervals. A combination of these two interval velocities results in a velocity of 2.3 km/s for the interval A^u to β, still slightly lower than the sonobuoy velocity of 2.58 km/s.

Physical properties measurements on board indicated that the interval between β' and β has *in situ* corrected vertical velocities about 2.0 km/s; this includes the contribution from the chalks in the 25 m above Horizon β. This velocity is lower than the one predicted by the reflection correlation method or from the sonobuoy data.

Although the correlations presented here are apparently at odds with the sonobuoy predictions and laboratory measurements, a discrepancy that can be partially explained, they agree well with the correlation calculations and semblance velocity measurements made at Site 391 (Benson et al., 1978; Sheridan, Pastouret, et al., 1978). A velocity inversion below the higher-velocity, 2.25 km/s, Great Abaco Member was calculated by the drilling correlation to give lower 1.98 km/s velocities for the Plantagenet and Hatteras formations, which agrees well with the correlations at Site 534. Averaging of many CDP (common depth point) semblance velocity measurements near Site 391 (Sheridan, Pastouret, et al., 1978) also gives a remote determination of this inversion, but these measurements are not precise because of the short 2400-m offset of the seismic hydrophone array. However, the CDP calculations do agree with the drilling correlations presented here.

Although the correlation technique is used to determine interval velocities at Site 534, and these results indicate discrepancies with velocities determined remotely by sonobuoys, and with corrected laboratory velocities (Table 18), these discrepancies are not really that bad. We have already partially explained the discrepancy with the sonobuoy data, because the sonobuoy solution was calculated assuming a single layer of constant velocity between A^u and β.

The other explanation for these discrepancies lies in the calculation errors inherent in each of the techniques. For example, in the drilling correlation, the unknowns about the exact convolution interference effects between thinly spaced impedance contrasts, as discussed earlier, make it uncertain at what exact part of the wavelet the observed physical-properties change in the hole should be correlated. This amounts to up to ± 0.02 s of uncertainty in the interval times between the reflectors being measured; when combined with the ± 10-m uncertainty in drilled depth, it can lead to as much as a 10% error in these calculated velocities. Another source of error in the drilling correlation technique is the slight structural relief in the reflection horizons being correlated; and there is also the fact that the position of the drill site is probably off the seismic line being measured by as much as a nautical mile, given the navigational accuracy of the site survey vessel. Thus variations in the interval times being measured could be ± 0.01 s in the case of Site 534, where the interfaces are sloping very gently, if at all. This uncertainty in the interval times introduces a slight error into the velocity determination, making the inaccuracy as much as 12%.

As far as the sonobuoy measurements are concerned, large errors can result because of what is assumed in the basic equations, such as the assumption that all velocity intervals have been detected by reflectors with moveout, and that constant velocities exist in the intervals calculated. Also, the wide-angle reflection technique samples a very wide area, several kilometers away from Site 534, where the velocities might be slightly different. Horizontal components of velocity, which are generally higher, are also sampled. Moreover, the equations themselves are approximations with a precision of 3 to 5%.

The laboratory measurements are precise, but assumptions are made about the weighting of different components of the lithology to give an average velocity for the interval to compare with the other measurements. Also, to correct the laboratory measurements to *in situ* values assumptions are made based on some knowledge of decompaction of various lithologies (Hamilton, 1976). This probably leads to a 10% accuracy.

Accordingly, the discrepancies seen in Table 18 are not significant. All the velocity numbers are within the errors of the various techniques. However, the net affect of these uncertainties was that the predicted depth to Horizon β of 1030 m (Table 17) is 55 m deeper than the drilled depth of 975 m at Site 534 (Table 18).

Obviously there is only one correct velocity structure at Site 534, which is somewhere within the range of values calculated by the three techniques presented in Table 18.

When drilling through the lower part of the Blake-Bahama Formation we encountered an abrupt increase in limestone below 1250 m. This lithologic break corresponds to a positive impedance contrast, as indicated by the physical properties measurements and the decrease in drilling rate. Seismic velocities, based on *in situ* corrected laboratory measurements, increased from 3.1 to 3.6 km/s. Apparently, the increased carbonaceous clay and shale content above 1250 m in the Blake-Bahama Formation contributes to the relatively lower velocity in the interval from 1050 to 1250 m. This shaly interval is different from the same interval drilled at Site 391, where more limestone and less shale were recovered. Thus the drilling at Site 534 demonstrates a marked facies change within the Blake-Bahama Formation in the interval between Horizons β and C.

Inspection of the seismic tie line between Sites 534 and 391 indicates that this facies change shows up in the changes in reflectivity for the β to C interval. Visible on line MC-88 of the *Robert Conrad* Cruise 2102 (Bryan et al., 1980) are the characteristic closely spaced reflections below Horizon β that are seen in most areas of the western North Atlantic seaward of Site 391 (Fig. 61). Between Sites 391 and 534 these closely spaced reflections disappear and the β to C interval becomes relatively more transparent. Such an acoustic change could be caused by more shale being present at Site 534 and more limestones being present at Site 391. Also, the calculated seismic velocities for this interval are different at the two sites, being 2.85 km/s at 534 versus 3.65 km/s at 391. This difference supports the observations of more shale in the same interval at Site 534.

Regarding the correlation of Horizon C, the drilling at Site 534 necessitated some revisions in the previously published results. The positive impedance contrast at 1250 m is correlated with a positive reflection wavelet at 7.72 s, giving a 2.85 km/s velocity for the overlying interval that agrees (within the uncertainty of the measurements) with the 2.99 km/s sonobuoy velocity and the 2.9 km/s *in situ* corrected laboratory velocity (Table 18).

However, the reflection at Site 534 at this depth, 7.72 s, had been correlated with Horizon C of Site 391 by Bryan et al. (1980). This correlation poses a problem, because at Site 391, Horizon C correlates with the top of the Cat Gap Formation and the transition from white limestone to red shaly limestone, whereas the positive impedance contrast at 1250 m at Site 534 is the top of the Berriasian bioturbated limestone of the bottom of the Blake-Bahama Formation. In an attempt to resolve this confusion, the original seismic tie line, MC-88 (Fig. 61), between Sites 534 and 391, was reexamined to trace the correlation of Horizon C between the two sites. The reexamination indicated that the wavelet for Horizon C at Site 391 did not carry to the wavelet at 7.72 s at Site 534, but to the next deeper wavelet at 7.77 s (Fig. 61). We correlate the wavelet at 7.77 s with the top of the Cat Gap red shaly limestones and designate this Horizon C at Site 534 (Fig. 60). This correlation gives an interval velocity of 3.90 km/s for the rocks of the Berriasian white limestones, close to the *in situ* corrected laboratory value of 4.0 km/s. This correlation of the well data to the seismic data is subject to alternate interpretations, based on the preliminary nature of the data and the

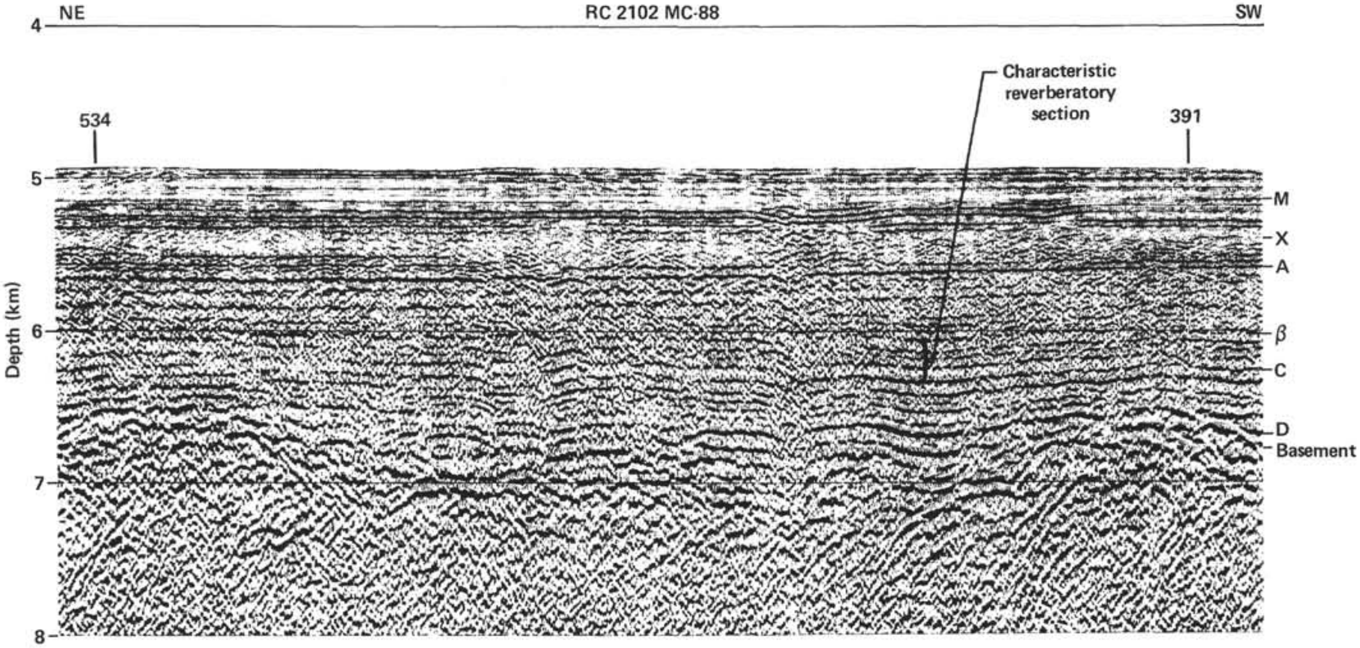

Figure 61. Multichannel seismic reflection profile made from the *Robert Conrad* showing the disappearance of the closely spaced reflections between Horizons β and C between Sites 391 and 534.

analysis to date. With the addition of logging and synthetic seismogram studies, we hoped to reevaluate and further delineate these correlations (see Sheridan, Bates et al., and Shipley, this volume).

It is evident, however, that the impedance contrasts at the top and bottom of the Berriasian–Tithonian limestone give positive reflection wavelets that can be carried over a wide area as a strong doublet with Horizon C. We designate the upper reflection of the doublet as reflector C′ (Fig. 60). This characteristic double positive wavelet of C′–C appears on other multichannel seismic reflection profiles to the north, such as the UTMSI line across the Blake Outer Ridge (Shipley et al., 1978). It appears that the white limestone at the base of the Blake-Bahama Formation, in contact with the red shaly limestones of the Cat Gap Formation, forms a strong amplitude pattern because of the convolution interference of the wavelets at these closely spaced (within 50 m) impedance contrasts.

In one case, on the UTMSI line the doublet C′–C (the top of the WNA-9 unit in Shipley et al. [1978]) begins to diverge in time section toward the northeast. It therefore becomes apparent that the C′ and C wavelets are distinct geological contacts that are nearly merged in the area of the Blake-Bahama Basin.

A recent interpretation of the western North Atlantic seismic stratigraphy (Vail et al., 1980) correlates the top of the WNA-9 unit with a hypothesized basal Valanginian unconformity, which would imply that C′ is such a hiatus. Indeed, the assignment of C′ within the Berriasian is close to the age proposed by Vail et al. (1980), and the abrupt change in lithology (decrease in clay content and increase in limestone) does imply a possible hiatus. Certainly an important paleoenvironmental change occurred at that Berriasian contact.

The net result of these revised correlations of Horizon C and reflector C′ is that the depth calculated for these deeper reflectors is shallower by some 70 m, as compared to the original predicted depths (Table 17).

Upon drilling through the Upper to Middle Jurassic sediments, the reflections between Horizons C and D were encountered. These reflections are being correlated with the impedance contrasts associated with the increase in turbiditic limestones relative to the general background shale lithology of Subunits 6a (Cat Gap Formation) and 7a. Marked increases in drilling time are associated with these limestone stringers (Fig. 62), and generally higher interval velocities are determined for the limestone units (e.g., 3.9 km/s for Subunit 6B based on *in situ* corrected laboratory measurements).

The contact between Lithologic Subunits 6a and 6b is very abrupt and marked by a sharp drilling break, which correlates with the positive reflection wavelet just below Horizon C, called reflector D′ here (Figs. 60 and 62). There is no biostratigraphic evidence for a sedimentary hiatus between Subunits 6a and 6b, but resolution in the Kimmeridgian–Tithonian interval is limited at best. If further studies of more Site 534 samples would suggest such an hiatus, they would be in agreement with the seismic data that show truncations at this reflector. Vail et al. (1980) suggest that there should be a deep-sea disconformity at 141 m.y. associated with their proposed global sea-level drop, and this correlation might agree with their suggestion.

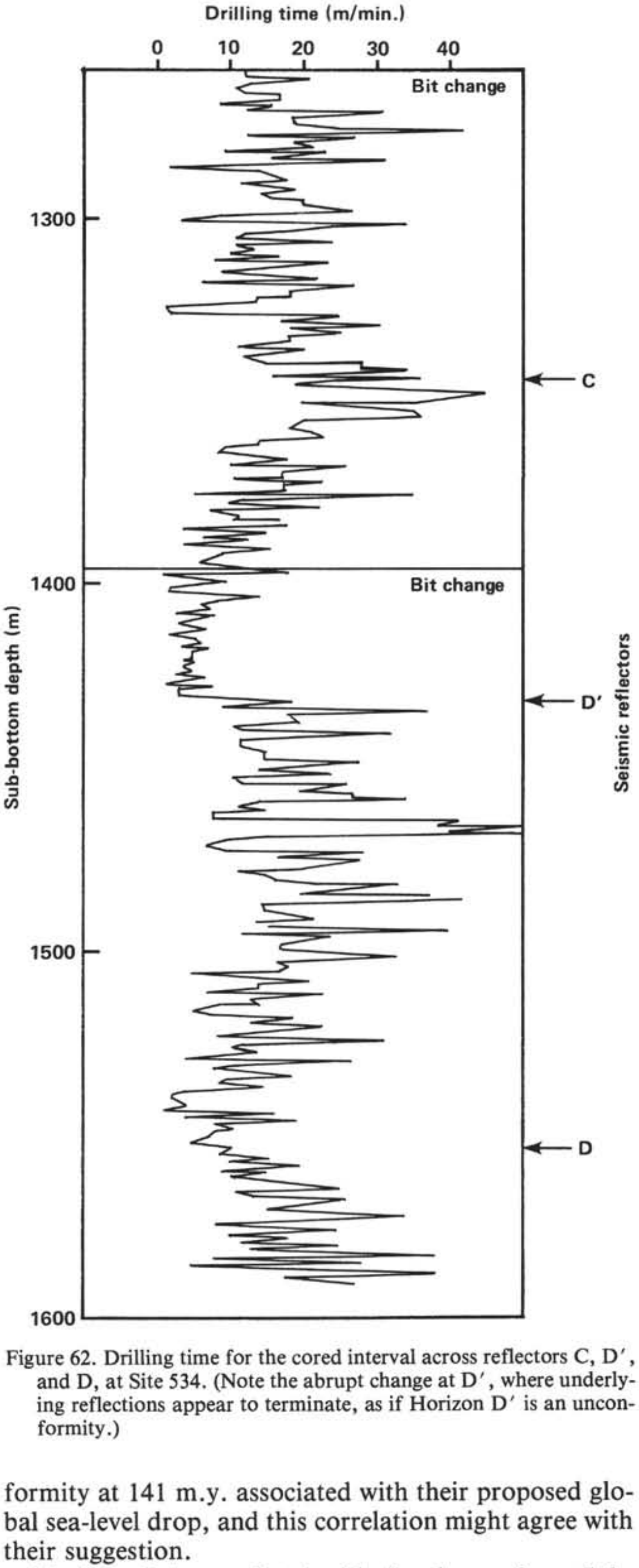

Figure 62. Drilling time for the cored interval across reflectors C, D′, and D, at Site 534. (Note the abrupt change at D′, where underlying reflections appear to terminate, as if Horizon D′ is an unconformity.)

Horizon D is correlated with the change from Subunit 7a, a more shaly lithology, to Subunit 7b, comprising more thick-bedded turbiditic limestone; the boundary is the limestone in Core 117 at 1552 m. Although coring recovery was quite poor in this interval, there is good indication of increasing limestones in Subunit 7b, based on the increased drilling times below 1550 m (Fig.

62). Unfortunately the poor recovery of material in this interval prevented a statistically meaningful distinction of a higher impedance or higher velocity acoustic unit that could be correlated with Subunit 7b, but it is probable that such a higher impedance exists for this more limestone-rich unit.

Given these correlations of Horizon D and D′, the calculated interval velocity between C and D′ is 3.06 km/s and between D′ and D is 4.00 km/s. These velocities generally agree with the 3.17 km/s velocity measured by sonobuoys and with the average *in situ* corrected velocity for the same intervals, 3.0 and 3.4 km/s (Table 18), although core recovery was poor so that the laboratory measurements might not be representative.

This correlation of Horizon D indicates that its depth at Site 534 is 46 m shallower than its predicted depth (Table 17), just as Horizon β has been found to be shallower than predicted because of the erroneous sonobuoy velocity in the A^u to β interval.

Basaltic oceanic basement was encountered at 1635 m in the bottom of Core 127, where a sharp contact exists between the middle Callovian soft red claystones and the hard igneous rock (Fig. 60). This occurrence is 180 m shallower than originally predicted (Table 17) for the proposed site. We had hoped to touch down in basalt in a place where the seismic reflection profiles showed basement just deeper than 8.0 s (Fig. 63). Given the velocities calculated by the site survey sonobuoys (Bryan et al., 1980), the depth to basement of 8.02 s corresponded to a calculated depth of 1819 m sub-bottom, which was just in reach of the engineering drill-string limit of the *Glomar Challenger*.

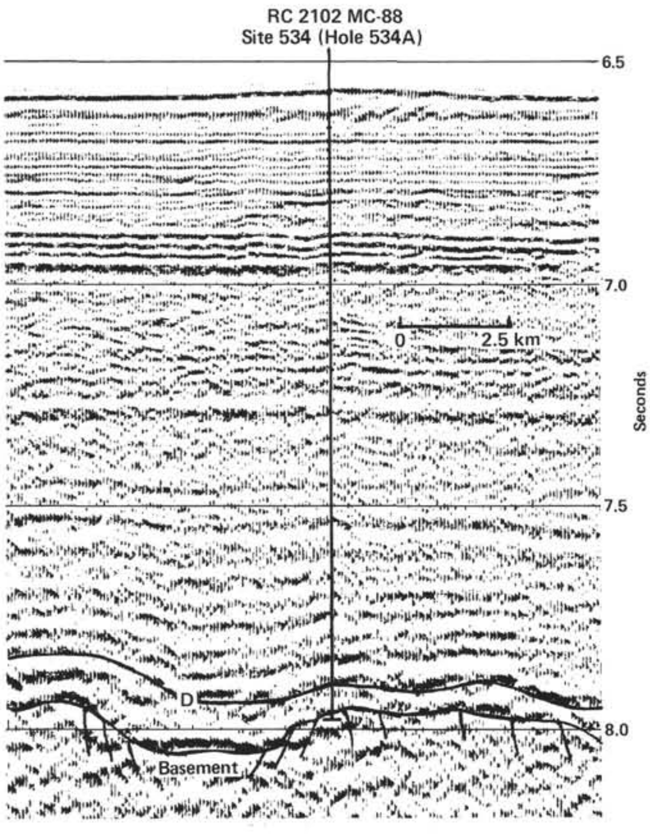

Figure 63. Best estimate of the location of Site 534 on nearby *Robert Conrad* seismic profile (line MC-88).

Apparently Site 534 is located a short distance (~0.5 n. mi.) away from the reference multichannel line, MC-88 (Fig. 63), where the local basement relief brings the basement reflector to 7.97 s. Such positioning uncertainties are inevitable when trying to reoccupy seismic lines, which themselves have uncertainty in positioning, and when using satellite and Loran C navigation systems.

Given these uncertains, we are pleased that the actual position of Hole 534A is so close to what we had hoped for. The prime goal of penetrating Horizon D, the oldest reflector in the western North Atlantic Ocean in reach of the *Challenger*'s drill, was achieved where the sediment interval from D to basement was thick enough to assure us of our seismic correlations.

Another reason for the basement depth being different than predicted is the inaccuracies of the sonobuoy velocities used to calculate depth. We have already discussed the affects of using the too high 2.58 km/s velocity for the A^u to β interval (Table 17), which resulted in Horizons β through D coming in 40 to 50 m shallower. For the D to basement interval, the 3.4 km/s seismic refraction velocity was assumed to apply for the entire interval. Now we know this is a wrong assumption. The refraction arrivals apparently come from head waves traveling horizontally along the upper part of Subunit 7b where the hard, high-velocity limestones occur. Indeed, the physical properties measurements for these limestones are in the 3.4 km/s range for those values measured parallel to bedding. However, the soft dark red and green claystones below the limestones of Subunit 7b are of a much lower velocity, as low as 2.2 km/s (uncorrected laboratory measurement). This results in a lower vertical velocity for this interval, which would have brought the basement to a predicted depth of 1730 m, only 90 m deeper than encountered. Thus the inherent velocity inaccuracies of the sonobuoy technique contributed half of the discrepancy in predicted depth, ±5% of total predicted depth, while the inherent navigational uncertainties contributed another ±5%.

Given the results, we are quite pleased with the site survey mapping and the precision of navigation of both the *Challenger* and *Conrad*. The officers and crews of both vessels should be commended, for without this precise work, the meaning of the seismic stratigraphy could not have been established. Moreover, the predictions of the feasibility of the drilling program could not have been made and proven correct. Often the geophysicist finds himself in the position of begging for more operational days to drill farther than he had predicted, especially at sites such as 534 where the objectives are so deep. Often higher velocities are found for the deeper rocks and the depth to basement is so deep it "races" ahead of the drill to unreachable depths. Fortunately, this did not happen at Site 534.

SUMMARY AND CONCLUSIONS

Continuous coring from 536 to 1666.5 m at Site 534 accomplished all the objectives established for the site, with the exception of obtaining a full suite of logs over the entire length of the hole. Because of bridging of the hole and large washouts, only density logs were successfully run on some portions of the hole. Drilling through seismic reflection Horizon D and into oceanic basement was the key to scientific achievement at this site. For the first time these oldest oceanic sediments beneath Horizon D have been sampled, and these samples reveal many aspects of the early North Atlantic Ocean that were often presumed to be quite different previously.

Lithostratigraphy and Biostratigraphy

The lithologic units penetrated at Site 534 between 0 and 1496 m sub-bottom are readily assigned to the formation erected for the North American Basin (Jansa et al., 1979) (Fig. 13). The red claystone, dark-colored claystone, olive gray limestone, and radiolarian silt and claystone between 1496 m and 1635 m on M-28 oceanic basement are quite different from and older than the Cat Gap Formation, the oldest known so far in the Atlantic Ocean. In descending order we encountered the following (Fig. 13):

1) From 0 to 2.1 m, in Core 534-1, penetrating 2.1 m with 2.1 m (100%) recovered, a gray nannofossil ooze and silty clay of the Quaternary Blake Ridge Formation. This unit (Unit 1) was sampled before the casing string to 531 m was placed.

2) From 536.3 to 696.5 m, in Cores 534A-1 to -18, penetrating 160.2 meters with 83.5 m (52%) recovered, chalks and intraclast chalks and dark green mudstones of the middle and lower Miocene Great Abaco Member of the Blake Ridge Formation (Unit 2).

3) From 696.5 to 723.5 m, in Cores 534A-19 to -21, penetrating 27 m with 8.4 m (31%) recovered, an interbedded zeolitic and siliceous, variegated mudstone, graded sandstone, and porcellanite of the upper Eocene Bermuda Rise Formation (Unit 3).

4) From 723.5 to 764.5 m, in Cores 534A-22 to -26, penetrating 41 m with 9.9 m (24%) recovered, a variegated claystone of the lower Maestrichtian Plantagenet Formation (Subunit 4a).

5) From 764.5 to 950.0 m, in Cores 534A-27 to -46, penetrating 185.5 m with 83.2 m (45%) recovered, a black to green carbonaceous claystone of the Cenomanian (Vraconian/uppermost Albian) through lower Aptian Hatteras Formation (Subunits 4b-d).

6) From 950.0 to 1342.0 m, in Cores 534A-47 to 91, penetrating 392 m with 298.4 m (76%) recovered, a bioturbated and laminated radiolarian-rich nannofossil limestone and chalk, grading upward into calcareous claystone and carbonaceous claystone redistributed shelf limestones and quartzose siltstones of the Barremian through the lower Berriasian Blake-Bahama Formation (Unit 5).

7) From 1342.0–1496 m, in Cores 534A-92 to -111, penetrating 154 m with 74.6 m (48%) recovered, a grayish red, calcareous claystone underlain by dark greenish gray claystone with interbedded limestone of the Tithonian through Oxfordian Cat Gap Formation (Unit 6).

8) From 1496 to 1635 m, in Cores 534A-112 to -127, penetrating 139 m with 39.8 m (29%) recovered, a dark-colored variegated claystone, underlain by olive gray pelletal limestone and radiolarian claystone, underlain by greenish black to brown nannofossil claystone, terminating in reddish almost massive claystone. This is a new unnamed lithostratigraphic unit (Unit 7) of the middle Callovian through at least part of the Oxfordian.

9) From 1635 to 1666.5 m, in Cores 534A-127 to -130, penetrating 31 m with 17.3 m (60%) recovered, a dark gray aphyric to sparsely microporphyritic basalt (Fig. 40). Green claystone and reddish brown siliceous limestone with "filaments" fill some of the 1- to 5-cm-thin fractures in the basalt and are present as thin (less than 7 cm) interbeds.

The preliminary biostratigraphy of the Jurassic, Cretaceous, and lower Tertiary sedimentary section is based on the interrelation of zonations using nannofossils, foraminifers, dinoflagellates, radiolarians, and calpionellids. The Kimmeridgian and younger biostratigraphy resembles that previously described for DSDP Hole 391C. The abyssal nature of the hemipelagic sediments deposited just above or below the carbon compensation depth (CCD) for foraminifers resulted in a stratigraphically patchy and often much impoverished foraminiferal record, without abundant planktonic forms. Nannofossils were most consistently present through the Jurassic to lower Tertiary, except in Jurassic and mid-Cretaceous dark shales. In those intervals organic walled microfossils and radiolarians assist in stratigraphic assignments.

Key biostratigraphic information for Site 534 (Fig. 13) is provided by:

1) The nannofossil zonations, which allow a twelve-fold subdivision in the middle Callovian through Albian strata.

2) An age assignment of middle Callovian to early Oxfordian for Cores 126 through 121, based on radiolarian biostratigraphy.

3) The *L. quenstedti, E.* aff. *uhligi* foraminifer assemblage characteristic of the *E. mosquensis* Zone in and below Core 99, which is not younger than early Tithonian, and Valanginian, Barremian, Aptian, and Vraconian datums between Cores 72 and 27.

4) The presence of Zone A (upper Tithonian) in Core 93, and of Zone B (close to the Tithonian/Berriasian boundary) in Cores 92 through 87, based on calpionellids.

5) Middle Callovian through Tithonian datum levels in Cores 127 through 91, and nine zones in Cores 90 through 27 (Berriasian through Vraconian) based on dinoflagellates.

6) A presumably *in situ* lower Maestrichtian *Globotruncana* foraminifer assemblage in Cores 23 to 26, and the upper Eocene nannoflora assigned to the *D. barbadiensis* to *G. saipanensis* Zones in Cores 19 to 21.

The Miocene stratigraphy at Site 534, as in Hole 391C, uses a combination of standard nannofossil and planktonic foraminiferal zonations; resolution is better than that in the older beds. There is good agreement in age assignment between the five microfossil disciplines for the majority of the Mesozoic–Cenozoic cores. It is particularly satisfactory that excellent dates exist on the basal sedimentary cores (127–124) (middle and late Callovian), on the cores (90–92) near the Jurassic/Cretaceous boundary, and in general at the bottom and top of the seven lithostratigraphic units. Discrepancies between nannofossil and dinoflagellate stratigraphies for the Callovian/Oxfordian, Oxfordian/Kimmeridgian, and Kimmeridgian/Tithonian boundaries and between nannofossils–foraminifers and dinoflagellates for the Hauterivian/Barremian boundary cannot be resolved at this time. Several lines of study may help to resolve these discrepancies: (1) reappraisal of the synchroneity of ranges of key taxa in the Blake-Bahama Basin and in the areas where the ranges were first established and were calibrated to a chronostratigraphic scale; (2) study of more deep-marine Mesozoic sections if and when such become available; (3) further study of foraminifers, nannofossils, and dinoflagellates in the Jurassic Atlantic margin basin (e.g., Portugal, Morocco, North American Atlantic shelf); and (4) improved calibration of the zones and datums or ranges to ammonite and calpionellid zones.

Depositional History

The thick Jurassic, Cretaceous, and Tertiary–Quaternary stratigraphic sequence is the result of relatively continuous slow and periodically fast sedimentation. There was mainly continuous, quiescent, 0.1 cm/10^3 yr. or less, hemipelagic "background" sedimentation at seafloor depths between the CCD for foraminifers and that for nannofossils. On this record is superimposed periodic sedimentation by turbidity currents, debris flows, or bottom currents of slope or shelf carbonate and carbonaceous claystone at average rates as high as 4 cm/10^3 yr. Three-quarters of this sediment (decompacted thickness) were deposited during the first 50 m.y. after the site formed at the mid-ocean ridge in the Callovian (154 Ma on the van Hinte time scale [1976b]). The overlying section, largely Miocene and younger, accumulated in the last 20 m.y. The main periods during which carbonates were redeposited occurred in the early part of the Early Cretaceous and in the Miocene; carbonaceous claystones were the dominant deposits in the basin in the mid-Cretaceous. Redeposited quartz sand and silt form a minor constituent of the cored section, which can be explained by the damming effect of the carbonate barrier platform to the west and southwest of the basin and by the very distal location of the site.

The basal sediments and several interbeds in the basalt are red, weakly laminated to massive claystones that contain some flattened burrows. There is no obvious basal ferromanganese horizon at Site 534. The color and sedimentary features point to oxidizing bottom waters without strong current activity in the middle Callovian basal deposits.

The Middle and Upper Jurassic brown and green black, radiolarian-rich claystone and redeposited limestones indicate hemipelagic sedimentation, modified by slope and shelf-derived turbidites and bottom-current transport. The various green, red, gray, and black colors largely reflect organic matter content and the sulfide surviving after diagenesis. Sedimentary structures indicate deposition of the black shale laminae largely by dilute turbidity currents. One alternative is that the black shales reflect periodic organic-matter input (mostly terrestrial) possibly related to fluctuating climate on land. In this case bottom water need not have been anoxic. Alternatively, pools of reduced bottom water may have existed for short periods on the Callovian seafloor.

Sedimentary structures, especially low-angle cross-bedding and winnowing effects, show that the Middle Jurassic Atlantic Ocean basin may have had some bottom circulation leading to possible contourite deposition. The Jurassic ocean surface waters sustained rich radiolarian faunas and nannofloras indicative of an ocean with a well-established surface circulation. The presence of these radiolarian faunas and nannofloras might suggest a continuous open marine connection to Tethys and probably the Pacific as well. This connection is also shown by the presence of Oxfordian primitive planktonic foraminifers. These are some of the oldest known and correlate with an abundance peak in the Mediterranean basin margins.

The major influx of pelagic and redeposited carbonates in the Berriasian to Barremian (Early Cretaceous) gradually changed to predominantly carbonaceous claystone accumulation during the Aptian to Cenomanian. The CCD shoaled sharply in the Barremian through Aptian and resulted in carbonate-depleted sediment. Many of the thin (<15 cm thick) carbonaceous claystones were deposited by distal turbidity currents. Ubiquitous, very fine laminations may be the result of extremely distal turbidites or nepheloid deposition. The organic matter is mostly terrigenous and less marine in origin, possibly reflecting a wet climate on land and an oxidizing environment on the seafloor. Alternatively, the sea bottom water may have been anoxic for at least some time. Based on the level of thermal maturation, kerogen type, and organic content, the carbonaceous claystone may be considered a potential gas source. There are distinct alterations (cycles) of primary and pedogenic (cf., illite to smectite) clay minerals and distinct peaks in organic abundance. The marine organic matter peaks correlate to similar peaks at other sites in the Atlantic Ocean. The variegated, oxidized late Aptian sequences contain minor silt layers and weather resistent clay minerals, which indicate a marked change in environment with improved bottom circulation, slower accumulation, or winnowing.

A surprising find was several tens of meters of thin, variegated claystone and interbedded zeolitic–siliceous mudstone, siltstone, and minor porcellanite of the Maestrichtian and the late Eocene (Fig. 13) where the Miocene/Cenomanian disconformity (discovered during Leg 44 at Site 391, 22 km southeastward) was expected. The postulation that there had been up to 800 m of erosion (mostly during the Oligocene), formulated on the basis of somewhat tenuous coalification data in the Aptian/Albian and Miocene strata (Dow, 1978), may need revision. Rather, we conclude that extensive sediment starvation in the Late Cretaceous and Paleogene Blake-Bahama Basin led to a low net sediment accumulation without large-scale sediment erosion.

In the lower Miocene gravity flows, one continuously graded unit over 10 m thick was observed that could be related to the same depositional event as that observed at nearby Site 391. Rather similar and coeval deposits have been found during DSDP cruises off Morocco, which suggests common causes for their formation. We are not certain if oversteepening of the shelf terrace due to Oligocene eustatic sea level lowering or Alpine tectonics (in the Atlas Mountains and Cuba-Antilles) or both was the cause of the large-scale Miocene gravity redeposition.

Physical Properties and Seismic Stratigraphy

Laboratory velocity measurements and *in situ* impedance calculations compare well with the correlation between seismic reflectors and drill hole lithologies and hiatuses. The possible errors in the different techniques of measuring velocities (laboratory versus seismic) place limitations on the certainty of the seismic correlations and the calculated impedance values for subjectively subdivided units. However, in the absence of computer modeling with log data, this is the best approach with the data available at sea.

The laboratory measurements, corrected to *in situ* values, showed generally higher values for limestones and cherty layers—2.4 to 4.0 km/s—and generally lower values for shales and claystones—2.0 to 2.9 km/s—as expected. There was a general increase of measured velocities and densities with depth for each lithology, claystone, chalks, and limestones.

While generally increasing with depth, the *in situ* corrected velocities and densities clearly document strong and abrupt inversions in four cases, at depths as deep as 1500 m (Fig. 13). These acoustic inversions produced slight inaccuracies in the sonobuoy velocities used to predict the depths at the site. The failure of the sonobuoys to detect any of the inversions led to 40 to 50 m discrepancies between predicted and drilled depths.

Important seismic correlations were made on key seismic reflectors at Site 534. Two "kinds" of reflectors were identified as: (1) those caused by strong bedding-plane impedance contrasts (facies changes) and the resulting convolution interference (e.g., A^c, β, C, and D); (2) those caused by unconformities and more subtle, associated impedance contrasts (e.g., A^u, β', C′, and D′). Reflectors β', C′, and D′ are inferred to be unconformities, on the basis of abrupt lithologic changes and truncations or downlap evident on seismic profiles. However, biostratigraphic resolution is insufficient to corroborate this interpretation. In Hole 534A the reflectors are presently assigned (Fig. 13) as follows:

Bedding Planes

A^c = upper Eocene porcellanitic claystone
β = Barremian turbiditic limestone
C = uppermost Tithonian or lowermost Berriasian interlayered
D = lower Oxfordian turbiditic limestone

Unconformities

A^u = lower Miocene/upper Eocene
β' = lower Albian/upper Aptian
C′ = upper Berriasian/lower Berriasian
D′ = Kimmeridgian/Kimmeridgian

The ages of Horizons A^c, β, and C at Site 534 agree with previously published correlations at Site 391 (Sheridan, Pastouret, et al., 1978; Benson et al., 1978) and at Sites 386 and 387 (Tucholke and Mountain, 1979; Tucholke, Vogt, et al., 1979). The age of Horizon D, drilled for the first time at Site 534, is younger than the basal Callovian, predicted by Bryan et al. (1980), and older than the Tithonian, predicted by Vail et al. (1980).

The ages of the unconformity reflectors A^u, β', C′, and D′ are determined to varying degrees. A^u and C′ are well bracketed. These ages agree with those hiatuses predicted to exist in the deep sea by Vail et al. (1980); these are the Oligocene and basal Valanginian hiatuses, which are times of rapid eustatic sea level falls. The ages of β' and D′ are less rigorously defined, but they could correlate with the mid-Aptian and mid-Tithonian (basal mid-Kimmeridgian) sea level falls and associated hiatuses, respectively, of Vail et al. (1980). The reason for this correlation of deep-sea and shelf unconformities is not understood, but it is clear that deep-sea processes must cause either nondeposition or erosion at these reflectors. Truncation is evident on some of these reflectors, so some small erosion also took place.

Age of Basement

The magnetostratigraphy of the sedimentary column of Hole 534A could not be ascertained aboard ship, but the direction of magnetization of the basaltic basement rocks is consistent with the Jurassic paleolatitude of the site. The age assignment of the basal beds to the middle Callovian has been verified by nannofossil and radiolarian stratigraphy. In order to reach basement within the engineering drill-string limit, Site 534 was positioned on the north flank of a fracture zone trough. As a result, basement was penetrated at a shallower depth than the sediments in the adjacent trough. However, because the seismic profiles suggest that the hemipelagic sediment cover on the basement at Site 534 formed more or less simultaneously in troughs and on highs, we are confident that the biostratigraphy of the basal sediments provides a reliable estimate of the minimum age for the basement at Site 534.

In support of this conclusion, the basal ages of previous Deep Sea Drilling Project sites on various seafloor magnetic anomalies are plotted in Figure 64. The magnetic anomalies are plotted at the distance from the center of the Mid-Atlantic Ridge along a flow line through Site 534 south of the Kane Fracture Zone. As a comparison, the paleomagnetic measurements of these same reversals, made in stratigraphic sections where the ages are known (Ogg, 1980; Lowrie et al., 1980), are plotted over the same anomalies. Note that the age of the basal sediments on the anomalies are within ±1 to 2 m.y. of the paleomagnetically determined age. This consistent relationship in so many cases implies that the basement ages determined by drilling are generally reasonably accurate.

Seafloor Spreading in the Middle and Late Jurassic

Drilling at Site 534 has contributed greatly to our understanding of the spreading rates for the central North Atlantic Ocean. The age of Horizon D, the deepest sedimentary reflector yet drilled, was found to be early Ox-

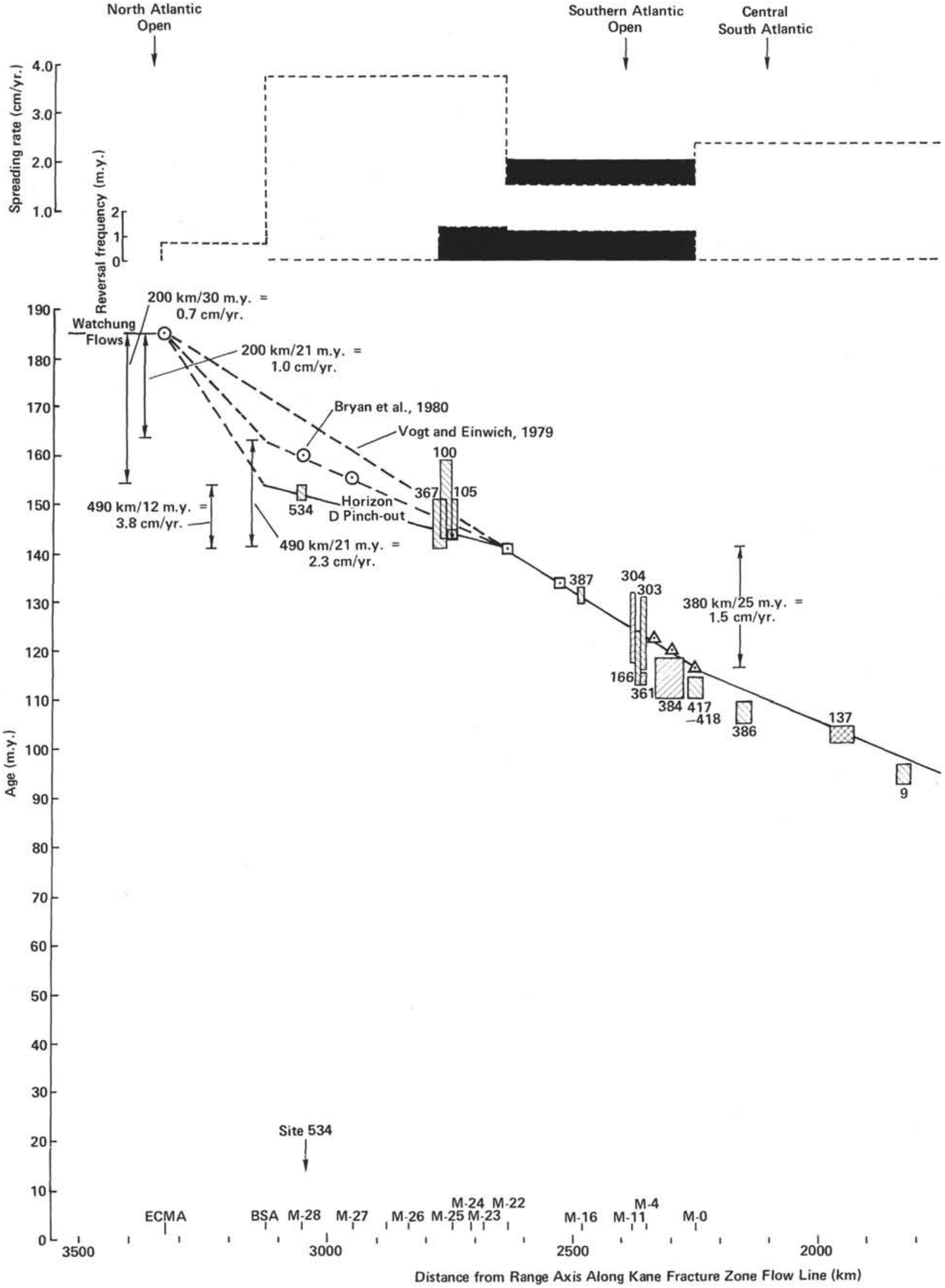

Figure 64. Plot of magnetic anomaly age versus distance along flow line through Site 534 indicates spreading rates. (ECMA = East Coast Magnetic Anomaly; BSA = Blake Spur Anomaly. Basement ages at the sites are based on drilling results as indicated in the legend.)

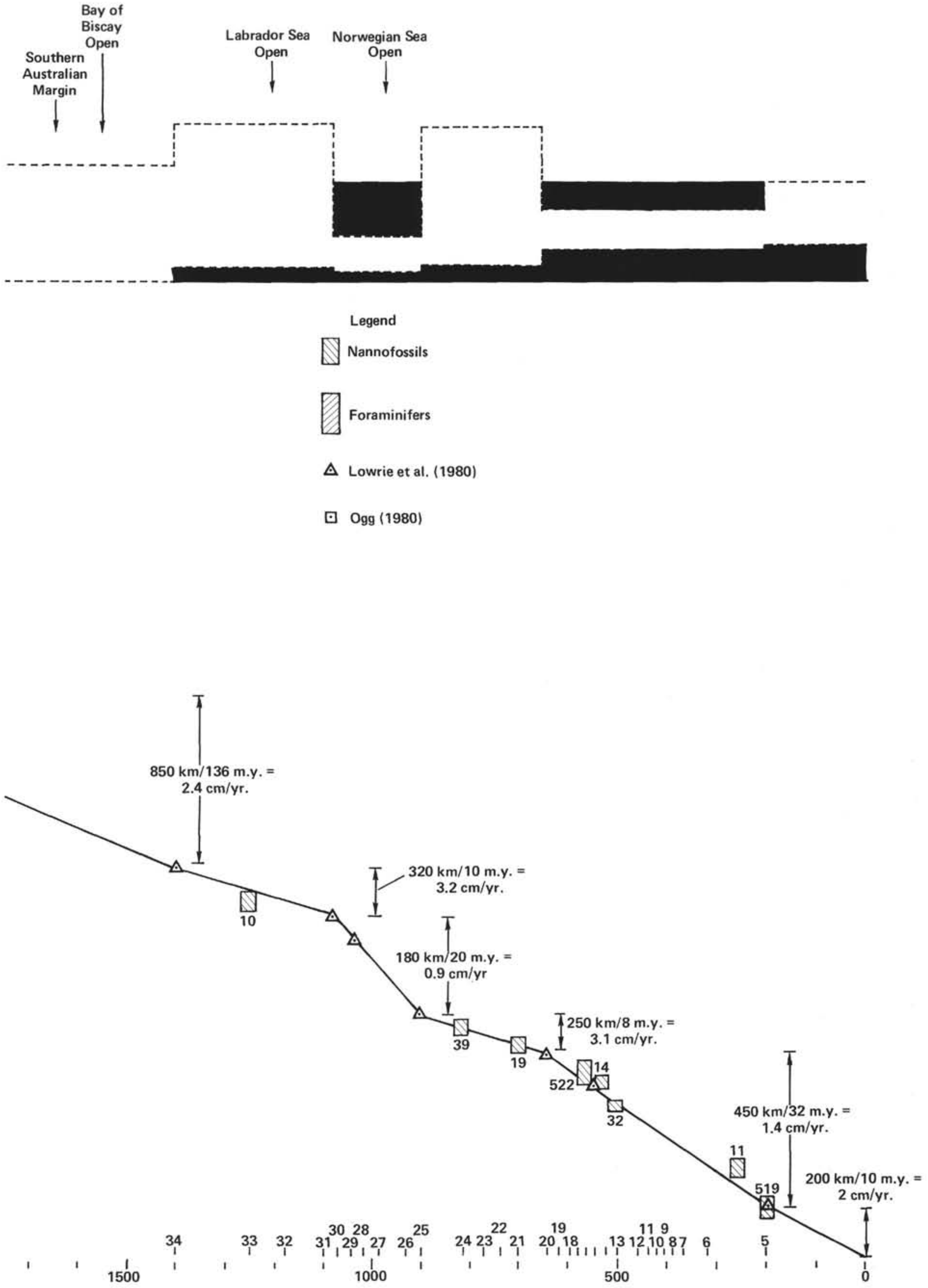

Figure 64. (Continued).

fordian. Assuming that constant sedimentation occurred during this interval, the age of the reflection horizon is thought to be approximately 149 m.y. on the van Hinte (1976b) time scale. Given that the seismic horizon has been mapped seaward to where it pinches out on Magnetic Anomaly M-27 (Fig. 64), it is possible to estimate the approximate age of this magnetic reversal. It happens that this early Oxfordian assignment for M-27 is in excellent agreement with the projected age for this anomaly, based on the paleomagnetic studies of Ogg (1980).

The sediments immediately above basement at Site 534 are dated as middle Callovian, about 154 m.y. old on the van Hinte (1976b) scale. This age for Magnetic Anomaly M-28 would also plot along a constant spreading rate curve, with the ages determined for M-22 through M-25 by Ogg (1980) (Fig. 64). A major achievement of Site 534, then, is the substantiation of Ogg's (1980) dates. These data indicate that magnetic reversals M-26 and M-27 both occurred in the Oxfordian. There data also imply that the sediments drilled at Sites 100 and 105 were deposited in the latest Oxfordian or early Kimmeridgian, which is in the range of the broad biostratigraphic determinations at those sites.

Following this argument, the Oxfordian dates for M-25, M-26, and M-27 and the Callovian date for M-28 require a 3.8 cm/yr. spreading rate for the Late Jurassic to Earliest Cretaceous (Fig. 64). It appears that the opening of the modern North Atlantic Ocean began with a pulse of very rapid spreading at rates >300% higher than the present rate. The implications of this rapid spreading for the origin of the Jurassic magnetic quiet zone are discussed elsewhere in this volume.

Age of Blake Spur Spreading-Center Jump

Mapping of the magnetic anomalies in the North Atlantic made it apparent that the corridor of ocean crust between the East Coast magnetic anomaly and the Blake Spur Anomaly had little or no equivalency on the African margin. Such asymmetry requires a spreading-center jump during the time of the Blake Spur Anomaly. Vogt (1973) observed this asymmetry and estimated an age of 175 m.y. for this jump; Vogt and Einwich (1979) continue to extrapolate this date (Fig. 64). Vogt (1973) admitted that this date was speculative and wrote: "The only adequate test for the hypothesis is to drill on the Blake Spur Anomaly."

Unfortunately, drilling directly on the Blake Spur Anomaly is not possible with *Challenger*'s present drill-string capabilities. Site 534 is the closest site possible to the Blake Spur from which to address the problem. As mentioned in the Background and Objectives section, sufficient seismic reflection mapping has been done to show a structure at the anomaly that is compatible with the spreading-center jump hypothesis. Drilling could add little more to proving that it did occur, although there are some suggestions of sub-basement stratification in the Blake Spur Ridge (Shipley et al., 1978) that might indicate an unusual basement type. These sub-basement reflectors could be caused by many things, but they are seen in other areas near the points of initiation of seafloor spreading. Apparently their formation relates to the presence of a new spreading center, in agreement with the spreading-center shift hypothesis.

However, drilling at Site 534 contributes to the dating of the Blake Spur spreading-center jump. Extrapolating the 3.8 cm/yr. spreading rate from the M-22 through M-28 anomalies to the Blake Spur indicates an age of 155 m.y., or early Callovian, for the event. This is significantly younger than the 175 m.y. age Vogt (1973) and Vogt and Einwich (1979) projected; and it is quite surprising to consider that such an event occurred so recently.

This surprising result is compatible with other regional tectonic data, however, and might help to explain several stratigraphic features. Stratigraphically the Callovian deposits around the North Atlantic marked the onset of a rapid, widespread transgression. Generally, the breakup of plates to form ocean crust is punctuated by a pulse of rapid subsidence and rapid transgression over the breakup unconformity on the continental margins. This widespread Callovian transgression, then, could be a record of the Blake Spur spreading-center jump and would be supportive evidence for the ages interpreted here.

REFERENCES

Ade-Hall, J. M., and Johnson, H. P., 1976. Paleomagnetism of basalts, Leg 34, *In* Yeats, R. S., Hart, S. R., et al., *Init, Repts. DSDP*, 34: Washington (U.S. Govt. Printing Office), 513.

Ager, D. V., 1975. The Jurassic world ocean (with special reference to the North Atlantic). In *Jurassic Northern North Sea Symposium*, Stavanger.

Alleman, F., Catalano, R., Fares, F., Remane, J., 1971. Standard calpionellid zonation (upper Tithonian-Valanginian) of the western Mediterranean province. *Proc. Second Plankt. Conf., Roma 1970*, II:1337-1340.

Arthur, M. A., 1979. North Atlantic Cretaceous black shales: the record at Site 398 and a brief comparison with other occurrences. *In* Sibuet, J.-C., Ryan, W. B. F., et al., *Init. Repts. DSDP*, 47, Pt. 2: Washington (U.S. Govt. Printing Office), 719-751.

Ascoli, P., 1976. Foraminiferal and ostracode biostratigraphy of the Mesozoic-Cenozoic, Scotian Shelf, Atlantic Canada. In *Proc. Int. Symp. Benthonic Foram Halifax, 1975.* Maritime Sed. Spec. Publ, 1:653-771.

Bader, R. G., Gerard, R. D., et al., 1970. *Init. Repts. DSDP*, 4: Washington (U.S. Govt. Printing Office).

Barnard, T., and Hay, W. W., 1974. On Jurassic coccoliths: a tentative zonation of the Jurassic of southern England and northern France. *Eclogae Geol. Helv.*, 67:563:585.

Barr, K. W., 1974. The Caribbean and plate tectonics—some aspects of the problem. *Verh. Naturforsch. Ges. Basel.*, 84(1):45-67.

Bartenstein, H., Bettenstaedt, F., and Bolli, H. M., 1957. Die Foraminiferen der Unterkreide von Trinidad, BWI-Cuche und Toco Formation. *Eclogae Geol. Helv.*, 50, Pt. 1:5-65.

________, 1966. Die Foraminiferen der Unterkreide von Trinidad, W.I.-Maridale Formation (Typlokalitat). *Eclogae Geol. Helv.*, 59, Pt. 1:129-175.

Bartenstein, H., and Bolli, H. M., 1973. Die Foraminiferen der Unterkreide von Trinidad, W.I.-Maridale Formation (Cotyplokolit). *Eclogae Geol. Helv.*, 66:389-418.

Bates, L., 1980. Synthetic seismogram model and the age and origin of Horizon D [Master's dissert.]. University of Delaware.

Baumgartner, P. O., De Wever, P., and Kocher, R., 1980. Correlation of Tethyan Late Jurassic-Early Cretaceous radiolarian events. *Cah. Micropaleontol.*, 2:23-72.

Benson, W. E., Sheridan, R. E., and Shipboard Scientific Party, 1978. Site 391: Blake-Bahama Basin. *In* Benson, W. E., Sheridan, R. E., et al., *Init. Repts. DSDP*, 44: Washington (U.S. Govt. Printing Office), 153-336.

Bernard, B. B., Brooks, J. M., and Sackett, W. M., 1978. Light hydrocarbons in Recent Texas continental shelf and slope sediments. *J. Geophys. Res.*, 83:4053-4061.

Bernoulli, D., 1972. North Atlantic and Mediterranean Mesozoic facies: a comparison. *In* Hollister, C. D., Ewing, J. I., et al., *Init. Repts. DSDP*, 11: Washington (U.S. Govt. Printing Office), 801-872.

Bielecka, W., and Geroch, S., 1974. Quelques foraminiferes du Jurassique superieur des Carpathes externes polonaises. *VI Coll. Africain Micropal., Tunis 1974. Ann. Mines. Geol. Tunis.*, 28:185-199.

Bleil, U., and Smith, B., 1980. Paleomagnetism of basalts, Leg 51. *In* Donnelly, T., Francheteau, J., Bryan, W., Robinson, P., Flower, M., Salisbury, M., et al., *Init. Repts. DSDP*, 51, 52, 53, Pt. 2: Washington (U.S. Govt. Printing Office), 1351-1361.

Bouma, A. H., and Hollister, C. D., 1973. Deep ocean basin sedimentation. *In* Middleton, G. M., and Bouma, A. H. (Eds.), *Turbidites and Deep-water Sedimentation.* Soc. Econ. Paleontol. Mineral. Short Course, pp. 79-118.

Bourbon, M., 1978. Mesozoic evolution of western North Atlantic and North Tethyan Margins: a comparison. *In* Benson, W. E., Sheridan, R. E., et al., *Init. Repts. DSDP*, 44: Washington (U.S. Govt. Printing Office), 949-969.

Boyce, R. E., 1976. Sound velocity-density parameters of sediment and rock from DSDP Sites 315-318 on the Line Islands Chain, Manihiki Plateau, and Tuamotu Ridge in the Pacific Ocean. *In* Schlanger, S. D., Jackson, E. D. et al., *Init. Repts. DSDP*, 33: Washington (U.S. Govt. Printing Office), 695-728.

Bryan, G. M., Markl, R. G., and Sheridan, R. E., 1980. IPOD Site Surveys in the Blake-Bahama Basin. *Mar. Geol.*, 35:43-63.

Bryan, W. B., 1972. Textural and mineralogical relations of basalts from Sites 100 and 105. *In* Hollister, C. D., Ewing, J. I., et al., *Init. Repts. DSDP*, 11: Washington (U.S. Govt. Printing Office), 873-876.

Bujak, J. P., and Williams, G. L., 1977. Jurassic palynostratigraphy of off-shore eastern Canada. *Proc. Symp. Strat. Micropaleontol. of Atlantic Basins and Borderlands, Delaware 1976:* New York (Elsevier), pp. 321-339.

Cande, S. C., Larson, R. L., and La Brecque, J. L., 1978. Magnetic lineations in the Pacific Jurassic quiet zone. *Earth Planet. Sci. Lett.*, 41:434-440.

Cardoso, J. N., Wardroper, A. M. K., Watts, C. D., Barnes, P. J., Maxwell, J. R., Eglinton, G., Mound, D. G., and Speers, G. C., 1978. Preliminary organic geochemical analyses: Site 391, Leg 44 of the Deep Sea Drilling Project. *In* Benson, W. E., Sheridan, R. E., et al., *Init. Repts. DSDP*, 44: Washington (U.S. Govt. Printing Office), 617-624.

Chamley, H., 1979. North Atlantic clay sedimentation and paleoenvironment since the Late Jurassic. *Am. Geophys. Union*, Maurice Ewing Series, 3:342-361.

Chen, P. Y., 1977. Table of key lines in X-ray powder diffraction patterns of minerals in clays and associated rocks. *Geol. Surv. Occasional Pap. 21*, Indiana.

Colom, G., and Rangheard, Y., 1965. Les couches a Protoglobigerines de l'Oxfordien spuerieur de l'Ile d'Ibiza et leurs equivalents a Majorque et dans le Domaine subbetique. *Rev. Micropalentol.*, 9: 29-36.

Cook, H. E., Johnson, P. D., Matti, J. C., and Zemmels, I. 1975. Methods of sample preparation and X-ray diffraction data analysis. *In* Hayes, D. E., Frakes, L. A., et al., *Init. Repts. DSDP*, 28: Washington (U.S. Govt. Printing Office), 999-1007.

Demaison, G. J., and Moore, G. T., 1980. Anoxic environments and oil source bed genesis. *Am. Assoc. Pet. Geol. Bull.*, 64:1179-1209.

Deroo, G., Herbin, J. P., Roucaché, J. R., Tissot, B., Albrecht, P., and Dastillung, M., 1978. Organic geochemistry of some Cretaceous claystones from Site 391, Leg 44, Western North Atlantic. *In* Benson, W. E., Sheridan, R. E., et al., *Init. Repts. DSDP*, 44: Washington (U.S. Govt. Printing Office), 593-598.

Dillon, W. P., Sheridan, R. E., and Fail, J. P., 1976. Structure of the western Blake-Bahama Basin as shown by 24-Channel CDP Profiling. *Geology*, 4:459-462.

Dow, W. G., 1978. Geochemical analyses of samples from Holes 391A and 391C, Leg 44, Blake-Bahama Basin. *In* Benson, W. E., Sheridan, R. E., et al., *Init. Repts. DSDP*, 44: Washington (U.S. Govt. Printing Office), 625-634.

Eberl, D., and Hower, J., 1976. Kinetics of illite formation. *Geol. Soc. Am. Bull.*, 87:1326-1330.

Enos, P., Freeman, T., 1978. Shallow-water limestones from the Blake Nose, Sites 390 and 392. *In* Benson, W. E., Sheridan, R. E., et al., *Init. Repts. DSDP*, 44: Washington (U.S. Govt. Printing Office), 413-461.

Espitalié, J., Laporte, J. L., Madec, M., Marquis, F., Leplzt, P., Paulet, J., Boutefeu, A., 1977. Méthode rapide de caratérizatiòn de roches mères, de leur potentiel pétrolier et de leur degré d'evolution. *Rev. Inst. Fr. Pet.*, 32:23-42.

Espitalié, J., and Sigal, J., 1963. Epistominidae du Lias sup. et du Bajocien du bassin de Majunga (Madagascar). Les genres Lamarckella et Garantella Kapt. Tchern. et Reinholdella Brotzen. *Rev. Micropaleontol.*, 6(2):109-119.

Fischer, A. G., and Arthur, M. A., 1977. Secular variations in the pelagic realm. *Soc. Econ. Paleontol. Mineral., Spec. Publ.*, 25:19-50.

Flood, R. D., 1978. X-ray mineralogy of DSDP Legs 44 and 44A, western North Atlantic. *In* Benson, W. E., and Sheridan, R. E., et al., *Init. Repts. DSDP*, 44: Washington (U.S. Govt. Printing Office), 516-521.

Freeman, T., and Enos, P., 1979. Petrology of Upper Jurassic-Lower Cretaceous limestones, DSDP, Site 391. *In* Benson, W. E., Sheridan, R. E., et al., *Init. Repts. DSDP*, 44: Washington (U.S. Govt. Printing Office), 463-477.

Gradstein, F. M., 1976. Biostratigraphy and biogeography of Jurassic Grand Banks Foraminifera. *Proc. Int. Symp. Benthonic Foram., Halifax, 1975.* Maritime Sed. Spec. Publ., 1:557-583.

________, 1978a. Biostratigraphy of Lower Cretaceous Blake Nose and Blake-Bahama Basin Foraminifers, DSDP, Leg 44, western North Atlantic Ocean. *In* Benson, W. E., Sheridan, R. E., et al., *Init. Repts. DSDP*, 44: Washington (U.S. Govt. Printing Office), 663-702.

________, 1978b. Jurassic Grand Banks Foraminifera. *J. Foraminiferal Res.*, 8:97-109.

Guex, J., and Davaud, E., 1982. Recherche automatique des associations unitaires en biochronologie. *Bull. Soc. Vaud. Sci. Nat.*, 76(361):53-69.

Habib, D., 1977. Comparison of Lower and Middle Cretaceous palynostratigraphic zonations in the western North Atlantic. *In* Swain, F. M. (Ed.), *Stratigraphic Micropaleontology of Atlantic Basin and Borderlands:* New York (Elsevier), pp. 341-367.

________, 1978. Palynostratigraphy of the Lower Cretaceous section at DSDP Site 391, Blake-Bahama Basin, and its correlation in the North Atlantic. *In* Benson, W. E., Sheridan, R. E., et al., *Init. Repts. DSDP*, 44: Washington (U.S. Govt. Printing Office), 887-898.

Hallam, A., 1975. *Jurassic Environments:* London (Cambridge University Press).

Hamilton, E. L., 1976. Variations of density and porosity with depth in deep-sea sediments. *J. Sediment. Petrol.*, 46:280-300.

Hamilton, G., 1979. Lower and Middle Jurassic calcareous nannofossils from Portugal. *Eclogae. Geol. Helv.*, 72(1):1-17.

Hand, J. H., Katz, D. L., and Verina, V. K., 1974. Review of gas hydrates with implication for ocean sediments. *In* Kaplan, I. R., (Ed.), *Natural Gases in Marine Sediments:* New York (Plenum Press), pp. 179-194.

Heezen, B. C., Hollister, C. D., and Ruddiman, W. F., 1966. Shaping of the continental rise by deep geostrophic contour currents. *Science*, 152:502-508.

Hesse, R., and Harrison, W. E., 1980. Abnormally low pore-water salinities in deep marine sections of the continental margins related to gas-hydrate (clathrate) occurrence. *Geol. Soc. Am. Abstract with Programs*, 12:446. (Abstract)

Hollister, C. D., Ewing, J. I., et al., 1972a. *Init. Repts. DSDP*, 11: Washington (U.S. Govt. Printing Office).

________, 1972b. Sites 102, 103, 104, Blake-Bahama Outer Ridge (northern end). *In* Hollister, C. D., Ewing, J. I., et al., *Init. Repts. DSDP*, 11: Washington (U.S. Govt. Printing Office), 135-218.

Honnorez, J., Von Herzen, R. P., in press. *Init. Repts. DSDP*, 70: Washington (U.S. Govt. Printing Office).

Jansa, L., Ascoli, P., and Remane, J., 1980. Calpionellid and foraminiferal-ostracod biostratigraphy at the Jurassic/Cretaceous boundary, offshore eastern Canada. *Riv. Ital. Paleontol.*, 86(1):67-126.

Jansa, L. F., Enos, P., Tucholke, B. E., Gradstein, F. M., and Sheridan, R. E., 1979. Mesozoic-Cenozoic sedimentary formations of the North American Basin, western North Atlantic. *In* Talwani, M., Hay, W., and Ryan, W. B. F., (Eds.), *Deep Drilling Results in the Atlantic Ocean: Continental Margins and Paleoenvironments.* Am. Geophys. Union, Maurice Ewing Series, 3:1-57.

Jansa, L., Gardner, J. V., and Dean, W. E., 1978. Mesozoic sequences of the Central North Atlantic. *In* Lancelot, Y., Siebold, E., et al., *Init. Repts. DSDP*, 41: Washington (U.S. Govt. Printing Office), 991-1031.

Klitgord, K. D., and Behrendt, J. C., 1979. Basin structure of the U.S. Atlantic margin. *Am. Assoc. Pet. Geol. Mem.*, 29:85-112.

Klitgord, K. D., and Grow, J. A., 1980. Jurassic seismic stratigraphy and basement structure of the western North Atlantic quiet zone. *Am. Assoc. Pet. Geol. Bull.*, 64:1658-1680.

Klitgord, K. D., and Schouten, H., 1977. The onset of seafloor spreading from magnetic anomalies. In *Symposium on the Geological Development of the New York Bight:* Palisades, New York (Lamont-Doherty Geological Observatory), pp. 12-13.

Maldonado-Koerdell, M., (Ed.), 1956. Estratigrafiá y paleontologiá del Jurásico Inferior y Medio Marino de la región central de la Sierra Madre Oriental, Mexico, Excursion C-8. 20^e Congr. Geol. Int., Mexico 1956.

Le Hegarat, G., and Remane, J., 1968. Tithonique superieur et Berriasien de la bordure cevenole. Correlation des Ammonites et des Calpionelles. *Geobios*, 1:7-70.

Lentin, J. K., and Williams, G. L., 1973. Fossil dinoflagellates—index to genera and species. *Can. Geol. Surv.*, 73-42:1-176.

Lippmann, F., 1973. *Sedimentary Carbonate Minerals:* New York (Springer-Verlag). 228 p.

Lowrie, W., Channell, J. E. T., and Alvarez, W., 1980. A review of magnetic stratigraphic investigations in Cretaceous pelagic carbonate rocks. *J. Geophys. Res.*, 85:3597-3605.

Luterbacher, H. P., 1972. Foraminifera from the Lower Cretaceous and Upper Jurassic of the northwestern Atlantic. *In* Hollister, C. D., Ewing, J. I., et al., *Init. Repts. DSDP*, 11: Washington (U.S. Govt. Printing Office), 561-593.

Lutze, G. F., 1960. Zur stratigraphie und Palaontologie des Callovien und Oxfordien in Nordwest-Deutschland. *Geol. Jahrb.*, 77:391-532.

McCave, I. N., 1979. Depositional features of organic carbon-rich black and green mudstones at DSDP Sites 386 and 387, western North Atlantic. *In* Tucholke, B. E., Vogt, P. R., et al., *Init. Repts. DSDP*, 43: Washington (U.S. Govt. Printing Office), 411-416.

Markl, R. G., Bryan, G. M., and Ewing, J. I., 1970. Structure of the Blake-Bahama Outer Ridge. *J. Geophys. Res.*, 75:4539-4555.

Medd, A. W., 1979. The Upper Jurassic coccoliths from the Haddenham and Gramlingay boreholes (Cambridgeshire, England). *Eclogae. Geol. Helv.*, 72:19-109.

Millioud, M. E., 1969. Dinoflagellates and acritarchs from some western European Lower Cretaceous type localities. *In* Brönniman, P., and Renz, H. H., (Eds.), *Proc. First Int. Conf. Planktonic Microfossils Geneva 1967* (Vol. 2): Leiden (E. J. Brill), 420-434.

Millot, G., 1970. *Geology of Clays:* New York (Springer-Verlag).

Moullade, M., 1966. Etude stratigraphique et micropaléontologique du Crétacé inférieur de la "fosse vocontienne." *Doc. Lab. Geol. Fac. Sci. Lyon*, (15):369.

________, 1974. Zones de Foraminifères du Crétacé inférieur mesogeen. *C. R. Acad. Sci. Ser. D*, 278(14):1813-1816.

________, 1980. Les Foraminifères du Valanginien hypostratotypique: Coupes d'Angles (Alpes de Haute Provence) et de Barret-le Bas (Drome). *In* Busnardo, R., Thieuloy, J. P., Moullade, M. (Eds.), *Hypostratotype mesogeen du Valanginien:* C.N.R.S. Res.

________, in press. Biostratigraphie du Crétacé inférieur: repartition des Foraminifères pelagiques et benthiques non neritiques (domaine tethysien). *In* Busnardo, R., (Ed.), *Synthese Biostratigraphique du Crétacé Inférieur*, 26th I.G.C., Paris.

Mountain, G. S., and Tucholke, B. E., 1977. Horizon β: acoustic character and distribution in the western North Atlantic. *EOS Trans. Am. Geophys. Union*, 58:406. (Abstract)

Mouterde, R., Enay, R., Carioux, E., Contini, D., Elmi, S., et al., 1971. Les zones du Jurassique en France. *C. R. Somm. Seances Soc. Geol. Fr.*, 6:1-27.

Oertli, H. J., 1963. *Faunes d'ostracodes du Mesozoique de France:* Leiden (E. J. Brill).

Ogg, J. G., 1980. Upper Jurassic magnetostratigraphy from northern Italy. *EOS Trans. Am. Geophys. Union*, 61:216. (Abstract)

________, 1981. Sedimentology and paleomagnetism studies of Jurassic pelagic limestones (*"Ammonitico rosso"* facies) [Ph.D. dissert.]. Scripps Institution of Oceanography, University of California, San Diego.

Ogg, J. G., Channell, J. G. T., Winterer, E. L., and Baumgartner, P. O., 1981. Magnetostratigraphy of Oxfordian and Kimmeridgian cherts and siliceous limestones of northern Italy. *Int. Assoc. Geomagn. Aeron. 4th Scientific Assembly, Edinburgh, Scotland, Abstracts and Program*, pp. 209-210.

Ohm, U., 1967. Zur Kenntnis der Gattungen Reinholdella, Garantella, und Epistomina (Foramin.). *Palaeontographica A*, 127:103-188.

Parsons, B., and Sclater, J. G., 1977. An analysis of the variation of ocean floor bathymetric and heat flow with age. *J. Geophys. Res.*, 82(5):803-827.

Pastouret, L., Auffret, G. A., and Chamley, H., 1978. Microfacies of some sediments from the Western North Atlantic: paleoceanographic implications. *In* Benson, W. E., Sheridan, R. E., et al., *Init. Repts. DSDP*, 44: Washington (U.S. Govt. Printing Office), 477-502.

Paull, C. K., and Dillon, W. P., 1979. The appearance and distribution of the gas hydrate reflector off the southeastern United States. *U.S. Geol. Surv. Open-File Rep.*

Pazdro, O., 1969. Middle Jurassic Epistominidae (Foraminifera) of Poland. *Stud. Geol. Pol.*, 27:1-92.

Pazdrowa, O., 1969. Bathonian *Globigerina* of Poland. *Ann. Soc. Geol. Pol.*, 39(1-3):41-56.

Remane, J., 1978. Calpionellids. *In* Haq, B. U., and Boersma, A. (Eds.), *Introduction to Marine Micropaleontology:* New York (Elsevier), pp. 161-170.

Rood, A. P., and Barnard, T., 1972. On Jurassic coccoliths: *Stephanolithion, Diadozygus* and related genera. *Eclogae. Geol. Helv.*, 65:327-342.

Rood, A. P., Hay, W. W., and Barnard, T., 1971. Electron microscope of Oxford clay coccoliths. *Eclogae. Geol. Helv.*, 64:245-272.

Roth, P. H., 1978. Cretaceous nannoplankton biostratigraphy of the Northwestern Atlantic. *In* Benson, W. E., Sheridan, R. E., et al., *Init. Repts. DSDP*, 44: Washington (U.S. Govt. Printing Office), 731-752.

Roth, P. H., and Bowdler, J. L., 1979. Evolution of the calcareous nannofossil genus *Micula* in the Late Cretaceous. *Micropaleontology*, 25:272-280.

Roth, P. H., and Thierstein, H., 1972. Calcareous nannoplankton: Leg 14 of the Deep Sea Drilling Project. *In* Hayes, D. E., Pimm, A. C., et al., *Init. Repts. DSDP*, 14: Washington (U.S. Govt. Printing Office), 421-485.

Ruget, C., 1973. Inventaire des microfaunes du Bathonien moyen de l'Algarve (Portugal). *Rev. Fac. Cienc. Univ. Lisboa, Ser. 2a-c*, 17(2):515-542.

Sclater, J. G., Hellinger, S., and Tapscott, C., 1977. The paleobathymetry of the Atlantic Ocean from the Jurassic to the Present. *J. Geol.*, 85(5):509-552.

Sclater, J. G., Jaupart, C., and Galson, D., 1980. The heat flow through oceanic and continental crust and the heat loss of the earth. *Rev. Geophys. Space Phys.*, 18(1):269-311.

Sheridan, R. E., 1978. Structure, stratigraphy, and petroleum potential of the Blake Plateau. *Offshore Technol. Conf. Proc. Houston, Texas*, pp. 363-368.

Sheridan, R. E., Enos, P., Gradstein, F., and Benson, W. E., 1978. Mesozoic and Cenozoic sedimentary environments of the western North Atlantic. *In* Benson, W. E., Sheridan, R. E., et al., *Init. Repts. DSDP*, 44: Washington (U.S. Govt. Printing Office), 971-980.

Sheridan, R. E., Pastouret, L., and Mosditchian, G., 1978. Seismic stratigraphy and related lithofacies of the Blake-Bahama Basin. *In* Benson, W. E., Sheridan, R. E., et al., *Init. Repts. DSDP*, 44: Washington (U.S. Govt. Printing Office), 529-546.

Sheridan, R. E., Windisch, C. C., Ewing, J. I., and Stoffa, P. L., 1979. Structure and stratigraphy of the Blake Escarpment based on seismic reflection profiles. *Am. Assoc. Pet. Geol. Mem.*, 29: 177-186.

Shipley, T. H., Buffler, R. T., and Watkins, J. S., 1978. Seismic stratigraphy and geologic history of Blake Plateau and adjacent western Atlantic continental margin. *Am. Assoc. Pet. Geol. Bull.*, 62:792–812.

Shipley, T. H., and Watkins, J. S., 1978. Fine-scale seismic stratigraphy of the western North Atlantic Basin. *Geology*, 6:635–639.

Sigal, J., 1977. Essai de zonation du Crétacé méditerranéen a l'aide des foraminifèrs planctoniques. *Geol. Mediterr.*, 4(2):99–108.

Simon, W. J., and Bartenstein, H. (Eds.) 1962. *Leitfossilien der Mikropalaeontologie:* Berlin (Gebr. Borntraeger).

Stainforth, R. M., Lamb, J. L., Luterbacher, H., et al., 1975. Cenozoic planktonic foraminiferal zonation and characteristics of index forms. *Univ. Kans. Paleontol. Contrib.*, 62:1–162 and appendix.

Thiede, J., 1979. History of the North Atlantic Ocean: evolution of an asymmetric zonal paleoenvironment in a longitudinal ocean basin. *In* Talwani, M., Hay, W., and Ryan, W. B. F. (Eds.), *Deep Sea Drilling Results in the Atlantic Ocean: Continental Margins and Paleoenvironment.* Am. Geophys. Union, Maurice Ewing Series, 3:275–296.

Thierstein, H. R., 1976. Mesozoic calcareous nannoplankton biostratigraphy of marine sediments. *Mar. Micropaleontol.*, 1:325–362.

Tissot, B., Deroo, G., and Herbin, P., 1979. Organic matter in Cretaceous sediments of the North Atlantic: contribution to sedimentology and paleogeography. *In* Talwani, M., Hay, W., and Ryan, W. B. F. (Eds.), *Deep Sea Drilling Results in the Atlantic Ocean: Continental Margins and Paleoenvironment.* Am. Geophys. Union, Maurice Ewing Series, 3:362–374.

Tucholke, B. E., and Mountain, G. S., 1979. Seismic Stratigraphy, lithostratigraphy, and paleosedimentation patterns in the North American Basin. *In* Talwani, M., Hay, W., and Ryan, W. B. F. (Eds.), *Deep Sea Drilling Results in the Atlantic Ocean: Continental Margins and Paleoenvironment.* Am. Geophys. Union, Maurice Ewing Series, 3:58–86.

Tucholke, B. E., and Vogt, P. R., 1979. Western North Atlantic: sedimentary evolution and aspects of tectonic history. *In* Tucholke, B. E., Vogt, P. R., et al., *Init. Repts. DSDP*, 43: Washington (U.S. Govt. Printing Office), 791–823.

Vail, P. R., Mitchum, R. M., Jr., Shipley, T. H., and Buffler, R. T., 1980. Unconformities of the North Atlantic. *Philos. Trans. R. Soc. London Ser. A*, 294:137–155.

Vail, P. R., Mitchum, R. M., Jr., and Thompson, S., III, 1977. Global cycles of relative changes in sea level. *Am. Assoc. Pet. Geol. Mem.*, 26:83–97.

van Andel, T. H., 1975. Mesozoic/Cenozoic calcite compensation depth and the global distribution of calcareous sediments. *Earth Planet. Sci. Lett.*, 26:187–195.

van Hinte, J. E., 1976a. A Cretaceous time scale. *Bull. Am. Assoc. Pet. Geol.*, 60(4):498–516.

_______, 1976b. A Jurassic time scale. *Bull. Am. Assoc. Pet. Geol.*, 60(4):489–497.

Vogt, P. R., 1975. Changes in geomagnetic reversal frequency at times of tectonic change: evidence for coupling between core and upper mantle processes. *Earth Planet. Sci. Lett.*, 25:313–321.

_______, 1973. Early events in the opening of the North Atlantic. *In* Tarling, D. H., and Runcorn, S. K. (Eds.), *Implications of Continental Drift to the Earth Sciences* (Vol. 2): New York (Academic Press), 693–712.

Vogt, P. R., Anderson, C. N., and Bracey, D. R., 1971. Mesozoic magnetic anomalies, sea floor spreading, and geomagnetic reversals in the southwestern North Atlantic. *J. Geophys. Res.*, 76: 4796–4823.

Vogt, P. R., and Einwich, A. M., 1979. Magnetic anomalies and sea floor spreading in the western North Atlantic, and a revised calibration of the Keathley (M) geomagnetic reversal chronology. *In* Tucholke, B. E., Vogt, P., et al., *Init. Repts. DSDP*, 43: Washington (U.S. Govt. Printing Office), 971–974.

Warren, J. S., 1973. Form and variation of the dinoflagellate *Sirmiodinium grossi* Alberti, from the Upper Jurassic and Lower Cretaceous of California. *J. Paleontol.*, 47:101–114.

Wernli, R. J., and Septfontaine, M., 1971. Micropaleontologie comparee du Dogger du Jura meridional (France) et des Prealpes Medianes palstiques romandes (Suisse). *Eclogae Geol. Helv.*, 63(3): 437–458.

Westermann, G. E. G., 1977. Comments to Hallam's conclusion regarding the first marine connection between the Eastern Pacific and western Tethys. *Milwaukee Public Museum, Spec. Publ.*, (2): 35–77.

_______, in press. Ammonite biochronology and biogeography of the circum-Pacific Middle Jurassic. *Syst. Assoc. Spec. Vol.*

Wind, F. H., 1978. Western Atlantic Upper Jurassic calcareous nannofossil biostratigraphy. *In* Benson, W. E., Sheridan, R. E., et al., *Init. Repts. DSDP*, 44: Washington (U.S. Govt. Printing Office), 761–773.

Zemmels, I., Cook, H. E., and Hathaway, J. C., 1972. X-ray mineralogy studies—Leg 11. *In* Hollister, C. D., Ewing, J. I., et al., *Init. Repts. DSDP*, 11: Washington (U.S. Govt. Printing Office), 729–789.

Date of Initial Receipt: March 30, 1982

SITE 534 HOLE CORE 1 CORED INTERVAL 0.0–2.1 m

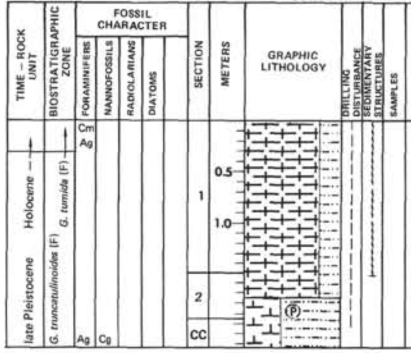

LITHOLOGIC DESCRIPTION

FORAMINIFER-NANNOFOSSIL OOZE

Section 1: foraminifer-nannofossil (silty) ooze, light olive gray (5Y 6/2) and light greenish gray (5GY 7/1) to bluish gray (5B 6/1), slight mottling.

Section 2:
0–25 cm: foraminifer-nannofossil (silty) ooze.
25–48 cm: nannofossil marl, greenish gray (5G 5/1), disseminated pyrite frequent.

SITE 534 HOLE CORE H1 CORED INTERVAL 2.1–87.5 m

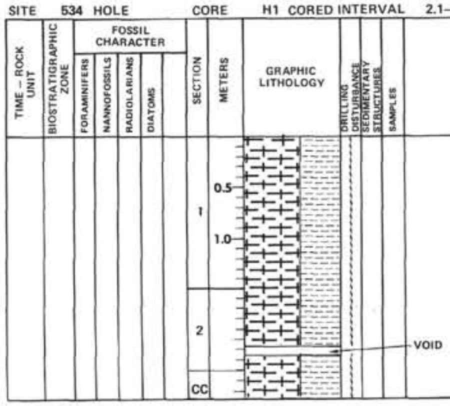

LITHOLOGIC DESCRIPTION

HIGHLY DEFORMED TO SOUPY SEDIMENTS

A wash core, highly deformed and contaminated by sand and rust flakes.

SITE 534 HOLE A CORE B1 CORED INTERVAL 1380.5–1395.5 m

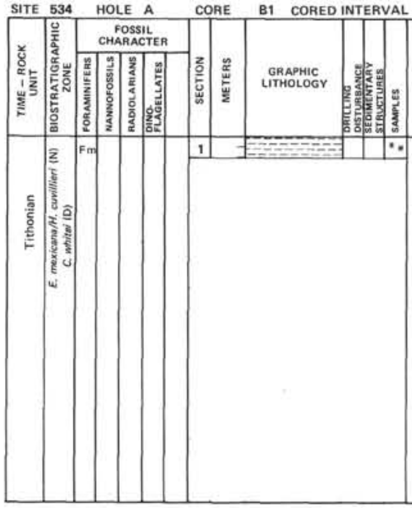

LITHOLOGIC DESCRIPTION

CALCAREOUS CLAYSTONE

CALCAREOUS CLAYSTONE; upper portion is dusky red (10R 3/3–10R 3/2); lower portion is greenish gray (5GY 5/1).

Smear Slide of darker red claystone has 15% needles of fine silt-size aragonite(?).

SMEAR SLIDE SUMMARY (%):

	1, 10 D	1, 10 D
Texture:		
Silt	15	12
Clay	85	88
Composition:		
Quartz	1	1
Mica	2	1
Clay	67	68
Zeolite	2	15
Carbonate unspec.	23	6
Calc. nannofossils	4	8
Plant debris	1	1

SITE 534 HOLE A CORE H1 CORED INTERVAL 0.0–531.0 m

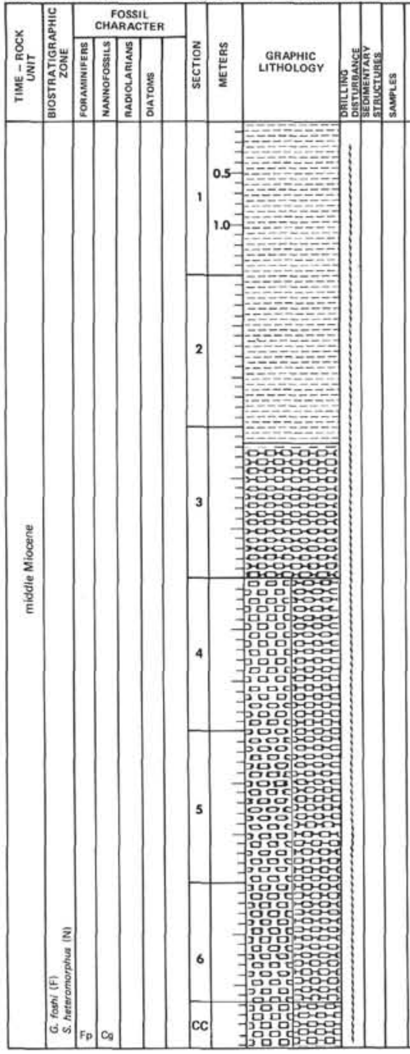

LITHOLOGIC DESCRIPTION

CHALK and OOZE

Sections 1 and 2: massive clay, gray to white (N5–5YR 8/1), calcareous.

Section 3:
15–150 cm: massive chalk, gray (5GY 6/1), with scattered burrow mottling.

Section 4: mixed calcareous ooze and chalk.

Whole core highly disturbed.

SITE 534 HOLE A CORE 2 CORED INTERVAL 545.8–555.4 m

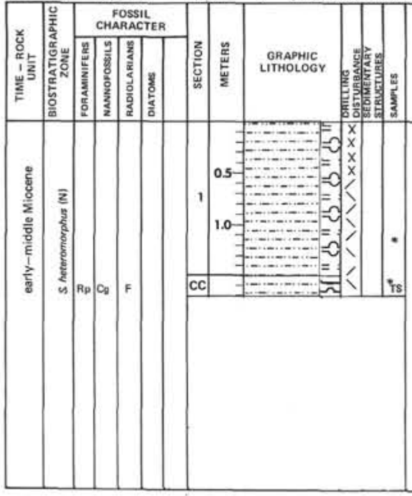

LITHOLOGIC DESCRIPTION

SILICEOUS MUDSTONE

Section 1: siliceous mudstone, grayish olive (10Y 4/2), highly fractured and disturbed. Mudstone is rich in pyrite.

Core-Catcher: becomes calcareous mudstone.

SMEAR SLIDE SUMMARY (%):

	1, 118 M	CC D	CC TS, M
Texture:			
Sand	6	–	–
Silt	44	20	100
Clay	50	80	–
Composition:			
Quartz	10	–	–
Clay	35	65	–
Pyrite	20	1	–
Carbonate unspec.	10	1	100
Foraminifers	–	1	–
Calc. nannofossils	4	20	–
Diatoms	16	4	–
Radiolarians	2	4	–
Sponge spicules	4	4	–

SITE 534 HOLE A CORE 3 CORED INTERVAL 555.4–565.0 m

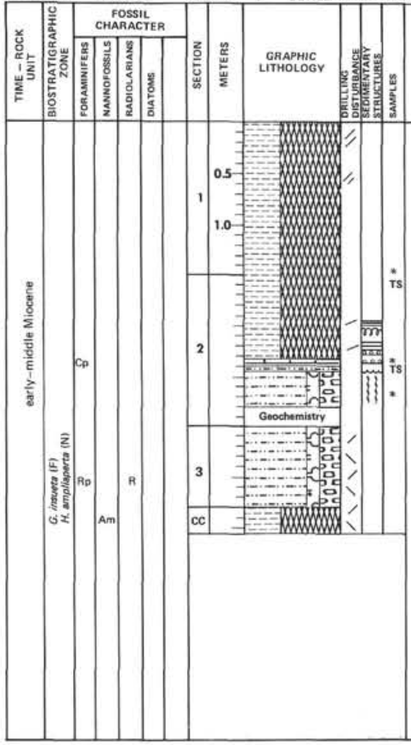

LITHOLOGIC DESCRIPTION

INTRACLASTIC CHALK and CHALK

Section 1: marly intraclastic chalk, grayish yellow green (5GY 7/2) with clay and chalk (5Y 8/4) intraclasts. Intraclasts elongated (1.5 cm x 0.3 mm) and oriented horizontally and more numerous below 90 cm.

Section 2:
50–90 cm: series of turbidites.

81–89 cm: foraminiferal chalk.

89–92 cm: mudstone, grayish olive (10Y 4/2); bioturbated.

93–130 cm: siliceous calcareous mudstone, grayish olive (10Y 4/2), moderately bioturbated.

Section 3:
80–103 cm: marly intraclastic chalk.

SMEAR SLIDE SUMMARY (%):

	1, 146 D	2, 98 M	2, 117 D
Texture:			
Sand	5	35	–
Silt	30	40	20
Clay	65	25	80
Composition:			
Quartz	–	–	2
Mica	–	1	–
Heavy minerals	–	5	–
Clay	42	11	53
Volcanic glass	1	–	–
Pyrite	1	–	3
Carbonate unspec.	20	15	10
Foraminifers	3	40	2
Calc. nannofossils	20	10	10
Diatoms	3	–	10
Radiolarians	3	1	3
Sponge spicules	5	15	3
Fish remains	1	–	1
Dolomite rhombs	1	–	–
Apatite	–	2	–
Siderite	–	–	3

SITE 534 HOLE A CORE 4 CORED INTERVAL 565.0–574.5 m

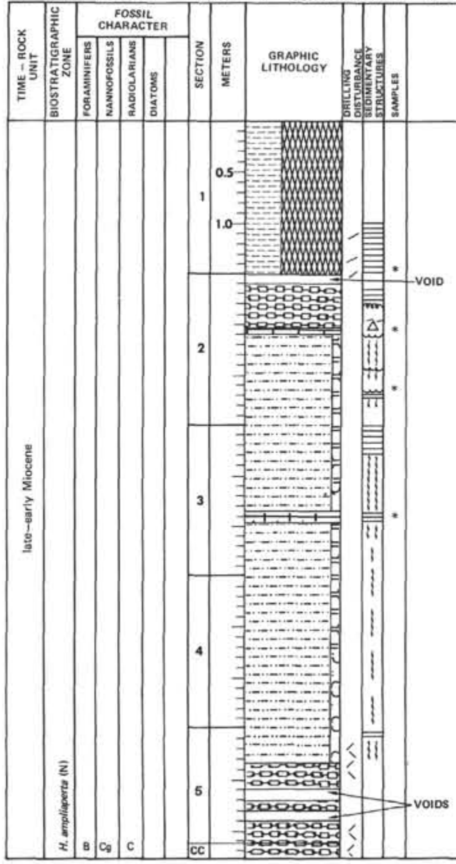

LITHOLOGIC DESCRIPTION

INTRACLASTIC CHALK

Section 1: marly intraclastic chalk, light bluish gray (5B 7/1) to pale greenish yellow (10Y 8/2) becoming very light gray (N8) down section. Intraclasts are gray–brown–green (5Y 3/2–5Y 4/4–10Y 4/2–10G 4/2) mudstone, elongated (up to 0.5 cm in length) and oriented horizontally; are absent from 100–150 cm.

Section 2:
10–58 cm: is calcareous chalk turbidite with basal coarse sand composed of *Arphistegina* foraminifers pinkish–yellowish gray (5YR 8/1–5Y 8/1).

58–150 cm: siliceous silty clay, light greenish gray (5G 6/1, 5G 8/1) to light olive gray (5Y 4/1, 5Y 6/1), may be *burrow mottled, laminated, or homogeneous; deposited by* bottom currents(;) (turbidites?).

Sections 3 and 4: similar to 58–150 cm of Section 2.

Section 5:
32–117 cm: homogeneous calcareous chalk, very light gray (N8) to yellowish gray (5Y 8/1).

SMEAR SLIDE SUMMARY (%):

	1, 146	2, 96	2, 113	3, 88
	D	M	D	D
Texture				
Sand	5	40	2	3
Silt	60	30	28	70
Clay	35	30	70	27
Composition:				
Quartz	–	–	5	6
Feldspar	–	–	–	1
Clay	34	5	81	1
Carbonate unspec.	50	50	–	37
Foraminifers	5	40	–	8
Calc. nannofossils	3	–,	–	30
Diatoms	1	3	7	7
Radiolarians	–	1	3	4
Sponge spicules	5	1	1	1
Fish remains	–	–	1	–
Apatite	1	–	–	–
Ostracod	1	–	–	–

SITE 534 HOLE A CORE 5 CORED INTERVAL 574.5–584.0 m

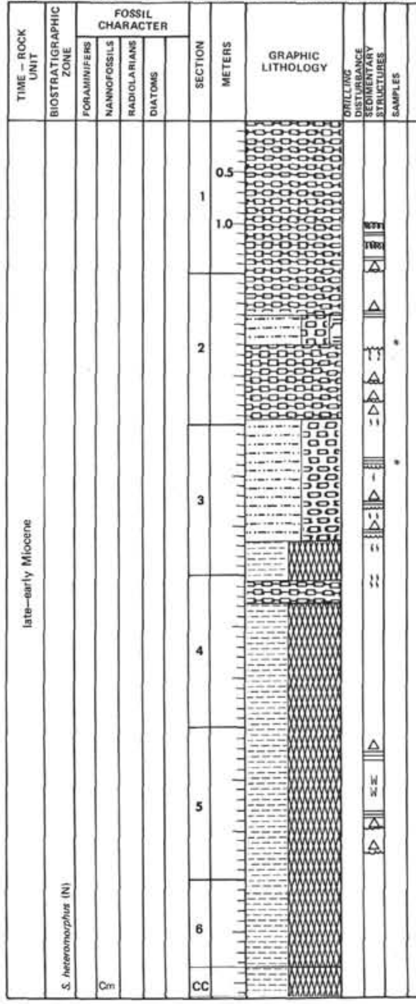

LITHOLOGIC DESCRIPTION

CALCAREOUS CHALK

Section 1: calcareous chalk, greenish gray (5G 6/1), homogeneous to 103 cm, then is laminated and convoluted. A fine-grained turbidite.

Section 2: a series of fining upward calcareous chalk turbidites, grays and greens (5Y 6/1, 5Y 8/1), interupted by a calcareous silty claystone bed.

Section 3: minor turbidites in calcareous silty clay, olive gray (5Y 4/1).

112–150 cm: massive marly chalk, yellowish gray (5Y 8/1) grading to pale olive (10Y 6/2) in Section 5 (probably tail of a turbidite).

Section 5: series of turbidites in intraclastic marly chalks.

SMEAR SLIDE SUMMARY (%):

	2, 69	3, 38
	D	M
Texture:		
Silt	35	40
Clay	65	60
Composition:		
Quartz	3	3
Clay	52	48
Glauconite	–	1
Pyrite	2	2
Carbonate unspec.	15	30
Foraminifers	3	3
Calc. nannofossils	10	5
Diatoms	3	3
Radiolarians	3	1
Sponge spicules	5	3
Fish remains	1	1
Plant debris	1	–
Dolomite rhombs	3	–

SITE 534 HOLE A CORE 6 CORED INTERVAL 584.0–593.5 m

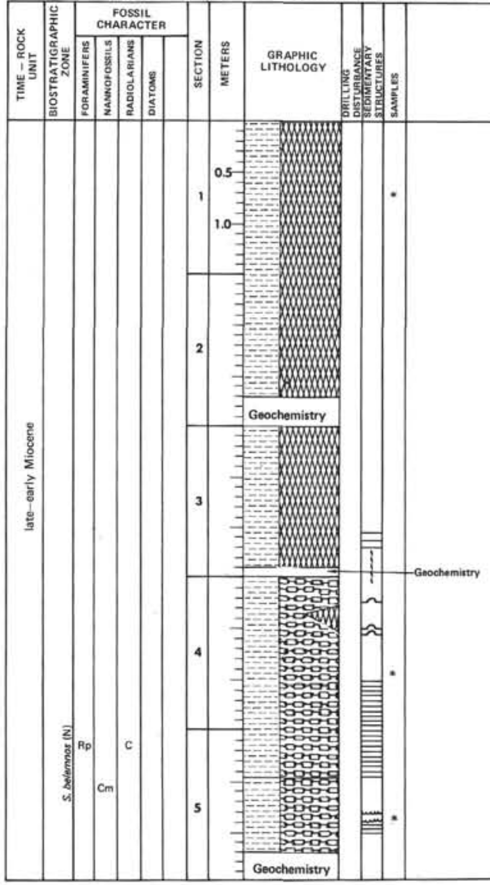

LITHOLOGIC DESCRIPTION

INTRACLASTIC CHALK

Sections 1, 2, and 3: marly intraclastic chalk, light olive gray (5Y 6/1), massive, intraclasts flattened and oriented horizontally, include siliceous silty clay (5B 5/1 and 5GY 2/1) and chalk (N8).

Section 4: wedge of intraclastic chalk is very coarse with clasts up to 1.8 cm in length; upper surface appears slumped. Section coarsens downward through first half and then the grain size is relatively constant with laminations formed by oriented siliceous mudstone clasts; coarse, laminated part deposited by bottom currents which wane up section.

Section 5:

85–95 cm: interbedded silts and carbonate.

95–120 cm: marly chalk.

SMEAR SLIDE SUMMARY (%):

	1, 70 D	4, 93 D	5, 88 M
Texture:			
Sand	–	3	5
Silt	55	57	65
Clay	45	40	30
Composition:			
Quartz	–	–	1
Clay	35	34	25
Glauconite	1	1	1
Carbonate unspec.	50	47	55
Foraminifers	1	5	5
Calc. nannofossils	10	6	8
Radiolarians	1	1	–
Sponge spicules	2	5	4
Dolomite rhombs	–	1	1

SITE 534 HOLE A CORE 7 CORED INTERVAL 593.5–603.0 m

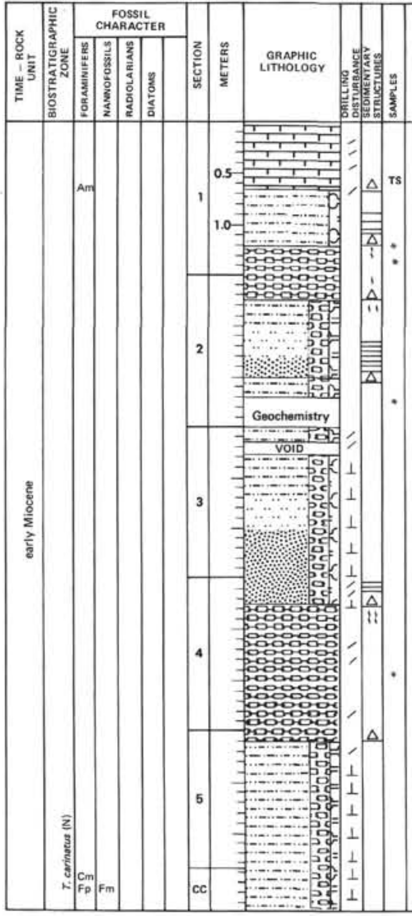

LITHOLOGIC DESCRIPTION

FORAMINIFERAL CHALK and CHALK

Section 1: foraminiferal chalk grading to foraminiferal sandstone at ~60 cm, yellowish gray (5Y 8/1) to light olive gray (5Y 6/1), probably the lower part of a turbidite. All laminae dip ~5°.

65–120 cm: siliceous mudstone grading to siltstone, olive gray (5Y 5/1) to medium bluish gray (5B 5/1), probably a turbidite.

120–150 cm: calcareous chalk, light to very light bluish-greenish gray (5BG 8/1, 5BG 9/1), bioturbated.

Section 2:

25–100 cm: siliceous, calcareous mudstone grading to sandstone, greenish to bluish gray (5G 5/1, 5B 6/1, 5Y 5/1), probably a turbidite cycle.

Section 3: siliceous, calcareous mudstone grading to sandstone, olive gray (5Y 5/1), turbidite deposition.

Section 4: calcareous chalk, very light yellowish olive gray (5Y 7/1), massive.

Section 5: siliceous calcareous mudstone, bluish gray (5B 6/1) to olive gray (5Y 5/1).

SMEAR SLIDE SUMMARY (%):

	1, 120 M	1, 135 D	2, 122 D	4, 93 D	1, 60 TS, M
Texture:					
Sand	10	–	–	–	60
Silt	15	50	30	30	22
Clay	75	50	70	70	18
Composition:					
Quartz	8	1	2	–	6
Clay	65	10	55	15	23
Pyrite	1	–	2	–	6
Carbonate unspec.	1	70	–	70	45
Foraminifers	–	–	–	–	19
Calc. nannofossils	10	10	25	10	–
Diatoms	–	1	5	–	–
Radiolarians	1	–	3	1	–
Sponge spicules	8	3	3	4	1
Silicoflagellates	1	–	–	–	–
Dolomite rhombs	5	5	–	–	–

SITE 534 HOLE A CORE 8 CORED INTERVAL 603.0–605.5 m

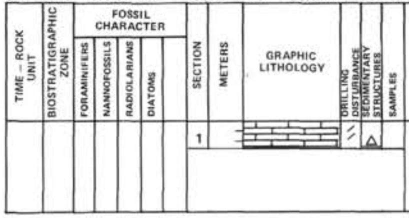

LITHOLOGIC DESCRIPTION

LIMESTONE

Limestone, light gray (N7), contains abundant sand-sized clasts of bluish-green gray (5BG 5/1) mudstone.

SITE 534 HOLE A CORE 9 CORED INTERVAL 605.5–612.5 m

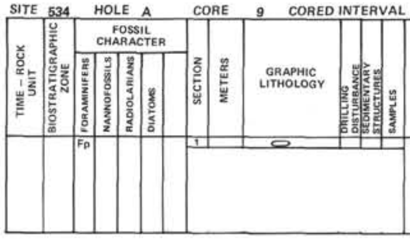

LITHOLOGIC DESCRIPTION

LIMESTONE

One piece, about 2 cm wide, of very light gray (N7) limestone with occassional darker clasts.

SITE 534 HOLE A CORE 10 CORED INTERVAL 612.5–622.0 m

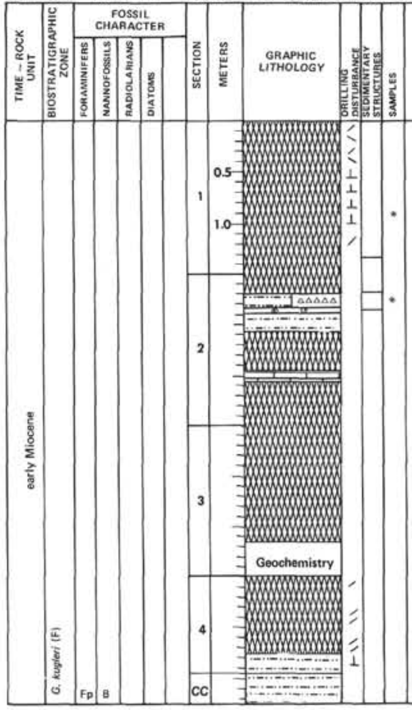

LITHOLOGIC DESCRIPTION

INTRACLASTIC CHALK and PORCELLANITE

Intraclastic chalk, very light olive gray (5Y 7/1) with 1–2 mm, horizontally oriented mudstone clasts. Clasts up to 1 cm below 135 cm; may be several debris flows.

Section 2:
20–30 cm: variegated medium bluish gray (5B 5/1) to dark olive gray (5Y 3/1) muddy porcellanite.
33–54 cm: olive gray (5Y 4/1) mudstone.

Section 4: bedding and contacts dip ~5–10°; Medium bluish gray (5B 5/1) and olive gray (5Y 5/1) mudstone clasts up to 5 mm long (rarely up to 2 cm). Olive gray mudstone at 75 cm.

SMEAR SLIDE SUMMARY (%):

	1, 90 D	2, 26 M
Texture:		
Sand	2	–
Silt	53	30
Clay	45	70
Composition:		
Quartz	1	3
Feldspar	–	1
Mica	–	1
Clay	20	43
Glauconite	–	1
Carbonate unspec.	68	1
Foraminifers	2	1
Calc. nannofossils	5	1
Diatoms	–	25
Radiolarians	1	15
Sponge spicules	3	5
Fish remains	–	1
Plant debris	–	1
Phosphatic grains	–	1

SITE 534 HOLE A CORE 11 CORED INTERVAL 622.0–631.5 m

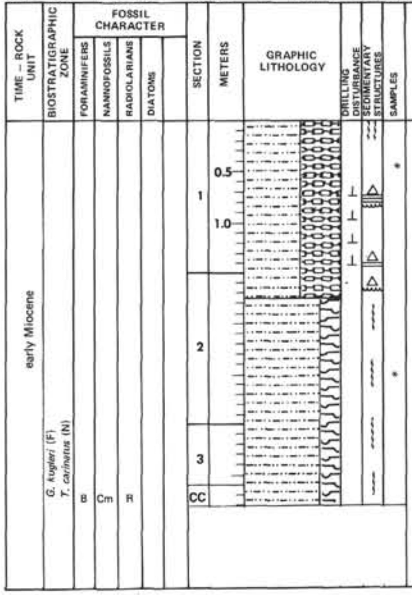

LITHOLOGIC DESCRIPTION

MUDSTONE

Section 1: calcareous mudstone (or silty claystone), medium bluish gray (5B 5/1) to olive gray (5Y 4/1), contains series of turbidites.

Section 2: diatomaceous silty claystone, olive gray (5Y 4/1), scattered burrows.

SMEAR SLIDE SUMMARY (%):

	1, 45 D	2, 97 D
Texture:		
Sand	2	3
Silt	35	20
Clay	63	77
Composition:		
Quartz	3	5
Mica	1	–
Clay	55	37
Glauconite	–	1
Pyrite	1	1
Carbonate unspec.	20	15
Foraminifers	3	1
Calc. nannofossils	10	10
Diatoms	–	20
Radiolarians	–	5
Sponge spicules	5	3
Fish remains	1	1
Plant debris	1	1

SITE 534 HOLE A CORE 12 CORED INTERVAL 631.5–641.0 m

TIME – ROCK UNIT | BIOSTRATIGRAPHIC ZONE | FOSSIL CHARACTER: FORAMINIFERS, NANNOFOSSILS, RADIOLARIANS, DIATOMS | SECTION | METERS | GRAPHIC LITHOLOGY | DRILLING DISTURBANCE | SEDIMENTARY STRUCTURES | SAMPLES | LITHOLOGIC DESCRIPTION

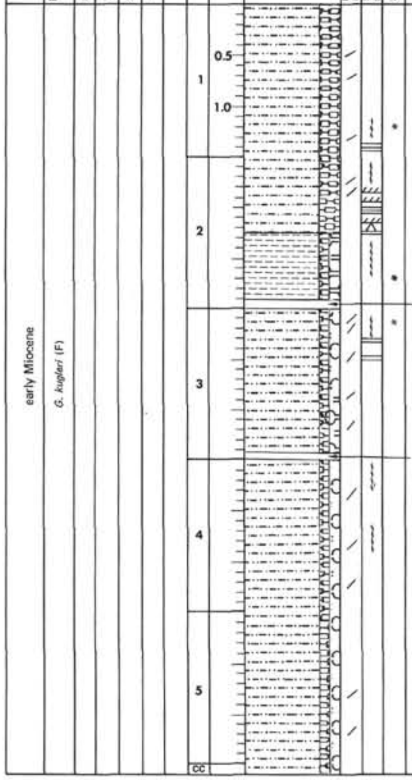

Geochemistry

5G 8/1

5GY 6/1 (mudstone clasts up to 0.8 cm in length)

Geochemistry

5GY 6/1

CLAYSTONE

Section 1: calcareous silty claystone, greenish gray (5GY 6/1), bioturbated, somewhat intraclastic; probably composed of several turbidite pulses.

Section 2: siliceous calcareous claystone, olive gray (5Y 4/1), somewhat bioturbated.

Sections 3 and 4: siliceous calcareous mudstone (as in Section 2) contains numerous small elongate mudstone chips.

SMEAR SLIDE SUMMARY (%):

	1, 120 D	2, 220 D	3, 12 D
Texture:			
Sand	3	–	–
Silt	25	20	15
Clay	72	80	85
Composition:			
Quartz	3	3	5
Mica	1	–	1
Heavy minerals	–	–	3
Clay	49	42	74
Glauconite	–	1	3
Pyrite	1	1	3
Carbonate unspec.	10	10	5
Foraminifers	5	1	–
Calc. nannofossils	15	15	1
Diatoms	5	15	–
Radiolarians	5	5	3
Sponge spicules	5	5	3
Fish remains	1	1	1
Plant debris	–	1	–

SITE 534 HOLE A CORE 13 CORED INTERVAL 641.0–650.5 m

TIME – ROCK UNIT | BIOSTRATIGRAPHIC ZONE | FOSSIL CHARACTER: FORAMINIFERS, NANNOFOSSILS, RADIOLARIANS, DIATOMS | SECTION | METERS | GRAPHIC LITHOLOGY | DRILLING DISTURBANCE | SEDIMENTARY STRUCTURES | SAMPLES | LITHOLOGIC DESCRIPTION

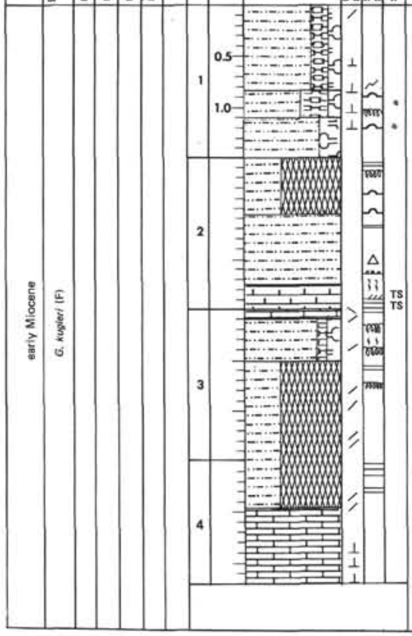

5GY 6/1

MUDSTONE and INTRACLASTIC CHALK

Section 1: siliceous calcareous mudstone, greenish gray (5GY 6/1), contains mudstone chips or clasts; becomes a debris flow ~70 cm, variable siliceous and calcareous contents.

Section 2: debris flow textures and structures continue with variable colors and lithologies – includes intraclastic chalks, redeposited shallow-water foraminiferal chalks, siltstones, and mudstones.

Section 3: debris flow continuous in upper portion. Lower part is marly intraclastic chalk, greenish gray (5G 8/1) with intraclasts becoming smaller and fewer down section.

Section 4: lower part is massive, light greenish gray (5GY 6/1) limestone, possibly turbiditic; intraclastic chalk probably a debris flow.

SMEAR SLIDE SUMMARY (%):

	1, 95 M	1, 113 M	2, 137 TS, M	2, 142 TS
Texture:				
Sand	7	–	50	50
Silt	33	30	30	30
Clay	60	70	20	20
Composition:				
Quartz	1	3	4	2
Clay	55	58	18	10
Glauconite	1	1	1	1
Pyrite	2	3	1	1
Carbonate unspec.	15	5	26	31
Foraminifers	5	–	35	40
Calc. nannofossils	4	–	–	–
Diatoms	4	15	–	6
Radiolarians	9	10	–	–
Sponge spicules	3	3	11	7
Fish remains	–	1	2	2
Plant debris	–	1	–	–
Dolomite rhombs	1	–	2	–

SITE 534 HOLE A CORE 14 CORED INTERVAL 650.5–660.0 m

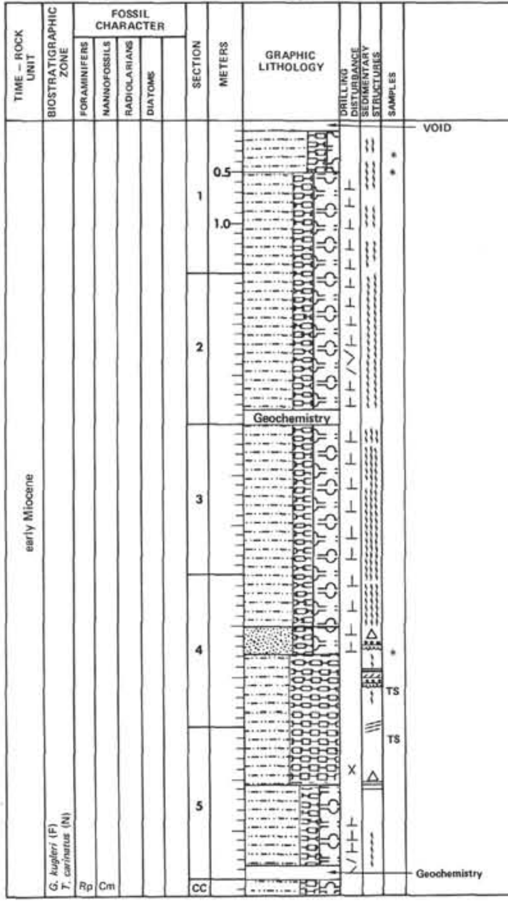

LITHOLOGIC DESCRIPTION

CLAYSTONE

Sections 1, 2, and 3: siliceous calcareous and calcareous siliceous silty claystone, grayish olive (10Y 4/2) to dark greenish gray (5GY 4/1), moderately bioturbated with occassional silty beds.

Section 4:
52–71 cm: sand grading into overlying silty, grayish olive (10Y 4/2) and light olive gray (5Y 5/2), probably terrigenous turbidite.

71–150 cm: marly calcareous chalk, yellowish gray (5Y 7/2 and 5Y 8/1), lightly bioturbated, probably two turbidites.

Section 5:
59–135 cm: calcareous siliceous silty claystone, olive gray (5Y 3/2) to greenish gray (5G 6/4) to medium bluish gray (5B 5/1), moderately bioturbated and fragmented.

SMEAR SLIDE SUMMARY (%):

	1, 35 M	1, 50 D	4, 75 D	4, 114 TS, M	5, 110 TS
Texture:					
Sand	5	–	10	20	10
Silt	40	25	45	30	40
Clay	55	75	45	50	50
Composition:					
Quartz	6	5	1	3	3
Mica	1	–	–	–	–
Heavy minerals	–	1	–	–	–
Clay	50	38	41	40	10
Glauconite	2	1	–	1	1
Pyrite	4	1	1	2	3
Carbonate unspec.	12	10	35	21	46
Foraminifers	4	–	3	18	30
Calc. nannofossils	5	10	10	5	–
Diatoms	4	15	1	4	3
Radiolarians	10	3	1	5	–
Sponge spicules	2	15	5	–	12
Fish remains	–	–	–	1	2
Plant debris	–	1	–	–	–
Dolomite rhombs	–	–	1	–	–

SITE 534 HOLE A CORE 15 CORED INTERVAL 660.0–669.5 m

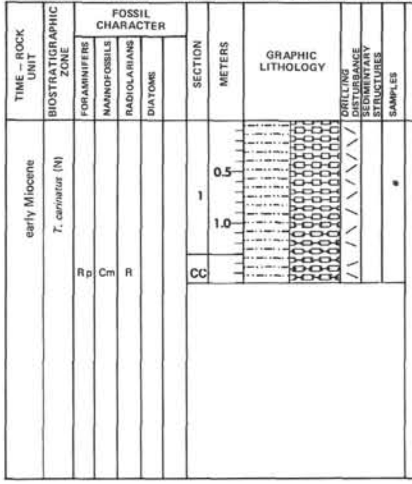

LITHOLOGIC DESCRIPTION

CHALK

Marly calcareous chalk, greenish gray (5GY 6/1), scattered burrow mottling and elongate, horizontally oriented dark clasts (up to 5 mm in length); may be upper end (fine tail) of debris flow seen in Core 17.

SMEAR SLIDE SUMMARY (%):

	1, 65 D
Texture:	
Silt	55
Clay	45
Composition:	
Quartz	1
Clay	40
Pyrite	1
Carbonate unspec.	43
Calc. nannofossils	6
Diatoms	2
Radiolarians	3
Sponge spicules	3
Dolomite rhombs	1

SITE 534 HOLE A CORE 16 CORED INTERVAL 669.5–678.5 m

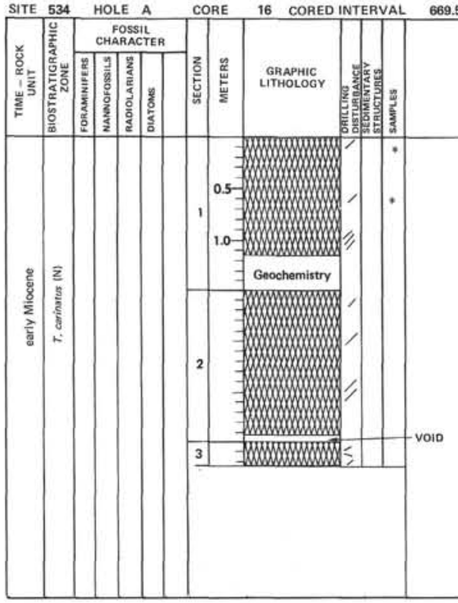

LITHOLOGIC DESCRIPTION

INTRACLASTIC CHALK

Intraclastic chalk, greenish gray (5GY 6/1). Clasts include light pinkish gray (5YR 9/1) and light bluish gray (5B 7/1) limestone and dark greenish gray (5GY 4/1), blue-green (5BG 5/1) and nearly black (5G 2/1) siliceous claystone. Clasts are elongate (1x5 mm) and oriented sub-horizontally, but some have up to 30°dip. In Section 2, the density of clasts increases toward base. Core may be fine tail (but getting coarser) of debris flow seen in Core 17.

SMEAR SLIDE SUMMARY (%):

	1, 11 M	1, 60 D
Texture:		
Silt	25	10
Clay	75	90
Composition:		
Quartz	2	–
Clay	10	30
Pyrite	1	2
Carbonate unspec.	55	50
Foraminifers	–	2
Calc. nannofossils	10	10
Diatoms	1	–
Radiolarians	–	1
Sponge spicules	3	6
Calcified radiolarians	10	–
Dolomite rhombs	8	–

SITE 534 HOLE A CORE 17 CORED INTERVAL 678.5–687.5 m

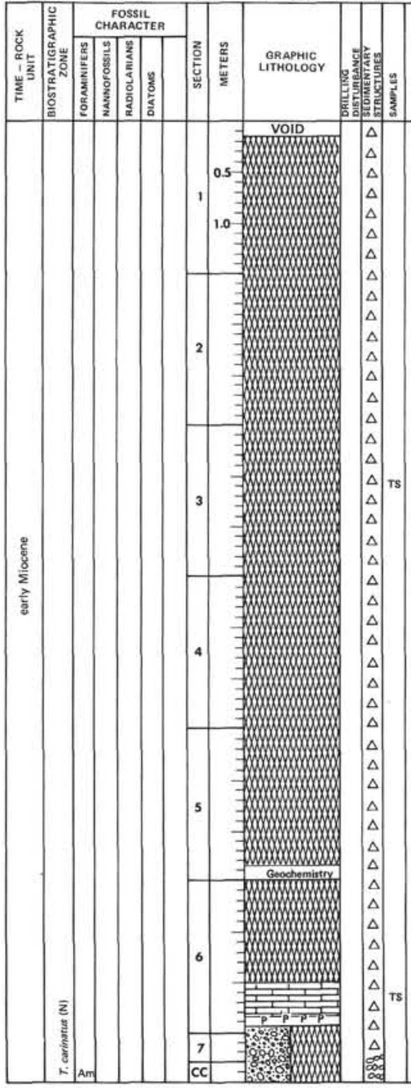

LITHOLOGIC DESCRIPTION

INTRACLASTIC CHALK

Intraclastic chalk, greenish gray (5GY 6/1). Clasts include mudstone (2–3 mm in length, up to 2 cm) dark greenish gray (5G 4/1 and 3/1) and medium bluish-greenish gray (5BG 5/1); limestone (3 mm in length) light pinkish gray (5YR 9/1) to yellowish gray (5Y 7/2), often deformed, and angular, undeformed carbonate (1–2 mm in length) shallow water origin, very light pinkish gray (5YR 8/1).

Density of clasts and overall grain size increase from top to bottom of core. At Section 5, matrix is a calcarenite and clasts may reach 2–3 cm in length. In Section 6 at 101–137 cm limestone clast, very light olive gray (5Y 6/1), contains mudstone clasts similar to those in chalk matrix. At 137–139 cm pyrite nodule. In Section 7 and Core-Catcher texture has become a rudite (calcareous conglomerate).

Whole core is a fining upward sequence, result of a massive debris flow.

NOTE: Section 7 is 35 cm in length.

SITE 534 HOLE A CORE 18 CORED INTERVAL 687.5–696.5 m

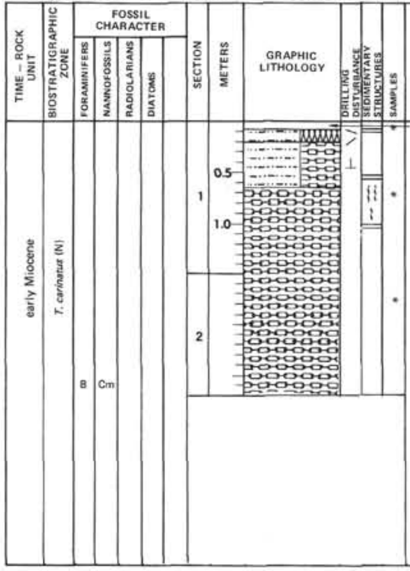

LITHOLOGIC DESCRIPTION

INTRACLASTIC CHALK

Intraclastic marly chalk, medium light gray (N6); grades to marly chalk, yellowish gray (5Y 8/1), light bluish gray (5B 7/1) and light greenish gray (5G 8/1); grades to chalk, pale olive (10Y 6/2) and yellowish gray (5Y 7/2). Marly chalk and chalk basically structureless.

SMEAR SLIDE SUMMARY (%):

	1, 4 M	1, 72 D	2, 30 D
Texture:			
Sand	15	–	–
Silt	50	40	30
Clay	35	60	70
Composition:			
Quartz	7	1	–
Mica	1	1	–
Heavy minerals	3	–	–
Clay	42	15	8
Pyrite	1	1	–
Zeolite	2	–	–
Carbonate unspec.	35	66	72
Foraminifers	1	2	2
Calc. nannofossils	5	10	13
Radiolarians	–	3	1
Sponge spicules	–	1	1
Fish remains	1	–	–
Plant debris	1	–	–
Dolomite rhombs	1	–	–

SITE 534 HOLE A CORE 19 CORED INTERVAL 696.5–705.5 m

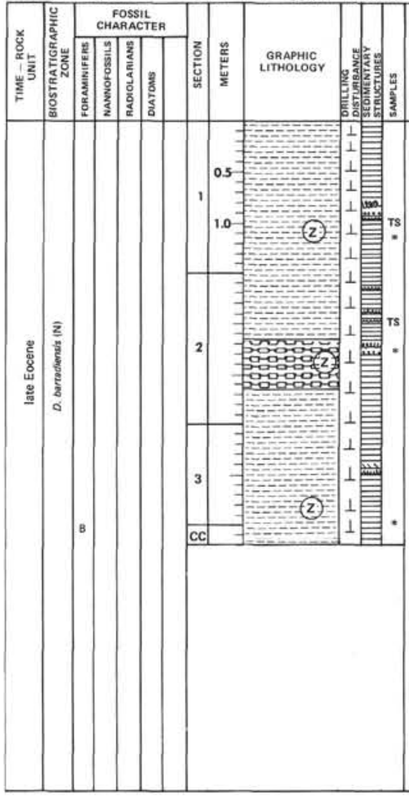

LITHOLOGIC DESCRIPTION

CLAYSTONE and CALCAREOUS CHALK

CLAYSTONE: grayish green (5G 5/2) to pale green (10G 6/2) to pink (10R 7/4) to pale yellowish green (10G 7/2) to grayish olive green (5GY 3/2) to yellowish gray (5GY 7/2).

CALCAREOUS CHALK: pale green (10G 6/2). Mostly parallel laminated, often speckled. Small white flecks, varicolored. In Section 1, 77–88 cm graded, probably turbidite, in Section 2, 40–48 cm graded, Bouma sequence, turbiditic, also 65–78 cm and in Section 3, 46–55 cm, graded, cross-laminated, probable turbidite.

Smear Slides: variable terrigenous biogenic silica content.

Thin Sections: Section 1, 97 cm is a zeolitic quartz-rich silt with a marly matrix. Section 2, 46 cm is a glauconitic quartz-rich pelmicrite or wackestone: biogenic component micrite and shell fragments.

SMEAR SLIDE SUMMARY (%):

	1, 112	2, 79	3, 99
	D	D	D
Texture:			
Sand	20	5	–
Silt	40	65	35
Clay	40	30	65
Composition:			
Quartz	15	7	5
Feldspar	5	–	–
Mica	2	1	–
Heavy minerals	1	1	1
Clay	15	33	50
Glauconite	7	1	–
Pyrite	TR	1	2
Zeolite	57	2	15
Carbonate unspec.	–	45	10
Foraminifers	–	1	–
Calc. nannofossils	–	5	5
Diatoms	–	–	15
Radiolarians	–	–	5
Sponge spicules	–	–	5
Fish remains	1	1	–
Other	–	–	1

SITE 534 HOLE A CORE 20 CORED INTERVAL 705.5–714.5 m

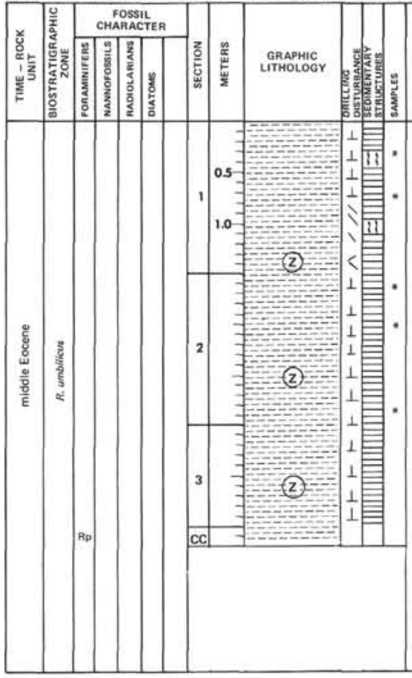

LITHOLOGIC DESCRIPTION

SILICEOUS and ZEOLITIC CLAYSTONE

Varicolored claystone, moderate olive brown (5Y 4/4), dusky yellowish green (5GY 5/2), olive (10Y 5/2), very pale orange (10YR 8/2), medium gray (N6), very pale orange (10YR 8/2) and intermediate colors. Mostly well *laminated, mottled, and burrowed in part, and reduction* spots.

Shipboard XRD:
Section 1, 135 cm: quartz, clinoptilolite, smectite, mixed layer clay (major); and calcite (minor).

Section 2, 114 cm: clinoptilolite, smectite, mixed layer clay (major); quartz, feldspar, and calcite (minor).

SMEAR SLIDE SUMMARY (%):

	1, 32	1, 73	2, 14	2, 50	2, 133
	M	D	M	D	D
Texture:					
Sand	60	70	20	30	75
Clay	40	30	80	70	25
Composition:					
Quartz	17	13	–	2	2
Feldspar	3	–	–	–	–
Mica	2	–	–	–	–
Heavy minerals	–	1	–	2	–
Clay	38	28	10	18	33
Glauconite	3	5	–	–	1
Pyrite	1	–	–	–	–
Zeolite	25	40	–	74	58
Carbonate unspec.	2	–	85	3	2
Calc. nannofossils	10	–	5	–	–
Radiolarians	–	–	–	–	2
Other	–	3	–	1	2

NOTE: Core 21, 714.5–723.5 m: no recovery.

SITE 534 HOLE A CORE 22 CORED INTERVAL 723.5–732.5 m

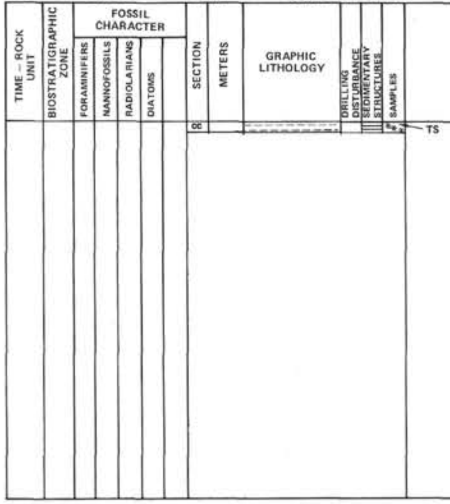

LITHOLOGIC DESCRIPTION

ZEOLITIC CLAYSTONE and SILTSTONE

A single piece of zeolitic claystone and siltstone: yellowish gray (5Y 6.5/2) and medium olive gray (5Y 4/2).

Smear Slides confirm quartz-rich terrigenous and zeolitic matrix. An impregnated Thin Section is a fine quartz silt, with zeolite, glauconite and abundant clay. Small volume of Fe-oxide(?) goethite.

SMEAR SLIDE SUMMARY (%):

	CC, 1	CC, 8	CC, 10
	D	M	D
Texture:			
Silt	60	10	65
Clay	40	90	55
Composition:			
Quartz	5	20	4
Heavy minerals	1	1	3
Clay	40	64	55
Glauconite	2	3	3
Zeolite	69	15	34
Carbonate unspec.	1	–	–
Other	1	–	3

SITE 534 HOLE A CORE 23 CORED INTERVAL 732.5–741.5 m

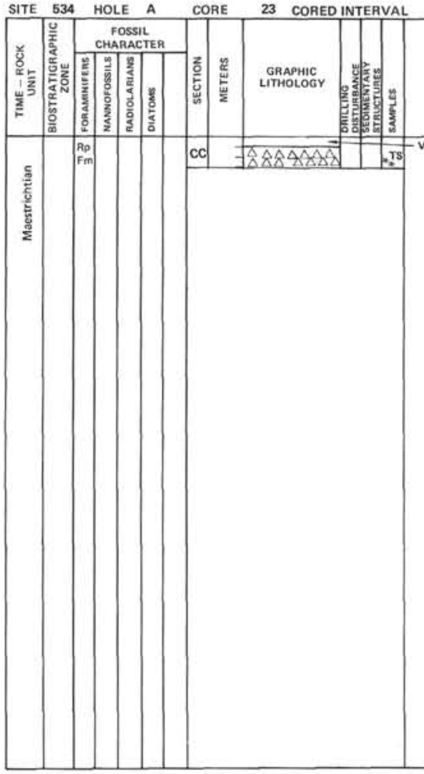

LITHOLOGIC DESCRIPTION

CLAYSTONE and PORCELLANITE

One piece of porcellanite 5 cm in diameter, dark yellowish brown (10YR 4/4) with a vitreous conchoidal fracture, patches of incomplete silicification.

Rest of Core-Catcher is claystone, grayish olive (10Y 4/4) with white (N9), reddish brown (2.5YR 4/4), and dark reddish brown (2.5YR 3/4) laminae. Claystone is burrowed throughout.

Thin Section of Core-Catcher is a chertified marly foraminifer chalk. Bioclasts of sponge spicules, and micritic lumps; terrigenous clay; cement is chert and calcite. Minor dolomite crystals, organic matter, and pyrite present. Most of the section is silicified. Unaffected patches contain well preserved planktonic foraminifers. Texture suggests redeposition either by traction or turbidity currents.

SMEAR SLIDE SUMMARY (%):

	CC, 23	CC, 24	CC
	D	M	TS, D
Texture:			
Sand	5	10	–
Silt	65	50	60
Clay	50	40	40
Composition:			
Quartz	28	15	–
Feldspar	3	1	–
Mica	3	7	–
Heavy minerals	1	1	–
Clay	40	40	20
Glauconite	5	4	1
Pyrite	–	–	3
Zeolite	17	28	–
Carbonate unspec.	3	1	2
Foraminifers	–	–	37
Radiolarians	–	–	7
Sponge spicules	–	–	2
Fish remains	–	–	2
Plant debris	–	–	1
Other	–	–	25

SITE 534 HOLE A CORE 24 CORED INTERVAL 741.5–750.5 m

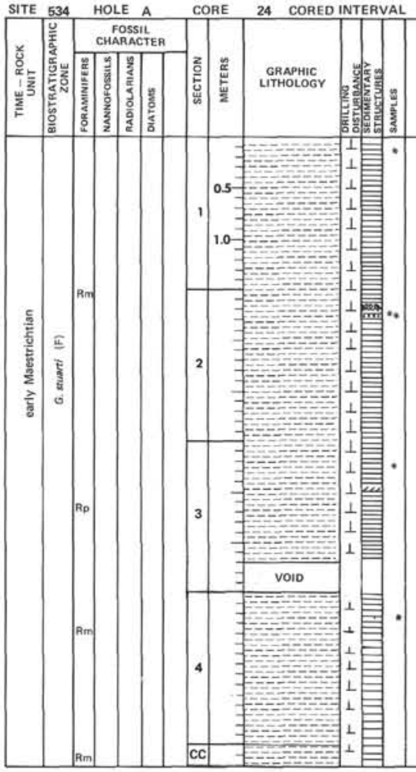

LITHOLOGIC DESCRIPTION

CLAYSTONE

Varicolored claystone with two-thirds of moderate reddish brown (10R 5/4); one-third greenish gray (5GY 6/1). Mostly well laminated, or banded on side of 0.5–2.0 cm; local microcross-lamination and burrows, and convolute lamination.

Smear Slide: note presence of well preserved radiolaria and zeolite (? clinoptilolite). Also note Section 4, 26 cm contains abundant phosphate particles and rare crystals of hyperthene. Note also that Core-Catcher contains abundant zeolite, devitrified volcanic glass, also small amounts of iron-oxide, apatite, sphere, chlorite, and siderite.

SMEAR SLIDE SUMMARY (%):

	1, 15	2, 23	2, 28	4, 26	CC
	D	D	D	M	D
Texture:					
Silt	10	15	15	15	50
Clay	90	85	85	85	50
Composition:					
Quartz	5	3	9	7	5
Feldspar	–	1	1	–	–
Mica	3	–	2	1	–
Heavy minerals	1	–	–	1	2
Clay	67	76	76	78	48
Volcanic glass	–	–	–	5	17
Glauconite	1	–	–	–	–
Pyrite	–	–	–	–	2
Zeolite	20	18	20	10	22
Fish remains	1	1	1	–	–
Plant debris	1	–	1	1	–
Other	1	1	–	48	–

SITE 534 HOLE A CORE 25 CORED INTERVAL 750.5–759.5 m

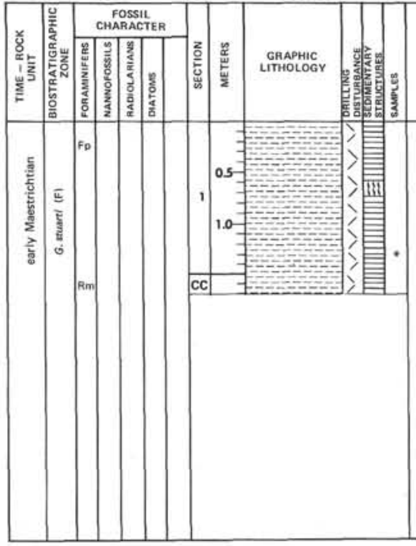

LITHOLOGIC DESCRIPTION

CLAYSTONE

The upper part of the core is two-thirds moderate reddish brown (10R 6/6) and one-third pale olive (10Y 6/2) by volume. Section 1 becomes progressively darker downwards to olive gray (5Y 3/2), showing parallel laminations. In Section 1, 80 and 90 cm rare small burrows are present, mostly moderate yellow (5Y 7/6). Much of the core strongly compressed by drilling. The Core-Catcher is particularly highly deformed, mostly olive gray.

SMEAR SLIDE SUMMARY (%):

	1, 134
	D
Texture:	
Silt	15
Clay	85
Composition:	
Quartz	5
Heavy minerals	1
Clay	64
Volcanic glass	5
Glauconite	1
Micronodules	1
Zeolite	20
Plant debris	2
Other	2

SITE 534 HOLE A CORE 26 CORED INTERVAL 759.5–764.5 m

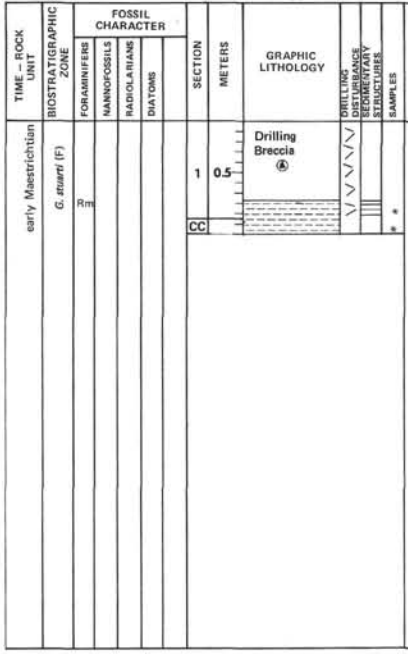

LITHOLOGIC DESCRIPTION

CLAYSTONE

Section 1, 0–87 cm is a drilling breccia composed of claystone fragments, the pieces get larger downwards. A chip of white porcellanite is present at 43 cm.

CLAYSTONE: grayish olive (10Y 4/2) to olive gray (5Y 3/2) is present from 85–96 cm in Section 1. A few thin bands less than 1 cm thick are composed of light olive brown (5Y 5/6) and grayish red (5R 4/2) claystone. A few burrows are present.

The Core-Catcher is composed of grayish red claystone (10R 4/2), mottled to light olive gray (5Y 6/1) to blackish red (5R 2/2). Again moderately burrowed with traces of parallel lamination.

SMEAR SLIDE SUMMARY (%):

	1, 90 D	CC, 12 D
Texture:		
Silt	15	10
Clay	85	90
Composition:		
Quartz	9	4
Feldspar	2	–
Mica	1	1
Heavy minerals	1	–
Clay	53	61
Volcanic glass	–	11
Glauconite	13	1
Pyrite	6	4
Zeolite	14	27
Fish remains	–	1

SITE 534 HOLE A CORE 27 CORED INTERVAL 764.5–774.0 m

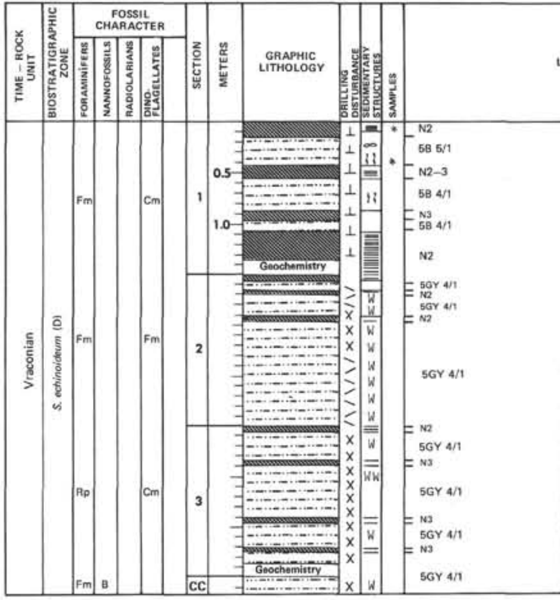

LITHOLOGIC DESCRIPTION

SILTY CLAYSTONE and CARBONACEOUS CLAYSTONE

Silty claystone is bluish gray (5B 5/1), dark bluish gray (5B 4/1) changing downward to dark greenish gray (5GY 4/1). Wavy bedding associated with or without current ripples and flaser bedding are observed throughout. Section 3 is horrifyingly disturbed by drilling. Silty clay layers are also characterized by burrows observed at Section 1, 18, 46, and 89 cm.

Carbonaceous claystone is grayish black (N2) to dark gray (N3) finely laminated. No burrows and only a few pyrite nodules are noted.

SMEAR SLIDE SUMMARY (%):

	1, 8 D	1, 40 D
Texture:		
Silt	20	30
Clay	80	70
Composition:		
Quartz/Feldspar	10	20
Mica	4	5
Heavy minerals	–	1
Clay	77	70
Glauconite	–	1
Pyrite	3	1
Zeolite	1	1
Fish remains	1	–
Plant debris	4	1

SITE 534 HOLE A CORE 28 CORED INTERVAL 774.0–783.5 m

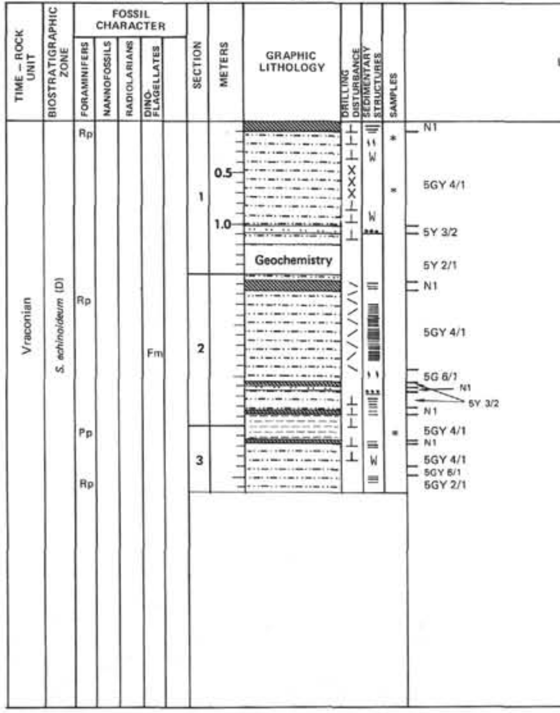

LITHOLOGIC DESCRIPTION

SILTY CLAYSTONE, CLAYSTONE, and CARBONACEOUS CLAYSTONE

Silty claystone and claystone are dark greenish gray (5GY 4/1) to olive black (5Y 2/1) and contain fair amount of plant debris. Wavy laminae at 17, 19, 28, and 92 cm in Section 1, and 45 cm in Section 2.

White colored laminae consisted of dominantly quartz and feldspar at 65 and 125 cm in Section 2 and at 32 cm in Section 3.

Carbonaceous claystone is black (N1) with finely divided fissiles.

SILTSTONE

Quartz and feldspar are dominant. Grading is not discernible but laminae are present.

SMEAR SLIDE SUMMARY (%):

	1, 17 D	1, 66 D	3, 9 D
Texture:			
Silt	25	30	15
Clay	75	70	85
Composition:			
Quartz/Feldspar	15	20	10
Mica	3	2	3
Heavy minerals	1	3	1
Clay	71	63	77
Volcanic glass	–	–	2
Glauconite	1	1	–
Pyrite	–	1	1
Zeolite	2	5	1
Carbonate unspec.	3	2	–
Calc. nannofossils	–	1	–
Fish remains	1	1	1
Plant debris	3	1	4

SITE 534 HOLE A CORE 29 CORED INTERVAL 783.5–793.0 m

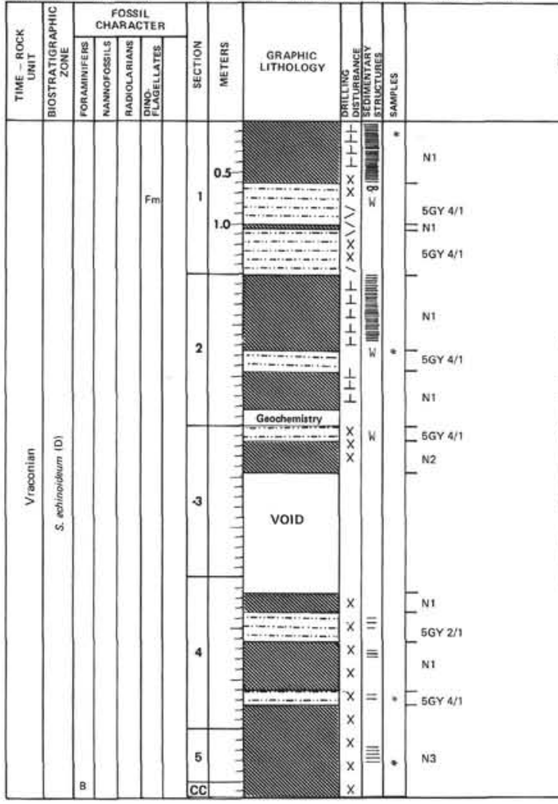

LITHOLOGIC DESCRIPTION

CARBONACEOUS CLAYSTONE and SILTY CLAYSTONE

CARBONACEOUS CLAYSTONE is black (N1), grayish black (N2) to dark gray (N3). Gray stringer at 30 cm in Section 5 contains quartz of sorted silt size. Wavy stringers at 19 and 24 cm in Section 3.

SILTY CLAYSTONE is dark greenish gray (5GY 4/1) to greenish black (5GY 2/1). Wavy laminae are in Section 1 at 62 and 71 cm, in Section 2 at 80 cm and in Section 4 at 40 and 115 cm.

SMEAR SLIDE SUMMARY (%):

	1, 12 D	2, 78 D	4, 120 D	5, 30 D
Texture:				
Sand	–	–	7	–
Silt	20	30	20	80
Clay	80	70	73	20
Composition:				
Quartz/Feldspar	7	13	15	67
Mica	5	5	5	2
Heavy minerals	1	1	3	1
Clay	72	70	73	20
Volcanic glass	5	–	–	–
Glauconite	–	1	–	1
Pyrite	1	2	–	3
Carbonate unspec.	–	–	–	1
Fish remains	1	1	1	–
Plant debris	8	3	3	2

SITE 534 HOLE A CORE 30 CORED INTERVAL 793.0–802.5 m

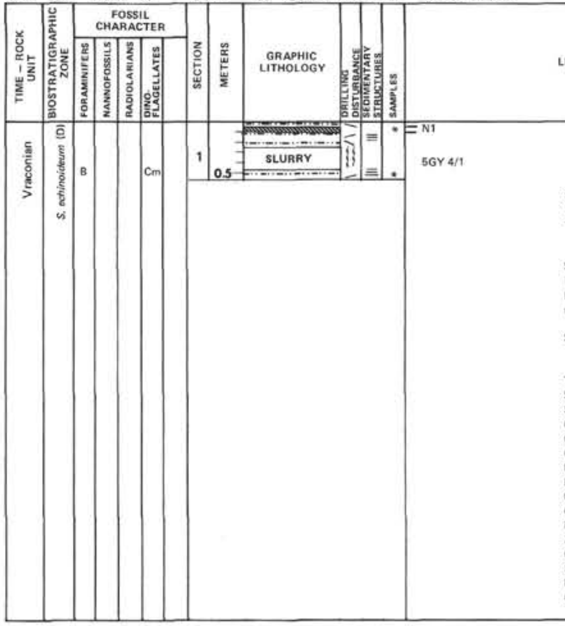

LITHOLOGIC DESCRIPTION

SILTY CLAYSTONE and CARBONACEOUS CLAYSTONE

SILTY CLAYSTONE is dark greenish gray (5GY 4/1). Lenticular laminae and wavy laminae dominante in this facies.

Smear slide observation shows concentration of quartz indicating some bottom currents. Other minerals are amphibole of metamorphic origin, brown and green mica, and microcline. A pyritized diatom is observed.

SMEAR SLIDE SUMMARY (%):

	1, 6 D	1, 52 D
Texture:		
Sand	–	5
Silt	20	30
Clay	80	65
Composition:		
Quartz/Feldspar	5	20
Mica	1	3
Heavy minerals	1	3
Clay	80	62
Glauconite	–	3
Pyrite	1	3
Zeolite	–	2
Carbonate unspec.	1	1
Fish remains	1	–
Plant debris	4	2
Other	3	3

SITE 534 HOLE A CORE 31 CORED INTERVAL 802.5–812.0 m

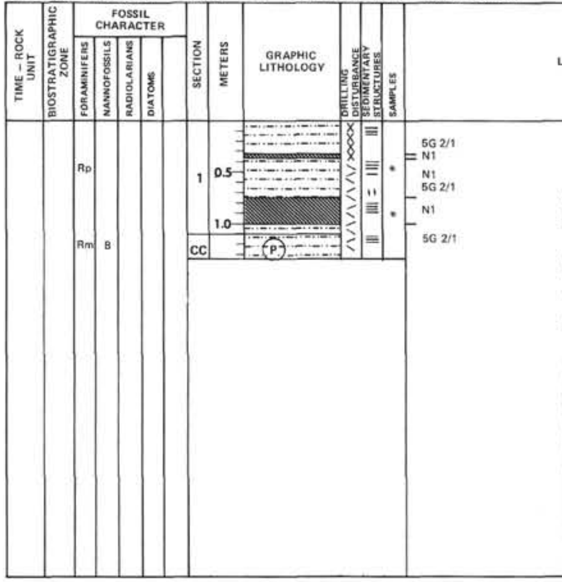

LITHOLOGIC DESCRIPTION

SILTY CLAYSTONE and CARBONACEOUS CLAYSTONE

SILTY CLAYSTONE is black (N1) to greenish black (5G 2/1) with laminae and stringer of greenish gray (5GY 6/1), some of which may be due to bioturbation.

CARBONACEOUS CLAYSTONE is black (N1), fissile, and tends to break on very thin laminae of greenish gray.

Pyrite nodule is present at 10 cm in Core-Catcher.

SMEAR SLIDE SUMMARY (%):

	1, 64 D	1, 92 D
Texture:		
Silt	30	10
Clay	70	90
Composition:		
Quartz/Feldspar	25	5
Mica	2	2
Heavy minerals	1	–
Clay	64	78
Glauconite	1	TR
Pyrite	2	2
Zeolite	–	1
Carbonate unspec.	1	–
Calc. nannofossils	1	–
Fish remains	–	2
Plant debris	3	10

SITE 534 HOLE A CORE 32 CORED INTERVAL 812.0–821.5 m

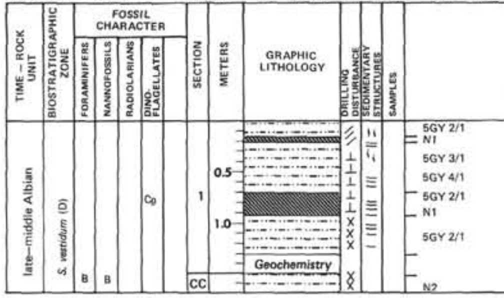

LITHOLOGIC DESCRIPTION

SILTY CLAYSTONE and CARBONACEOUS CLAYSTONE

SILTY CLAYSTONE is greenish black (5GY 2/1), dark greenish gray (5GY 3/1), and greenish gray (5GY 4/1). Silty stringer, wavy laminae and burrows are present.

CARBONACEOUS CLAYSTONE is greenish black (5GY 2/1) to black (N1) with occasional very thin laminae of greenish gray (5GY 6/1).

SITE 534 HOLE A CORE 33 CORED INTERVAL 821.5–831.0 m

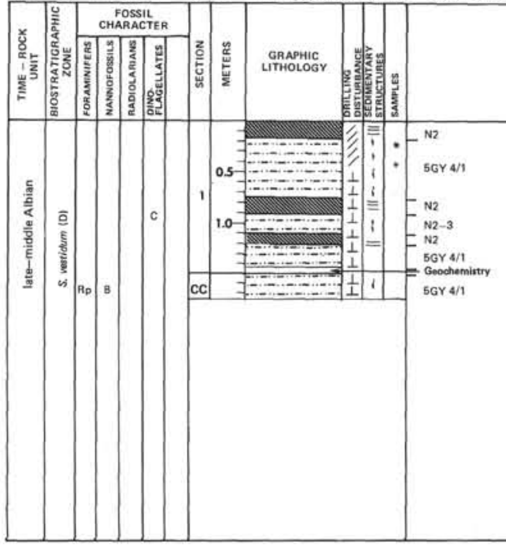

LITHOLOGIC DESCRIPTION

SILTY CLAYSTONE and CARBONACEOUS CLAYSTONE

SILTY CLAYSTONE is grayish black (N2), dark gray (N3) to dark greenish gray (5GY 4/1). Moderately to highly burrowed especially at 33 and 70 cm.

CARBONACEOUS CLAYSTONE is grayish black (N2) with tiny stringers and fine laminae.

SMEAR SLIDE SUMMARY (%):

	1, 21	1, 42
	D	D
Texture:		
Silt	15	25
Clay	85	75
Composition:		
Quartz/Feldspar	7	10
Mica	3	10
Heavy minerals	1	1
Clay	83	74
Glauconite	–	1
Pyrite	1	2
Carbonate unspec.	2	1
Plant debris	2	1
Other	1	–

SITE 534 HOLE A CORE 34 CORED INTERVAL 831.0–840.5 m

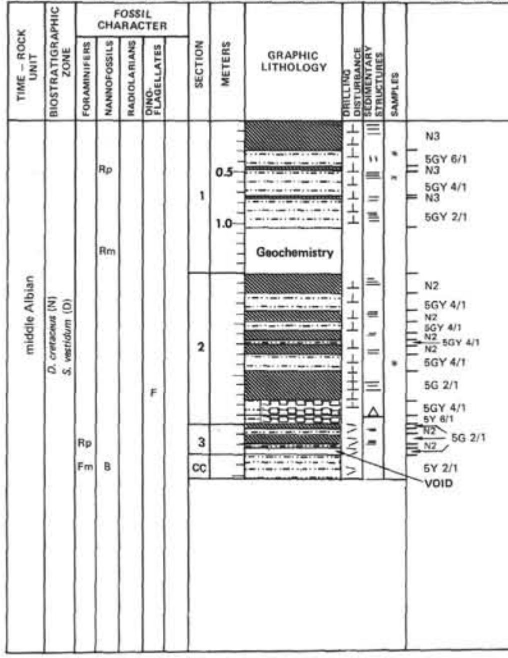

LITHOLOGIC DESCRIPTION

CARBONACEOUS CLAYSTONE and SILTY CLAYSTONE

CARBONACEOUS CLAYSTONE is grayish black (N2). Dark gray (N3) and greenish black (5GY 2/1). No burrows are observed. Silty laminae are present in places. Pyrite concentration at 12 cm in Section 2.

SILTY CLAYSTONE is greenish gray (5GY 6/1), dark greenish gray (5GY 4/1) and greenish black (5GY 2/1). Tiny burrows are observed at 37 cm in Section 1. Wavy and flaser laminae developes frequently especially at 70 cm in Section 1 and at 25 cm in Section, which are determined to be calcilutite.

Marly chalk occurs in two layers at 132 and 140 cm in Section 2, and are of turbidite origin.

SMEAR SLIDE SUMMARY (%):

	1, 34	1, 50	2, 89
	D	D	D
Texture:			
Silt	25	45	65
Clay	75	55	35
Composition:			
Quartz	4	15	60
Feldspar	–	2	4
Mica	17	9	4
Heavy minerals	–	1	1
Clay	69	64	24
Glauconite	–	–	1
Pyrite	2	6	2
Carbonate unspec.	3	–	–
Plant debris	3	3	2
Other	–	–	2

SITE 534 HOLE A CORE 35 CORED INTERVAL 840.5–850.0 m

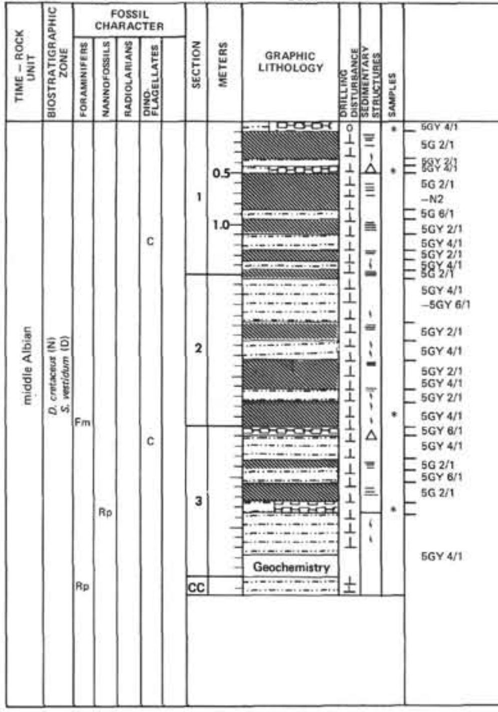

LITHOLOGIC DESCRIPTION

CARBONACEOUS CLAYSTONE and
SILTY CLAYSTONE

CARBONACEOUS CLAYSTONE is greenish black (5G 2/1, 5GY 2/1) and grayish black (N2). Very fine laminae and stringers are frequent throughout.

SILTY CLAYSTONE is greenish black (5GY 2/1), dark greenish gray (5GY 4/1) and greenish gray (5GY 6/1, 5G 6/1), moderately burrowed.

Indurated chalks or marly chalks are found 0–8 and 46–50 cm in Section 1 and 4–9 and 81–83 cm in Section 3 and are deposited by calciturbidite.

SMEAR SLIDE SUMMARY (%):

	1, 8	1, 49	2, 136	3, 81
	D	D	D	D
Texture:				
Silt	30	20	15	20
Clay	70	80	85	80
Composition:				
Quartz	–	5	5	–
Mica	–	3	10	1
Heavy minerals	–	2	2	–
Clay	48	36	75	45
Glauconite	–	–	1	–
Pyrite	–	1	1	–
Zeolite	–	–	3	–
Carbonate unspec.	50	40	4	45
Calc. nannofossils	1	10	–	5
Plant debris	1	3	2	4

SITE 534 HOLE A CORE 36 CORED INTERVAL 850.0–859.5 m

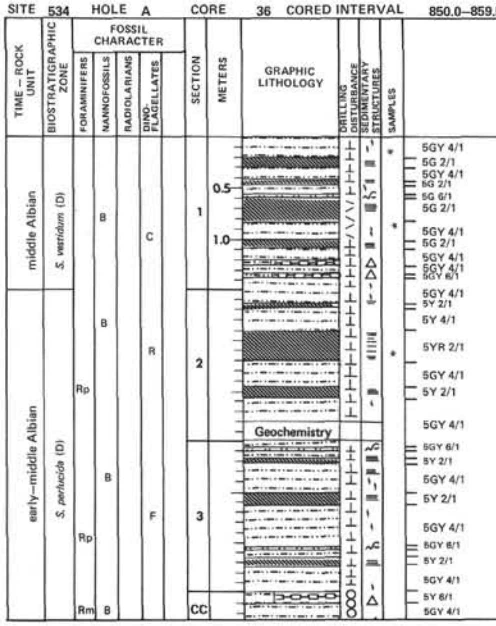

LITHOLOGIC DESCRIPTION

CARBONACEOUS CLAYSTONE and
SILTY CLAYSTONE

CARBONACEOUS CLAYSTONE is brownish black (5YR 2/1), olive black (5Y 2/1) and greenish black (5G 2/1). Very fine laminated with stringers in places.

SILTY CLAYSTONE is dark greenish gray (5GY 4/1) with numerous burrows and a few stringers.

Marly chalk and limestone is greenish gray (5G 6/1, 5GY 6/1) and light olive gray (5Y 6/1). Some show normal grading.

SMEAR SLIDE SUMMARY (%):

	1, 14	1, 138	2, 64
	D	D	D
Texture:			
Silt	30	90	17
Clay	70	10	83
Composition:			
Quartz	13	4	}3
Feldspar	4	1	
Mica	8	2	2
Heavy minerals	1	–	–
Clay	68	17	82
Pyrite	–	–	1
Carbonate unspec.	2	75	2
Plant debris	3	1	10

SITE 534 HOLE A CORE 37 CORED INTERVAL 859.5–869.0 m

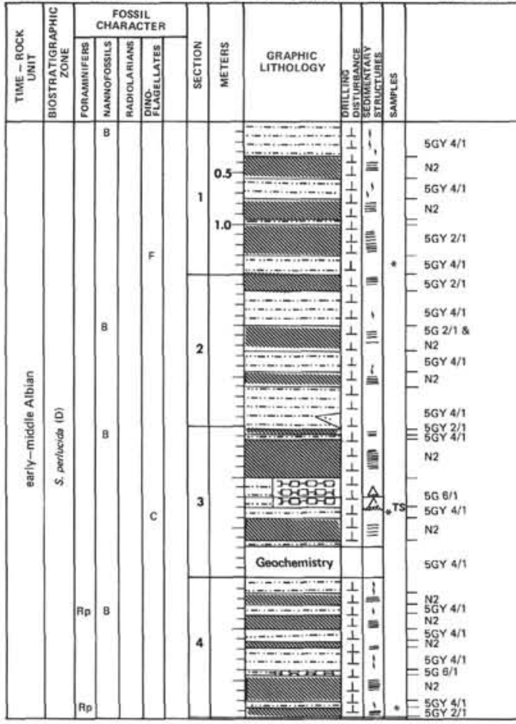

LITHOLOGIC DESCRIPTION

CARBONACEOUS CLAYSTONE and
SILTY CLAYSTONE

CARBONACEOUS CLAYSTONE is grayish black (N2), greenish black (5GY 2/1, 5G 2/1) with fine laminae. Stringers with wavy and flaser laminae appear to concentrate in carbonaceous claystones rather than silty claystones.

SILTY CLAYSTONE is greenish gray (5GY 4/1) with burrows and laminae in places.

Marly chalk and indurated chalk is greenish gray (5G 6/1) up to 17 cm thickness, based by erosional contact. Bouma sequences B–E(?) observed.

Thin Section at Section 3, 82–84 cm shows oolitic texture.

SMEAR SLIDE SUMMARY (%):

	1, 140	3, 55	3 83	4, 128	3, 83
	D	D	M	D	TS, M
Texture:					
Sand	–	–	–	–	35
Silt	25	20	50	15	50
Clay	75	80	50	85	15
Composition:					
Quartz	} 18	1	3	6	10
Feldspar					
Mica	5	1	–	2	1
Heavy minerals	–	–	1	1	–
Clay	70	13	10	72	9
Glauconite	–	–	–	–	1
Pyrite	–	1	–	3	–
Carbonate unspec.	1	50	30	2	35
Foraminifers	–	–	–	–	10
Calc. nannofossils	1	20	10	3	–
Fish remains	–	–	–	1	–
Plant debris	3	2	1	10	1
Other	–	12	45	–	22

SITE 534 HOLE A CORE 38 CORED INTERVAL 869.0–878.0 m

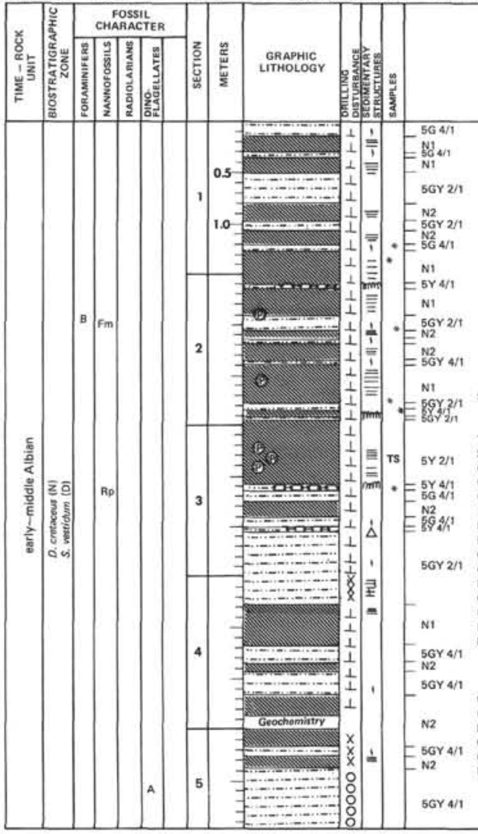

LITHOLOGIC DESCRIPTION

CARBONACEOUS CLAYSTONE and
SILTY CLAYSTONE

CARBONACEOUS CLAYSTONE is black (N1), grayish black (N2), and olive black (5Y 2/1), laminated but is more homogeneous in the lower sections. Pyrite concentration at 20–40 cm in Section 3. Quartzose stringers less than millimeters are examined by Smear Slides (Section 1 137 cm and Section 2, 57 cm.

SILTY CLAYSTONE is greenish black (5GY 2/1) and dark greenish gray (5G 4/1, 5GY 4/1) with burrows in places.

Marly chalk is olive gray (5Y 4/1) with distorted current laminae observed at 10 cm in Section 1 and 60 and 100 cm in Section 3.

SMEAR SLIDE SUMMARY (%):

	1, 122 D	1, 137 M	2, 57 M	2, 128 D	2, 137 M	3, 65 D
Texture:						
Silt	15	95	80	30	95	90
Clay	85	5	20	70	5	10
Composition:						
Quartz	} 8	74	62	5	64	3
Feldspar		10	5	–	10	–
Mica	1	3	5	15	5	–
Heavy minerals	1	1	3	–	3	1
Clay	75	5	18	74	5	5
Glauconite	–	1	–	1	–	–
Pyrite	3	1	2	3	2	1
Carbonate unspec.	1	2	–	–	5	72
Calc. nannofossils	1	–	–	–	–	15
Fish remains	–	–	1	–	–	–
Plant debris	10	3	4	2	3	3

	3, 38 TS
Composition:	
Quartz	5
Mica	10
Clay	60
Carbonate unspec.	10
Plant debris	15

SITE 534 . HOLE A CORE 39 CORED INTERVAL 878.0–887.0 m

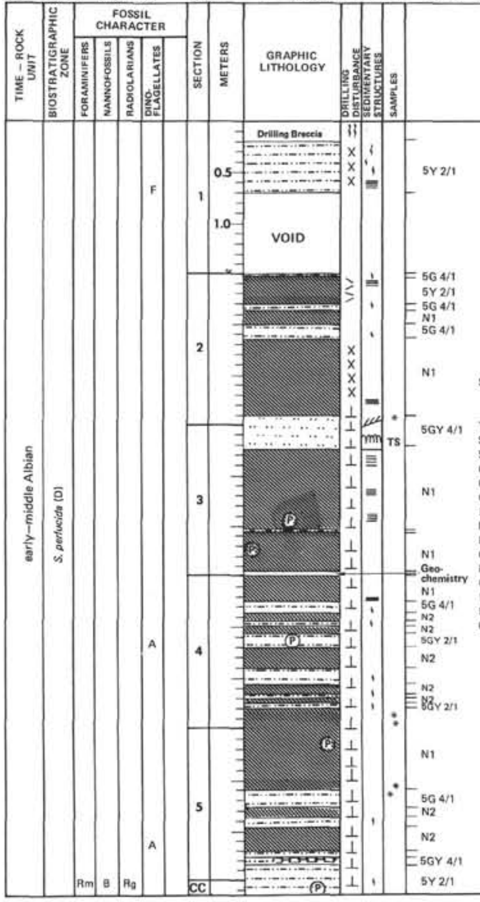

LITHOLOGIC DESCRIPTION

CARBONACEOUS CLAYSTONE and
SILTY CLAYSTONE

CARBONACEOUS CLAYSTONE is black (N1), grayish black (N2) and olive black (5Y 2/1). Although silty string occurs in places, carbonaceous claystones are quite thick. Pyrite concentration in Sections 3 and 5.

SILTY CLAYSTONE is olive black (5Y 2/1), dark greenish gray (5G 4/1, 5GY 4/1) and greenish black (5GY 2/1), and burrows occur frequently.

Quartz-rich calciturbidite, 32 cm thick occurs between 140 cm of Section 2 and 22 cm of Section 3. Climbing ripples are observed in visual and Thin Section observations.

SMEAR SLIDE SUMMARY (%):

	2, 145 D	4, 135 D	4, 142 D	5, 54 D	5, 62 D	3, 18 TS
Texture:						
Sand	50	–	2	1	2	5
Silt	45	10	8	14	15	60
Clay	5	90	90	85	83	35
Composition:						
Quartz	75	5	5	5	4	35
Feldspar	5	–	1	1	–	–
Mica	10	2	2	3	1	–
Heavy minerals	2	1	1	1	–	–
Clay	3	76	70	66	74	30
Pyrite	1	3	4	2	2	–
Carbonate unspec.	–	–	–	–	–	25
Fish remains	–	1	2	1	1	–
Plant debris	4	12	15	12	18	–
Other	–	–	–	–	–	10

SITE 534 HOLE A CORE 40 CORED INTERVAL 887.0–896.0 m

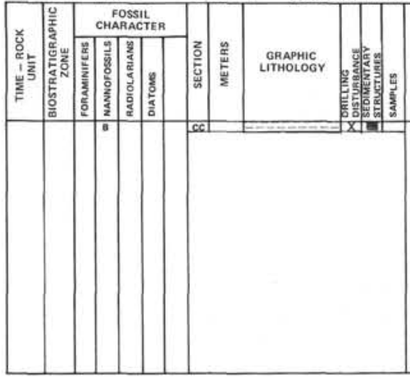

LITHOLOGIC DESCRIPTION

CLAYSTONE

Grayish green (5G 5/2) fissile-bearing claystone are dominant in the upper 5 cm, intercalated by pale yellowish green (10GY 7/2) homogeneous silty claystone. The silty claystone is very silty and composed mainly of quartz, feldspar, and mica, suggesting silty layers in the variegated claystone member.

Lower part is a 4 cm thick dusky green (5G 3/2) claystone with very pale green laminae of less than 1 mm and a thin flake of dark gray (N3) claystone.

From colors and interbedded silt layer, this core belongs to the variegated member.

SITE 534 HOLE A CORE 41 CORED INTERVAL 896.0–905.0 m

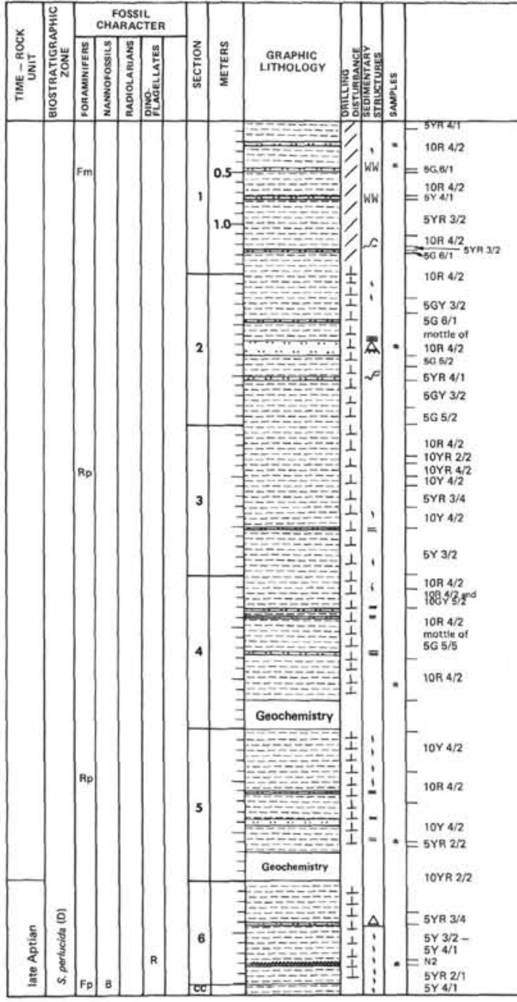

LITHOLOGIC DESCRIPTION

VARIEGATED CLAYSTONE

The claystone color varies from dark reddish brown (5YR 3/2, 3/4, 2/2), very dark brown (10YR 2/2), dark grayish brown (4/2), grayish red (10R 4/2), greenish olive (10Y 4/2), greenish olive green (5GY 3/2), brownish gray (5G 5/2), greenish gray (5G 6/1), dark olive gray (5Y 3/2), dark gray (5Y 4/1), dark gray (5YR 4/1), brownish black (5YR 2/1) to grayish black (N2).

Numerous siltstones are observed with the one at 75 cm in Section 2, being 8 cm thick and composed of quartz with less than 10% carbonate.

One carbonaceous claystone occurs at 80 cm in Section 6 with 5% plant debris.

SMEAR SLIDE SUMMARY (%):

	1, 23	1, 44	2, 75	4, 101	5, 110	6, 81
Texture:	D	D	D	D	D	D
Sand	–	–	15	–	–	–
Silt	20	30	60	15	10	10
Clay	80	70	25	85	90	90
Composition:						
Quartz	25	10	54	} 5	5	3
Feldspar	5	1	1	}		
Mica	4	3	7	3	2	2
Heavy minerals	1	1	2	–	–	1
Clay	62	77	20	–	90	87
Glauconite	–	–	2	5	–	–
Pyrite	1	1	5	–	–	1
Zeolite	–	–	–	2	–	–
Carbonate unspec.	3	2	2	2	1	1
Calc. nannofossils	–	1	5	–	–	–
Plant debris	3	4	3	2	2	5

SITE 534 HOLE A CORE 42 CORED INTERVAL 896.0–905.0 m

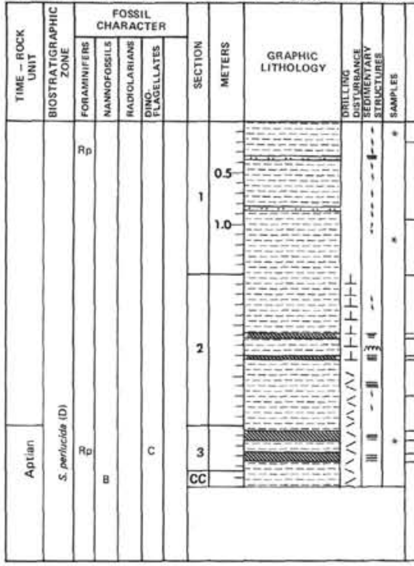

LITHOLOGIC DESCRIPTION

VARIEGATED CLAYSTONE and CARBONACEOUS CLAYSTONE

Variegated claystone in Section 1, and carbonaceous claystone-bearing silty claystone in Sections 2 and 3. Section 1 is brownish gray (5G 5/2), dark gray (5Y 4/1), dark olive gray (5Y 3/2), and greenish gray (5G 6/1). Sections 2 and 3 are dark greenish gray (5GY 4/1), greenish black (5GY 2/1) and brownish black (5YR 2/1).

Quartzose silt layers characterize the variegated intervals.

SMEAR SLIDE SUMMARY (%):

	1, 12	1, 115	3, 12
	D	D	D
Texture:			
Silt	10	5	10
Clay	90	95	90
Composition:			
Quartz	3	3	3
Mica	3	1	1
Heavy minerals	1	1	–
Clay	89	91	85
Glauconite	3	–	–
Pyrite	–	2	–
Carbonate unspec.	–	–	1
Fish remains	–	1	–
Plant debris	1	1	10

SITE 534 HOLE A CORE 43 CORED INTERVAL 914.0–923.0 m

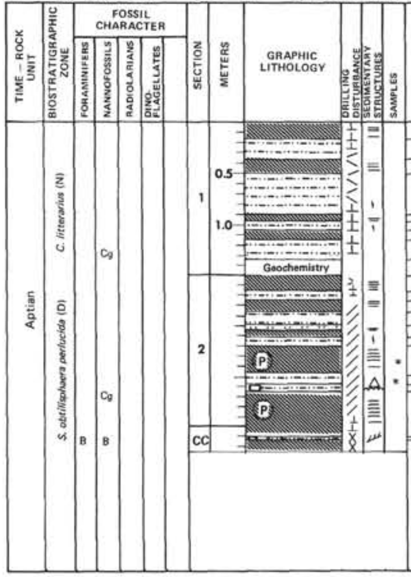

LITHOLOGIC DESCRIPTION

CARBONACEOUS CLAYSTONE

Carbonaceous claystone is calcareous, grayish black (N2), dark gray (N3), greenish black (5G 2/1), and olive black (5Y 2/1) laminae and silt stringers are frequent. Pyrite concretions void in center, is observed at 145 cm in Section 2.

SILTY CLAYSTONE

Dark greenish gray (5G 4/1), medium bluish gray (5B 5/1), and greenish gray (5GY 6/1). Colors tend to be greenish, due to nannofossil content.

SMEAR SLIDE SUMMARY (%):

	2, 89	2, 109
	D	D
Texture:		
Silt	15	25
Clay	85	75
Composition:		
Quartz	3	3
Mica	2	–
Heavy minerals	1	–
Clay	67	59
Zeolite	2	–
Carbonate unspec.	10	25
Calc. nannofossils	10	10
Plant debris	5	2

SITE 534 HOLE A CORE 44 CORED INTERVAL 923.0–932.0 m

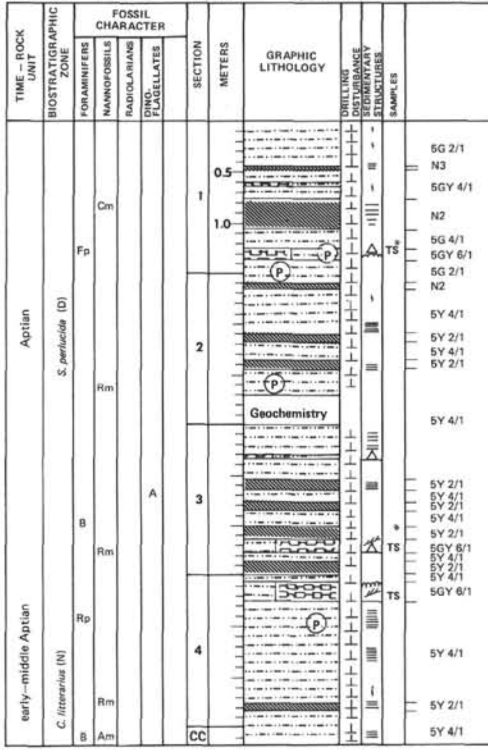

LITHOLOGIC DESCRIPTION

CARBONACEOUS CLAYSTONE and SILTY CLAYSTONE

CARBONACEOUS CLAYSTONE is grayish black (N2), dark gray (N3), and olive black (5Y 2/1). Carbonaceous layers are thin, 5–10 cm average, and tend to be massive.

SILTY CLAYSTONE is greenish black (5G 2/1), dark greenish gray (5GY 4/1), and olive gray (5Y 4/1). This layer too appears to be massive, sometimes associated with burrows. Pyrites are present.

Main compositions of caliciturbidites are pellet with small amount of foraminifer indicating shallow water origin.

SMEAR SLIDE SUMMARY (%):

	1, 121 D	3, 102 D	1, 125 TS	3, 123 TS	4, 23 TS
Texture:					
Sand	–	–	30	70	75
Silt	30	15	55	10	10
Clay	70	85	15	20	15
Composition:					
Quartz	3	5	10	3	2
Feldspar	–	–	1	1	–
Mica	2	2	1	–	1
Clay	42	68	40	30	30
Carbonate unspec.	35	5	39	61	60
Foraminifers	–	–	5	2	5
Calc. nannofossils	15	10	–	–	–
Plant debris	3	10	4	3	2

SITE 534 HOLE A CORE 45 CORED INTERVAL 932.0–941.0 m

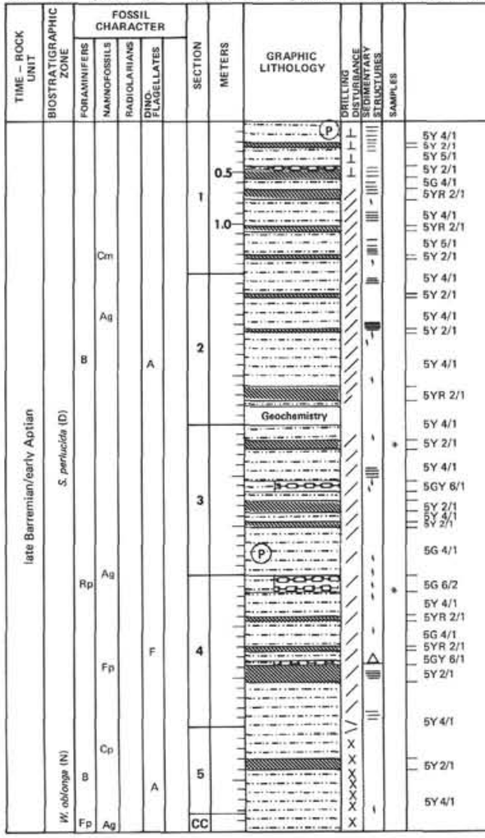

LITHOLOGIC DESCRIPTION

SILTY CLAYSTONE and CARBONACEOUS CLAYSTONE

CALCAREOUS SILTY CLAYSTONE is *olive gray* (5Y 4/1), light olive gray (5Y 6/1), and dark greenish gray (5G 4/1). Fine laminated intervals are between 52–58 and 88–93 cm in Section 2; 26–33, 68–73, 87–94, 111–117 cm in Section 3; 38–43, 55–71, 104–115, 120–129 cm in Section 4; and 15–30 and 50–59 cm in Section 5.

MARLY CHALK with burrows occurs 55–68 cm in Section 3 and 0–14 cm in Section 4, which is greenish gray (5GY 6/1).

CARBONACEOUS CLAYSTONE is olive black (5Y 2/1) and brownish black (5YR 2/1), dominantly less than 5 cm thick with $CaCO_3$ up to 30 %.

SMEAR SLIDE SUMMARY (%):

	3, 20 D	4, 11 D
Texture:		
Silt	25	10
Clay	75	90
Composition:		
Quartz	3	3
Mica	1	1
Clay	72	48
Carbonate unspec.	6	20
Calc. nannofossils	3	20
Plant debris	15	1
Other	–	7

SITE 534 HOLE A CORE 46 CORED INTERVAL 941.0–950.0 m

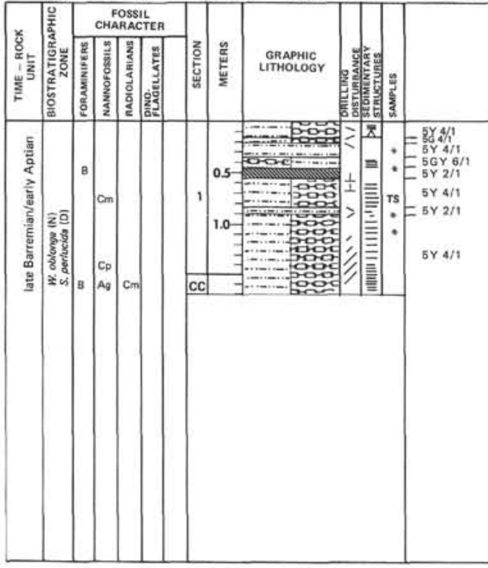

LITHOLOGIC DESCRIPTION

NANNOFOSSIL CHALK

Marly nannofossil chalk is dark greenish gray (5G 4/1) to olive gray (5Y 4/1), highly laminated. Laminations are 0.2–0.4 mm thick, and of clay-sized quartz and micrite. Within a micrite layer, 10–15% radiolarians, mostly replaced by calcite are present.

Carbonaceous layer contains 48% $CaCO_3$. Pyrite is observed.

SMEAR SLIDE SUMMARY (%):

	1, 30 D	1, 46 D	1, 90 D	1, 105 D	1, 76 TS
Texture:					
Silt	20	30	50	30	
Clay	80	70	50	70	
Composition:					
Quartz	4	25	–	5	10
Mica	1	4	–	–	–
Heavy minerals	–	3	–	–	–
Clay	58	63	40	47	50
Pyrite	1	–	–	–	–
Carbonate unspec.	2	2	48	30	30
Foraminifers	–	–	–	–	5
Calc. nannofossils	30	–	10	15	–
Sponge spicules	1	–	–	–	–
Plant debris	3	3	2	3	–

SITE 534 HOLE A CORE 47 CORED INTERVAL 950.0–959.0 m

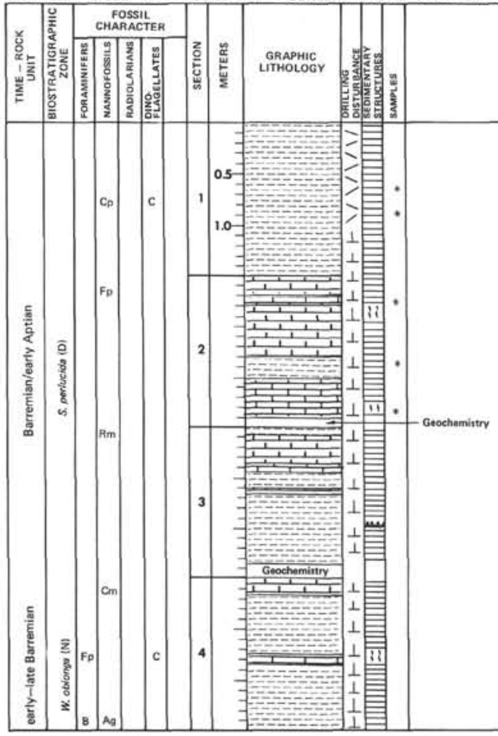

LITHOLOGIC DESCRIPTION

CALCAREOUS CLAYSTONE, NANNOFOSSIL CLAYSTONE, and DOLOMITIC LIMESTONE

Upper part (Section 1) marly, silty, and nannofossil claystone ranging from light olive gray (5Y 6/1) to greenish black (5G 2/1) to dark greenish gray (5G 4/1); several thin intercalations of dolomitic limestone (Section 2) and carbonaceous claystone olive black (5Y 2/1) in Sections 3 and 4.

Ammonite found at Section 3, 150 cm.

Mostly parallel laminated with moderately to highly burrowed intervals; pyrite nodule at Section 1, 87 cm.

SMEAR SLIDE SUMMARY (%):

	1, 67 D	1, 89 D	2, 27 D	2, 89 D	2, 136 D
Texture:					
Silt	50	20	40	20	20
Clay	50	80	60	80	80
Composition:					
Quartz	2	2	–	2	2
Mica	–	1	–	–	–
Clay	35	42	40	40	20
Pyrite	1	–	1	2	1
Carbonate unspec.	35	5	43	5	60
Calc. nannofossils	25	35	15	33	15
Plant debris	2	15	1	15	2
Other	–	–	1	3	–

SITE 534 HOLE A CORE 48 CORED INTERVAL 959.0–963.5 m

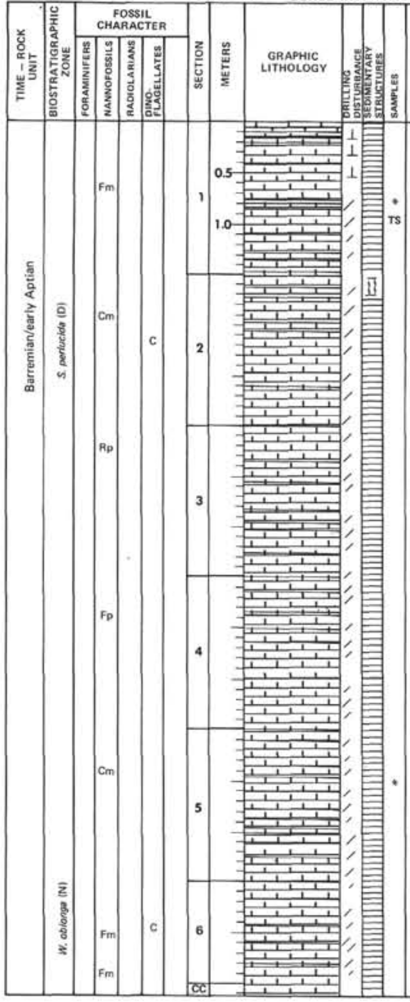

LITHOLOGIC DESCRIPTION

NANNOFOSSIL-CHALK and CALCAREOUS LIMESTONE

Mostly nannofossil-chalk of varying shades of gray (5Y 5/1–5Y 6/1) through greenish gray (5G 3/1–5Y 2/1) with all intermediate shades. Lighter shades are more silt-size rich (dolomitic); the darker shades are more clay and organic rich, frequently associated with pyrite. Almost whole core very finely parallel laminated with minor burrowed intervals. The dark intervals often begin suddenly then grade into lighter, but not invaribly. Laminae density is about 20 cm in the finely laminated intervals.

In Thin Section, Section 1, 98 cm, the calcareous limestone is a carbonaceous radiolarian micrite (wackestone). Radiolaria are all sparite filled. Thin shell fragments, quartz and mica are also present.

SMEAR SLIDE SUMMARY (%):

	1, 50 D	5, 51 D
Texture:		
Silt	30	15
Clay	70	85
Composition:		
Quartz	2	1
Feldspar	1	–
Mica	–	1
Clay	5	10
Pyrite	1	–
Carbonate unspec.	73	37
Calc. nannofossils	17	40
Fish remains	–	1
Plant debris	1	7
Other	–	3

SITE 534 HOLE A CORE 49 CORED INTERVAL 963.5–972.5 m

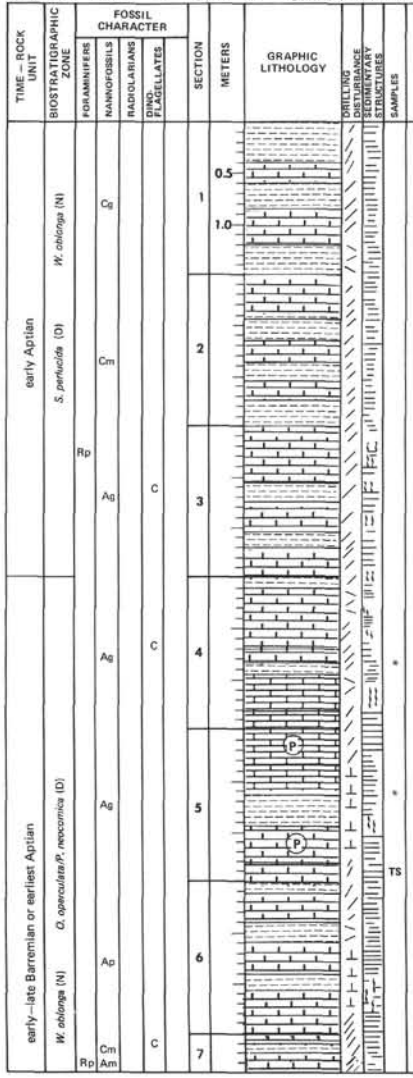

LITHOLOGIC DESCRIPTION

NANNOFOSSIL CHALK and CALCAREOUS CLAYSTONE

Alternations of calcareous claystone and nannofossil chalk ranging from dark gray (N3), light gray (N7), gray (5Y 4/1), dark greenish gray (5GY 4/1), to olive gray (5Y 6/1).

Mostly very finely laminated with occasional moderately to highly burrowed intervals, locally laminations wavy or convoluted. Occasionally graded, massive, non-burrowed units up to 3 cm thick are likely to be calciturbidites, local pyrite stringers.

In thin section the calcareous claystone is a carbonaceous pelletal micrite (wackestone). Pellets 15%, quartz silt 3%, micrite are clay matrix 75%, organics 5%, pyrite 3%. The pellets, which are spherical, may be micrite-filled radiolaria. Slight lamination may be intensified by diagenetic compaction.

SMEAR SLIDE SUMMARY (%):

	4, 84	5, 61
	D	D
Texture:		
Silt	15	25
Clay	85	75
Composition:		
Feldspar	1	1
Clay	48	7
Pyrite	2	1
Carbonate unspec.	4	75
Calc. nannofossils	13	15
Plant debris	12	1
Other	20	–

SITE 534 HOLE A CORE 50 CORED INTERVAL 972.5–981.5 m

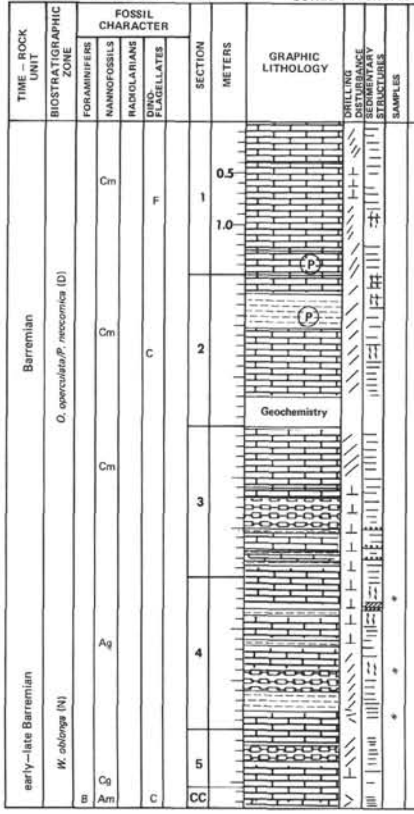

LITHOLOGIC DESCRIPTION

MARLY NANNOFOSSIL CHALK, CALCAREOUS CHALK, and CALCAREOUS CLAYSTONE

Blue gray (5Y 6/1), medium light gray (N6), dark gray (N3), and light greenish gray (5B 7/1).

Mostly very finely laminated, occasional massive, burrowed and graded intervals. Greenish gray (5B 7/1) intervals normally the most bioturbated.

Occasional intervals show grading, parallel laminations, and microcross-lamination signifying turbidite deposition.

Pyrite nodules deform the laminae.

SMEAR SLIDE SUMMARY (%):

	4, 38	4, 90	4, 136
	D	D	D
Texture:			
Silt	7	20	13
Clay	93	80	87
Composition:			
Quartz	4	3	7
Feldspar	2	–	3
Mica	1	–	–
Clay	13	30	3
Glauconite	1	–	–
Pyrite	3	–	2
Carbonate unspec.	39	54	50
Calc. nannofossils	35	10	27
Fish remains	–	–	1
Plant debris	–	1	2
Other	2	2	5

SITE 534 HOLE A CORE 51 CORED INTERVAL 981.5–990.5 m

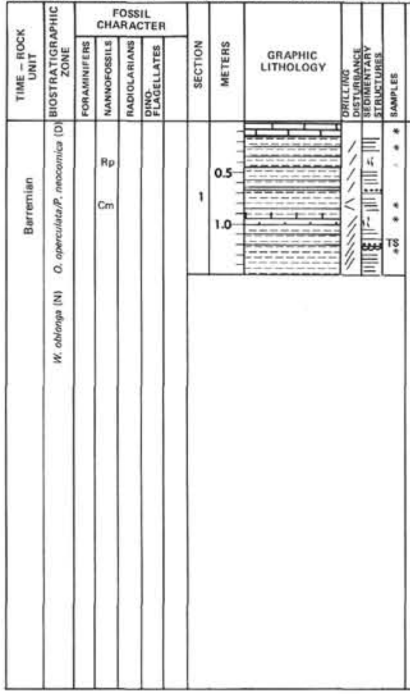

LITHOLOGIC DESCRIPTION

DOLOMITE LIMESTONE, CALCAREOUS CLAYSTONE and MARLY NANNOFOSSIL CHALK

Greenish gray (5G 6/1) to medium bluish gray (5B 5/1) dolomitic limestone; olive black (5Y 2/1) to grayish black (N2) dolomitic nannofossil chalk; and greenish gray (5GY 4/1) calcareous claystone.

Mostly finely parallel laminated with up to 15 cm thick burrowed intervals; up to 15 cm intervals with grading, and parallel lamination of the D–E intervals of Bouma sequences. Base of calciturbidites contains some sand-sized carbonate.

The Thin Section (Section 1, 139–141 cm) of marly nannofossil chalk is a radiolarian biomicrite. Bioclasts include shallow water carbonate material (ooids, algae fragments, pellets, shells). Rare quartz grains. Sparry calcite in radiolarian shells. Micrites matrixs replaced by microspar-sized calcite.

SMEAR SLIDE SUMMARY (%):

	1, 10 D	1, 27 D	1, 81 D	1, 97 D	1, 125 D
Texture:					
Sand	–	–	2	5	3
Silt	5	–	20	20	30
Clay	95	–	78	75	63
Composition:					
Quartz	1	5	2	15	4
Feldspar	–	–	–	–	2
Mica	–	2	–	2	–
Heavy minerals	2	3	2	4	4
Clay	–	–	–	60	42
Volcanic glass	1	–	–	–	–
Carbonate unspec.	96	70	81	9	20
Calc. nannofossils	–	20	15	10	30

SITE 534 HOLE A CORE 52 CORED INTERVAL 990.5–999.5 m

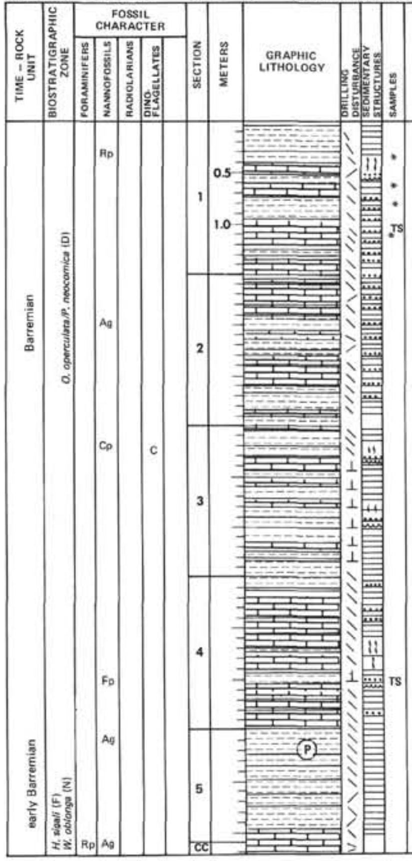

LITHOLOGIC DESCRIPTION

CALCAREOUS CLAYSTONE, CALCAREOUS CHALK and MARLY NANNOFOSSIL CHALK

CLAYSTONE, greenish gray (5GY 6/1) to dark greenish gray (5GY 4/1) to olive gray (5Y 4/1) to light olive gray (5Y 4/1) to olive black (5Y 4/1).

CALCAREOUS CHALK and MARLY NANNOFOSSIL-CHALK, greenish gray (5GY 6/1) to dark greenish gray (5GY 4/1).

Parallel laminated and minor burrowed intervals intercalated with graded, microcross-laminated dolomitic limestone. Base of these calciturbidites is silt-sized; Bouma C–E and D–E intervals.

Smear slides contain some zeolite (to 9%). A Thin Section of marly nannofossil chalk (Section 1, 71–73 cm) is a biomicrite (wackestone). Bioclasts of shell fragments, radiolaria, and sponge spicules, 25%; quartz and biotite, 1%; clay-rich micrite and opal-Ct, 74%. One feldspathic volcanic grain noted.

SMEAR SLIDE SUMMARY (%):

	1, 38 D	1, 62 D	1, 83 D	1, 113 D
Texture:				
Silt	20	30	40	50
Clay	80	70	60	50
Composition:				
Quartz	2	2	3	2
Feldspar	–	–	1	–
Mica	–	–	2	–
Clay	47	25	43	53
Pyrite	–	1	1	1
Carbonate unspec.	30	40	10	40
Calc. nannofossils	15	15	37	5
Sponge spicules	1	–	–	–
Plant debris	3	2	5	–
Other	2	15	–	–

SITE 534 HOLE A CORE 53 CORED INTERVAL 999.5–1008.5 m

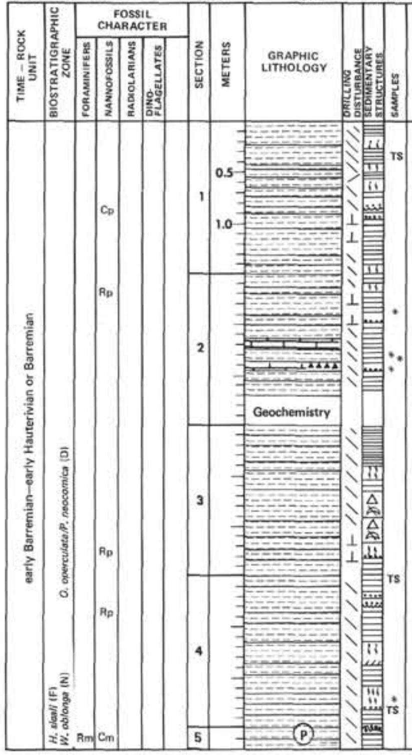

LITHOLOGIC DESCRIPTION

LIMESTONE, CALCAREOUS CLAYSTONE and CALCAREOUS CHERT

LIMESTONE, dark greenish gray (5GY 4/1) to greenish gray (5GY 6/1) to light bluish gray (5B 7/1); claystone are dark greenish gray (5GY 4/1) to greenish black (5G 2/1).

Mostly parallel laminated with occasional up to 8 cm thick intervals which are graded with scoured bases and show *microcross-lamination* and *rarely micro-convolute* lamination. Bouma A–E and combinations present. Sand-sized carbonates, concentrated at base of some calciturbites.

Many of the limestones are dolomitic. Small volumes of calcareous chalcedonic quartz chert of replacement origin are present. Three Thin Sections (Section 1, 38 cm; Section 4, 11 and 78 cm) are silty bioclastic micrites (packstones and wackestones). Section 4, 11–13 cm contain abundant shallow water carbonate (shells, benthic foraminifers, echinoderm plates, algae, ooids, micrites, intraclasts).

SMEAR SLIDE SUMMARY (%):

	2, 39 D	2, 80 D	2, 85 D	2, 92 D	4, 122 D
Texture:					
Silt	–	20	50	30	–
Clay	–	80	50	70	–
Composition:					
Quartz	2	1	2	2	5
Mica	–	TR	–	–	–
Heavy minerals	–	TR	–	–	–
Clay	5	47	40	56	25
Pyrite	1	2	–	1	TR
Carbonate unspec.	90	5	46	20	25
Calc. nannofossils	–	12	8	10	20
Sponge spicules	–	–	–	–	TR
Fish remains	–	1	–	–	–
Plant debris	1	5	2	1	1
Other	–	12	2	10	15

SITE 534 HOLE A CORE 54 CORED INTERVAL 1008.5–1017.5 m

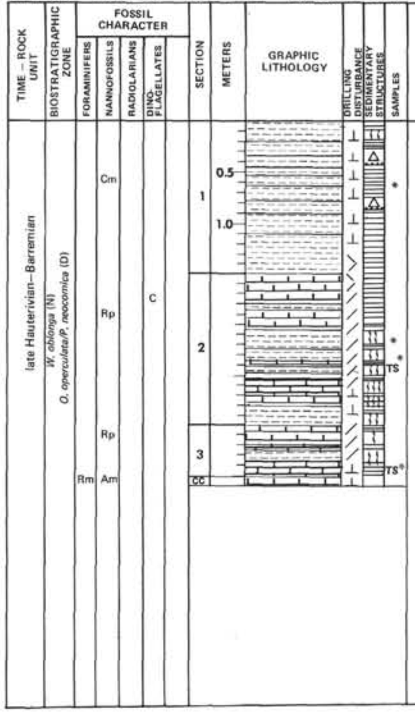

LITHOLOGIC DESCRIPTION

CALCAREOUS CLAYSTONE, DOLOMITE LIMESTONE and MARLY NANNOFOSSIL CHALK and FINE GRAINED CALCAREOUS SILTSTONE

Colors range from light greenish gray (5GY 5/1) and dark greenish gray (5GY 5/1) to olive gray (5Y 4/1) to dark yellowish brown (10YR 4/2). The claystones are generally darker than the chalks and limestones.

Mostly finely parallel laminated with moderately to highly burrowed intervals (chondrites). Several graded intervals up to 9 cm thick, but fewer than Core 53 (calciturbidites).

In Smear Slide many lithologies are dolomitic; claystones contain unusually well-preserved calcareous nannoplankton. A Thin Section at Section 2, 98–100 cm is a biomicrite (wackestone) with a shallow water calcareous assemblage of shells, algae, ooids, echinoderm plants. Quartz is concentrated at base of this turbidite. Clay-rich upper part less recrystallized. Thin Section at Section 3, 49–51 cm is a pelleted packstone of similar provenance.

SMEAR SLIDE SUMMARY (%):

	1, 68 D	2, 68 D	2, 81 D	3, 45 D
Texture:				
Silt	20	25	50	50
Clay	80	75	50	50
Composition:				
Quartz	5	2	–	10
Clay	31	55	24	47
Pyrite	1	–	TR	2
Carbonate unspec.	10	10	70	10
Calc. nannofossils	35	18	5	15
Fish remains	–	–	–	1
Plant debris	3	3	1	–
Other	15	12	–	25

SITE 534 HOLE A CORE 55 CORED INTERVAL 1017.5–1026.5 m

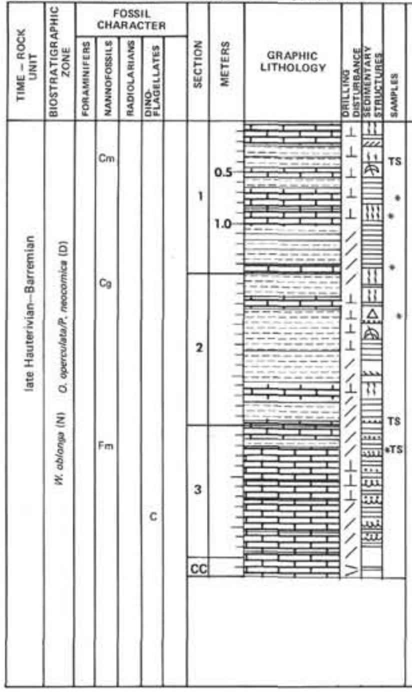

LITHOLOGIC DESCRIPTION

MARLY LIMESTONE and CALCAREOUS CLAYSTONE

Colors medium light gray (N6), light bluish gray (5B 7/1), light olive gray (5Y 6/1), and greenish gray (5GY 6/1).

Finely parallel laminated, or vaguely parallel laminated with frequent burrowed intervals. Toward base of core graded, intervals with microcross-laminations (up to 11 cm thick become abundant); calciturbidites.

Several molluscan shell fragments, *Inoceramus*, present.

Bases of calciturbidites contain up to 15% sand-sized carbonate. Poorly preserved radiolaria, converted to chalcedonic quartz present (up to 15%), also pyritized diatoms. Section 1, 70 cm in Thin Section is a radiolarian micrite. Section 1, 45 cm is a partially recrystallized sandy micritic limestone. Section 2, 149 cm is a siliceous micrite. Shallow water material (ooids, algae, pisoliths, echinderm plates, micritic intraclasts) preserved in Section 1, 145 cm.

SMEAR SLIDE SUMMARY (%):

	1, 76	1, 92	1, 144	2, 64	3, 24
	D	D	D	D	D
Texture:					
Sand	5	5	–	–	15
Silt	35	35	–	20	25
Clay	60	60	–	80	60
Composition:					
Quartz	1	2	–	2	3
Heavy minerals	–	–	–	1	–
Clay	22	40	10	45	30
Pyrite	1	–	–	–	–
Carbonate unspec.	50	30	75	5	40
Calc. nannofossils	10	20	5	10	10
Plante debris	TR	3	–	5	2
Other	16	5	10	33	15

SITE 534 HOLE A CORE 56 CORED INTERVAL 1026.5–1035.5 m

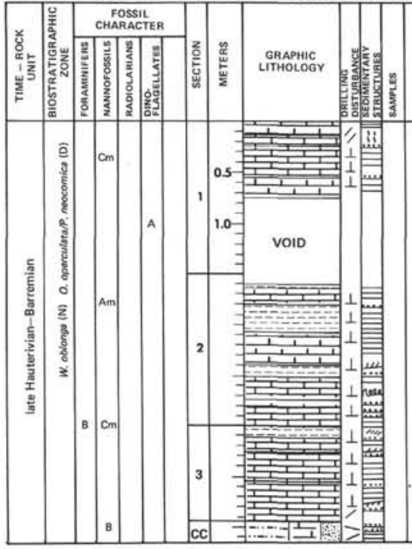

LITHOLOGIC DESCRIPTION

CALCAREOUS MUDSTONE, MARLY NANNOFOSSIL CHALK, and CALCAREOUS SILTSTONE

MARLY NANNOFOSSIL CHALK is medium light gray (N6), dark gray (N3), and light olive gray (5Y 6/1), finely laminated or moderately to strongly burrowed.

CALCAREOUS MUDSTONE is medium dark gray (N4) to dark gray (N3), often massive, or vaguely graded with few burrows, locally carbonaceous.

CALCAREOUS SILTSTONE is gray (5Y 6/1) to greenish gray (5GY 5/1), graded, parallel lamination, few burrows; basal few cm is calcareous siltstone or silty limestone, rest is homogeneous gray calcareous siltstone; interpreted as calcereous turbidite (Bouma C–D, E, D–E).

SITE 534 HOLE A CORE 57 CORED INTERVAL 1035.5–1044.5 m

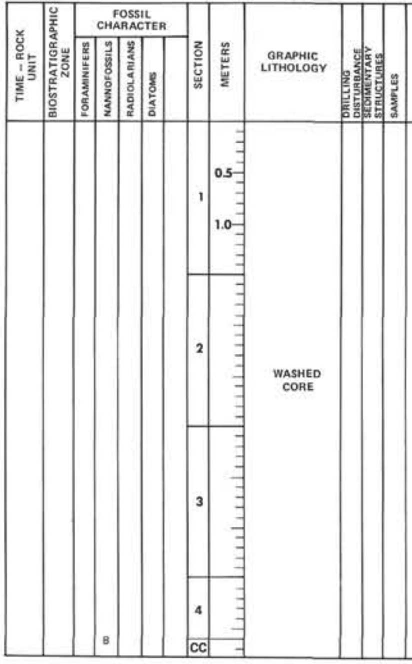

LITHOLOGIC DESCRIPTION

CUTTINGS ONLY

Cuttings from cave-ins of sides of hole during re-entry.

SITE 534 HOLE A CORE 58 CORED INTERVAL 1044.5–1053.5 m

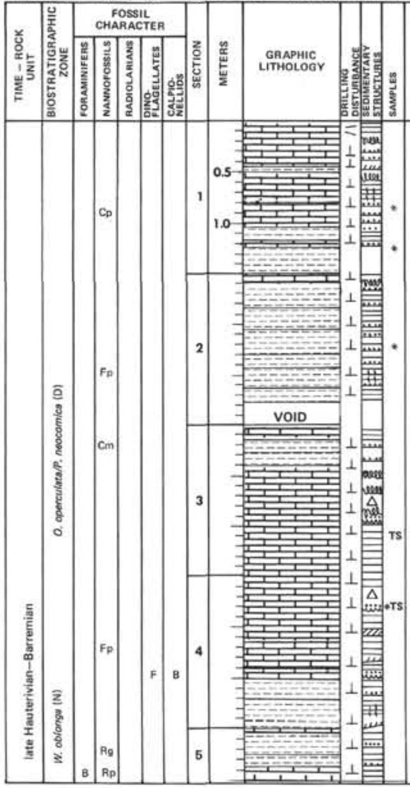

LITHOLOGIC DESCRIPTION

MARLY NANNOFOSSIL CHALK, CALCAREOUS CLAYSTONE, CALCAREOUS SILTSTONE, and CALCAREOUS SANDSTONE

MARLY NANNOFOSSIL-OOZE is light gray (N7), very finely parallel laminated, or moderately to strongly burrowed.

CALCAREOUS CLAYSTONE is greenish gray (5G 6/1) massive and weakly graded at base of units, typically <6 cm thick; usually no burrows, or small chondrites.

CALCAREOUS SILTSTONE is dark greenish gray (5G 4/1) fine- to medium-grained siltstone showing cross- and parallel-laminations, units up to 10 cm thick.

CALCAREOUS SANDSTONE is dark greenish gray (5G 4/1), base of major turbidite intervals up to 1 m thick, graded and cross-laminated. Some may be shallow carbonate platform and continental basement lithologies.

NOTE: In Section 3 major convolute-laminated and intraclast-bearing debris flow unit.

Thin Section at Section 3, 127 cm and Section 4, 18–21 cm are calcareous quartzose siltstones to fine sandstone (quartzarenite) with quartz, feldspar, and mica abundant.

SMEAR SLIDE SUMMARY (%):

	1, 89 M	1, 126 M	2, 75 M	4, 30 M
Texture:				
Sand	2	10	15	60
Silt	10	10	10	5
Clay	88	80	75	35
Composition:				
Quartz	3	1	15	50
Feldspar	–	2	1	2
Mica	1	–	2	1
Heavy minerals	1	1	–	2
Clay	50	67	59	35
Carbonate unspec.	3	1	1	8
Calc. nannofossils	40	25	20	1
Plant debris	2	3	2	1

SITE 534 HOLE A CORE 59 CORED INTERVAL 1053.5–1062.5 m

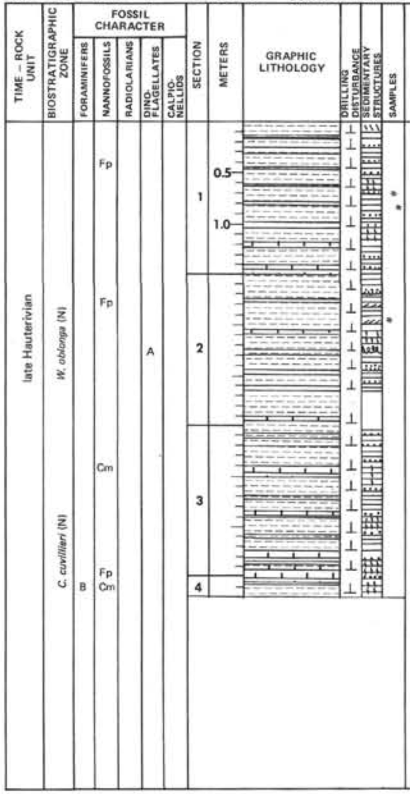

LITHOLOGIC DESCRIPTION

CALCAREOUS CLAYSTONE, MARLY NANNOFOSSIL-CHALK, CALCAREOUS SILTSTONE, and CALCAREOUS SANDSTONE

CALCAREOUS CLAYSTONE is greenish gray (5G 6/1) clasts up to 8 cm thick, massive or weakly graded at base; usually no burrows. Some intervals carbonaceous.

MARLY NANNOFOSSIL-CHALK is light gray (N7). Very finely laminated, often moderately to highly burrowed intervals up to 15 cm thick. This section consists mainly of partly recrystallized micritic "limestone" with few well-preserved calcareous nannofossils.

CALCAREOUS SILTSTONE is dark greenish gray (5G 4/1) and occurs as graded units up to 10 cm thick, at the base of the calcareous claystone intervals (1–2 mm) as in the upper part of sand turbidites, parallel and cross-laminated.

CALCAREOUS SANDSTONE is dark greenish gray (5G 4/1) turbidites (Bouma B–C–D–E, C–D–E, D–E) with convolute and laminations.

The thin sections are all turbidites calcareous quartzose sandstones and siltstones of terrigenous provenance plus some bioclastic carbonate (echinoderm plates and spires, shells, benthic foraminifers, and rare micritized pellets).

SMEAR SLIDE SUMMARY (%):

	1, 72 M	1, 86 M	2, 49 M
Texture:			
Sand	2	–	1
Silt	5	5	5
Clay	93	92	94
Composition:			
Quartz	2	1	3
Feldspar	1	–	2
Heavy minerals	–	1	–
Clay	71	69	89
Palagonite	1	–	–
Zeolite	15	1	–
Calc. nannofossils	5	25	3
Plant debris	5	3	3

SITE 534 HOLE A CORE 60 CORED INTERVAL 1062.5–1071.5 m

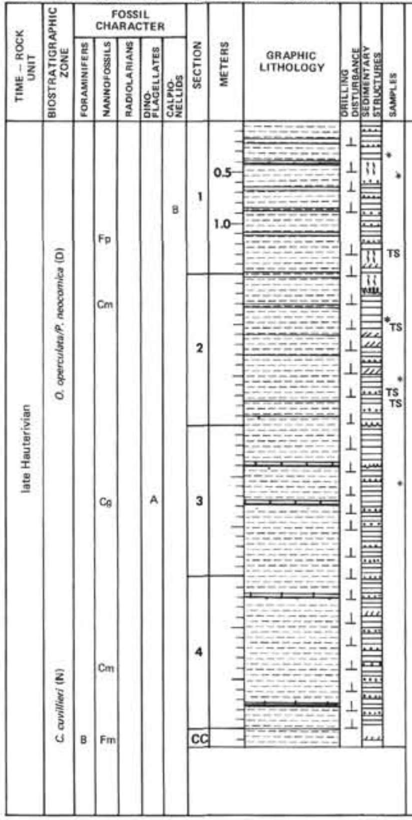

LITHOLOGIC DESCRIPTION

CALCAREOUS CLAYSTONE, MARLY NANNOFOSSIL-CHALK, CARCAREOUS SILTSTONE, and SILTY LIMESTONE

CALCAREOUS CLAYSTONE is greenish gray (5G 6/1) units up to 6 cm thick, massive or weakly lamininated or graded at base; usually no burrows, or very small chondrites. Some intervals carbonaceous.

MARLY NANNOFOSSIL-CHALK is light gray (N7). Very finely laminated with micro-cutoffs of individual laminae, some intervals moderately to highly burrowed intervals up to 20 cm thick.

CALCAREOUS SILTSTONE is dark greenish gray (5G 4/1) and occurs as graded units up to 10 cm thick, at the base of the calcareous claystone intervals (1–3 mm), and in upper part of sand turbidities. Parallel and cross-laminated.

SILTY LIMESTONE, several up to 0–20 m turbiditic intercalations.

In Thin Section, Section 1, 134–137 cm is a calcareous siltstone; 17% bioclasts including thin shell fragments; 37% terrigenous, quartz, plagioclase, mica, microcline, polycrystalline quartz, chlorite; 43% cement of sparry calcite; 3% carbonaceous turbiditic deposition. Thin Section, Section 2, 58–60, 136–137, 138–140 and Section 3, 18–20 cm are all very similar in composition and diagenesis.

SMEAR SLIDE SUMMARY (%):

	1, 34	1, 59	2, 47	2, 103	3, 57
	M	M	M	M	M
Texture:	1	–	1	3	2
Silt	5	10	7	15	5
Clay	94	90	92	82	93
Composition:					
Quartz	1	–	1	3	1
Feldspar	2	–	1	3	1
Heavy minerals	1	–	–	–	1
Clay	87	65	46	82	68
Zeolite	–	5	–	1	5
Carbonate unspec.	5	–	–	1	1
Calc. nannofossils	1	20	50	10	15
Plant debris	2	10	2	5	8

SITE 534 HOLE A CORE 61 CORED INTERVAL 1071.5–1080.5 m

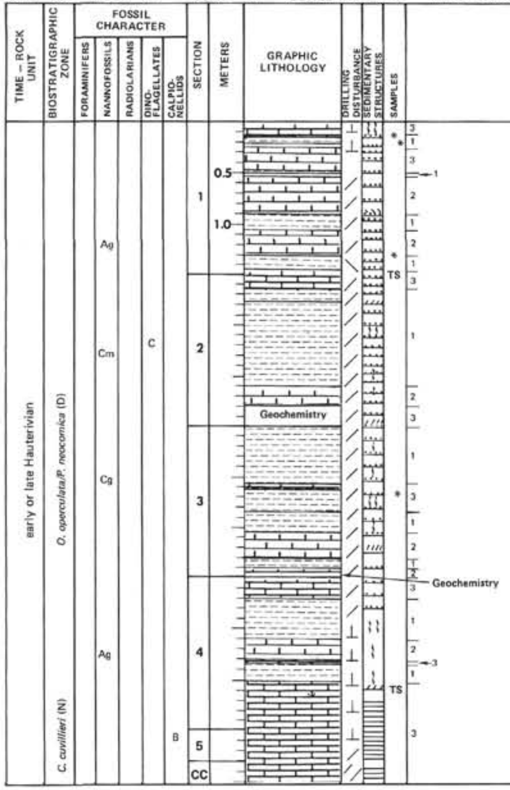

LITHOLOGIC DESCRIPTION

CALCAREOUS CLAYSTONE, MARLY CHALK, and MARLY LIMESTONE

1 – CALCAREOUS CLAYSTONE, dark gray (N2–N3), is homogeneous, but usually with a thin (0.5–1 cm) laminated gray (N4–N5) silty graded layer at base; typically coccolith-rich.

2 – MARLY CHALK is either very finely laminated gray (5Y 5/1) with rare burrowing, or light gray (5Y 6/1–5Y 7/1) moderately to highly bioturbated with disrupted laminae.

3 – MARLY LIMESTONE is medium gray (N5) to medium dark gray (N4), usually cross-bedded or laminated, graded. Sometimes sandy or silty as well as marly.

In Thin Section, Section 2, 17–19 cm is a quartzose calcareous siltstone with 4% shells and other bioclasts; 35% terrigenous including quartz, plagioclase, muscovite, biotite, hornblende, and chlorite. Matrix and cement is 57%; 3% pyrite. Both thin sections are well sorted. Matrix extensively recrystallized to sparry calcite.

SMEAR SLIDE SUMMARY (%):

	1, 15	1, 21	1, 130	3, 68
	M	M	M	D
Texture:				
Sand	–	10	10	50
Silt	3	25	20	30
Clay	97	65	70	20
Composition:				
Quartz	–	3	25	41
Feldspar	–	3	6	5
Mica	–	1	4	10
Heavy minerals	–	2	1	15
Clay	20	70	67	20
Zeolite	–	4	2	–
Carbonate unspec.	78	3	2	1
Calc. nannofossils	2	10	10	3
Plant debris	1	5	3	5

SITE 534 HOLE A CORE 62 CORED INTERVAL 1080.5–1089.5 m

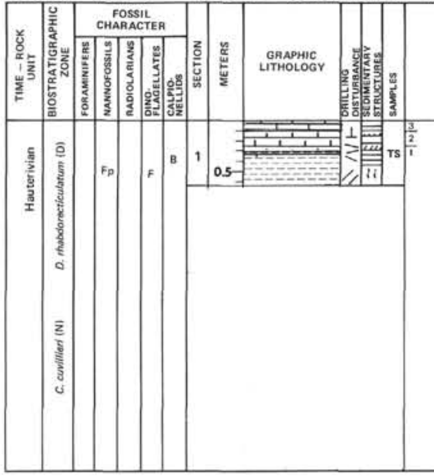

LITHOLOGIC DESCRIPTION

CALCAREOUS CLAYSTONE, MARLY CHALK, and SANDY LIMESTONE

1 – CALCAREOUS CLAYSTONE, dark gray (N2–N3) homogeneous little burrowed graded units up to 10 cm thick.

2 – MARLY CHALK, light gray (5Y 5/1) to gray (5Y 5/1), either very finely parallel laminated or moderately to highly burrowed units.

3 – SANDY LIMESTONE, medium gray (N5), graded and cross-laminated turbiditic unit.

A Thin Section at Section 1, 15–17 cm is a calcareous quartz arenite. Bioclasts (17%) shells, echinoderm plates and rare arenaceous foraminifers; 35% terrigenous (quartz, plagioclase, orthoclase, microcline, penthite, muscovite, biotite, chlorite, epidite, amphibole); 41% clay and sparry calcite matrix and cement, 4% micritic pellets; and 3% pyrite. Quartz grains show pressure solution against shells. Quartz well sorted and graded; a turbidite.

SITE 534 HOLE A CORE 63 CORED INTERVAL 1089.5–1098.5 m

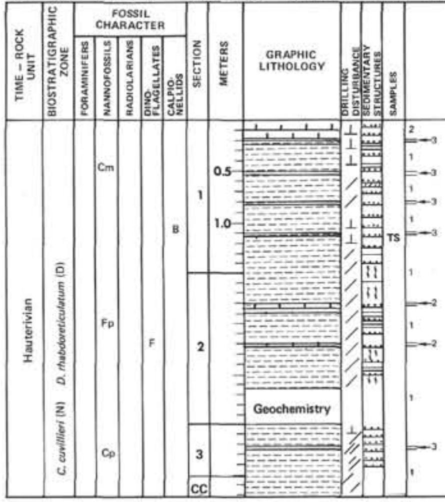

LITHOLOGIC DESCRIPTION

CALCAREOUS CLAYSTONE, MARLY CHALK, and CALCAREOUS SILTSTONE

1 – CALCAREOUS CLAYSTONE, medium light gray (N6) to dark gray (N3), often carbonaceous. Small graded units up to 6 cm thick, usually massive and with small chondrite burrows.

2 – MARLY CHALK, medium light gray (N6) to dark gray (N3) and light olive gray (5Y 6/1). Very finely laminated with small truncations of individual laminae. Alternating intervals are moderately to highly burrowed (up to 25 cm).

3 – CALCAREOUS SILTSTONE, thin parallel and cross-laminated partings at base of turbiditic calcareous claystones.

In Thin Section, Section 1, 116–118 cm, is a calcareous quartzose siltstone to fine sandstone; 2% bioclast of shells and sponge spicules; 30% terrigenous quartz, mica, plagioclase; 57% calcite cement; 6% organic particles, 5% micrite pellets, large micrite intraclasts, and clay-rich laminae.

SITE 534 HOLE A CORE 64 CORED INTERVAL 1098.5–1107.5 m

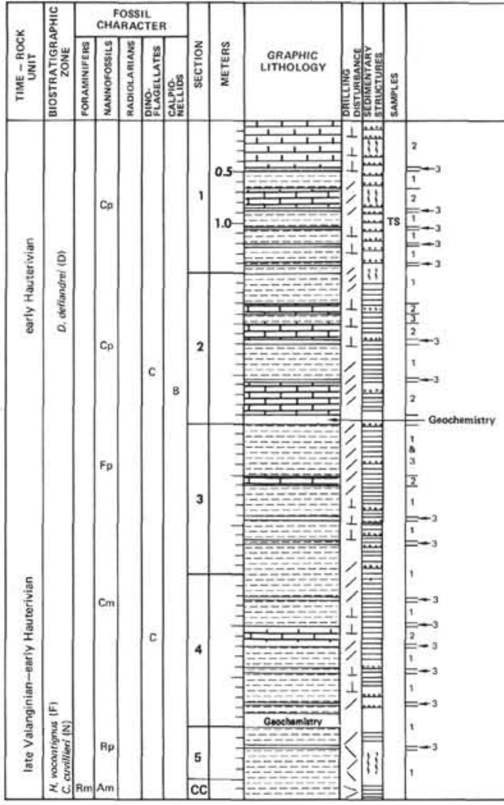

LITHOLOGIC DESCRIPTION

CALCAREOUS CLAYSTONE, MARLY CHALK, and CALCAREOUS SILTSTONE

1 – CALCAREOUS CLAYSTONE, medium light gray (N6) to dark gray (N3), often carbonaceous small graded units up to 5 cm thick, usually massive and with small chondrite burrows.

2 – MARLY CHALK, medium light gray (N6) to dark gray (N3) and light olive gray (5Y 6/1). Very finely laminated with small microcross-laminated cement. Alternating intervals are moderately to highly burrowed (up to 25 cm).

3 – CALCAREOUS SILTSTONE, gray (5G 4/1), thin parallel or cross-laminated partings at base of turbiditic calcareous claystone.

A Thin Section at Section 1, 115–116 cm is a calciturbidite with rare fine shell fragments and quartz grains and residual organic particles in a matrix of micrite partly recrystallized to microspar-sized calcite. The sparry calcite probably replaces radiolarian. Note that the replaced(?) radiolarian are spherical, thus cemented prior to extensive compactions.

SITE 534 HOLE A CORE 65 CORED INTERVAL 1107.5–1116.5 m

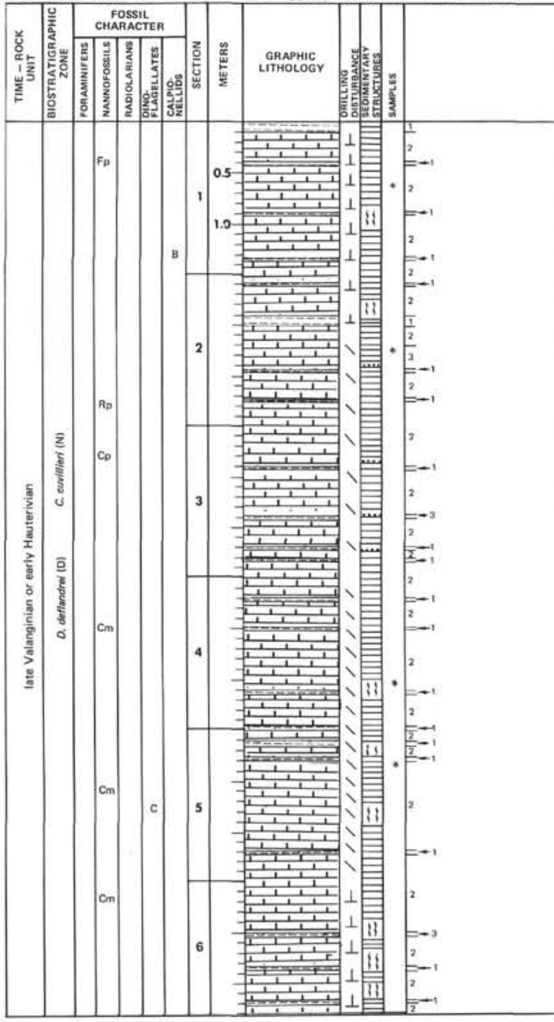

LITHOLOGIC DESCRIPTION

CALCAREOUS CLAYSTONE, MARLY CHALK, and CALCAREOUS SILTSTONE

1 – CALCAREOUS CLAYSTONE, dark gray (N2–N3), homogeneous, but usually with a thin (0.5 cm) laminated gray (N4–N5) silty graded layer at base; typically contains abundant, well-preserved coccolith.

2 – MARLY CHALK, gray (5Y 5/1), is finely laminated with few burrows or light gray (5Y 6/1–5Y 7/1) moderately to highly burrowed with disturpted laminae.

3 – CALCAREOUS SILTSTONE, medium gray (N5), three thin (<5 cm) graded and parallel laminated intervals, clearly turbiditic in origin.

Lithologies and sedimentary features very similar to Core 64, but fewer turbiditic claystones.

SMEAR SLIDE SUMMARY (%):

	1, 65 M	2, 75 D	4, 105 M	5, 35 M
Texture:				
Sand	15	–	–	2
Silt	30	2	10	3
Clay	55	98	90	95
Composition:				
Quartz	10	1	1	2
Feldspar	3	3	1	1
Mica	5	–	–	1
Heavy minerals	2	–	–	1
Clay	70	94	75	50
Zeolite	1	–	1	1
Calc. nannofossils	6	1	20	41
Plant debris	3	1	2	3

SITE 534 HOLE A CORE 66 CORED INTERVAL 1116–1125.5 m

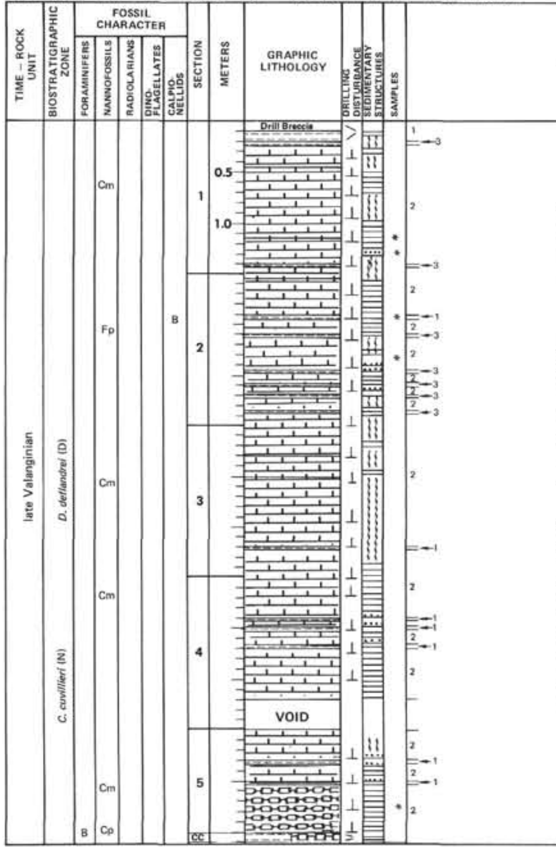

LITHOLOGIC DESCRIPTION

CALCAREOUS CLAYSTONE, MARLY CHALK, and CALCAREOUS SILTSTONE

1 – CALCAREOUS CLAYSTONE, dark gray (N2–N3), homogeneous, or with tiny chondrite burrows, often unit is thin (0.5–1 cm) graded or parallel laminated silty layer at base (turbiditic?).

2 – MARLY CHALK. Three distinct types present: 1) light gray (5Y 6/1) very finely laminated with few burrows, 2) dark gray (N2–N3) also very finely laminated with few burrows in units up to 20 cm thick, and 3) light gray (5Y 6/1) moderately to very highly laminated with traces of original parallel laminations as is in 1).

3 – CALCAREOUS SILTSTONE, medium gray (N5) graded, very finely laminated, e.g. 2.5 cm interval in Section 4 (42.0–44.5 cm).

Note the sharp distinction between the three lithologies seen in Cores 64–68 is now becoming more diffuse, particularly the distinction between burrowed and finely laminated intervals.

SMEAR SLIDE SUMMARY (%):

	1,113 D	1, 130 M	3, 45 D	3, 86 D	5, 77 M
Texture:					
Sand	2	1	1	1	1
Silt	5	1	3	1	3
Clay	93	98	96	98	96
Composition:					
Quartz	3	2	1	1	2
Feldspar	1	–	1	–	1
Mica	–	–	–	–	1
Heavy minerals	1	2	–	1	1
Clay	42	92	72	87	52
Zeolite	2	–	1	–	1
Carbonate unspec.	–	–	20	10	–
Calc. nannofossils	50	4	5	–	40
Plant debris	1	–	–	1	2

SITE 534 HOLE A CORE 67 CORED INTERVAL 1125.0–1130.0 m

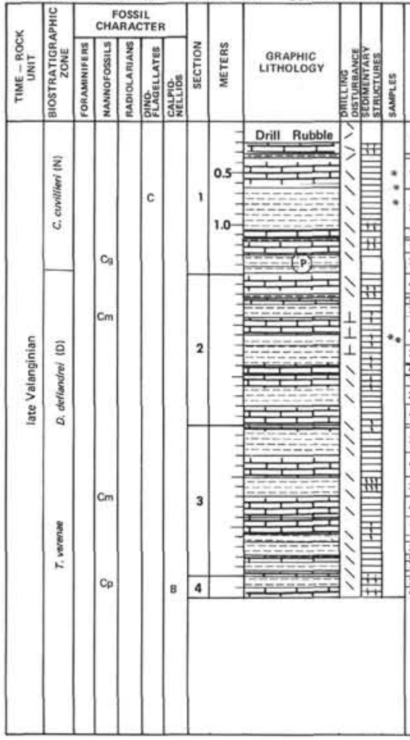

LITHOLOGIC DESCRIPTION

MARLY LIMESTONE, CALCAREOUS CLAYSTONE, CLAYSTONE, and MARLY LIMESTONE

1 – MARLY LIMESTONE, light bluish gray (5B 7/1) to dark greenish gray (5GY 4/1), laminated and highly burrowed.

2 – CALCAREOUS CLAYSTONE, light olive gray (5Y 6/1) to greenish black (5GY 2/1) laminated.

3 – CLAYSTONE, olive gray (5Y 4/1) to greenish black (5G 2/1), massive to moderately laminated.

4 – MARLY LIMESTONE and CHALK, light olive gray (5Y 6/1) to pale yellowish brown (10YR 6/2), laminated.

Note that relative to Cores 65–67 burrowed zones are fragments, c. f. graded claystones. The turbiditic siltstones have completely gone. A minor lithology is claystone greenish gray (5GY 6/1) to dark greenish gray (5G 4/1), massive, cabonaceous is seen at Section 1, 21–23 cm.

SMEAR SLIDE SUMMARY (%):

	1, 50	1, 67	1, 80	2, 62	2, 67
	D	M	D	M	D
Texture:					
Sand	–	–	–	–	10
Silt	5	15	10	20	10
Clay	95	85	90	80	80
Composition:					
Quartz	–	5	2	8	2
Feldspar	–	–	–	TR	–
Mica	–	–	1	5	–
Heavy minerals	–	–	–	1	–
Clay	27	48	50	52	57
Pyrite	1	3	1	2	–
Carbonate unspec.	60	5	15	5	30
Calc. nannofossils	10	35	22	15	15
Plant debris	–	4	–	10	–
Other	2	–	6	2	15

SITE 534 HOLE A CORE 68 CORED INTERVAL 1130.0–1139.0 m

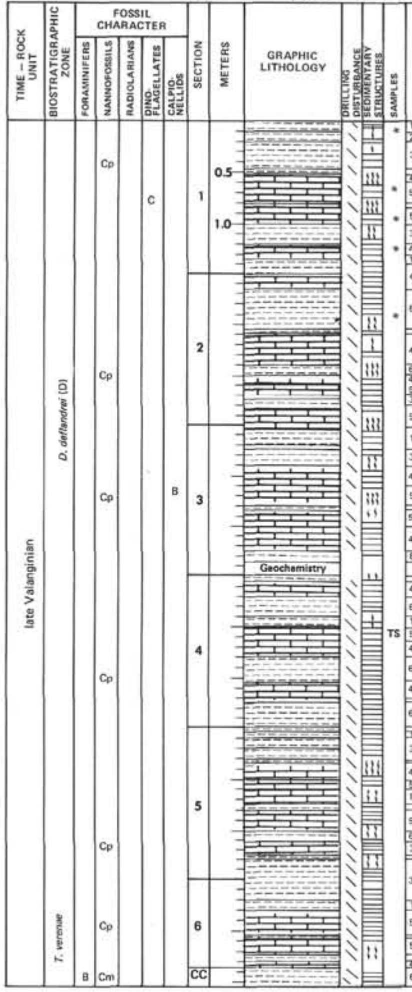

LITHOLOGIC DESCRIPTION

CLAYSTONE, MARLY CLAYSTONE, SILTY CLAYSTONE, MARLY LIMESTONE, LIMESTONE, and CLAYEY LIMESTONE

1 – CLAYSTONE, olive gray (5Y 4/1) to olive black (5Y 2/1), laminated to massive.

2 – MARLY CLAYSTONE, greenish gray (5GY 6/1) to dark greenish gray (5G 4/1), laminated and intensely burrowed.

3 – MARLY SILTY CLAYSTONE, greenish gray (5G 6/1) to greenish black (5GY 2/1), laminated and moderately burrowed.

4 – MARLY LIMESTONE, light olive gray (5Y 6/1) to dark greenish gray (5GY 4/1), laminated.

5 – LIMESTONE, light gray (N7) to light bluish gray (5B 7/1), intensely burrowed with rare laminae.

6 – CLAYEY LIMESTONE, light olive gray (5Y 6/1) to pale yellowish brown (10YR 6/2), laminated.

7 – MINOR LITHOLOGY, claystone, greenish gray (5GY 6/1) to dark greenish gray (5G 4/1), massive, carbonaceous; occurs Section 2, 20–55 cm, Section 3, 130–135 cm, Section 4, 30–44, 85–90, 130–150 cm, Section 5, 130–133, and in Core-Catcher.

A Thin Section at Section 4, 54 cm is a micaceous siltstone with rare micritic intraclasts.

SMEAR SLIDE SUMMARY (%):

	1, 7	1, 68	1, 95	1, 125	2, 42
	D	D	D	D	D
Texture:					
Silt	45	70	40	70	30
Clay	55	80	60	80	70
Composition:					
Quartz	–	–	2	2	1
Feldspar	1	1	–	–	–
Clay	36	68	40	69	38
Pyrite	1	2	–	2	–
Carbonate unspec.	30	13	55	5	55
Calc. nannofossils	3	11	2	17	4
Plant debris	2	2	1	5	1
Dolomite	25	–	–	–	1

SITE 534 HOLE A CORE 69 CORED INTERVAL 1139.0–1148.0 m

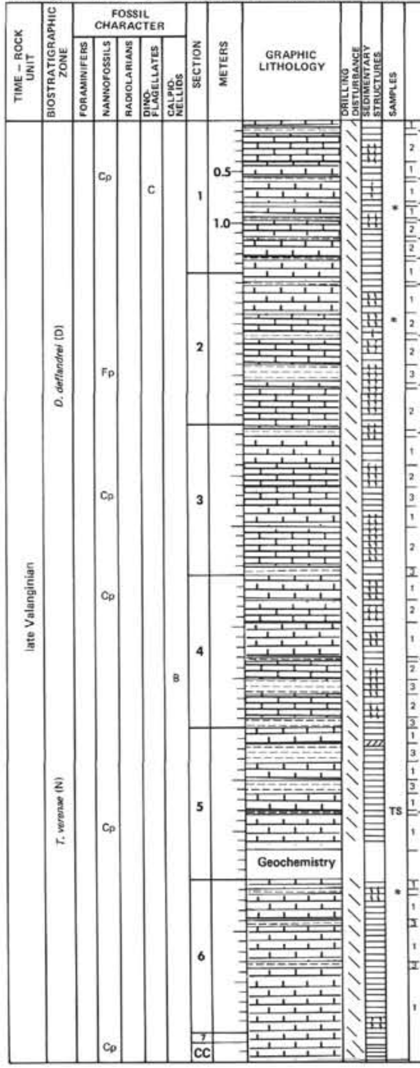

LITHOLOGIC DESCRIPTION

MARLY LIMESTONE, LIMESTONE, and
CALCAREOUS CLAYSTONE

1 – MARLY LIMESTONE, medium light gray (5Y 6/1) to dark grayish green (5GY 4/1) or dark gray (N3) with progressive variations between. Laminae in the darker material are better defined and close spaced. Abundant white particles are calcified radiolaria. Laminae often irregular.

2 – LIMESTONE, very light bluish gray (5B 8/1–N7), intensely has traces of original lamination. Many burrow types. These are often dark bluish gray (5B 4/1) streaks and spots that seem to be associated with burrows (pyritic?). Lithology often grades into into the marly limestone.

3 – CLAYSTONE, black (N1) to greenish black (5G 2/1) carbonaceous nannofossil-rich; frequently with minor laminations. Often has graded silt towards base (turbiditic), is also greenish gray (5GY 6/1) to dark greenish gray (5GY 4/1) homogeneous claystone. Occasionally has small burrows at top. Usually layers <1 cm thick. Normally associated with the darker laminated beds.

Note: A nodule of black chert in Section 7, 5–10 cm.

Thin Section at Section 5, 87–88 cm is a radiolarian calcareous quartzose siltstone with pyrite and phosphatic layers. Many of the radiolaria are pyritized.

SMEAR SLIDE SUMMARY (%):

	1, 87 M	2, 45 D	6, 11 M
Texture:			
Sand	9	–	–
Silt	11	55	30
Clay	80	45	70
Composition:			
Quartz	2	–	–
Clay	75	10	33
Pyrite	3	–	–
Carbonate unspec.	2	86	45
Calc. nannofossils	13	3	6
Plant debris	4	1	1
Other	1	–	15

SITE 534 HOLE A CORE 70 CORED INTERVAL 1148.0–1157.0 m

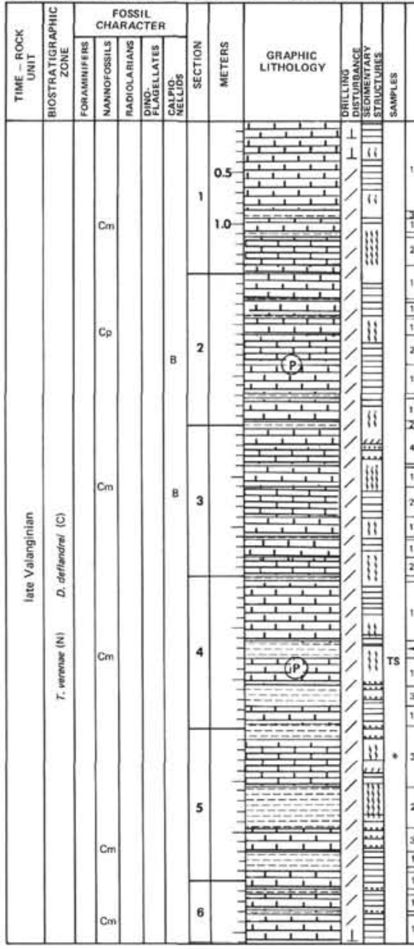

LITHOLOGIC DESCRIPTION

MARLY LIMESTONE and CHALK, LIMESTONE, CLAYSTONE, and CALCAREOUS CLAYSTONE

1 – MARLY LIMESTONE and CHALK, 1) medium light gray (5Y 6/1) and light olive gray. Few, regular, locally swirly laminations. Abundant white particles (micrite elipses) elongated parallel to bedding. 2) Dark gray (N3–N4), densely laminated, white particles again common.

2 – LIMESTONE, light gray to very light gray (N7–N8). Often has traces of original laminations. Grades into marly limestone and chalk. Often has dark bluish gray (5B 4/1) streaks. Often strongly burrowed.

3 – CLAYSTONE, 1) black (N1–N2) to greenish black (5G 2/1), often carbonaceous, and with pyrite nodules. 2) Greenish gray (5GY 5/1) to dark greenish gray (5GY 4/1), homogeneous, but often has burrows at top if adjacent to a burrowed unit.

4 – CALCAREOUS CLAYSTONE, dark greenish gray (5G 3/1), slightly burrowed calcareous claystone, probably a burrowed equivalent of the dark gray marly limestone.

Thin Section at Section 4, 88 cm is a radiolarian micrite. Radiolaria are poorly preserved and replaced by calcite. Where the radiolarian shells are densely parked pressure solution features are evident.

SMEAR SLIDE SUMMARY (%):

	5, 23 M
Texture:	
Silt	20
Clay	80
Composition:	
Quartz	1
Mica	1
Clay	36
Carbonate unspec.	48
Calc. nannofossils	12
Plant debris	2

SITE 534 HOLE A CORE 71 CORED INTERVAL 1157.0–1166.0 m

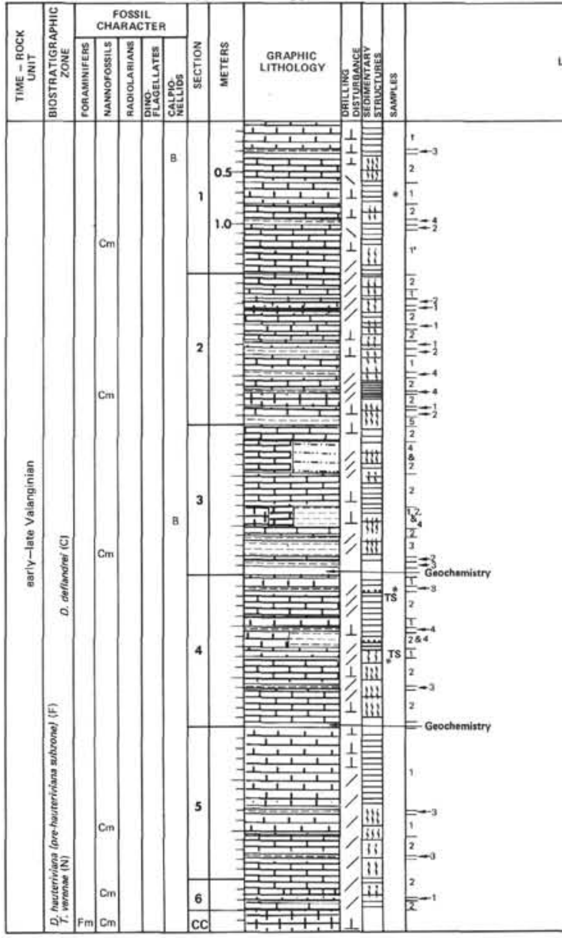

LITHOLOGIC DESCRIPTION

MARLY CHALK, LIMESTONE, CALCAREOUS CLAYSTONE, and CARBONACEOUS CLAYSTONE

1 – MARLY CHALK, medium light gray (N6), medium dark gray (N4), light olive gray (5Y 6/1), even fine laminations with abundant white particles concentrated parallel to laminations. Some a bit darker, olive gray (5Y 4/1) and dark gray (N3), also with white particles.

2 – LIMESTONE, light gray (N7) and light bluish gray (5B 7/1), often with faint lamination, and traces of original bedding.

3 – CALCAREOUS CLAYSTONE, dark greenish gray (5GY 4/1) to grayish olive (10Y 4/2), occurs most often interbedded with limestone.

4 – CLAYSTONE, grayish black (N2), massive or very slightly graded, carbonaceous.

Note that Core 71 contains more burrowed units than Core 70. A few graded intervals may be turbidites; parallel laminated units produced by some type of bottom current.

Thin Section at Section 4, 17–18 cm is a radiolarian micrite. Radiolaria mostly elongate replaced by calcite. Some quartz grains and mica with minor phosphate and pyrite Section 4, 135–137 cm is a dolomitic micrite with numerous dolomite rhombs. Terrigenous component of quartz, mica, and clay.

SMEAR SLIDE SUMMARY (%):

	1, 71 M	4, 16 TS, D	4, 84 TS, M
Texture:			
Silt	10	15	15
Clay	90	85	85
Composition:			
Quartz	2	2	5
Mica	–	1	3
Heavy minerals	1	–	1
Clay	31	17	63
Carbonate unspec.	45	60	5
Calc. nannofossils	20	10	15
Fish remains	–	1	–
Plant debris	TR	3	5
Other	1	8	3

SITE 534 HOLE A CORE 72 CORED INTERVAL 1166.0–1175.0 m

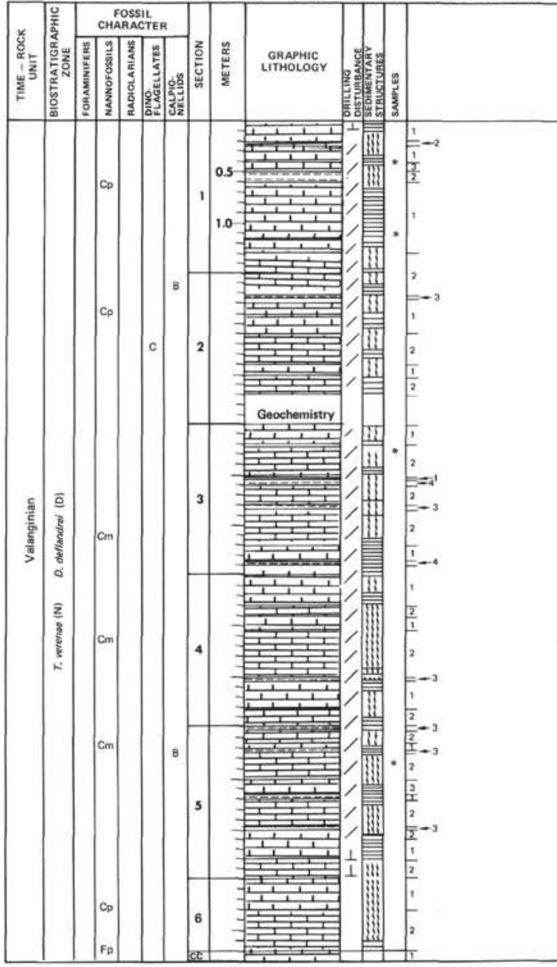

LITHOLOGIC DESCRIPTION

MARLY CHALK, LIMESTONE, CALCAREOUS CLAYSTONE, and CARBONACEOUS CLAYSTONE

1 – MARLY CHALK, 1) medium dark gray (N4) with light olive gray (5Y 6/1); very finely laminated, alternates of darker and lighter laminae 0.3 mm; some laminae carbonaceous; 2) olive gray (5Y 4/1) and dark gray (N3) as above 1) but darker; black (N2) carbonaceous laminae up to 0.3 cm thick.

2 – LIMESTONE, light gray (N7) and light bluish gray (5B 7/1), very highly burrowed, with rare traces of primary lamination, and micro-stylolites; locally pelletoid texture especially within burrows.

3 – CALCAREOUS CLAYSTONE, dark greenish gray (5G 4/1) to grayish olive (10Y 4/2), often graded, few burrows.

4 – CARBONACEOUS CLAYSTONE, black (N2) and dark (N3–N4), massive, unburrowed.

SMEAR SLIDE SUMMARY (%):

	1, 41 D	1, 140 D	3, 28 M	5, 35 D
Texture:				
Sand	–	5	–	–
Silt	5	10	35	10
Clay	95	85	65	90
Composition:				
Quartz	3	–	10	2
Feldspar	1	–	–	–
Mica	–	–	6	–
Heavy minerals	–	–	1	–
Clay	15	45	42	10
Pyrite	1	4	1	–
Carbonate unspec.	60	30	5	73
Calc. nannofossils	20	20	20	10
Plant debris	–	1	15	–
Other	1	–	–	5

SITE 534 HOLE A CORE 73 CORED INTERVAL 1175.0–1184.0 m

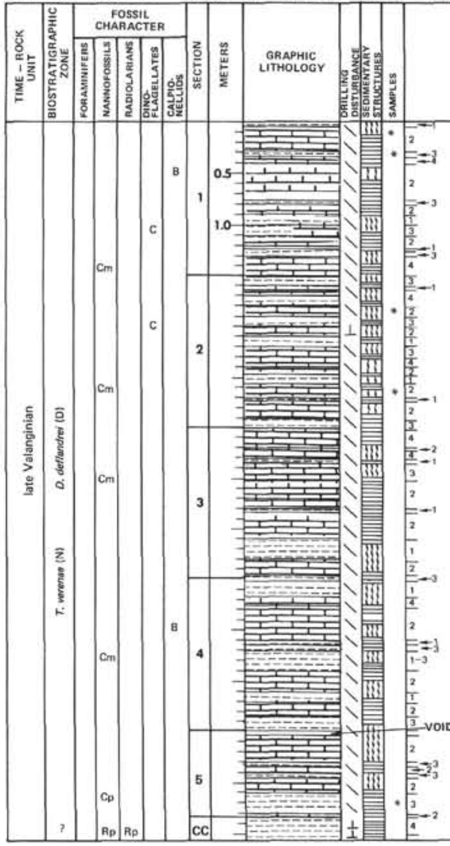

LITHOLOGIC DESCRIPTION

CLAYSTONE, LIMESTONE, CALCAREOUS
CLAYEY LIMESTONE, and MARLY CHALK

1 – CLAYSTONE, olive gray (5Y 4/1) to greenish black (5G 2/1), moderatley laminated and massive.

2 – LIMESTONE, light gray (N7) to light bluish gray (5B 7/1), moderately to intensely burrowed.

3 – CALCAREOUS CLAYSTONE, greenish gray (5G 6/1) to dark greenish gray (5G 4/1), laminated and burrowed, grading into marly chalk.

4 – CLAYEY LIMESTONE, light brownish gray (5YR 6/1) to olive gray (5Y 4/1), laminated. Grades into marly chalk.

Differs from Core 72 with fewer, thinner intervals of burrowed limestone Very little carbonaceous material; more claystone.

SMEAR SLIDE SUMMARY (%):

	1, 10	1, 30	2, 33	2, 115	5, 70
	D	M	D	M	M
Texture:					
Silt	10	10	10	10	10
Clay	90	87	90	90	90
Composition:					
Quartz	–	1	2	–	–
Clay	10	30	20	41	39
Pyrite	–	–	1	1	–
Zeolite	–	–	–	–	2
Carbonate unspec.	85	27	45	7	26
Calc. nannofossils	5	40	25	50	40
Fish remains	–	–	–	–	3
Plant debris	–	2	1	1	3
Other	–	–	5	–	–

SITE 534 HOLE A CORE 74 CORED INTERVAL 1184.0–1193.0 m

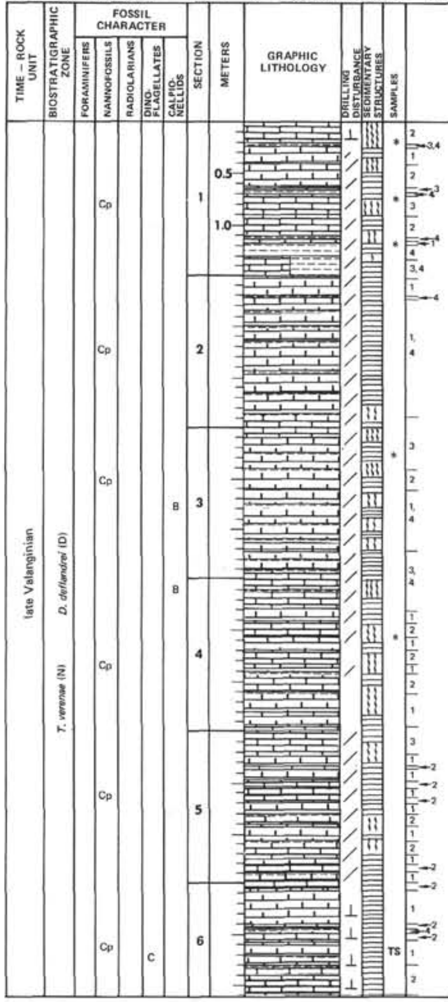

LITHOLOGIC DESCRIPTION

MARLY LIMESTONE, MARLY CHALK, LIMESTONE,
CLAYSTONE, and CARBONACEOUS CLAYSTONE

1 – MARLY LIMESTONE and MARLY CHALK, gray (5Y 6/1) to light gray (5Y 7/1). White particles common (? flattened radiolaria). Occasional macro-bioclast (e. g. shell and aptychi) and burrows dark gray (5Y 4/1). Often has claystone laminae.

2 – LIMESTONE, light gray (N7) to light bluish gray (5B 7/1), burrowed, often darker gray toward base, grading down into laminated marly limestone.

3 – MARLY LIMESTONE, dark gray (5Y 4/1–5Y 5/1), moderately burrowed, intensely associated with claystone laminae. Burrows disrupt the laminated intervals.

4 – CLAYSTONE, black (N1) to dark gray (N2) to (5Y 3/1) often carbonaceous. Also dark greenish gray (5GY 4/1) to greenish gray (5G 5/1). Claystones are homogeneous with rare chondrite burrows and other minor bioturbation at top, and often have graded siltstone (dark gray) below which is microcross-laminated. Core 74 has more carbonaceous material than Core 75.

The Thin Section at Section 6, 71–73 cm is a clay-rich radiolarian micrite. Radiolarians are strongly flattened and replaced by calcite.

SMEAR SLIDE SUMMARY (%):

	1, 20	1, 74	1, 119	3, 26	4, 58
	M	M	D	M	M
Texture:					
Sand	1	1	10	3	2
Silt	14	9	20	13	8
Clay	85	90	70	84	90
Composition:					
Quartz	1	–	4	–	3
Feldspar	–	–	1	–	–
Mica	–	–	–	–	1
Heavy minerals	–	–	2	–	1
Clay	45	42	43	38	6
Pyrite	–	–	3	1	2
Carbonate unspec.	20	25	7	19	21
Calc. nannofossils	30	30	30	40	29
Plant debris	4	3	10	2	7

SITE 534 HOLE A CORE 75 CORED INTERVAL 1193.0–1202.0 m

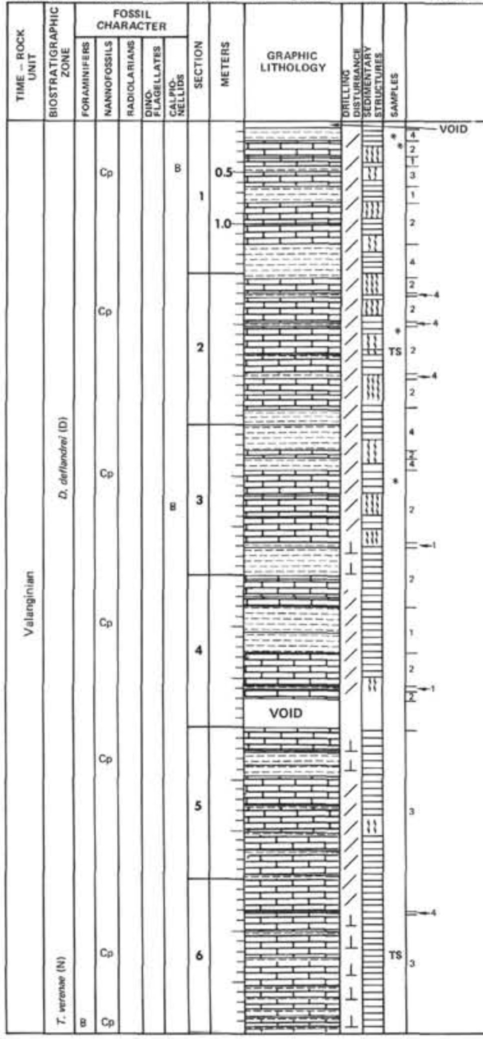

LITHOLOGIC DESCRIPTION

CALCAREOUS CLAYSTONE, LIMESTONE, and MARLY CHALK

1 – CALCAREOUS CLAYSTONE, olive gray (5Y 4/1) with laminae of light olive gray (5Y 6/1) and massive cm layers of olive black (5Y 2/1), grades into marly chalk.

2 – LIMESTONE, light bluish gray (5B 7/1) to light olive gray (5Y 6/1). Laminae visible, but always intensely burrowed.

3 – LIMESTONE, light olive gray (5Y 6/1) to olive gray (5Y 4/1), as above but finely laminated, with massive claystone partings up to 1 cm thick.

4 – MASSIVE CLAYSTONE, olive gray to dark greenish gray (5Y 4/1–5GY 4/1) and olive gray (5Y 4/1) to greenish black ((5G 2/1). Burrowed limestones still abundant in Core 76, but little carbonaceous material. Intensity of burrowing decreases down the core.

Thin Section at Section 2, 82–83 cm is a radiolarian micrite in which most of the radiolaria are replaced by calcite, a few are pyritized. At Section 6, 80 cm is a radiolarian calcareous claystone with calcite and pyrite-replaced radiolarian in a dense clay matrix.

SMEAR SLIDE SUMMARY (%):

	1, 19 D	1, 22 M	2, 58 M	3, 58 D
Texture:				
Sand	2	–	–	–
Silt	18	15	10	30
Clay	80	85	90	70
Composition:				
Quartz	1	1	1	1
Heavy minerals	1	–	1	–
Clay	57	47	65	10
Pyrite	2	2	–	–
Carbonate unspec.	15	20	–	80
Calc. nannofossils	20	25	30	5
Plant debris	–	2	2	1
Other	2	3	1	3

SITE 534 HOLE A CORE 76 CORED INTERVAL 1202.0–1211.0 m

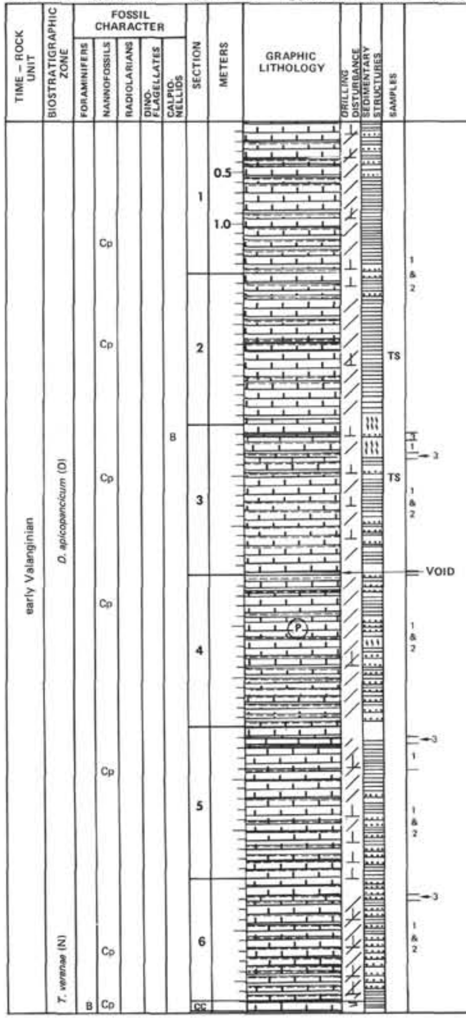

LITHOLOGIC DESCRIPTION

MARLY LIMESTONE and CHALK, LIMESTONE, and CLAYSTONE

1 – MARLY NANNOFOSSIL LIMESTONE and CHALK, gray (5Y 5/1 and 5Y 4/1–5Y 6/1) with abundant calcified radiolaria. Laminae about 1 mm to 1 cm sort of alternating carbonate-rich and clay-rich material. The clay-rich laminae are dark green-gray and organic-rich (Smear Slide Section 4, 15 cm), and resemble the other claystone layers.

2 – CLAYSTONE, dark greenish gray (5GY 4/1 and 5GY 5/1), nannofossil and terrestrial organic-rich, typically 1–2 cm thick, usually has microcross-bedded silty layer beneath and indications of upward grading at base. Well defined intervals (38) this core.

3 – LIMESTONE, light gray (5Y 7/1 and N8) limestone usually shows disrupted laminae. Typically 6 cm in thickness. Three definite and 4 partially developed zones in the 6 sections.

Note this core is marked by return of turbiditic claystones. Core 77 has much more bioturbation. Core 77 is similar to Core 74.

Thin Section: Section 2, 81 cm is a very finely laminated radiolarian micrite. Section 3, 53 cm is a typical radiolarian micrite.

SITE 534 HOLE A CORE 77 CORED INTERVAL 1211.0–1215.5 m

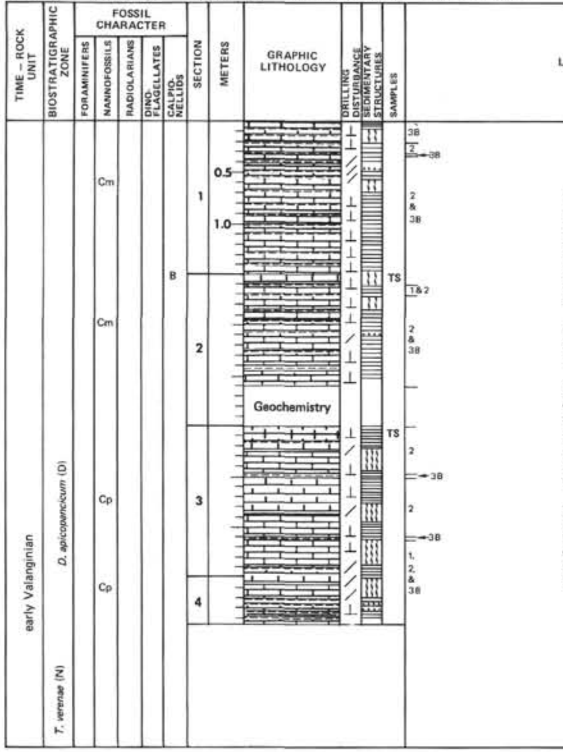

LITHOLOGIC DESCRIPTION

MARLY CHALK, LIMESTONE, CALCAREOUS CLAYSTONE, and CARBONACEOUS CLAYSTONE

1 – MARLY CHALK:
A: medium dark gray (N4) and light olive gray (5Y 6/1), scattered white particles but not as abundant as cores above with alternating light (calcareous) and dark (clay-rich) laminae.

B: dark gray (N3) and olive gray (5Y 4/1) of essentially the same composition, but darker color; tends to occur above the burrowed limestones and marly chalk.

2 – LIMESTONE: light gray (N7) to light bluish gray (5B 7/1) limestone show remnants original laminations and more abundant than in Core 76.

3 – CLAYSTONES:
A: dark gray (N3) to black (N1) massive and organic-rich, several cm thick.

B: dark greenish gray (5G 4/1) to greenish black (5GY 2/1), massive, thinner than the black claystones; rarely has silty laminated base and grading upward appearance (less than Core 76).

Thin Section at Section 2, 15–17 cm is radiolarian micrite. All the radiolarian shells have been dissolved and infilled by sparry calcite. The micritic matrix is partly recrystallized to microspar-size calcita. Section 3, 9–11 cm is a silty micritic limestone, 7% replaced radiolaria, 15% terrigenous, 75% cement, and 3% pyrite.

SITE 534 HOLE A CORE 78 CORED INTERVAL 1218.5–1224.5 m

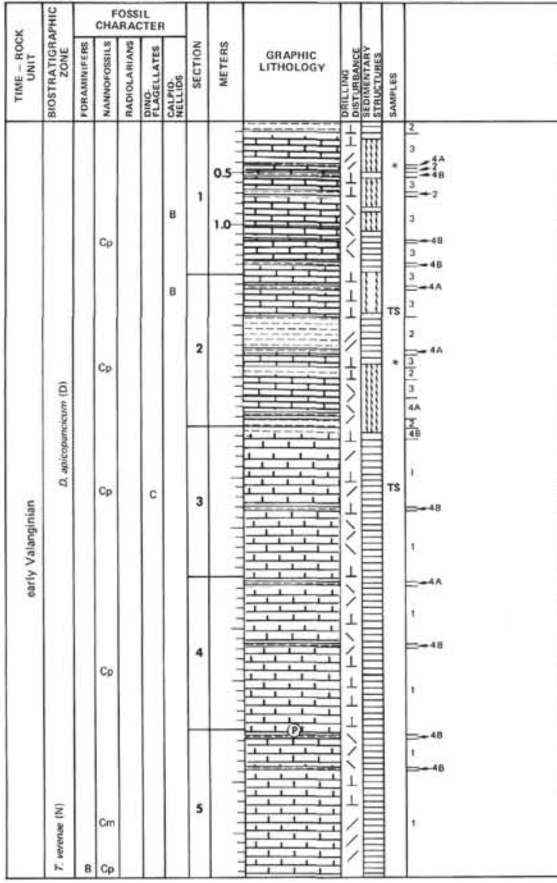

LITHOLOGIC DESCRIPTION

MARLY CHALK, CLAYSTONE, and LIMESTONE

1 – MARLY CHALK, light gray (N7) and light olive gray (5GY 6/1); often with white particles (radiolaria) clay bedding laminae; grades into darker laminated medium dark gray (N6) and olive gray (5Y 4/1).

2 – CLAYSTONE (silty), dark greenish gray (5G 4/1), greenish black (5GY 2/1), medium gray (N5); occurs with green and black claystones; minor intervals of calcareous silty claystone and carbonaceous claystone.

3 – LIMESTONE, light gray (N8) light gray (N7), light bluish gray (5B 7/1) with darker burrow fills and vague laminations.

4 – CLAYSTONE:
A: dark gray (N3) to grayish black (N2) massive, a few cm thick.

B: dark greenish gray (5GY 4/1) to greenish black (5GY 2/1), massive, few cm thick.

Sections 1 and 2 are burrowed and have claystone while Sections 3–5 are uniformly laminated chalks with occasional claystone layers. Much more uniform than previous cores.

Thin Section: Section 2, 33–35 cm is a radiolarian micrite with all the radiolaria replaced by sparry calcite and pyrite. Section 3 at 78 cm is very similar.

SMEAR SLIDE SUMMARY (%):

	1, 42 M	2, 139 M
Texture:		
Silt	20	15
Clay	80	85
Composition:		
Quartz	5	3
Mica	3	1
Clay	63	42
Carbonate unspec.	5	10
Calc. nannofossils	15	40
Plant debris	4	2
Other	3	1

SITE 534 HOLE A CORE 79 CORED INTERVAL 1224.5–1233.5 m

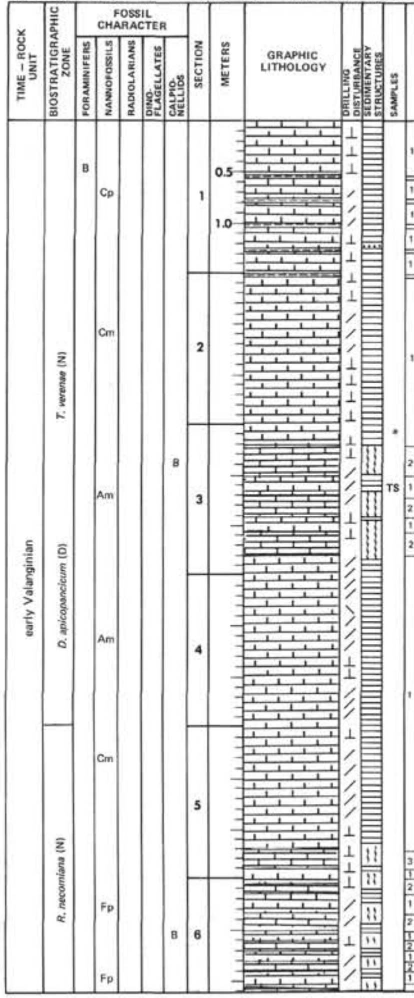

LITHOLOGIC DESCRIPTION

MARLY CHALK, LIMESTONE, and CLAYSTONE

1 – MARLY CHALK, light gray (N7) and light olive grey (5Y 6/1), uniformly and finely laminated with rare fossils and scattered white particles (calcified radiolaria); varies to darker laminite, medium olive gray (N4) and olive gray (5Y 4/1).

2 – LIMESTONE, light gray (N7) to light bluish gray (5B 7/1), massive bioturbated, generally with vague and wavy laminations.

3 – CLAYSTONE, dark gray (N3) to grayish black (N2), massive, may be coarser and somewhat graded at base, occur only in first 2 sections.

The first 2 sections continue trend of Core 78 in that they have no burrowed units. There is no green clay after Section 2 and no black claystone in this core.

A Thin Section of the limestone (Section 3, 71–73 cm) is a radiolarian micrite. Radiolaria are quite well preserved and replaced by calcite; rare quartz grains, mica, and minor phosphate. Several of the laminae are densely packed with radiolaria, others are more scattered.

SMEAR SLIDE SUMMARY (%):

	3, 10 D
Texture:	
Sand	2
Silt	3
Clay	95
Composition:	
Quartz	1
Feldspar	1
Mica	1
Heavy minerals	1
Clay	43
Carbonate unspec.	30
Calc. nannofossils	20
Plant debris	3

SITE 534 HOLE A CORE 80 CORED INTERVAL 1233.5–1242.5 m

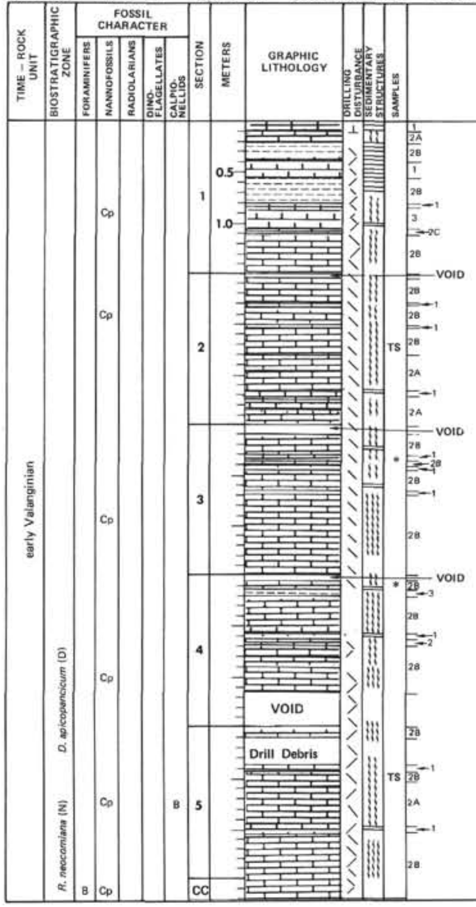

LITHOLOGIC DESCRIPTION

MARLY CHALK, LIMESTONE, and CLAYSTONE

1 – MARLY CHALK, light olive gray (5Y 6/1) to olive gray (5Y 4/1) and brownish gray (5YR 4/1) laminated, sometimes dark greenish gray (5G 4/1). Smear slides nannofossil-rich.

2 – LIMESTONE:

A: very light gray (N8), to light bluish gray (5B 7/1), intensely burrowed and sometimes with laminae.

B: pinkish gray (5YR 8/1) and greenish gray (5GY 6/1) laminated in places, intensely burrowed.

C: pinkish gray (5YR 8/1) and greenish gray (5GY 6/1) laminated.

3 – CLAYSTONE, olive gray (5Y 4/1) to greenish black (5G 2/1).

4 – SILTY LIMESTONE (minor lithology), greenish gray (5G 6/1) to dark greenish gray (5G 4/1), laminated and intensely burrowed.

By contrast Core 81 is mostly well laminated with little burrowed limestone. A Thin Section at Section 5, 47 cm is a micritic limestone with occasional pyritized radiolaria. Section 2, 79–81 cm is also a radiolarian micrite. Some radiolaria infilled by micrite, others with sperry calcite. Very densely packed radiolarian zones may result from current winnowing.

SMEAR SLIDE SUMMARY (%):

	2, 65 D	3, 35 D	4, 19 D
Texture:			
Sand	–	1	1
Silt	1	10	10
Clay	99	89	89
Composition:			
Quartz	–	2	2
Feldspar	1	1	1
Heavy minerals	1	3	3
Clay	62	20	50
Carbonate unspec.	30	24	10
Calc. nannofossils	5	50	29
Plant debris	1	–	5

SITE 534 HOLE A CORE 81 CORED INTERVAL 1242.5–1251.5 m

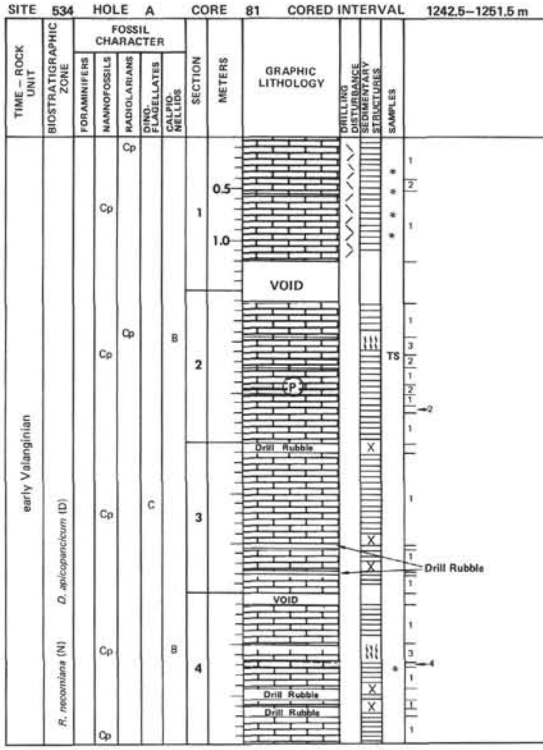

LITHOLOGIC DESCRIPTION

LIMESTONE, CLAY-RICH LIMESTONE, and CLAYSTONE

1 – LIMESTONE, light brownish gray (5YR 6/1) and light olive gray (5Y 6/1) with laminae of dark greenish gray (5GY 4/1).

2 – LIMESTONE, olive gray (5Y 4/1) to olive black (5Y 2/1) with laminae of light olive gray (5Y 6/1).

3 – LIMESTONE, very light gray (N8) to dark greenish gray (5G 4/1) laminated and burrowed at top and base; intensely burrowed inbetween.

4 – CLAYSTONE (minor lithology), dark greenish gray (5G 4/1) and olive black (5Y 2/1).

Core 82 by contrast contains much more pure limestone. Thin Section at Section 2, 79–81 cm is a radiolarian micrite. Radiolaria are replaced with micrite or sparry calcite, a few pyritized. Minor phosphate (? base debris). Some laminations are densely packed with radiolaria.

SMEAR SLIDE SUMMARY (%):

	1, 35	1, 53	1, 79	1, 94	4, 77
	D	D	M	D	M
Texture:					
Sand	–	2	1	5	2
Silt	5	5	2	7	4
Clay	95	83	97	88	94
Composition:					
Quartz	1	1	2	7	1
Feldspar	1	1	1	1	1
Heavy minerals	–	2	1	1	1
Clay	82	40	61	70	41
Carbonate unspec.	5	2	5	10	54
Calc. nannofossils	10	50	30	10	50
Plant debris	1	5	1	1	2

SITE 534 HOLE A CORE 82 CORED INTERVAL 1251.5–1260.5 m

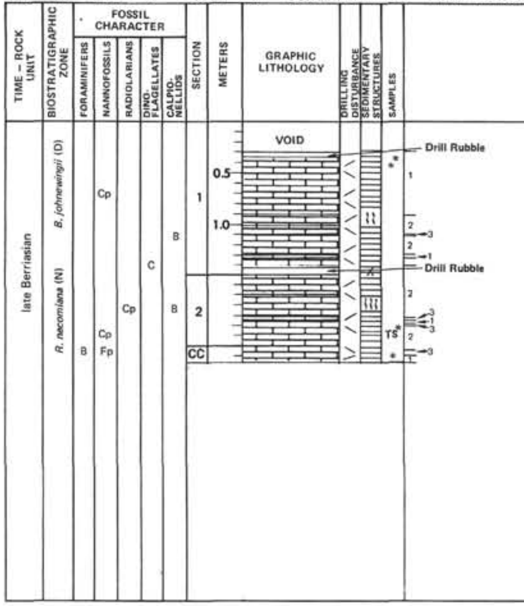

LITHOLOGIC DESCRIPTION

LIMESTONE and CLAY-RICH LIMESTONE

1 – LIMESTONE, light brownish gray (5YR 6/1) and olive gray (5Y 6/1) with dark greenish gray (5GY 4/1), laminated. Sometimes wavy laminae occur near gradational contacts with bioturbated limestones.

2 – LIMESTONE, very light gray (N8) to dark greenish gray (5G 4/1), moderately to intensely burrowed.

3 – CLAY-RICH LIMESTONE, olive gray (5Y 4/1) to olive black (5Y 2/1) with light olive gray (5Y 6/1), laminated.

Smear slides all contain abundant calcareous nannofossils. Thin Section (Section 2, 40–42 cm) is a radiolarian micrite with very fine shell fragments and numerous radiolaria replaced by calcite. Some of the radiolaria are flattened. Micro-stylolites around some of the radiolarian shells.

SMEAR SLIDE SUMMARY (%):

	1, 32	1, 44	2, 55	CC
	D	D	M	D
Texture:				
Silt	17	14	17	7
Clay	83	86	83	93
Composition:				
Quartz	6	5	4	2
Clay	47	48	49	43
Carbonate unspec.	7	6	7	13
Calc. nannofossils	40	41	42	40

SITE 534 HOLE A CORE 83 CORED INTERVAL 1260.5–1268.0 m

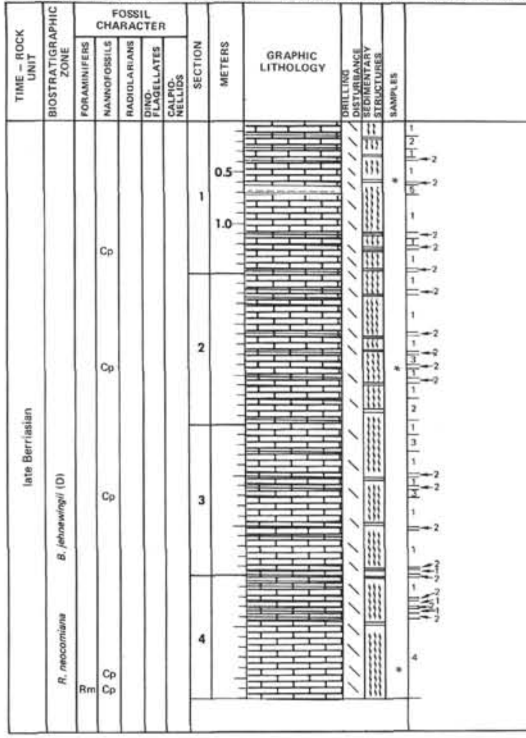

LITHOLOGIC DESCRIPTION

LIMESTONE, CLAY-RICH LIMESTONE, and SILTSTONE

1 – LIMESTONE, light bluish gray (5B 7/1) to light greenish gray (5GY 8/1) to light gray (N7) to greenish gray (5GY 6/1), hard and finely well-cemented calcilutite which is moderately to highly burrowed. Burrow-fill interval often light gray (N7) to medium gray (N5). In places a nodular texture is present, nodules up to 1.5 cm in diameter with greenish gray streaks around edges (? pressure solution effects). Virtually unlaminated.

2 – LIMESTONE, light olive gray (5Y 6/1) greenish gray (5GY 6/1), olive gray (5Y 4/1), brownish gray (5YR 4/1) and intermediate. A few shells and aptici. Several dark ?carbonaceous laminae – finely laminated, and few burrows.

3 – LIMESTONE, mixed type of 1 and 2. Highly burrowed, but original lamination still visible.

4 – LIMESTONE, as in 1 but more oxidized, grayish red (5R 4/2) to moderate red (5R 4/6) to grayish orange pink (10R 8/2).

5 – SILTSTONES, mixed, light olive gray (5Y 6/1).

SMEAR SLIDE SUMMARY (%):

	1, 61	1, 22	4, 94
	D	D	D
Texture:			
Sand	–	–	1
Silt	3	7	2
Clay	97	93	97
Composition:			
Quartz	4	–	1
Heavy minerals	–	–	1
Clay	52	64	15
Carbonate unspec.	17	9	12
Calc. nannofossils	27	27	70
Plant debris	–	–	1

SITE 534 HOLE A CORE 84 CORED INTERVAL 1286.0–1277.0 m

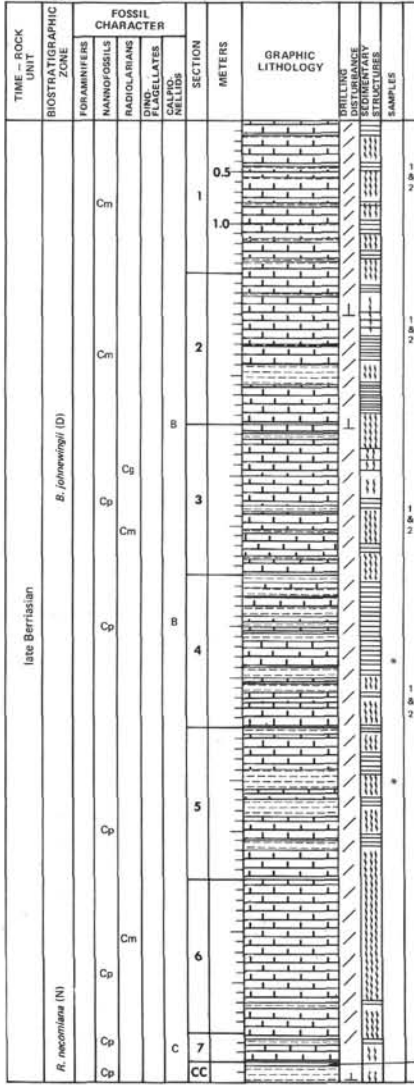

LITHOLOGIC DESCRIPTION

MARLY NANNOFOSSIL CHALK and NANNOFOSSIL CHALK

1 – MARLY NANNOFOSSIL CHALK, greenish gray (5GY 6/1) to 5G 5/1), transitional to limestone and very heavily burrowed. Burrows can be both darker and lighter in tint than the host sediments. In most cases bioturbation has severely disrupted and original laminated texture. A variety of burrow types.

2 – NANNOFOSSIL CLAYSTONE, dark greenish gray (5GY 4/1 and 5Y 4/1). Laminae of clay-rich material are spaced about 0.5–0.3 mm apert. Occasionally a clay-rich layer is up to 1.5 mm thick (rare).

These two lithologies smoothly alternate with about a 20–50 cm spacing between laminated zones. The main lithology is therefore both 1 and 2 combined, some more distinct towards base of core. No hint of red tints seen in core.

SMEAR SLIDE SUMMARY (%):

	4, 84	5, 52
	D	D
Texture:		
Sand	1	1
Silt	2	2
Clay	97	97
Composition:		
Quartz	2	2
Mica	1	TR
Heavy minerals	–	2
Clay	25	30
Carbonate unspec.	5	5
Calc. nannofossils	66	60
Plant debris	1	1

SITE 534 HOLE A CORE 85 CORED INTERVAL 1277.0–1286.0 m

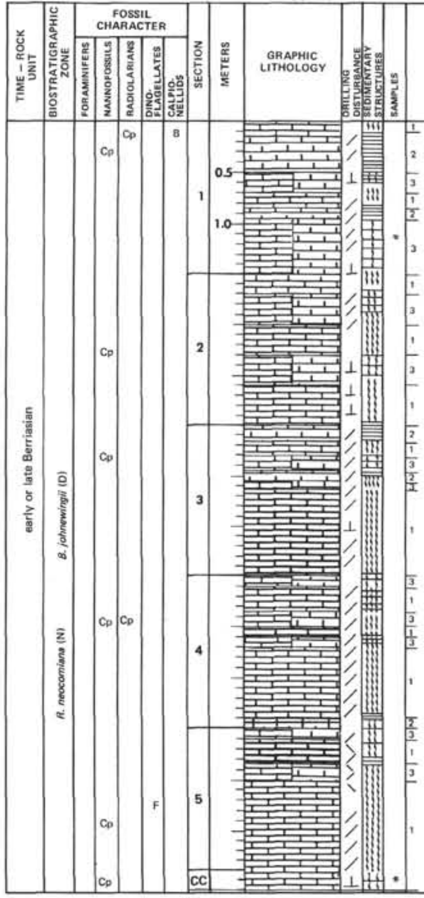

LITHOLOGIC DESCRIPTION

LIMESTONE and NANNOFOSSIL CHALK

1 – LIMESTONE, bluish white (5B 9/1) to light bluish gray (5B 7/1) to light greenish gray (5GY 8/1); highly burrowed and vaguely laminated. Laminations which are present are dark greenish to gray (5G 4/1) clay-rich, and reach 1–2 cm in width, though usually are 1–3 mm.

2 – MARLY NANNOFOSSIL-CHALK, light olive gray (5Y 6/1) and olive gray (5Y 4/1) to greenish gray (5G 6/1) and medium bluish gray (5B 5/1); well-laminated.

3 – Combination of 1 and 2, burrowed but laminations clearly visible. In Section 1, 85 cm a microfault. Section 2, 75 cm has incipient micronodule texture, Section 4, 8–100 cm has stylolites and micro-faults. In general, the limestones become purer and more abundant downward in the core.

SMEAR SLIDE SUMMARY (%):

	1, 111	CC
	M	D
Texture:		
Silt	15	10
Clay	85	90
Composition:		
Quartz	1	1
Mica	1	1
Heavy minerals	–	1
Clay	51	25
Glauconite	1	–
Carbonate unspec.	15	65
Calc. nannofossils	25	7
Diatoms	1	–
Radiolarians	1	2
Fish remains	1	–
Plant debris	3	TR

SITE 534 HOLE A CORE 86 CORED INTERVAL 1286.0–1295.0 m

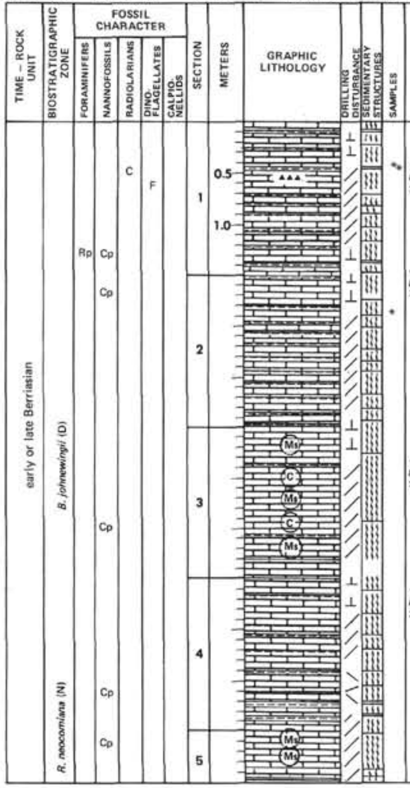

LITHOLOGIC DESCRIPTION

LIMESTONE and CLAYSTONE

1 – LIMESTONE, bluish white (5B 9/1) to very light gray (N8) limestone. Chondrites especially noticible. May show incipient micronodules structure, microfaults and microstylolites. Vague laminations of dark green color, very fine (< 1 mm) clay laminae. Laminations are usually wavy and may be cut by other laminations, no obvious grading or other sedimentary structures.

2 – CLAYSTONE, dark greenish gray (5GY 4/1), usually <0.5 cm in width. Bottoms and tops normally sharp and pass into a series of thinner laminations.

Section 1, 54 cm, gray vitreous chalcedonic quartz chert nodule. Section 3, 60 cm, micronodular texture. This core continues the trend of Core 84. All laminated chalks have disappeared.

SMEAR SLIDE SUMMARY (%):

	1, 40	1, 46	2, 38
	D	M	M
Texture:			
Sand	1	2	3
Silt	4	4	7
Clay	95	94	90
Composition:			
Quartz	–	1	3
Feldspar	–	–	2
Mica	–	–	1
Clay	39	64	49
Carbonate unspec.	30	15	17
Calc. nannofossils	30	30	28

SITE 534 HOLE A CORE 87 CORED INTERVAL 1295.0–1304.0 m

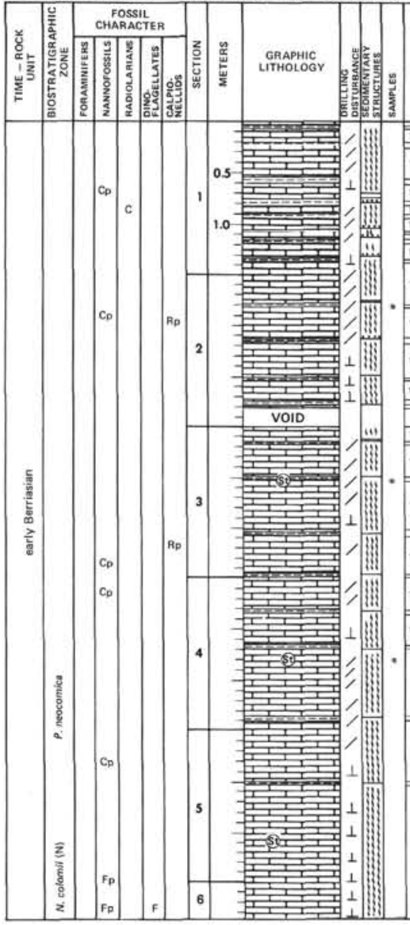

LITHOLOGIC DESCRIPTION

LIMESTONE and CLAYSTONE

1 – LIMESTONE, light gray (N8) to light gray (N7) moderately to highly burrowed, locally micronodular often with medium to dark gray (N3) claystone laminae which are wavy and anastomosing. These laminae are composed of claystone.

2 – CLAYSTONE, dark greenish gray (5GY 2/1) calcareous, merges with limestone. A few thin beds are graded and parallel-laminated over 1–2 mm at base. These are partially turbiditic.

Stylolites prominent in Section 3, 87 cm and Section 5, 87–97 cm.

SMEAR SLIDE SUMMARY (%):

	2, 32	3, 52	4, 84
	M	M	M
Texture:			
Silt	15	30	15
Clay	85	70	85
Composition:			
Quartz	1	2	1
Mica	2	2	2
Heavy minerals	1	–	–
Clay	60	49	45
Pyrite	2	–	–
Carbonate unspec.	20	35	10
Calc. nannofossils	10	10	40
Fish remains	1	–	1
Plant debris	3	2	1

SITE 534 HOLE A CORE 88 CORED INTERVAL 1304.0–1313.0 m

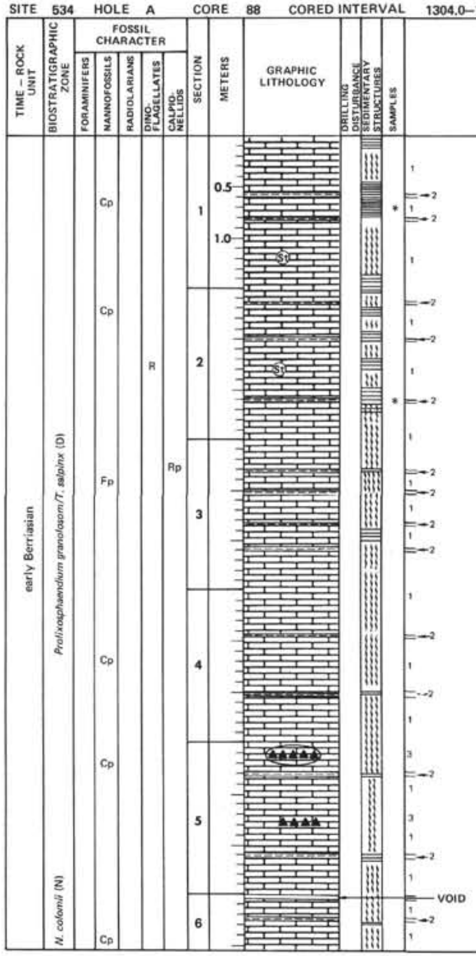

LITHOLOGIC DESCRIPTION

LIMESTONE, CALCAREOUS CLAYSTONE, and CHERT

1 – LIMESTONE (major lithology), very light gray (N8) to greenish gray (5GY 6/1) and light bluish gray (5B 7/1), moderate to intense burrowing with varying amounts of lamination. Stylolites present throughout the core.

2 – CALCAREOUS CLAYSTONE (minor lithology), greenish gray (5G 6/1) to dark greenish gray (5G 4/1), sometimes burrowed but mostly laminated. Most of the minor laminae appear to be composed of this lithology. All laminae are somewhat wavy, often stylolitic.

3 – CHERT (minor lithology), light gray (N7) to light bluish gray (5B 7/1), slightly mottled, vitreous, chalcedonic chert formed by replacement.

Facies similar to Cores 87 and 89.

SMEAR SLIDE SUMMARY (%):

	1 70 M	2, 111 M
Texture:		
Silt	15	10
Clay	85	90
Composition:		
Quartz	2	2
Feldspar	1	–
Mica	1	1
Clay	62	70
Carbonate unspec.	25	20
Calc. nannofossils	8	5
Plant debris	1	1
Other	–	1

SITE 534 HOLE A CORE 89 CORED INTERVAL 1313.0–1322.0 m

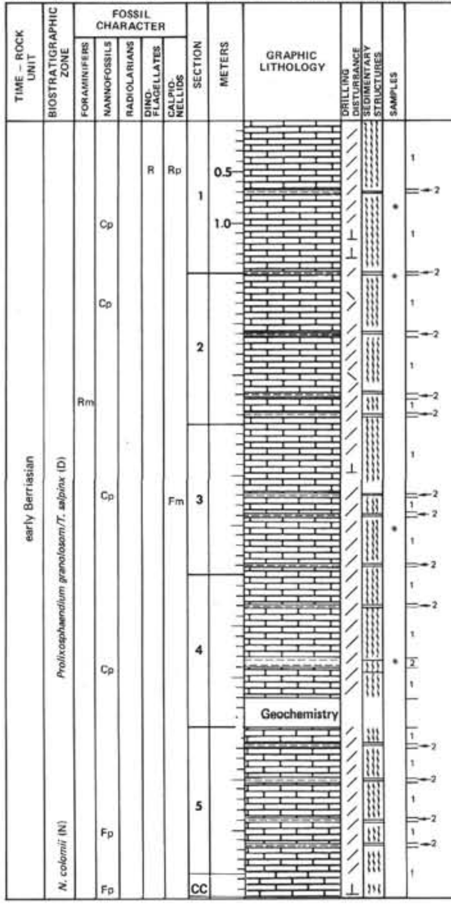

LITHOLOGIC DESCRIPTION

LIMESTONE and CALCAREOUS CLAYSTONE

1 – LIMESTONE (major lithology), very light gray (N8) to greenish gray (5GY 6/1) and light bluish gray (5B 7/1), moderate to intense burrowing. Stylolites present throughout the core.

2 – CALCAREOUS CLAYSTONE (minor lithology), greenish gray (5GY 6/1), to dark greenish gray (5GY 6/1), laminated. Most laminae in the limestone are composed of this lithology. Laminae are mostly wavy.

Section 3, 63 cm, is a possible microbreccia of unknown origin.

SMEAR SLIDE SUMMARY (%):

	1, 89 D	2, 7 D	3, 103 D	4, 87 D
Texture:				
Silt	25	25	25	25
Clay	75	75	75	75
Composition:				
Mica	1	1	1	2
Clay	71	–	58	45
Zeolite	2	1	–	1
Carbonate unspec.	20	25	35	35
Calc. nannofossils	5	5	5	15
Fish remains	–	–	–	1
Plant debris	1	1	1	1

SITE 534 HOLE A CORE 90 CORED INTERVAL 1322.0–1331.0 m

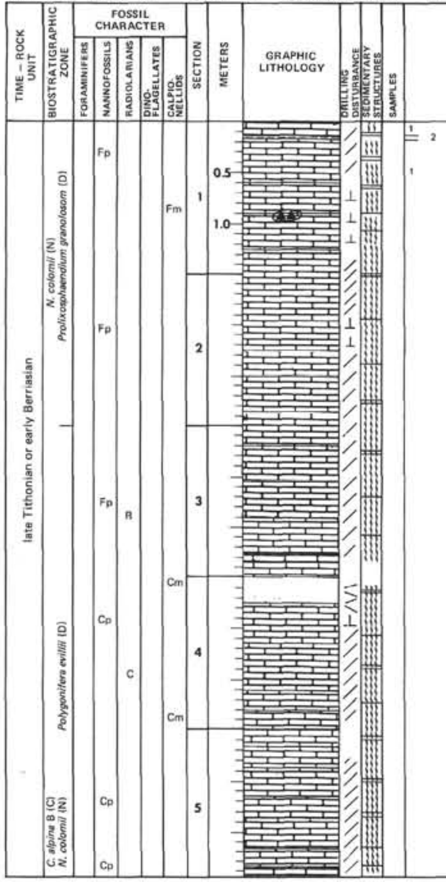

LITHOLOGIC DESCRIPTION

LIMESTONE, CALCAREOUS CLAYSTONE, and CHERT

1 – LIMESTONE (major lithology), very light gray (N8) to bluish white (5B 9/1), bioturbated, with chondrites, stylolites, and a few laminae of green clay. A lesser amount is more greenish (light greenish gray [5B 7/1]) and has more vertical-type burrows, more incipient nodular texture and more laminae of green clay.

2 – CALCAREOUS CLAYSTONE (minor lithology), mostly chalk greenish gray (5G 4/1) varying to greenish black (5GY 2/1) with some brownish gray (5YR 4/1) tints; massive to laminated (usually wavy), thin stringers usually anastomosing.

3 – CHERT (minor lithology), light bluish gray (5B 7/1) nodules of vitreous replacement chert.

Section 2, 20–30 cm; chondrites very abundant. Section 4, 90–95 cm, is a microbreccia. Section 5, 70–90 cm has a micronodular texture. Base of core becomes more greenish otherwise like Core 89.

SITE 534 HOLE A CORE 91 CORED INTERVAL 1331.0–1340.0 m

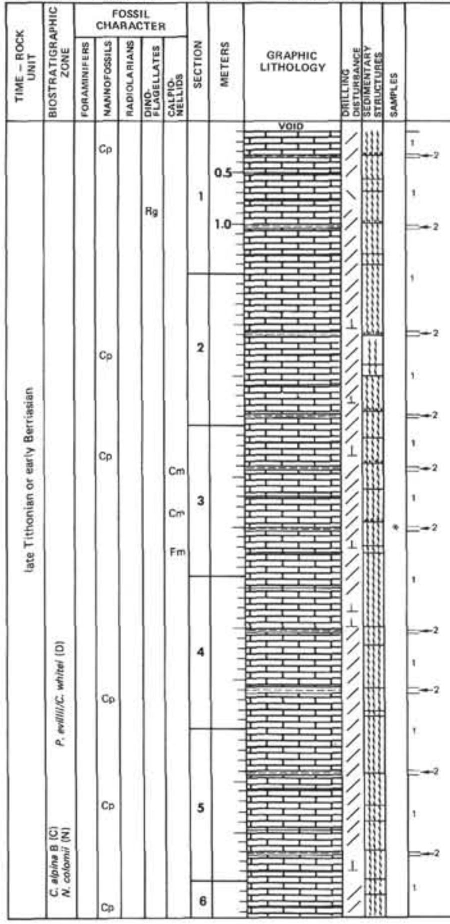

LITHOLOGIC DESCRIPTION

LIMESTONE and CALCAREOUS CLAYSTONE

1 – LIMESTONE (major lithology), two color types, 1) very light gray (N8) to bluish white (5B 9/1) and 2) light greenish gray (5G 8/1) to light bluish gray (5B 7/1). Both are extensively burrow mottled; the darker type has more clay stringers and more stylolites. The greenish color is probably clay.

2 – CALCAREOUS CLAYSTONE (minor lithology), dark greenish gray (5G 4/1). Massive to laminated, both plane and wavy, thin anastomosing stringers.

Section 2, 130–140 cm: has an incipient micronodular texture; Section 3, 135–140 cm, contorted clay seam is possibly a slump structure; Section 9, 50–55 cm, microfaults; Section 5, 91 cm, light bluish white siliceous limestone(?) proto-chert nodule; 122–127 cm partially silicified limestone with a microslumped structure.

SMEAR SLIDE SUMMARY (%):

	3, 100 M
Texture:	
Silt	20
Clay	80
Composition:	
Quartz	1
Mica	2
Heavy minerals	1
Clay	84
Zeolite	1
Carbonate unspec.	15
Calc. nannofossils	25
Plant debris	7

SITE 534 HOLE A CORE 92 CORED INTERVAL 1340.0–1349.0 m

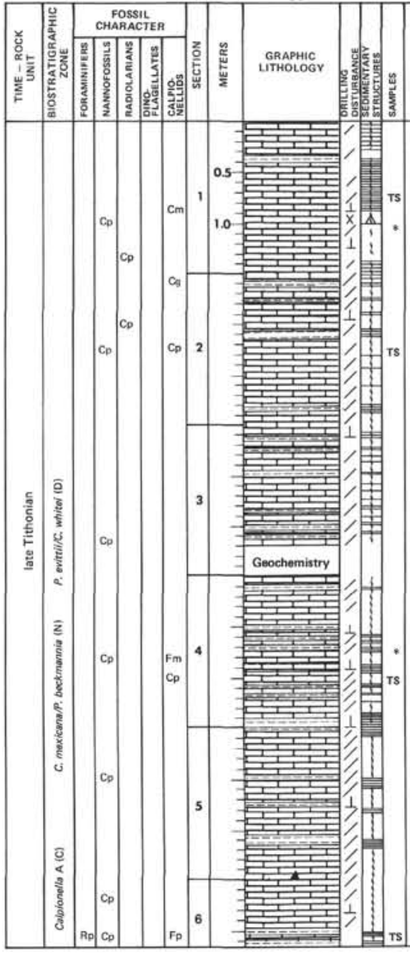

LITHOLOGIC DESCRIPTION

INTERBEDDED LIMESTONE and CLAYSTONE

LIMESTONE (biomicrite) of two color types:
Light gray (N8, N7) to ligh brownish gray (5YR 6/1), with some stylolites.

Pale red (5YR 6/2) to grayish red (5R 5/2), with gray mottling.

Both types are moderately to heavily burrowed, contain calpionellids and spar-replaced radiolarians, and generally have wavy clay seams.

NANNOFOSSIL CLAYSTONE of two color types:
Dark gray (N3, N4).

Dusky red (10R 3/4) to reddish black (10R 2/1).

Both types are finely laminated, have sharp lower contacts, and commonly have diffuse upper contacts to limestones.

The first red coloration is in Section 2, 41 cm; more abundant and dark red colors toward base.

Microbreccia layers (about 1 cm thick) at Section 1, 82 and 129 cm and Section 6, 35 cm.

Siliceous limestone nodules and burrow fillings at Section 1, 110 cm, Section 3, 73 cm, Section 4, 93 and 125 cm, Section 5, 89 and 140 cm, and Section 6, 35 cm. Nodular limestone texture at Section 5, 77–90 cm.

Thin sections of limestones show partial microspar recrystallization of micrite.

SMEAR SLIDE SUMMARY (%):

	4, 73 M	1, 102 M
Texture:		
Silt	15	10
Clay	85	90
Composition:		
Quartz	1	1
Mica	2	2
Clay	58	60
Carbonate unspec.	5	30
Calc. annnofossils	30	5
Fish remains	–	1
Plant debris	2	1
Apatite	2	–

SITE 534 HOLE A CORE 93 CORED INTERVAL 1349.0–1353.5 m

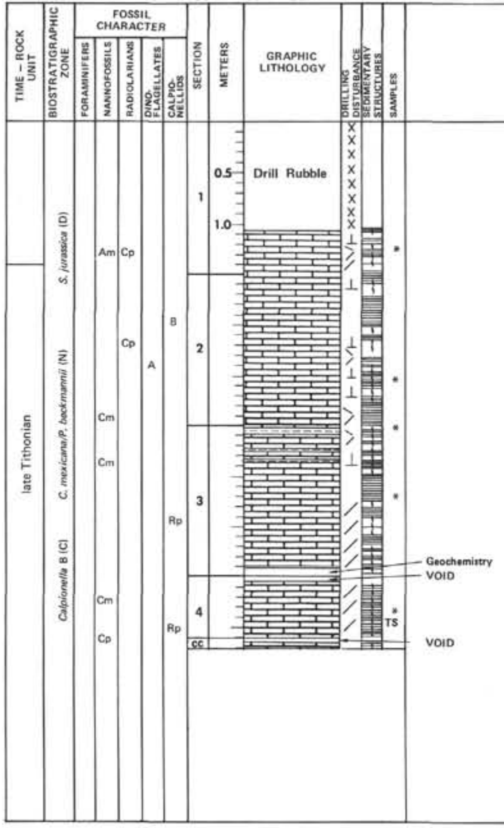

LITHOLOGIC DESCRIPTION

INTERBEDDED LIMESTONE, MARLY LIMESTONE, and CLAYSTONE

LIMESTONE (biomicrite), light gray (N7) to greenish gray (5GY 6/1), moderately to intensely bioturbated.

MARLY LIMESTONE (biomicrite), greenish gray (5GY 6/1, 5GY 5/1), laminated and wavy laminated by clay seams.

MARLY LIMESTONE (biomicrite), pale red (5R 6/2) to grayish red (5R 4/2). Either laminated or intensely bioturbated.

NANNOFOSSIL CLAYSTONE, grayish red (5R 4/2) to very dusky red (10R 2/2), laminated and slightly burrowed.

Limestone and marly limestones contain spar-replaced radiolaria, rare calpionellids, and calcispheres.

(Minor lighology at Section 2, 98–106 cm) nannofossil claystone, dark greenish gray (5GY 4/1), laminated.

Shell fragment *(Inoceramus?)* at Section 3, 47 cm. Laminations dip 10° in Section 2, 120–135 cm. Possible synsedimentary slump at Section 3, 105–110 cm. Siliceous limestone nodules in claystone (type 4) at Section 3, 35–42 cm.

SMEAR SLIDE SUMMARY (%):

	1, 125 D	2, 100 D	3, 7 M	3, 70 D	4, 38 D
Texture:					
Sand	–	–	–	–	2
Silt	15	10	10	20	15
Clay	85	90	90	80	83
Composition:					
Quartz	1	1	1	1	1
Mica	–	1	1	–	–
Heavy minerals	–	1	–	–	–
Clay	48	68	65	35	48
Carbonate unspec.	45	2	4	60	35
Calc. nannofossils	5	25	25	3	15
Fish remains	–	–	1	–	–
Plant debris	–	1	1	–	–
Fe oxide	1	–	2	1	1

SITE 534 HOLE A CORE 94 CORED INTERVAL 1353.5–1362.5 m

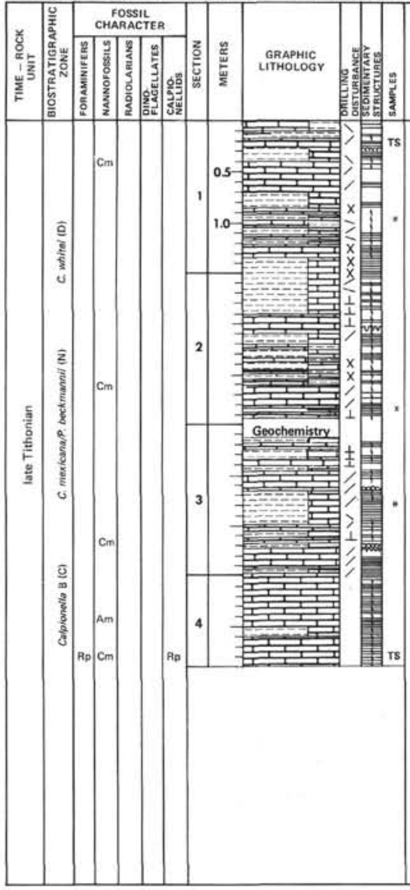

LITHOLOGIC DESCRIPTION

INTERBEDDED CLAYSTONE, MARLY LIMESTONE, and LIMESTONE

CALCAREOUS CLAYSTONE, grayish brown (5YR 3/2) to dusky brown (5YR 2/2) to dark reddish brown (10R 3/4), massive to laminated, moderately fissil, commonly grades into marly chalk.

MARLY LIMESTONE CHALK (biomicrite), pale red (5R 6/2) to grayish red (5R 4/2, 10R 4/2); slightly to moderately bioturbated; commonly mottled with greenish gray (5GY 8/1). Thin sections show 5–20% spar-replaced radiolaria and rare calpionellids in micrite. Radiolaria are flattened and are concentrated in discontinuous laminae. Abundant *Saccocoma*.

LIMESTONE (biomicrite), very light gray (N8) to light bluish gray (5B 7/1), to light greenish gray (5GY 8/1), 5G 8/1, 5GY 6/1); moderately bioturbated with vague wavy clay-rich laminations.

Minor lithology, Section 2, 136–138 cm nannofossil claystone, dark greenish gray (5G 4/1), faintly laminated.

Microbreccia layers (1 cm thick) at Section 3, 101 and 141 cm.

Siliceous limestone nodules, pale red (5R 6/2), elongate, 0.5–1.5 cm in length, Section 2, 39 cm and Section 4, 2 cm.

Nodular textures of limestone and claystone at Section 3, 116–118 and 132–135 cm. Possibly a compaction-boudinage effect.

Shell fragment (aptychus?) at Section 1, 82 cm.

SMEAR SLIDE SUMMARY (%):

	1, 98 D	2, 138 D	3, 80 D
Texture:			
Silt	10	10	15
Clay	90	90	85
Composition:			
Quartz	–	–	1
Mica	–	1	1
Heavy minerals	–	–	TR
Clay	73	75	74
Carbonate unspec.	20	3	3
Calc. nannofossils	6	20	18
Fe oxide	1	1	2

SITE 534 HOLE A CORE 95 CORED INTERVAL 1362.5–1371.5 m

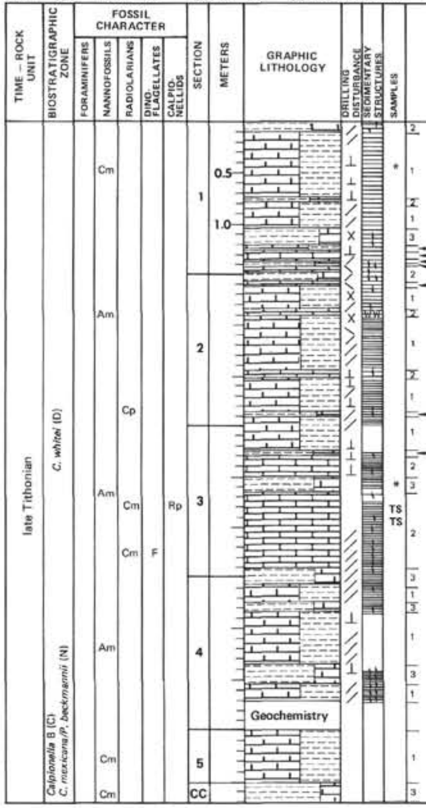

LITHOLOGIC DESCRIPTION

INTERBEDDED CLAYSTONE, LIMESTONE, and MARLY CHALK

1 – CALCAREOUS CLAYSTONE to MARLY NANNOFOSSIL CHALK, grayish red (5R 4/2) to grayish brown (5YR 3/2); mottled and interbedded with greenish gray (5G 6/1–5G 4/1). Generally laminated, but usually slightly to moderately bioturbated (especially chondrites burrows).

2 – LIMESTONE (radiolarian biomicrite), light gray (N7, N6), greenish gray (5GY 6/1), or pale bluish gray (5B 7/1) with dusky blue (5PB 3/2) laminations caused by variable radiolaria/micrite ratios. Thin section has rare calpionellids, calcispheres, and micritized *Saccocoma*. Partial microspar and dolomite recrystallization.

3 – CALCAREOUS CLAYSTONE to MARLY CHALK, greenish gray (5G 6/1) to dark greenish gray (5G 4/1). Laminated and slightly bioturbated.

Claystone to limestone contacts are sharp with occasional burrows at top of limestones.

Laminations dip 5–15° through most of core.

Calcite-filled fractures at Section 1, 103 cm and Section 2, 31–35 and 92–95 cm.

XRD analysis of reddish claystone (lithology 1) at Section 2, 40 cm shows significant aragonite.

SMEAR SLIDE SUMMARY (%):

	1, 45 D	3, 58 D
Texture:		
Silt	15	5
Clay	85	95
Composition:		
Quartz	1	–
Mica	2	2
Clay	46	45
Carbonate unspec.	15	5
Calc. nannofossils	35	45
Plant debris	1	3

SITE 534 HOLE A CORE 96 CORED INTERVAL 1371.5–1380.5 m

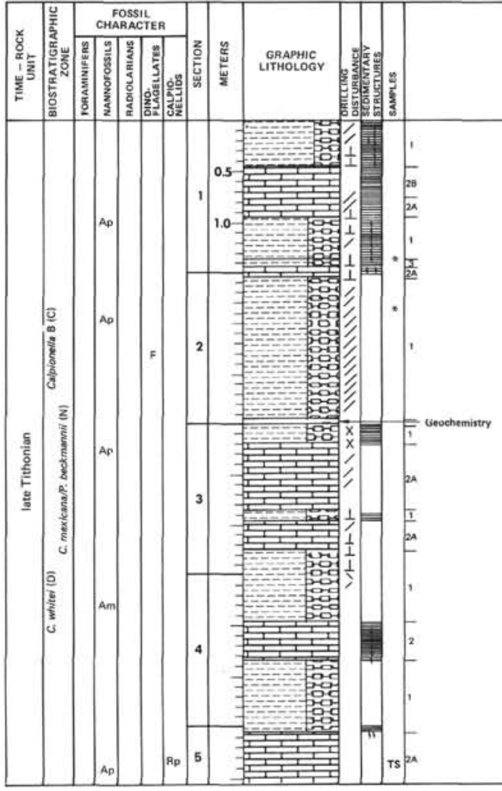

LITHOLOGIC DESCRIPTION

CALCAREOUS CLAYSTONE to MARLY CHALK
with INTERBEDDED LIMESTONE

1 – CALCAREOUS CLAYSTONE to MARLY NANNOFOSSIL CHALK, grayish red (5R 4/2) to grayish brown (5YR 3/2, 5YR 2/2) with mottles and bands of greenish gray (5G 6/1–5G 4/1). Generally laminated with minor bioturbation (especially chondrites burrows).

2 – LIMESTONE (radiolarian biomicrite), moderately bioturbated, vaguely laminated. Two color types:
A: greenish gray (5GY 6/1–5GY 4/1) with interbeds or mottles of light grayish red (5R 4/2–5R 6/2), commonly marly. Thin section has abundant *Saccocoma* and calcified sponge spicules.
B: medium light gray (N6) with dusky blue (5PB 3/2) laminations, minor lithology.

3 – minor lithology Section 1, 137–142 cm – calcareous claystone, dark greenish gray (5G 4/1).

Laminations at Section 1, 65–73 cm dip 10° . Apthycus fragment at Section 1, 107 cm. Burrows are occasionally filled with dark gray to black material.

SMEAR SLIDE SUMMARY (%):

	1, 139	2, 35
	M	D
Texture:		
Silt	15	10
Clay	85	90
Composition:		
Quartz	1	1
Mica	1	1
Clay	62	50
Carbonate unspec.	10	15
Calc. nannofossils	25	30
Fish remains	–	1
Plant debris	1	2

SITE 534 HOLE A CORE 97 CORED INTERVAL 1380.5–1389.5 m

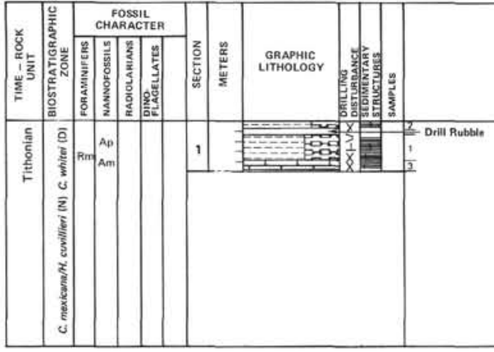

LITHOLOGIC DESCRIPTION

CALCAREOUS CLAYSTONE

1 – CALCAREOUS CLAYSTONE to MARLY LIMESTONE, *grayish red (10R 4/2, 10R 3/2)* laminated to moderately burrowed. Chondrites burrows common.

Minor Lithologies:
2 – Section 1, 0–3 cm: fragment of calcareous clay, very dusky red (10R 2/2).
3 – Section 1, 40–46 cm: fragment of limestone, pale red (5R 6/2) to grayish red (10R 4/2), laminated and slightly burrowed.

SITE 534 HOLE A CORE 98 CORED INTERVAL 1389.5–1395.5 m

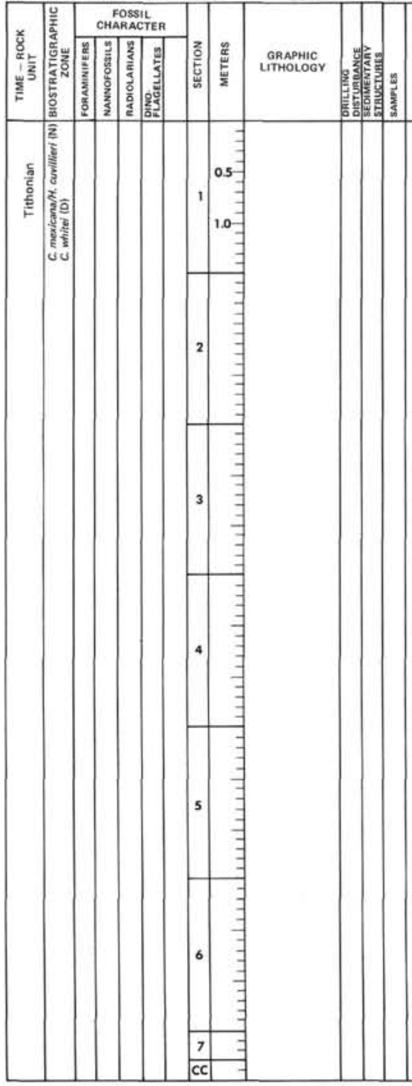

LITHOLOGIC DESCRIPTION

Only a trace of recovery.

SITE 534 HOLE A CORE 99 CORED INTERVAL 1395.5–1401.0 m

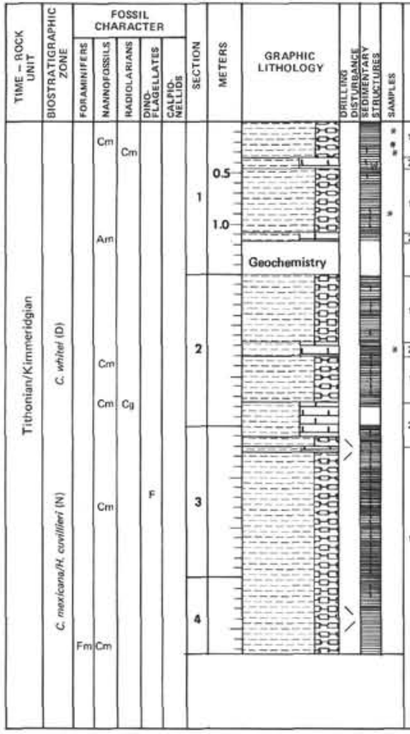

LITHOLOGIC DESCRIPTION

CALCAREOUS CLAYSTONE to MARLY CHALK

1 – CALCAREOUS CLAYSTONE to MARLY CHALK (clayey biomicrite), dark reddish brown (10R 3/4) to very dusky red (10R 2/2) with mottles and bands of dark greenish gray (5G 4/1). Laminated, but commonly with burrows (especially chondrites). Smear slides have variable amounts of nannofossils, dolomite, and needles of possibly aragonite. *Saccocoma* in thin section.

2 – NANNOFOSSIL CLAYSTONE, dark greenish gray to greenish black (5GY 4/1–5GY 2/1); laminated with minor gray burrows.

Minor lithologies:
Section 1, 25–35 cm: dolomitic marly limestone (spare biomicrite), greenish gray (5GY 6/1) to olive gray (5Y 4/1), laminations of variable clay content. Thin section has flattened radiolaria and rare fragments of bivalve shells.

Section 2, 132–147 cm: carbonaceous calcareous claystone, greenish black (5G 2/1), laminated.

SMEAR SLIDE SUMMARY (%):

	1, 10 D	1, 22 D	1, 30 M	1, 90 D	2, 75 M
Texture:					
Silt	30	20	20	10	10
Clay	70	80	80	90	90
Composition:					
Quartz	3	2	1	–	1
Mica	1	–	–	–	1
Clay	26	42	57	63	60
Pyrite	9	2	–	–	–
Zeolite	4	–	–	–	–
Carbonate unspec.	9	15	30	20	6
Foraminifers	1	1	–	–	–
Calc. nannofossils	20	22	10	15	30
Fish remains	3	2	1	2	–
Plant debris	2	3	–	–	2
Aragonite	22	11	–	–	–

SITE 534 HOLE A CORE 100 CORED INTERVAL 1401.0–1410.0 m

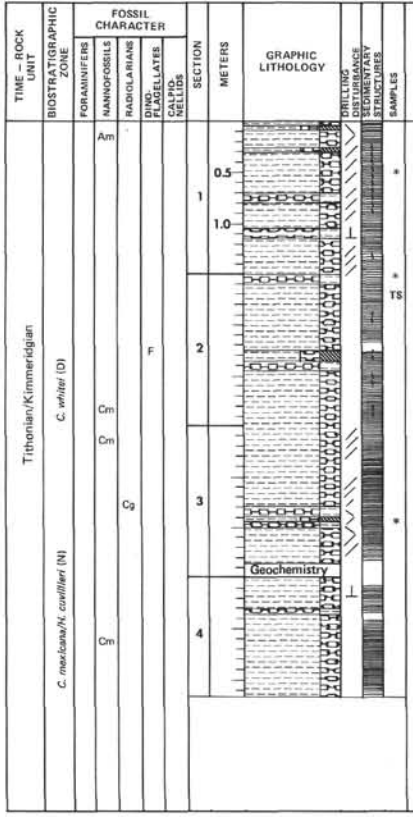

LITHOLOGIC DESCRIPTION

CALCAREOUS CLAYSTONE and MARLY CHALK

CALCAREOUS CLAYSTONE, grayish red (10R 4/2) to very dusky red (10R 2/2), commonly with mottles and bands of light olive gray (5Y 6/1) to dark greenish gray (5GY 4/1). Laminated with some burrows (especially in the greenish gray zones). Smear slides have 25% silt-sized carbonate needles interpreted as aragonite.

MARLY CHALK (minor lithology), light olive gray (5Y 6/1) to dark greenish gray (5GY 4/1). Laminated with moderate bioturbation. Thin Section (Section 2, 17 cm) has a clayey biomicrite texture with abundant silt-sized bioclasts. May be aragonite needle-bearing.

CARBONACEOUS CALCAREOUS CLAYSTONE (minor lithology), olive black (5Y 2/1) to brownish black (5YR 2/1); laminated.

Ammonite fragments and other shell pieces having pearly luster preserved are abundant in the grayish red claystone (especially Section 2, 100 cm–Section 3, 150 cm). Original aragonite?

Pyrite nodule at top of Section 1. Radial crystal structure.

Thin (2–3 mm) white (pale pink) layers occur at about 30 cm intervals.

SMEAR SLIDE SUMMARY (%):

	1, 50 D	2, 2 M	3, 93 M
Texture:			
Silt	30	40	25
Clay	70	60	75
Composition:			
Quartz	1	–	2
Mica	–	–	4
Heavy minerals	1	–	1
Clay	55	49	60
Carbonate unspec.	5	10	10
Calc. nannofossils	10	5	8
Fish remains	1	–	2
Plant debris	1	1	10
Aragonite	25	35	3

SITE 534 HOLE A CORE 101 CORED INTERVAL 1410.0–1419.0 m

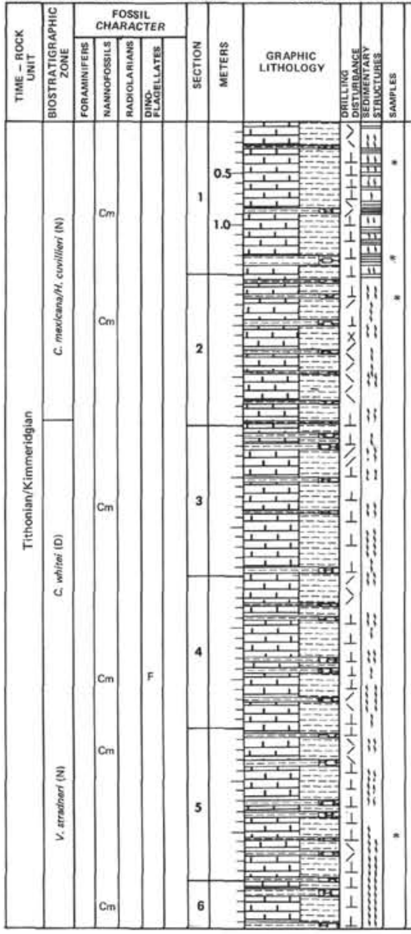

LITHOLOGIC DESCRIPTION

CALCAREOUS CLAYSTONE to MARLY NANNOFOSSIL CHALK

CALCAREOUS CLAYSTONE to MARLY NANNOFOSSIL CHALK *(major lithology), grayish red (10R 4/2)* to grayish brown (5YR 3/2) to moderate brown (5YR 3/4), has mottles of greenish gray along bedding. Massive to thin bedded with slight to moderate bioturbation (abundant chondrites).

CALCAREOUS CLAYSTONE (minor lithology), medium bluish gray (5B 5/1) to greenish gray (5G 6/1). Massive to vaguely laminated, commonly bioturbated. Carbonaceous in the layer at Section 5, 104–105 cm.

SMEAR SLIDE SUMMARY (%):

	1, 40	1, 138	2, 25	5, 103
	D	M	D	M
Texture:				
Silt	5	5	5	15
Clay	95	95	95	85
Composition:				
Quartz	1	2	–	4
Feldspar	–	–	–	1
Mica	1	–	–	4
Heavy minerals	–	–	–	1
Clay	74	80	53	74
Zeolite	–	–	–	2
Carbonate unspec.	5	5	10	3
Calc. nannofossils	15	10	35	5
Fish remains	2	1	1	–
Plant debris	1	2	–	6
Fe-oxide	1	–	1	–

SITE 534 HOLE A CORE 102 CORED INTERVAL 1419.0–1428.0 m

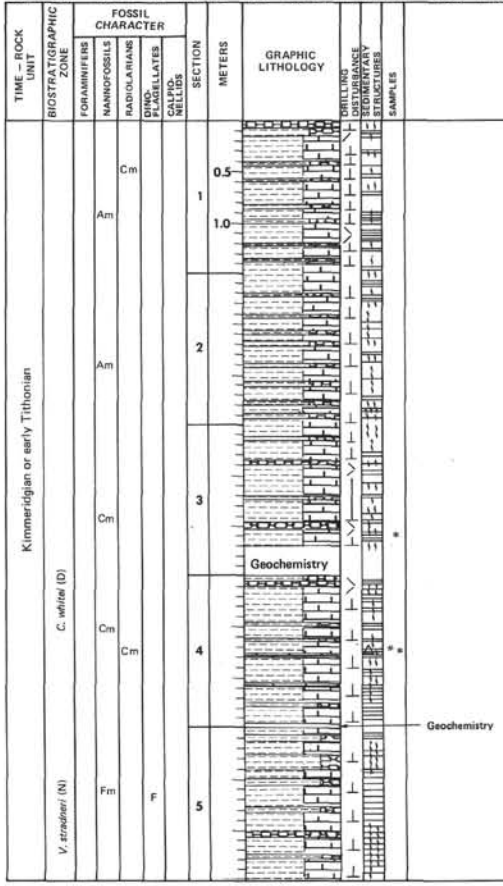

LITHOLOGIC DESCRIPTION

CALCAREOUS CLAYSTONE

CALCAREOUS (NANNOFOSSIL) CALYSTONE, grayish brown (5YR 3/2) to moderate brown (5YR 3/4) to grayish red (5R 4/2); massive to thin bedded, slight to moderate bioturbation. Up to 5% organic debris in smear slide.

CALCAREOUS CLAYSTONE (minor lithology), medium bluish gray (5B 5/1) to light olive gray (5Y 5/2) to dark greenish gray (5G 4/1); moderately bioturbated with vague, wavy laminations. Occurs mainly as very thin interbeds in the grayish brown claystone.

CHALK (minor lithology), light gray (N7) to light olive gray (5Y 6/1); moderate bioturbation (especially chondrites). This lithology appears mainly in lower part of core.

SMEAR SLIDE SUMMARY (%):

	3, 110	4, 71	4, 74
	D	M	D
Texture:			
Silt	–	–	18
Clay	–	–	82
Composition:			
Quartz	5	–	2
Mica	1	–	–
Heavy minerals	1	–	–
Clay	65	10	69
Carbonate unspec.	6	78	6
Calc. nannofossils	15	10	15
Fish remains	1	1	1
Plant debris	5	1	3
Other	–	–	4

SITE 534 HOLE A CORE 103 CORED INTERVAL 1428.0–1437.0 m

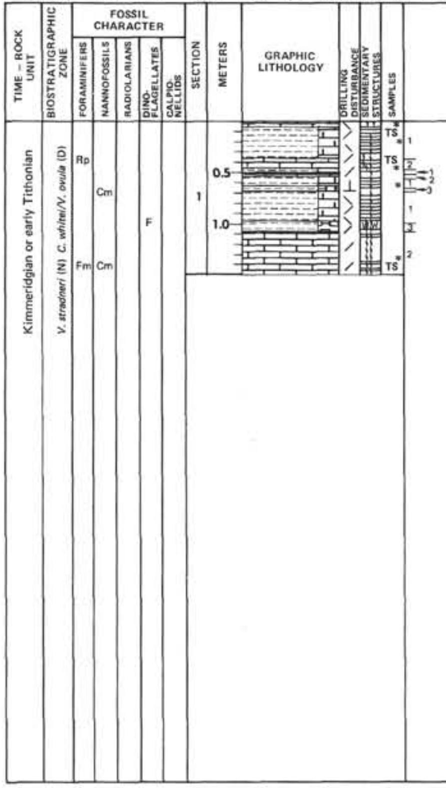

LITHOLOGIC DESCRIPTION

INTERBEDDED NANNOFOSSIL CLAYSTONE and LIMESTONE

1 – NANNOFOSSIL CLAYSTONE, grayish brown (5YR 3/2) to moderately brown (5YR 3/4) to grayish red (5R 4/2); massive to thin bedded; slight to moderate bioturbation. Thin section shows that burrow fillings are microspar commonly with geopetal texture. Few mollusc fragments present.

2 – LIMESTONE (biomicrite to pelletal microsparite), mottled light gray (N7), medium light gray (N6), and light bluish gray (5B 7/1) commonly with greenish gray (5GY 6/1, 5Y 6/1) and light brownish gray 5YR 6/1); massive to laminated; slight to moderate bioturbation. Thin section of a burrowed limestone (Section 1, 44 cm) has coarse microspar-filled burrows; microspar-replaced bioclasts of radiolaria and mollusc fragments, and overgrown echinderm fragments in micrite/microspar. Thin section of a laminated limestone (Section 1, 133 cm) is a biomicrite with 20% small pellets.

3 – CALCAREOUS CLAYSTONE (minor lithology), light gray (N6) to medium bluish gray (5B 5/1); massive.

Microbreccia layer (0.5 cm thick) at Section 1, 96 cm.

SMEAR SLIDE SUMMARY (%):

	1, 2 M	1, 20 D	1, 48 D	1, 68 D	1,132 M
Texture:					
Sand	–	–	1	–	2
Silt	10	40	19	10	68
Clay	90	60	80	90	30
Composition:					
Quartz	–	3	3	11	3
Mica	–	1	1	3	–
Heavy minerals	–	1	–	7	–
Clay	–	47	71	47	19
Pyrite	–	1	3	9	–
Carbonate unspec.	98	16	6	6	78
Calc. nannofossils	–	26	8	11	–
Fish remains	–	2	3	3	–
Plant debris	2	3	5	3	–

SITE 534 HOLE A CORE 104 CORED INTERVAL 1437.0–1446.0 m

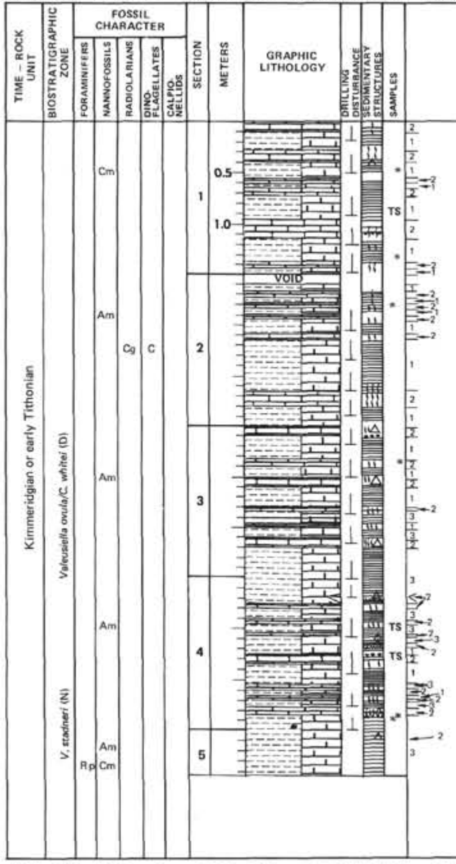

LITHOLOGIC DESCRIPTION

INTERBEDDED NANNOFOSSIL CLAYSTONE and LIMESTONE

1 – NANNOFOSSIL CLAYSTONE to MARLY CHALK, (pelagic bivalve-rich radiolarian biomicrite), medium dark gray (N3); finely laminated with moderate bioturbation. Thin section has abundant calcified radiolaria and small pelagic bivalves with overgrowths, plus zone of pelletal biomicrite. Commonly has sparite bands, discontinuous.

2 – LIMESTONE (pelletal to biomicrite), light gray (N7), finely laminated to banded to highly burrowed. Several beds have upward-fining graded texture. Turbidite origin.

3 – NANNOFOSSIL CLAYSTONE to MARLY CHALK, (micrite to pelagic bivalve biomicrite), grayish brown (5YR 3/2) to moderate brown (5YR 3/4) to grayish red (5R 4/2). Texture same as lithology 1. More abundant in lower part of core.

Sparite bands in marly chalks have fibrous texture and are discontinuous. May be related to overgrowth on pelagic bivalves.

Shallow-water foraminifera found in some of the limestones.

Microbreccia at Section 1, 110 cm.

SMEAR SLIDE SUMMARY (%):

	1, 49 D	1,135 M	2, 31 M	3, 38 M	4, 137 D	4, 139 M
Texture:						
Sand	1	2	–	1	–	50
Silt	24	18	10	44	25	20
Clay	75	80	90	55	75	30
Composition:						
Quartz	3	1	1	–	4	1
Feldspar	–	2	–	–	–	–
Mica	1	–	–	–	1	–
Heavy minerals	–	–	–	–	1	–
Clay	57	–	21	–	46	30
Pyrite	4	–	3	–	3	1
Zeolite	3	–	3	–	–	–
Carbonate unspec.	3	97	55	99	6	50
Calc. nannofossils	26	–	11	–	22	13
Fish remains	1	–	2	–	2	2
Plant debris	2	–	4	1	3	1
Aragonite	–	–	–	–	12	–

SITE 534 HOLE A CORE 105 CORED INTERVAL 1446.0–1455.0 m

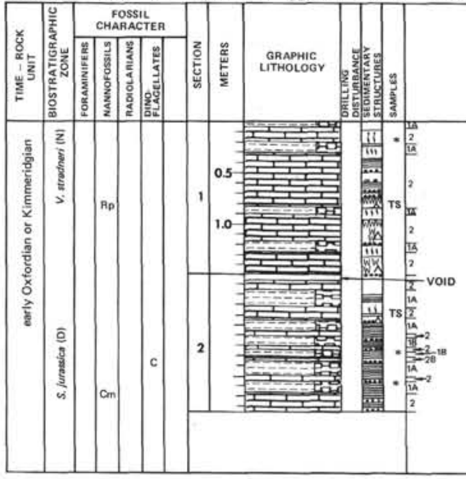

LITHOLOGIC DESCRIPTION

INTERBEDDED LIMESTONES and CLAYSTONE

1 – CALCAREOUS CLAYSTONE of two color types: A: dark greenish gray (5GY 4/1).

B: grayish red (5R 4/2) to blackish red (5R 2/2) to grayish brown (5YR 3/2). Weakly laminated to massive with small burrows. May have fine pelagic bivalves.

2 – LIMESTONE (packed shell-pellet microsparite to radiolarian biomicrite), light greenish gray (5GY 6/1) to light bluish gray (5B 7/1). Two texture types: A: fine-grained biomicrite. Thin section has micritized radiolaria, fine pellets, and tiny pelagic bivalves; often in thin (1–2 cm or less) beds interbedded with claystone. These show boudinage and other compression features.

B: medium- to coarse-grained bioclast-pelletal microsparite to biomicrite, often with graded bedding, laminations, and convolute-laminations. Sand-sized, round, micrite pellets in the thin section may be micritized ooids. Occasional benthic foraminifera. Erosional bases. Turbidite origin evident.

SITE 534 HOLE A CORE 106 CORED INTERVAL 1455.0–1464.0 m

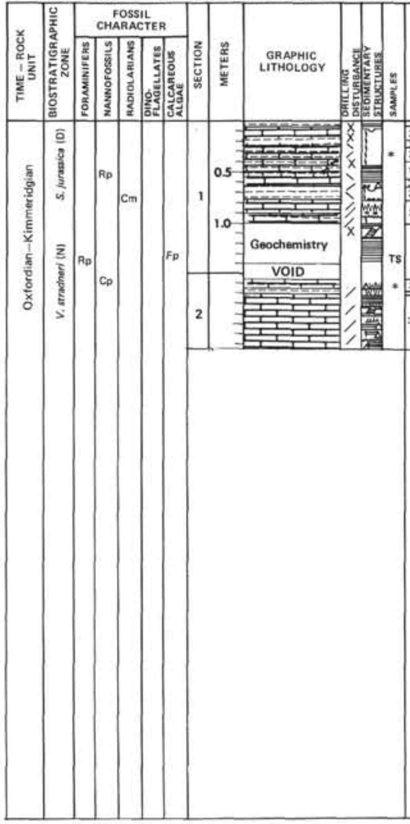

LITHOLOGIC DESCRIPTION

INTERBEDDED LIMESTONES and CALCAREOUS CLAYSTONE

1 – CALCAREOUS CLAYSTONE, dark greenish gray (5GY 4/1) to greenish black (5GY 2/1); laminated. Smear slides contain abundant calcite laths which could be crushed fine pelagic bivalves, and up to 10% clastics.

2 – LIMESTONE (micrite to microspar), greenish gray (5GY 6/1) to dark greenish gray (5GY 4/1); massive with bioturbation. Thin Section (Section 1, 31 cm) has less than 5% bioclasts which are microspar replaced.

3 – LIMESTONE (packed skeletal-pelletal sparite), yellowish gray (5Y 8/1) to light olive gray (5Y 6/1) with olive gray (5Y 4/1) laminae at the top of the beds. Sand- to silt-sized grading upward common. Probable turbidites of shallow-water origin. Thin Section (Section 1, 134 cm) has 10% ooids, 25% pellets and micritized grains, and 15% bioclasts including foraminifera in a sparite cement.

Section 1:
79–82 cm: contorted bedding in limestone.

82–88 cm: clasts of fine-grained limestone in a coarse calcareous matrix.

96–140 cm: single turbidite of limestone (lithology 3). Bouma A–C.

Section 2:
31–39 cm: current laminations in granular limestone (lithology 3).

SMEAR SLIDE SUMMARY (%):

	1, 37 M	2, 15 M
Texture:		
Silt	30	40
Clay	70	60
Composition:		
Quartz	4	6
Feldspar	3	4
Mica	1	1
Clay	63	55
Carbonate unspec.	25	30
Calc. nannofossils	2	2
Plant debris	2	2

SITE 534 HOLE A CORE 107 CORED INTERVAL 1464.0–1468.5 m

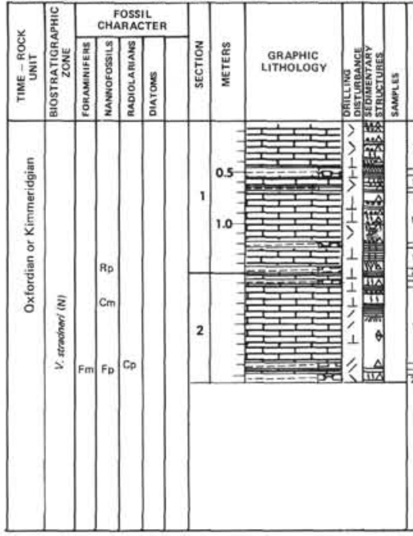

LITHOLOGIC DESCRIPTION

INTERBEDDED LIMESTONES and CALCAREOUS CLAYSTONE

1 – LIMESTONE, light olive gray (5Y 6/1) to dark greenish gray (5G 4/1); coarse-grained at base, generally fining upward to darker laminated beds. Bases are scoured, burrows (chondrites) only in fine-grained tops of sequences. *Probably turbidites of shallow-water origin.*

2 – CALCAREOUS CLAYSTONE (minor lithology), dark greenish gray (5G 4/1) to greenish black (5GY 2/1); generally interbedded with upper parts of the limestone turbidites. Grayish brown (5YR 3/2) to dusky brown (5YR 2/2) at base of Section 2.

Section 1:
24 cm: small slumps in bedding.

70–74 cm: claystone clasts in granular limestone.

93 cm: flute casts at base of granular limestone bed.

Section 2:
40–92 cm: normal graded texture has an interval (60–80 cm) of reverse grading in continuous granular limestone.

At least 15 turbidite pulses recovered in this core.

SITE 534 HOLE A CORE 108 CORED INTERVAL 1468.5–1477.5 m

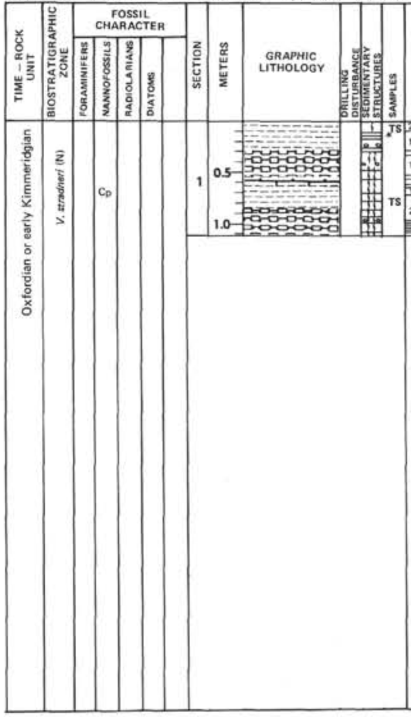

LITHOLOGIC DESCRIPTION

CALCAREOUS CLAYSTONE

1 – CALCAREOUS CLAYSTONE, grayish red (5R 4/2) to moderate red (5R 5/4), has some burrow-mottled, massive. Thin section (Section 1, 74 cm) has up to 50% microspar and no bioclasts. Rare fibrous calcite seams.

2 – LIMESTONE (micrite) (minor lithology), grayish pink (5YR 6/2); with chondrites burrows.

3 – CALCAREOUS CLAYSTONE, (minor lithology), greenish gray (5GY 5/1); probably reduced product of reddish claystone.

Section 1:
0–9 cm: large burrow in pink limestone with green reduction halo.

23–25 cm: small limestone nodules in clay. Microfault breaks shell fragment nearby.

39 cm: microbreccia layer.

78–87 cm: series of graded red silty claystones with 1–3 cm repetitions.

SMEAR SLIDE SUMMARY (%):

	1, 18 D
Texture:	
Silt	40
Clay	60
Composition:	
Quartz	1
Feldspar	2
Clay	54
Carbonate unspec.	38
Calc. nannofossils	2
Plant debris	2
Dolomite	1

SITE 534 HOLE A CORE 109 CORED INTERVAL 1477.5–1486.5 m

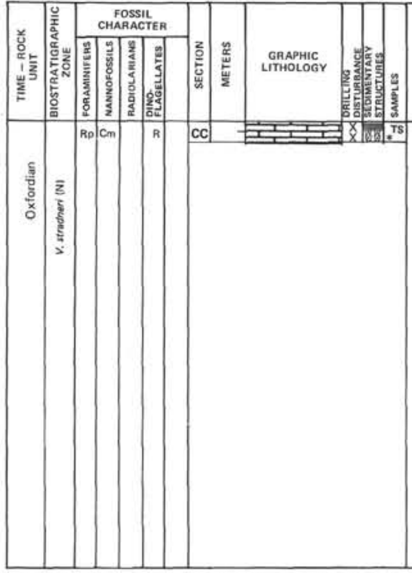

LITHOLOGIC DESCRIPTION

LIMESTONE

LIMESTONE (packed pellet sparite), light olive gray (5Y 6/1) with laminae of olive gray (5Y 4/1). Thin section has 45% pellets and micritized grains and 10% bioclasts (mollusc, foraminifera, and echinoderm fragments) in a microspar-sparite matrix. Probably redeposited shallow water material.

NANNOFOSSIL CLAYSTONE, (minor lithology [fragments only]), dark greenish gray (5GY 4/1), laminated.

CHERT, (minor lithology [fragments only]), yellowish brown (5YR 4/3).

SMEAR SLIDE SUMMARY (%):

	CC D
Texture:	
Silt	20
Clay	80
Composition:	
Quartz	2
Feldspar	1
Clay	58
Carbonate unspec.	12
Calc. nannofossils	25
Plant debris	2

SITE 534 HOLE A CORE 110 CORED INTERVAL 1486.5–1495.5 m

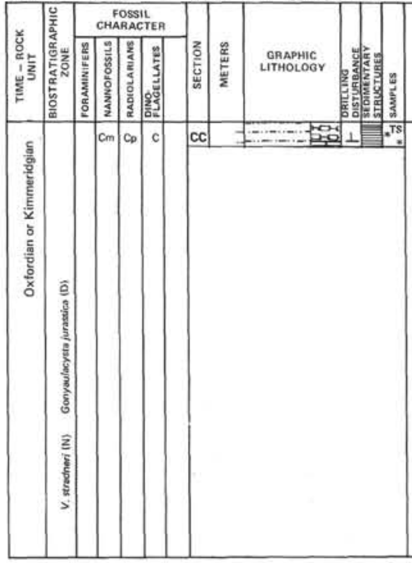

LITHOLOGIC DESCRIPTION

CLAYSTONES

CALCAREOUS SILTY CLAYSTONE, (0–21 cm), grayish brown (5YR 3/2); thin-bedded to massive, slight bioturbation. Interbedded by:

A: claystone, greenish gray (5G 6/1) at 13 cm.

B: limestone (micrite to silt-sized pelletal microsparite), very light gray (N8) to light greenish gray (5G 8/1); with incipient nodular texture 0–2 and 19 cm.

NANNOFOSSIL-RICH SILTY CLAYSTONE, (21–27 cm), medium gray (N5) and dark bluish gray (5B 4/1); laminated to massive. No obvious bioturbation.

SMEAR SLIDE SUMMARY (%):

	CC, 12 D	CC, 22 M
Texture:		
Silt	32	35
Clay	68	65
Composition:		
Quartz	2	2
Feldspar	1	1
Heavy minerals	–	2
Clay	56	53
Carbonate unspec.	30	12
Calc. nannofossils	10	27
Plant debris	1	3

SITE 534 HOLE A CORE 111 CORED INTERVAL 1495.5–1504.5 m

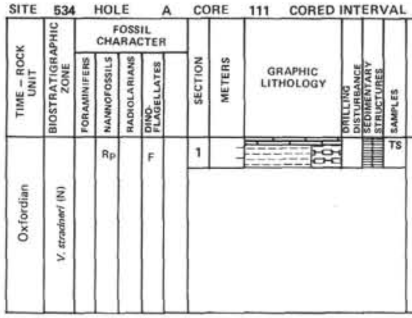

LITHOLOGIC DESCRIPTION

LIMESTONE and CALCAREOUS CLAYSTONE

LIMESTONE (micrite [0–7 cm]), medium gray (N5), vaguely laminated, slight bioturbation. Uniform micrite in thin section with only scattered microspar patches.

CALCAREOUS CLAYSTONE, (7–28 cm), interbedded grayish brown (5G 6/1) to dark greenish gray (5G 4/1), minor bioturbation.

SITE 534 HOLE A CORE 112 CORED INTERVAL 1504.5–1513.5 m

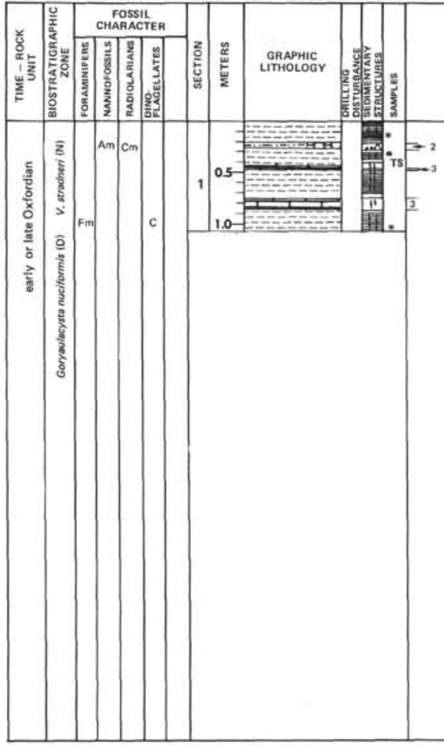

LITHOLOGIC DESCRIPTION

CLAYSTONES with INTERBEDDED LIMESTONE

1 – CLAYSTONE of several color types:

A: greenish gray (5G 6/1, 5GY 6/1), nearly devoid of nannofossils, bioturbated.

B: grayish red (5R 4/2) to dusky red (5R 3/4), up to 30% nannofossils.

C: olive gray (5Y 4/1), otherwise similar to type B.

Sharp contacts between type A and other types. Greenish type C is probably a red type B which is reduced; often seen as mottles in the red. Burrows pass from greenish gray type A into other types.

2 – CALCAREOUS SILTSTONE (minor lithology), light greenish gray (5G 8/1), nannofossil-rich. Always overlies type A claystone and underlies types B and C, suggesting that it is basal member of thin (3–5 cm thick) clay-rich turbidites.

3 – LIMESTONE (micrite [minor lithology]), light gray (N8) to greenish gray (5GY 6/1), massive. Two isolated pieces recovered.

SMEAR SLIDE SUMMARY (%):

	1, 11 D	1, 31 M	1, 109 D
Texture:			
Silt	20	25	15
Clay	80	75	85
Composition:			
Quartz	3	7	2
Mica	–	2	–
Heavy minerals	–	1	–
Clay	60	41	78
Pyrite	2	2	2
Carbonate unspec.	4	17	7
Calc. nannofossils	28	26	9
Fish remains	2	2	1
Plant debris	1	2	1

SITE 534 HOLE A CORE 113 CORED INTERVAL 1513.5–1522.5 m

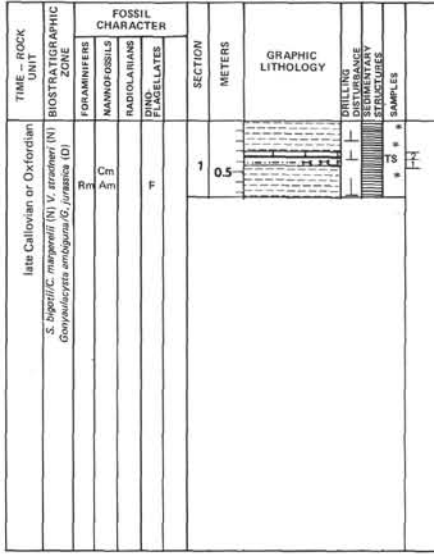

LITHOLOGIC DESCRIPTION

CLAYSTONES with INTERBEDDED LIMESTONE

1 – CLAYSTONES of a variety of color types including dark greenish gray (5GY 4/1), brownish gray (5YR 4/1), olive gray (5Y 4/1), and grayish red (5R 4/2) to dusky red (5R 3/4). Some types are calcareous and have excellent nannofossil preservation, others are nearly devoid of nannofossils. Laminated to burrow mottled.

2 – CALCAREOUS SILTSTONE (pelletal marly micrite), greenish gray (5GY 5/1). Thin Section (Section 1, 29–31 cm) has 10% quartz and mica silt.

3 – LIMESTONE (pelmicrite), greenish gray (5G 5/1), laminated.

SMEAR SLIDE SUMMARY (%):

	1, 9	1, 25	1, 55
	D	M	M
Texture:			
Sand	–	1	–
Silt	15	14	85
Clay	85	85	15
Composition:			
Clay	71	82	35
Carbonate unspec.	23	13	3
Calc. nannofossils	5	4	60
Fish remains	1	1	2

SITE 534 HOLE A CORE 114 CORED INTERVAL 1522.5–1531.5 m

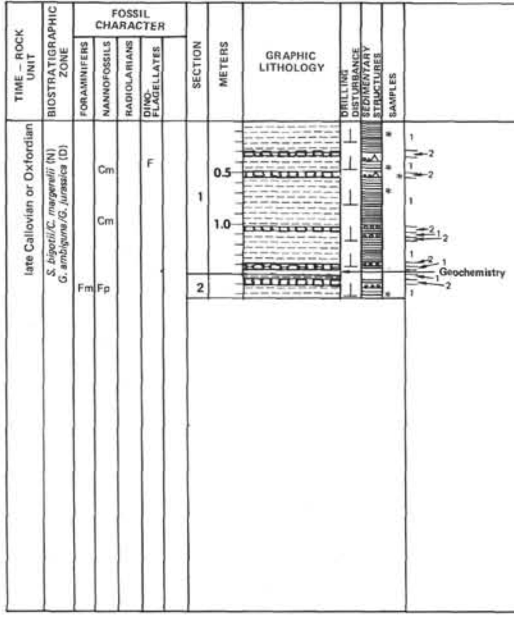

LITHOLOGIC DESCRIPTION

CLAYSTONES and MARLY CHALK

1 – CLAYSTONE of a variety of colors including medium brown (5YR 3/4) (dominant), dark reddish gray (10R 3/4), olive gray (5Y 4/1), grayish red (10R 4/2), pale red (5R 6/2), and dark greenish gray (5GY 4/1). Color banded on 3–6 cm scale.

2 – MARLY CHALK to CALCAREOUS CLAYSTONE, dark gray (N3) to dark greenish gray (5GY 4/1); generally in 0.5–1.0 cm layers.

Burrows are rare.

Graded fine silt to claystone sequences occur frequently.

SMEAR SLIDE SUMMARY (%):

	1, 12	1, 49	1, 59	1, 69	2, 21
	D	D	D	D	D
Texture:					
Sand	–	–	1	–	–
Silt	10	13	15	15	7
Clay	90	87	84	85	93
Composition:					
Quartz	5	4	2	2	2
Mica	1	1	1	1	–
Clay	72	27	73	83	80
Pyrite	3	3	1	–	1
Carbonate unspec.	3	–	3	11	13
Calc. nannofossils	11	60	17	2	2
Fish remains	1	1	1	1	–
Plant debris	4	4	2	–	2

SITE 534 HOLE A CORE 115 CORED INTERVAL 1531.5–1540.5 m

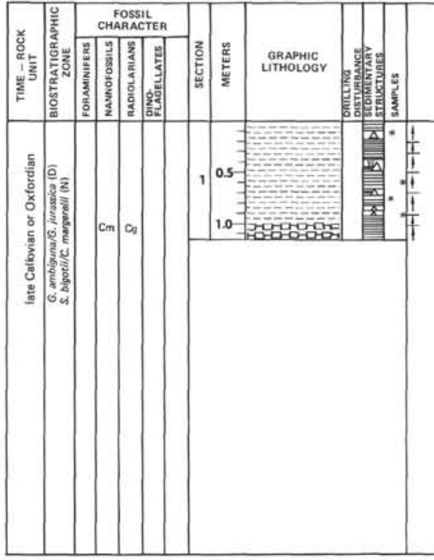

LITHOLOGIC DESCRIPTION

CLAYSTONES

CLAYSTONE to CALCAREOUS CLAYSTONE, variety of color bands including dark reddish brown (10R 3/4), dark gray (N3), grayish green (5GY 6/1), olive black (5Y 2/1), and brownish gray (5YR 3/2, 5YR 4/1). Bands are 0.5–7.0 cm thick. Has some mottling. Grading on a very fine-grained scale seen in some layers.

A typical sequence is a finely laminated dark green silty claystone passing upward into a reddish brown with greenish gray mottling, then a massive dark gray layer.

SMEAR SLIDE SUMMARY (%):

	1, 11	1, 62	1, 76	1, 94
	D	D	M	D
Texture:				
Silt	10	15	10	30
Clay	90	85	90	70
Composition:				
Quartz	4	5	5	2
Feldspar	–	1	2	1
Heavy minerals	–	–	1	–
Clay	60	67	83	67
Carbonate unspec.	10	10	2	25
Calc. nannofossils	25	15	4	3
Plant debris	1	2	3	2

SITE 534 HOLE A CORE 116 CORED INTERVAL 1540.5–1549.5 m

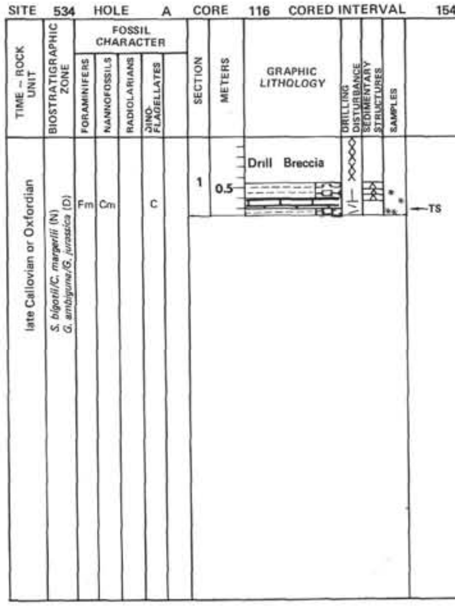

LITHOLOGIC DESCRIPTION

CALCAREOUS CLAYSTONES with INTERBEDDED LIMESTONE

CALCAREOUS CLAYSTONES, variety of colors including blackish red (5R 2/2), dark gray (N3) with streaks, and olive gray (5Y 4/1). The typical sequence is a sharp contact of a reddish claystone over a dark gray with olive mottling of the red type at the contact, then a transition upward from reddish to dark gray. Grading seen at contacts in fine-grained material. Turbidite origin.

LIMESTONE (biomicrite [minor lithology]), greenish gray (5GY 6/1), weakly laminated. Convolute laminations in basal 2 cm. Rare burrows near top. Thin section has 10–15% echinoderm plates, 10% calcified radiolaria, and 3% quartz in a fine pelmicrite matrix.

SMEAR SLIDE SUMMARY (%):

	1,52	1, 69	1, 72	1, 76
	D	D	M	D
Silt	35	40	–	25
Clay	65	60	–	75
Composition:				
Quartz	3	3	2	2
Feldspar	1	1	–	1
Clay	52	45	–	56
Carbonate unspec.	40	45	95	30
Calc. nannofossils	2	4	3	10
Plant debris	2	2	–	1

SITE 534 HOLE A CORE 117 CORED INTERVAL 1549.5–1558.5 m

TIME – ROCK UNIT	BIOSTRATIGRAPHIC ZONE	FOSSIL CHARACTER: FORAMINIFERS	NANNOFOSSILS	RADIOLARIANS	DINO-FLAGELLATES	SECTION	METERS
late Callovian or Oxfordian	*S. bigotii/C. margerelii* (N) *Ctenidodinium pachydermum* (D)		Cm		F	1	0.5

LITHOLOGIC DESCRIPTION

CLAYSTONES and LIMESTONE

Drilling breccia of clay chips (0–7 cm).

Interbedded CLAYSTONE (7–26 cm), greenish black (5G 2/1), and NANNOFOSSIL CLAYSTONE, dusky brown (5YR 2/2). Color boundaries are fairly sharp.

LIMESTONE (biomicrite [26–56 cm]), light olive gray (5Y 6/1) to light gray (N7). Base has laminated and convolute bedding; grades upward into laminated beds with dark clasts; an intraclast layer is near the top (oriented white clasts). Calciturbidites with C–D units.

SMEAR SLIDE SUMMARY (%):

	1, 10 D	1, 24 M
Texture:		
Silt	15	10
Clay	85	90
Composition:		
Quartz	1	1
Mica	1	–
Clay	63	70
Pyrite	1	3
Carbonate unspec.	4	4
Calc. nannofossils	27	19
Fish remains	2	1
Plant debris	1	2

SITE 534 HOLE A CORE 118 CORED INTERVAL 1558.5–1567.5 m

TIME – ROCK UNIT	BIOSTRATIGRAPHIC ZONE	FOSSIL CHARACTER: FORAMINIFERS	NANNOFOSSILS	RADIOLARIANS	DINO-FLAGELLATES	SECTION	METERS
late Callovian or early Oxfordian	*Ctenidodinium pachydermum* (D) *S. bigotii/C. margerelii* (N)		Cm Fp	Cp	F	1	0.5 1.0

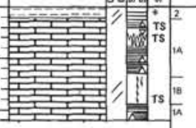

LITHOLOGIC DESCRIPTION

LIMESTONES

1 – LIMESTONES of two textural types:
A: pelmicrite, light olive gray (5Y 6/1) to greenish gray (5GY 6/1); graded bedding and laminated. Bouma sequence B–D–E common. Thin section has overgrowths on echinoderm plates and rare benthic foraminifera.

B: micrite, greenish gray (5G 6/1) and dark greenish gray (5GY 4/1), massive and slightly bioturbated. Thin section has 5% calcified radiolarian dense micrite.

2 – CLAYSTONE, olive gray (5Y 4/1) to dark greenish gray (5GY 4/1), slight bioturbation and vague laminations.

Microbreccias(?) in limestones at 19 and 41 cm. Thin Section at 19 cm is very similar to type A limestone; 10–15% calcified radiolaria and echinoderm plates. Breccia(?) texture is not apparent in thin section.

Both limestone types were probably redeposited.

SMEAR SLIDE SUMMARY (%):

	1, 3 D
Texture:	
Silt	10
Clay	90
Composition:	
Clay	81
Pyrite	1
Carbonate unspec.	7
Calc. nannofossils	9
Fish remains	1
Plant debris	1

SITE 534 HOLE A CORE 119 CORED INTERVAL 1569.5–1572.0 m

TIME – ROCK UNIT	BIOSTRATIGRAPHIC ZONE	FOSSIL CHARACTER: FORAMINIFERS	NANNOFOSSILS	RADIOLARIANS	DINO-FLAGELLATES	SECTION	METERS
late Callovian–early Oxfordian	*S. bigotii/C. margerelii* (N)		Cm		F	1	0.5 1.0

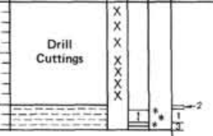

LITHOLOGIC DESCRIPTION

CLAYSTONES

1 – CLAYSTONES of three color types:
A: blackish red (5R 2/2)

B: olive gray (5Y 4/1)

C: black (N1), nannofossil-rich

Three rhythmic sequences, or parts thereof, are present. The sequence proceeds from olive to red claystone with a possible black clay background.

SMEAR SLIDE SUMMARY (%):

	1, 106 D	1,114 M	1, 120 M
Texture:			
Sand	–	–	1
Silt	10	5	4
Clay	90	95	95
Composition:			
Clay	84	90	75
Carbonate unspec.	8	5	3
Calc. nannofossils	6	4	21
Fish remains	1	1	1
Plant debris	1	–	–

SITE 534 HOLE A CORE 120 CORED INTERVAL 1572.0–1581.0 m

TIME – ROCK UNIT	BIOSTRATIGRAPHIC ZONE	FORAMINIFERS	NANNOFOSSILS	RADIOLARIANS	DINO-FLAGELLATES	SECTION	METERS
late Callovian or early Oxfordian	*S. bigotii/C. margerelii* (N) *Lithodinia jurassica, Stephanelytron redcliffense* (D)		Rp			1	0.5
		B	Rp	Ag	F		

GRAPHIC LITHOLOGY / DRILLING DISTURBANCE / SEDIMENTARY STRUCTURES / SAMPLES

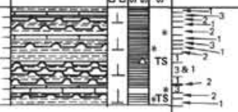

LITHOLOGIC DESCRIPTION

CLAYSTONE, RADIOLARIAN SILTSTONE, and LIMESTONE

1 – CLAYSTONE, dusky blue green and dusky purple (5BG 3/2 and 5P 3/2), grayish blue green (5BG 5/2) to dark greenish gray (5GY 4/1); finely laminated with a streaky texture due to small burrows.

2 – RADIOLARIAN SILTSTONE, dark greenish gray (5G 4/1), laminated; occurs in thin layers or lenses. Eleven beds (0.5 cm maximum thickness) in section; 35–45% radiolaria, silica replaced (often by chalcedonic quartz).

3 – LIMESTONE (pelmicrite to packed skeletal pelmicrite), light gray (N7) to greenish gray (5GY 6/1). Graded bedding with parallel laminations at 40–48 cm, massive otherwise. Thin section (48 cm) has 15–20% silicified radiolaria, 10% shell fragments, and 2% echinoderm plates in pelmicrite.

SMEAR SLIDE SUMMARY (%):

	1, 29	1, 43	1, 87	1, 90
	D	D	D	D
Texture:				
Sand	–	–	–	1
Silt	14	3	17	23
Clay	86	97	83	76
Composition:				
Quartz	–	–	15	–
Feldspar	–	–	2	–
Mica	–	–	3	–
Heavy minerals	–	–	1	–
Clay	88	12	58	47
Pyrite	–	–	2	5
Carbonate unspec.	9	75	9	4
Calc. nannofossils	3	13	7	–
Radiolarians	–	–	–	45
Fish remains	–	–	1	–
Plant debris	–	3	2	3

SITE 534 HOLE A CORE 121 CORED INTERVAL 1581.0–1590.0 m

TIME – ROCK UNIT	BIOSTRATIGRAPHIC ZONE	FORAMINIFERS	NANNOFOSSILS	RADIOLARIANS	DINO-FLAGELLATES	SECTION	METERS
late Callovian or early Oxfordian	*S. bigotii/C. margeretii* (N) *Hystrichogonyaulax pectinigera* (D) *P. evittii* (D)		Rp	Ag			
			Rp		C	1	
					C		0.5

GRAPHIC LITHOLOGY / DRILLING DISTURBANCE / SEDIMENTARY STRUCTURES / SAMPLES

LITHOLOGIC DESCRIPTION

RADIOLARIAN CLAYSTONE and SILTSTONE overlying MARLY LIMESTONE

RADIOLARIAN-RICH CLAYSTONE (0–18 cm), dark greenish gray (5GY 4/1), calcareous, massive; with radiolarian siltstone, greenish black (5GY 2/1), non-calcareous, finely laminated.

LIMESTONE (sparse biomicrite [18–60 cm]), greenish gray (5GY 6/1), massive. Thin Section (Section 1, 26 cm) has 5–10% radiolaria replaced by pyrite, 5% radiolaria replaced by calcite, and 3% shell and echinoderm fragments in a clay-rich micrite.

SMEAR SLIDE SUMMARY (%):

	1, 2	1, 3	1, 8	1, 14
	M	M	D	D
Texture:				
Silt	20	3	20	17
Clay	80	97	80	83
Composition:				
Quartz	11	3	3	–
Feldspar	2	–	–	–
Mica	1	1	2	–
Heavy minerals	–	–	1	–
Clay	59	82	60	40
Pyrite	3	2	3	–
Carbonate unspec.	1	–	2	56
Calc. nannofossils	–	1	–	4
Radiolarians	21	9	26	–
Fish remains	1	1	1	–
Plant debris	2	1	2	–

SITE 534 HOLE A CORE 122 CORED INTERVAL 1590.0–1594.0 m

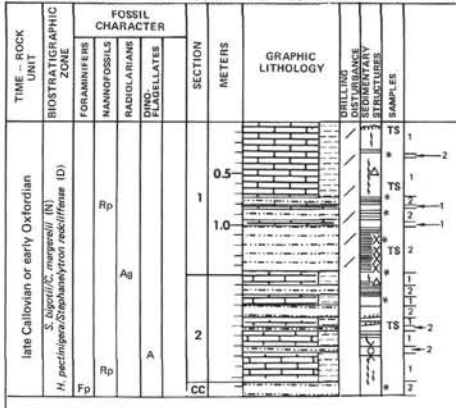

LITHOLOGIC DESCRIPTION

INTERBEDDED MARLY LIMESTONE and CLAYSTONE

1 – MARLY LIMESTONE (pelletal micrite to bioclastic pelletal microsparite), olive gray (5Y 5/1–5Y 4/1). Basal (1–5 cm) part of beds is often a laminated silty carbonate which grades up to the finer-grained massive main part of the bed. Chondrites occur throughout, but upper part of bed in contact with claystone has more bioturbation. Density of pellets and bioclasts (pelagic bivalve shells, pyritized radiolaria, benthic foraminifera, echinoderm fragments, and calcispheres) increases in basal part of some beds. Thickness of beds ranges from 10–35 cm.

2 – CLAYSTONE, grayish blue green (5BG 3/2), dusky blue green (5BG 3/2), medium bluish gray (5B 5/1), and dark greenish gray (5GY 4/1), with abundant streaks of greenish black (5G 3/1); laminated or banded. Interbedded by RADIOLARIAN CLAYEY SILTSTONE, dark greenish gray (5GY 4/1); occurs as bands or lenses within claystone levels with 3–10 cm repetition interval between thin (0.5–1.0 cm) layers. Thin sections show radiolaria to be filled by quartz or chert; matrix is same composition as claystone; contains 40–50% radiolarians.

Section 1:
0–7 cm: wavy or contorted bedding in medium-grain limestone. Thin section is a bioclastic pelletal microspar.

145 cm: claystone, grayish black (N2) laminated, possibly carbonaceous, 1 cm thick.

Beds and laminations dip 5–15°.

Thin Section (Section 2, 70 cm) of claystone contains a sand-sized phosphate concretion with concentric laminations, and occasional pyrite-replaced radiolaria.

SMEAR SLIDE SUMMARY (%):

	1, 31	1, 70	1, 88	1, 112	1, 145	2, 24	CC	1, 2	1, 66	1, 128	2, 50
	D	D	D	M	M	D	D	TS	TS	TS	TS
Texture:											
Sand	–	–	–	–	–	–	–	1	–	–	–
Silt	5	5	7	50	5	2	30	65	–	10	23
Clay	95	95	93	50	95	98	70	34	100	90	77
Composition:											
Quartz	–	–	3	15	5	–	6	6	1	2	2
Feldspar	–	–	1	–	–	–	–	–	–	–	–
Mica	–	–	2	–	1	–	–	–	–	1	1
Heavy minerals	–	–	–	–	–	–	15	–	–	TR	TR
Clay	20	20	86	44	85	25	2	18	30	70	44
Volcanic glass	–	–	–	–	–	–	65	–	–	–	–
Pyrite	–	–	–	–	1	–	–	1	1	5	3
Carbonate unspec.	74	80	3	–	3	75	1	70	68	2	49
Calc. nannofossils	5	–	–	–	2	–	–	–	–	–	–
Radiolarians	–	–	–	40	–	–	–	5	–	20	–
Fish remains	–	–	1	–	–	–	1	TR	–	–	–
Plant debris	1	–	–	1	3	–	3	–	–	–	–
Other	–	–	3	–	–	–	7	–	–	–	–

SITE 534 HOLE A CORE 123 CORED INTERVAL 1594.0–1603.5 m

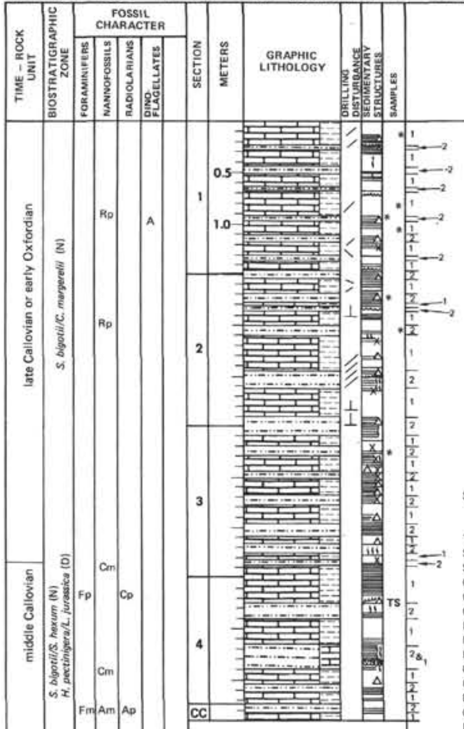

LITHOLOGIC DESCRIPTION

INTERBEDDED MARLY LIMESTONE and CALCAREOUS SILTY CLAYSTONE

1 – MARLY LIMESTONE (pelletal micrite to pelsparite), olive gray (5Y 4/1); massive, often with a graded silt (pelletal) base with laminations. Sharp basal contacts, commonly grades upward into claystone. Thin section (Section 4, 24 cm) is sparsely bioclastic with fine bivalve shells, pyritized radiolarians, and calcispheres, and has 30% pellets (0.08–0.1 mm).

2 – CALCAREOUS SILTY CLAYSTONE, often carbonaceous; olive black (5Y 2/1) with dusky yellowish green (10GY 3/2) and brownish black (5YR 2/1) layers; laminated to intensely bioturbated and mottled. Darker color toward base of core. Contains periodic lenses or bands of radiolarian silt. Smear slides have 25% quartz and mica silt and 15–20% nannofossils. Darker zones are more bioturbated.

Most beds dip 5–10°.

Section 1, 0–6 cm: claystone, grayish red (5R 4/2) to very dusky red (10R 2/2), massive with occasional greenish clay.

SMEAR SLIDE SUMMARY (%):

	1, 13	1, 85	1, 92	1, 106	2, 25	2, 58	3, 27	4, 24
	M	M	D	D	M	M	M	TS
Texture:								
Sand	–	–	–	–	1	1	–	–
Silt	–	5	10	5	70	79	40	50
Clay	–	95	90	95	29	20	60	50
Composition:								
Quartz	5	2	2	3	24	20	15	–
Feldspar	–	–	–	–	–	TR	TR	–
Mica	–	2	3	TR	1	7	10	–
Heavy minerals	–	–	TR	TR	–	TR	TR	–
Clay	40	45	73	40	20	63	45	12
Glauconite	3	–	–	–	–	–	–	–
Pyrite	–	–	2	–	–	2	1	1
Carbonate unspec.	20	5	2	55	2	2	10	–
Foraminifers	–	–	–	–	–	–	–	TR
Calc. nannofossils	25	45	10	TR	5	5	17	75
Radiolarians	–	–	–	–	48	–	–	–
Fish remains	3	–	–	–	–	–	–	–
Plant debris	3	–	7	2	–	1	2	–
Other	–	1	1	–	–	–	–	5

SITE 534 HOLE A CORE 124 CORED INTERVAL 1603.5–1612.5 m

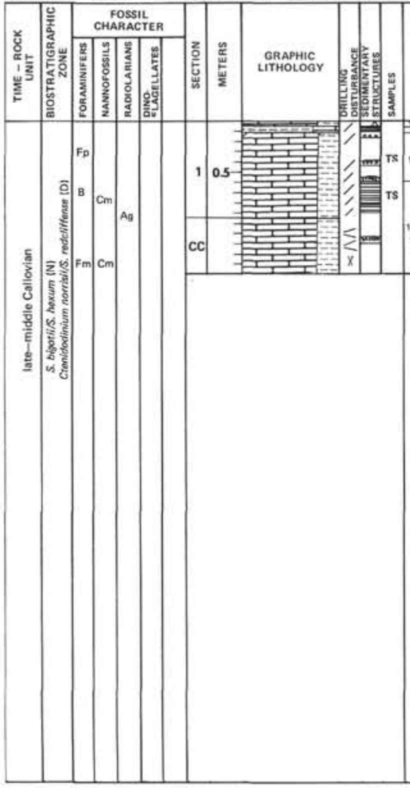

LITHOLOGIC DESCRIPTION

INTERBEDDED MARLY LIMESTONE and NANNOFOSSIL CLAYSTONE

1 – MARLY LIMESTONE (pelletal micrite), olive gray (5Y 4/1) to medium gray (N5) to light olive gray (5Y 6/1); massive to vaguely laminated, commonly with chondrite burrows. Base of beds are usually coarsely laminated with grading upward sequence common; commonly have contorted basal laminations. Middle portion of beds commonly have bands of slightly different grain-size or color. Thin Section (Section 1, 40 cm) has 40% pellets (0.05–0.1 m), 10% fine bivalve shells, and rare pyritized radiolaria and phosphate debris.

2 – NANNOFOSSIL CLAYSTONE, greenish black (5G 2/2) to black (N1) with dark greenish gray (5GY 4/1) laminae (especially near limestone contacts). Laminated with flakes of plant debris. Rare stringers of radiolarian silt.

Basal contacts of limestone to claystone are usually sharp; upper contacts can be gradational.

Section 1:
10–15 cm: *nannofossil claystone bed, olive black* (5Y 2/1) with upward fining grading, abundant plant debris, and burrows at top. Contains glauconite and phosphate.

Core-Catcher:
44–57 cm: drilling breccia.

SMEAR SLIDE SUMMARY (%):

	1, 39 TS
Texture:	
Silt	50
Clay	50
Composition:	
Quartz	1
Clay	30
Pyrite	1
Calc. nannofossils	63
Other	5

SITE 534 HOLE A CORE 125 CORED INTERVAL 1612.5–1621.5 m

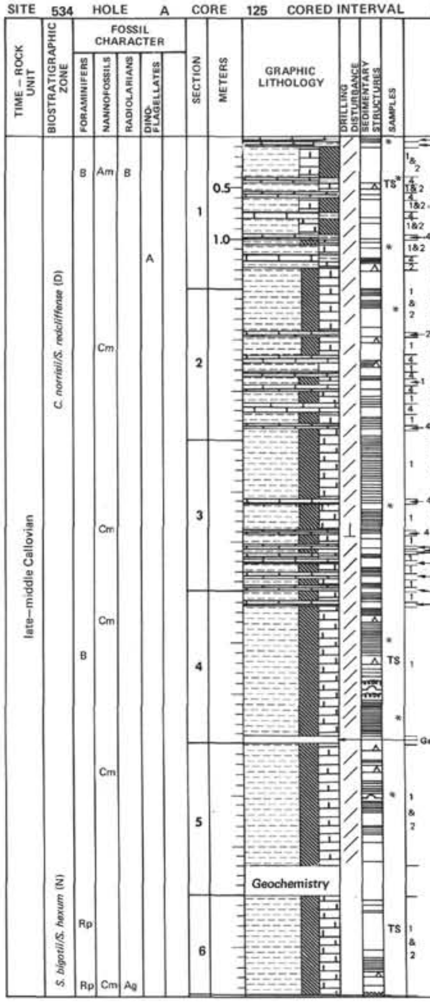

LITHOLOGIC DESCRIPTION

NANNFOOSSIL CLAYSTONES with INTERBEDDED MARLY LIMESTONE

1 – NANNOFOSSIL CLAYSTONE to CARBONACEOUS NANNOFOSSIL CLAYSTONE, greenish black (5G 2/1) to olive black (5Y 2/1); predominately laminated, with possible chondrites burrows (compressed); usually has speckled texture (radiolaria and plant debris), commonly with graded appearance. Abundant black laminae. Pyrite in some laminae.

2 – NANNOFOSSIL CLAYSTONE, predominantly dark greenish gray (5G 4/1) with streaks and mottles of grayish blue green (5BG 5/2), dusky green (5G 3/2), and grayish green (5G 5/2) creating a discontinuous streaky texture. Contains dark gray specks and possible small-scale bioturbation.

These claystones contain thin interbeds of:

3 – MARLY RADIOLARIAN SILTSTONE, dark greenish gray (5GY 4/1) to greenish black (5GY 2/1); occurs as thin 0.5–1.0 cm) bands of lenses with sharp contacts. About 30–40 such levels in core. Contains about 40–50% radiolarians.

4 – MARLY LIMESTONE (pelmicrite to micrite [minor lithology]), greenish gray (5GY 6/1) to olive gray (5Y 4/1); massive to faintly laminated at base, often with graded texture. Occasional chondrite burrows, generally containing pyrite. These limestones occur only in upper three sections.

Slumping with shear planes and contorted or folded beds in Section 4, 83–97 cm; Section 5, 46–52 cm; and possibly base of Section 6. Soft sediment deformation of limestone beds in Section 3.

Zones of elongate platy intraclasts (1 mm–2.5 cm long) of greenish claystone in Section 4, 62–68 cm (very small clasts); Section 5, 46–52 cm; and Section 6, 68–71 cm.

Thin Section of layer at Section 4, 68 cm has phosphate grains (sand-sized, concentric laminations), glauconite, Fe-oxide, pyritized radiolarians, micrite pellets, and rare bivalve shell fragments within the claystone clasts or claystone matrix.

Thin Section (Section 6, 72 cm) of black claystone (lithology 1) has 5% pyrite or pyritized radiolarian fragments, 5% quartz silt, mica, rare foraminifera, fine bivalve shells, phosphatic debris, and a phosphate concretion in a calcareous claystone matrix with organic material and pyrite and Fe-oxide.

Beds dip 5–15°.

SMEAR SLIDE SUMMARY (%):

	1, 4 M	1, 45 D	1, 110 D	2, 21 D	3, 67 D	4, 48 D
Texture:						
Silt	–	5	–	–	5	10
Clay	–	95	–	–	95	90
Composition:						
Quartz	–	1	5	–	1	2
Mica	–	1	3	–	–	2
Heavy minerals	–	1	1	–	–	TR
Clay	35	30	65	65	25	60
Pyrite	3	–	2	2	–	2
Carbonate unspec.	–	60	2	5	74	5
Calc. nannofossils	20	5	20	25	1	20
Radiolarians	40	–	–	–	3	3
Fish remains	–	–	–	1	–	–
Plant debris	–	2	2	–	1	5
Other	2	–	–	2	–	–

	4, 124 D	5, 50 M	1, 45 TS, M	4, 69 TS	6, 31 TS
Texture:					
Silt	–	15	–	5	5
Clay	–	85	–	95	95
Composition:					
Quartz	2	2	1	4	4
Mica	3	8	–	1	1
Heavy minerals	–	–	–	TR	–
Clay	52	82	25	78	68
Glauconite	1	–	–	1	–
Pyrite	3	1	–	4	5
Carbonate unspec.	5	–	74	10	22
Calc. nannofossils	15	3	–	–	TR
Diatoms	–	–	–	–	TR
Radiolarians	15	–	–	1	TR
Fish remains	–	2	–	1	TR
Plant debris	4	1	–	–	–

SITE 534 HOLE A CORE 126 CORED INTERVAL 1621.5–1630.5 m

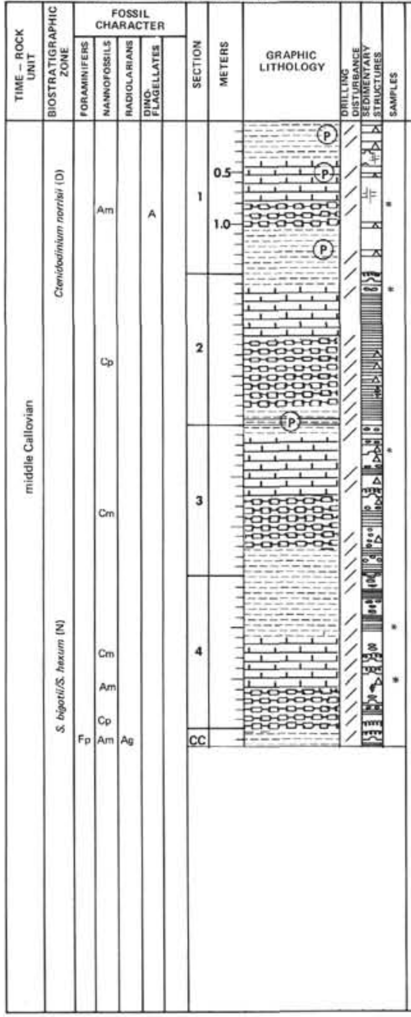

LITHOLOGIC DESCRIPTION

CARBONACEOUS CLAYSTONE to
NANNOFOSSIL CLAYSTONE

1 – CARBONACEOUS CLAYSTONE to NANNOFOSSIL CLAYSTONE, greenish black (5G 2/1) to olive black (5Y 2/1) with dark greenish gray (5G 4/1); finely laminated in general, but massive or with graded texture in many bands. Several bands have intraclasts of small platy elongate greenish claystone, often grading upward; intraclasts are usually ≤2 mm. Abundant specks and flakes of plant debris. Radiolarian siltstone layers (1 mm–1 cm thickness) are present, commonly partially replaced by pyrite. Scattered radiolarians or pyrite grains (replaced radiolarians or plant debris?). Smear slides of claystone have variable (10–25%) nannofossil and calcareous fine silt content. Intraclasts of greenish claystone have 30–40% nannofossils.

Section 3:
75–134 cm: calcareous claystone, varegated grayish red (5R 4/2), dusky red (5R 3/4), olive black (5GY 4/1), and greenish gray (5G 4/1). Textures similar to major lithology.

Section 4:
95 cm–Core-Catcher, base: nannofossil claystone, dark greenish gray (5G 4/1) to very dusky red (10R 2/2) to greenish black (5G 2/1). Textures similar to major lithology, but reduced organic matter content.

Slumping with shear planes and contorted bedding at several levels.

Section 3:
80–97 cm: zone with large flattened intraclasts of claystone up to 3 cm in length.

Bedding dips 10–15°, some possible current ripples.

SMEAR SLIDE SUMMARY (%):

	1, 84 D	2, 17 D	3, 27 D	4, 50 D	4, 100 D
Texture:					
Sand	1	1	1	1	–
Silt	10	6	2	2	3
Clay	89	93	97	97	97
Composition:					
Quartz	4	5	–	1	1
Feldspar	1	1	1	–	2
Mica	–	TR	–	–	1
Heavy minerals	–	–	–	1	TR
Clay	80	55	55	69	63
Volcanic glass	–	TR	–	–	–
Palagonite	1	1	1	–	1
Pyrite	–	2	–	–	–
Zeolite	–	–	–	–	1
Carbonate unspec.	5	3	–	5	5
Calc. nannofossils	5	30	40	20	25
Radiolarians	–	–	1	–	–
Plant debris	5	4	1	4	1

SITE 534 HOLE A CORE 127 CORED INTERVAL 1630.5–1639.5 m

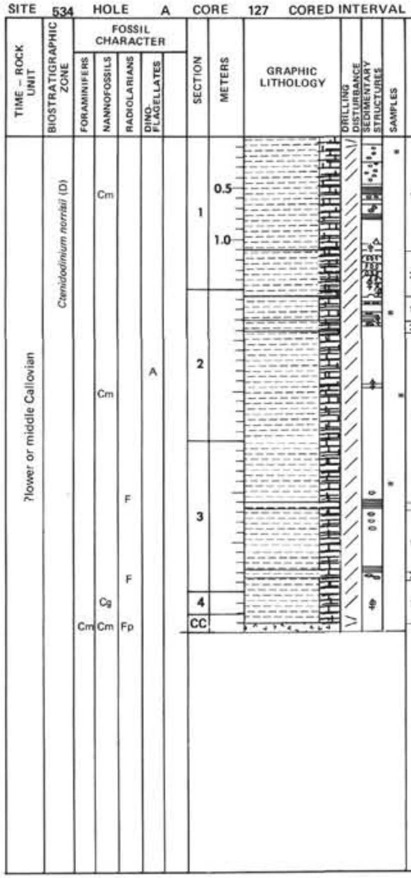

LITHOLOGIC DESCRIPTION

NANNOFOSSIL CLAYSTONE overlying BASALT

1 – NANNOFOSSIL CLAYSTONE (major lithology), grayish brown (5YR 3/2) to dusky brown (5YR 2/2) with some levels of grayish olive green (5GY 3/2) to grayish green (10G 4/2); massive to irregular laminated. Contains several radiolarian sand lenses or bands of 0.5–1.0 cm thickness of greenish gray. White flattened specks (fine shells?) common in Sections 3 and 4; can form laminations. Some levels contain plant debris.

2 – NANNOFOSSIL CLAYSTONE to MARLY LIMESTONE, grayish green (10GY 5/2), olive black (5Y 2/1), and dark greenish gray (5GY 4/1); laminated and partially carbonaceous.

Several beds of both claystone types contain small (1–2 mm) intraclasts of claystone.

Section 1, 110 cm–Section 2, 4 cm: zone of large (up to 3 cm) flattened claystone clasts of greenish, grayish, and reddish gray shades.

Bedding inclinations of 10–20°.

Core-Catcher:
10–20 cm: basalt, grayish black (N2) with white feldspar laths and filled vesicles. Thin section has variolitic feldspar texture.

SMEAR SLIDE SUMMARY (%):

	1,19 M	2, 28 D	2, 109 D	3, 42 D
Texture:				
Sand	50	–	–	–
Silt	10	5	10	15
Clay	40	95	90	85
Composition:				
Quartz	3	2	4	3
Feldspar	1	–	–	–
Mica	1	1	1	2
Heavy minerals	–	TR	TR	–
Clay	30	58	70	65
Pyrite	–	1	–	1
Carbonate unspec.	5	2	2	3
Calc. nannofossils	15	35	20	25
Radiolarians	50	–	–	–
Plant debris	1	1	2	1
Other	–	–	1	–

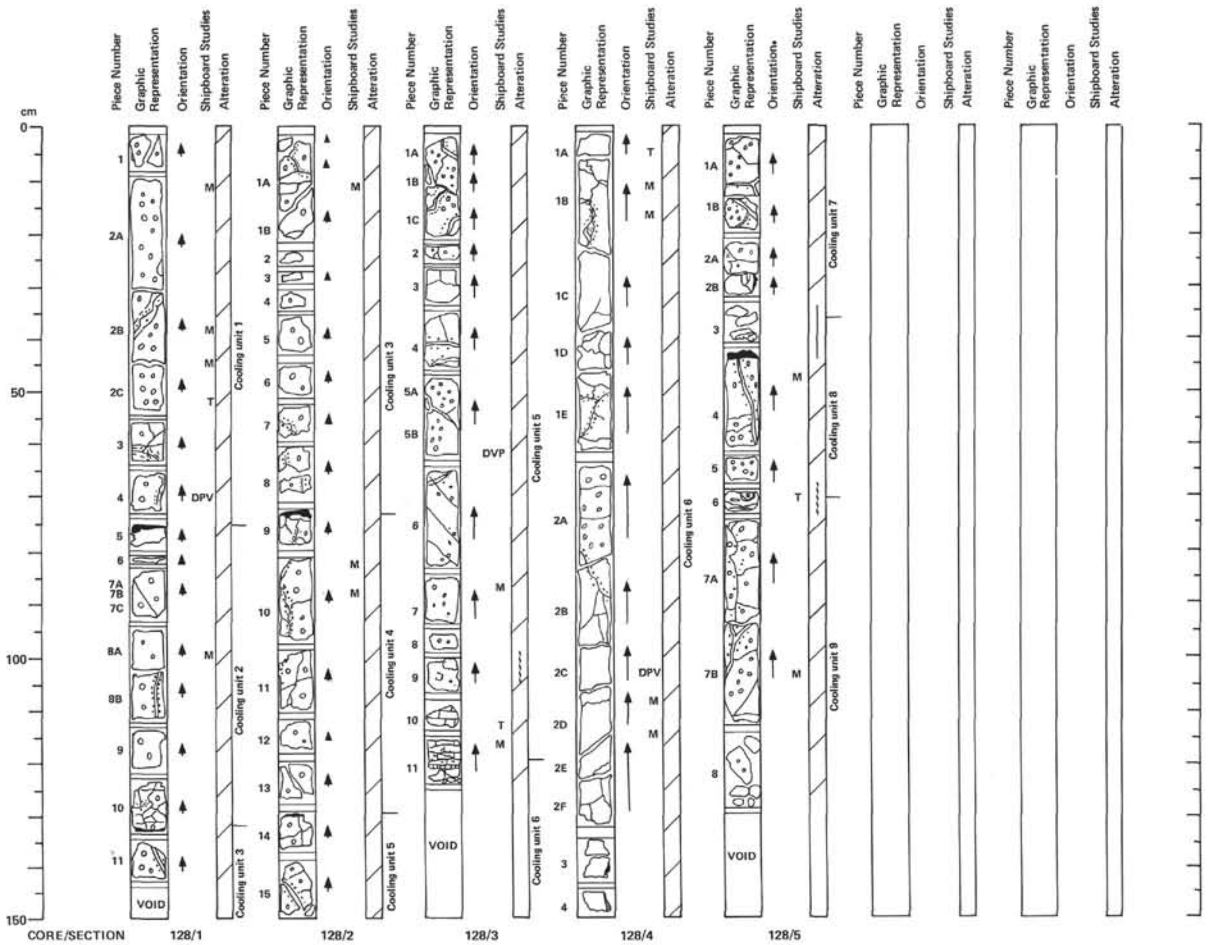

76-534A-128

Depth: 1639.5–1648.5 m

SECTION 1:

BASALT: dark gray (N3) with black speckles (claystone opaques?) and medium dark gray (N4) amygdules (circular), both about 1 mm in diameter, fine grained (<1 mm), aphyric, and sparsely to moderately vesicular (generally infilled). Common calcite veins, up to 2 mm across. Common greenish black (5GY 2/1) to dark greenish gray (5G 4/1) alteration products along fractures and with calcite in veins, sometimes moderate yellowish brown (10YR 5/4). Thin pyrite films common along some fractures.

GLASSY BASALT: *grayish black (N2) to greenish black (5GY 2/1) depending on extent of alteration, aphyric,* and very fine grained(?). Occurs as thin (up to 2 cm) thick layers apparently on margins of cooling units – e.g., 75 and 131 cm (reverse side of Piece 10).

CALCAREOUS CLAYSTONE: dark reddish brown (10R 3/4) 76–77, and 79–81 cm (Pieces 5 [part] and 6). Contains irregular fragments(?) of glassy basalt <2 cm across, especially in Piece 5, where there is a calcite mass (1 x 2 cm) grayish blue green (5BG 3/2) in color.

PIECES 2A, B, C: more amygdaloidal than rest of core section. Top 1 cm of Piece 2A, finer grained and less vesicular (possible chilled margin).

SECTION 2:

BASALT: identical to Section 1. Black infilled vesicles appear to be more abundant in the vicinity of fractures.
Top of Piece 14: 5 mm glassy basalt underlain by 5 mm finer grained non-vesicular basalt.
Top of Piece 9: 1 cm glassy basalt underlain by 5 mm finer grained non-vesicular basalt.

SECTION 3:

BASALT: aphyric, dark gray (N3) with scattered vesicles filled with dark green smectite(?). Moderately fractured *with some calcite-veins (with some green smectite? mixed). Very similar to basalt in Section 1 and 2. Vesicles* gray mixture of calcite and smectite (altered glass?) and yellowish palagonite(?).

CLAYEY LIMESTONE (limey claystone?): Piece 10 and the top part of Piece 11 is reddish brown clayey limestone, massive, and no sediment structures. Piece 11 (top part) is reddish brown clayey limestone with several white calcite veins. Large, horizontal calcite vein occurs approximately halfway down sample. Calcite in vein is fibrous (texture perpendicular to vein). Small calcite-veined basalt fragments in limestone just above vein. *Basalt below vein is aphyric and black.*

SECTION 4:

BASALT: aphyric, dark gray (N3), vesicular, moderately altered with scattered fractures and calcite-filled (plus smectite?) veins as marked. Vesicles are small (~0.5–1.0 mm) and many are filled with dark green smectite(?) and white calcite. Piece 2A has one side with calcite-filled vesicles and the other with smectite-filled vesicles. Several small pyrite crystals in Piece 1E. Glassy margins on back sides of Pieces 3 and 4. Clay-filled vesicles appear to occur around veins. Grain size appears to coarsen from top of Piece 1A to about 16 cm, then uniforms below. Piece 1A and top of 1B appear to be more fine-grained than rest of section.

SECTION 5:

BASALT: dark gray (N3) aphyric, vesicular with vesicules partly filled with dark green smectite(?). Calcite and smectite veins common as marked. Glassy margins (altered to clay) in Pieces 2B and 4 mark boundaries of cooling units. Top of Piece 4 is chilled. Piece 6 contains a piece of basalt surrounded on one side by mixed calcite and yellowish brown palagonite(?). Outer coating of quartz on one side of sample with calcite layer just below. See drawing:

LIMESTONE: small piece of reddish limestone in rubble of Piece 3.

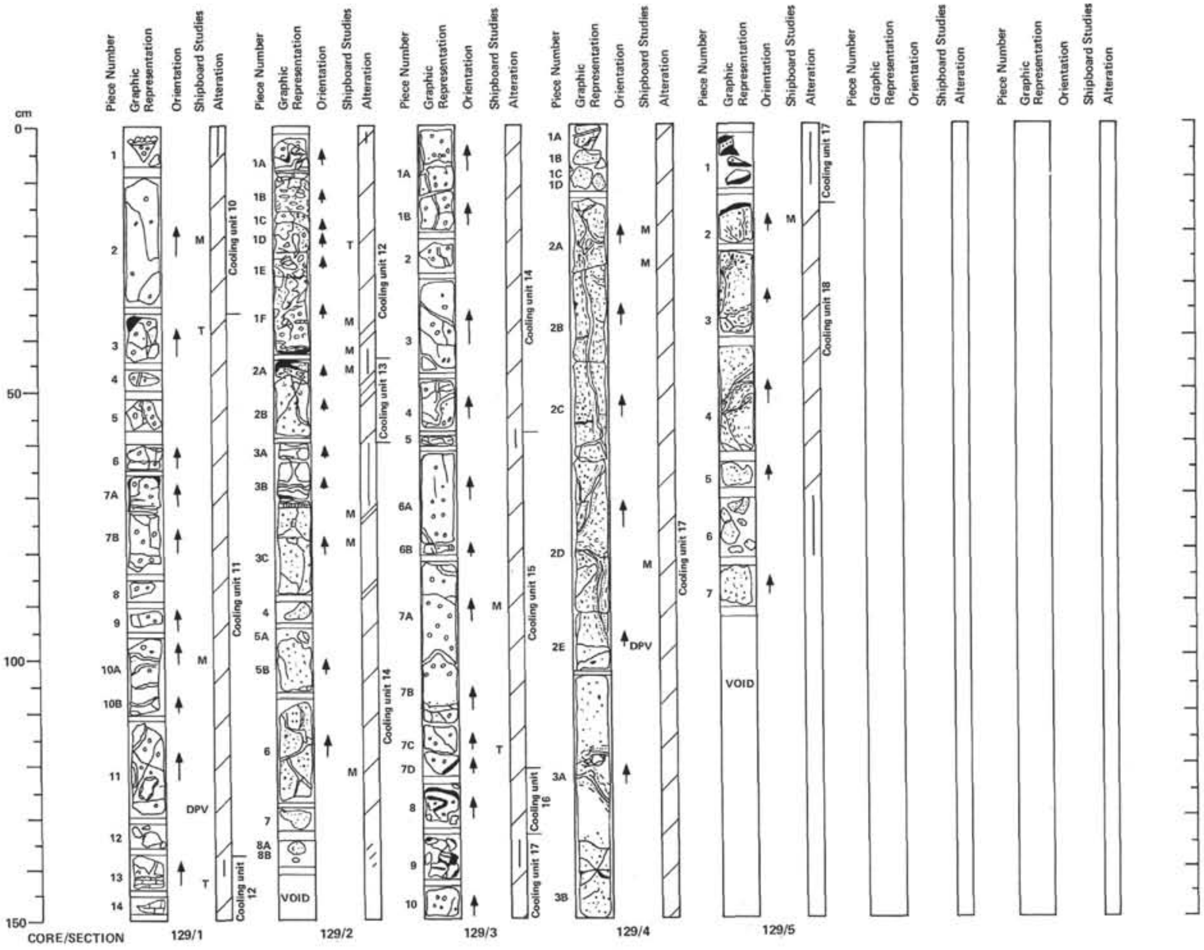

76-534A-129 **Depth: 1648.5–1657.5 m**

SECTION 1:

BASALT: dark gray (N3), aphyric with scattered vesicles filled with white calcite and dark green smectite(?). Vesicles are longer and more numerous in Pieces 4 through 7B. Calcite- and smectite(?)-filled veins are common (as marked). Fibrous calcite grows perpendicular to fractures in some cases. Piece 1 is aphanitic and highly altered (all vesicles filled). One surface has an outer coating of spherulitic (botryoidal) quartz overlying green clays then a thin discontinous white calcite layer over altered basalt. See drawing:

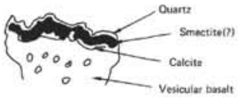

Pieces 3 and possibly 7 have glassy margins.

CLAYEY LIMESTONE: reddish brown, siliceous? aphanitic/massive with no obvious sedimentary structures (Pieces 13 and 14). Piece 13 shows a sharp contact between claystone and basalt as shown below:

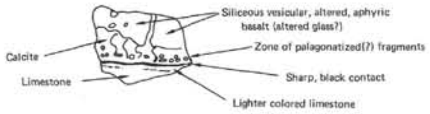

SECTION 2:

VESICULAR BASALT: fine-grained, moderately altered throughout. Vesicles about 0.1 mm at top of section, gradually increasing to about 1 mm in diameter. Piece 1A contains several fractures which may have been infilled with red metalliferrous sediment, with quartz veins in the bottom half intermingling with the sediment in the middle. Pieces 1B–1F are brecciated basalt fragments in a matrix of hydrothermal quartz and calcite. Greenish color possible smectite. Piece 2A appears to be capped by glassy basalt with an altered zone below. Piece 2B is a fractured basalt. Pieces 3A and 3B contain quartz infilled with hydrothermal calcite. Piece 3C is a basalt (fractured) capped by an altered zone of quartz, red sediment(?) and calcite. Remainder of section is fractured vesicular basalt; Piece 6 contains hydrothermal quartz.

SECTION 3:

BASALT: aphyric, vesicular, dark gray (N3), with scattered calcite veins. Smectite-filled fractures are less common. Grain size appears uniform throughout except in Pieces 8 and 9 where basalt appears finer grained near glassy (altered) margins. Vesicles filled with green smectite(?) and some calcite. Brownish clay(?) mixed with calcite in some veins. Piece 5 is highly altered to calcite and smectite. Piece 8 has glassy margins on 3 sides with a sinuous pattern of aphyric basalt inbetween; intense calcite and smectite(?) alteration of outside edges of glass. Fragments comprising Piece 9 have glassy margins, several dark glassy(?) bands, and calcite/smectite alteration.

SECTION 4:

VESICULAR BASALT: moderately altered with frequent fracturing, sometimes filled with hydrothermal quartz and palagonite. Piece 2A is quartz filled about half its length, gradually changing to a quartz/palagonite vein. Some of the vesicles are beginning to be filled with calcite. Piece 2B contains basalt with a palagonite/quartz vein, some of the altered zone being also composed of palagonite. In the top half, the vesicles are mostly calcite filled. Piece 2C is similar; however, 2D is typified by a distinct loss of vesicles. Pieces 2A and C contain vesicles of 1 mm diameter whereas the size and frequency diminish very rapidly. In the middle of Piece 2D the vesicles are again present, but less numerous. Their size range is about 1–2 mm. This trend continues until Piece 3B where vesicles are again numerous.

SECTION 5:

VESICULAR BASALT: moderately altered with frequent fractures, mostly filled with hydrothermal quartz. Pieces in 1 are glassy basalt. Piece 2 has a glassy top; some calcitic vesicles present. The remainder of the section is fairly similar with about a 50:50 ratio of glass and calcite-filled vesicles. Piece 7 contains 100% calcite vesicles.

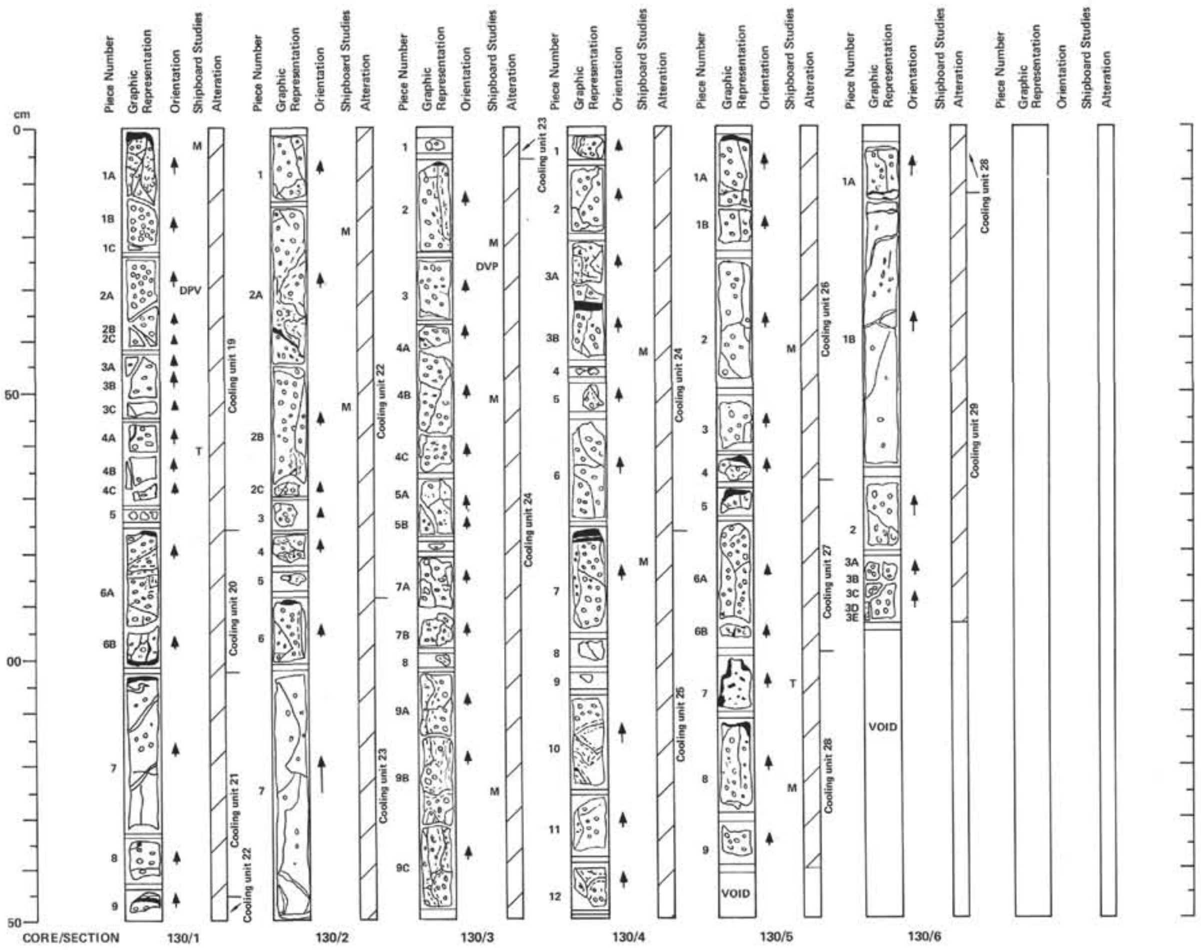

76-534A-130

Depth: 1657.5–1666.5 m

SECTION 1:

BASALT: dark gray (N3) aphyric and vesicular. Vesicles 0.1–1.0 mm diameter, usually filled with dark mineral (celadonite, smectite?), about 30% filled with calcite (more locally at Pieces 7 and 8), a few filled with pyrite or calcedony. Generally grains are two small to see but plagioclase laths >1 mm are apparent in Pieces 2, 3, and 4. Fractures are occasionally filled with calcite in Pieces 6 and 7, others may be filled with celadonite or clay. Alteration rims apparent only in Piece 6. Pyrite scattered along fractures.

Chilled margins at 0, 98, and 143 cm are very narrow (3–5 mm) and have lost most of glassy luster. Margin at 143 cm is highly fractured and may be alteration zone.

Possible chilled margin at 76 cm.

SECTION 2:

BASALT: dark gray (N3) aphyric and vesicular. Vesicles 0.1–1.0 mm diameter usually filled with dark (N1) mineral possibly celadonite or smectite, about 30% filled with calcite, a few with quartz and pyrite. Plagioclase laths usually large enough to be seen by eye, 0.5–1.0 mm. Fractures are filled with white (N9) calcite, clear quartz, black (N1) and/or light olive brown (5Y 5/6) mineral. Alteration rims are narrow, less than 2 mm, light brown (5YR 5/6) to dark yellowish orange (10YR 6/6) in color.

Chilled margin at 90 cm (top of Piece 6), very narrow, and preserved only at top of piece.

Glassy vein at 80 and 40 cm (oblique).

SECTION 3:

BASALT: as described in previous 2 sections. Chilled margin at top of Piece 2.

Black infilled and light gray infilled vesicles show antipathetic distribution, former closer to fractures.

SECTION 4:

BASALT: as in previous 3 sections. Very dense, chilled margins(?) in top of Piece 3 and top of Piece 7. Neither is glassy.

Margin at top Piece 3B may be a vein/fracture.

SECTION 5:

BASALT: as in previous 4 sections. Chilled glassy margin exhibited at top of Pieces 1A, 4, 5, and 8.

Piece 7 differs in having no vesicles, considerable glass, very fine-grained with no macroscopic plagioclase. May be a holohyaline or hypocrystaline basalt.

Piece 7 contains glassy fragments.

SECTION 6:

APHYRIC BASALT: with clay- and calcite-filled vugs. Possible glassy margins at base of Piece 1A and top of Piece 1B. Calcite veins sparse in Piece 1B. Pieces in this section are otherwise homogeneous.

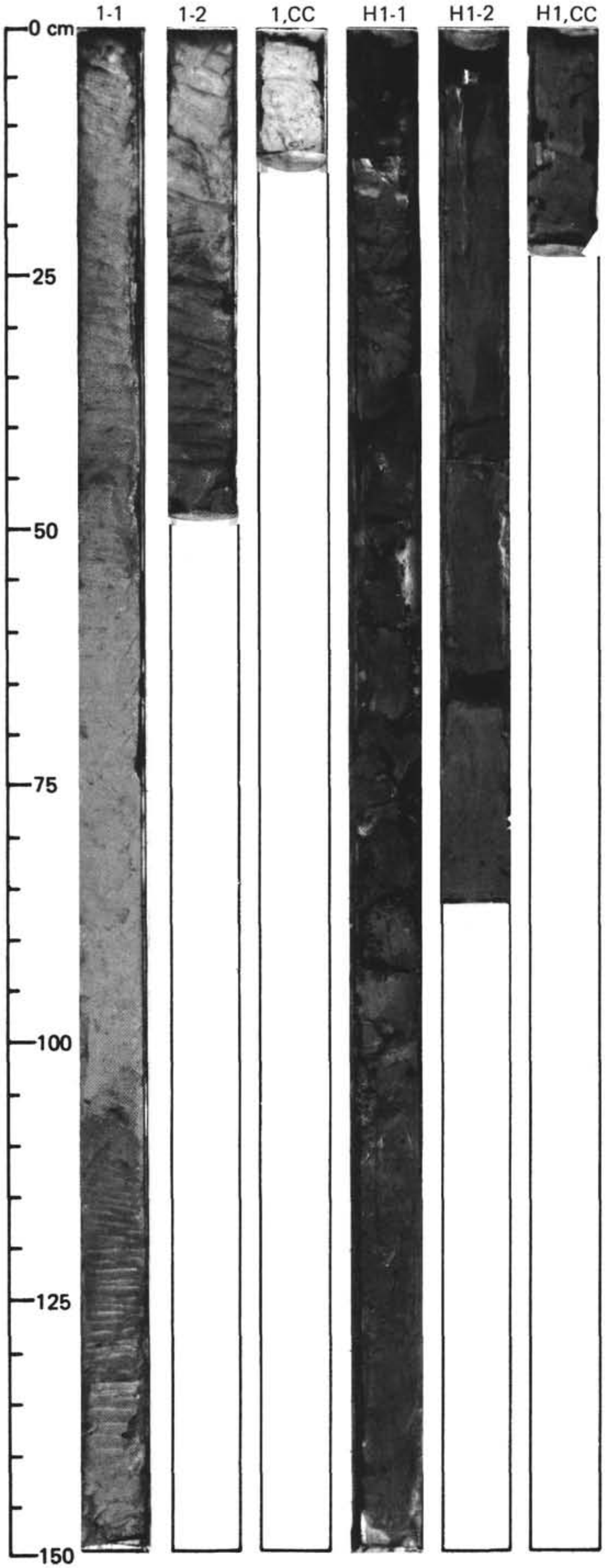
1-1
1-2
1,CC
H1-1
H1-2
H1,CC
0 cm
25
50
75
100
125
150

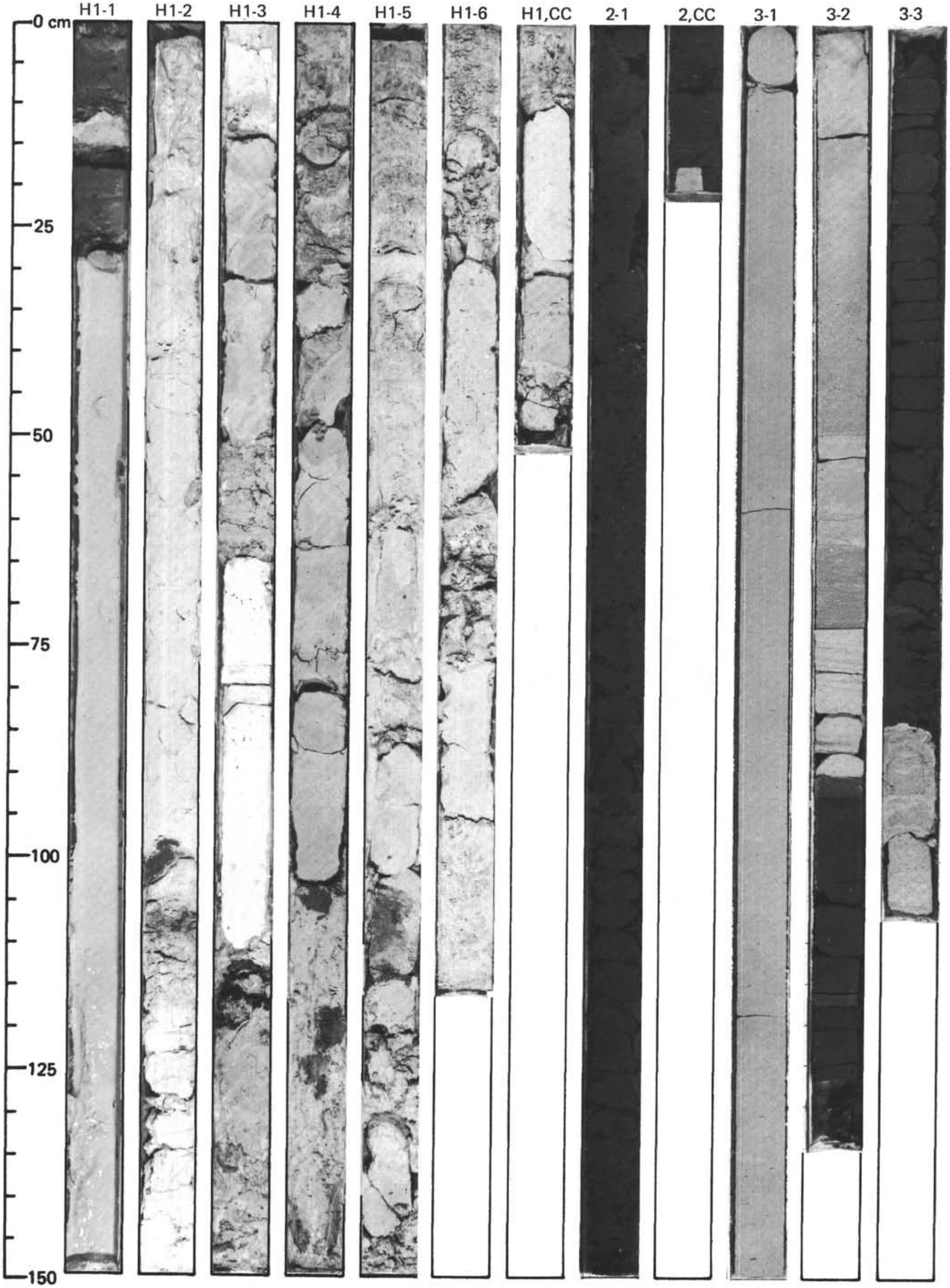
H1-1
H1-2
H1-3
H1-4
H1-5
H1-6
H1,CC
2-1
2,CC
3-1
3-2
3-3
0 cm
25
50
75
100
125
150

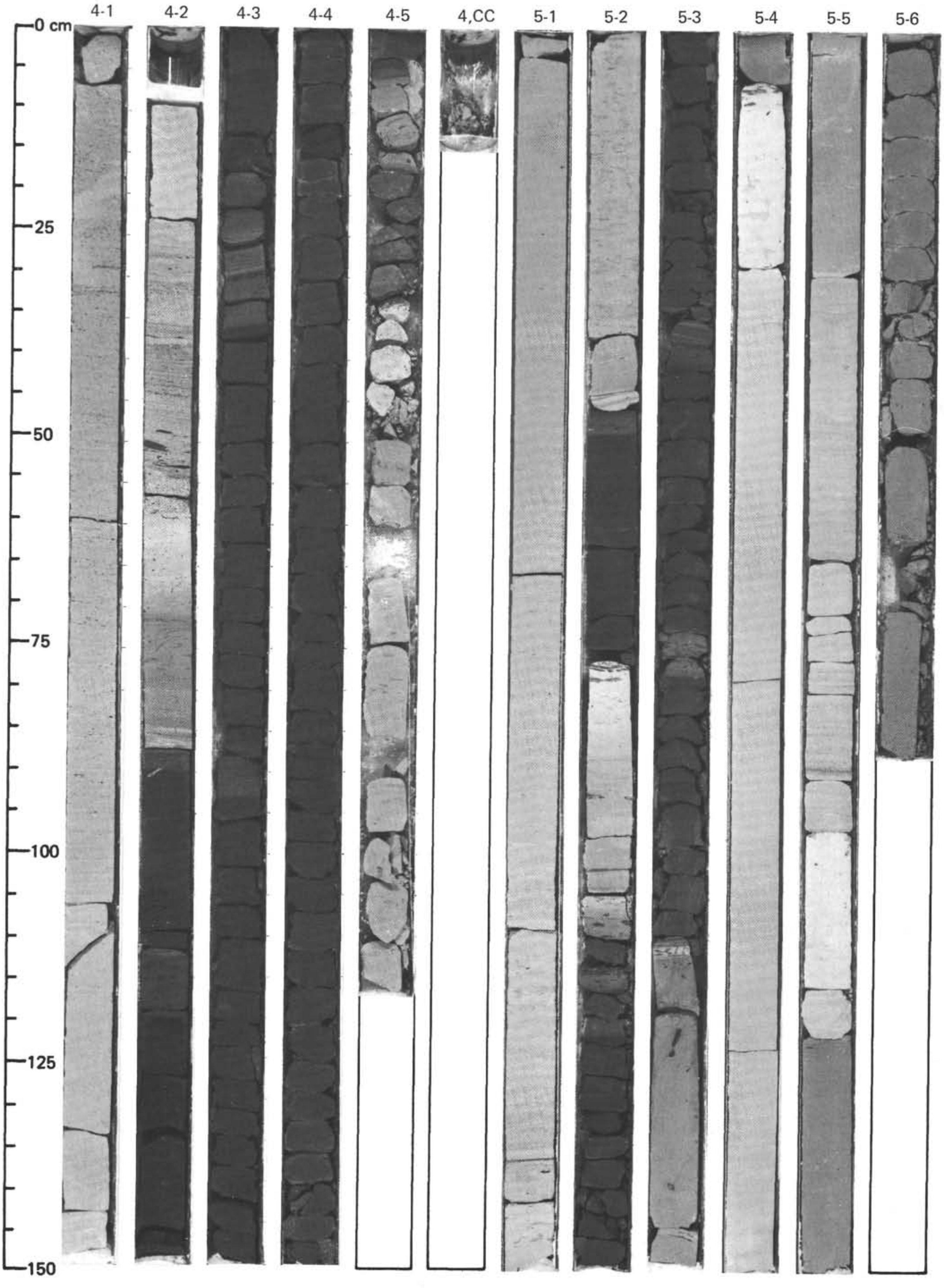
4-1
4-2
4-3
4-4
4-5
4,CC
5-1
5-2
5-3
5-4
5-5
5-6
0 cm
25
50
75
100
125
150

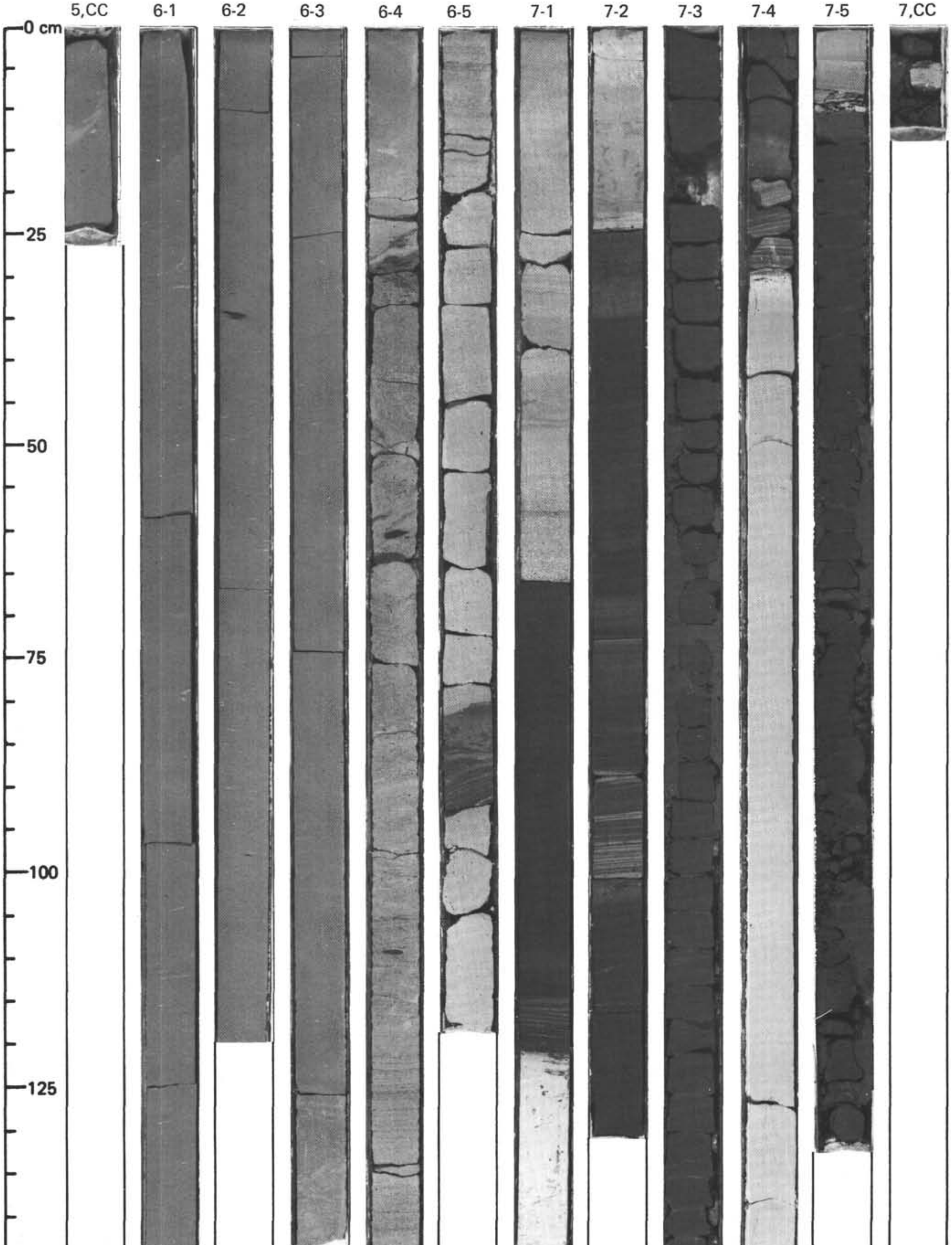
5,CC
6-1
6-2
6-3
6-4
6-5
7-1
7-2
7-3
7-4
7-5
7,CC
0 cm
25
50
75
100
125
150

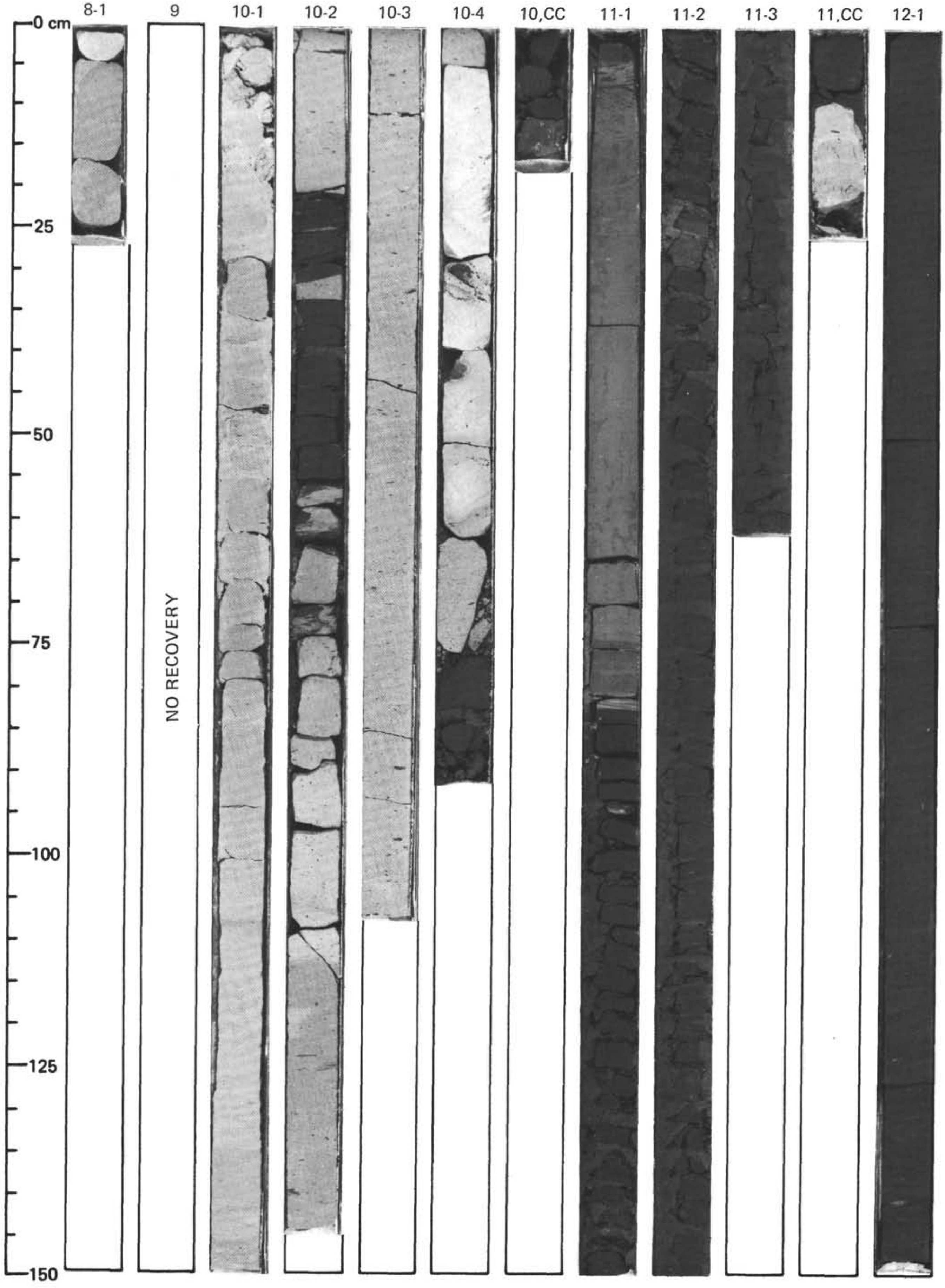
8-1
9
10-1
10-2
10-3
10-4
10,CC
11-1
11-2
11-3
11,CC
12-1
0 cm
25
50
75
100
125
150
NO RECOVERY

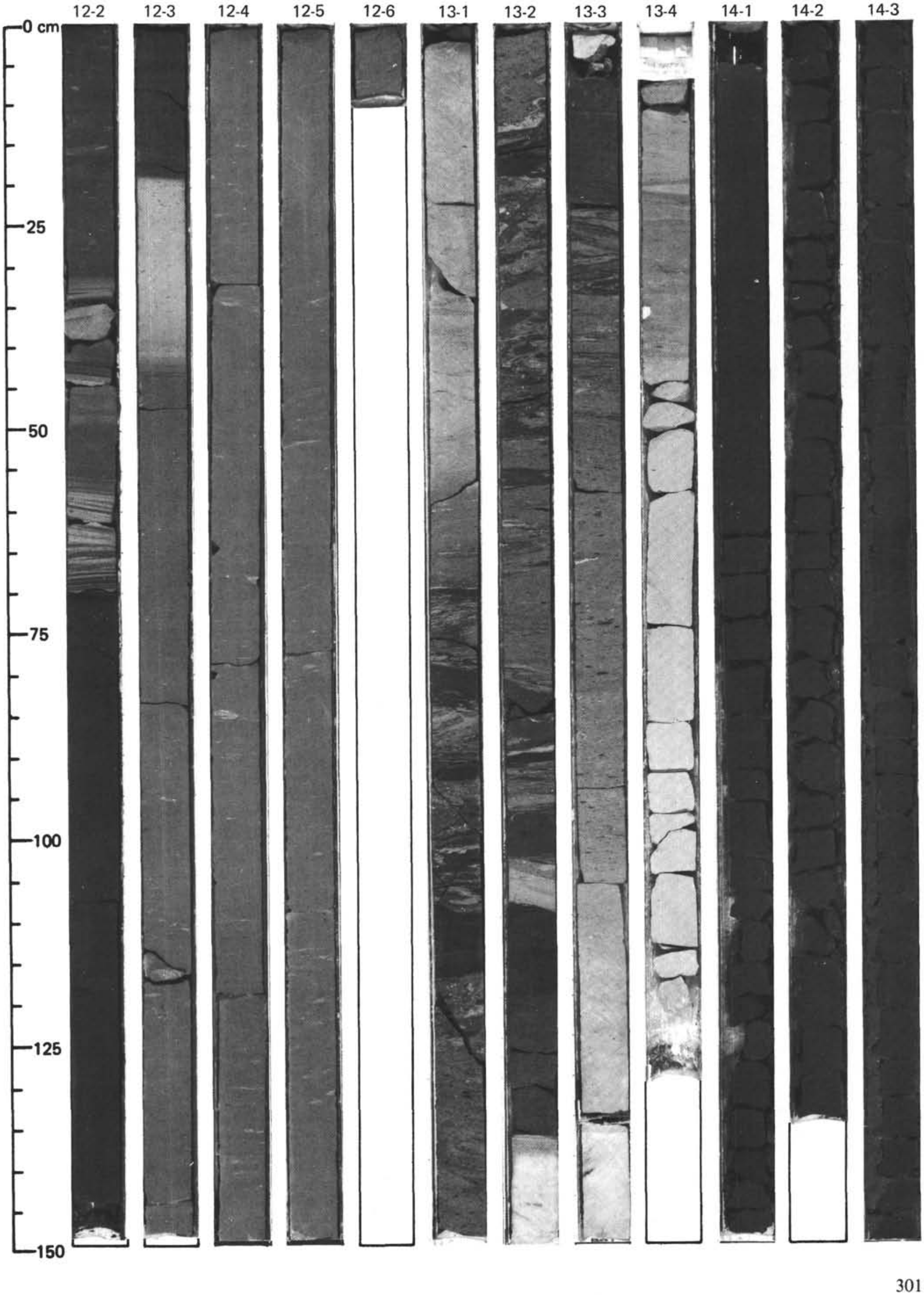
12-2
12-3
12-4
12-5
12-6
13-1
13-2
13-3
13-4
14-1
14-2
14-3
0 cm
25
50
75
100
125
150

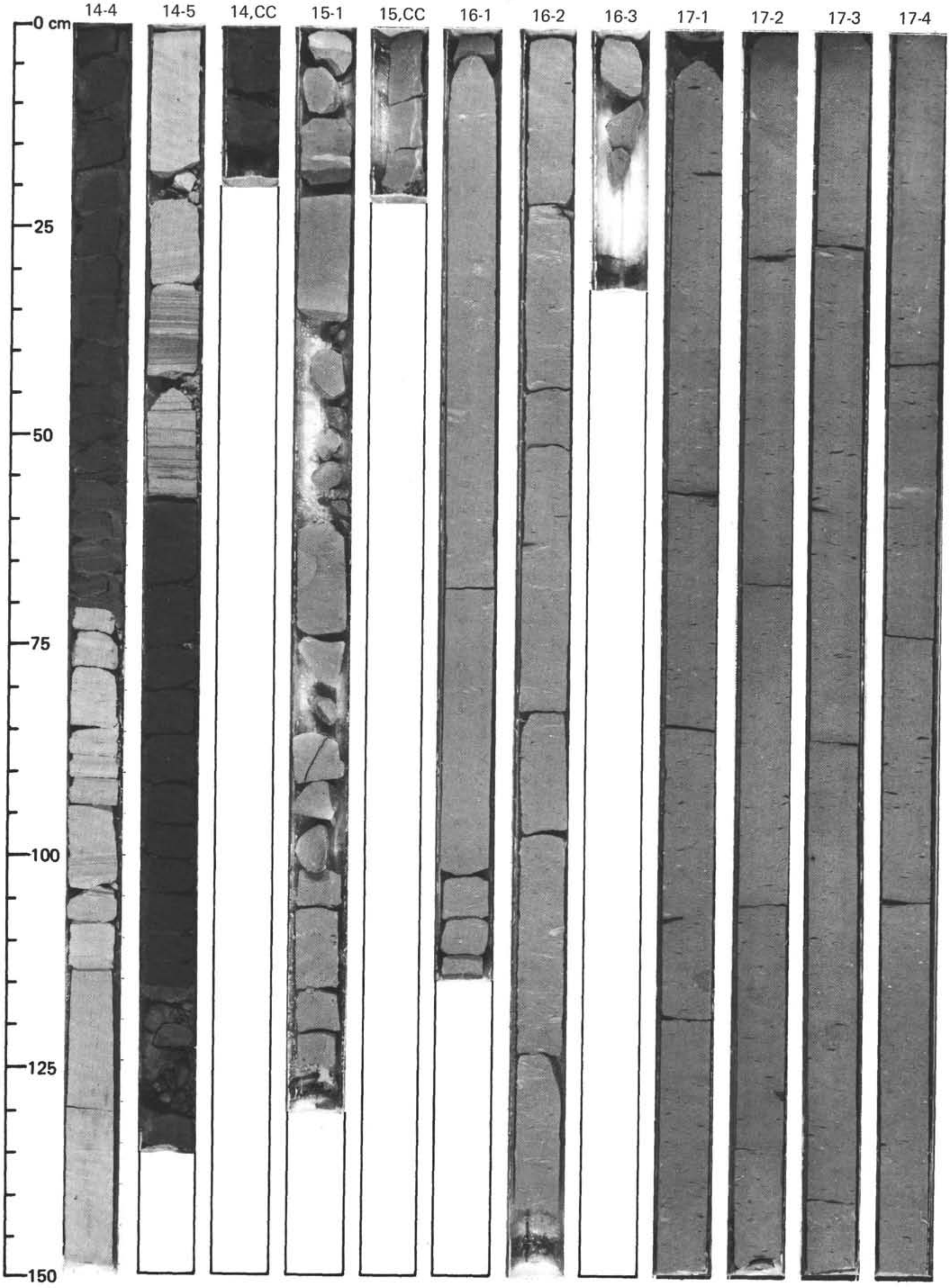
0 cm
25
50
75
100
125
150
14-4
14-5
14,CC
15-1
15,CC
16-1
16-2
16-3
17-1
17-2
17-3
17-4

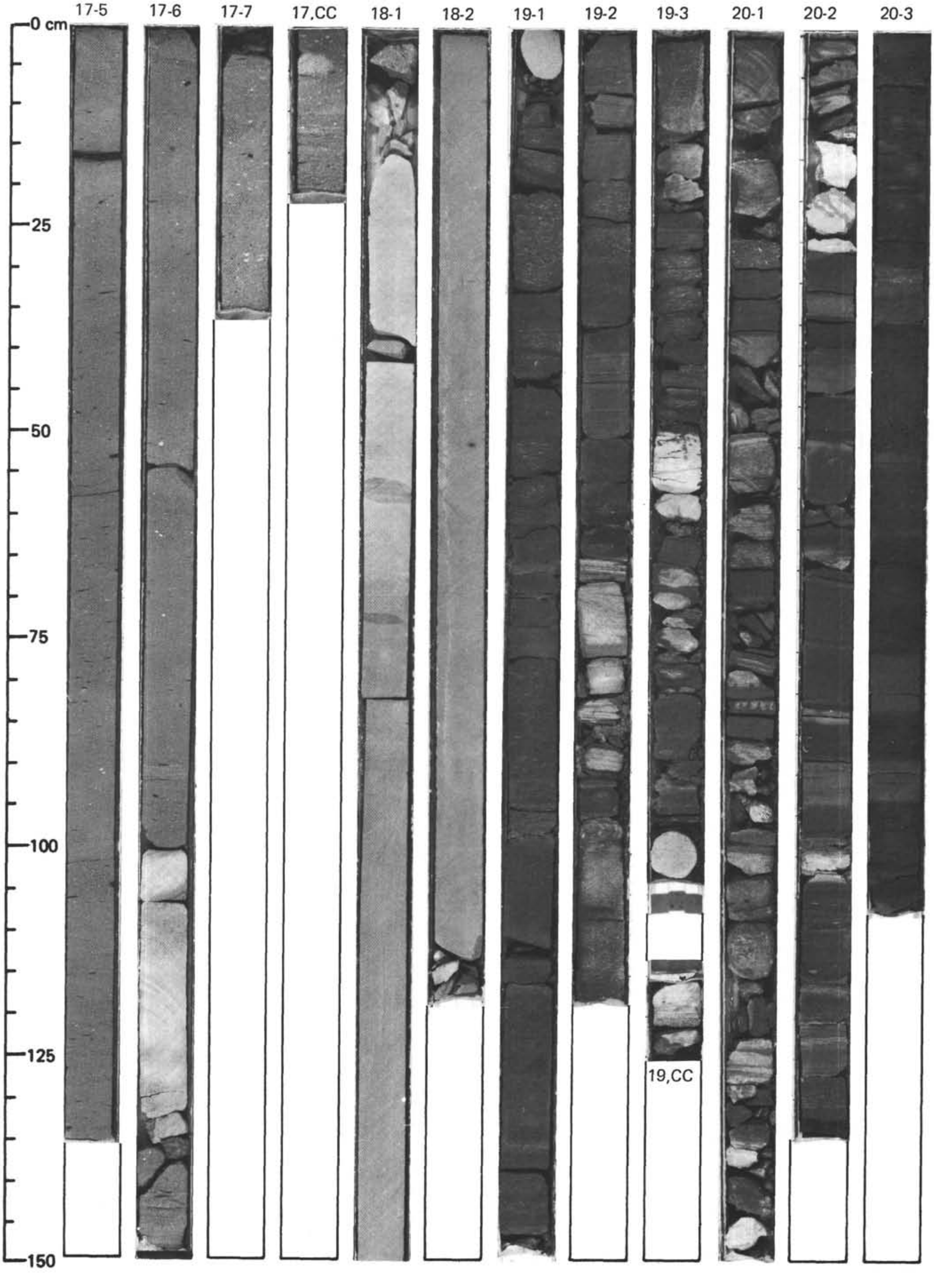
17-5
17-6
17-7
17,CC
18-1
18-2
19-1
19-2
19-3
20-1
20-2
20-3
0 cm
25
50
75
100
125
150
19,CC

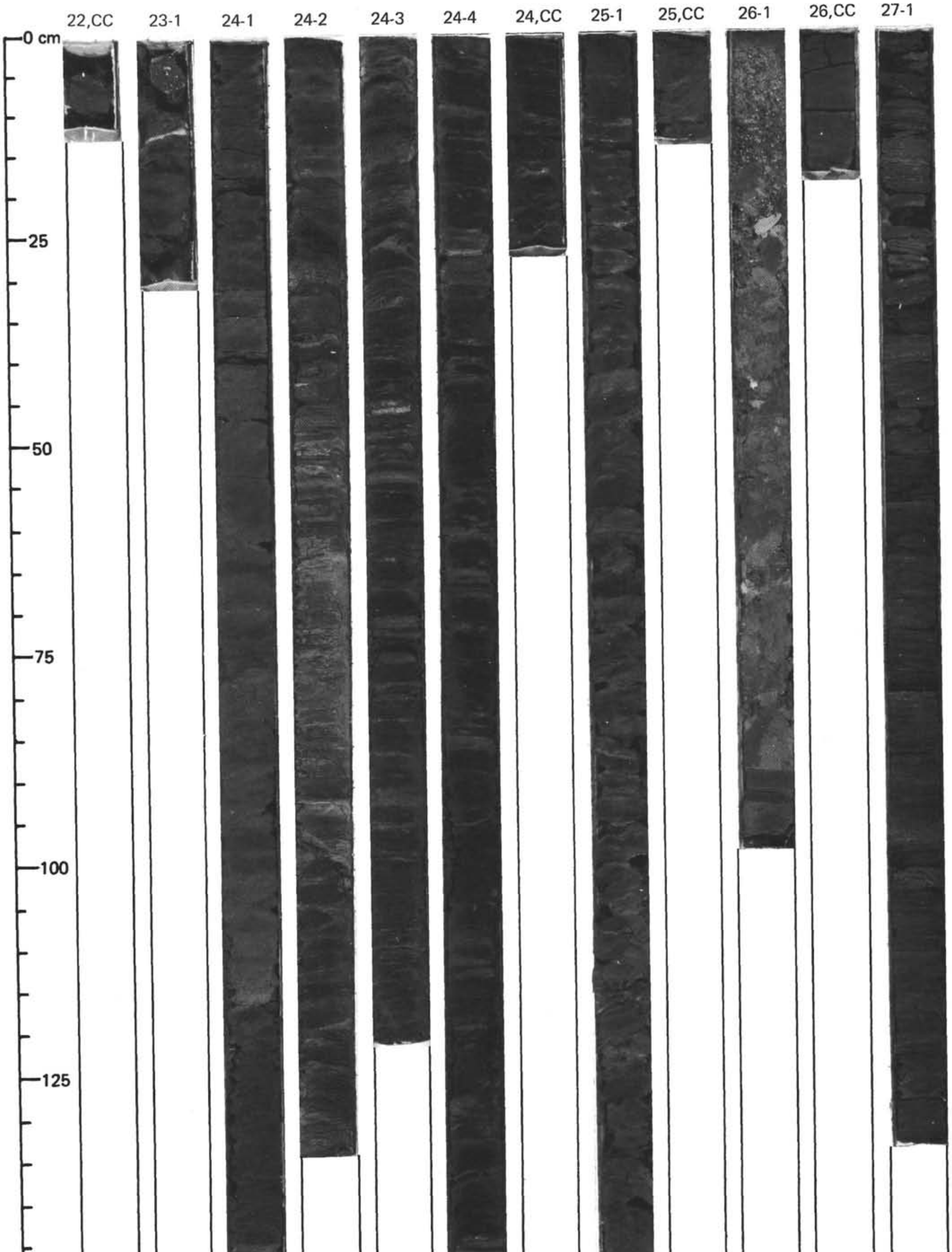
22,CC
23-1
24-1
24-2
24-3
24-4
24,CC
25-1
25,CC
26-1
26,CC
27-1
0 cm
25
50
75
100
125
150

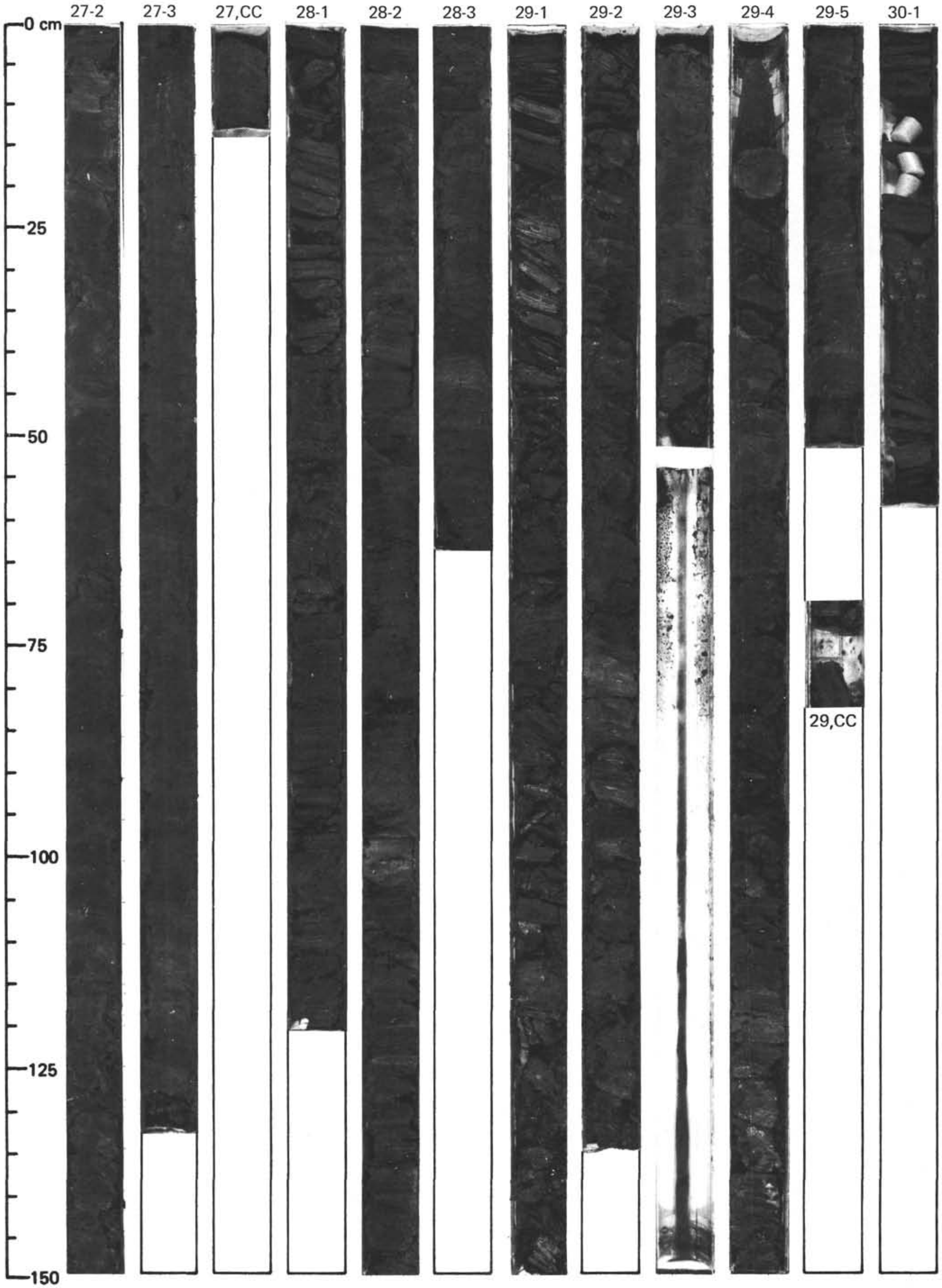
27-2
27-3
27,CC
28-1
28-2
28-3
29-1
29-2
29-3
29-4
29-5
30-1
0 cm
25
50
75
100
125
150
29,CC

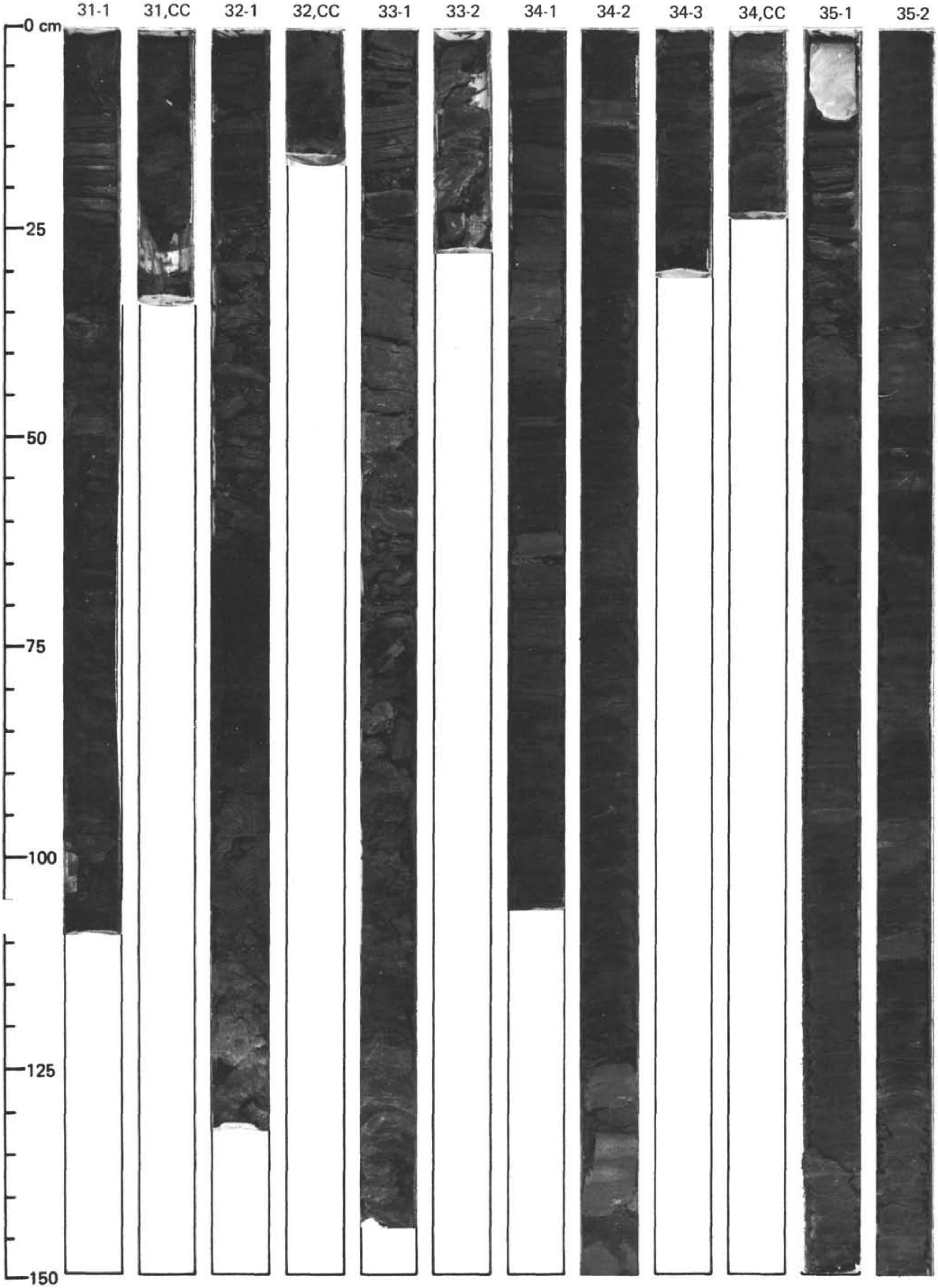
31-1
31,CC
32-1
32,CC
33-1
33-2
34-1
34-2
34-3
34,CC
35-1
35-2
0 cm
25
50
75
100
125
150

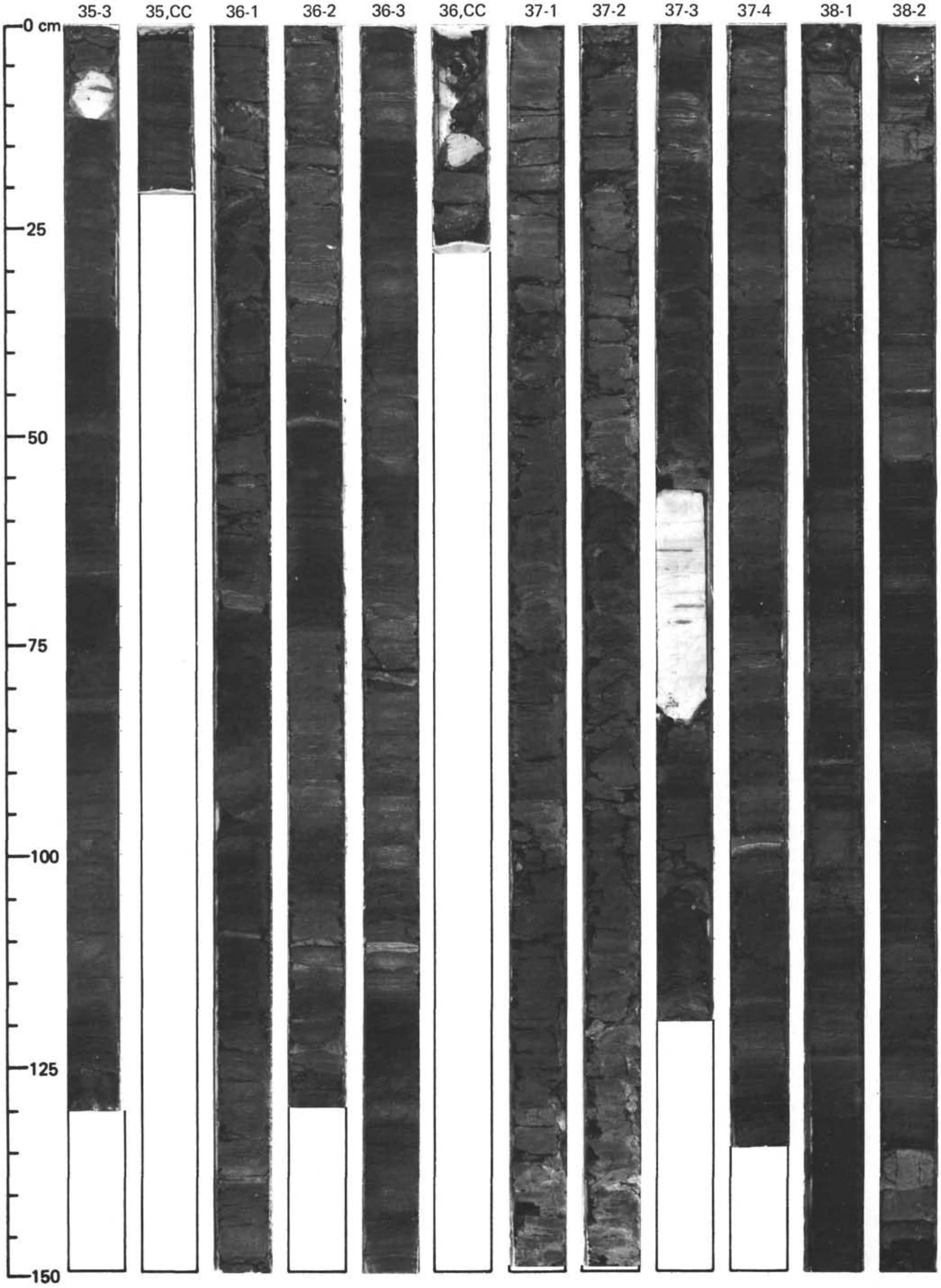
35-3
35,CC
36-1
36-2
36-3
36,CC
37-1
37-2
37-3
37-4
38-1
38-2
0 cm
25
50
75
100
125
150

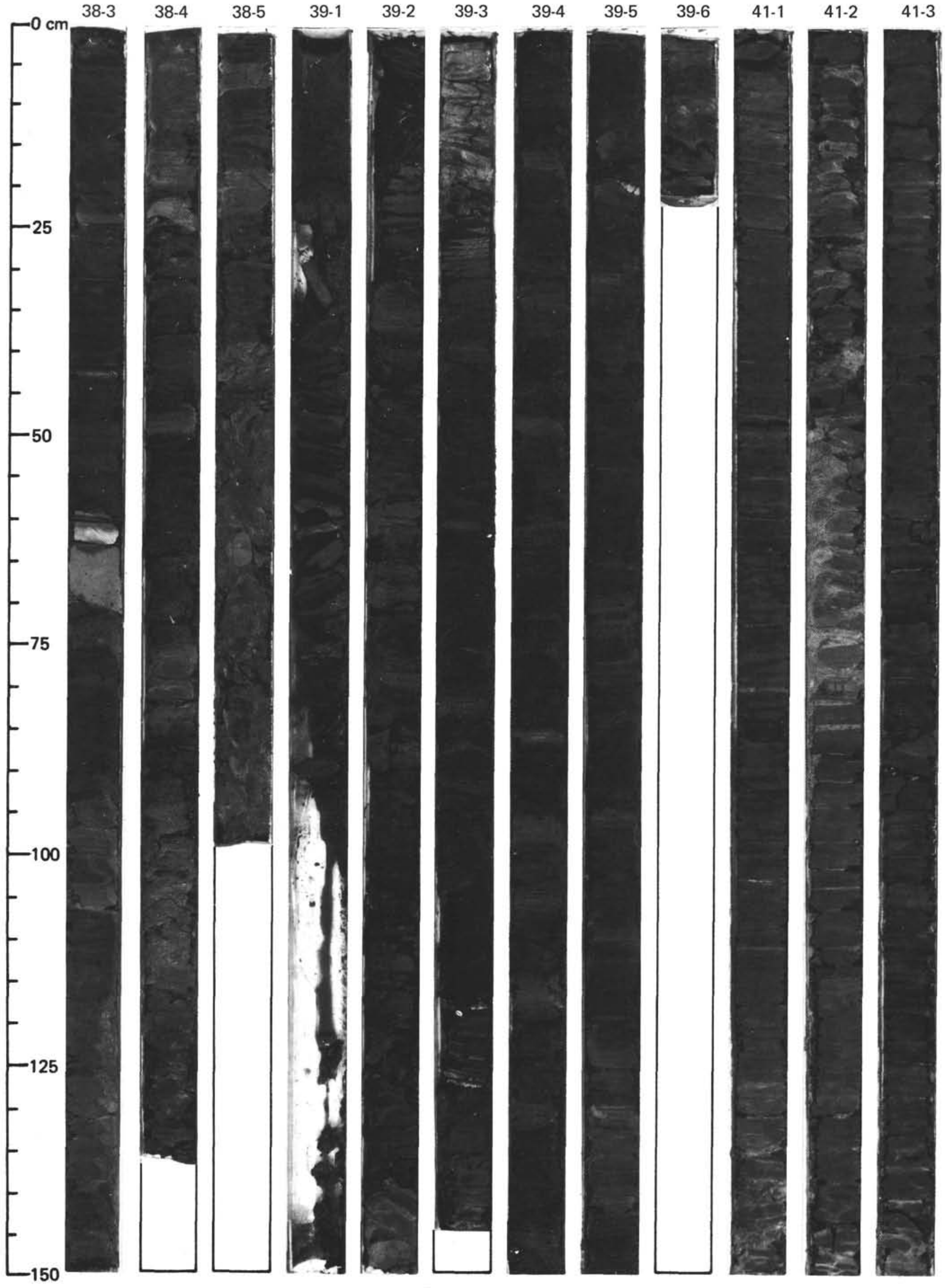
38-3
38-4
38-5
39-1
39-2
39-3
39-4
39-5
39-6
41-1
41-2
41-3
0 cm
25
50
75
100
125
150

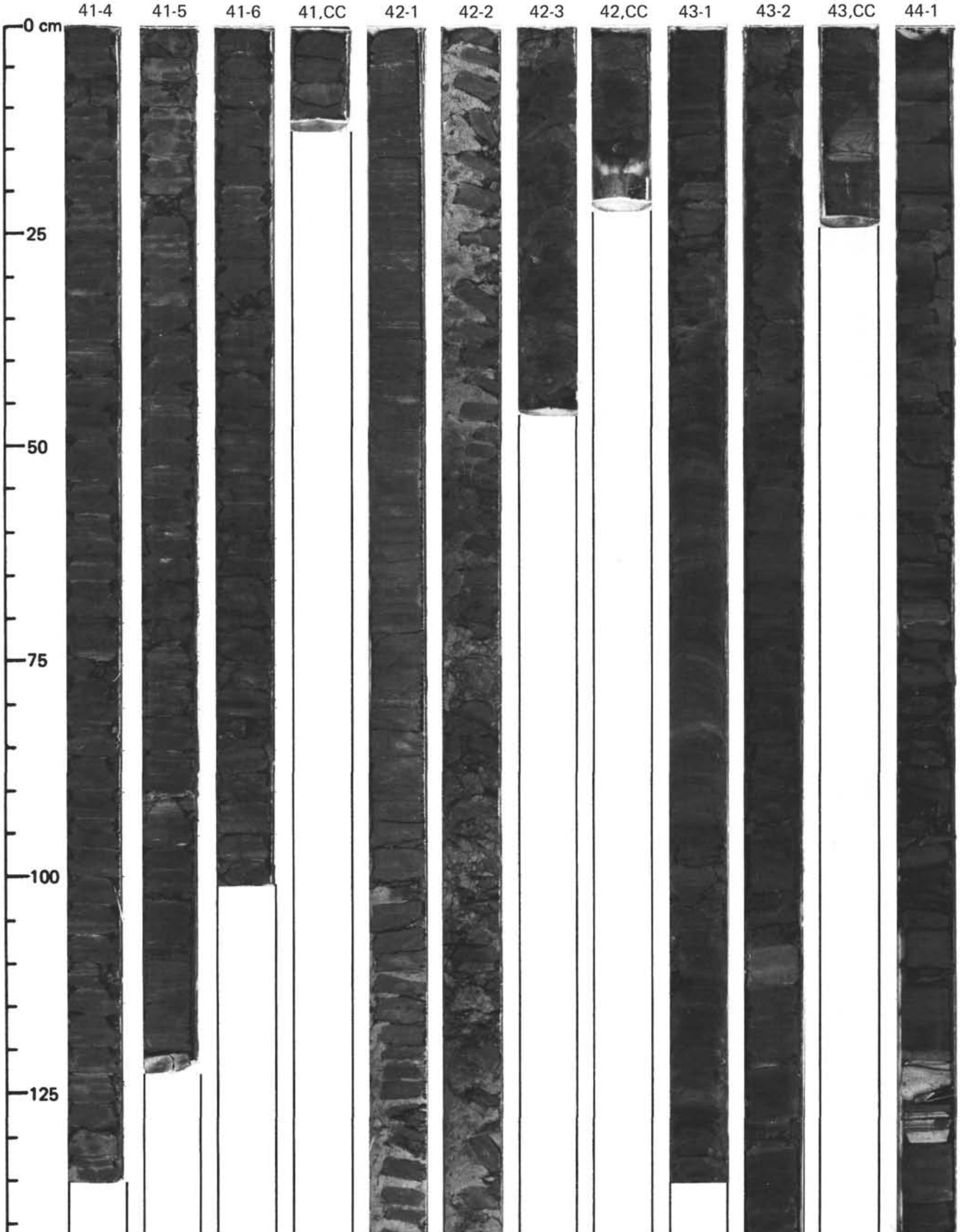
41-4
41-5
41-6
41,CC
42-1
42-2
42-3
42,CC
43-1
43-2
43,CC
44-1
0 cm
25
50
75
100
125
150

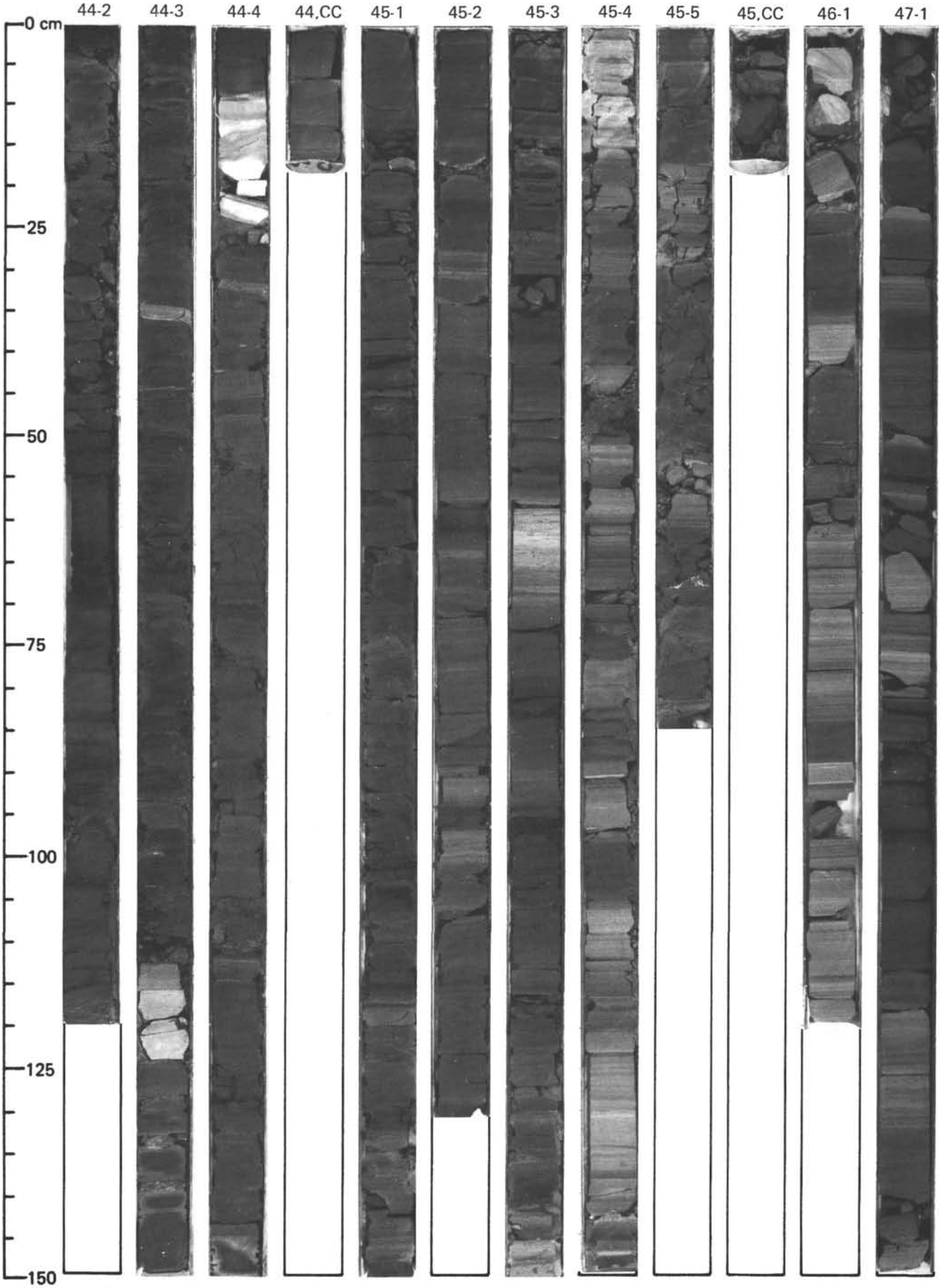
44-2
44-3
44-4
44,CC
45-1
45-2
45-3
45-4
45-5
45,CC
46-1
47-1
0 cm
25
50
75
100
125
150

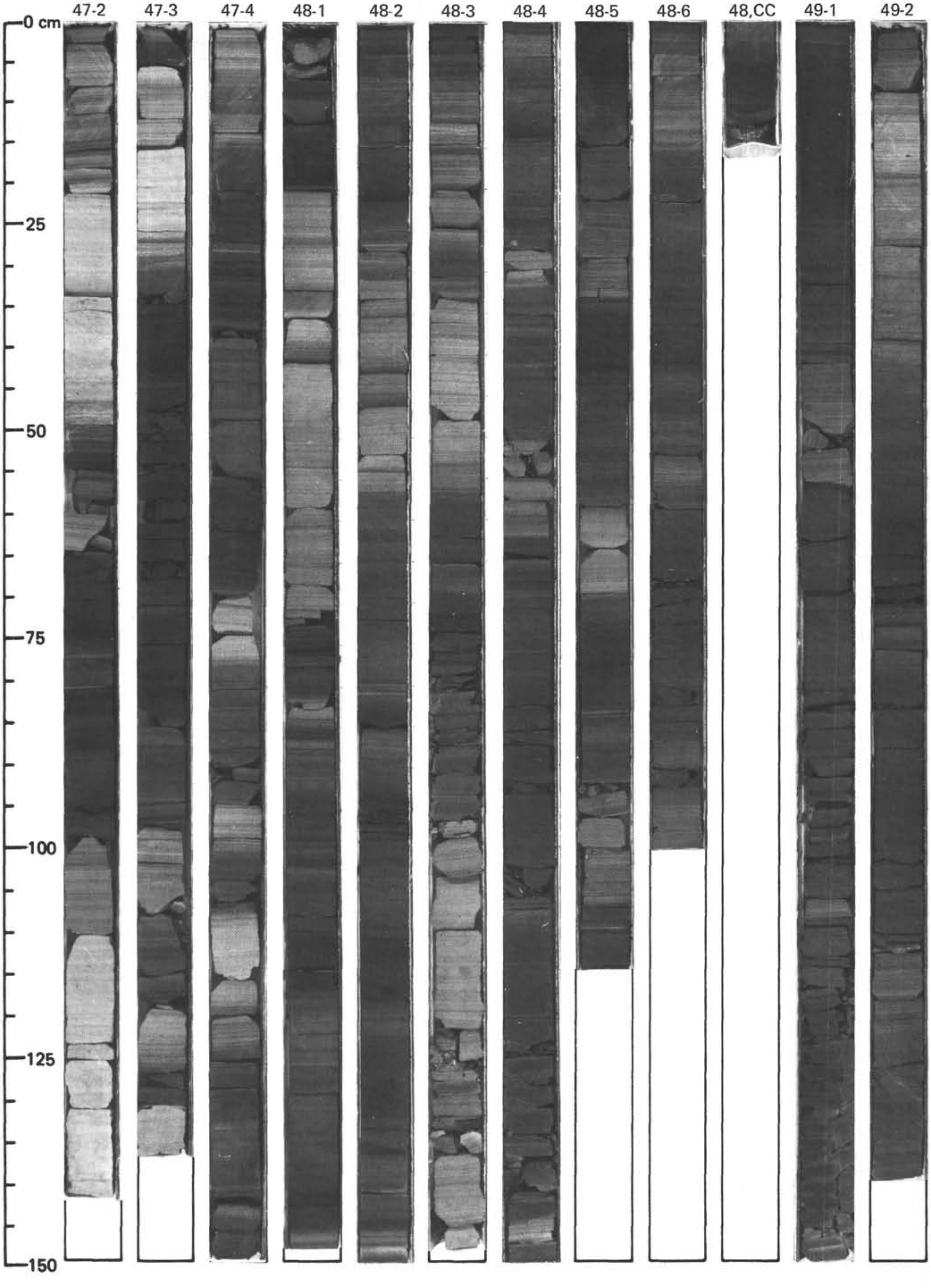
47-2
47-3
47-4
48-1
48-2
48-3
48-4
48-5
48-6
48,CC
49-1
49-2
0 cm
25
50
75
100
125
150

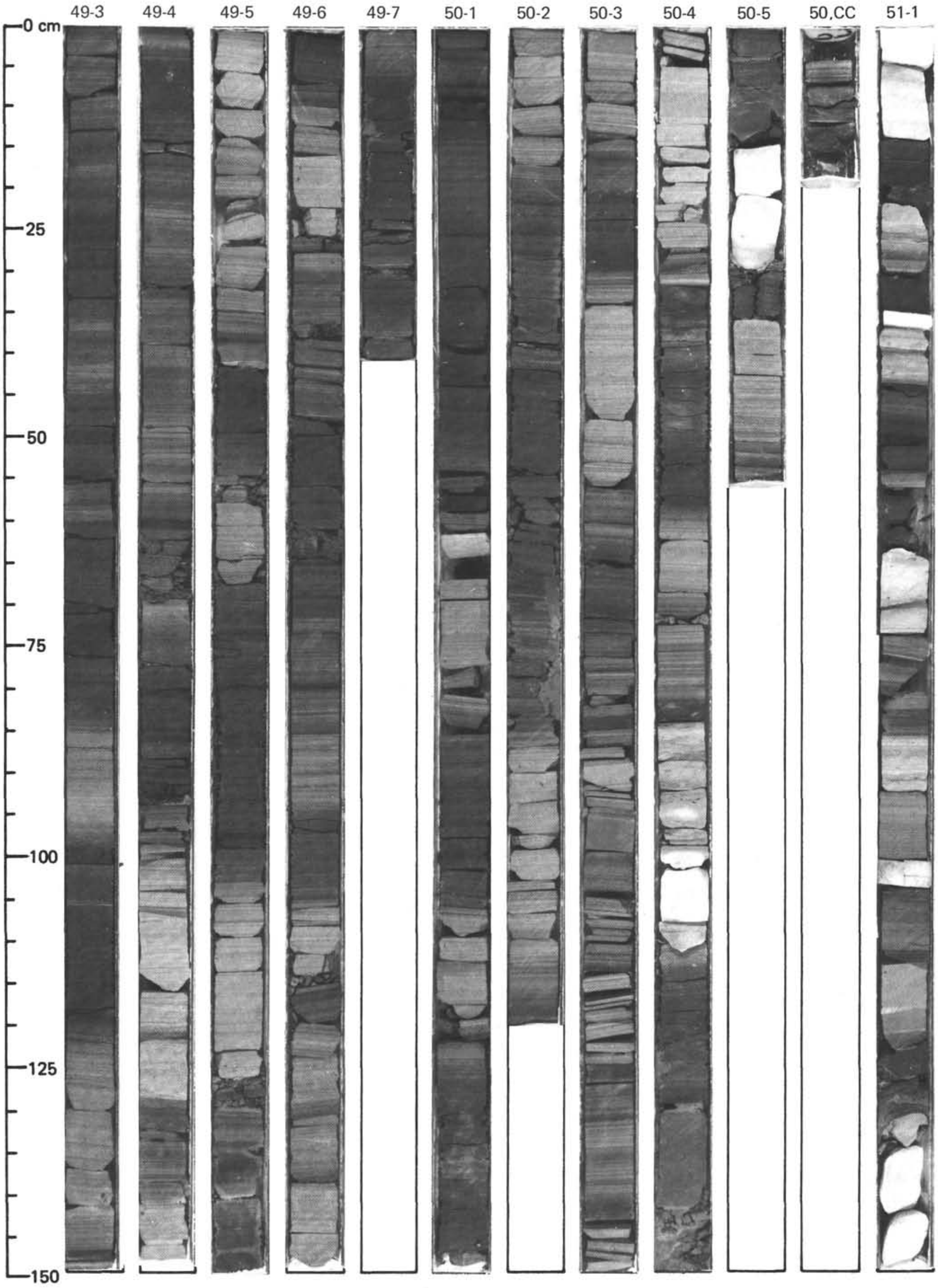
49-3
49-4
49-5
49-6
49-7
50-1
50-2
50-3
50-4
50-5
50,CC
51-1
0 cm
25
50
75
100
125
150

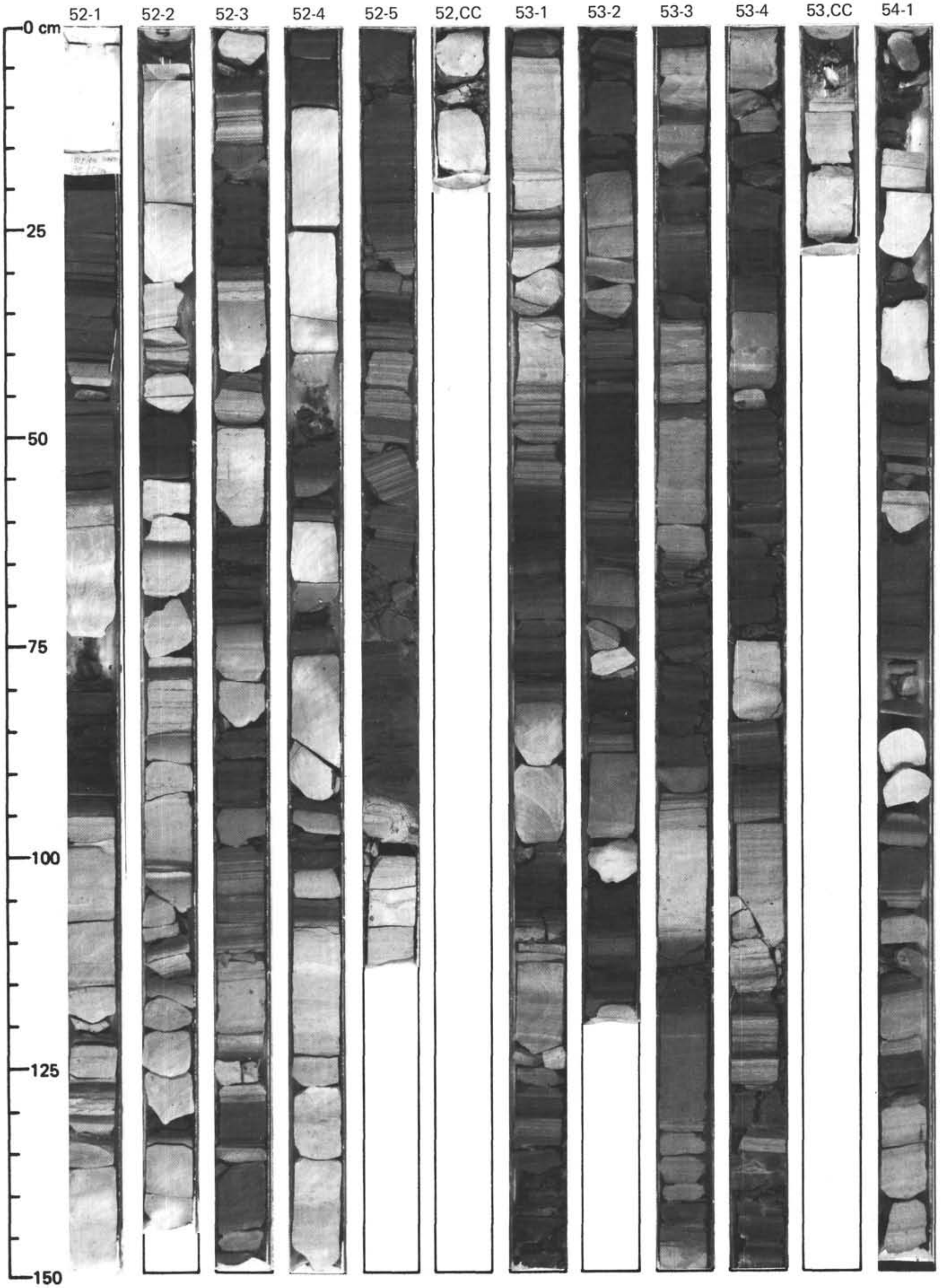
52-1
52-2
52-3
52-4
52-5
52,CC
53-1
53-2
53-3
53-4
53,CC
54-1
0 cm
25
50
75
100
125
150

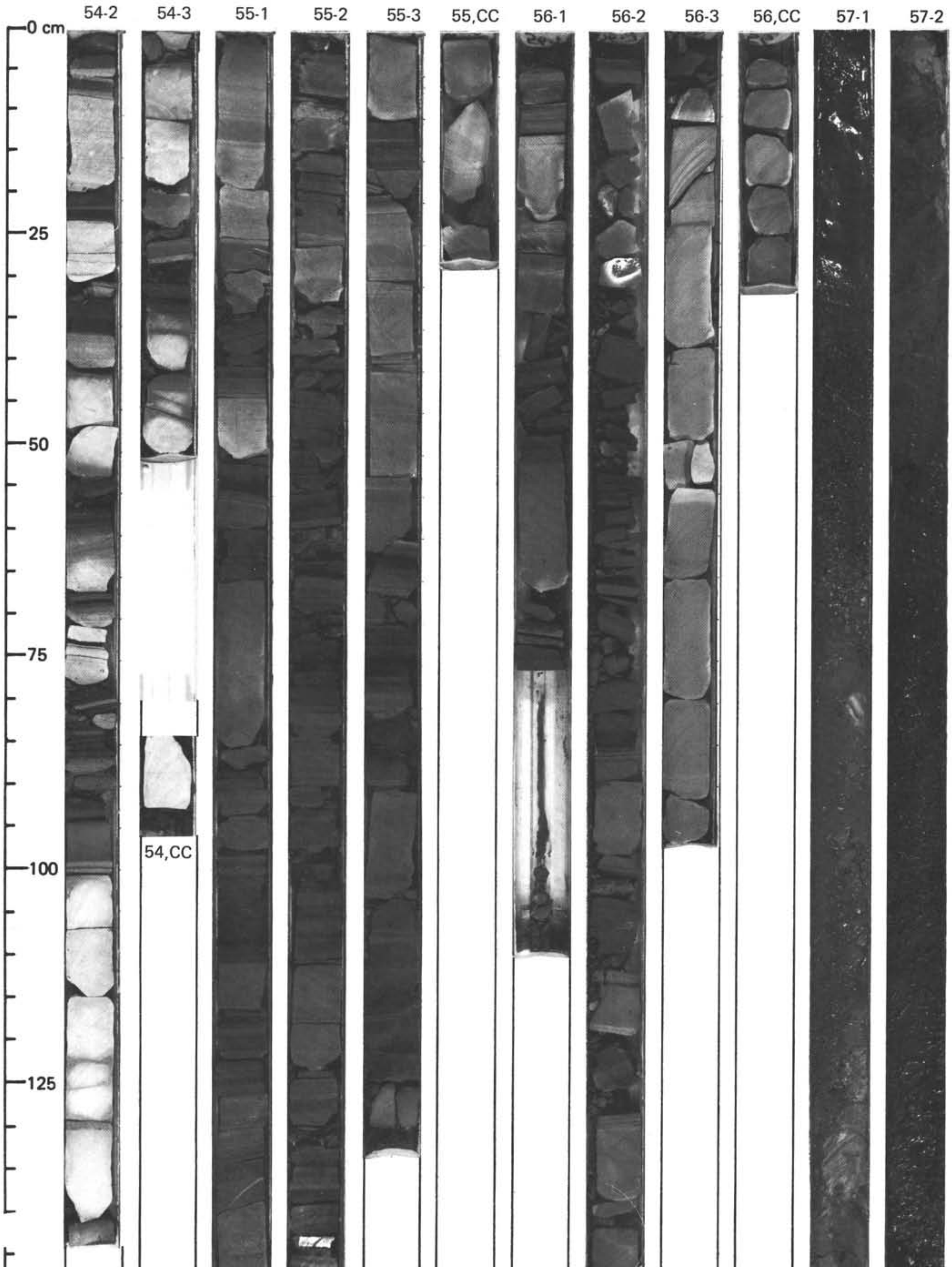
54-2
54-3
55-1
55-2
55-3
55,CC
56-1
56-2
56-3
56,CC
57-1
57-2
0 cm
25
50
75
100
125
150
54,CC

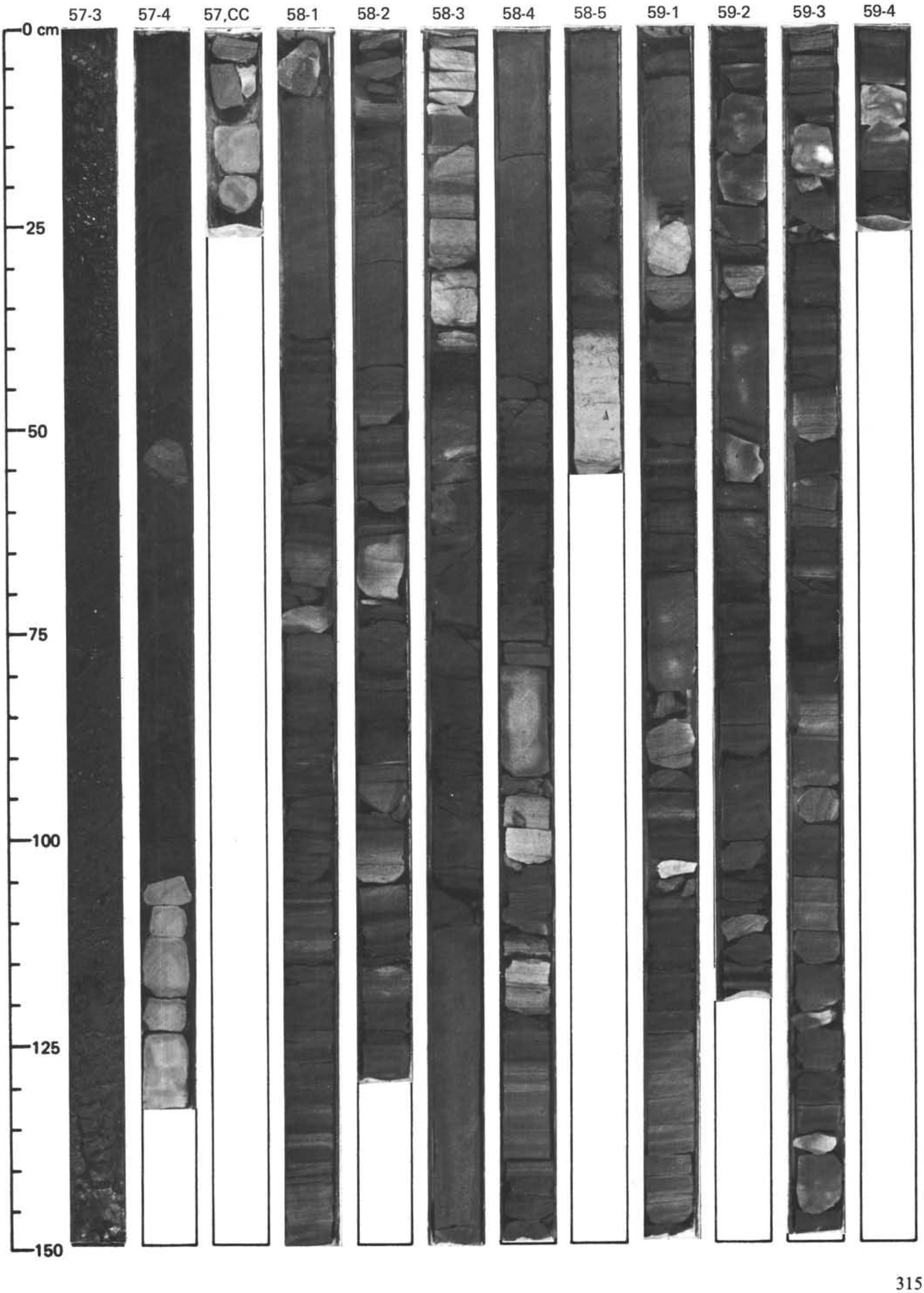
57-3
57-4
57,CC
58-1
58-2
58-3
58-4
58-5
59-1
59-2
59-3
59-4
0 cm
25
50
75
100
125
150

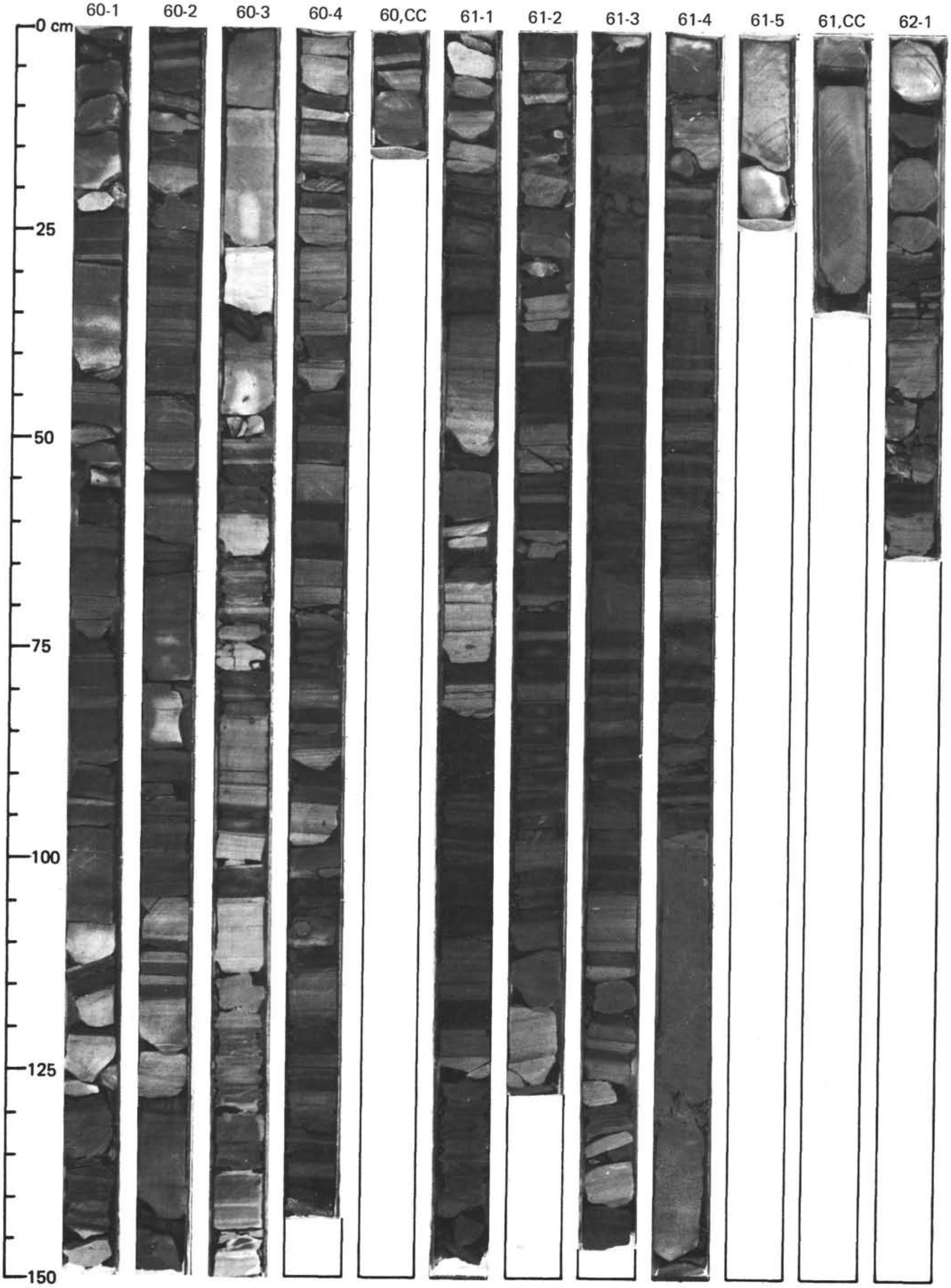
60-1
60-2
60-3
60-4
60,CC
61-1
61-2
61-3
61-4
61-5
61,CC
62-1
0 cm
25
50
75
100
125
150

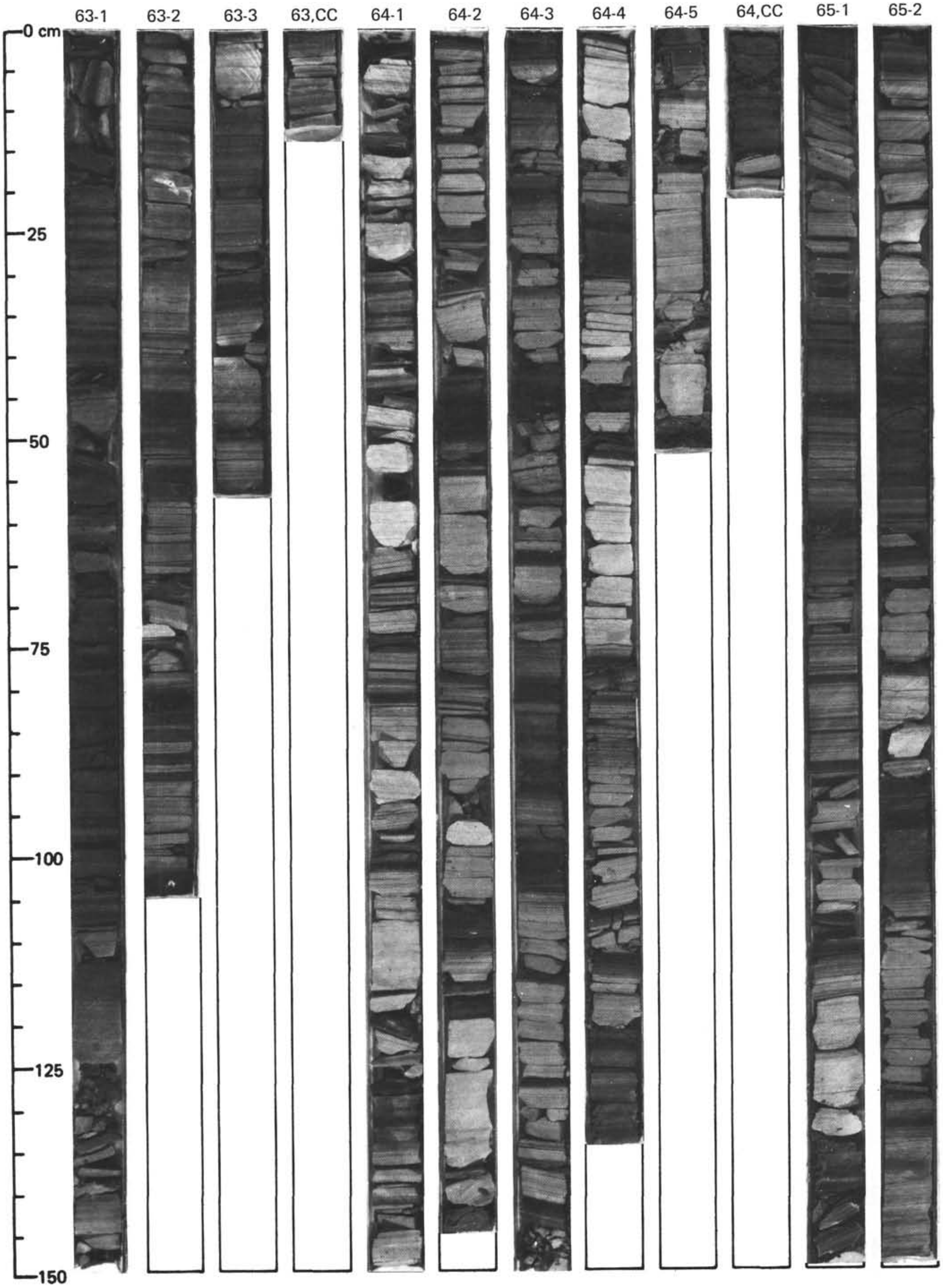
63-1
63-2
63-3
63,CC
64-1
64-2
64-3
64-4
64-5
64,CC
65-1
65-2
0 cm
25
50
75
100
125
150

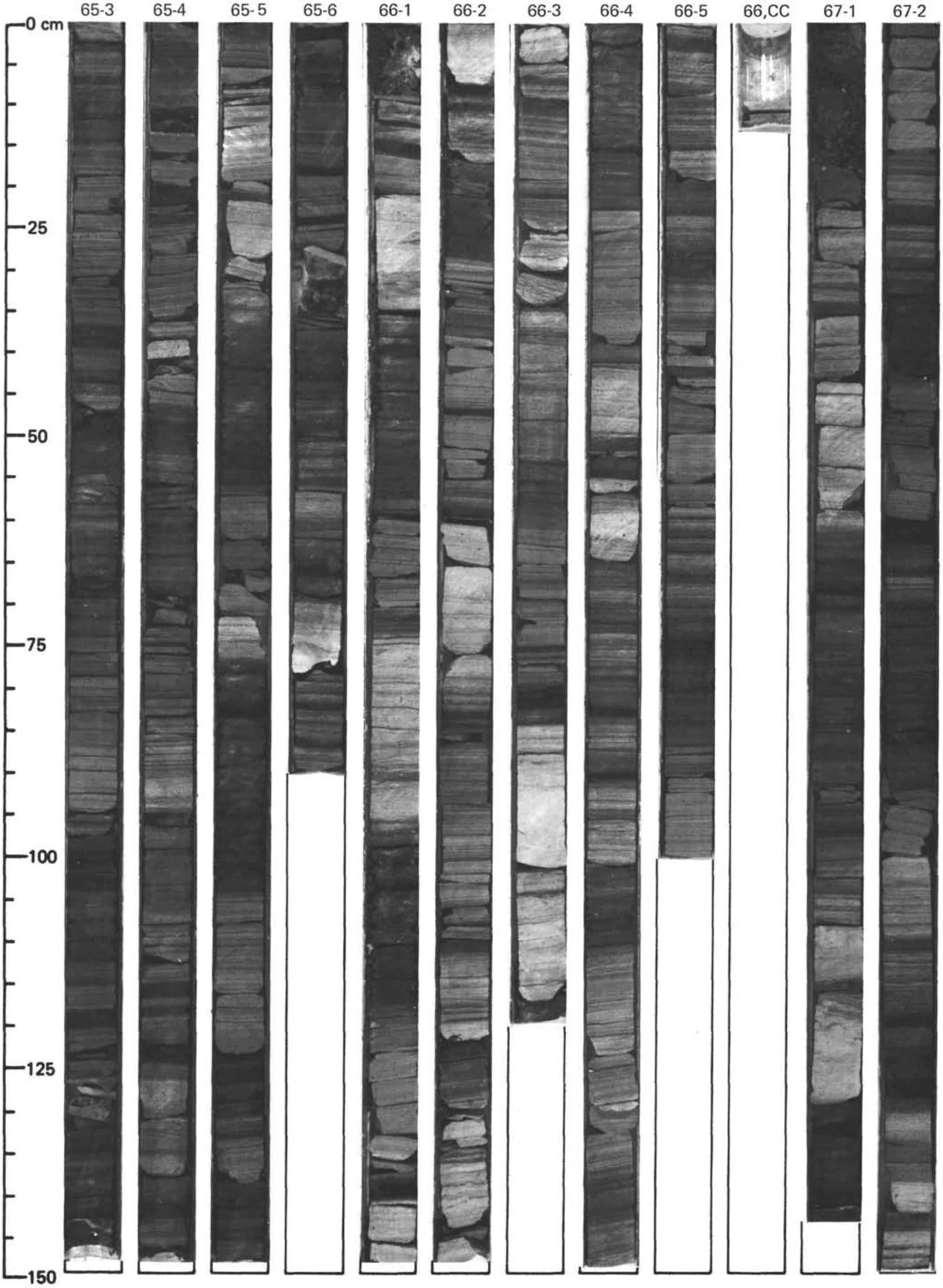
65-3
65-4
65- 5
65-6
66-1
66-2
66-3
66-4
66-5
66,CC
67-1
67-2
0 cm
25
50
75
100
125
150

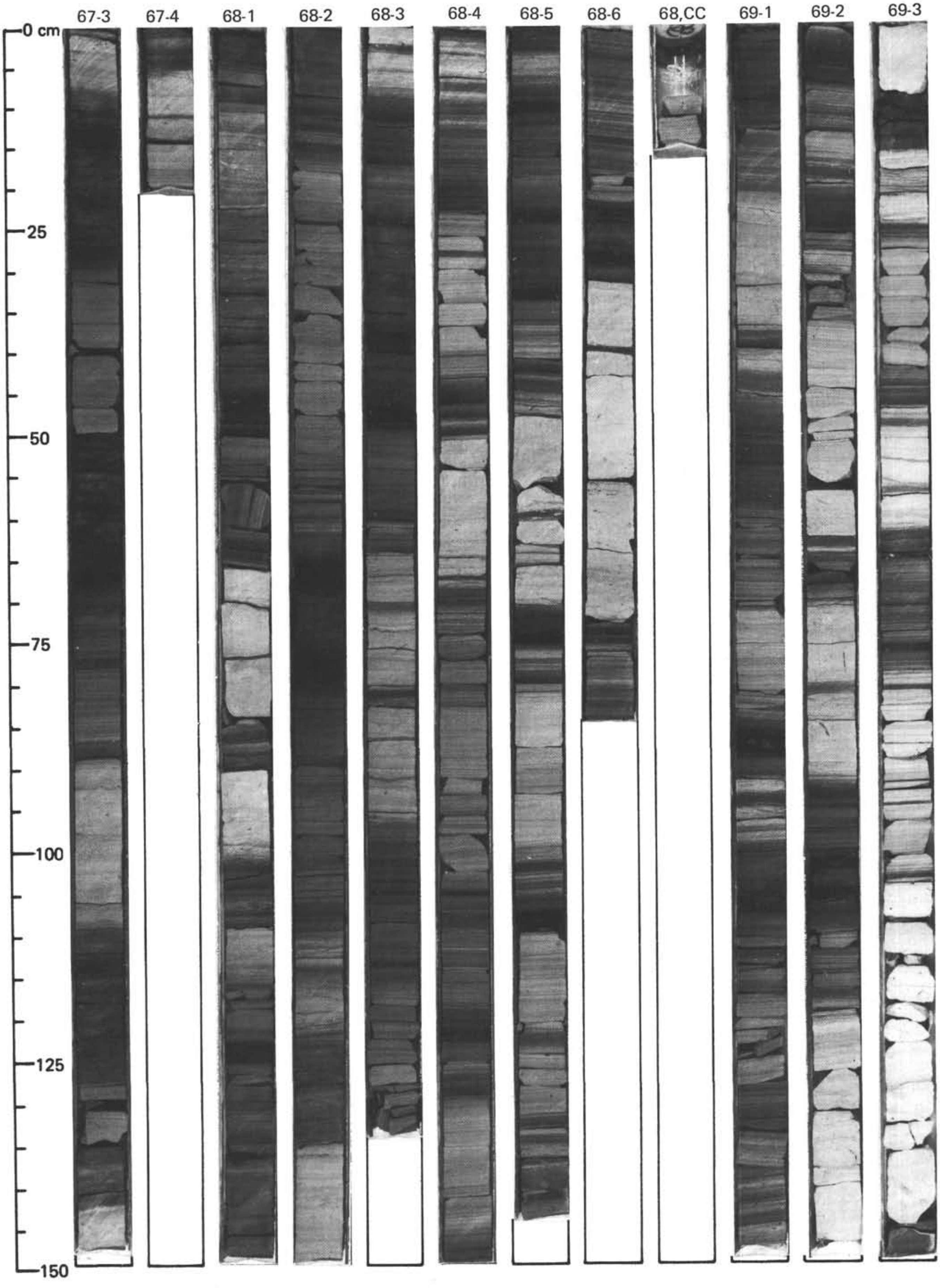
67-3
67-4
68-1
68-2
68-3
68-4
68-5
68-6
68,CC
69-1
69-2
69-3
0 cm
25
50
75
100
125
150

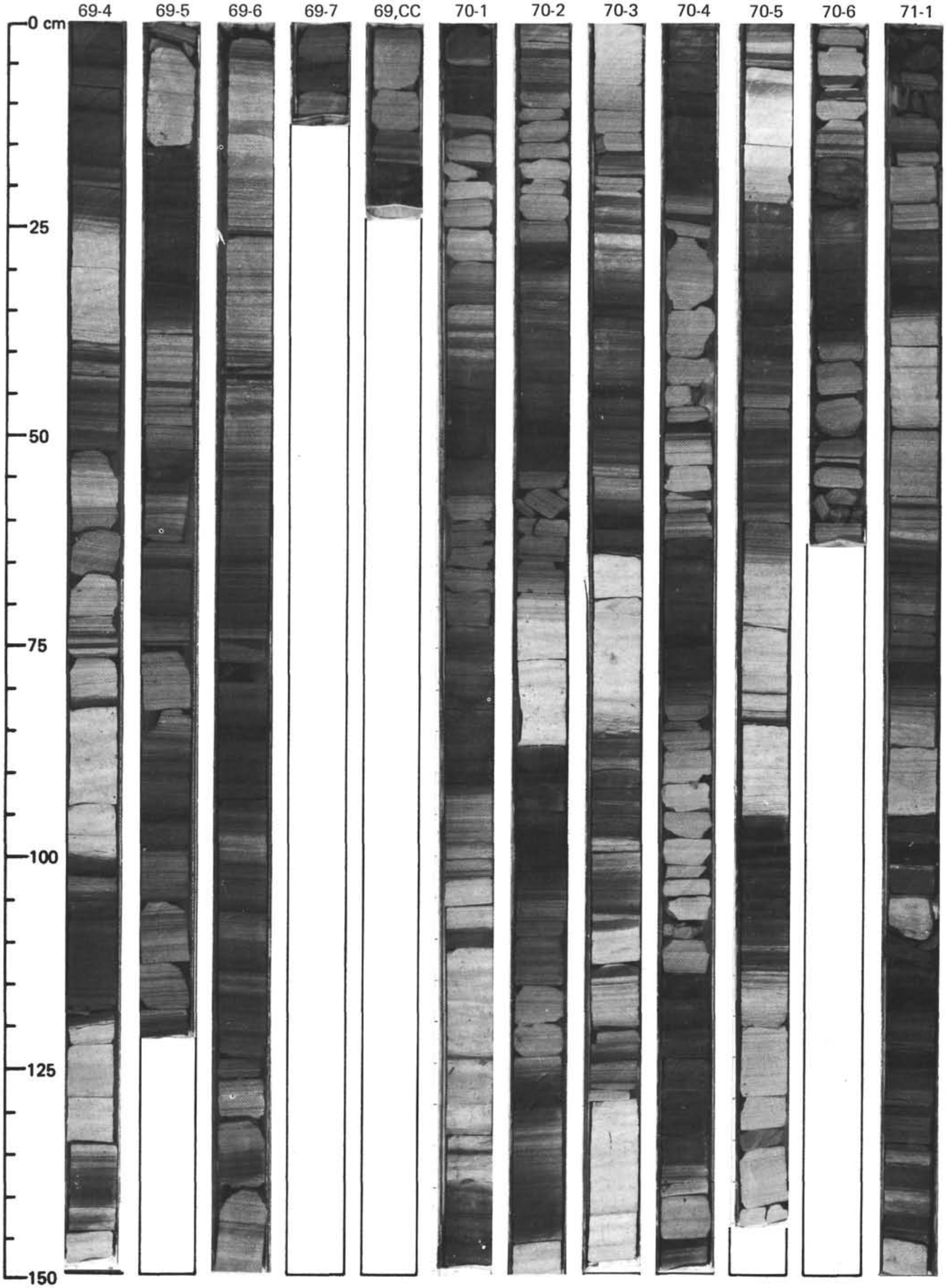
69-4
69-5
69-6
69-7
69,CC
70-1
70-2
70-3
70-4
70-5
70-6
71-1
0 cm
25
50
75
100
125
150

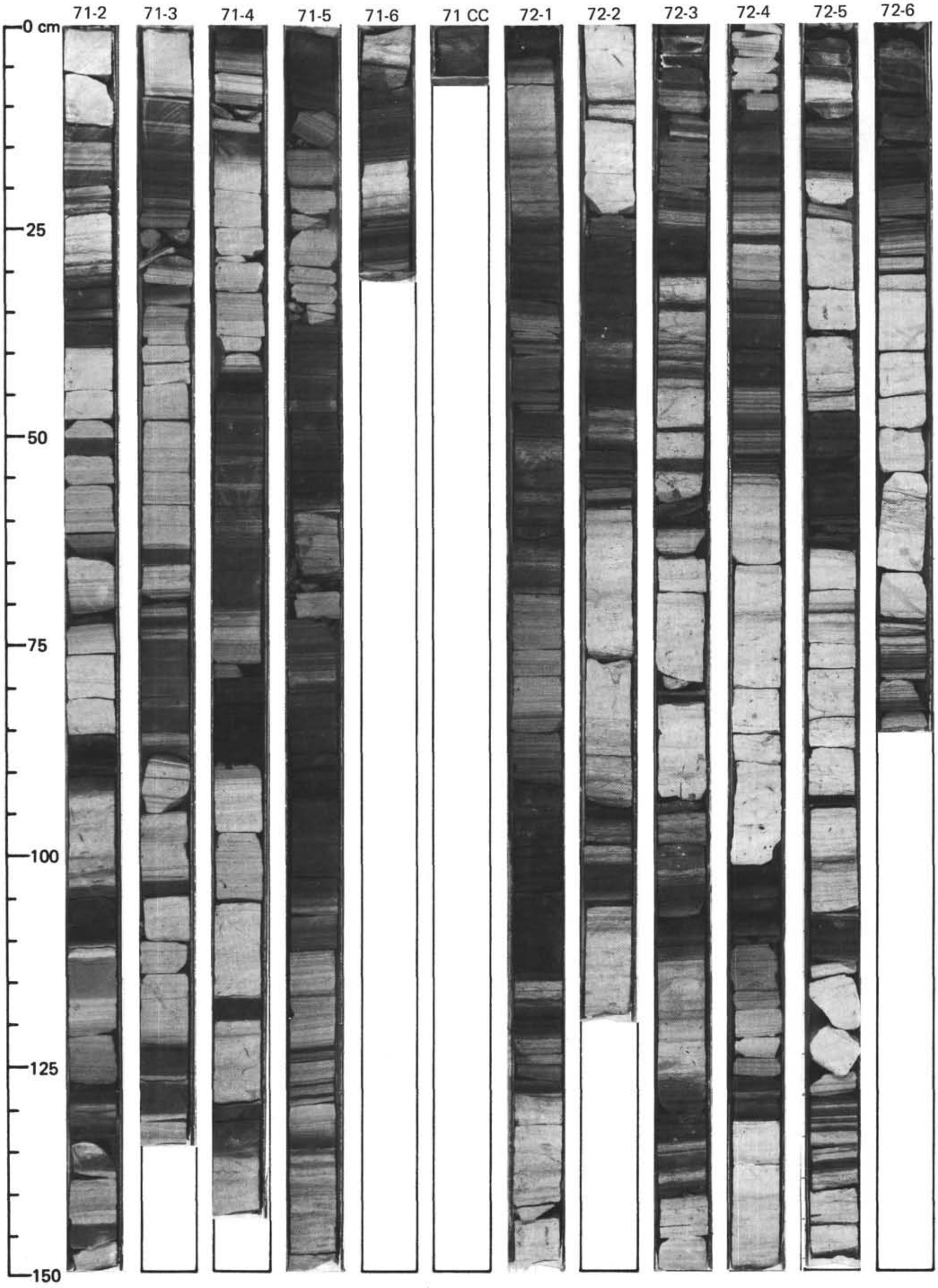
71-2
71-3
71-4
71-5
71-6
71 CC
72-1
72-2
72-3
72-4
72-5
72-6
0 cm
25
50
75
100
125
150

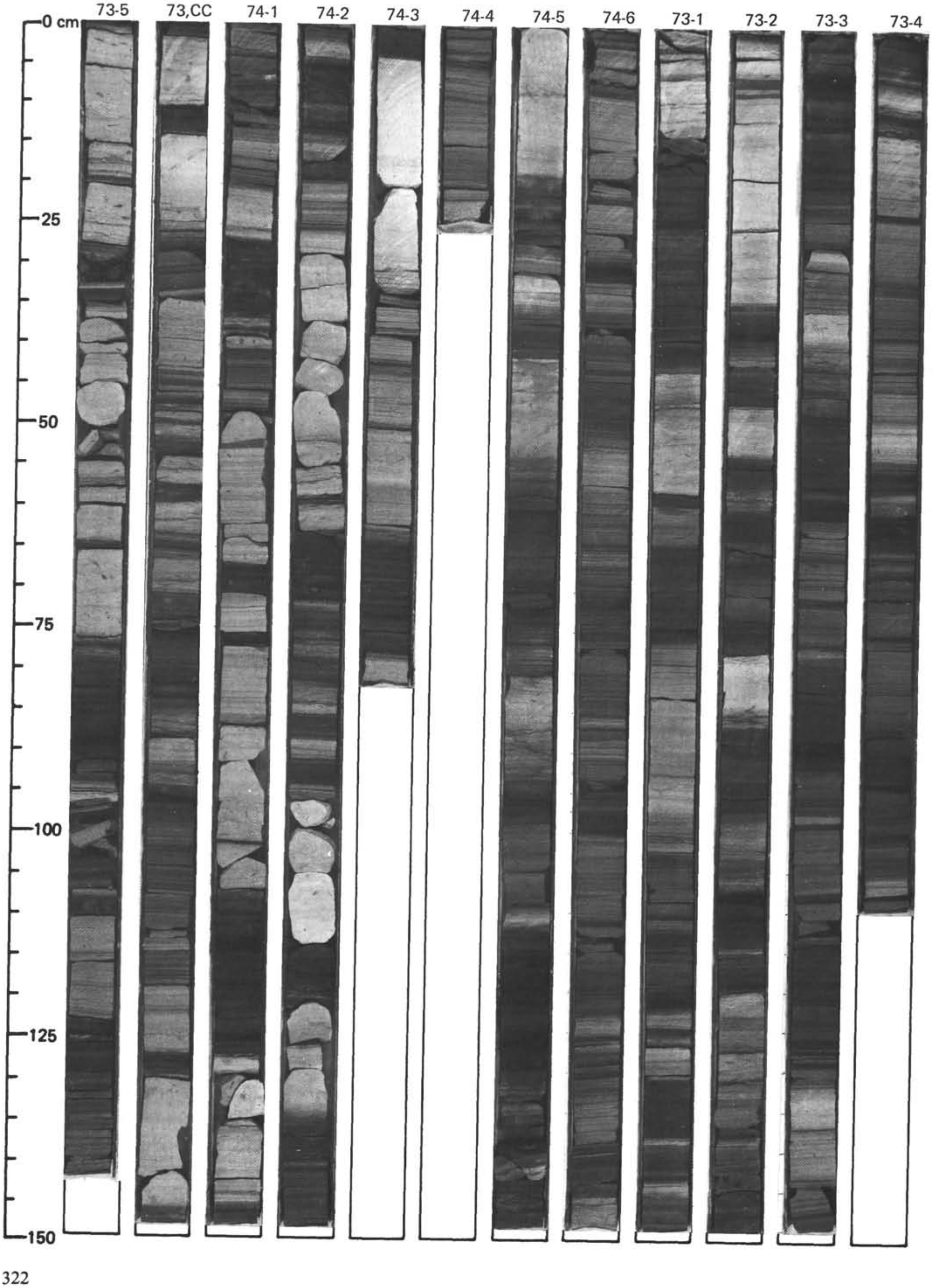
0 cm
25
50
75
100
125
150
73-5
73,CC
74-1
74-2
74-3
74-4
74-5
74-6
73-1
73-2
73-3
73-4

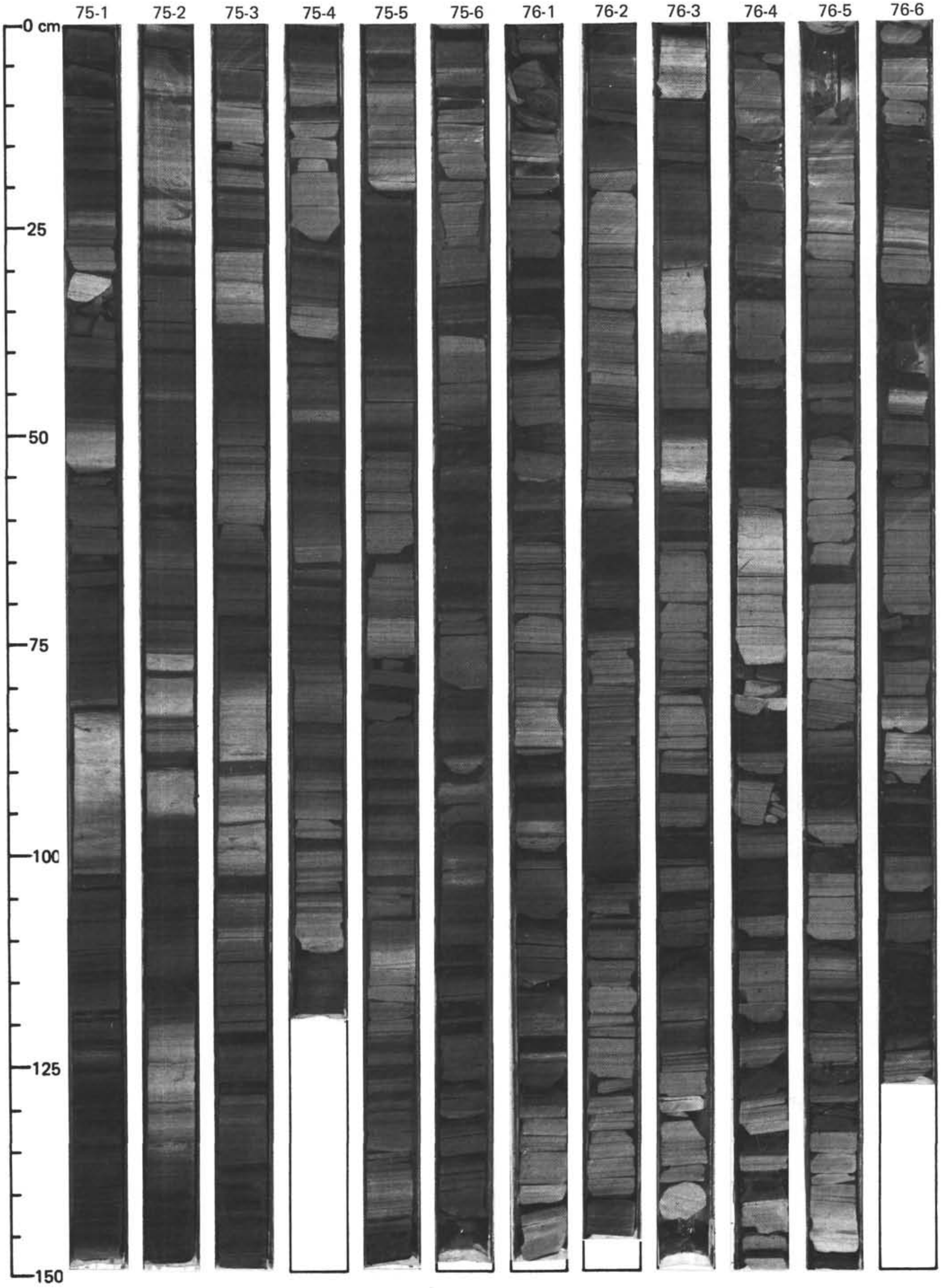
75-1
75-2
75-3
75-4
75-5
75-6
76-1
76-2
76-3
76-4
76-5
76-6
0 cm
25
50
75
100
125
150

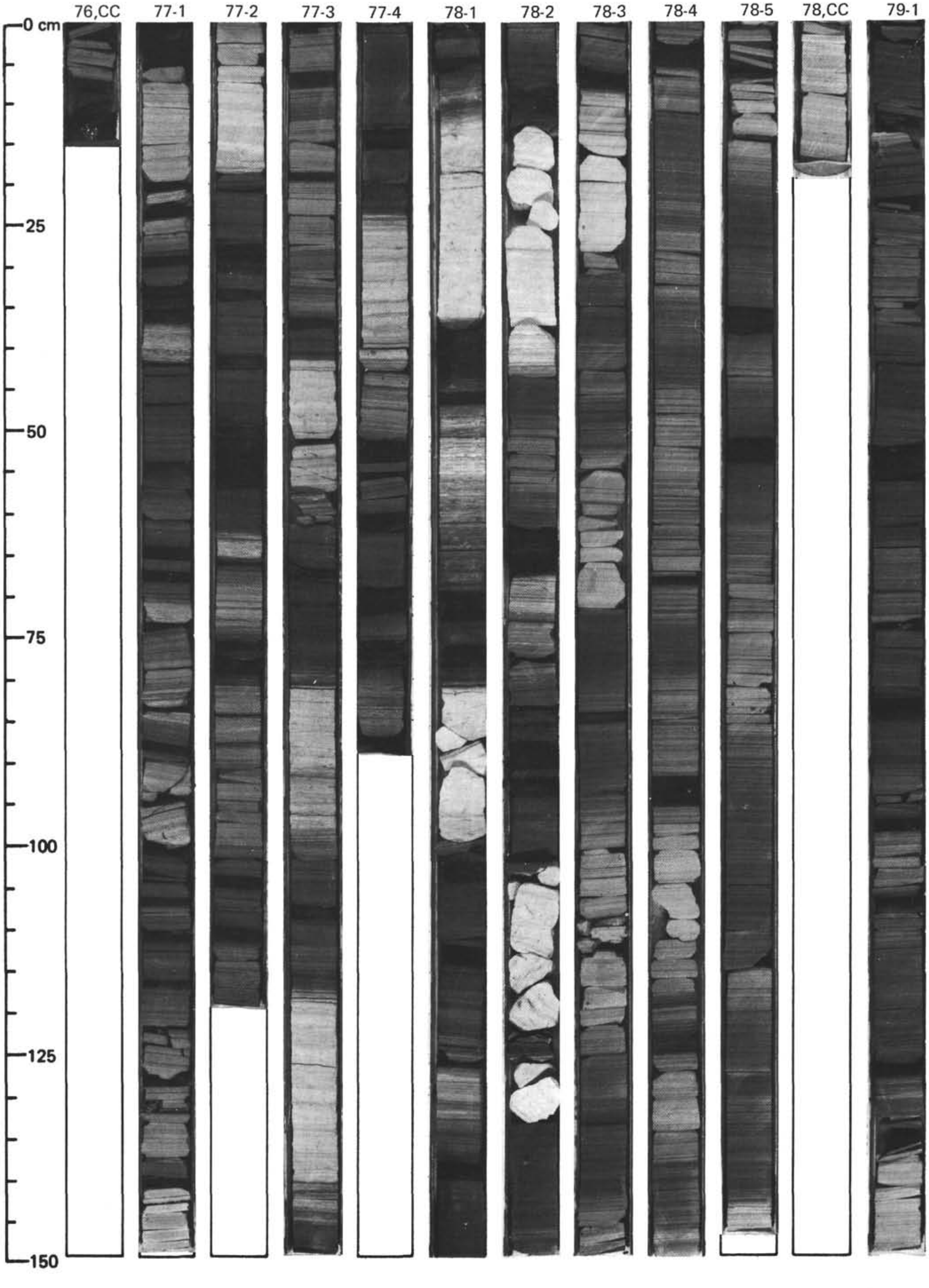
76,CC
77-1
77-2
77-3
77-4
78-1
78-2
78-3
78-4
78-5
78,CC
79-1
0 cm
25
50
75
100
125
150

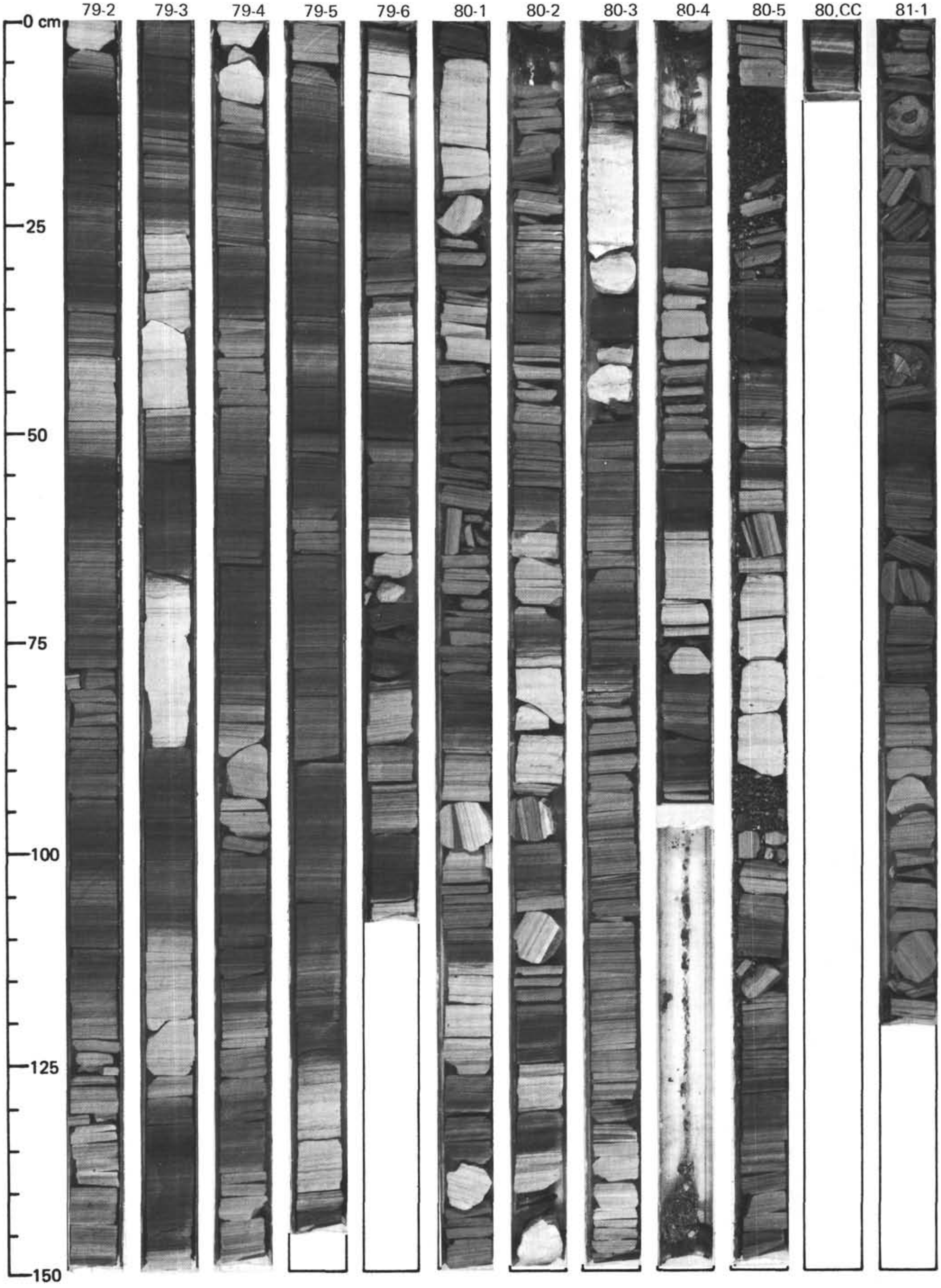
79-2
79-3
79-4
79-5
79-6
80-1
80-2
80-3
80-4
80-5
80,CC
81-1
0 cm
25
50
75
100
125
150

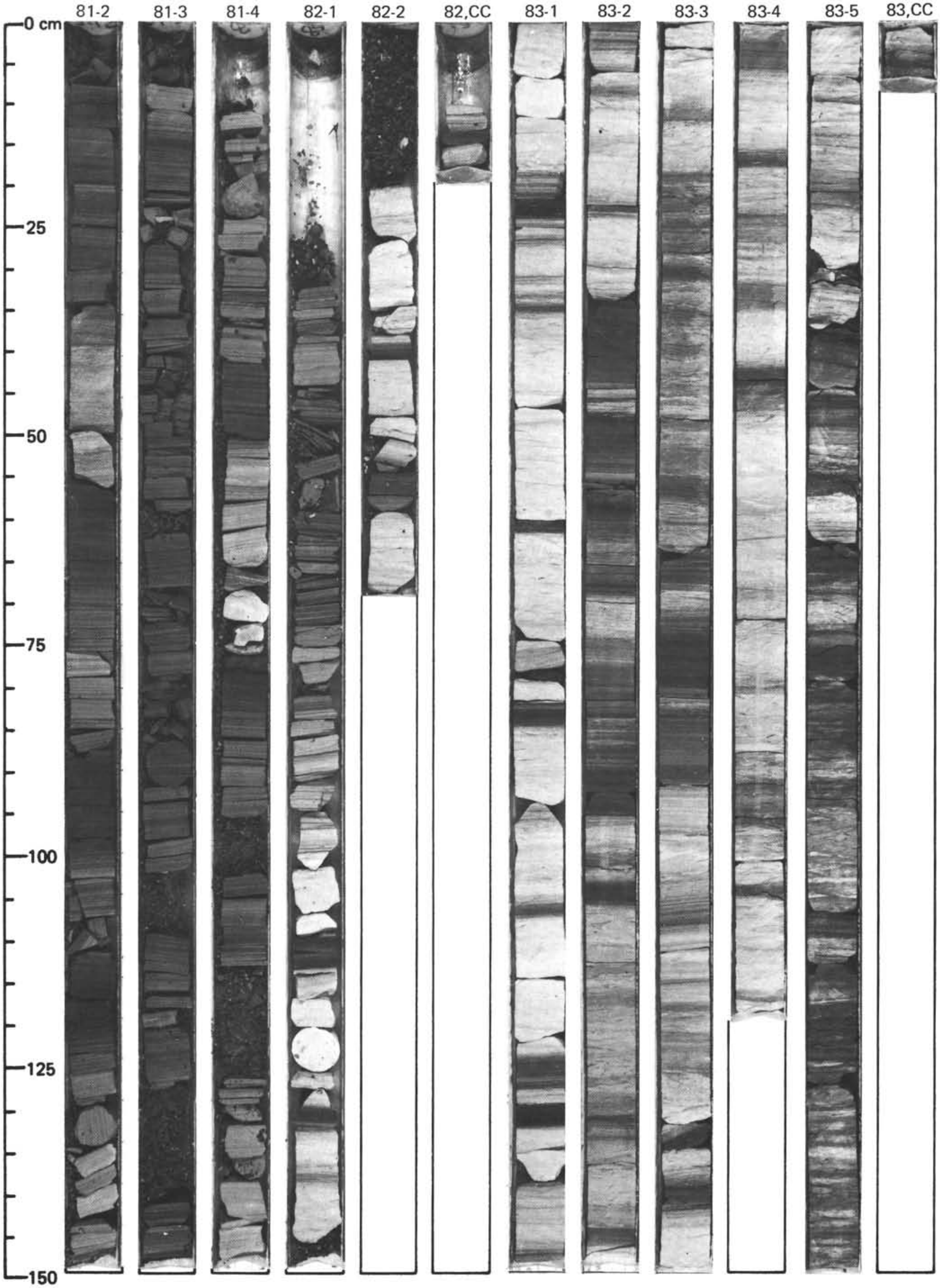
81-2
81-3
81-4
82-1
82-2
82,CC
83-1
83-2
83-3
83-4
83-5
83,CC
0 cm
25
50
75
100
125
150

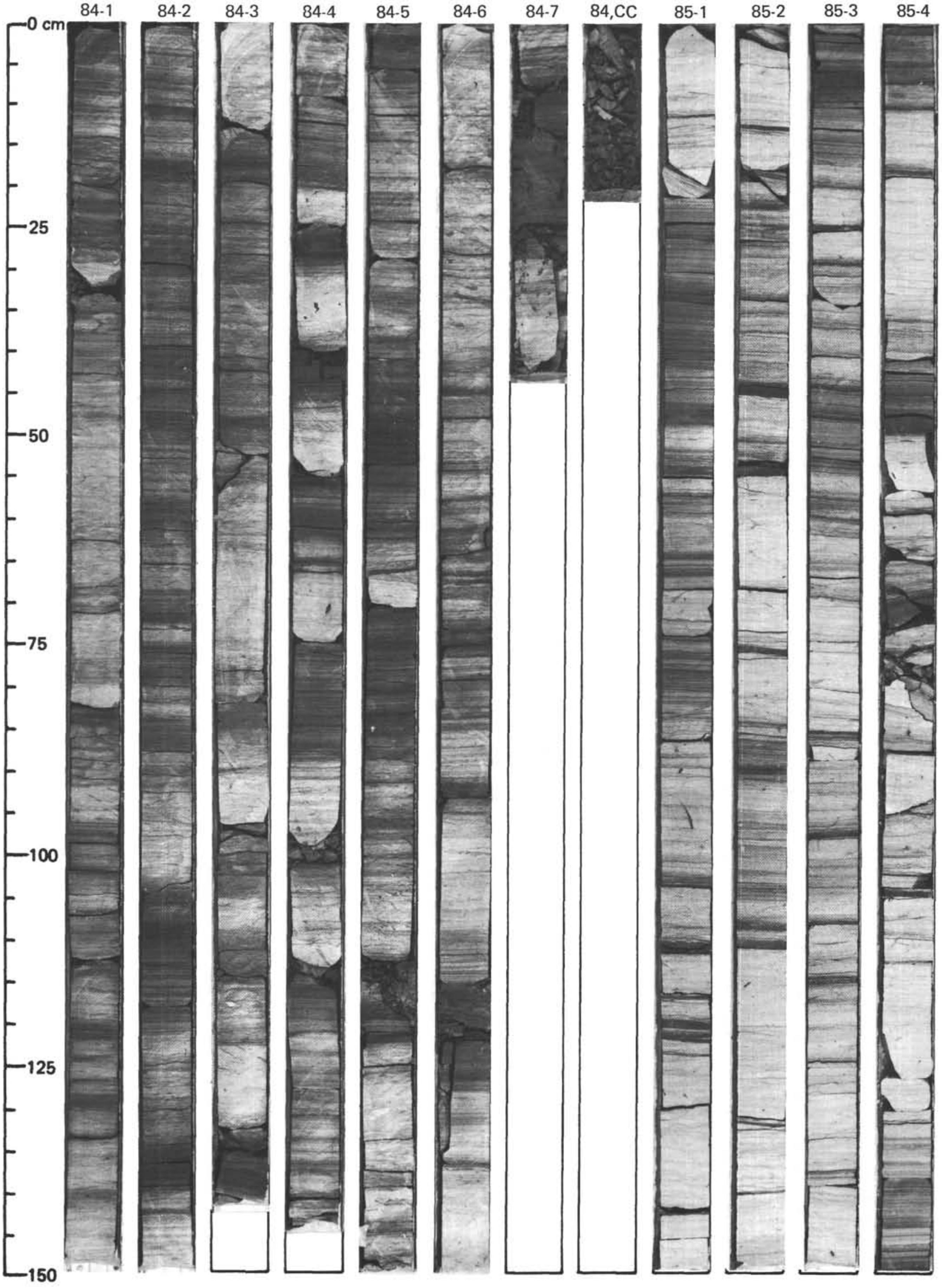
84-1
84-2
84-3
84-4
84-5
84-6
84-7
84,CC
85-1
85-2
85-3
85-4
0 cm
25
50
75
100
125
150

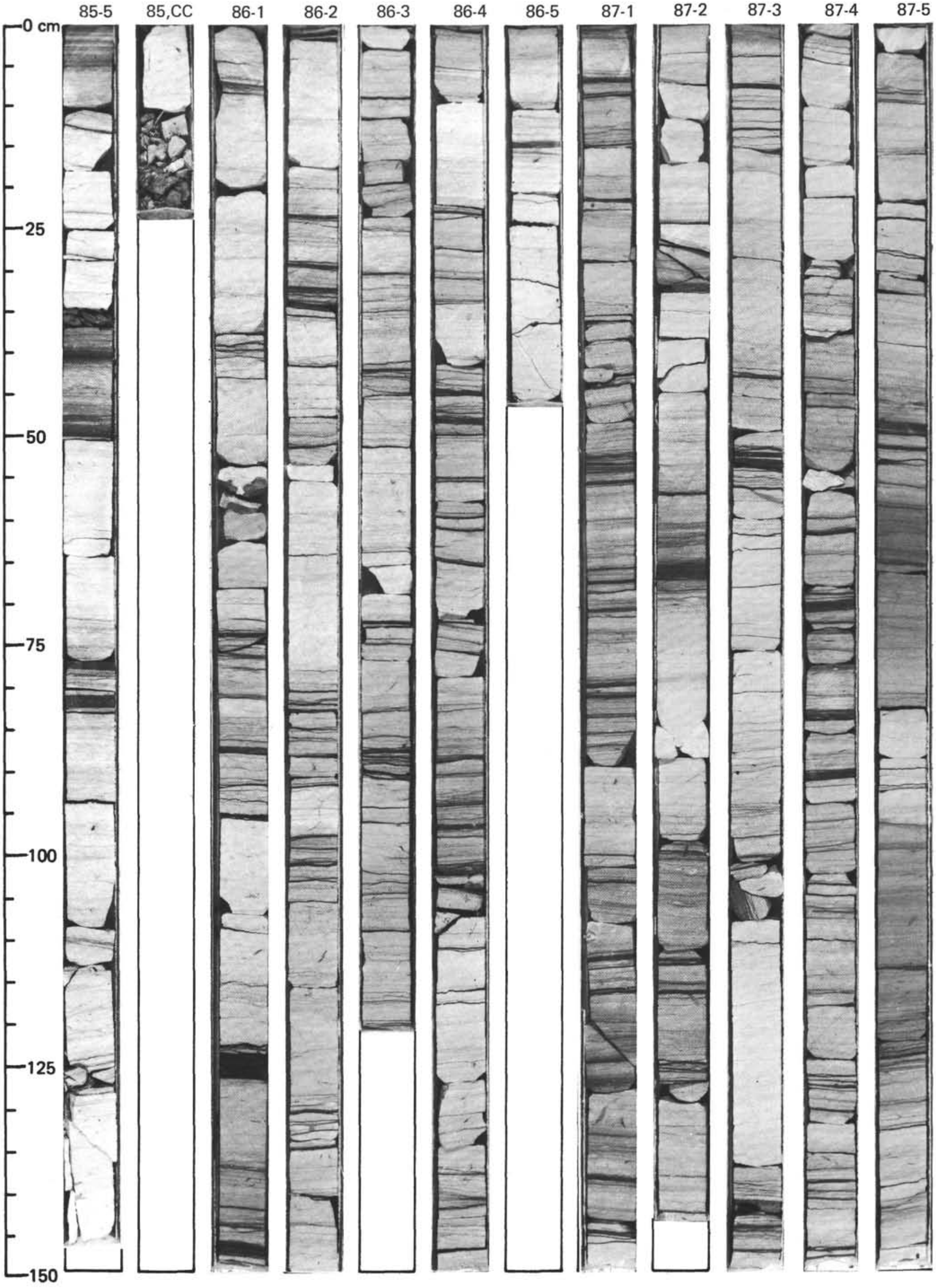
85-5
85,CC
86-1
86-2
86-3
86-4
86-5
87-1
87-2
87-3
87-4
87-5
0 cm
25
50
75
100
125
150

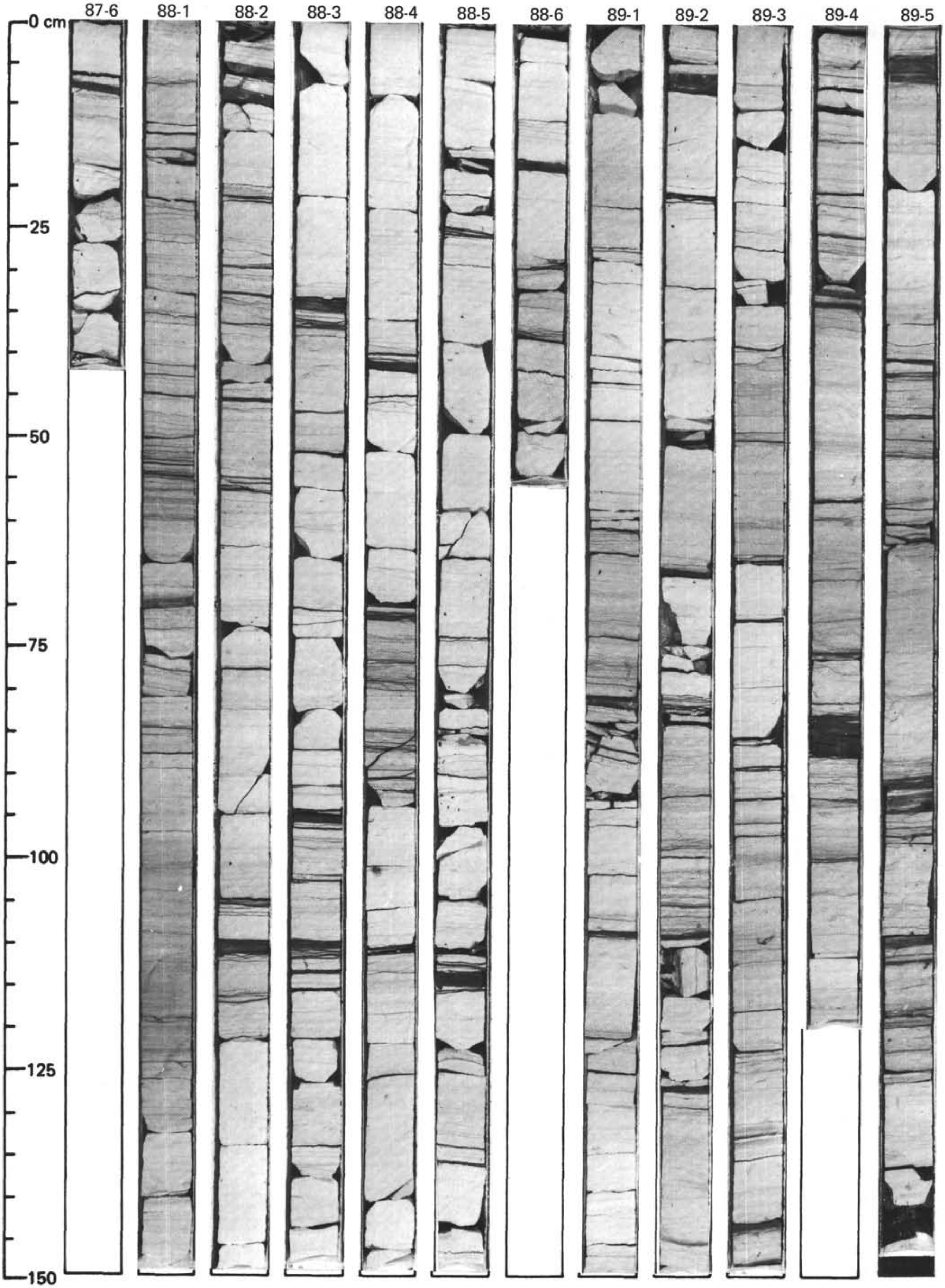
0 cm
25
50
75
100
125
150
87-6
88-1
88-2
88-3
88-4
88-5
88-6
89-1
89-2
89-3
89-4
89-5

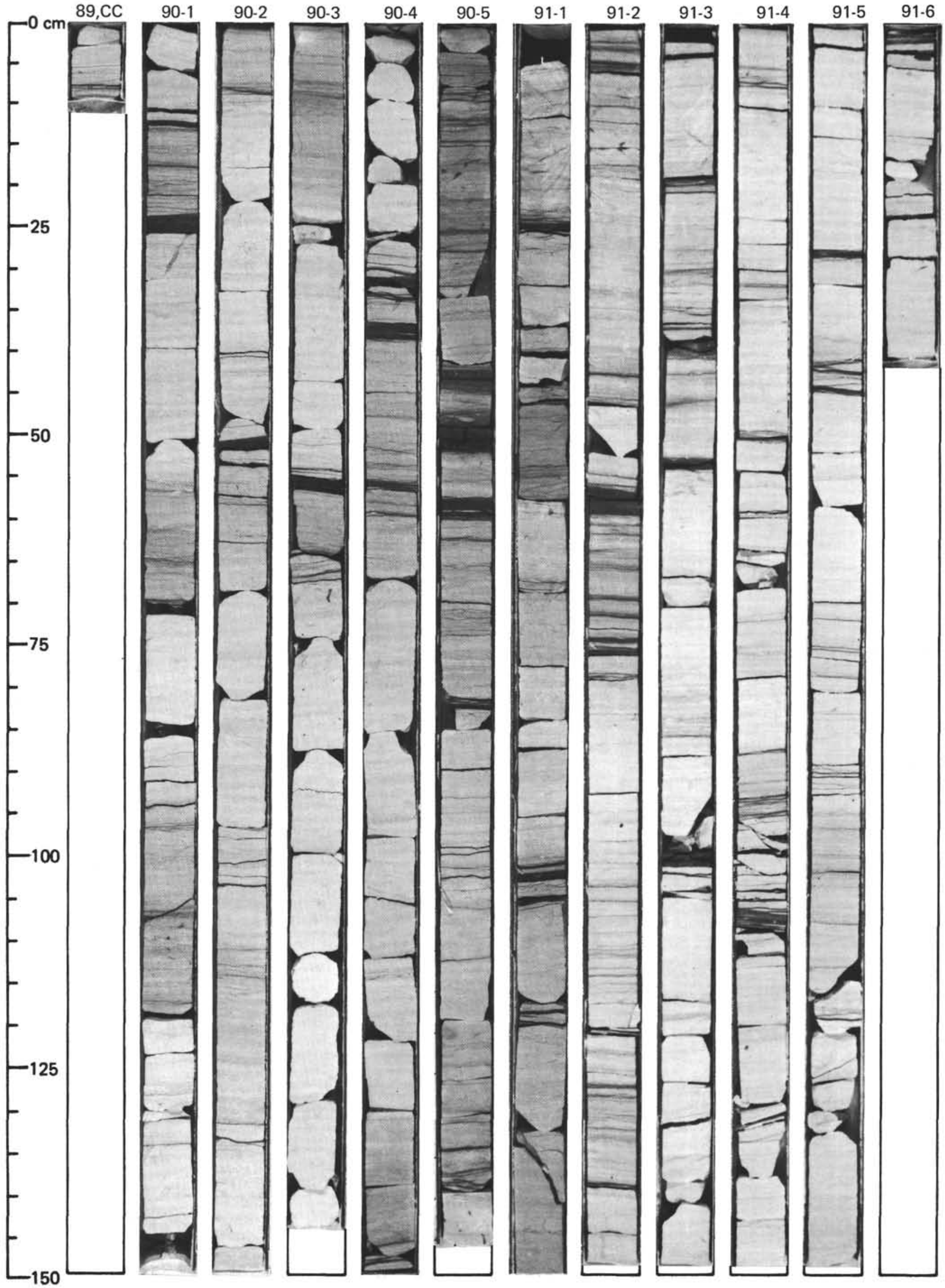
0 cm
25
50
75
100
125
150
89,CC
90-1
90-2
90-3
90-4
90-5
91-1
91-2
91-3
91-4
91-5
91-6

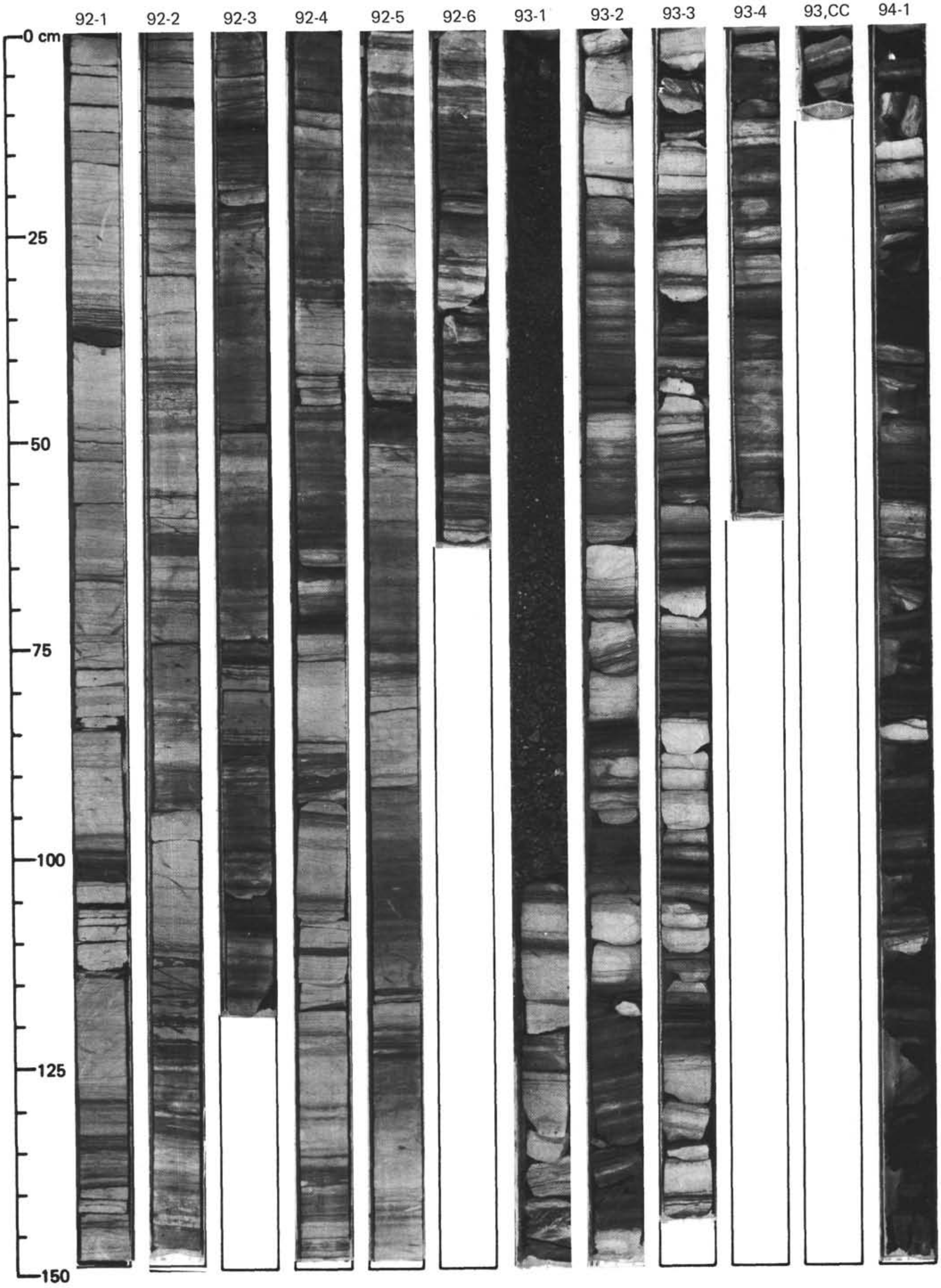
92-1
92-2
92-3
92-4
92-5
92-6
93-1
93-2
93-3
93-4
93,CC
94-1
0 cm
25
50
75
100
125
150

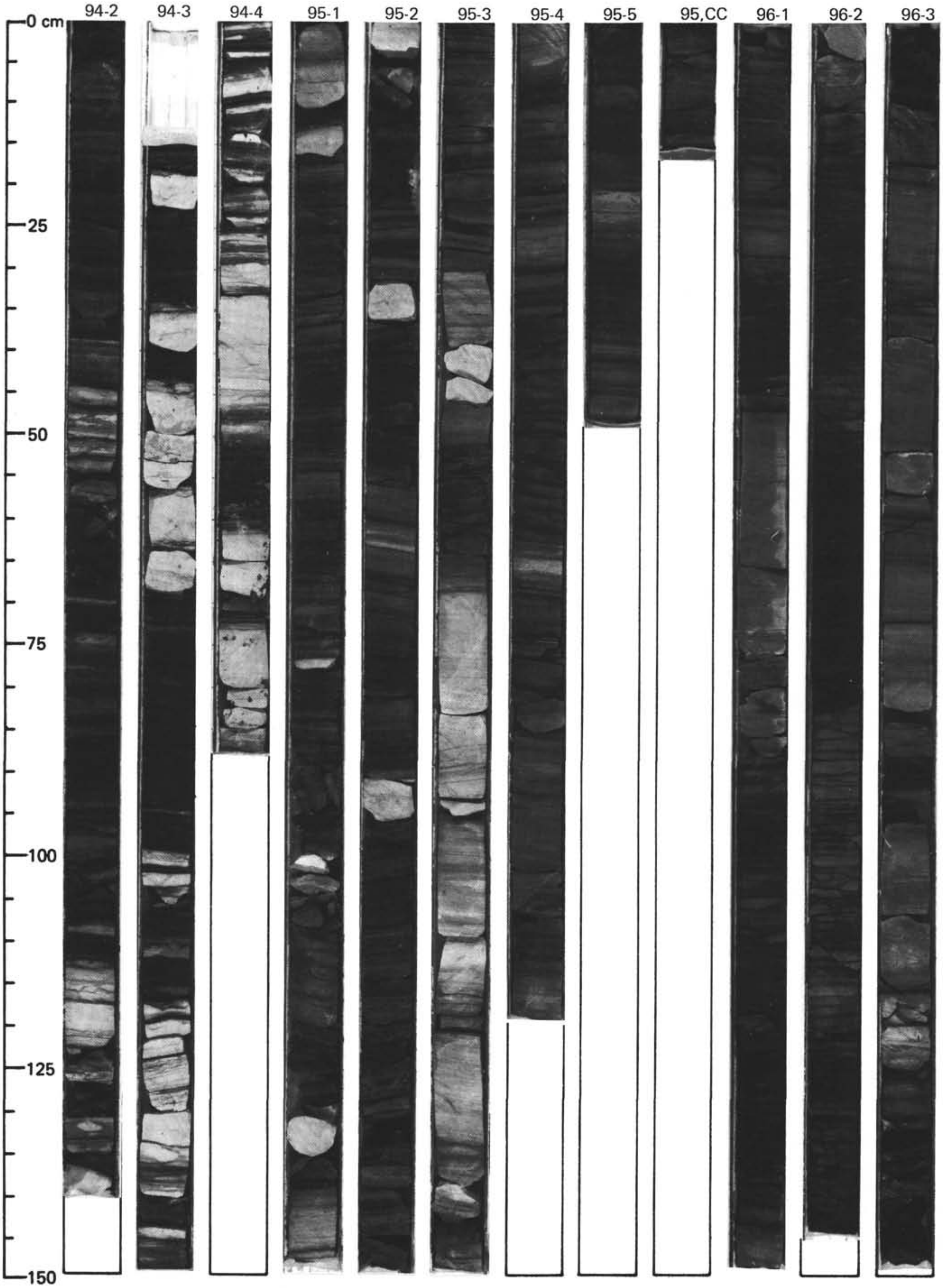
0 cm
25
50
75
100
125
150
94-2
94-3
94-4
95-1
95-2
95-3
95-4
95-5
95,CC
96-1
96-2
96-3

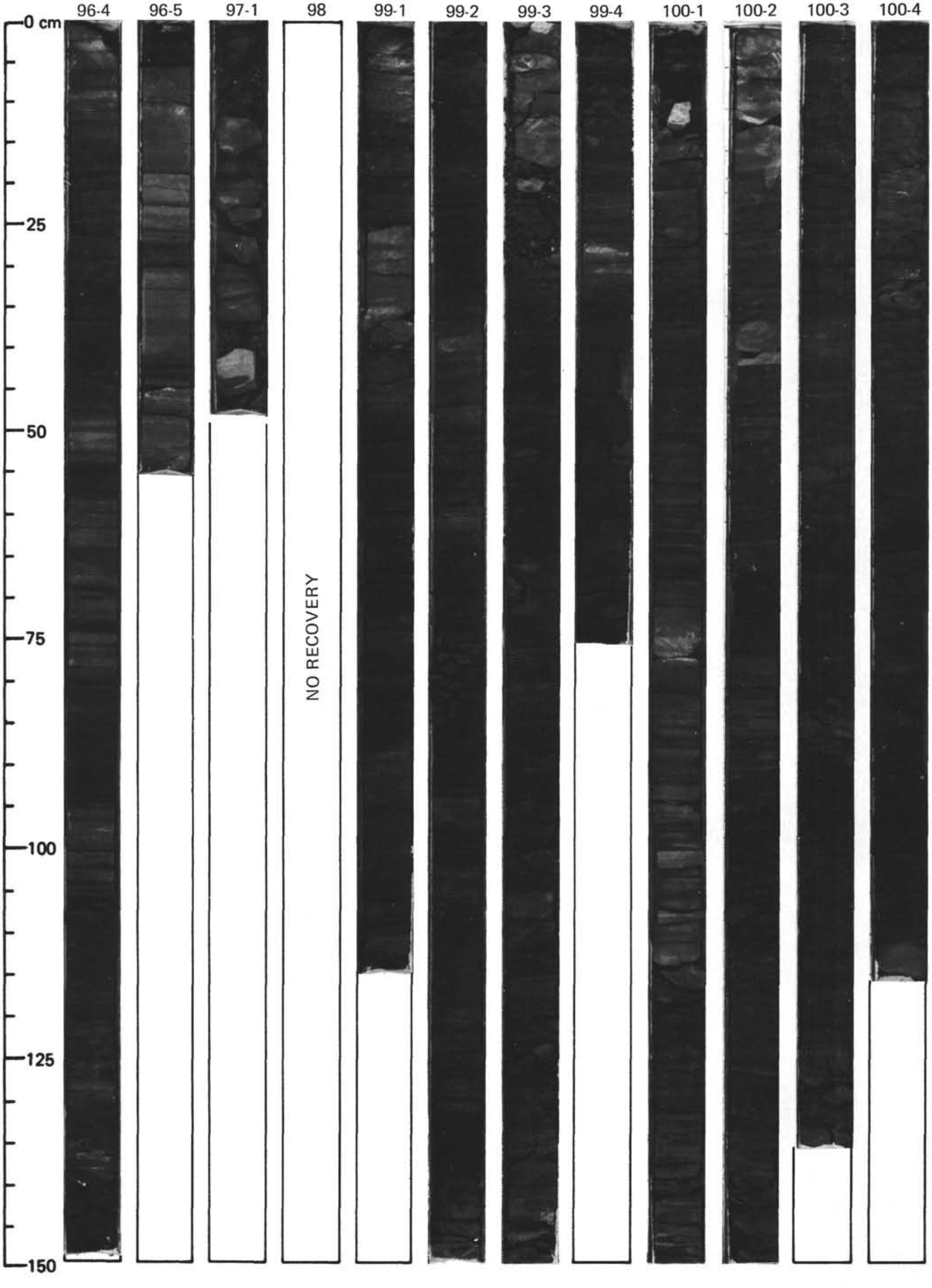
96-4
96-5
97-1
98
99-1
99-2
99-3
99-4
100-1
100-2
100-3
100-4
0 cm
25
50
75
100
125
150
NO RECOVERY

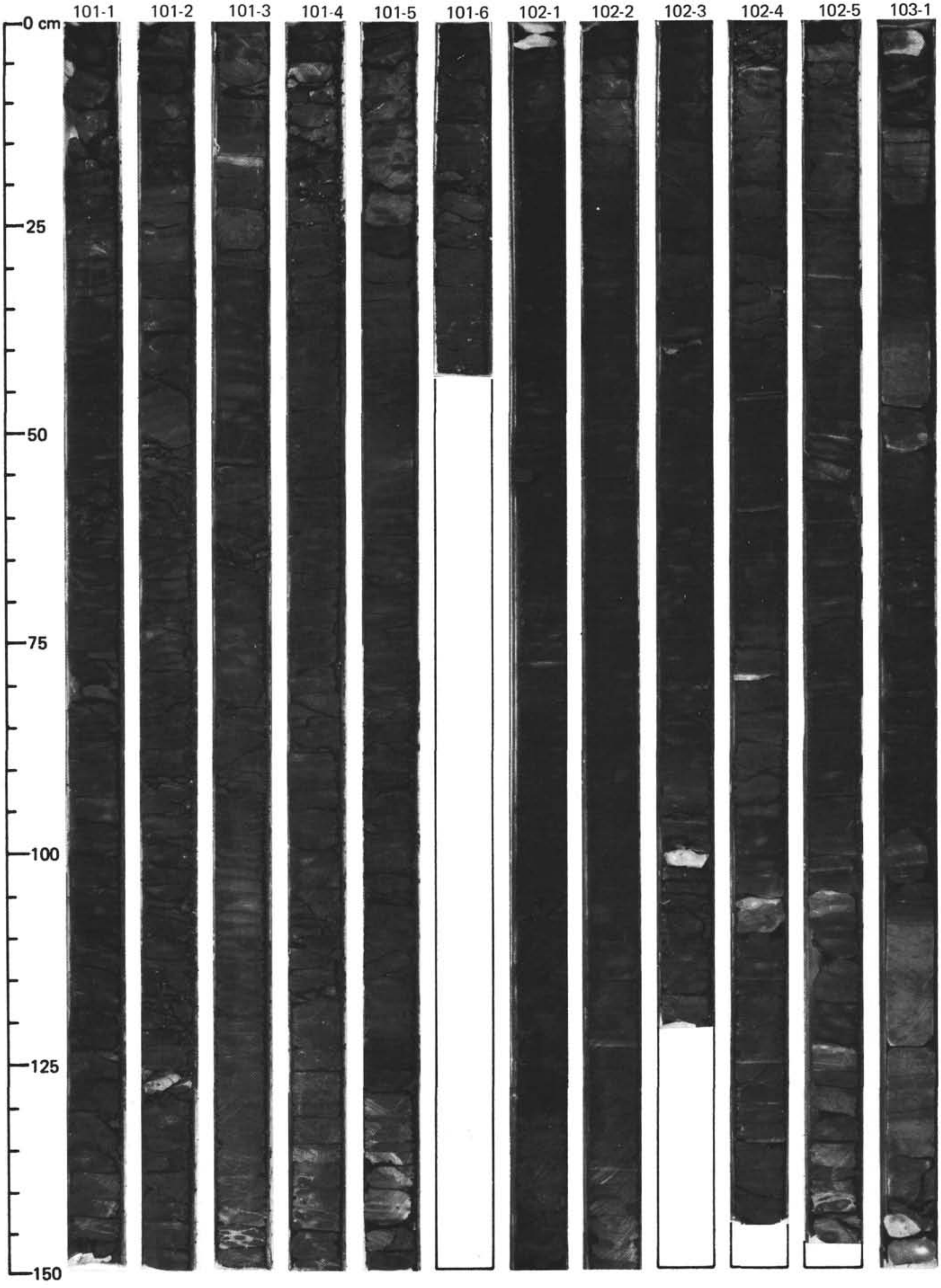
101-1
101-2
101-3
101-4
101-5
101-6
102-1
102-2
102-3
102-4
102-5
103-1
0 cm
25
50
75
100
125
150

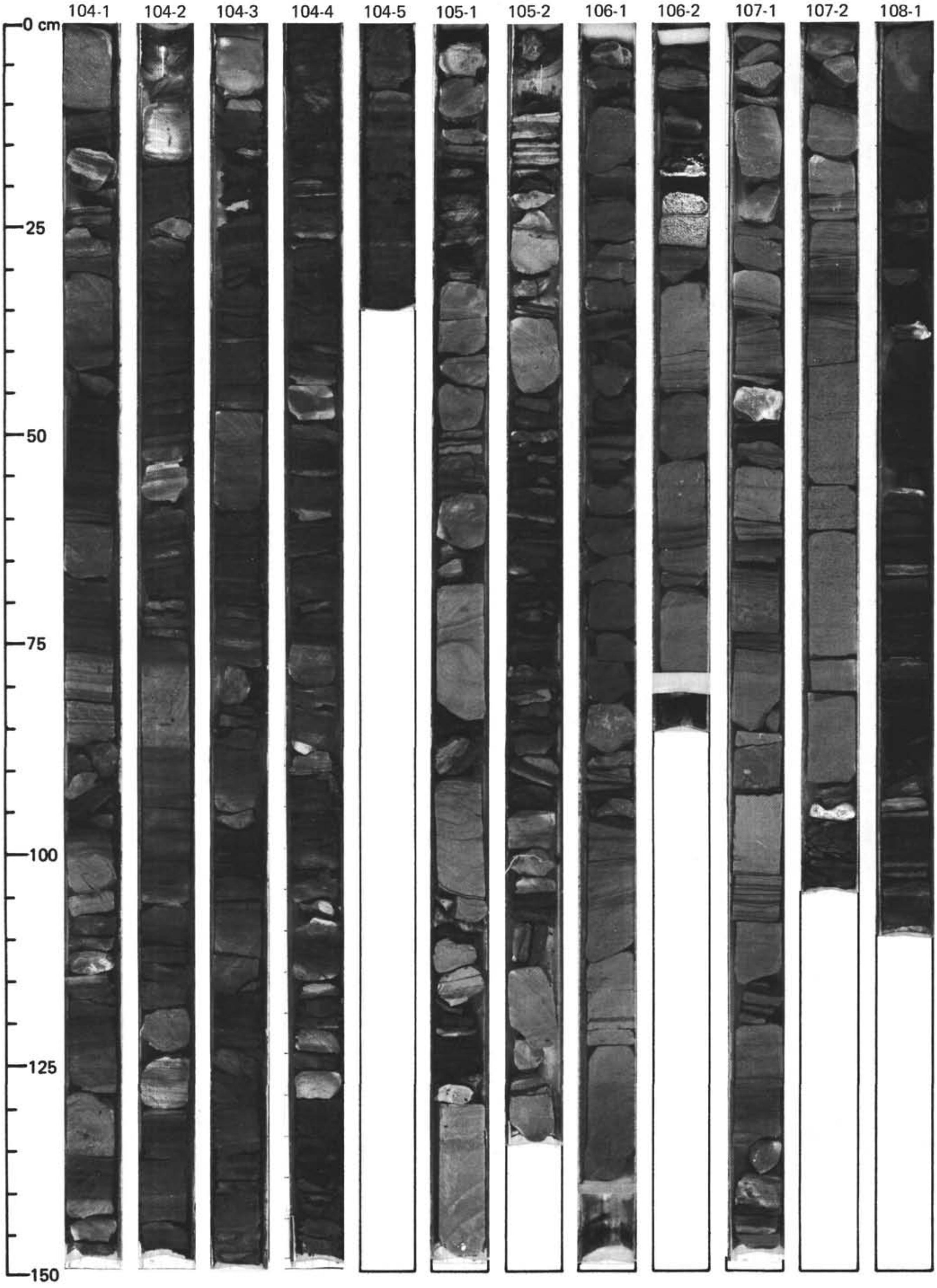
104-1
104-2
104-3
104-4
104-5
105-1
105-2
106-1
106-2
107-1
107-2
108-1
0 cm
25
50
75
100
125
150

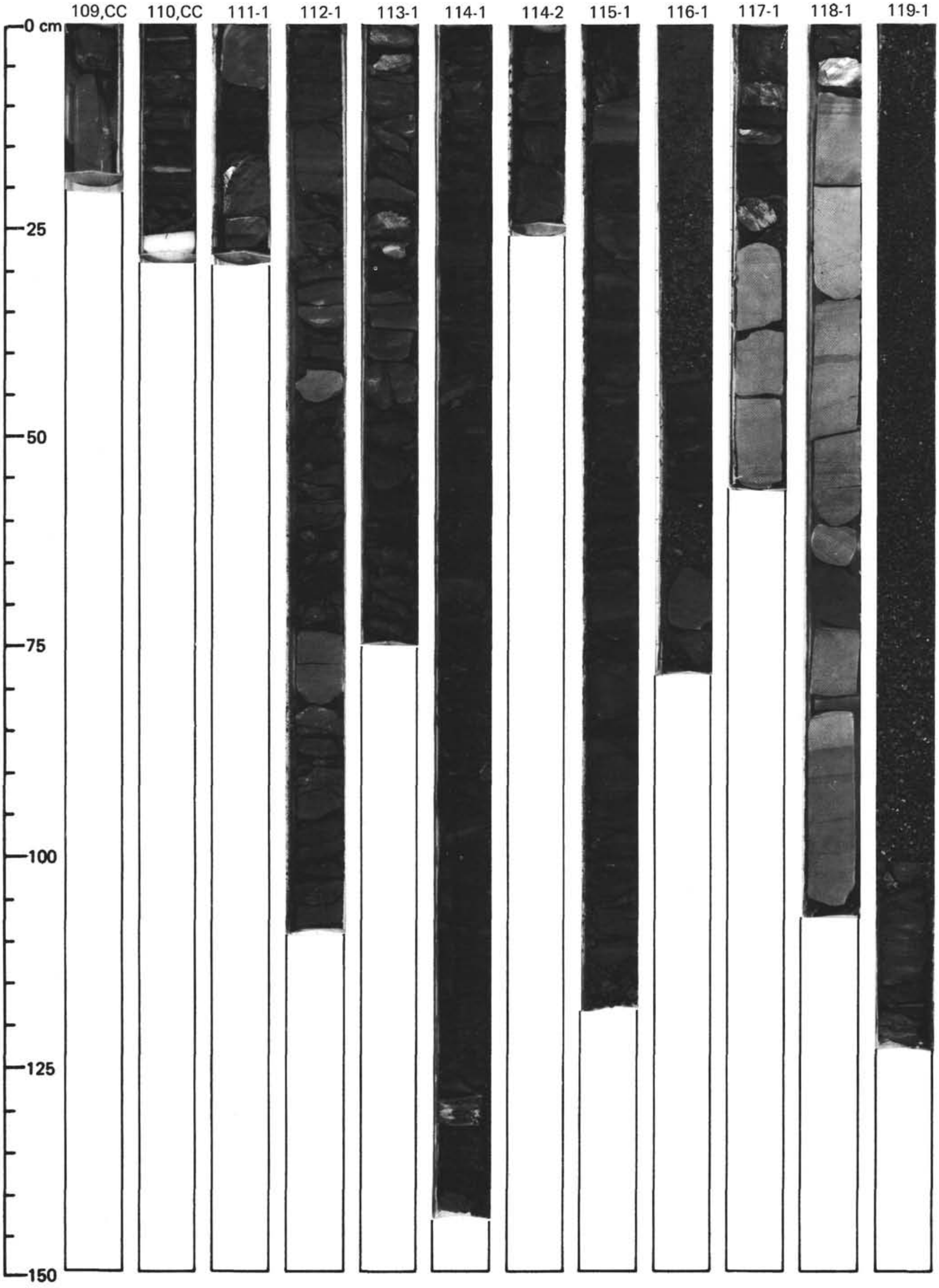
109,CC
110,CC
111-1
112-1
113-1
114-1
114-2
115-1
116-1
117-1
118-1
119-1
0 cm
25
50
75
100
125
150

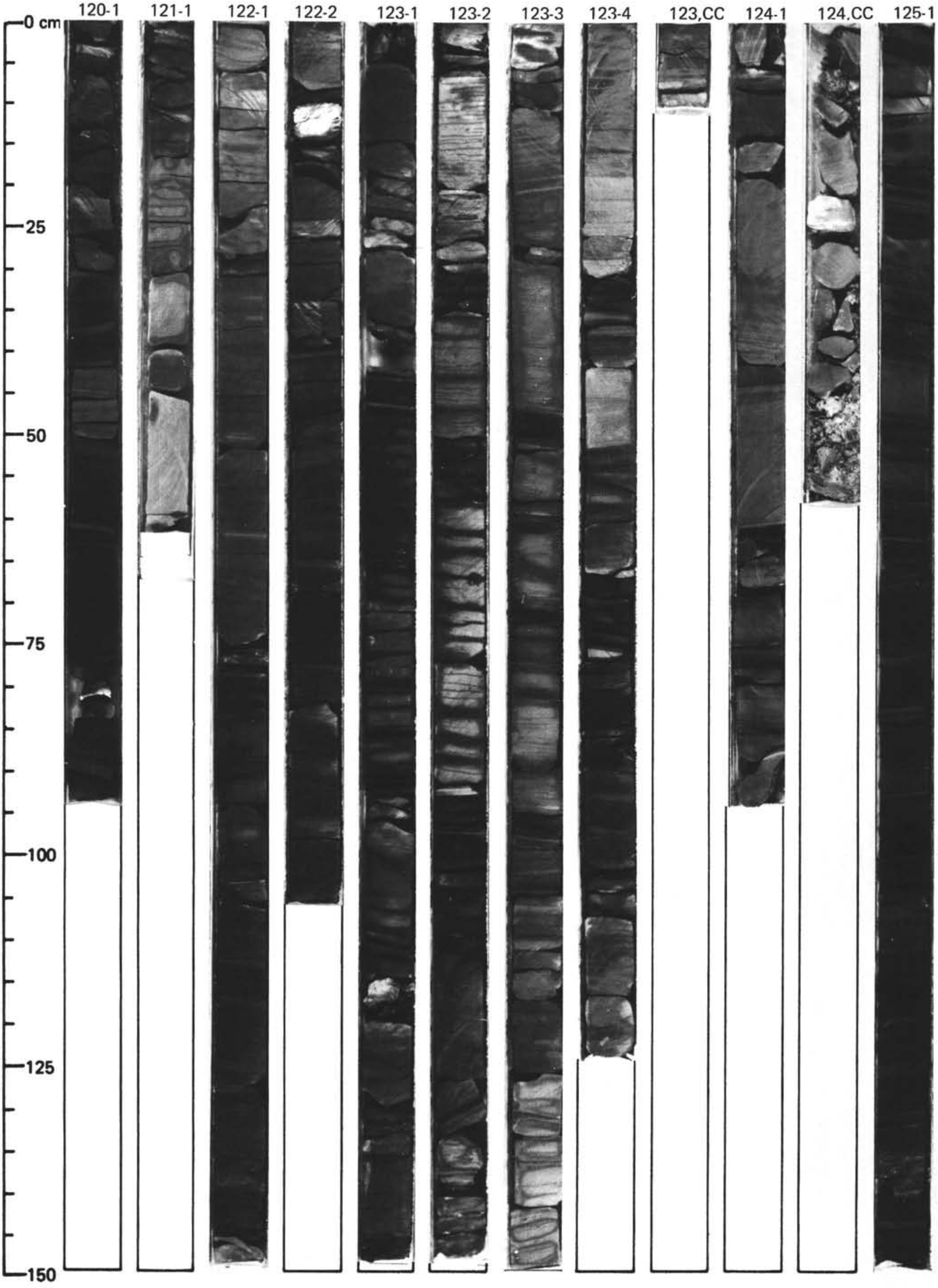
120-1
121-1
122-1
122-2
123-1
123-2
123-3
123-4
123,CC
124-1
124,CC
125-1
0 cm
25
50
75
100
125
150

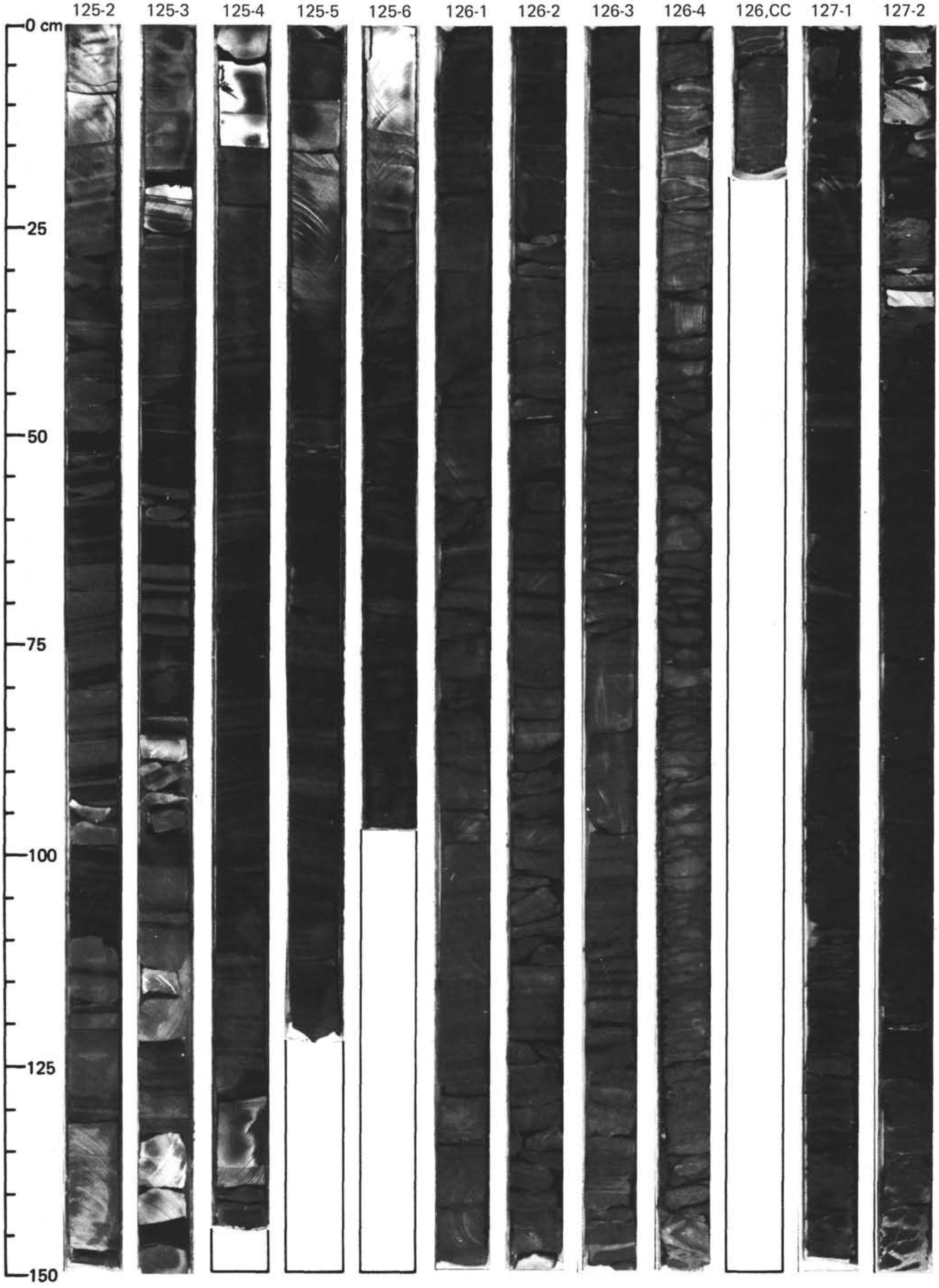
125-2
125-3
125-4
125-5
125-6
126-1
126-2
126-3
126-4
126,CC
127-1
127-2
0 cm
25
50
75
100
125
150

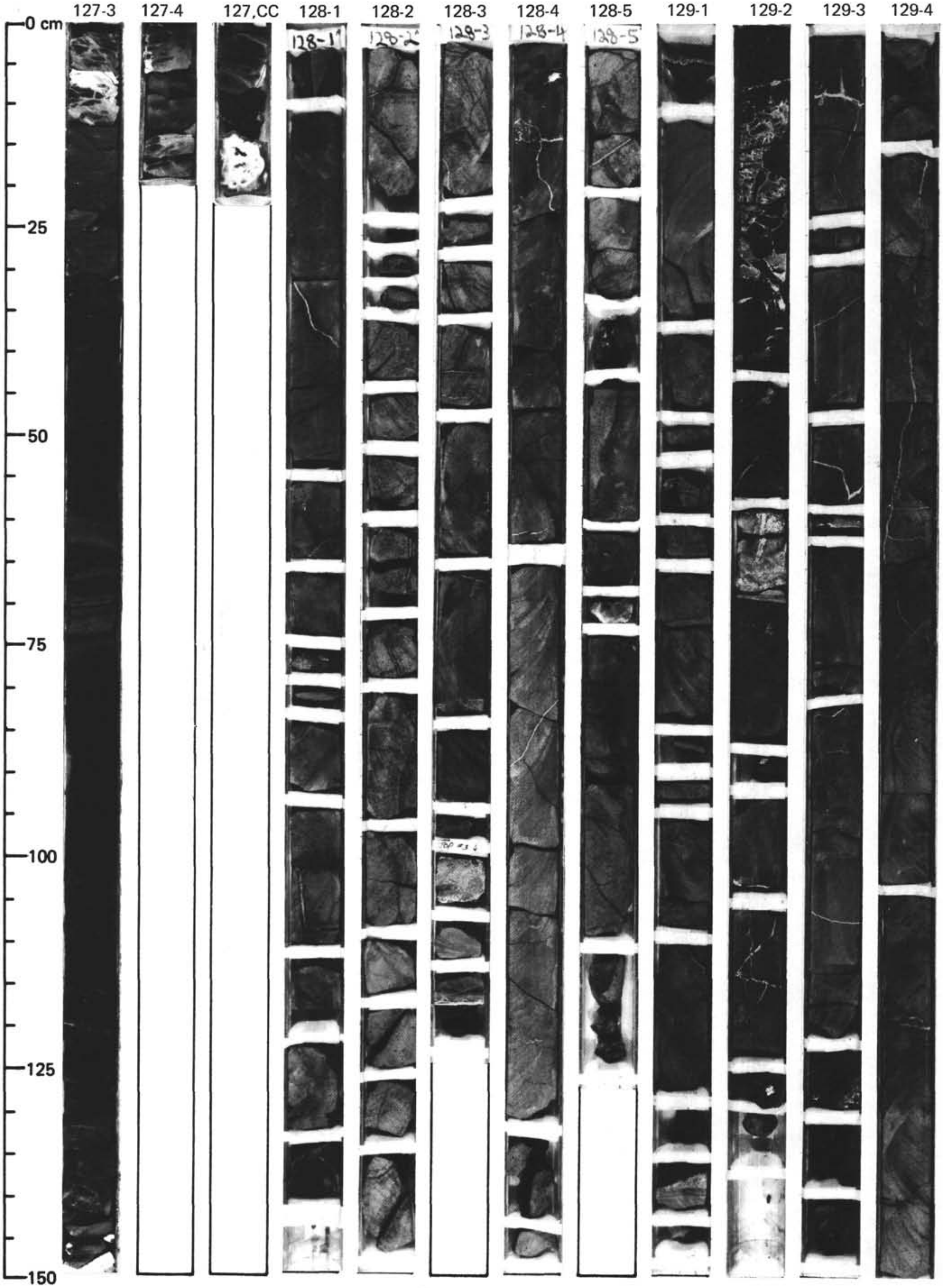
127-3
127-4
127,CC
128-1
128-2
128-3
128-4
128-5
129-1
129-2
129-3
129-4
0 cm
25
50
75
100
125
150

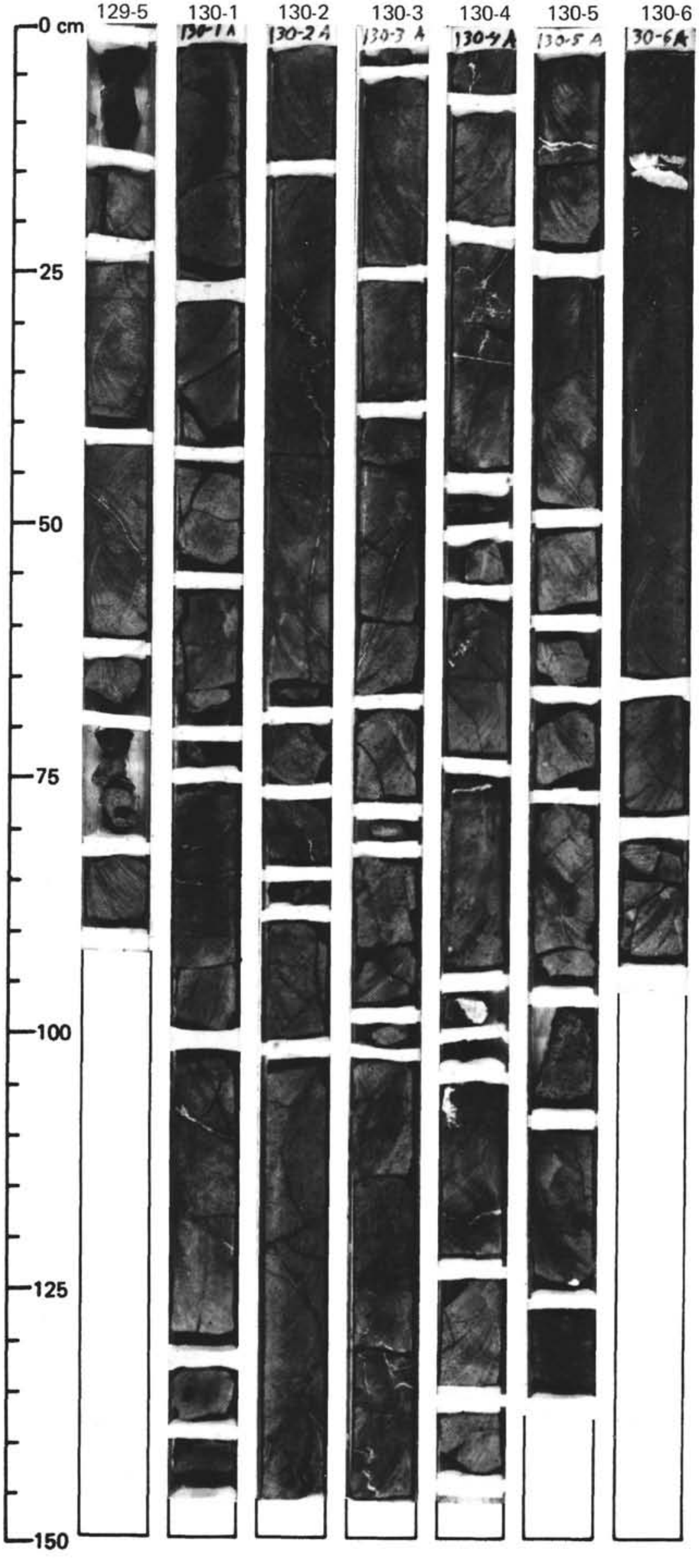
0 cm
25
50
75
100
125
150
129-5
130-1
130-2
130-3
130-4
130-5
130-6
130-1 A
130-2 A
130-3 A
130-4 A
130-5 A
30-6 A